UNIVERSITY OF SOUTHAMPTON

FACULTY OF SCIENCE

School of Chemistry

Flexoelectricity in Liquid Crystals

Volume 2 of 2

by

Daniel Jackson

Thesis for the degree of Doctor of Philosophy

July 2007

UNIVERSITY OF SOUTHAMPTON

ABSTRACT

FACULTY OF ENGINEERING SCIENCE AND MATHEMATICS

SCHOOL OF CHEMISTRY

Doctor of Philosophy

FLEXOELECTRICITY IN LIQUID CRYSTALS

By Daniel Jackson

A rich variety of symmetric and non-symmetric liquid crystal dimers have been synthesised and studied in order to investigate their structure property relations; in particular their flexoelectric properties.

The project is introduced in Chapters 1 and 2 where Chapter 1 gives a brief general background to liquid crystals and liquid crystal synthesis, and Chapter 2 gives a more detailed background to the flexoelectric effect.

The research can be broadly divided into two parts. Chapters 3 and 4 focus on seven conventional non-symmetric liquid crystal dimer series containing two mesogenic groups ether linked through a flexible spacer. These non-symmetric dimers all contain a cyanobiphenyl mesogenic group at one end and either a poly-fluorinated biphenyl or a phenyl-cyclohexyl-alkane mesogenic group at the other. Almost all these materials possess nematic phases (and in one series a smectic phase) and show strong flexoelectric coupling to an applied field with some experiments yielding very large values for the flexoelastic ratio.

Chapter 5 focuses on two series of bent core liquid crystal dimers, where the long chain spacer is divided by a catechol or resorcinol based disruptor group. The disruptor is located in the centre of the molecule and symmetric cyanobiphenyl mesogenic groups are at each end. These materials show a curious odd-even effect in the nematic-isotropic transition temperatures which is further investigated in Chapter 6 by reducing the symmetry of the compounds and studying the changes in the transitional properties. This was achieved in one series by changing the relative position of the catechol linking group along the spacer chain or, in a different series, by altering one of the mesogenic end groups to a di-fluorinated biphenyl (a mesogenic moiety studied in Chapter 3).

The liquid crystal properties were investigated by optical microscopy, differential scanning calorimetry and deuterium NMR spectroscopy. The flexoelastic ratios were determined from the dependence of the tilt in the optic axis on an applied electric field.

Acknowledgments

For me, this PhD has been a journey – and a long one at that! As with any long journey there have been a huge number of people supporting me along the way and here I have an opportunity to thank them.

Every journey has a beginning and mine really started at St Mary's College in Southampton, a mere forty minutes walk from the university – it was here that I fell in love with chemistry and decided that I was going to do a PhD in the subject (probably earlier then most). It was here that I met and was taught for four years by Terry Simmonds the then head of Chemistry. Even at university I do not think I have ever met anyone with such an infectious enthusiasm for chemistry. Clearly (and rightly) convinced that chemistry was the most fascinating, useful, rewarding and important academic subject on the curriculum he was an inspiration to me. In fact I did not fully appreciate how large an impact he had made on my academic career in the subject until I was forced to make the adjustment to learning from other tutors at university – a culture shock which nearly saw me quit my degree. Terry's instinctive and precise knowledge of such a wide range of chemistry was set a very high standard to aspire to and one which I am convinced I have still not suitably obtained, PhD or not! I am however convinced that the most important period of learning in this subject comes at A-level and to him I owe a deep sense of gratitude for the time, energy and patience he willingly gave me ensuring a rock solid foundation in chemistry which has and will last me my career.

Moving on to university, the two most significant figures in my nearly nine-year (!) affiliation, were Martin and Geoffrey who tirelessly supervised my somewhat extended PhD. Martin's work really started some years before when he, beyond all other members of staff in the department took care to keep an eye on me during my undergraduate years. During my attempts to survive the culture shock which was doing an undergraduate degree Martin, on more than one occasion and, I think, without always realising it, provided me with the encouragement I needed to persevere and not give up. Indeed it was only at the end of my degree that I found out how much he had kept an interest in my well-being, through the friends and housemates of mine whom he knew. Martin, in a double-act with James, wooed me into reconsidering a PhD as an option after having lost confidence in my ability

during my final year in undergraduate. So in many respects I owe him not just my PhD but also my undergraduate degree as well.

Geoffrey has taken the leading role in supervising my PhD and, as such, has worn the brunt of my disappointments and been architect of my successes. He has worked tirelessly to educate me in the science of liquid crystals, explaining to me with great patience the background I needed to know to understand the subject I was studying. He was and is always generous with his time with everyone who is in his group holding an interest in not just their academic advance but also their personal well-being. The hours which Geoffrey has poured into my work is phenomenal and unlike any other supervisor in the department. His eye for detail and determination to get the best result possible meant that he not only read the liquid crystal science in my reports but also worked his way through the organic chemistry and experimental sections. His care over my work has been both constant and complete, and I am greatly indebted to him for always going beyond what is required of him as a supervisor to get the best out of my work.

Second in the line of fire after my supervisors is my advisor George, who in spite of his extremely busy schedule, always took the time to help advise, listen, explain (in some cases decode) the science I was attempting to write about in my Thesis. With a wit which is razor sharp and sense of humour which is a dry as the Sahara, George has been both kind and sensitive at the times I have needed it, offering practical advice, suitably cruel questions in my transfer viva and suffered has my sometimes hounding attempts to get his time and attention. I, to this day, do not know anyone else from whom he runs from quite as fast as me! And as a reward, I presented him with a Thesis to read which was almost as along as his.

From there I should move to my parents who, I can imagine, never dreamt this journey would take so long, have supported me unfailingly throughout. Wherever possibly they have made every attempt to lighten my load to allow me the space to do the work that needed to be done, but also to have a chance to relax between times. During these past years they have shared not only the highs and lows of the PhD, but also the many ups and downs of my personal life during this time – and there have been many. Whilst I matured and my approach to life changed, they maintained a constant support to me regardless of how well or not I was handling the situation they provided love, support, time, money and service to me throughout, never stopping and never counting the cost. They exemplified Paul's teaching to the Corinthians on love

and even in the final hours, Dad was helping with corrections and printing whilst Mum waited on us providing much needed coffee and food. As much as I owe Geoffrey and Martin for their direct support of my PhD I owe my parents more for their support of me generally through this testing time.

During the majority of the time I spent throughout my Thesis, my now ex-finaceé Zoe spent much of her time supporting me in spite of the battles she was fighting in her own life. The effort which we put in to help each other overcome the goals we had set ourselves in some respects cost us our relationship. During this time, she spent many hours, supporting me in ways which few if any saw. Her patience with me was un-ending and she bore with me during times when it all seemed hopeless (these moments happen in all PhDs I am reliably told). Not more so then when I was ill, she, along with my parents, bore the brunt of getting me back to fighting fitness. I am blessed that she has become as good a friend to me now as she was partner to me when I was doing my PhD. It is to the support which was unseen to everyone else that I thank her most whole-heartedly for.

There are three things which a PhD student needs to get right before starting, a good supervisor, a good area of study and a good group to work in. The Grossel group has been all that and more. Having working in it for nearly 2 PhDs worth of time I have seen many changes in the group dynamic as colourful characters (which seems to be a constant trait of Grosselites) have come and gone. To mention everyone would take too long in what is already going to be a rather extended acknowledgments section. However during my stay I have been blessed with two very close friends, more like family, in the form of James and Polski. James I knew in my undergraduate years and played a vital role in helping me make the decision to undertake the PhD and then, when life turned upside-down, patently listened to me as I tried hard to figure out this thing called life often keeping him awake in the early hours when clearly he needed to go to sleep! Always loyal and always ready to help – even for an 8 hour round trip to the midlands at midnight. One of my first recollections of Polski was his attempts at helping me purify a starting material. I was unable to do this and he took a couple of hours out of his afternoon to help me. This was an event which would repeat itself as he selflessly gave his time to help me, be it in the lab, online game or refitting a printer (which he did not so much help as do single handed such was my lack of skill for the task). You cannot make it through life without good friends, and I have been blessed to have these two in my life to be mine.

A few other notable mentions in the group include Alan who has been patience personified whilst I shared his fume-cupboard in my final year of writing up. He has endured my disorganisation and maintained a sense of humour which is disturbingly similar to my own (you may want to get that seen to Alan!). Andrew must clearly be mentioned as the inspiration for my use of the PhD comics in on my cover pages and Jon's general organisation in the lab, bringing order to chaos, printers to bear, computers to heel and Martin (almost) under control has been legendary. Georgie has given the group the much needed 'feminine touch' which we wayward men would have otherwise lacked, but I must particularly thank her for reading no less than two of my long chapters whilst herself battling to finish her PhD. In the midst of her stresses she took the time to work through two particularly poorly written chapters making invaluable suggestions struggling with an area of science which is hard at the best of times. I could go on, but thanks should also go to Sophie who helped me in my early years of PhDing, Michael, Alex, Andy, Chris, Francesco, Alain the plethora of project students (and anyone else I may have missed) all of whom have contributed to five enjoyable years in the group.

Outside of the Grossel group is Azizah and Tim who ran several deuterium NMR experiments which are included in the Thesis.

Within the department there are many people who should be thanked, these include Neil and Joan in NMR; the ever patient John and Julie in mass spectrometry; Claire, dealing with all matters financial in my PhD; Sally for answering with just about every other kind of departmentally related question I have ever had; Bevy for looking after me when letters had to be written, Thesis submission problems arose... (the list goes on...); and all the other administration staff who, over the years have kept the department and me afloat when all around was sinking.

Beyond the Chemistry department I must also thank Merck in Chilworth for providing a large portion of the funding, numerous materials, microscopy cells and expertise without which my research would have been impossible. All the staff at Merck were extremely helpful and readily gave up time to help me in my many desperate times working at Chilworth. I should especially like to thank Doina Ionescu, Cecile Schott and Kevin Adlem for their help in supervising my PhD from the industrial perspective. During my postgraduate work it was they who were my first port of call at Merck, locating information and showing me the complexities of making flexoelectric measurements on my samples. When a synthetic chemist attempts to do

physical chemical measurements, patience is a must and theirs with me was seemingly endless!

Also I should thank Prof. John Seddon for his work with X-ray diffraction experiments and the time he took to introduce me to Cliff Jones in the BLCS meeting.

Finally there has been huge support from friends, Lili, Phil, Louise, Moina, Alex, Faith and Hannah to name but a few. Many have listened particularly in the last days to my endless 'it's nearly finished' and then me explaining to them what was left to be done, to them, who have left chemistry years ago. The staff at St. Mary's College, particularly Bryn, who lent me their support whilst I was both teaching and PhDing at the same time, and the classes whom I taught, particularly my Year 10 (now Year 11 class of 2007) classes both of whom gave much colour to my time there (by request Sam and Izy wanted a specific mention – well girls here is it, as promised!).

I would very much like to thank all the members of SonRise Church, particularly Pastor Mary, who have continually supported me, most importantly in prayer during my entire time at University.

This leads me to the most important thank you. I entered into this PhD without thinking to ask my Heavenly Father whether this was the path He wanted me to take. In spite of that, from the very first day when I cried out to Him because it was all going wrong, He has lovingly taken care of me. He surrounded me with the best colleagues, family and friends I could hope for and blessed me with success when I was least expecting it. He has remained completely faithful and utterly constant in my life which has undergone several quantum leaps of change during this time. It is to Him that I ultimately owe my talents in this subject and the people who have supported me in achieving what I have in this work.

It is to Him that any glory from this Thesis rightly belongs, and I pray that He blesses me in the next chapter of my life as much as He as in this one.

Volume 1

Chapter 5

Examining cyanobiphenyl dimers with a kink in the spacer

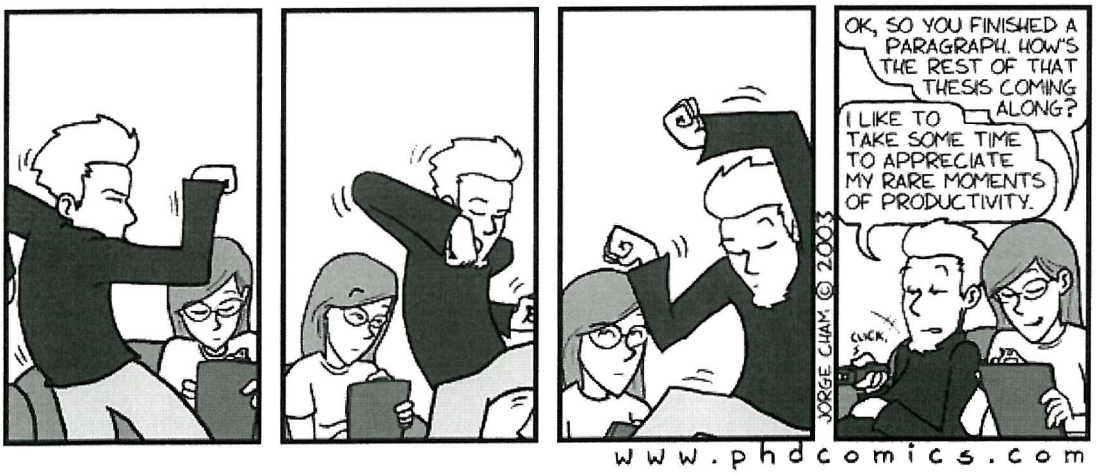

"Piled Higher and Deeper" by Jorge Cham
www.phdcomics.com

Used with permission

5. Examining cyanobiphenyl dimers with a kink in the spacer

5.1. Introduction

With the knowledge that large switching angles and switching speeds could be obtained from conventional dimers such as those discussed in Chapters 3 and 4, our early design strategy for maximising the flexoelastic ratio focused more heavily on manipulating the shape of the materials through insertion of new chemical groups. Rather than subtly altering the chemical characteristics (i.e. changing the mesogenic moieties) resulting in an alteration in the order and the conformational distribution, the overall shape of the molecule was altered through the use of a small aromatic unit in the middle of the chain. The effect was to create a small or moderate angular kink in the molecule which was intended to increase the number of bent conformers in the nematic phase and reduce the melting point. The greater number of bent conformers should increase the average flexoelectric coefficients, $\bar{e}$, and possibly reduce the elastic constant, $\overline{K}$. Such materials would be advantageous for use in display devices. There is also the possibility that the new group could kink the dimer too much resulting in an increase in $\overline{K}$ and $\Delta\varepsilon$.

5.1.1. Symmetric cyanobiphenyl dimers

It is known that reducing the molecular linearity of the liquid crystal destabilises liquid crystalline phase.[1] Therefore distorting the shape of a dimer, making the molecule less linear, is expected to destabilise the liquid crystal phase.

The cyanobiphenyl group was selected as the mesogenic group of choice for a number of reasons. Primarily the group has been shown to stabilise nematic phases due to its shape and large longitudinal dipole. Groups like the Schiff-base moieties were avoided because they are prone to hydrolyse[2] and the lower melting dimers tend to give smectic phases[3] at low temperatures. Equally, at this stage, fluorinated groups such as those described in Chapter 3 were not used as they were not sufficiently mesogenic. Although terphenyl groups are known to stabilise the nematic phase they also tend to raise the melting points making flexoelastic ratios practically difficult to measure or use in a final device.[4] The cyanobiphenyl group, also used in other flexoelectric dimers, comes from a readily available precursor and is known to give large flexoelastic ratios in conventional dimers.[5]

It is also the consistent component in all the non-symmetric dimers reported in this Thesis making the cyanobiphenyl moiety the best candidate for use in flexo-studies of mesogens with this molecular architecture.

5.1.2. The use of disruptors in polymeric systems

It is well-known in polymer compounds that substituted aromatics can be used to lower the melting point by disrupting the molecular shape of the polymer.[6, 7] If the introduction of a disruptor significantly unfavourably alters the length-to-breadth ratio of the molecule the result is expected to also reduce the mesophasic properties of the system. With a large nematic range, however, it is intended that the cost in a sacrificial loss of liquid crystal stability is offset by gaining access to the mesophase at a lower temperature. In deciding upon which disruptor group to use, there were several considerations. The group would have to possess a shape which kinked the spacer group sufficiently to bias the conformational distribution towards less linear conformers without destroying the liquid crystallinity altogether. Incorporating this group into the structure had to be synthetically straightforward with as few steps as possible (if necessary, more synthetically sophisticated structures could be attempted once proof of concept was demonstrated). There appeared to be literally hundreds of group which could have been used to introduce a kink in the molecule. However there were some constraints on the selection of a given group, in particular:

- It should promote more of a bent structure than the corresponding conventional dimers.
- Starting material should be commercially available and preferably cheap.
- Where possible it should not complicate the electronic structure of the material by the introduction of unnecessary hetro-atoms as this could complicate our understanding of where the molecular dipole lies and how this is affecting the flexoelectric behaviour.
- It should not be so large as to destroy any liquid crystallinity
- It needs to be stable to the synthetic reaction conditions.
- The product needs to be thermally stable to melting and cooling cycles used in the analysis of the liquid crystalline properties.

- The starting material should ideally be compatible with the types of molecular building blocks already available. (i.e. to react with the α,ω-bromoalkylcyanobiphenyl unit, there needs to be a nucleophilic centre on the disruptor unit)

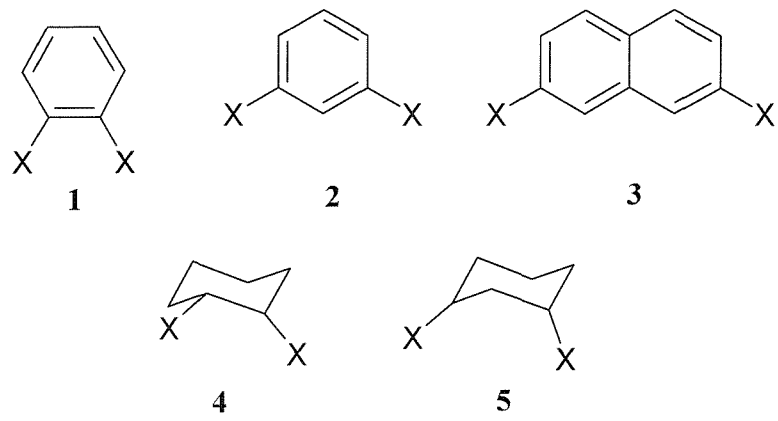

Figure 5.1 Variety of cyclic ring systems which were considered as disruptor units to generate a bend in the dimer structure. X represents either an oxygen or methylene unit.

This leaves a short list of only a few potential cores which are shown in Figure 5.1. Synthetically, it is simpler to have hydroxyl groups at X rather than forming a methylene link. The presence of oxygen in this position has the advantage of promoting the stability of the nematic phase even though it does raise the melting point slightly.[8] Other linking groups such, as esters which produce phthalate ester cores, were also considered (and attempted in a few cases) however, these were generally found to raise the melting points and lower nematic to isotropic transitions. There were advantages and disadvantages to each group. Groups **1** and **2** were very cheap to buy and reactions involving double alkyl substitutions are well-known[9] however, there is a tendency for catechol and resorcinol to oxidise, especially under alkaline conditions. Naphthan-1,7-diol trimers are known[10] and are predominantly monotropic. The size of the naphthylene unit is also larger and increases the melting point significantly. Groups **4** and **5** were interesting as the slightly flexible nature the cyclohexyl ring would be expected to help reduce the melting point and increase solubility[11] however **4** is not commercially available and **5** is available but only as a mixture of *cis* and *trans* isomers. Thus catechol and resorcinol were used as

core groups to produce a range of kinked dimers based around a 1,2- and 1,3-substituted benzene ring core.

For clarity the mnemonics of the series considered in this chapter are given with their full systematic names in Figure 5.2.

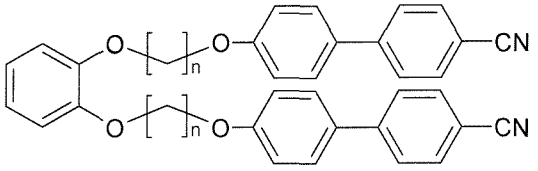

Cat(OnOCB)$_2$ (Chapter 5)
1,2-bis-[α-(4'-cyanobiphen-4-yloxy)alkyl-ω-oxy]benzene

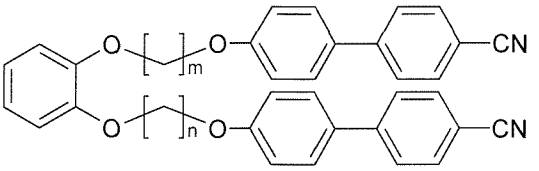

Cat(OmOCB)(OnOCB) (Chapter 6)
1-[α-(4'cyanobiphenyl-4-oxy)alkyl1-ω-oxy]-2-[α'-(4'cyanobiphenyl-4-oxy)alkyl-ω'-oxy]benzene

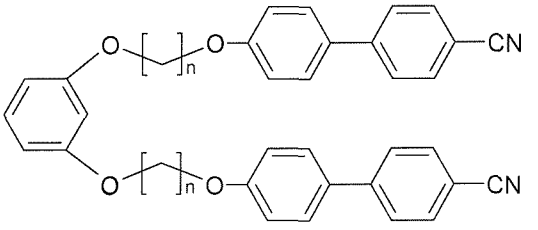

Res(OnOCB)$_2$ (Chapter 5)
1,3-bis-[α-(4'-cyanobiphen-4-yloxy)alkyl-ω-oxy]benzene

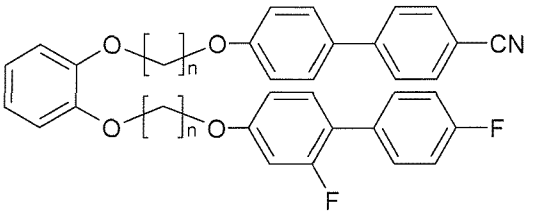

Cat(OnOCB)(OnOBF$_2$) (Chapter 6)
1-[α-(4'cyanobiphen-4-yloxy)alkyl-ω-oxy]-2-[α-(2,4'-difluorobiphenyl-4-yloxy)alkyl-ω-oxy]benzene

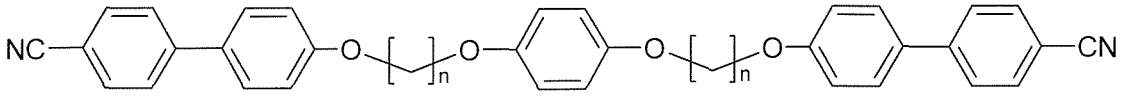

Qui(OnOCB)$_2$ (Chapter 5)
1,4-bis-[α-(4'-cyanobiphen-4-yloxy)alkyl-ω-oxy]benzene

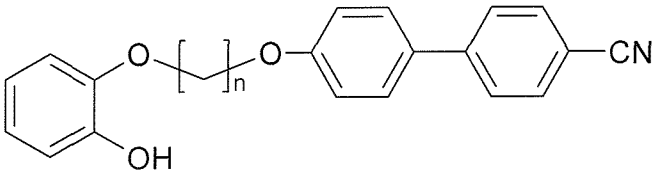

Cat(OnOCB)(OH) (Chapter 6)
1-[α-(4'cyanobiphen-4-yloxy)alkyl-ω-oxy]-2-hydroxybenzene

Figure 5.2 Structrures, mnemonics and systematic names for the dioxybenzene substituted liquid crystal dimers considered in Chapters 5 and 6.

5.1.3. Quinone linked dimer systems

It has very recently come to our attention that a small range of dimeric compounds with a 1,2- or 1,3-dioxybenzene core have been synthesised and characterised.[12, 13] A reference in these recent papers refers to an earlier publication in which a subset of the 1,3-dioxybenzene kinked dimers with symmetric cyanobiphenyl mesogenic groups is given.[14] A short consideration of this work is given subsequent to the conclusions in this chapter. The 1,4-dioxybenzene based analogues made by Furuya *et al.*[15] have been known for a considerably longer length of time and these results are given below.

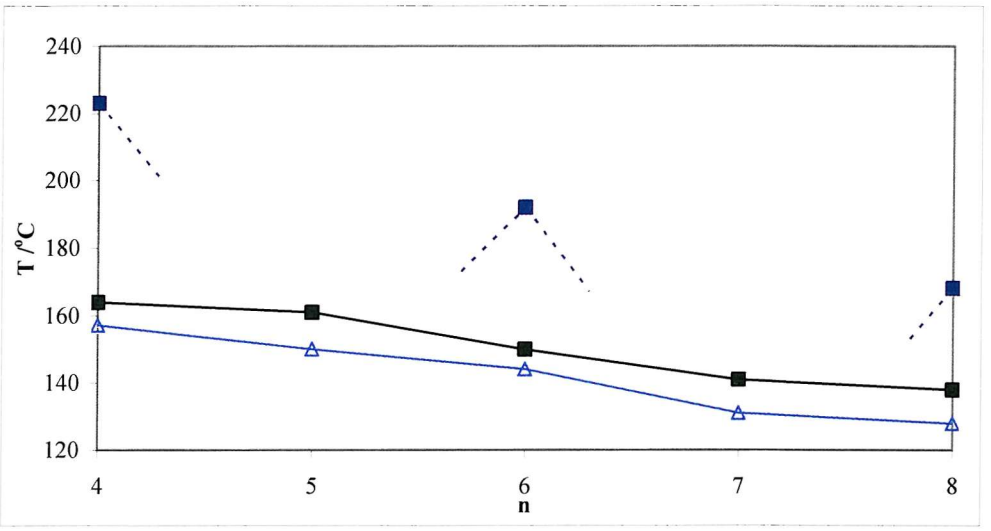

Figure 5.3 The temperatures of transition for 1,4-dioxybenzene core dimers where ■ denotes T_{CrN} for Qui(OnOCB)$_2$ and T_{CrI}; ■ denotes T_{NI} for Qui(OnOCB)$_2$ and Δ denotes T_{NI} for CBO(2n+6)OCB.[16]

The Qui(OnOCB)$_2$ dimers are likely to form linear geometries in the nematic and so it is not surprising that the examples in Figure 5.3 were nematogenic and show both high melting and N-I transitions, which are both larger than the corresponding conventional cyanobiphenyl dimers (Note that CBO(2n+6)OCB is plotted in Figure 5.3 to take into account the double spacer and the extra atoms in the disruptor group). This is not surprising as the *para*-substituted aromatic ring serves to elongate the structure and to make it more rigid. The other significant feature of Furuya's dimers is that there are no recorded transitions for the odd dimers. This is not as profound as it may first appear. It was shown by Attard *et al.*[17] that the constant high melting point of the odd dimers was much larger than their T_{NI} and by introducing a side alkyl group on the core, the melting

point could be lowered enough to access the nematic phase. With these results in mind it would be prudent to look at another set of series of dimers, where examples with bent and linear disruptor groups have been made, and examine the effect of introducing a kink in the molecule.

5.1.4. Phthalate, isophthalate and terephthalate ester linked liquid crystal dimers

Benzene ester disruptors in liquid crystal dimers (phthalate (1,2-), isophthalate (1,3-) and terephthalate (1,4-)) are known compounds reported by Attard and Douglass.[18, 19] The behaviour of Schiff-base moieties compared to cyanobiphenyl moieties is substantial both in terms of chemical stability and mesogenic behaviour. Similarly the difference in transition temperatures between ester (as in these examples) and ether spacer linkers (as in the materials reported later) is known to be significant.[20] However, in spite of these differences, the comparison between *ortho-*, *meta-* and *para-* substituted benzene cores may give some insight as to what will happen in the corresponding cyanobiphenyl dimers. The structures of the considered materials are shown in Figure 5.4 and the transition temperatures given in Table 5.1.

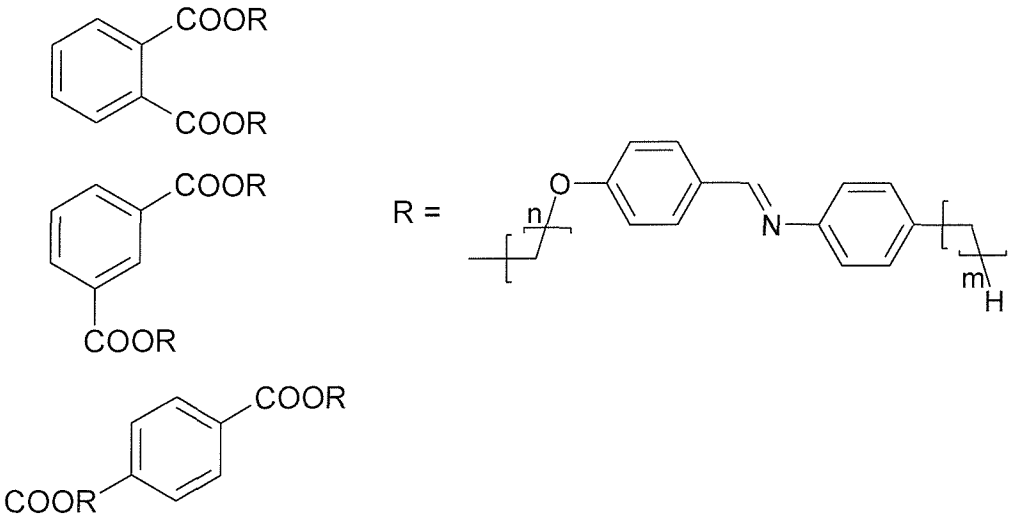

Figure 5.4 Structure of phthalate, isophthalate and terephthalate core, Schiff-base liquid crystal based dimers. For the purposes of this analysis, n=3-6 and m=4.

Table 5.1 gives the transition temperatures (available in the literature) for these series. For the purposes of this Thesis, however, we shall restrict ourselves to a simple analysis of the nematic-isotropic transitions for each series (see Figure 5.5).

	m = 4															
	n	Cr		SmF/I		SmB		SmC		SmA		N		I		
Ortho	3	•	100	•	(38)	•			(58)	•	(64)	•	(67)	•		
	4	•	86	•		•			(50)	•			(56)	•		
	5	•	83			•			(49)	•	(60)	•	(62)	•		
	6	•	81			•			(57)	•			(65)	•		
Meta	3	•	116									•	(104)	•		
	4	•	96			•							(79)	•		
	5	•	104							•	(85)	•	(101)	•		
	6	•	83	•	(57)	•	(62)	•	(64)	•	(79)	•	(81)	•		
Para	5	•	140								(132)	•	148	•		
	6	•	114											•		

Table 5.1 Table of transition temperatures in °C for phthalates, isophthalates and terephthalate core dimers for m = 4 and n = 3 - 6. [18, 19] Only data for n = 5, 6 for the terephthalates was available.

The most significant feature is that almost all the mesophases are monotropic. In fact only the nematic phase of the *para*-substituted core for n = 5 is enantiotropic. This is expected as the materials become more linear and the liquid crystal phase more stable.

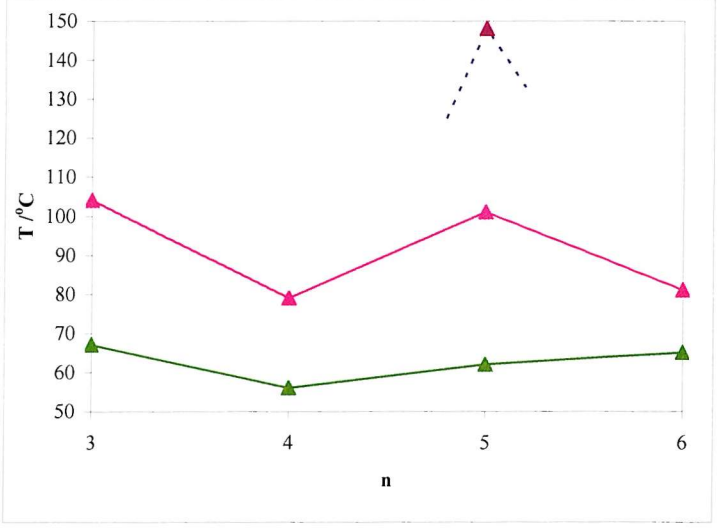

Figure 5.5 N-I transition temperatures for the three series reported in Table 5.1 where ▲ denotes the phalate core series, ▲ denotes the isophthalate core series and ▲ denotes the terephthalate core series.

The plethora of different mesophases seen is almost certainly a consequence of the mesogenic moieties used. Schiff-base mesogenic groups are known for exhibiting a

variety of different smectic phases so it is not surprising that such a rich liquid crystal polymorphism is observed. However the nature of these phases change with different disruptor groups as they cause the molecule to be more kinked. Cyanobiphenyl dimers do not show such a rich morphology and as we shall see later in the series that are studied, almost exclusively, only nematic phases are observed.

For the phthalate based dimers, the melting points are reduced as the substitution on the disruptor becomes closer. However, they fall by less than the corresponding T_{NI} resulting in the monotropic behaviour. In the case of the cyanobiphenyl 1,4-dioxybenzene linked dimers, the nematic phase is much more stable and from this we might be tempted to predict that the 1,2- and 1,3-dioxybenzene core dimers should be stable enough to produce an enantiotropic nematic phase for some spacer lengths.

In these series the nematic phase of the odd members appears to be generally more stable than for the even, however the extent of the odd-even effect is lessened the more bent the molecule becomes so much so that the phthalate cores show no appreciable alternation.

It is unwise to form firm expectations based on trends seen on a group of materials which are very different in structure and chemical composition compared to 1,2-dioxybenzene linked, cyanobiphenyl dimers. However the decrease in melting point and phase stability, the increase in observable smectic character and the reduction in the degree of alternation between odd and even members appear to show some basic changes with shape which may well be mimicked by the proposed dioxybenzene core dimers.

5.2. Synthesis of novel kinked symmetric dimers.

5.2.1. Details of the synthesis

Synthesis of the 1,2-dioxybenzene and 1,3-dioxybenzene based dimers was achieved by reaction of a cyanobiphenyloxy-α-alkyl-ω-bromide with catechol or resorcinol, respectively. Synthesis of the alkylating agent is described in full in Chapter 3 with experimental details given in Chapter 7.

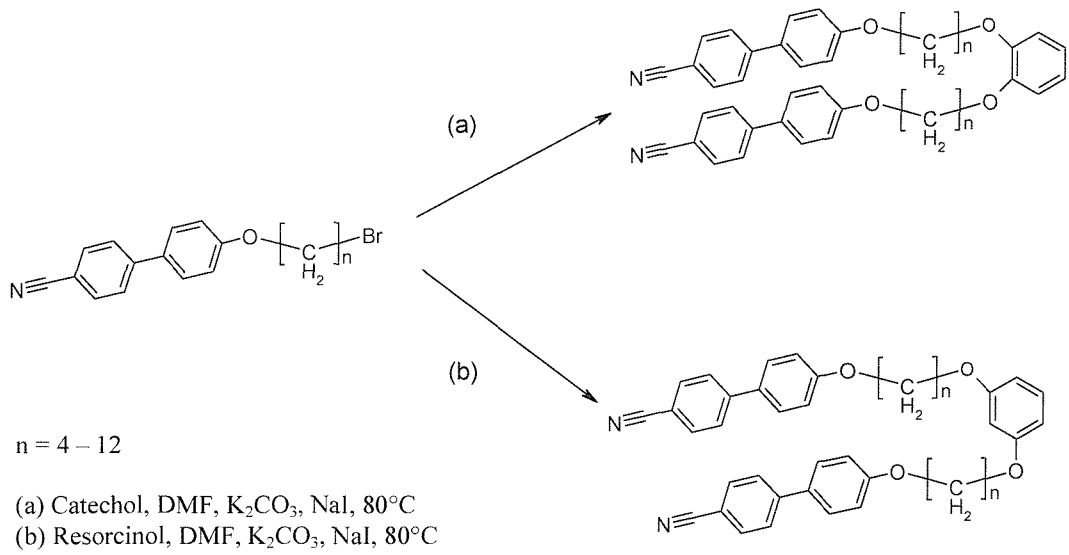

Figure 5.6 Synthesis of (a) 1,2-dibenzoxy-bis-(α-alkyl-ω-oxycyanobiphenyl) dimer ($Cat(OnOCB)_2$); (b) 1,3-dibenzoxy-bis-(α-alkyl-ω-oxycyanobiphenyl) dimer ($Res(OnOCB)_2$).

Chain length n	1,2-dibenzoxybis-(α-alkyl-ω-oxycyanobiphenyl)	1,3-dibenzoxybis-(α-alkyl-ω-oxycyanobiphenyl)
4	52%	38%
5	46%	37%
6	34%	74%
7	24%	59%
8	68%	52%
9	45%	70%
10	92%	64%
11	60%	71%
12	63%	24%

Table 5.2 Yields of pure product obtained for $Cat(OnOCB)_2$ and $Res(OnOCB)_2$ series where n = 4 – 12.

The synthetic route for each series is given in Figure 5.6 and the range of yields are listed in Table 5.2. It should be noted that in the case of the 1,2-dioxybenzene substituted materials the synthesis was conducted over the course of a year and not in numerical order (e.g. 7 was attempted first). The variation in yields is, therefore, due to a number of factors relating to the nature of the materials. These include increasing experience and range of different techniques to achieve higher yields and purity. The final optimum procedure is reported in Chapter 7 although some of the problems associated with the

syntheses are considered here. In the case of the reactions with resorcinol, lower yields were generally found when the chain length was short where the cyanobiphenyl group is close to the aromatic ring and so, presumably inhibiting the second substitution resulting in yields as low as 38% for n = 4. When the chain is very long, where the chain presumably gets in the way of the second substitution, the yields are also adversely affected (e.g. for n = 12; yield = 24%). Although the double alkylation of the catechol appears straightforward, control of the reaction to obtain good yields was less trivial. The aerial oxidation of dihydroxy-benzenes to form a di-ketonic group which spontaneously oxidizes to a variety of dark brown organic biproducts is well-known[21] and is vastly accelerated in the basic conditions necessary for alkylation. Quantifying this process is impossible, but can be crudely assessed based on the yield of the reaction. The most straightforward way of reducing this side reaction is to remove the oxygen from the system by nitrogen purging the solvent for up to 30 min immediately before use and maintain a positive pressure of nitrogen over the reaction during its course. In spite of this, some oxidation inevitably did take place. The solvent of choice for this reaction was dry, HPLC grade DMF, due to its high boiling point and solubilising properties. In each case the anion was preformed (visible by the clear change in colour to a pale blue on addition of base before the onset of oxidation).

Generally the reaction was left for an extensive period of time. Even with the sodium iodide as the catalyst better yields were generally obtained if the reaction was left for seven days rather than three and certainly better than just overnight. Given that this alkylation is an SN_2 type reaction occurring twice there are two steps in the process. From qualitive analysis of the electronic inductive (I+) and mesomeric (M+/-) effects of each successive alkylation, the second deprotonation and alkylation is likely to be the rate determining step (since formation of the anion will be destabilised by an I+ movement of charge into the aromatic ring resonating to ortho and para positions). Thus it would be expected that a significant quantity of monosubstituted material would be produced and this is indeed what is observed. Such is the difference in acidity of the protons that sodium hydride is used in preference to potassium or caesium carbonate when deprotonating the second hydroxyl group in the non-symmetric syntheses (described in

Chapter 6) however, curiously, the use of sodium hydride in the symmetric synthesis made no difference to the yield when used in symmetric synthesis.

It should also be noted that literature preparations of dialkylated catechols also include procedures involving ethanol and potassium hydroxide. This method was attempted but gave a chronic yield of 8% with a poor recovery of starting materials. NMR of the crude showed no major biproduct. As such the procedure was not pursued any further. Procedures involving phase catalysts tended to use DCM or chloroform as the organic solvent. Since the previous reaction gave poor yields at low temperatures (comparable to refluxing chloroform) this method was not investigated further.

Workup was generally achieved by one of two methods depending on the availability of a vacuum with sufficiently low pressure to be able to remove DMF below 90 degrees by rotary evaporation. Where this was not possible workup was achieved by precipitation of the product by addition of water followed by filtration through celite and washing with water. In one case (n = 8) crystallisation from neat DMF was achieved but this was never repeatable and the crystal structure is given later in Figure 5.7.

Synthesis of the 1,3-disubstituted materials was achieved by a very similar method. DMF was removed by rotary evaporation and treated exactly as for the 1,2-dioxybenzene series.

Purification had to be achieved through column chromatography. However, in the case of the 1,2-dioxybenzene compounds, this was complicated by the monomer and dimer having very similar Rf values irrespective of the solvent polarity. This was due, coincidently, to the polarity of the free aromatic -OH group on the monomer being equivalent in its attraction to the silica compared to the extra molecular weight on the disubstituted dimer. This became increasingly more problematic as the spacer length became longer. It was fortuitous that the 1,3-dioxybenzene derivatives were more easily purified as the separation by column chromatography was considerably better.

The monosubstituted catechols are discussed in Chapter 6 and fully characterised in Chapter 7.

5.2.2. Molecular characterization

Insolubility of the cyanobiphenyl moiety is widely known by those chemists who handle it in the synthetic lab. Generally chlorinated organics are the solvents of choice. These

materials were no exception as they tended to dissolve only in THF, DMF and chlorinated solvents at room temperature. This limited the solvents available for both chromatography and crystalisation. In the case of the latter, a variety of solvents were used with little success and then only for even dimers.

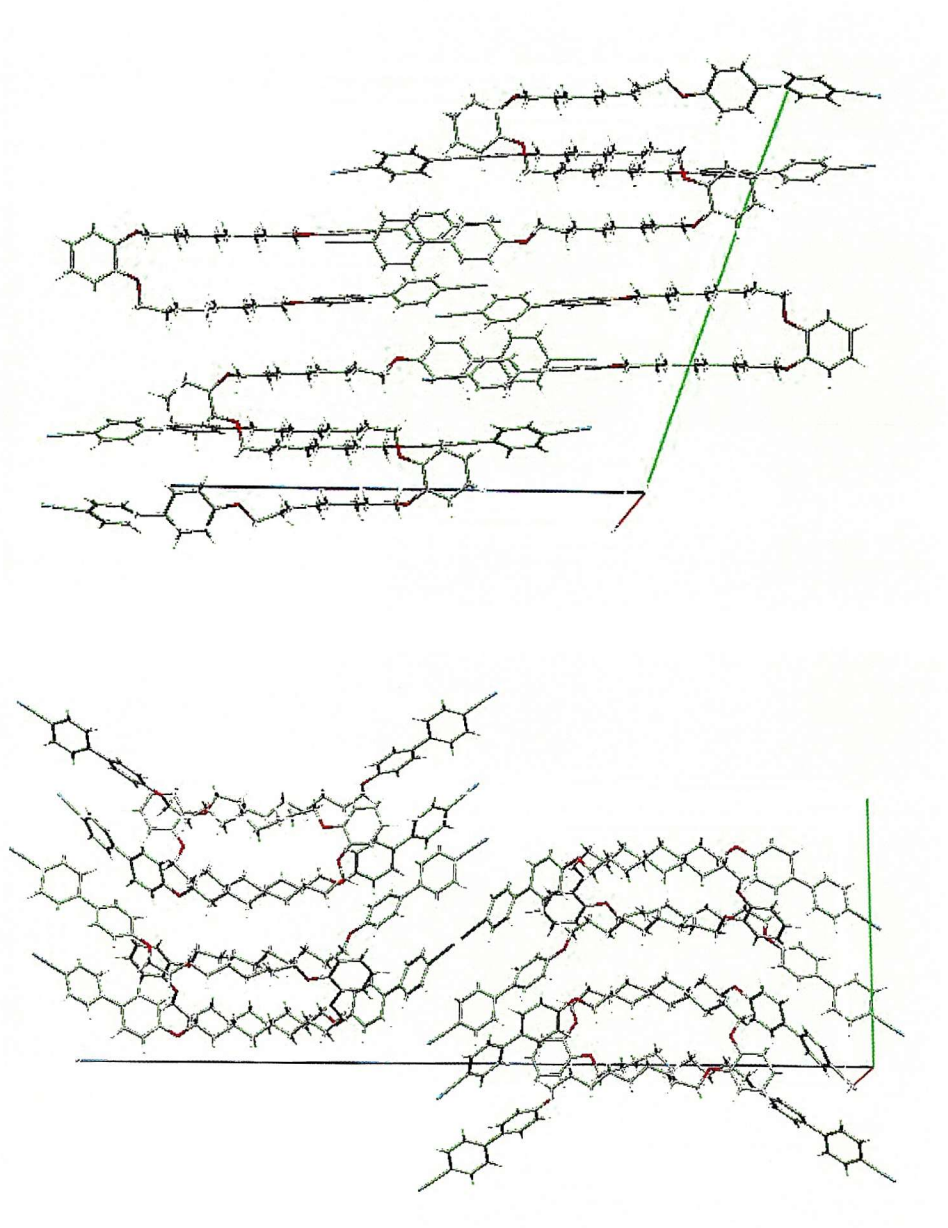

Figure 5.7 The unit cell of (top) Cat(O8OCB)$_2$ containing six molecules, three in the asymmetric unit (found in Appendix E); (bottom) Cat(O9OCB)$_2$ containing 8 molecules, 1 in the asymmetric unit (found in Appendix E).

Indeed until very close to completion of this Thesis, no odd dimers had been successfully crystallised and studied via single crystal X-ray diffraction. However we have data now for Cat(OnOCB)$_2$ where n = 8 and 9 which n = 8 crystallised from DMF and n = 9 was recrystallsied from ethyl acetate.

We cannot reliably use conformational information from the crystal structure to predict the conformational distribution in the nematic. However, it does reveal what structure the crystal is likely to be melting from and, may offer some clues as to why the transition temperatures behave as they do with changing parity. Also, as a straightforward crystallographic comparison, they are interesting as the structure is very different to that seen for conventional dimers.

Comparing the two structures for n = 8 and 9 (see Figure 5.7) we see that there are a number of similarities between them. Their overall conformational structure is U-shaped, the significance of which we will discuss later. Fundamentally each molecule can be thought of in two parts, the aliphatic region which consists of the two methylene spacers and the aromatic parts which consists of the two cyanobiphenyl groups and the 1,2-dioxybenzene moiety. These regions appear to effectively separate in the crystal with the aliphatic chains packing most closely together and the aromatic groups, particularly the cyanobiphenyls arranging themselves to maximise a number of favourable intermolecular interactions. The geometry of the aromatic groups in both cases suggest weak hydrogen bonding between the cyano nitrogen and aromatic protons on a neighbouring biphenyl which are similar to those found in di-cyanobenzene.[22] The biphenyls tend to adopt a T-shaped geometry from quadrupolar interactions (edge-to-face contacts) between the rings.[23, 24]

For both molecules these short contacts along with those originating from the ether links are likely to be opportunistic interactions rather than structure directing which probably results simply from efficient molecular packing.

On closer inspection of the unit cell and the crystal data given in Table 5.3 we see that the symmetry of the unit cell is different for each molecule and curiously, in spite of the more disordered spacer chain, it is the Cat(O9OCB)$_2$ which has the higher symmetry. We can also see that in both crystal structures the molecules are packed head-to-tail, however the n = 9 has a 1:1 packing whereas n = 8 has a 1:2 ratio which is an artefact of the

differing symmetry. Again, we cannot read too much into these differences as each crystal was obtained from different solvent system however this arrangement forms a pseudo-layer structure which is best appreciated when rotating the crystal structure rather than from a stationary picture (see the attached CD).

$C_{49}H_{52}N_2O_4$	a = 9.4379(3) Å	T = 120(2) K
RMM = 720.92	b = 24.5343(10) Å	λ = 0.71073 Å
Triclinic P-1	c = 27.8878(11) Å	Dc = 1.213 Mg/m^3
V = 5920.8(4) $Å^3$	α = 109.848(2)°	μ = 0.076 mm^{-1}
Z = 6	β = 96.750(2)°	0.10 x 0.10 x 0.06 mm^3
R_1 = 0.0576	γ = 97.960(2)°	Pale beige shard

$C_{50}H_{56}N_2O_4$	a = 8.8233(2) Å	T = 120(2) K
RMM = 749.01	b = 17.7886(4) Å	λ = 0.71073 Å
Orthorhombic Pbca	c = 52.8278(12) Å	Dc = 1.200 Mg/m^3
V = 8291.5(4) $Å^3$	α = 90.00°	μ = 0.075 mm^{-1}
Z = 8	β = 90.00°	0.05 x 0.05 x 0.02 mm^3
R_1 = 0.1294	γ = 90.000°	White shard

Table 5.3 Crystal data for (top) Cat(O8OCB)$_2$; (bottom) Cat(O9OCB)$_2$

The parity of the spacer chain does result in some difference between the two structures. The biggest difference is in the conformation where n = 8 is clearly more linear than that of n = 9. This results from not only the natural shape of the all-trans odd spacer, but also from the larger number of gauche links in both chains.

Primarily, however, there is a common conformational shape which is the closed U-shape and although we cannot draw conclusions about conformations in the nematic from the crystal structure, we can consider that this *may* be *a* plausible conformation in the nematic. If we also consider the entropy of melting (given in Table 5.6) we see that there is very little variation in $\Delta S_{melt}/R$ with change in parity and all these values are comparable to those seen for the CBOnOCB series.[25] From this we may speculate that any change in conformation at melting is likely to be neither drastic nor particularly different for either the odd or even dimers.

5.3. Physical data for the 1,2-dibenzoxybis-(-α-alkyl-ω-oxycyanobiphenyl) series

The examination of the materials via optical microscopy to study their phase behaviour revealed a variety of unexpected results. As we shall see, the nature of the phase (i.e. nematogenic) was expected, however, the variation in the transition temperature as a

function of spacer length was not. Beyond the microscope obtaining reliable physical data on the 1,2-dioxybenzene disruptor series to unravel the mysteries of its behaviour proved capricious. The DSC data, X-ray scattering data and ^{2}H NMR spectroscopy gave a series of results which were either uninformative, perplexing or both.

5.3.1. Optical microscopy

It is well known that the cyanobiphenyl dimers tend to favour nematic phases.[25] It is, therefore, not surprising that the entire series synthesised show purely nematogenic behaviour albeit monotropic in some cases. Most of the materials generally show Schlieren textures consisting of two and four brush defects (see Figure 5.8 and 5.9) consistent with a uniaxial nematic. In some materials in the catechol series there are a remarkably large number (or though not exclusively) of two brush defects which are thought to be indicative of a biaxial nematic phase.[26]

There is evidence that certain members of the series exhibit different crystal phases depending on the temperature, rate of cooling, mechanical stress and the conditions of crystallisation (i.e. from solvent or from the melt). For example, $n = 8$ for the Cat(OnOCB) series melts sharply from solvent crystallised solid at 126 °C to an isotropic liquid. On cooling it forms a nematic at 115 °C and then can be supercooled and crystallised at about 100-105 °C. If this crystal phase is cooled rapidly and/or subjected to mechanical stress a second crystal phase is induced and has been observed under the microscope. Apart from the texture of the two crystal phases being quite different, the structure of each crystal phase is unlikely to be similar as their respective melting points are quite different.

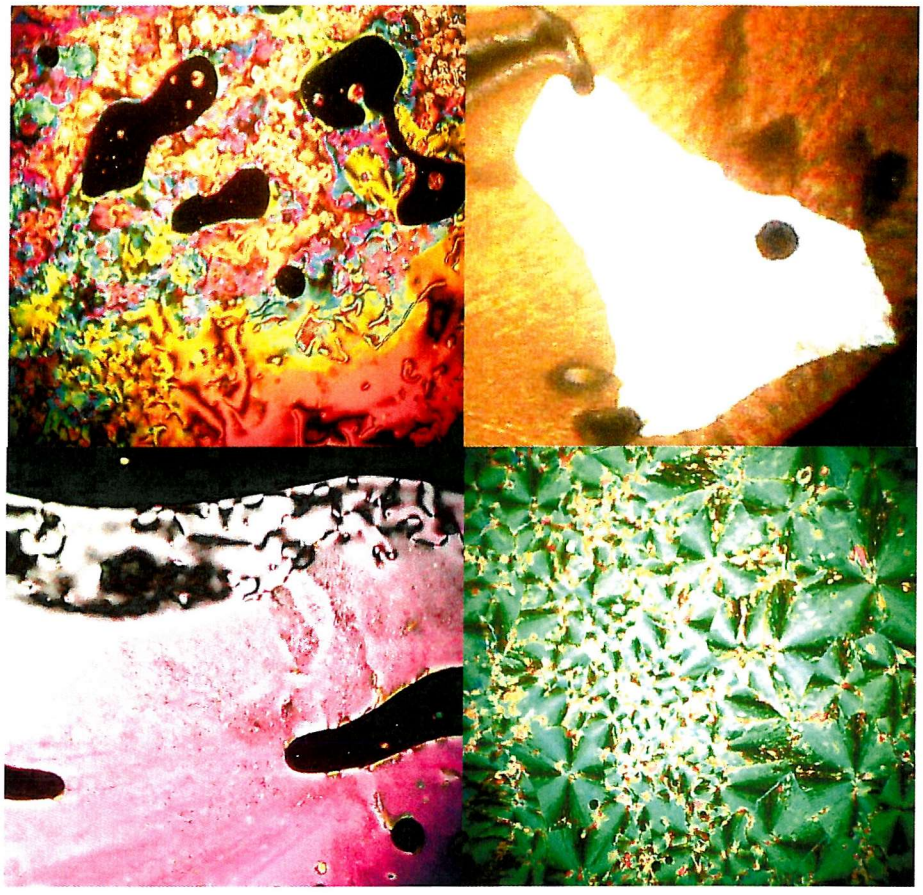

Figure 5.8 All optical texture pictures were taken on cooling showing nematic phases Cat(O4OCB)$_2$ taken at 141 °C, 0.99T_{NI} (top left); Cat(O5OCB)$_2$ taken at 92 °C, 0.99T_{NI} (top right – note the bright region is the liquid crystal texture, the darker areas are regions which are crystallising); Cat(O6OCB)$_2$ taken at 122 °C, 0.99T_{NI} (bottom left); Cat(O7OCB)$_2$ taken at 74 °C, 0.96T_{NI} (bottom right) .

The first crystal phase, formed on cooling, melts at ~109 °C into a nematic which clears at 115 °C and appears to be enantiotropic. The second crystal phase is similar to that formed from solvent crystallisation as it melts at 126 °C to an isotropic liquid. This behaviour is reproducible and observed in the DSC traces for subsequent heating/cooling cycles. This behaviour is observed in some of the other members of the series (e.g. n = 6 and n = 10) and seen quite clearly in the DSC although it is not so easily observed under the microscope.

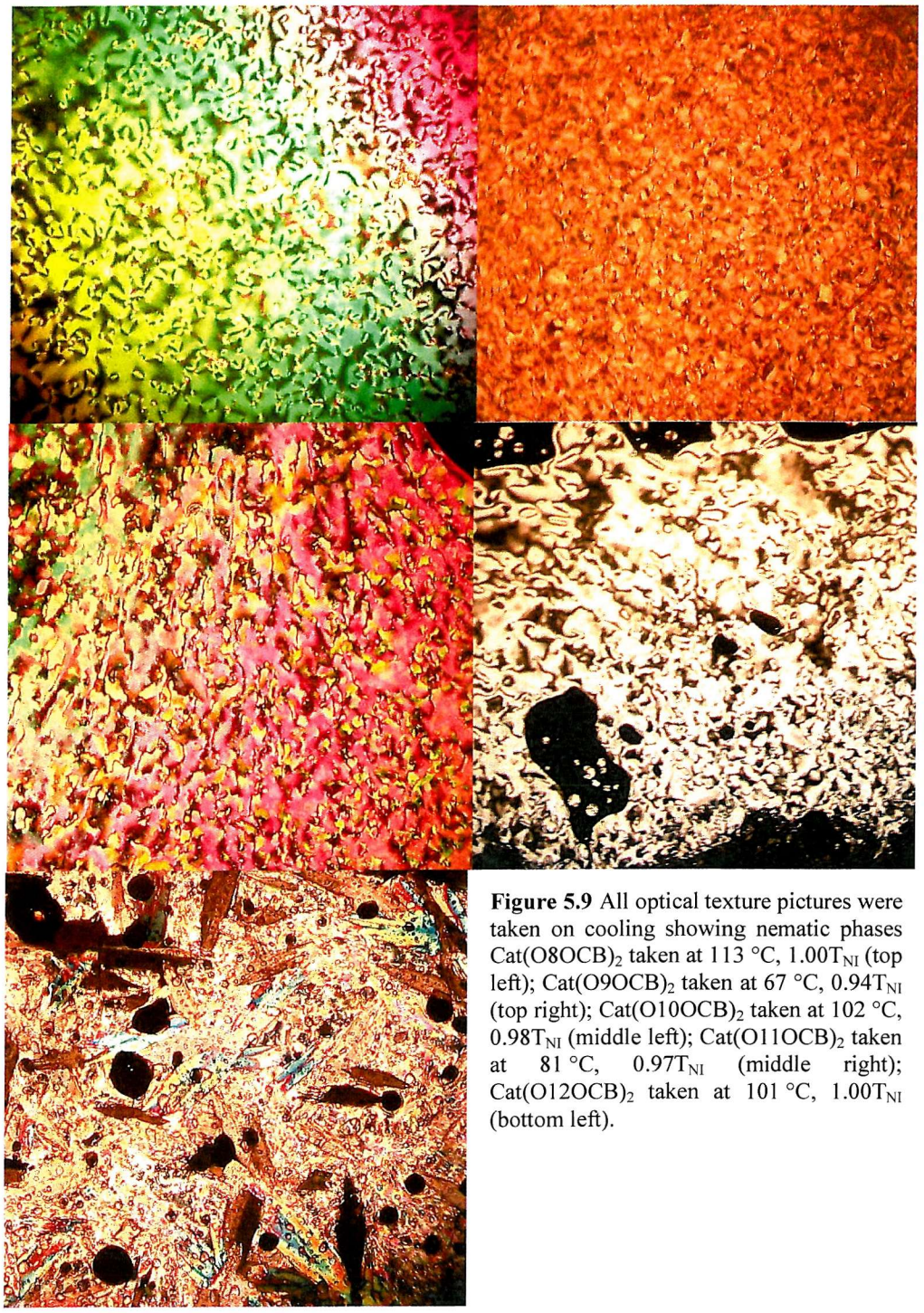

Figure 5.9 All optical texture pictures were taken on cooling showing nematic phases $Cat(O8OCB)_2$ taken at 113 °C, $1.00T_{NI}$ (top left); $Cat(O9OCB)_2$ taken at 67 °C, $0.94T_{NI}$ (top right); $Cat(O10OCB)_2$ taken at 102 °C, $0.98T_{NI}$ (middle left); $Cat(O11OCB)_2$ taken at 81 °C, $0.97T_{NI}$ (middle right); $Cat(O12OCB)_2$ taken at 101 °C, $1.00T_{NI}$ (bottom left).

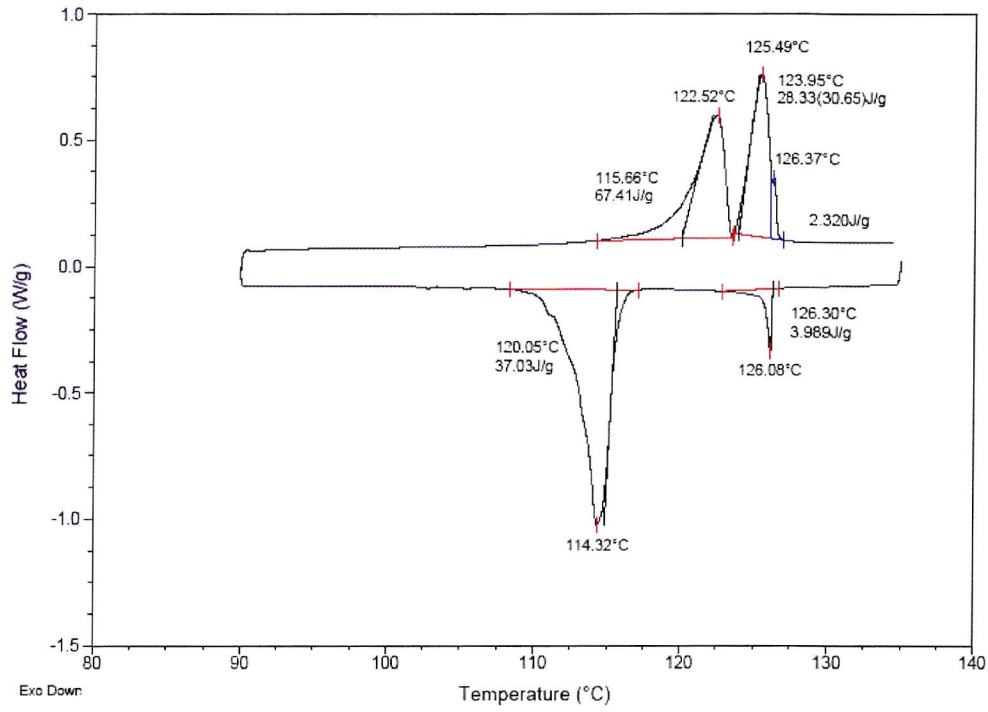

Figure 5.10 DSC plot of the first heating and cooling cycle for Cat(O6OCB)$_2$. Endothermic transitions are given as peaks (e.g. on heating) and exothermic transitions are given as troughs (e.g. on cooling). Here we see on heating, two separate melting peaks corresponding to the two different crystal structures in the solid. The second peak vanishes for subsequent heating cycles as this polymorph is apparently favoured by solvent crystallisation.

Figure 5.10 shows that there are two large exothermic transitions which correspond to melting transitions. From microscopy observations made on the sample the two large exothermic transitions correspond to two different crystal forms in the same solid melting. Often this transition is only seen in the first heating cycle and successful observation of these different melting transitions under the microscope (when the sample is not a thin film) is capricious. This is compounded by the fact the microscope only can see a small region of the sample. Where, under the microscope, the two crystal forms coexist, it is possible to see some regions melt prior to others at temperatures corresponding to those seen in the DSC experiments. Where this sort of polymorphic behaviour is seen, data for the melting points is generally taken from the DSC results (corrected to the microscope calibration).

5.3.2. Phase behaviour

5.3.2.1. Relating the structural conformers to the phase behaviour

In Chapter 3 we built up a theory guided picture of how first uniaxial monomers behaved, then biaxial monomers, and then finally we looked at flexible molecules like liquid crystal dimers. It was noted that introducing the flexible spacer complicated the calculations considerably since not only did they need to account for the geometry of the spacer, but also its conformational energy, the length, the parity as well as the anisotropy of the mesogenic groups.

Analysis of the liquid crystal properties of the dimers showed that whilst it was tempting to consider the dimers in their all-trans form, this failed to quantitatively explain their properties. For example, it would be expected that for the linear even dimers the ordering should be like that of a monomer when in fact it is the bent (seemingly less anisotropic) odd dimers which behave more like monomers. Similarly for the entropy of transition (which is related to the ordering) the values for the even dimers are substantially larger than would have been expected for a simple linear molecule like a monomer.

These differences are accounted for by the molecular field theory which includes all the different conformations with the coupling between the orientation and conformational order. It is found that the anisotropic environment favours the more elongated conformers over the bent conformers subject to the constraints of the conformational energy needed to adopt such a conformer.

From this we can conclude that looking at the all-trans or even a handful of conformations does not give any reasonable quantitative indication of how the dimers behave in the liquid crystal. However, this simplistic approach does provide some qualitative appreciation of the odd-even effect in simple dimers. Therefore we may be able to use this approach to gain some understanding of how the more complicated 1,4-, 1,2- and, later in Section 5.4.2.1, 1,3- substituted dioxybenzene dimers behave.

We have seen in Figure 5.3 how the 1,4- dimer showed a large odd-even effect in T_{NI}.

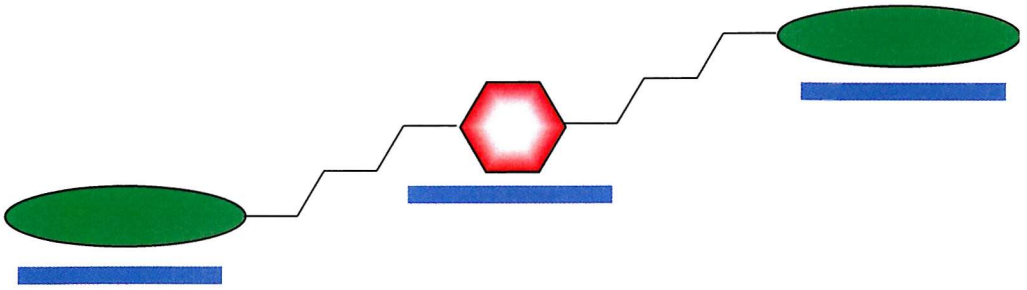

Figure 5.11 Sketch of a 1,4- substituted dimer with an even number of atoms in the linking spacers in the all-trans form. The mesogenic groups depicted in green are parallel to the *para* substituted benzene (shown in red) emphasised by the blue lines.

Considering the shape of the all-trans conformer it can be seen in Figure 5.11 that for even spacers the mesogenic groups are parallel to each other and to the central group resulting in a highly anisotropic shape. The rigid central core helps support the anisotropy along the molecule.

The odd spacers appear very similar except, as shown in Figure 5.12 they are no longer parallel to the central group and the benefit of the rigidity of the linker is not only lost, but it counts against the anisotropy in the molecule reducing the nematic stability considerably.

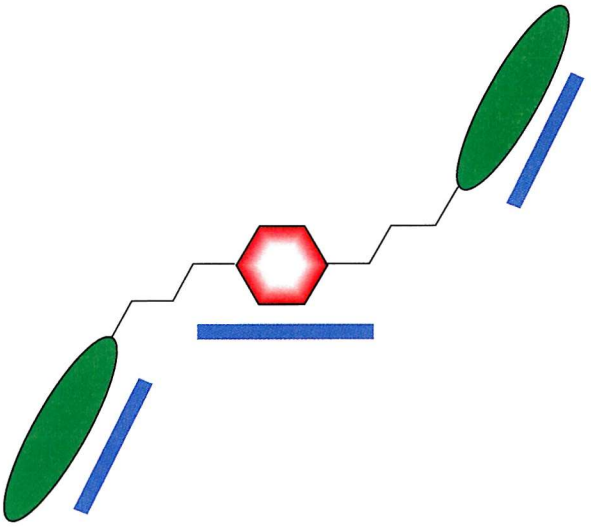

Figure 5.12 Sketch of a 1,4- substituted dimer with an odd number of atoms in the linking spacers in the all-trans form. The mesogenic groups depicted in green are not parallel to the *para* sunstituted benzene (shown in red) emphasised by the blue lines.

It should be noted however that the 'odd' spacer is in fact overall still even as each spacer arm has been increased by one methylene each (over all two) symmetrically. However this result still does not fully explain the very large odd-even effect observed.

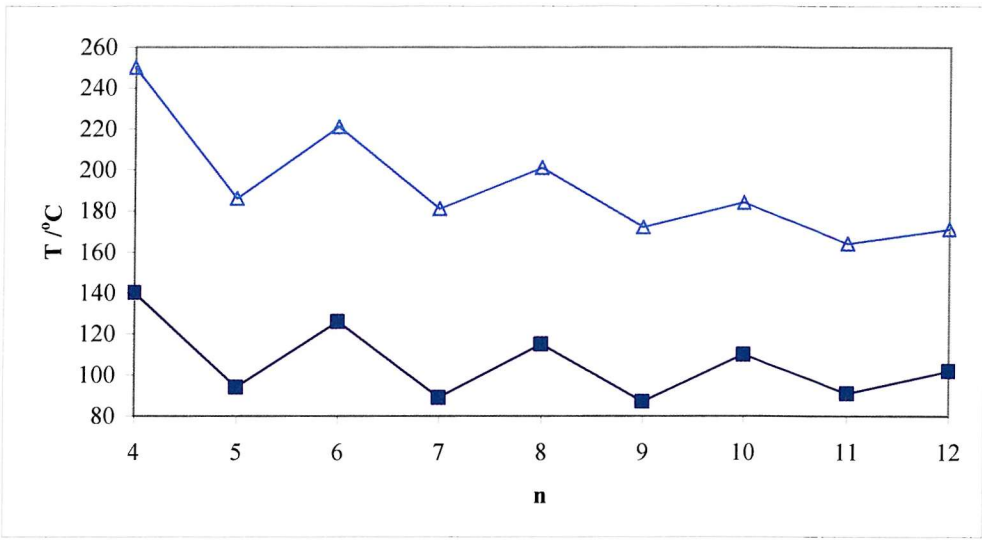

Figure 5.13 Nematic to isotropic transition temperatures for Cat(OnOCB)2 and CBOnOCB. Here, ■ denotes T_{NI} for Cat(OnOCB)2 and Δ denotes T_{NI} for CBOnOCB.

Looking at the data for T_{NI} for $Cat(OnOCB)_2$ we see that there is a distinct odd-even effect as the spacer length increases. The behaviour which we observe is typical of an odd-even alternation similar to that observed in T_{NI} for the CBOnOCB dimers (see Figure 5.13). A full comparative analysis between these two series is undertaken in Section 5.3.2.3. As with the 1,4-dioxybenzene linked dimers we should note that each spacer arm increments by one symmetrically meaning that there should be no odd members and hence we would expect there to be an odd-even effect.

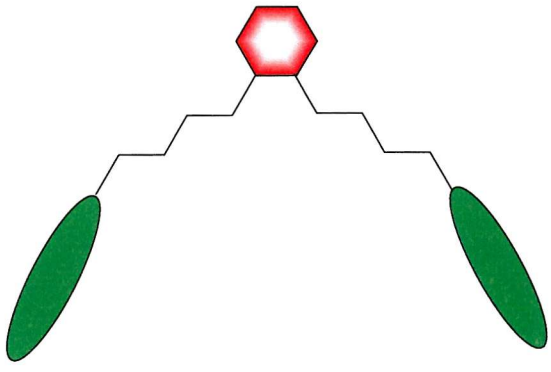

Figure 5.14 Sketch of a 1,2- substituted dimer with an even number of atoms in the linking spacers in the all-trans form.

Considering the all-trans examples for a typical even dimer (an example is given in Figure 5.14) we see that the mesogenic groups are not parallel and the structure seems highly bent which is unlikely to be compensated for by the central ring. However comparing the 1,2- and 1,4- dimers we see why there would be such a difference in the nematic stability as the 1,4- conformer is, by comparison, highly anisotropic.

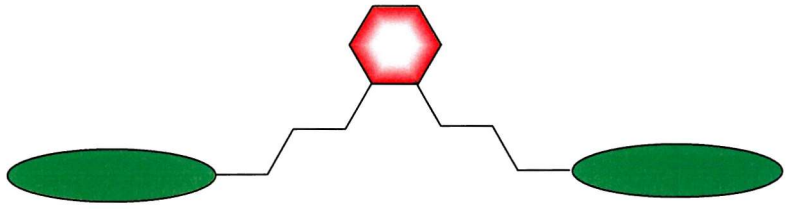

Figure 5.15 Sketch of a 1,2- substituted dimer with an odd number of atoms in the linking spacers in the all-trans form.

The confusion arises when we consider a typical odd dimer such as that given in Figure 5.15. Here we see that the mesogenic groups are parallel and, despite the small length-to-breadth ratio, the molecule is considerably more anisotropic than the even analogue. So we are left with two problems to consider for the 1,2- substituted dimers (the 1,3- dimers are considered later).

1) Why do the dimers show a distinct odd-even effect in T_{NI}?
2) Why are the even dimer nematics more stable than the odd?

We have very little evidence to support any further speculation and selecting certain conformers out of the distribution is known to give unreliable results. So we propose a sketch view of what the dominant conformers in the distribution may look like and comment the observations we have to support this view and what evidence could be gathered given the facilities.

To address the issue of the presence of the odd-even effect, it can be considerd that the end link in the chain is gauche and not trans. This, although unintuitive, has been shown to be the more stable form. If we make the change to the diagrams in Figure 5.14 and 5.15 we can see that this does decrease the length-to-breadth ratio in both cases, but in terms of the overall shape, it does not make the even dimer sufficiently more anisotropic than the odd dimer.

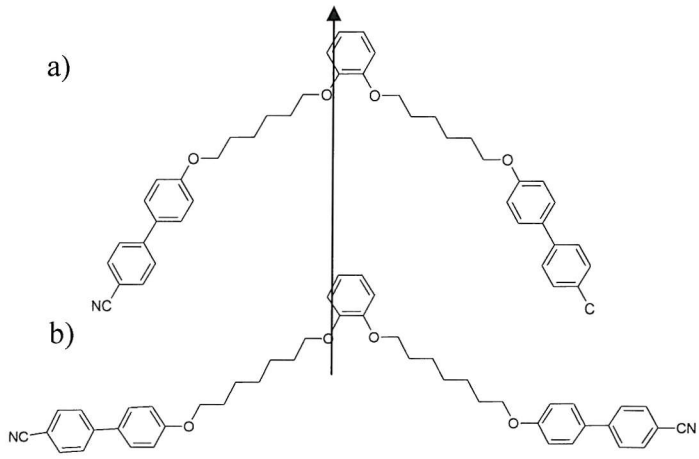

Figure 5.16 Odd and even dimers showing the axis which aligns to the director as bisecting the benzene ring in the centre of the molecule. The mesogenic groups in (a) the even dimers are closer to being parallel than the odd dimers in (b) which are almost perpendicular to this axis of alignment.

Another way to see how we could get an odd-even effect is to re-define the major axis of the molecule. Thus far we have assumed that the axis which lines up parallel to the director being the line that runs from one cyano group to the other. However if we take this axis as the line which bisecting the benzene ring disruptor then we can see that the even dimers have mesogenic groups roughly parallel to this axis whereas the odd dimers have their mesogenic moieties pointing out at an angle to this (see Figure 5.16 (a) and (b)). Given the flexibility of the chains we can imagine it more likely that they would adopt a range of conformations which would make the molecules less broad about this axis than in the all-trans form (see Figure 5.17).

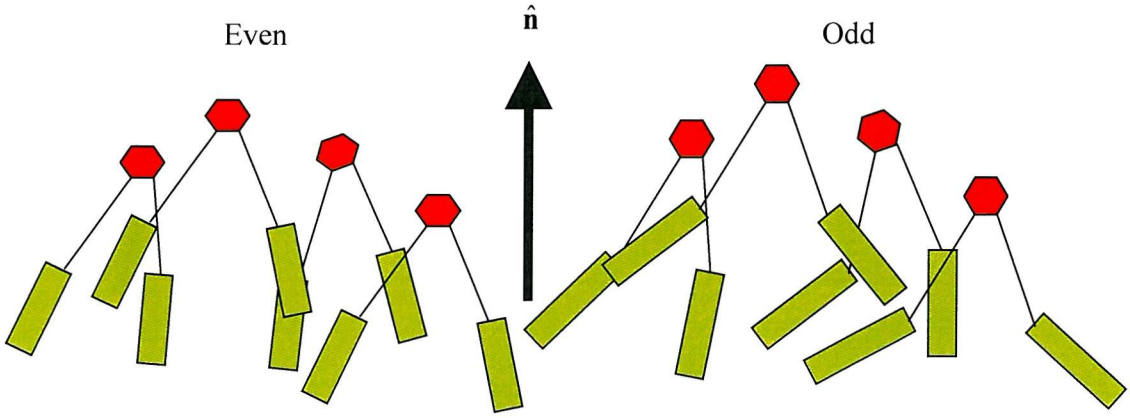

Figure 5.17 Diagram of how the dominant odd and even dimer conformers in the distribution may vary.

From what we understand from conventional dimers, the even dimers would form more conformers which bring the mesogenic groups parallel to the molecular long axis than the odd. Therefore a range of U-shaped conformers could give the odd-even effect in T_{NI} as we observe it for Cat(OnOCB)$_2$.

It is unclear why this should be the case when clearly opening up the molecule gives a more favourable length-to-breadth ratio in the case of the odd dimer. We shall see that the closed form is the conformation adopted in the crystal structure and that the entropy of transition is not unusually large as we may have predicted if the arms were opening up in the melting transition.

There are possible experiments in which we could gather more information to better understand how the compounds are behaving in the nematic phase. The two suggested experiments involve measuring the dielectric anisotropy and X-ray scattering experiments.

Investigating $\Delta\varepsilon$ in an aligned sample would, depending on the conformational distribution, either be very large or relatively small. Assuming the dimers adopt a U-shaped conformation, in an aligned sample the dielectric anisotropy would be very large and positive. If the molecular arms are spread out in the aligned sample the dipoles would cancel and thus reduce $\Delta\varepsilon$ would be small. These measurements are not trivial and without the proper equipment and expertise have therefore not been conducted.

Another way of studying the nematic phase is through X-ray diffraction experiments to determine the molecular spacing in the nematic. Prof. Seddon of Imperial College kindly agreed to study the Cat(O6OCB)$_2$ and the Cat(O7OCB)$_2$ compounds. In spite of being able to see the nematic, he was only able to determine the wide-beam scattering rather than the crucial narrow-beam scattering from the end to end spacing. Further attempts to obtain this data have so far been unsuccessful at the time of writing.

5.3.2.2. Comparing Cat(OnOCB)$_2$ to nOCB monomers

Given the molecular shape of these materials we could view them like two monomer units which are tethered to some core (in this case a catechol unit). The more independent the arms are, the more we would expect the behaviour to reflect that of the corresponding

monomer (in this case nOCB) both in terms of the absolute value of the transition temperatures and how they vary as a function of spacer length.

n	T_{NI} /°C TSm_AIa /°C nOCB	T_{NI} /°C Cat(OnOCB)$_2$
4	(76)	(140)
5	68	(94)
6	76	126
7	74	89
8	80	(115)
9	80	87
10	84a	(110)
11	88a	(91)
12	90a	(102)

Table 5.4 T_{NI} for series Cat(OnOCB) and OnCB for spacer and terminal chain n = 4 – 12. Here ( ) denotes a monotropic transition.

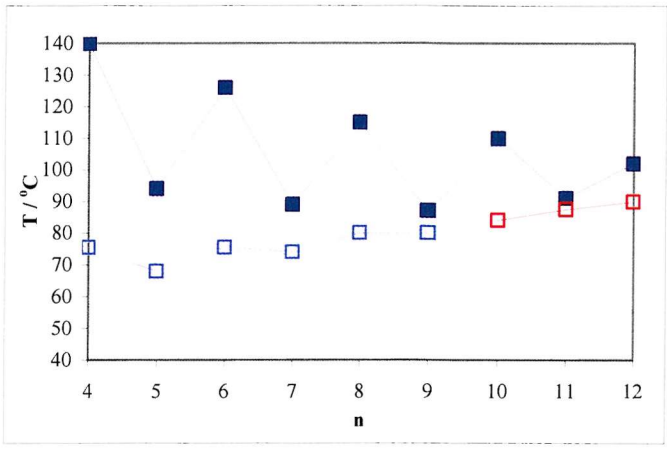

Figure 5.18 T_{NI} for nOCB and Cat(OnOCB)$_2$ where ■ denotes T_{NI} for Cat(OnOCB)$_2$, □ denotes T_{NI} for nOCB and □ denotes T_{SmAI} for nOCB.

From these results (shown in Table 5.4 and Figure 5.18) we see that the dimers behave much more like typical dimeric materials with a distinct odd-even effect in T_{NI} and isotropic transition temperatures generally higher than the corresponding monomers. Although T_{NI}s of the two series are quite similar, the behaviour of the transition temperatures differs between the two series considerably. The size of the alternation in the odd-even effect is considerably more pronounced for the dimers and increasing the chain length has the effect of destabilising the nematic phase for the Cat(OnOCB)$_2$ series whereas for the monomers the nematic phase is stabilised up to the emergence of the smectic phase. The smectic behaviour in the monomers particularly emphasises the differences between the behaviour of these two materials. If we understand the lamellar stabilisation being related to a microphase separation of the long chains and the biphenyl units, then the dioxybenzene linking group is acting as a solubilising agent which destabilises any smectic phase which may have otherwise emerged. The degree to which the presence of one arm affects the other in the dimer is not known, however it is clear that by tethering the arms together they certainly do not act like two independent units.

5.3.2.3. Comparing Cat(OnOCB)$_2$ to CBOnOCB (short)

The Cat(OnOCB)$_2$ series (where $n = 4 - 12$) are all nematogenic although many members are monotropic; the data this are given in Table 5.5.

n	Cr		N		I
4	•	174	•	(144)	•
5	•	139	•	(94)	•
6	•	120	•	126	•
7	•	80	•	89	•
8	•	126	•	(115)	•
9	•	75	•	87	•
10	•	113	•	(110)	•
11	•	89	•	91	•
12	•	113	•	(102)	•

Table 5.5 The transition temperatures in °C for the Cat(OnOCB)$_2$ homologues. Melting points are taken from the solvent crystallised form. The ( ) indicates a monotropic transition.

The structural complexity of these materials makes giving a simple explanation for their behaviour difficult. In this section we will attempt to discuss the evidence to support the suggested geometries suggested in Section 5.3.2.1 existing in the phase by comparison with a variety of different series.

For the purpose of clarification, symmetric cyanobiphenyl dimers with spacers of comparable length to the length of one arm of Cat(OnOCB)$_2$ are referred to as short chain CBOnOCB dimers. Materials which have the same number of methylenes as in both arms (i.e. 2n) are referred to as long chain dimers. Here we compare Cat(OnOCB)$_2$ against CBOnOCB (where in both cases n = 4 – 12). The reason for choosing the CBOnOCB series is that the Cat(OnOCB)$_2$ series exhibits an odd-even effect which is more comparable to the parity change in the short chain dimers rather than keeping a constant parity (e.g. for 2n). Compared to the symmetric short chain cyanobiphenyls (see Figure 5.18) the odd-even effect in both the T_{NI} transition and the melting points are similar in appearance to that seen in conventional dimers. However there are several differences, the most crucial being the comparative difference in temperature. The CBOnOCB series have much more stable nematic to isotropic transitions than the 1,2-dioxybenzene homologues. Considering there is such a large disparity between the T_{NI} of the two series for a given spacer length, it is difficult to envisage the Cat(OnOCB)$_2$ molecules

completely opened out. The more opened out the structure, the more anisotropic the molecule is which we would expect to be reflected in higher T_{NI}. This supports the view that the molecules are more likely to be U-shaped, rather than completely opened up to a more linear structure. If the conformers are predominantly U-shaped they will have a small length-to-breadth ratio, and so it would not surprising that the many of the Cat(OnOCB)$_2$ series possesses sufficiently low T_{NI}s rendering the nematic phases monotropic. The remaining enantiotropic nematics (for n = 6, 7 and 9) are more a reflection on lower melting points than higher T_{NI}s.

The attenuation in the T_{NI} as n increases is less than that of the conventional dimers. Since the dilution effect of adding two CH_2 groups in the kinked dimers is greater than adding one CH_2 to a conventional dimer, this trend must lie in the difference in conformational shape between the two series. Because, on average, the length-to-breadth ratio in the kinked dimers is smaller than the conventional dimer, any increase in the length of the Cat(OnOCB)$_2$ dimer will be proportionally larger than for the corresponding CBOnOCB dimer.

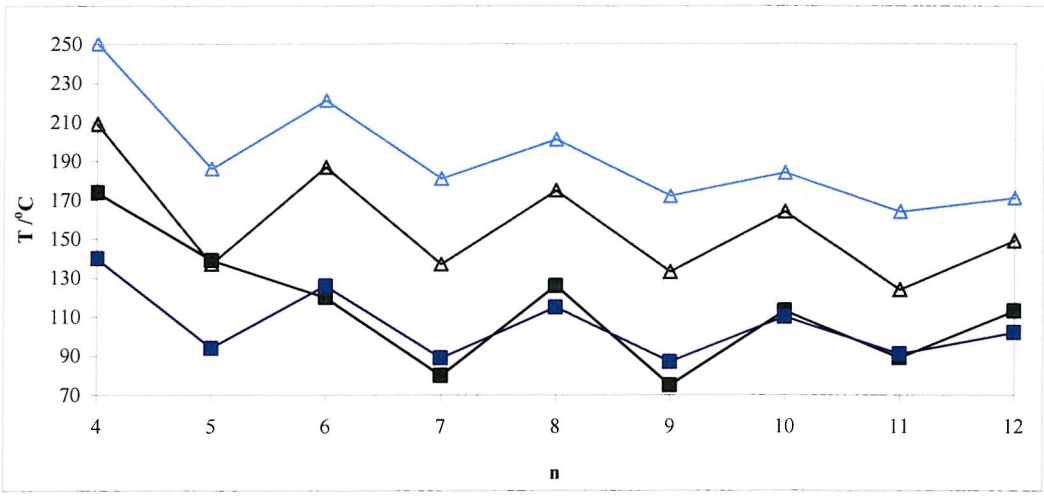

Figure 5.19 The transition temperatures as a function of the methylene spacer of Cat(OnOCB)$_2$ and CBOnOCB where n = 4 – 12, where Δ represents T_{NI} CBOnOCB and Δ represents T_{CrN} CBOnOCB; ■ represents T_{NI} Cat(OnOCB)$_2$ and ■ represents T_{CrI} and T_{CrN} Cat(OnOCB)$_2$.

The melting points of the Cat(OnOCB)$_2$ series are significantly lower (generally about 40 – 50 °C) than the CBOnOCB series which is significant as there is nearly a 50% increase in mass in the novel series (see Figure 5.19). The melting transitions do show an odd-

even effect for materials where n > 6. The drop in the melting point for n = 4 compared to n = 8 for the CBOnOCB series is about 35 °C compared to the difference of 45 °C in the kinked series. Since we know that the solvent crystallised, crystal structures for n = 4 and 8 are primarily the same (see Appendix E), it can be assumed that the change in melting points for the even members is purely due to the increase in the aliphatic chain length. The odd dimers appear to have a substantially different crystal structure owing to the marked difference in the melting points and in $\Delta S_{CrN}/R$ (see Table 5.6) compared to the even members.

5.3.2.4. Comparing Cat(OnOCB)$_2$ to CBO(2n+4)OCB (long)

By looking at monomers and short chain dimers we have previously only considered the closed geometries, comparison with the long CBO(2n+4)OCB series (even members) considers the open geometry.

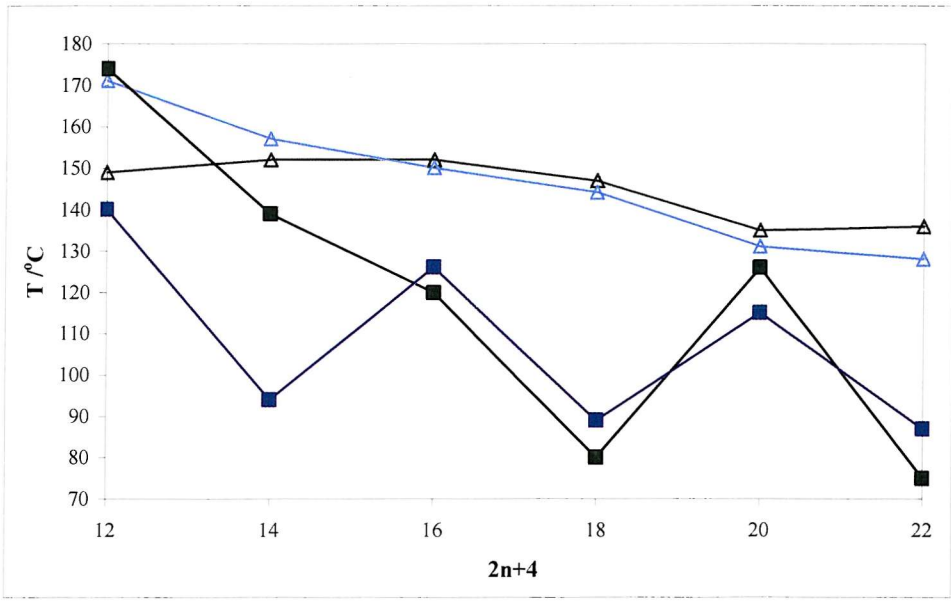

Figure 5.20 The transition temperatures as a function of the methylene spacer for Cat(OnOCB)$_2$ and CBO(2n+4)OCB where n = 4 – 12, where Δ represents T_{NI} for CBO(2n+4)OCB and Δ denotes T_{CrN} for CBO(2n+4)OCB; ■ represents T_{NI} for Cat(OnOCB)$_2$ and ■ represents T_{CrI} and T_{CrN} for Cat(OnOCB)$_2$.

To do this we have taken only the even members of the long chain symmetric cyanobiphenyl dimers such that the spacer includes both the arms of the Cat(OnOCB)$_2$ dimer and the extra four atoms from the catechol and oxygen linkers thus we have plotted transition temperatures for CBO(2n+4)OCB (see Figure 5.20).The role of the catechol

unit by comparison to four extra carbons in the chain is quite different in that it is effectively a rigid gauche link in the centre of the chain. The aromatic-oxygen-aliphatic link creates a slightly wider internal angle than a methylene-methylene link in the simple dimer chain.

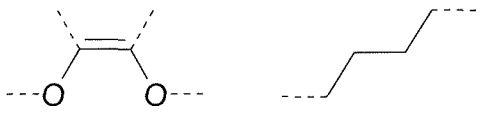

Figure 5.21 Diagram comparing the all-trans methylene chain compared to a section of the 1,2 dioxybenzene liner demonstrating they are of comparable length.

Simply looking at the all-trans chain and the 1,2-dioxbenene linker we may be surprised to see that there are similarities between them (see Figure 5.21) both in terms of length and the direction which the end groups point (that being anti-parrallel).

Considering the plot of the transition temperatures in Figure 5.19, where the CBOnOCB series increases by two carbons there is no odd-even effect observed. Instead there is a steady decline in the T_{NI} in contrast with the odd-even effect seen in the Cat(OnOCB)$_2$ series. The melting points for CBO(2n+4)OCB also show a smooth change varying by less than 20 °C over the series compared to the odd-even variations which range between 20 – 45 °C. The shape and variation in Cat(OnOCB)$_2$ in both the melting points and the T_{NI} transitions are so different that it leaves little doubt that the dominant shapes in the conformation distributions of the two series are substantially different.

This series is also contrasted against the 1,4-dioxybenzene-*bis*-(α-alkyl-ω-oxycyanobiphenyl) synthesized by Furya *et al.* at section 5.4.4 where the N - I transitions for each substituted (*ortho*, *meta* and *para*) dioxybenzene dimer series are compared.

5.3.3. Entropy of transition

The entropy of transition for this series was complicated by the small nematic ranges, the monotropic behaviour of many of the members and a curious tail feature at the N - I transition on cooling which was observed for all of the plots for this series. Being certain of the purity of the material, we were led to conclude that the long tail coming from the transition was probably due to the long chains in the material becoming entangled on cooling. The time taken for the material to become orientationally more ordered whilst

the medium became increasingly viscous resulted in a tail being formed. Reducing the rate of cooling appeared to make little difference to the length of the tail, however reticulated structures were not observed under the microscope.

Figure 5.22 is a more detailed view of the trace shown in Figure 5.10 highlighting several features of the plot. Because of presence of this tail (Figure 5.22 C), there is a significant discrepancy between $\Delta S_{NI}/R$ heating (where available) compared to cooling. Since many of the materials are either monotropic or the N-I transition is overlapped by the peak from the Cr-N transition because the range is so small, there are very few reliable $\Delta S_{NI}/R$ values on heating. The length of the tail and where to determine the transition has been completed leads a higher level of uncertainty pertaining to the accuracy of the results.

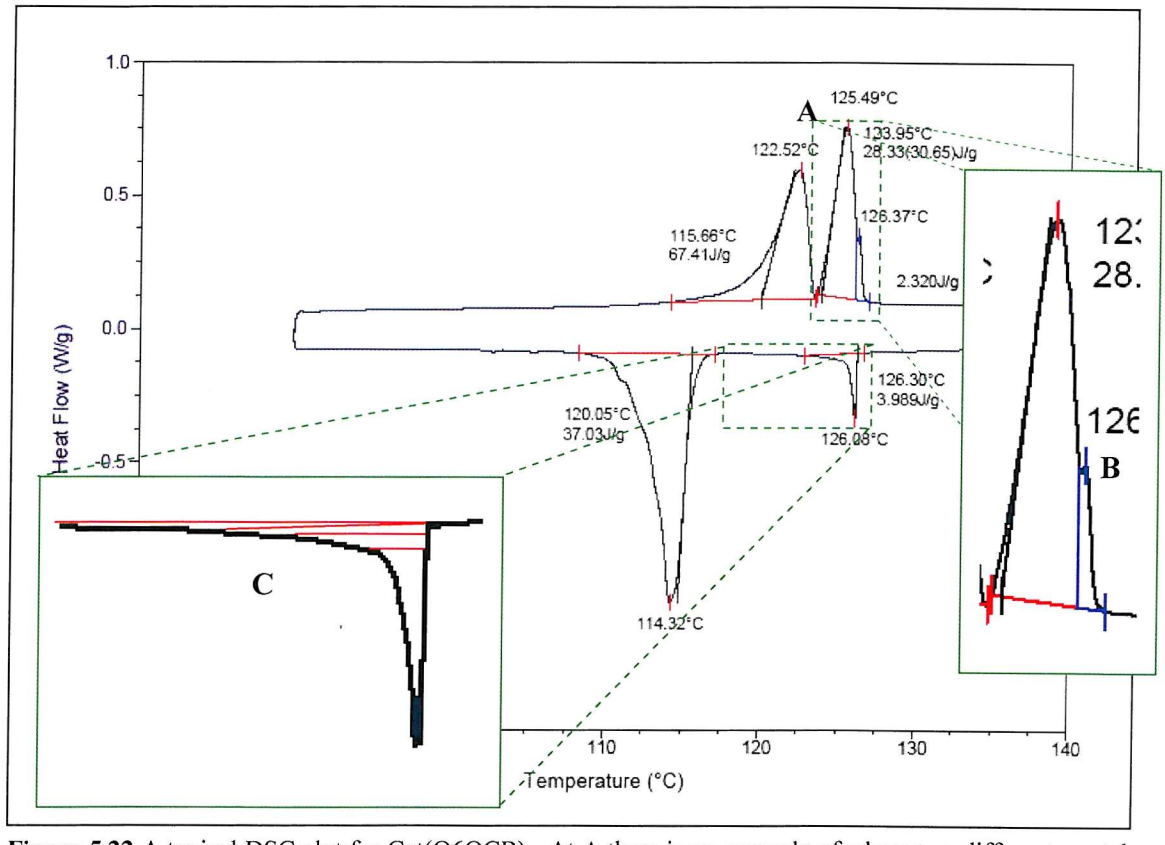

Figure 5.22 A typical DSC plot for Cat(O6OCB)$_2$. At **A** there is an example of where two different crystal structures melt at two distinctively different temperatures, the latter is not normally observed under the microscope, but makes the N - I transition impossible to analyse properly (shown at **B**). **C** shows a close view of the tail seen on all examples in this series. The red lines indicate the possible points to evaluate the area under the peak. The considerable variation in position can result in a difference of more than 50% in the area under the curve (the enthalpy). This cycle was heated and cooled at 10 °C/min.

Because so many of the series only show monotropic behaviour, the data for $\Delta S_{NI}/R$ in Table 5.6 is taken from the cycle only cooling only. First analysis of the data (see Figure

5.23) suggests a reassuring consistency showing an odd-even trend which, according to theory for conventional dimers, is expected behaviour. The odd-even effect shows the even members having a larger $\Delta S_{NI}/R$ than the odd following a similar trend to the CBOnOCB (short chain) series.

n	$\Delta H_{CrN(CrI)}$ /kJmol^{-1}	$\Delta S_{CrN(CrI)}/R$	ΔH_{NI} /kJmol^{-1}	$\Delta S_{NI}/R$
4	52.3	14.1	3.29	0.96
5	52.3	15.3	Not measured	Not measured
6	48.1	14.8	4.53	1.37
7	49.9	16.3	0.57	0.19
8	50.8	15.8	4.92	1.53
9	38.6	13.7	0.98	0.32
10	60.1	18.7	6.45	2.00
11	68.3	23.1	4.73	0.57
12	94.1	27.7	6.55	2.20

Table 5.6 Entropy data for melting and N – I transition. ( ) indicates a transition directly into the isotropic

Given that the catechol based dimers have twice the number of spacer atoms per molecule, we might expect the entropy of transition to be large; perhaps larger than the symmetric cyanobiphenyls.

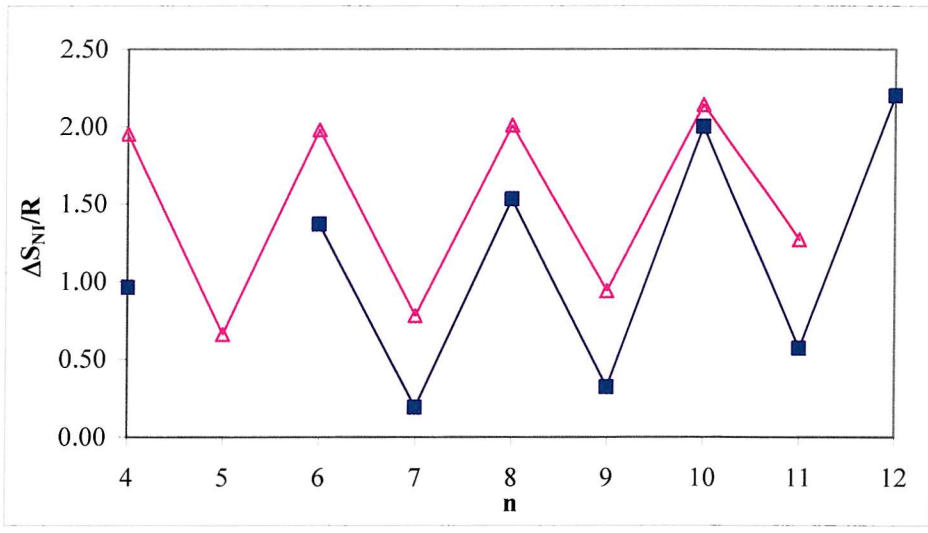

Figure 5.23 The entropy of transition for $Cat(OnOCB)_2$ against spacer length contrasted against the CBOnOCB (short chain) series where ■ is $\Delta S_{NI}/R$ for $Cat(OnOCB)_2$ and △ is $\Delta S_{NI}/R$ for CBOnOCB.

This is not the case suggesting that the 1,2- substituted dimers are considerably more disordered in the liquid crystal phase compared to the corresponding members of the

CBOnOCB series. The conformational contribution to the transitional entropy can be explained using the conformational arrangement shown in Figure 5.17. The even dimers, order themselves in such a way as to stabilise the more linear conformers as is thought to be the case in CBOnOCB. This will raise the entropy of transition as seen in the even dimers. The odd dimers have to undergo a far higher energetic cost to achieve this conformational linear stabilisation and therefore the more linear conformers are less well stabilised. Therefore the orientational order and conformational distribution of the odd dimers more closely resembles that of the isotropic than the even dimers. The entropic difference for the odd dimers is lower at the transition and hence there is an odd-even effect observed.

5.4. Physical data for the 1,3-dioxybenzene *bis*(-α-alkyl-ω-oxycyanobiphenyl) series

Given the nematogenic nature of the Cat(OnOCB)$_2$ series it was expected that the Res(OnOCB)$_2$ series would also be nematogenic. Given the observations made about the Schiff-base phthalates, it might be reasonable to expect the transitions and melting points to be intermediate between the *ortho* and *para* substituted benzene core cyanobiphenyl dimers. A direct comparison and analysis of the effect of changing the substitution of the core will be made at the end of this section.

5.4.1. Optical microscopy

The crystal-crystal transitions which arise from polymorphism in the crystal structure in in the 1,3-dioxybenzene core dimers was more apparent by both DSC and optical microscopy than in the 1,2-dioxybenzene dimers. All members of the series show monotropic nematic phases (compared to the higher melting crystal polymorphs), however this is more due to the generally higher melting points observed in the 1,3-dioxybenzene dimers compared to the 1,2- analogues rather than the lack of stability of the nematic phase.

In several cases it was difficult to take an adequate picture of the optical texture of the nematic phase as the onset of crystallisation occurred before the liquid crystal phase formed. In the case of n = 7 this meant the picture was not always very sharp and in the case of n = 5 only small droplets not easily seen in the picture, showed a nematic phase.

Generally, all of the observed nematic textures were not so easily identifiable with less schlieren textures compared to the 1,2-dioxybenzene cores dimers (see Figure 5.25). What evidence there was of two and four brush defects showed no particular bias in the type observed. The features that identified the phase were a combination of the thread-link texture, the low viscosity and the small flashes which occurred as the top coverslip was subjected to mechanical stress.

There was also evidence of polymorphism by the shape of the crystals which formed. This is evident in the picture for n = 5 (which shows at least two distinct types of crystals growing seen in Figure 5.25) but was also observed for n = 6, 7, 8 and 10 (See Figure 5.24). Viewed through the microscope there are apparently only two different types of crystal which form, one shape being more stable than the other.

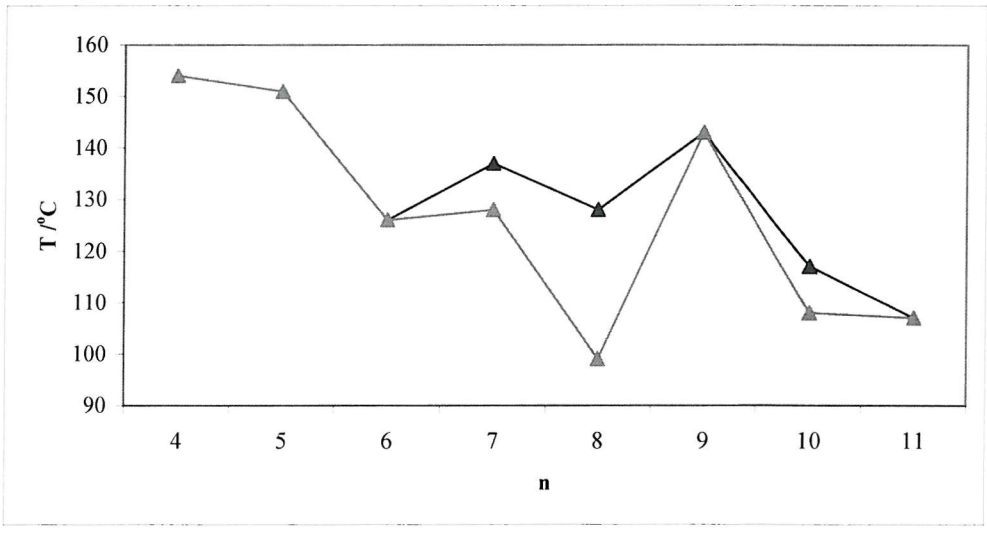

Figure 5.24 The different crystal melting points arising from the polymorphism in the crystalisation from the melt. Here ▲ denotes T_{Cr1Cr2}/T_{Cr1} and ▲ denotes T_{Cr2I}.

The results in Figure 5.24 show that with respect to the thermal stability of the *less* stable crystal phase, some of the dimers could appear to be enantiotropic. A trait seen for n = 8 for the 1,2-dioxybenzene series.

Unfortunately no crystals could be grown of high enough quality for X-ray structural studies to probe the crystal structure.

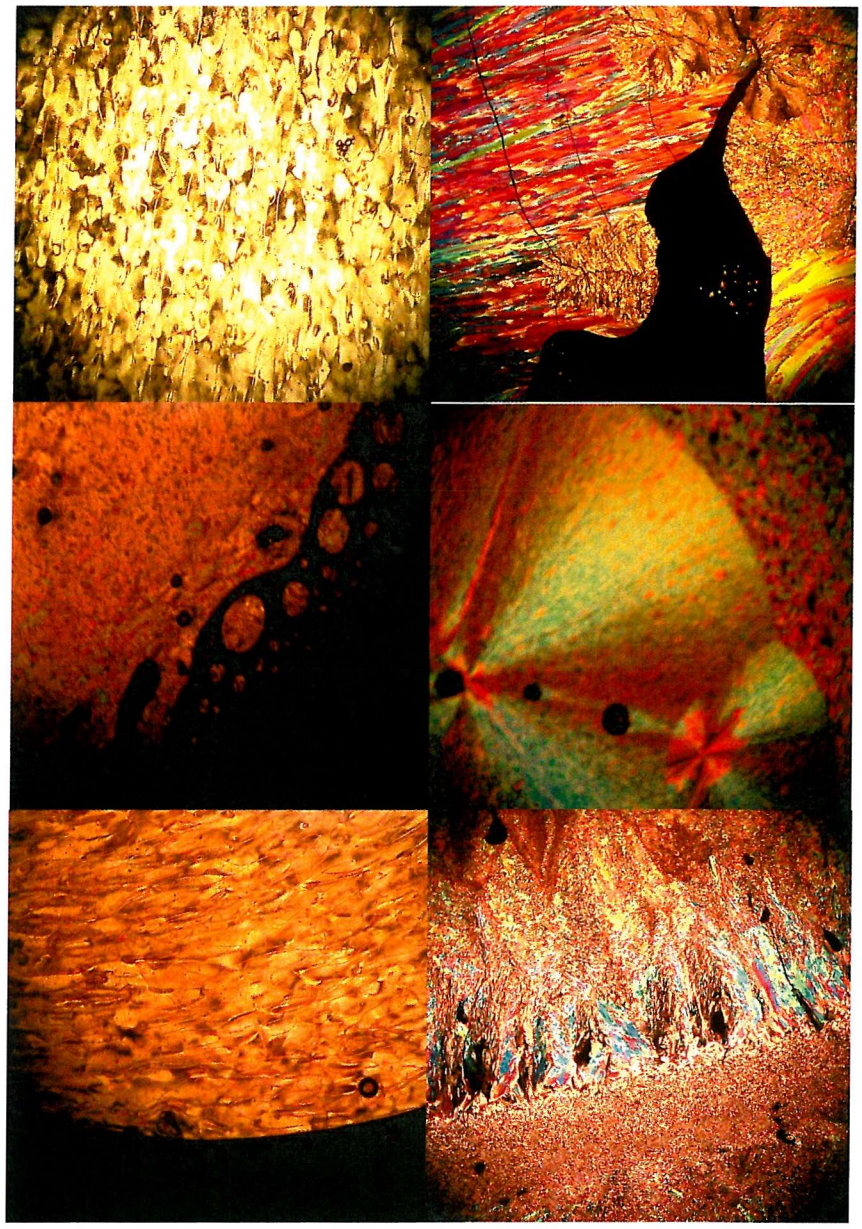

Figure 5.25 All optical texture pictures were taken on cooling showing nematic phases Res(O4OCB)$_2$ taken at 126°C, 1.00T_{NI} (top left); Res(O5OCB)$_2$ taken at 107°C, 0.99T_{NI} (top right); Res(O6OCB)$_2$ taken at 106°C, 0.98T_{NI} (top-middle left); Res(O7OCB)$_2$ taken at 102°C, 0.99T_{NI} (top-middle right); Res(O8OCB)$_2$ taken at 104°C, 0.98T_{NI} (bottom-middle left); Res(O9OCB)$_2$ taken at 101°C, 1.00T_{NI} (bottom-middle right).

5.4.2. Phase behaviour

There are many similarities between the properties of the 1,3-dioxybenzene dimers and 1,2-dioxybenzene analogues and their phase behaviour. Many of the same arguments apply and so will not be repeated here.

5.4.2.1. Relating the structural conformers to the phase behaviour

The 1,2- and 1,4- dimer all-trans conformers were examined in an attempt to explain the odd-even effect. There was very little correlation between the shape in the open all-trans and the behaviour observed in the T_{NI}. The only way of understanding these materials properly would be to do the calculations using the molecular field theory however this is a non-trivial task and so we have attempted to explain the behaviour in the N-I transition temperatures using a more simplistic qualitative analysis. The all-trans conformers do not satisfactorily rationalise the observed behaviour in conventional dimers and therefore for the 1,2-dioxybenzene dimers, the behaviour has been explained by adapting the conformational shape to the data on the series that was available as a basis for speculation on how the materials behave in the nematic.

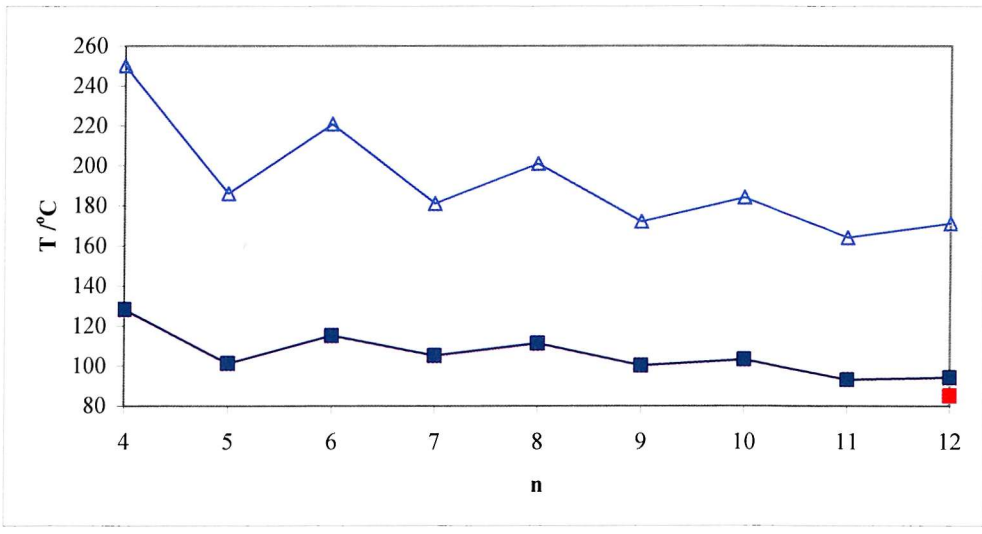

Figure 5.26 T_{NI} transitions for the Res(OnOCB)$_2$ series where ■ represents for Res(OnOCB)$_2$, ■ represents T_{SmAN} and Δ represents T_{NI} for CBOnOCB.

Considering the 1,3-substituted dimers (see Figure 5.26, transition temperatures given in Table 5.8), we note that again there is an odd-even effect as n increases and that the

alternation in the effect is small in comparison with the $Cat(OnOCB)_2$ (not shown in Figure 5.26) and the CBOnOCB dimers.

If we apply the reasoning that we used for the 1,2- substituted materials it becomes clear that there are two problems:

1) With the change in substitution position, the odd dimers have their mesogenic end groups more in line with the director rather than the even which should reverse the odd-even effect in T_{NI} – which we can see is not the case (see Figure 5.26).
2) The substitution position increases the molecular width, making the already broad molecule possibly too broad to form a liquid crystal phase.

With this we are left to consider the all-trans dimers and what we find is that there is very little difference between the odd and the even in terms of the anisotropy.

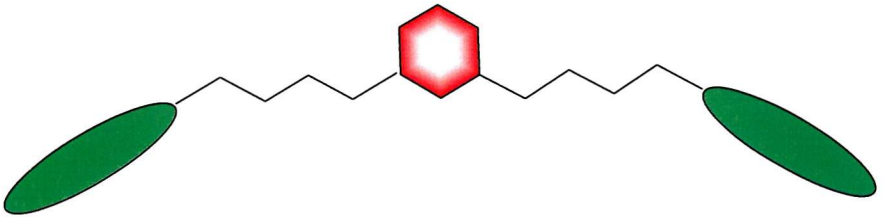

Figure 5.27 Sketch of a 1,3- substituted dimer with an even number of atoms in the linking spacers in the all-trans form.

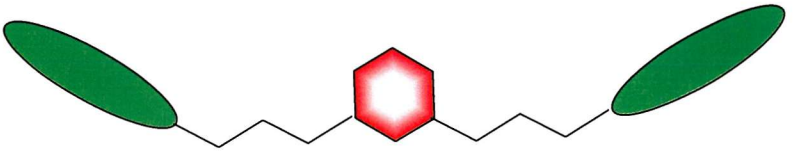

Figure 5.28 Sketch of a 1,3- substituted dimer with an odd number of atoms in the linking spacers in the all-trans form.

Trying to see any significant anisotropic difference between the even (see Figure 5.27) and odd (see Figure 5.28) is not possible in such a qualitative fashion. Given the subtlety of the odd-even effect in this series this should be unsurprising. The fact that there is so little difference between the odd and even dimers points us in the right direction; we would expect this series to have a less stable nematic phase than the 1,4-dimers, which is true, and we would expect there to be less alternation in the odd-even effect than in the

1,2- and 1,4- dimers which again is true. However, this ultimately leads us back to the original comment that explaining patterns in these dimers (especially where the differences in T_{NI} between odd and even are so small) cannot be satisfactorily achieved using these qualitative methods. So for this series a satisfactory explanation can only be explained through modelling.

5.4.2.2. Comparing Res(OnOCB)$_2$ with nOCB monomers

Unlike the 1,2-dioxybenzene dimers, the 1,3- substitution pattern allows the spacer chains more freedom to adopt more linear geometries with less steric interference.

n	T_{NI} /°C TSm_AIa /°C nOCB	T_{NI} /°C Res(OnOCB)$_2$
4	(76)	(128)
5	68	(101)
6	76	(115)
7	74	(105)
8	80	(111)
9	80	(100)
10	84a	(103)
11	88a	(93)
12	90a	(102)

Table 5.7 T_{NI} for series Res(OnOCB)$_2$ and OnCB for spacer n = 4 – 12. ( ) denotes a monotropic transition

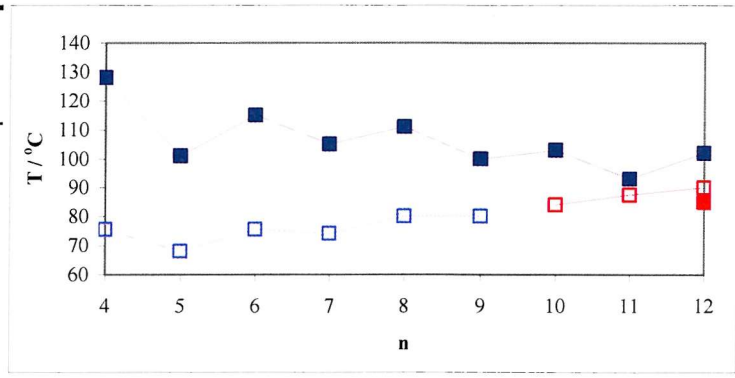

Figure 5.29 T_{NI} for nOCB and Res(OnOCB)$_2$ where ■ denotes T_{NI} for Res(OnOCB)$_2$, ■ denotes T_{SmAN} for Res (OnOCB)$_2$, □ denotes T_{NI} for nOCB and □ denotes TSmAI for nOCB.

As with the Cat(OnOCB)$_2$ series, the 1,3-substituted analogues show an odd-even effect more pronounced than seen in the monomer series. Again we see that the monomer T_{NI} stabilises with increasing chain length (here the chain length is adding to the anisotropy of the molecule) but for the dimer there is a subtle decrease in the nematic stability. Compared to the Cat(OnOCB)$_2$ series we can see that Res(OnOCB)$_2$ compounds behaves more like the nOCB series in that there is an emergence of a SmA phase for n = 12 however this is less stable than seen in 12OCB and a less pronounced odd-even effect in the dimer T_{NI}. This perhaps suggests that since the arms are more spaced apart they are more free to behave independently like the monomers, this not withstanding, the 1,3-dioxybenzene tether still stabilises the nematic phase relative the monomer and destabilises the formation lamellar phases.

5.4.2.3. Comparing Res(OnOCB)$_2$ with CBOnOCB (short)

As with the 1,2-dioxybenzene dimers the 1,3- analogue dimers will be compared to the CBOnOCB series first and then compared to the long chain dimers. Since much of geometric arguments are the same, this analysis shall be brief.

n	Temperature /°C								
	Cr_1		Cr_2		Sm A		N		I
4	•	154	•	(137)	•		•	(128)	•
5	•	151	•	(146)	•		•	(101)	•
6	•	126	•	(120)	•		•	(115)	•
7	•	137	•	(128)	•		•	(105)	•
8	•	128	•	(99)	•		•	(111)	•
9	•	143	•		•		•	(100)	•
10	•	117	•	(108)	•		•	(103)	•
11	•	107	•		•		•	(93)	•
12	•	106	•		•	(85)	•	(94)	•

Table 5.8 Table of 1,3-dioxybenzene dimers phase transitions from microscope observations including Cr-Cr transitions observed on cooling only. Cr_2 transitions in red are obtain from DSC data corrected to the microscope calibration.

There is an interesting polymorphism resulting in crystal-crystal transitions observed for n = 7, 8 and 9 (shown in Table 5.7 and Figure 5.30) briefly mentioned in Section 5.4.1. This will be expanded upon more fully in the entropy section where measurements by DSC show more examples in this series where similar polymorphism occurs.

The entrance of the smectic phase at n = 12 is curious and possibly visible due to the lower melting points for the longer spacer lengths and hence access to lower temperatures through supercooling. That is to say that it is possible for smectic phases to exist for the other compounds in the Res(OnOCB)$_2$ series but they have too low a transition to be observed. Each material was supercooled by approximately 30 °C (transitions for some materials, e.g. n = 5, were obtained by observing droplets on the microscope slide).

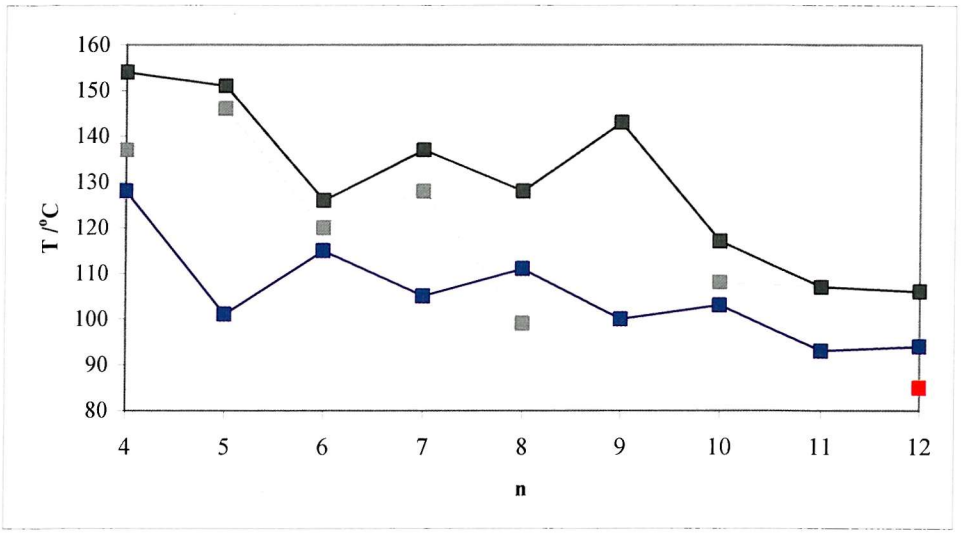

Figure 5.30 The melting points and polymorphic melting points and liquid crystal transition temperatures for the Res(OnOCB)$_2$ series where ■ represents Cr_1-I, ■ represents Cr_2-Cr_1 or Cr_2-N, ■ represents N-I and ■ represents SmA-N.

Figure 5.30 shows the T_{NI} which attenuates rapidly becoming almost constant by n = 11 and 12. The Cr_2 data is plotted from a combination of optical microscopy and DSC data as reported in Table 5.7. These Cr_2 transitions show a more consistent odd-even effect which, interestingly, is out of phase with the alternation in T_{NI} which stops about n = 10. Comparing the liquid crystal phase transitions of Res(OnOCB)$_2$ with CBOnOCB we see that the alternation in T_{NI} is significantly lower in the kinked dimers (see Figure 5.31) compared to the conventional dimers. Since the degree of conformational change between odd and even members of the series is expected to be small (as discussed in Sections 5.4.2.1 and 5.3.2.1) this result in not surprising. The significantly lower T_{NI} is likely to be due to a number of reasons. Primarily there are likely to be many more bent conformers in the conformational distribution for a given member of the Res(OnOCB)$_2$ series both due to the presence of the core group and the fact there are two flexible chains. Secondly the benzene core and the additional chains are non-mesogenic and so will further dilute the mesogenicity by comparison, destabilising the liquid crystal phase.

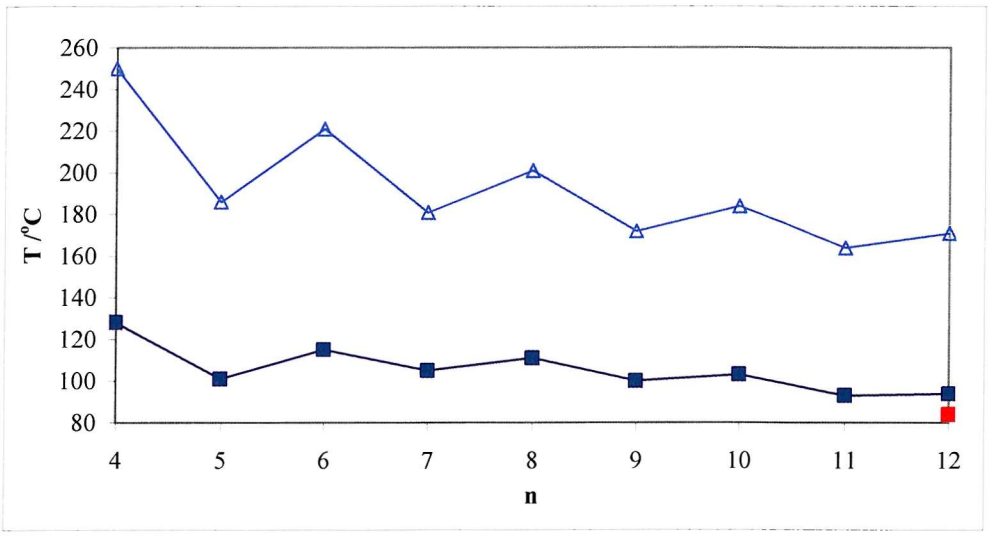

Figure 5.31 Temperature transitions for N-I and SmA-N transitions for CBOnOCB and Res(OnOCB)$_2$, where ■ is the T_{NI} and ■ is the T_{SmAN} for Res(OnOCB)$_2$ Δ is the T_{NI} transition for CBOnOCB.

Finally, as described before, if the U-shaped dimers become more stabilised by the longer spacer group and occupy a larger proportion of the conformational distribution, this would be likely to stabilise a smectic phase which would not be seen in the CBOnOCB series. Greater evidence for this could be gained by measuring the spacing between the layers for Res(O12OCB)$_2$.

5.4.2.4. Comparing Res(OnOCB)$_2$ with CBO(2n+5)OCB

Comparing the CBO(2n+5)OCB series with Res(OnOCB)$_2$ gives an interesting result. As was the case for the 1,2-dioxybenzene dimers, to account for the extra atoms represented by the resorcinol unit, the kinked dimers are compared to a chain length of 2n + 5 in the simple cyanobiphenyl dimers. In Figure 5.32, taking the members of the CBO(2n+5)OCB series (which correspond in length to the elongated Res(OnOCB)$_2$ conformer) generates a non-alternating trend compared to the odd-even alternation seen in the Res(OnOCB)$_2$ series. However, the difference in magnitude of T_{NI} between the two series is somewhat less than was observed for the Cat(OnOCB)$_2$ dimers. There is clearly some difference in the character of the Res(OnOCB)$_2$ dimers giving rise to the odd-even effect, but the alternations are so small that there may be some relationship between the shapes of both sets of dimers. That is the arms of the 1,3-dioxybenzene dimers are

substantially more opened out than compared to the corresponding 1,2-dioxybenzene analogues.

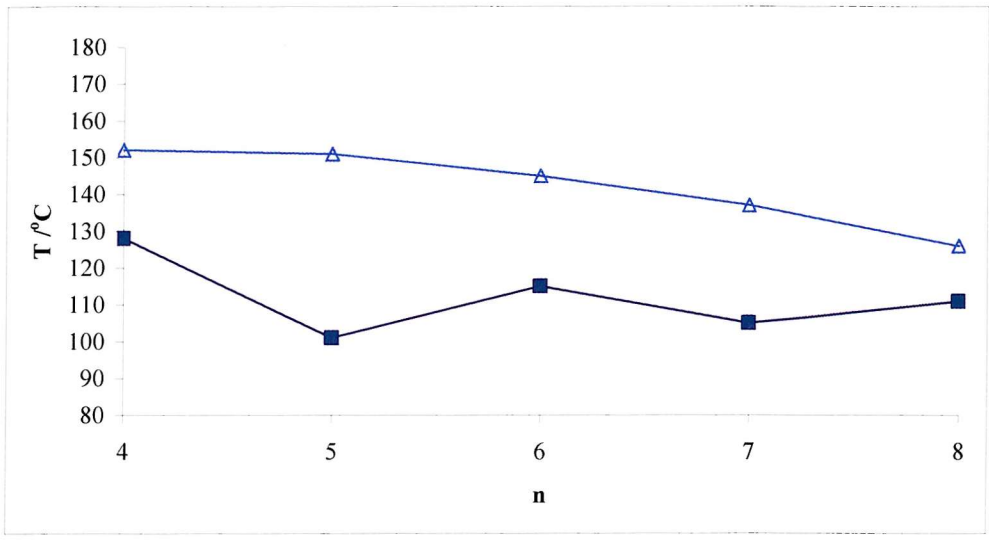

Figure 5.32 The N-I temperature transitions as a function of the methylene spacer for Res(OnOCB)$_2$ and CBOnOCB. Δ denotes T_{NI} CBOnOCB and ■ denotes T_{NI} Res(OnOCB)$_2$.

Again, the stability in the nematic phase for the CBO(2n+5)OCB series will benefit from linearising the molecule through small torsional rotations in the long chain whereas the kinked dimers have two shorter chains which will be able to accommodate less torsional rotation for the same cost in energy.

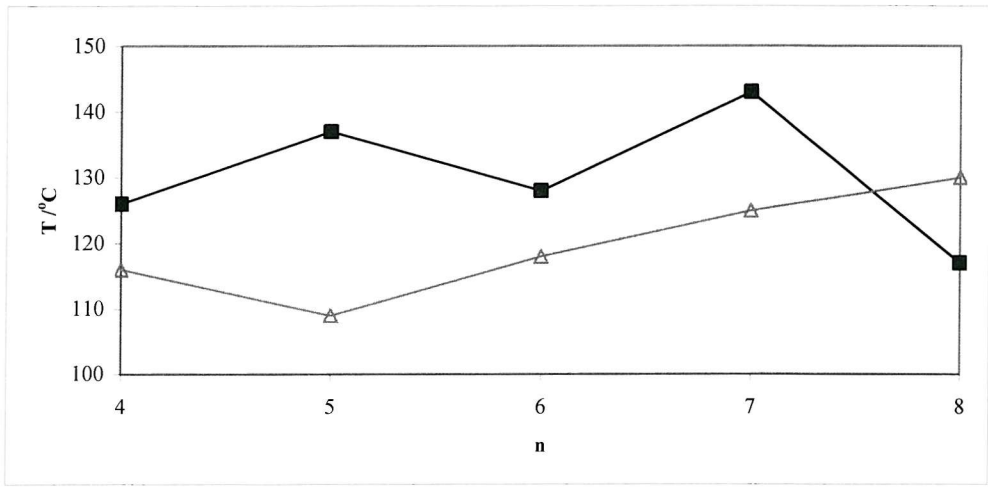

Figure 5.33 The melting transitions for Res(OnOCB)$_2$ and CBOnOCB. Here, Δ denotes T_{CrN} CBOnOCB and ■ denotes T_{CrIN} Res(OnOCB)$_2$.

The more interesting comparison is actually by considering the melting points (see Figure 5.33). All the CBO(2n+5)OCB series are enantiotropic compared to the Res(OnOCB)$_2$ series which are all monotropic. However, for most examples the Cr-N transition for the CBO(2n+5)OCB series is smaller than the Cr_1-I or even some of the lower Cr_2-I transitions. This suggests that the packing in the crystal for both polymorphs is very different to that of the CBOnOCB series which is likely to follow the same structure as those known for shorter spacer groups in the same series.[27, 28] In the absence of a proper X-ray structure it is hard to comment further on the crystal structure of the Res(OnOCB)$_2$ series. It should however be noted that the molecular mass of the CBO(2n+5)OCB and the Res(OnOCB)$_2$ series are roughly the same, but the 1,3-dioxybenzene substituted dimers have two extra hetro atoms (oxygens) and a planar aromatic ring, which are likely to form favourable electrostatic interactions. This would lead to higher melting points for the kinked crystal conformer.

To conclude, as predicted, the 1,3-dioxybenzene dimers do not behave like the CBO(2n+5)OCB series either in terms of melting point or the variation in the transition temperatures as a function of n. The nematic phase is less stable than either the long (2n+5) or short (n) spacer chain members of the symmetric cyanobiphenyl series which is probably due to the complicated conformational distribution arising from the inclusion of the disrupting group.

5.4.3. Entropy of transition

The entropy of transition for the Res(OnOCB)$_2$ series was somewhat easier to measure compared to the Cat(OnOCB)$_2$ series however measurements are complicated by the monotropic nature of the compounds. As described in previous chapters, each material was run through 4 heat/cool cycles and an average of the data was taken and plotted.

We see in Figure 5.34 and Table 5.9 that the lack of data points is again making analysis of any trend almost impossible. However, we can note an overall increase in entropy as the spacer length increases is in keeping with theoretical prediction and similar to the increase seen in the corresponding CBOnOCB materials. The problems of tails in the data were not so prevalent in the Res(OnOCB)$_2$ DSC traces which, if related to the chains being entangled, can be understood as the result of the arms being further apart due to the particular motif on the ring.

n	ΔH_{NI}/kJmol^{-1}	$\Delta S_{NI}/R$
4	2.52	0.76
5	Not Observed	
6	2.29	0.72
7	4.49	1.43
8	3.52	1.12
9	Not Observed	
10	5.97	1.93
11	5.45	1.80
12	5.97	1.94

Table 5.9 Table of the enthalpy and entropy of transition for Res(OnOCB)$_2$

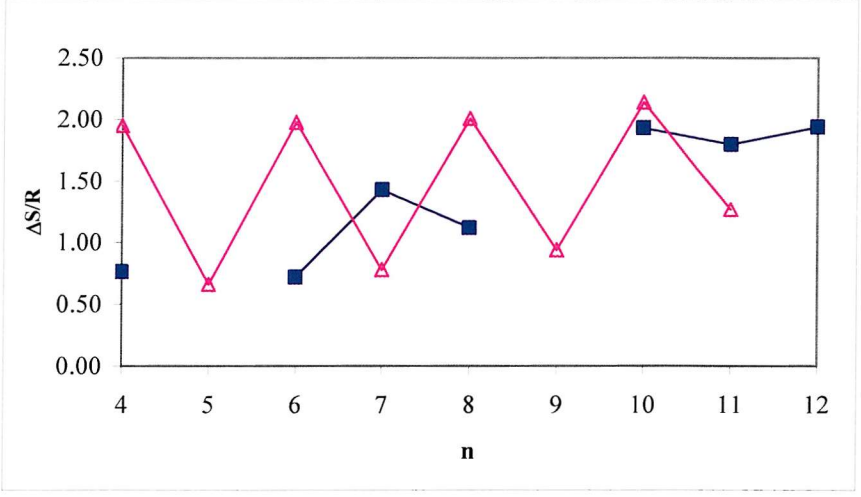

Figure 5.34 The change in transitional entropy for Res(OnOCB)$_2$ and CBOnOCB as a function of spacer length.

Assessment of the odd-even effect in the data is complicated by the lack of data points at n = 5 and 9 due to the onset of crystallisation before the N-I transition is reached. The most important observation would be that the effect is going contrary to expectation for n = 6 – 8 and then following the expected trend for n = 10 – 12. The data for n = 6 – 9 is consistent across the average, suggesting that the data are correct. With the inherent lack of data points any further speculation on the trends would be unwise.

5.4.4. Assessing the affect of the angular change in the core on the nature and stability of the phase

Comparing the liquid crystal phase behaviour between the 1,2-, 1,3- and 1,4- substituted benzene rings we can see the significant effect different cores has on the stability of the materials. The conformational structure of the linear 1,4- dimers appear vastly different to

that of the 1,2- and 1,3- dimers although the decline in the T_{NI} for the 1,4- substituted dimers appears that when, n = 12, (by extrapolation) would give T_{NI} transitions similar to that of the bent core dimers (see Figure 5.35). The massive difference in T_{NI} for the 1,4-dioxybenzene dimers compared to the 1,2- and 1,3- analogues is a strong indicator for the big difference in the conformational distribution for the apparently more anisotropic 1,4-dimers compared to the seemly bent *ortho* and *meta* substituted dimers.

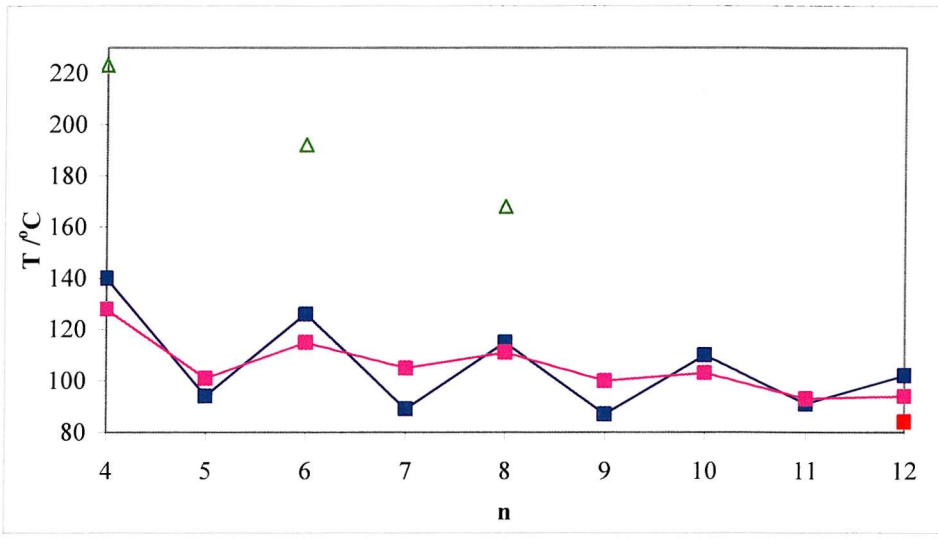

Figure 5.35 The transition temperatures of the 1,2-, 1,3-, 1,4- dioxybenzene core cyanobiphenyl dimers as a function of spacer length. Where Δ denotes T_{NI} for Qui(OnOCB)$_2$,[15] ■ denotes T_{NI} for Res(OnOCB)$_2$, ■ denotes T_{SmAN} for Res(OnOCB)$_2$ and ■ denotes T_{NI} for Cat(OnOCB)$_2$.

Both the 1,4- dimers[15] and the 1,2- dimers show a much larger alternation in the odd-even effect. Strictly speaking the 1,4- substituted dimers do not show an odd-even effect, however it was demonstrated by Attard *et al.*[17] that by lowering the melting point of the dimer by introducing a non-mesogenic aliphatic side-chain to the quinone unit, does show a visible odd-even effect for this series. Thus for the Qui(OnOCB)$_2$ series it is assumed that the odd members show nematic phases which are simply too monotropic to have been observed. Despite not knowing the precise T_{NI} for odd members, we know from the melting points[15] that the odd-even effect for the N-I transitions are likely to be larger than both the 1,2- and 1,3- substituted dimers. The large alternation in both the 1,2- and 1,4- series suggests the Res(OnOCB)$_2$ dimers have the greatest number of non-linear conformers in the distribution since changes in parity affect the T_{NI} the least. This should

give rise to these materials giving the best flexoelastic ratios (so long as the elastic constants are not sufficiently large). It is of course a pity that these materials are all monotropic and as such cannot be measured in the pure systems.

Comparing the trends in these results to the phthalate ester disrupted symmetric Schiff-base dimers shown in Figure 5.4, we see that where the phthalate esters core dimers showed a small odd-even alternation in the T_{NI} for only the intermediate 1,3-substitution isophthalate esters, both the 1,2- and 1,3-dioxybenzene core dimers show an odd-even effect. It should be noted that the significant difference in mesogenic groups makes any further comparison irrelevant, however it does show that the phase behaviour of these types of bent core dimer are affected in a more complicated way than simply the change in shape caused by the introduction of the aromatic core.

5.5. Conclusions

The synthesis of the 1,2-dioxybenzene and 1,3-dioxybenzene linked cyanobiphenyl liquid crystal dimers proved to be a challenging task. However, once these materials were made and satisfactorily purified, understanding their transitional behaviour proved to be even more difficult. The curious odd-even effect in the melting points and temperature transitions defied any simple explanation of how, conformationally, the materials behaved. Similarly these compounds show an odd-even effect in the N-I transitional entropy demonstrating a considerable difference in the orientational and conformational ordering between dimers with different parities.

For the Cat(OnOCB)$_2$ series comparisons with cyanobiphenyl monomers and dimers showed that, counter-intuitively, the Cat(OnOCB)$_2$ series behaves most like the CBOnOCB, i.e. the short chain symmetric dimers. Given that, structurally the CBOnOCB dimers are significantly smaller than the Cat(OnOCB)$_2$ analogues this is particularly surprising. From these comparisons we currently infer that the molecules tend to adopt U-shaped conformations in the nematic and this appears to fit the behaviour which we have observed although until more concrete evidence is obtained, remains conjecture.

The Res(OnOCB)$_2$ series possess similar properties relating to the N-I temperature transitions. The transitional entropies are easily understood due to the lack of data for some members of the series. The dominant conformers in the distribution for this series is even less certain than for the Cat(OnOCB)$_2$ series. The odd-even alternation is more

subtle than for the 1, 2-dioxybenzene core dimers and still the series which the Res(OnOCB)$_2$ series behaves most similarly to is the CBOnOCB series.

Of the two series the Cat(OnOCB)$_2$ was the more interesting as it showed some enantiotropic compared to Res(OnOCB)$_2$ which were all monotropic. It was unfortunate that the flexoelastic ratio of these materials could not be determined due to non-availability of HAN cells at Merck which remained unavailable up to the date of Thesis submission.

In spite of this, the interesting behaviour of these materials in terms of their transitional properties and how they might relate to their structure inspired a study on non-symmetric variants on the 1,2-oxybenzene systems which is continued in Chapter 6 and to some extent supports the supposition about the U-shaped conformers in the nematic phase.

Note: It came to our attention that there exists work recently published[12, 13] on 1,2 and 1,3-dioxybenzene dimers (referred to in the papers as trimers). These papers also refer to a paper published in 2005.[14] In particular transition temperatures for members of the Res(OnOCB)$_2$ series are published and these are in agreement with our results. Their interpretation of the conformation of catechol dimers in the nematic phase is also that it forms a U-shaped structure.

5.6. References

1. P. J. Collings, M. Hird, *Introduction to Liquid Crystals*. Taylor and Francis: Ed. G.W. Gray, J. W. Goodby, A. Fukuda 2001.
2. G. W. Gray, K. J Harrison, J. A. Nash, *Electron. Lett.*, **1973**, 9, 130.
3. G. S. Attard, R. W. Date, C. T. Imrie, G. R. Luckhurst, S. J. Roskilly, J. M.; Seddon, L. Taylor, *Liq. Cryst.*, **1994**, 16, 529.
4. G. W. Gray, K. J Harrison, J. A. Nash, *J. Chem. Soc., Chem. Comm.*, **1974**, 431.
5. H. J. Coles, B. Musgrave, M. J. Coles, J. Willmott,, *J. Chem. Mater.*, **2001**, 11, 2709.
6. D. L. Brydon, I. S. F., J. Emans, D. M. Smith, T. Bowen, I. W. Harvey, *Polymer Journal*, **1993**, 34, 4481.
7. P. Castell, A. Serra, M. Galia, *J. Poly. Sci. Part A: Poly. Chem.*, **2003**, 41, 1536.
8. A. P. J. Emerson, G. R. Luckhurst, *Liq. Cryst.*, **1991**, 10, 861.

9. B. Mohr, V Enkelmann, G. Wegner,, *J. Org. Chem.*, **1994**, 59, 635.
10. P. J. Barnes. Ph.D. Thesis. University of Southampton, 1994.
11. C. A. Hunter, *J. Chem. Soc., Chem. Comm.*, **1991**, 749.
12. A. Yoshizawa, A. Y., M. Watanabe, *Liq. Cryst.*, **2007**, 34, 633.
13. A. Yoshizawa, H. K., F. Ogasawara, Y. Nagashima, T. Kawaguchi, *Liq. Cryst.*, **2007**, 34, 547.
14. A. Yoshizawa, H. Kinbara, T. Narumi, A. Yamaguchi, *Liq. Cryst.*, **2005**, 32, 1175.
15. H. Furuya, K. Asahi, A. Abe, *Polymer Journal*, **1986**, 18, 779.
16. G. R. Luckhurst, *Liq. Cryst.*, **2005**, 32, 1335.
17. G. S. Attard, C. T. Imrie, *J. Chem. Mater.* , **1992**, 4, 1246.
18. G. S. Attard, A. G. Douglass, *Liq. Cryst.*, **1997**, 22, 349.
19. A. G. Douglass. Ph.D. Thesis. University of Southampton, 1998.
20. A. Abe, H. Furuya, Su Yong Nam, S. Okamoto, *Acta Polymerica*, **2003**, 46, 437.
21. S. G. Broadbridge. Ph.D. Thesis. University of Southampton, 1998.
22. C.van Rij, D.Britton, *Acta Crystallogr.,Sect.B:Struct.Crystallogr.Cryst.Chem.*, **1977**, (1301).
23. E.G.Cox, D.W.J.Cruickshank, J.A.S.Smith, *Proc.R.Soc.London,Ser.A* **1958**, 247, 1.
24. J.Trotter, *Acta Crystallogr.*, **1961**, 14, 1135.
25. J. W. Emsley, G. R. Luckhurst, G. N. Shilstone, I. Sage, *Mol. Cryst. Liq. Cryst.*, **1984**, 102, 223.
26. Y. Galerne, *Mol. Cryst. Liq. Cryst.*, **1998**, 323, 211.
27. L. Malpezzi, S. Bruckner, E. Galbiati, G. R. Luckhurst, *Mol. Cryst. Liq. Cryst.*, **1991**, 195, 179.
28. L. Malpezzi, S. Bruckner, D. R. Ferro, G. R. Luckhurst, *Liq. Cryst.*, **2001**, 28, 357.

Chapter 6

Investigating the mesogenic behaviour of non-symmetric kinked dimer motifs

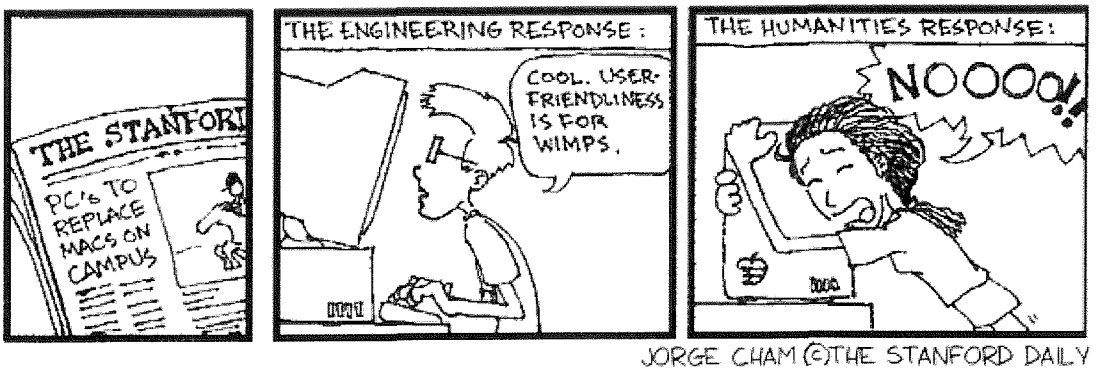

"Piled Higher and Deeper" by Jorge Cham
www.phdcomics.com

Used with permission

6 Investigating the mesogenic behaviour of a non-symmetric kinked dimer motifs

6.1 Introduction

The synthesis of the symmetric 1,2- and 1,3-dioxybenzene linked dimers yielded some interesting results. They provided several unanswered questions concerning the ordering of the materials, as well as the conformational distribution in the nematic phase which gave rise, in both series, to an unexpected odd-even effect. As seen in the non-symmetric conventional dimers considered in Chapter 3, we would expect that altering the symmetry of the 1,2-dioxybenzene linked materials would have an impact on the melting point and the liquid crystal phase transitions.[1-3] By synthesising two series where the symmetry has been deliberately destroyed, we shall investigate how the melting points and phase behaviour is altered. This change in symmetry was achieved by either changing the position of the core group (the 1,2-dioxybenzene ring) in relation to the end groups by making the spacer lengths inequivalent, or by keeping the spacer groups the same and altering one of the mesogenic groups (the options are sketched in Figure 6.1).

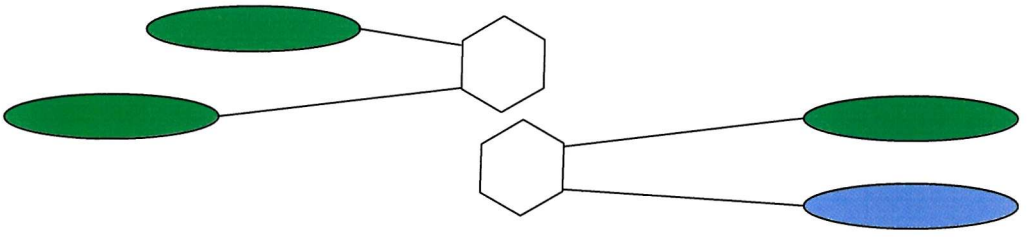

Figure 6.1 Sketch of bent core dimers where the chemical symmetry is broken by either changing the spacer length (left) or altering the mesogenic group (right).

Changing the position of the core group in relation to the end mesogenic groups requires the total length of the spacer arms (and indeed the empirical formula) to be kept same but altering the number of carbon atoms in each arm. The total length chosen for this study was 16 allowing five different combinations of dimer to be synthesised (12-4, 11-5, 10-6, 9-7 and 8-8 already described in Chapter 5). In terms of the difference in the spacer length we may expect the behaviour of the 8-8 and 12-4 isomers to be the most disparate with some odd-even alternation corresponding to pairs of odd and even pairs of spacer arms.

Based on the results for the $CBOnOBF_2$ series detailed in Chapter 3 and that the majority of the $Cat(OnOCB)_2$ dimers presented in Chapter 5 were monotropic, the 2,4'-difluorinated-4-oxybiphenyl mesogenic group was chosen allowing the biggest drop in melting point with the best stability of the nematic phase.

6.2 Synthesis of monomers

The use of the term 'monomer' in the context of this Chapter relates to those compounds with a single mesogenic group. This includes either monosubstituted catechol by an alkyl oxycyanobiphenyl (e.g. Cat(OH)(OnOCB)) as well as a bromo-alkyloxydifluorobiphenyl alkylating agent (e.g. F_2BOnBr). These materials are the first stage building blocks on the way to synthesizing the more complicated non-symmetric, kinked dimers.

In each case either the bromo or the 1-oxy-2-hydroxybenzene groups are not mesogenic groups in their own right and, similar to the reasons leading to the definition of liquid crystal dimer and trimers established in Chapter 1, these materials both fall in the category of monomers.

6.2.1 Catechol based monomers

The first synthesis of the mono-substituted catechols resulted as a biproduct of the symmetric catechol synthesis and was isolated during purification of these disubstituted materials. By experience it was found that generally the interaction of the aromatic -OH group with silica on the column was roughly the same as that for the disubstituted dimers making purification non-trivial and the quantity and/or purity of the monomers was sufficiently low that they were unsuitable for use in further reactions. A clean method of synthesis was required and discovered largely by accident in an attempt to optimize the yield of the disubstituted catechols.

Following a synthesis route which required deprotonation using potassium fluoride as a base in acetonitrile,[4] the result was exclusively a monosubstituted catechol in spite of there being 2.2 equivalents of the alkylating agent. The conclusion, subsequently confirmed by experiment, was that the acetonitrile, at high concentration, was not able to solubilise the monosubstituted product.

This process was optimised and the mono-alkylation of catechol is now performed using acetonitrile with an excess catechol and potassium carbonate as a base. The low solubility

of the mono-substituted catechol in acetonitrile causes the material to precipitate out and thus halts further alkylation. This reaction has become a useful tool to access non-symmetric catechol based dimers discussed later. A series of materials were synthesised (n = 4 – 12) see Scheme 6.1.

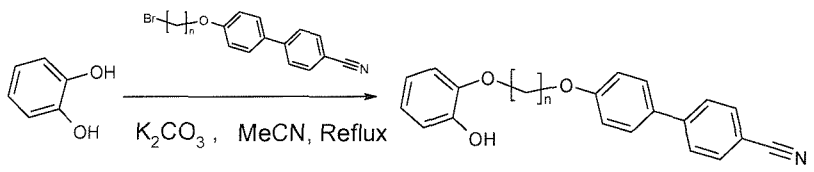

Scheme 6.1 Reaction of catechol with cyanobiphenyloxyalkyl bromide to give the monosubstituted catechol exclusively.

Generally the syntheses proceeded smoothly giving good yields (available in Chapter 7) with the exception of n = 4 and 5 which gave yields of 10% and 15% respectively. Here the mixture of short chain monomer and excess catechol formed an emulsion when extracted from the quenched reaction mixture. Separation of the product from the catechol, was therefore, complicated resulting in excessive handling losses.

Although these intermediates were not synthesised for their liquid crystalline behaviour it was not surprising that there was some evidence of a monotropic nematic phase in some members of the series.

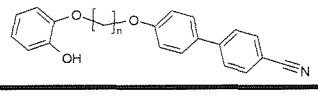

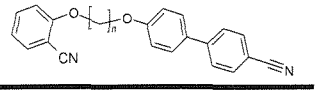

n	Cr		N		I	I_{gl}	Cr		N		I
4	•	195			•	164	•	112	•	(68)	•
5	•	98	•	(43)	•		•	115	•		•
6	•	147			•	113	•	102	•	(58)	•
7	•	109	•	(60)	•		•	92	•		•
8	•	131			•	114	•	96	•	(58)	•
9	•	100	•	(65)	•		•	80	•		•
10	•	123	•	(93)	•		•	75	•	(63)	•
11	•	100	•	(65)	•		•	72	•	(53)	•
12	•	125	•	(79)	•		•	67	•	(58)	•

Table 6.1 Transition temperatures in °C for the monosubstituted catechol dimer and for comparison those of the CBOnO2CP.[5] I_{gl} denotes the isotropic – glass transition marking the upper limit of the unobserved N –I transition.

All the materials in the Cat(OnOCB)(OH) series are monotopic (see table 6.1). Most members were so monotropic that it was not easy to obtain a clear full nematic texture as

the transition often occurred during crystallisation. The most readily available series for comparison to these materials was the ortho-cyanophenyl series (CBOnO2CP).[5] Briefly considering the phase behaviour, there is an odd-even alternation in the melting points for the catechol materials which is not seen in the CBOn2CP series (see Figure 6.2). The overall trend for both series is that the melting points and N-I phase transitions become smaller as n increases and also that any odd-even effects seen attenuate as n increases.

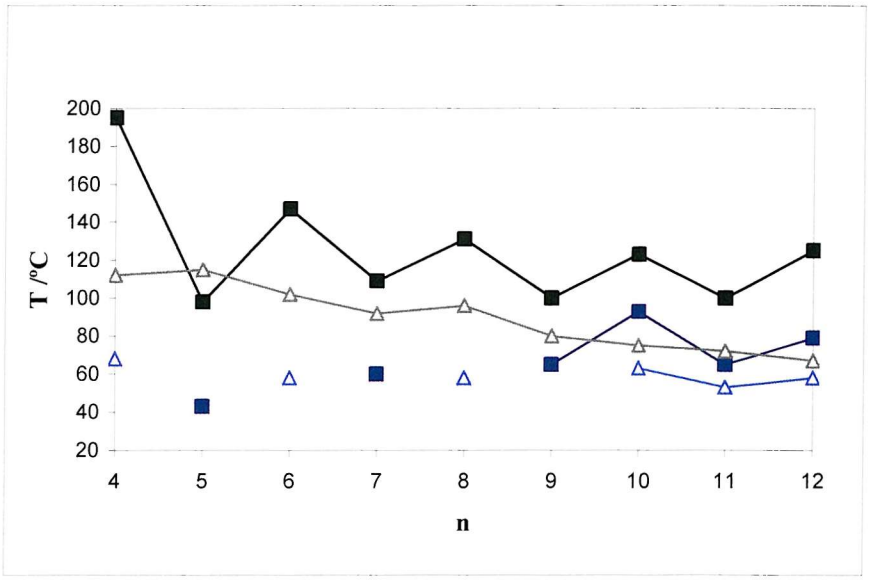

Figure 6.2 Transition temperatures for Cat(OnOCB)(OH) and CBOnO2CP. Here ■ denotes T_{CrI} for Cat(OnOCB)(OH), Δ denotes $T_{CrI/CrN}$ for CBOnO2CP, ■ denotes T_{NI} for Cat(OnOCB)(OH) and Δ denotes T_{NI} for CBOnO2CP.

In both series shown in Figure 6.2, the trend in T_{NI} shows an odd-even effect for larger spacers ($n > 9$). Neither series show any enantiotropic behaviour which, given the off axis dipolar group and the non-mesogenic phenyl group is not surprising. In addition several examples did not exhibit any liquid crystal phase. It is perhaps curious that the linking groups containing an odd number of carbon atoms for the catechol based molecules have a detectable nematic phases whereas for the even examples only the Cr–I transition is observed. This behaviour is reversed for the 2-cyanophenyl materials. These apparently contradictory results can be explained by regarding the melting points trends of both series and then relating them in turn to the respective T_{NI} transition data. Since both materials are monotropic, the observation of a monotropic phase will depend on the degree to which it is possible to supercool. How easily a material supercools will depend on how readily the material self-seeds in the bulk, the thickness of the film and to what

degree the surface interactions provide nucleation points. By supercooling the materials to a point where the material freezes we can obtain an upper limit for T_{NI}.

The catechol based material shows a pronounced odd-even effect in both the melting and N – I transitions. Where n is even the melting points are sufficiently high that crystallisation is favoured before the material can be supercooled to T_{NI} and thus where n < 9 only the odd members, with lower melting points, have an observable monotropic nematic phase. As expected the odd-even effect attenuates as n increases for both melting and T_{NI} transitions and the melting points decrease with increasing n for both odd and even members. This attenuation and drop in the melting points allows the observation of the monotropic phase for n > 9.

For the CBOnO2CP series the melting point trend shows no alternation reducing continuously as n increases. The liquid crystal phase shows an odd-even effect but this is much less pronounced compared to the Cat(OnOCB)(OH) series. Again this is only completely observable when the melting points are low (n > 10). In the case where n < 10, because there is no alternation in the melting point, the nematic phase is only observed where the T_{NI} is highest which is in the even members.

6.2.2 Examining the role of the hydroxyl group

The role of the hydroxyl group compared to the cyano group clearly influences both the melting and N – I transitions shown by the differences in the phase behaviour seen in Figure 6.2. The difference between these behaviours lie in the nature of the supramolecular contacts. Although some H-bonding contacts would be expected to be observed from a C≡N···H contact (we know this from the short contacts in the crystal structures in Chapter 5), the H-O···H should be more dominant. The formation of a supramolecular dimer (two monomers held together by supramolecular contacts) is unlikely, given their low melting points (compared to that expected for the resulting supramolecular trimer). However, in crystals the size of the H-bonding contact is sensitive to the linearity of the contact,[6] it is reasonable to assume that this is true in the nematic phase. Therefore, any major changes to the conformational distribution would also affect the supramolecular contact as this will influence how linear (and hence strong) any H-bond formed will be. The expected result would be an increase in the nematic

stability with stronger H-bonding (so long as the H-bonding interaction promotes a more favourable length-to-breadth ratio).[7]

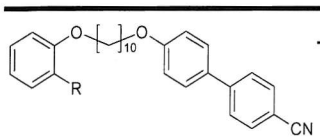

R	Cr		N		I
OH	•	123	•	93	•
CN	•	75	•	63	•
OMe	•	67	•	46	•

Table 6.2 Transition temperatures of the cyanobiphenyl monomers with n = 10 and three different groups at position R. (R = CN[5])

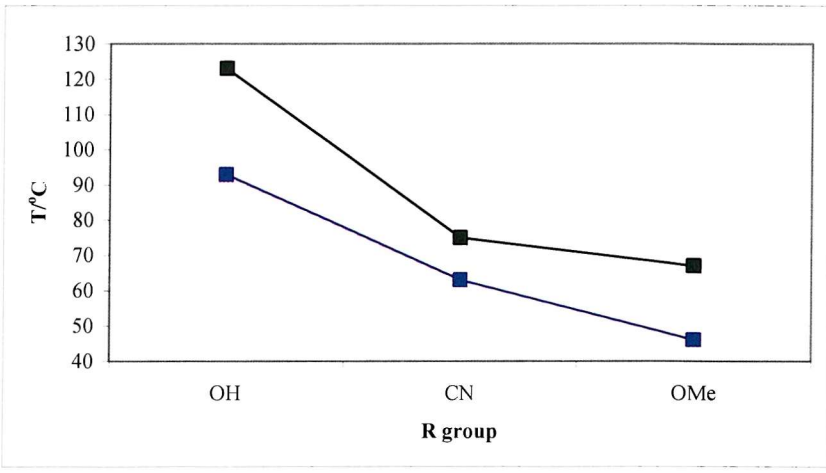

Figure 6.3 Transitional temperatures of cyanobiphenyl monomers with n = 10 and three different groups at position R, where ■ is T_{CrI} and ■ is T_{NI}.

This was tested by synthesising a material with an -OMe group in the 2 position thus destroying the hydrogen bond (see Table 6.2). As can be seen in Figure 6.3 the melting point for R = -OH is considerably higher than R = -CN or OMe. This is not surprising as the system in the crystal is static and the local interactions are fixed at the optimum angle for hydrogen bonding for Cat(O10OCB)(OH). We might not, therefore, have expected such a decrease in the T_{NI} since liquid crystal systems are dynamic and change as the molecules flow.

Interestingly there is a significant difference in the nematic phase stability of nearly 50 °C. This can be rationalised in terms of change in anisotropy, (from molecular shape/size; OMe > CN > OH) and in terms of electrostatic interaction (OH > CN > OMe). This means that we might expect T_{NI} of the hydroxyl compound to be the largest

by a significant amount. The oxygen contributes the largest electrostatic attraction for the smallest perturbation in linear shape, the latter being generally considered more important than the former.

6.2.3 α-(2,4'-difluorobipheny-4-oxy)alkyl-ω-bromide alkylating agent

To create the non-symmetric 1-[α-(4'cyanobiphen-4-yloxy)alkyl-ω-oxy-]-2-[α-(2,4'-difluorobiphenyl-4-yloxy)alkyl-ω-oxy-]-benzene series described in Section 6.2, an alkylating agent analogous to the α-(cyanobiphenyloxy)alkyl-ω-bromide series had to be synthesized. This was done in much the same way as for the cyanobiphenyl analogues using a ten fold excess of the dibromoalkane in acetone with 4-hydroxy-2,4'-difluorobiphenyl shown in Scheme 6.2.[8] The members of the series produced were mostly oils. No members showed any liquid crystalline behaviour even when, in some cases, cooled to below -20 °C (performed on the DSC rather than on the microscope) where they underwent an isotropic glass transition.

n	mp /°C	I_{gl}/°C
4	oil	
5	oil	
6	53	
7	oil	~-20
8	53	
9	oil	-22
10	53	

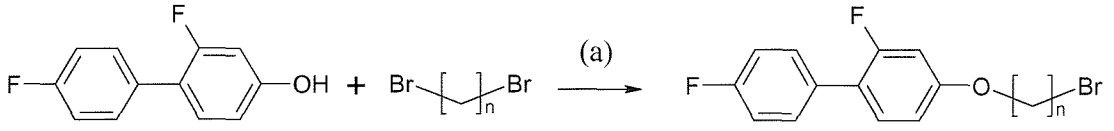

(a) Acetone (reflux), K_2CO_3, NaI

Scheme 6.2 Williamson synthesis of the α-(2,4'-difluorobipheny-4-oxy)alkyl-ω-bromide series.

These materials were somewhat harder to purify than the analogous cyanobiphenyls as they were far more readily solubilised by the excess dibromoalkane which behaved as an eluent, moving the product through the column before separation could take place. This was overcome by distilling off the majority of the dibromoalkane under vacuum and then separating the remainder by column chromatography. The yields for these materials are somewhat more modest than those for the cyanobiphenyl analogues owing to the extra stage in purification; they are found in Chapter 7.

6.3 Synthesis of novel kinked non-symmetric dimers.

Attempting to synthesize these types of dimer took the chemistry to a slightly more complex level. From the outset it was unlikely that any materials made were going to make practically useful flexoelectric materials since they would be likely to be extremely monotropic. However, the effect of making these changes on the compounds with already low melting points was attractive as they could potentially have been used with symmetric kinked dimers to make eutectic mixtures. Also making the comparisons of these materials to the conventional dimers gave another possible opportunity to try and elucidate what was giving rise to the peculiar odd-even effect in the transition temperatures.

This section describes the general synthetic problems surrounding these two sets of novel materials in an attempt to justify the methods described in the Experimental section.

6.3.1 Details of the synthesis

It was found that synthesis of the non-symmetric dimers tended to require the use of a stronger base to deprotonate the remaining phenolic proton. Although it was shown that excess potassium carbonate or caesium carbonate would deprotonate the remaining hydroxyl group of the mono-substituted catechols, it was found that sodium hydride gave better yields using a smaller excess. There is a literature precedent[9] for using carbonate in these types of non-symmetric catechol substitutions, but this was only available a considerable time after the synthesis of these materials had been completed. Potassium hydroxide has been reported to work[10] in similar materials however sodium hydride was used as the base of choice for these reactions as it acts in an entirely non-nucleophilic fashion. The disadvantage is that these reactions were moisture sensitive and the hydride had to be activated by removing the mineral oil by continual washing with petrol under dry nitrogen.

The number of solvents which were available and known to solubilise both the starting materials and products were limited. Butanone and acetone could not be used as they polymerise in the presence of hydride. THF was shown to give modest yields but the solvent of choice was still DMF which both solubilised the materials and had a boiling (or rather decomposition) point higher than other solvents available allowing the reaction

to be conducted at temperatures of 100 °C whilst also being relatively easy to remove under vacuum after the reaction (unlike the remaining candidates which included cyclohexanone and DMSO). The only disadvantage of DMF was the necessity to keep the solvent dry for use with hydride. Vacuum distillation was the most likely option although the use of excess sodium hydride in fresh HLPC grade DMF, degassed by dry nitrogen, gave comparable results with a less cumbersome preparation being required.

6.3.2 Cat(OmOCB)(OnOCB)

The aim of this synthesis was to make a short series of materials where the catechol unit effectively moved down the chain with the total spacer length remaining the same. Thus each member of the series (other than n = m = 8) was synthesized under the conditions shown in Scheme 6.3.

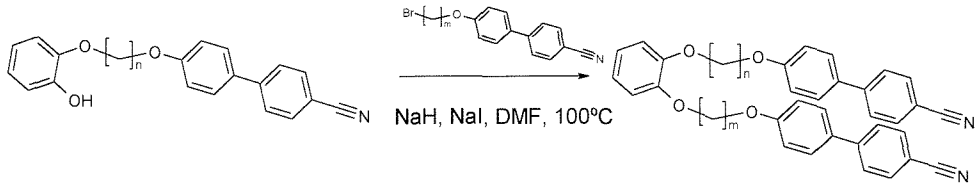

Scheme 6.3 Reaction scheme for non-symmetric catechol [Cat(OmOCB)(OnOCB)] dimers where the two spacer lengths are inequivalent and the total number of carbon atoms of m and n add up to 16.

m	n	Yield %
12	4	10
11	5	51
10	6	46
9	7	16
8	8	68

Table 6.3 Yields for Cat(OmOCB)(OnOCB) where m and n represent the spacer lengths as shown in Scheme 6.3. Quantities produced from the synthesis are given in Chapter 7.

The yields from these reactions, shown in Table 6.3, were moderate to low, particularly for m = 12 and 9. The reason for this is unclear as there seemed very little unreacted material after the reaction and no other spots were observed by TLC other than product and some baseline material. By NMR of the crude product there was neither evidence of the alkyl bromide undergoing elimination nor any other significant side reaction.

6.3.3 Cat(OnOCB)(OnOBF$_2$)

Synthesis of the non-symmetric kinked cyanobiphenyl fluorobiphenyl dimer was completed similarly to that described in Section 6.2.1.1. The corresponding α-(2,4'-difluorobipheny-4-oxy)alkyl-ω-bromide was added and the reaction conducted under the conditions shown in Scheme 6.4.

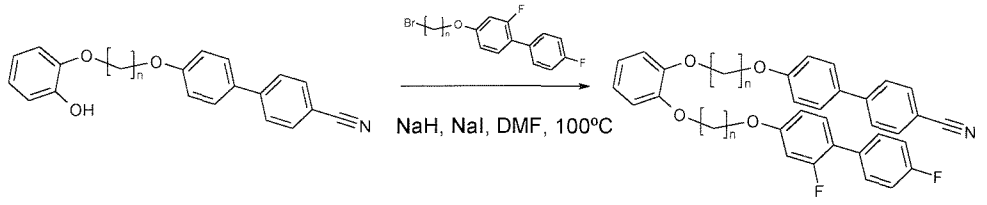

Scheme 6.4 Reaction scheme for the preparation of the non-symmetric catechol dimers [Cat (OnOCB)(OnOBF$_2$] where the two mesogenic groups are inequivalent.

n	Yield %
4	24
5	38
6	48
7	30
8	30
9	49
10	21
11	23

Table 6.4 Yields of the non-symmetric dimers Cat(OnOCB)(OnOBF$_2$) shown in Scheme 6.4.

Product yields were generally poor with no reaction giving better than 50% yield. The starting materials were all pure by NMR that is to 5%, so contaminant in the starting material is an unlikely explanation for the poor yields. There was still excess sodium hydride present when the reaction was quenched and there was no bi-product which could be detected either by NMR or by TLC. There was significant discolouring of the product (brown) which was removed by column chromatography; this could have been a result of degradation of the reactants. Thermal degradation of the product is unlikely as none of these materials decomposed on the microscope slide and there was no evidence such moieties undergoing this extent of chemical attack under these conditions.

6.3.4 Analysing the molecular characterization

Characterising these materials both to identify them and to determine their purity was often very difficult. Identifying the materials themselves was often best done by mass spectroscopy where the monotropic mass could be identified uniquely. This said, the molecular mass of all the materials in the Cat(OmOCB)(OnOCB) series are identical since they are structural isomers. In their NMR and IR spectra, this series showed almost no differences between them, only the ^{13}C spectra showed slight differences in the carbon signals originating from atoms in the chains based on the lack of symmetry. The best characteristic indication of which material had been made, came from the T_{NI} which, as we shall see, did alternate with changing position of the core group. Identification of the members of the Cat(OnOCB)($OnOBF_2$) series was much more straightforward as both mesogenic groups gave sufficiently different signals in the ^{1}H and ^{13}C NMR spectrum that each group could be identified unambiguously.

The most common impurities seen in these materials are the unreacted starting materials. Both starting materials can be easily identified by ^{1}H NMR (although quantifying the impurity is often less straightforward). The alkylating agent can be seen from the triplet peak coming at ~3.5 ppm corresponding to the protons adjacent to the bromine atom. The mono-substituted catechol gives a multiplet at ~6.7 ppm (data found in Chapter 7) which corresponds to the four protons on the catechol aryl group itself. Even in non-symmetric dimers, the protons on fully substituted catechol dimers give these protons as an unresolved singlet using a 400 MHz spectrometer. This result is consistent with results from predictive NMR programs.

Each compound gave NMR spectra with peaks consistent with the identification of the intended product and showed no impurities to an accuracy of 95%. IR and mass spectra supported these conclusions on identification and purity based on the NMR data.

6.4 Analyzing the physical data for Cat(OnOCB)(OmOCB)

Analysing the physical data of these materials led to the discovery of an interesting property in both of these non-symmetric series. Many of these materials were observed to supercool over very large ranges and several show a large number of two brush defects which thought to be indicative of a biaxial nematic. Another test for the identification of

this phase is the size of the $\Delta S/R_{NI}$ which should be particularly small if the nematic phase is biaxial.

6.4.1 Optical microscopy

Optical microscopy was used for these materials to examine their optical textures and to determine their phase behaviour. The samples were set up in much the same way as described in previous chapters, that is the solid was mounted on a cover slip, melted and another cover slip placed on top to produce a thin film. This was then examined on a microscope and viewed between crossed polarisers.

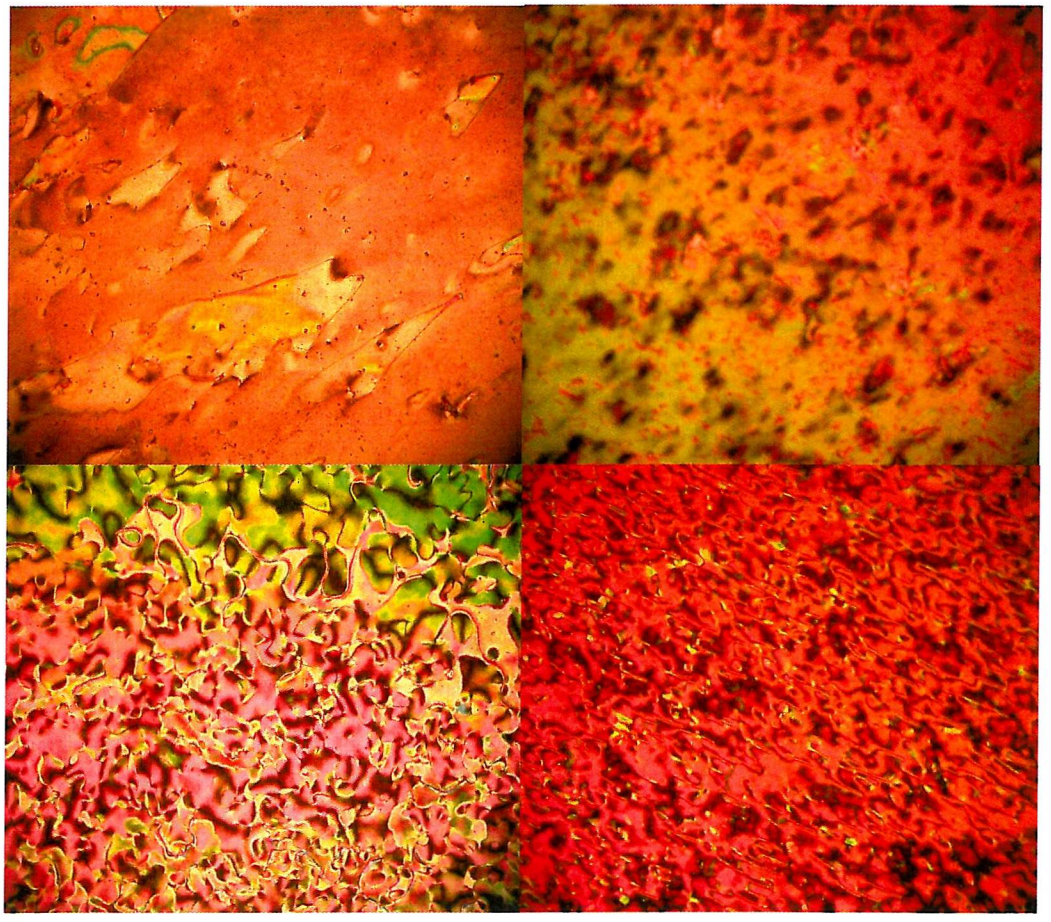

Figure 6.4 All optical texture pictures were taken on cooling showing the nematic phases Cat(O9OCB)(O7OCB) taken at 77 °C, $0.97T_{NI}$ (top left); Cat(O10OCB)(O6OCB) taken at 89 °C, $0.93T_{NI}$ (top right); Cat(O11OCB)(O5OCB) taken at 78 °C, $0.98T_{NI}$ (bottom left); Cat(O12OCB)(O4OCB) taken at 89 °C, $0.94T_{NI}$ (bottom right).

There were many similarities in the behaviour of these materials; their phase behaviour is discussed in full later. The Cat(OmOCB)(OnOCB) dimers all showed a thread-like

optical texture characteristic of a nematic, this is not always well captured by the camera as the threads are fine and not easily brought into focus (see Figure 6.4). Each of the materials flashed when pressure was applied to the cover-slip close to T_{NI} (i.e. when the liquid was less viscous and less well ordered). Some materials, had a distinctly more pronounced schlieren texture than others (e.g. m/n = 11/5 and 12/4). These optical textures were a mixture of two- and four-brush defects in all cases. Each material supercooled by some considerable margin (noted in Table. 6.5) and remained as a viscous liquid even after the application of considerable mechanical stress. This included pressing the slides together using a spatula and even rubbing the coverslips together off the heating stage.

6.4.2 Phase behaviour

Regrettably, given what is known about the phase behaviour of the symmetric $Cat(O8OCB)_2$ dimer it was unlikely that any of the other materials were going to exhibit enantiotropic phases. However, there are several interesting features about this series given that they are isomeric. Included in the data in Table 6.5 are the temperatures at which the materials crystalise on cooling under the conditions used to observe the material with the optical microscope.

m	n	Cr		N		I	Crystallise
8	8	•	126	•	118	•	101
9	7	•	107	•	89	•	59
10	6	•	124	•	118	•	56
11	5	•	99	•	85	•	~25
12	4	•	121	•	111	•	< 25

Table 6.5 Transition temperatures in °C for non-symmetric and symmetric dimers Cat(OmOCB)(OnOCB) where n + m = 16. Temperature of <25 °C indicates samples which supercooled to room temperature (taken to be 25 °C) and remained in the nematic phase for several hours.

As described earlier, the degree of supercooling is very much dependent on the conditions. There is generally a trend that the greater the difference in arms lengths, the greater the super cooling range and the harder it is for the material to crystallise even at these low temperatures. It should also be noted that for m = 11 and 12, these cells were subject to mechanical stress (moving the slides and pressing down on the sample with a cover slip and still crystallisation did not occur). After several minutes m = 11, n = 5

formed a nematic glass whereas m = 12 was still a liquid crystal after several hours. Crystallisation occurred when the sample was left at room temperature over night. The difference in time to crystallise between the 11/5 and 12/4 dimers is not surprising as it can be imagined that mis-matching the different spacer lengths makes forming the crystal harder resulting in the observed supercooling.

The phase behaviour is also interesting (see Figure 6.5) Here we see an odd-even alternation in both the melting and N – I transition as a result of simply moving the catechol moiety along the chain. If we understand the structure to be U-shaped as described in Chapter 5, then this odd-even effect is not surprising since the parity of both chains is the same even if the lengths are different. In that respect the non-symmetric molecules with different parity find themselves in a geometric environment which would be very similar to that of the symmetric case and so should generally behave in similar way, i.e. 9/7 and 11/5 both have odd parity arms and as such are expected to (and do) give a lower T_{NI} than 10/6 and 12/4 which have even parity. The differences would be expected to come in the temperature of melting and N-I transition and this is the case. For the even dimers, the more non-symmetric the material becomes, the lower T_{NI} and T_{CrI} become.

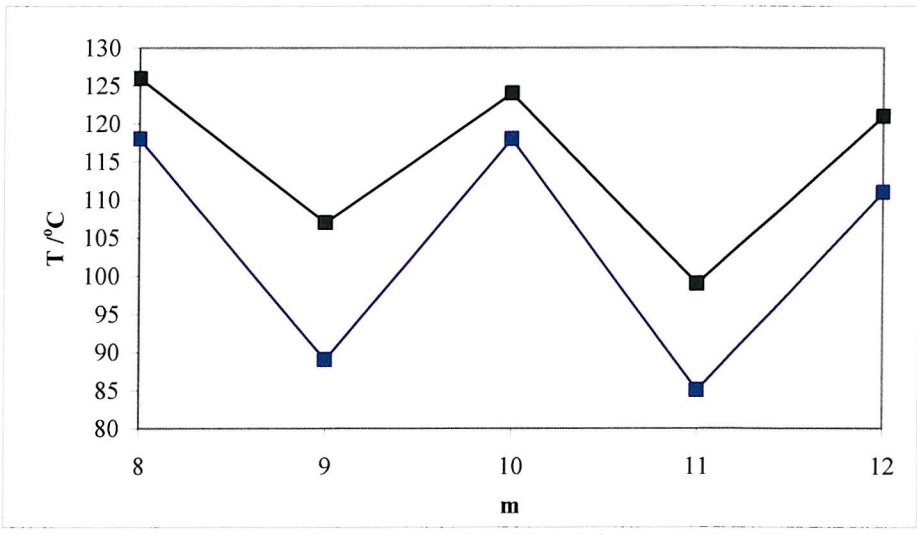

Figure 6.5 The transition temperatures of Cat(OmOCB)(OnOCB) as a function of the spacer length where ■ denotes T_{CrI} and ■ denotes T_{NI}

However, the difference between 8/8 and 12/4 dimers is still not very large and is certainly smaller than the effect of changing the parity. Thus we can conclude that the

effect of the different conformational shape caused by changes in the spacer parity is much greater than significant changes in symmetry of the molecule, i.e. by changing the position of the 1,2-dioxybenzene linker with respect to the mesogenic end groups.

6.4.2.1 Comparing these results with the symmetric dimers [Cat(OnOCB)$_2$]

There are three interesting questions which arise from the data:

- What happens when m is even and n is odd?
- How do these results compare to those for the symmetric dimers?
- Can the phase behaviour be replicated by mixing the appropriate symmetric dimers?

The first question cannot be well answered. Time did not allow an in depth study to be made although one sample of 10/5 was made in poor yield and with impurities. This not withstanding, we know the difference in T_{NI} between 8/8 and 10/6 is very small so it is reasonable to compare 10/5 with 7/7 and 8/8 as shown in Table 6.6 and Figure 6.6.

m/n	Cr		N		I
7/7	•	80	•	89	•
10/5	•	112	•	(103)	•
8/8	•	126	•	(118)	•

Table 6.6 Transition temperatures in °C for Cat(OmOCB)(OnOCB) where n + m = 14 - 16

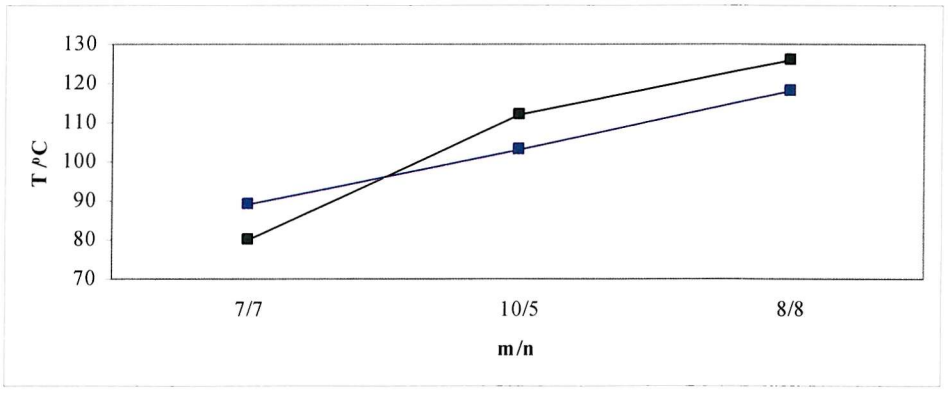

Figure 6.6 Transition temperatures for the three compounds listed in Table 6.6, where ■ denotes T_{NI} and ■ denotes $T_{CrN/CrI}$.

The interesting feature shown in Figure 6.7 is the linear increase in T_{NI} with increasing spacer length. Also it is important to note that this is the first truly 'odd' dimer which has

been studied (odd because the sum of the length of the two arms has an odd parity) and that T_{NI} is above that of the 7/7 dimer.

Another interesting comparison would be to see the effect of increasing n whilst keeping m constant and comparing this to the corresponding dimers. This was done with a short series of 10/n dimers where n = 4, 5 and 6. The data is given in Table 6.7 and displayed graphically in Figure 6.8

m/n	Cr		N		I
10/4	•	110	•	117	•
10/5	•	112	•	(103)	•
10/6	•	124	•	(118)	•

Table 6.7 Transition temperatures in °C for Cat(OmOCB)(OnOCB) where m = 10 and n = 4 – 6.

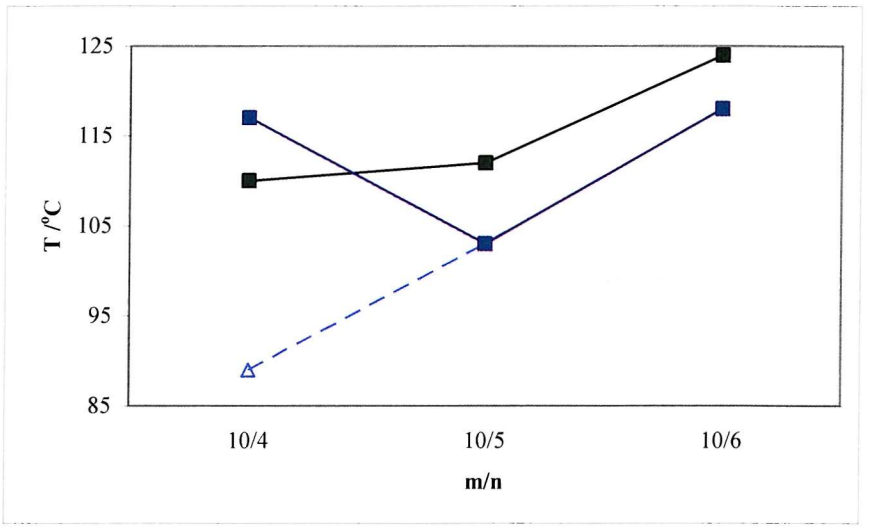

Figure 6.7 Melting points and N-I transition temperatures for the materials in Table 6.7. Where ■ denotes T_{NI}, ■ represents $T_{CrN/CrI}$ and Δ denotes T_{NI} for the corresponding length of symmetric dimer, m/n = 7/7 and 8/8 (i.e. n = m).

Although not much can be gleaned from a series with just three members, we see that there is what appears to be an odd-even effect in T_{NI} as n increases. Also there is a clear difference between m/n = 10/4 and m/n = 7/7. This suggests that the effect of two even spacer groups, even though they are non-symmetric, results in a higher T_{NI} because the mesogenic units are more co-linear with the molecular long axis.

The melting points show a moderate increase as n increases. This is not surprising as we can assume that molecular packing in the crystal becomes easier the more similar the length of the arms.

Comparing the n + m = 16 non-symmetric series with the 1,2-dioxybenzene dimers has been done by plotting the transition temperatures for Cat(OmOCB)(OnOCB) against those for $Cat(OmOCB)_2$ and $Cat(OnOCB)_2$. The comparison of the melting points is shown in Figure 6.9 and N – I transitions in Figure 6.8.

Considering T_{NI} for the symmetric and non-symmetric dimers (see Figure 6.8) once again we see that there is very different behaviour for the odd members compared to the even dimers. Looking at the even dimers we see that the symmetric examples show an increasing dissimilarity as the difference in m and n gets bigger. The T_{NI} for the non-symmetric dimers appear to be the mean of those for the symmetric T_{NI}s for 10/6 but in the case of 12/4 clearly the longer spacer group is dominating here. This is understood simply because T_{NI} of the 12/4 is significantly closer to that of $Cat(O12OCB)_2$ rather than $Cat(O4OCB)_2$.

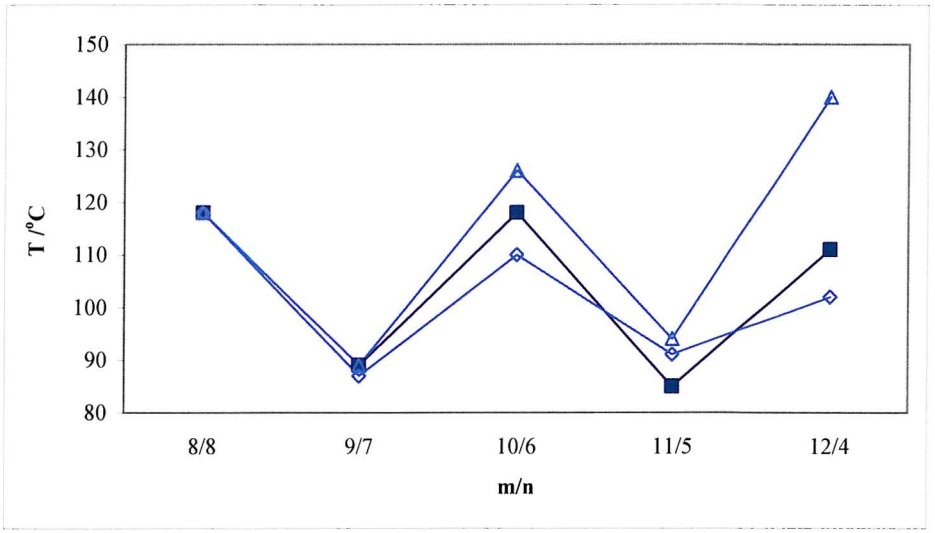

Figure 6.8 The N-I transition temperatures for non-symmetric 1,2-dioxybenzene dimers against the long and short chain symmetric analogues. Where ■ denotes T_{NI} for Cat(OmOCB)(OnOCB), ◊ denotes T_{NI} for $Cat(OmOCB)_2$ and Δ represents T_{NI} for $Cat(OnOCB)_2$.

Taking the suggested idea that the dimers tend to form U-shaped conformers in the nematic, we would see that the shorter spacer has much less rotational freedom due to the

proximity to the longer arm. It is not unreasonable to assume that the absence of the mobility in the shorter chain will result in behaviour dominated by the longer chain. Therefore we would expect, hypothetically, the dimers 11/4 and 12/4 to be more similar in their respective behaviours to the symmetric analogue of the longer arm; that is 11/11 and 12/12. Whereas if n were longer, for example, 11/10 and 12/10, we would expect to be closer to the mean of the two symmetric dimers. Where the odd members are concerned the $T_{NI}^{m/n}$ is slightly lower than T_{NI}^{m} and T_{NI}^{n} analogues. This can offer some insight to the nematic environment for the odd systems since subtle changes in shape appear to affect the stability of the phase more than for members with an even parity. It suggests the odd members have a nematic phase whose stability is far more sensitive to changes in shape.

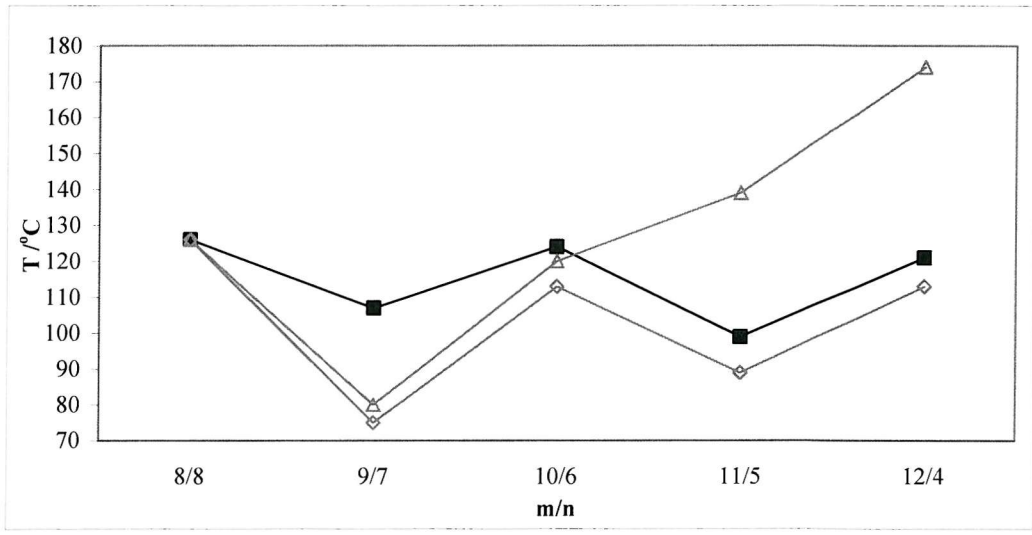

Figure 6.9 Melting transitions for non-symmetric 1,2-dioxybenzene dimers as a function of the long and short chain symmetric analogues. Here ■ denotes T_{CrI} Cat(OmOCB)(OnOCB), ◇ denotes T_{CrI} for Cat(OmOCB)$_2$ and △ denotes T_{CrI} for Cat(OnOCB)$_2$.

Considering the melting points, we see there is a more substantial difference between the two symmetric systems (see Figure 6.9). The smaller chain members have a much higher melting point allowing access to the very monotropic nematic transitions for n = 4 and 5. It is interesting to note that the melting points in the non-symmetric series seem to mimic that of the longer chain analogues rather than the shorter chain examples. There is a slight

increase in the melting point but generally there is an odd-even effect which is similar in nature to that of the Cat(OmOCB)$_2$ examples (with the exception of m/n = 9/7).
This is potentially of great benefit as it appears to suggest that making a large disparity between the lengths of the spacer chains results in a slight increase in T_{NI} without a large increase in the melting point and a very long supercooling range.

6.4.2.2 Examining the phase behaviour of mixtures of symmetric dimers

We can examine the effect by mixing two of the component symmetric materials and examining the resultant mixture under the microscope to determine the transition temperatures. The mixture was made by measuring out equal quantities (by mole) of each of the symmetric dimers and then mixing them by dissolving them first in DCM, mixing and then allowing the solvent to evaporate. The solid was then heated into the less viscous isotropic phase using a hot air gun and mechanically mixed by gentle shaking. The mixture was allowed to cool to room temperature when a solid was formed. This was then examined under the microscope under normal conditions described in the optical microscopy section.
Using a sketched diagram of a binary mixture of varying compositions melting giving mixtures of crystal and/or nematic we can see that at some composition mixture there will be heated through a eutectic point where the two crystal phases melt directly into the nematic (or indeed the reverse; shown in Figure 6.10) or isotropic if the mixture is monotropic (see Figure 6.11).
Figures 6.10 and 6.11 show the two extremes where T_{NI} for the mixture is either completely enantiotropic or monotropic regardless of the composition. This, of course, does not have to be the case, but makes the point without the diagram having to appear overly complicated. Bearing this in mind, unless at the eutectic point, there will always be effectively two melting points corresponding to one crystal and then the other.

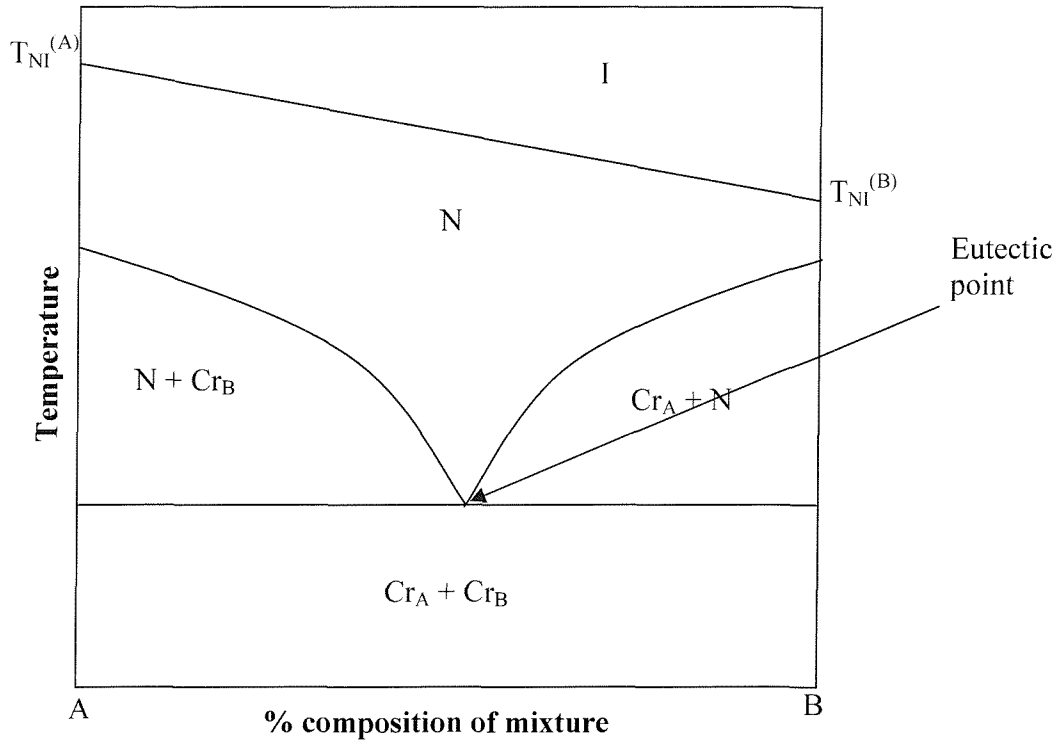

Figure 6.10 Phase diagram of a two component mixture which melts into a nematic at the eutectic point. Percentage compositions ranges from 0 – 100% of A, left to right. Note the eutectic point varies depending on the properties of the components (T_{mp} and ΔS_{mp}) and does not have to be at equimolar composition.

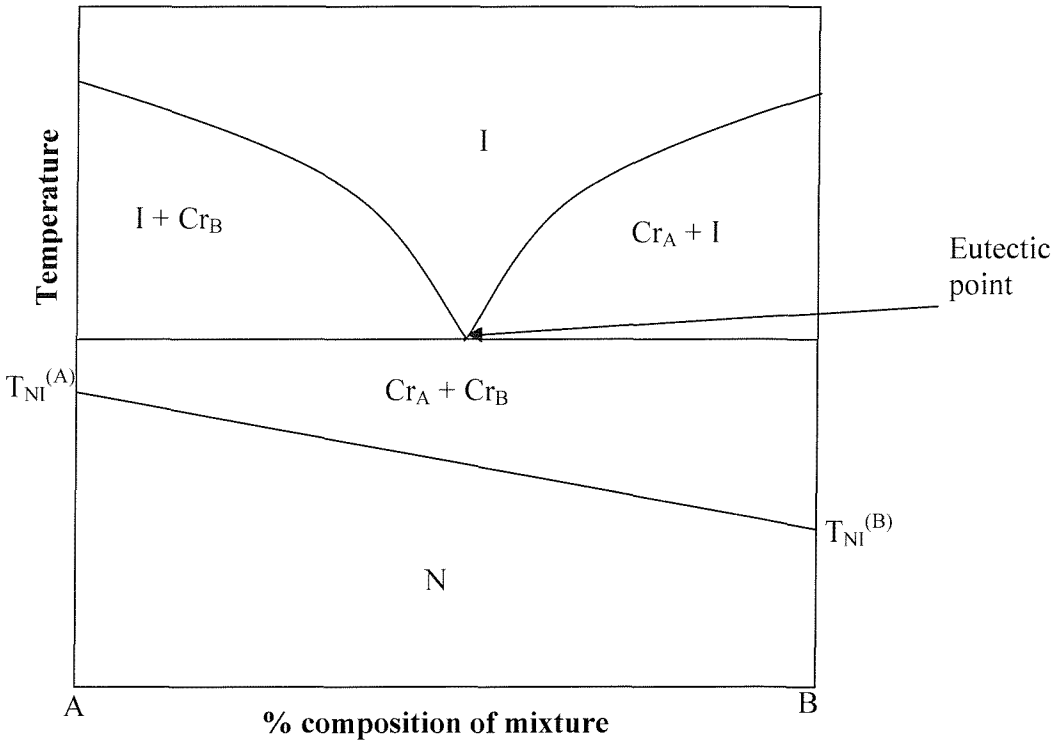

Figure 6.11 Phase diagram of a two component mixture which melts into the isotopic. Percentage compositions ranges from 0 – 100% of A, left to right. Note the eutectic point varies depending on the properties of the components (T_{mp} and ΔS_{mp})and does not have to be at 50% composition.

In order to avoid confusion, all plots of melting points will show both transitions in different shades of grey where the darker will always be the transition into I or N. m will always be taken as the larger spacer number in the composition (e.g. m/n = 10/6) and, although the eutectic point is not known, based on microscope observations we can assume that the diagram in Figure 6.12 is essentially valid. (Note that for mixtures 11/5 and 12/4 the mixture melts into the isotropic phase.)

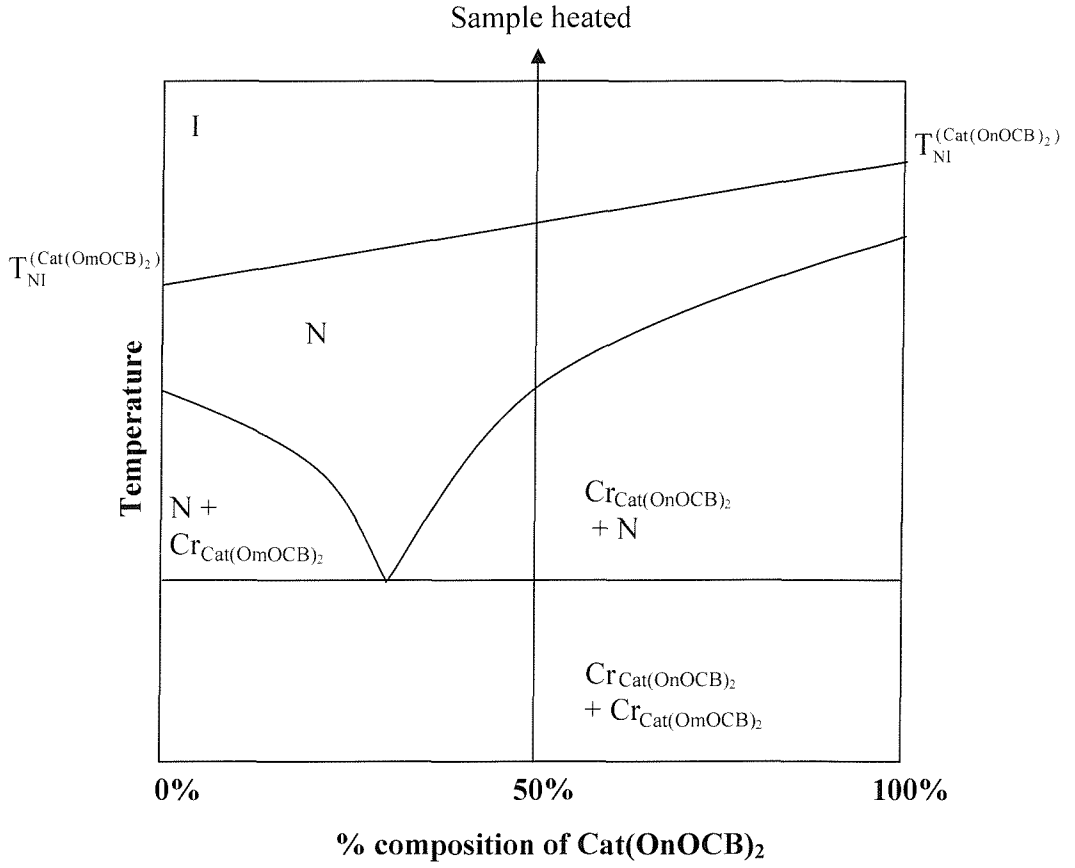

Figure 6.12 Sketch of the phase diagram for mixtures of symmetric 1,2-dioxybenzene dimers where m represents the long chain dimer and n the short chain. The eutectic point is unknown but assumed, from microscopy observations, to be where the composition has more of the long chain dimer.

From this understanding we can examine the phase behaviour at an equimolar composition. The transition temperatures are given in Table 6.8 followed by a table of T_{NI} (Table 6.9) and a table of T_{CrN}/T_{CrI} (Table 6.10) which includes data for the pure non-symmetric and symmetric systems for comparison.

m/n	Cr_m		Cr_n		N		I	Crystallise
8	•	126	•	126	•	(118)	•	101
9/7	•	56	•	83	•	89	•	<25
10/6	•	109	•	116	•	119	•	69
11/5	•	94	•	134	•	(85)	•	43
12/4	•	144	•	159	•	(94)	•	62

Table 6.8 Transition temperatures (in °C) for the equimolar mixtures $Cat(OmOCB)_2/Cat(OnOCB)_2$. Here m represents the longer chain length and n the shorter and Cr_m denotes the melting point of $Cat(OmOCB)_2$ and Cr_n the melting point of $Cat(OnOCB)_2$.

m/n	Cat(OmOCB)(OnOCB)	$Cat(OmOCB)_2$	$Cat(OnOCB)_2$	Mixture
9/7	(89)	87	89	89
10/6	(118)	(110)	126	119
11/5	(85)	(91)	(94)	(85)
12/4	(111)	(102)	(140)	(94)

Table 6.9 Comparing the N - I transitions (in °C) for the pure non-symmetric and symmetric 1,2-dioxybenzene dimers and the equimolar mixtures $Cat(OmOCB)_2/Cat(OnOCB)_2$. Here m represents the longer chain length and n the shorter.

m/n	Cat(OmOCB)(OnOCB)	$Cat(OmOCB)_2$	$Cat(OnOCB)_2$	Mixture Cr_m	Mixture Cr_n
9/7	107	75	80	56	83
10/6	124	113	120	109	116
11/5	99	89	139	94	134
12/4	121	113	174	144	159

Table 6.10 Melting transitions (in °C) for the pure non-symmetric and symmetric 1,2-dioxybenzene dimers and the equimolar mixtures $Cat(OmOCB)_2/Cat(OnOCB)_2$. Here m represents the longer chain length and n the shorter and Cr_m denotes the melting point of $Cat(OmOCB)_2$ and Cr_n the melting point of $Cat(OnOCB)_2$.

Examining the results in Table 6.8 we see that in two cases the nematic phase is enantiotropic. In the case of 9/7 this is not surprising as the nematic phases of both materials are enantiotropic. However, for 10/6 although T_{NI} of the mixture has fallen compared to the symmetric dimer n = 6, the melting point has fallen sufficiently for the material to be enantiotropic. It should also be noted that the supercooling range was vastly increased as a result of mixing these materials. This behaviour is similar to that observed for the pure non-symmetric systems although crystallisation does tend to occur more readily in the mixtures for these.

Table 6.9 shows the T_{NI} for the pure non-symmetric and symmetric systems as well as the equimolar mixtures and here we can see the similarity between the pure non-symmetric dimers and the mixtures of symmetric dimers.

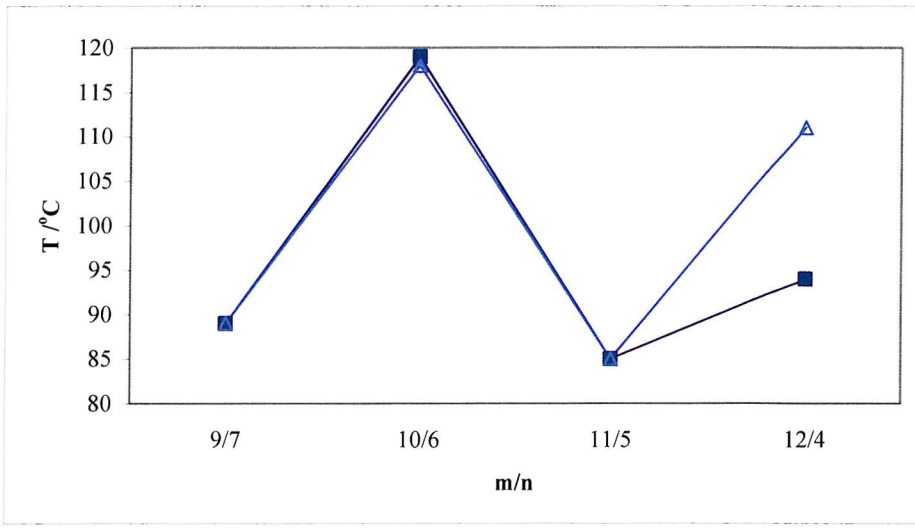

Figure 6.13 T_{NI} as a function of spacer length for the pure non-symmetric Cat(OmOCB)(OnOCB) and the equimolar mixture $Cat(OmOCB)_2/Cat(OnOCB)_2$. Here ■ represents T_{NI} for the mixture and Δ represents T_{NI} for the pure non-symmetric dimers.

This similarity is seen more clearly when the transition temperature is plotted, as in Figure 6.13, however, we can see that there is almost no difference between the pure and mixed systems until the 12/4 dimer where the disparity between the arms is much larger. Table 6.10 compares the differences in the melting points and these are plotted in Figure 6.14. Here we have two melting points for the mixture where Cr_n probably corresponds more to the dissolution of the crystal in the molten Cr_m than an actual melting.

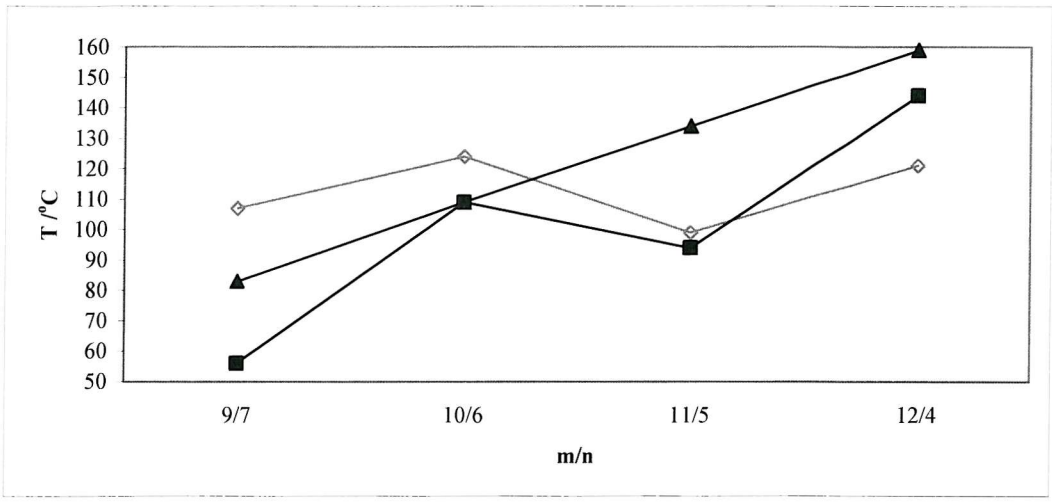

Figure 6.14 Melting point as a function of spacer length for the pure non-symmetric Cat(OmOCB)(OnOCB) and the equimolar mixture Cat(OmOCB)$_2$/Cat(OnOCB)$_2$. Here ■ represents the Cr_m-N/Cr_m-I transitions and ▲ the Cr_n-N/Cr_n-I transitions for the mixture and ◊ represents Cr-I transitions for the non-symmetric dimers.

However, what is striking is the lack of an odd-even alternation in Cr_n. This is perhaps due to the higher melting, shorter dimer simply dissolving at increasingly higher temperatures as n became smaller given the similarity in molecular structure.

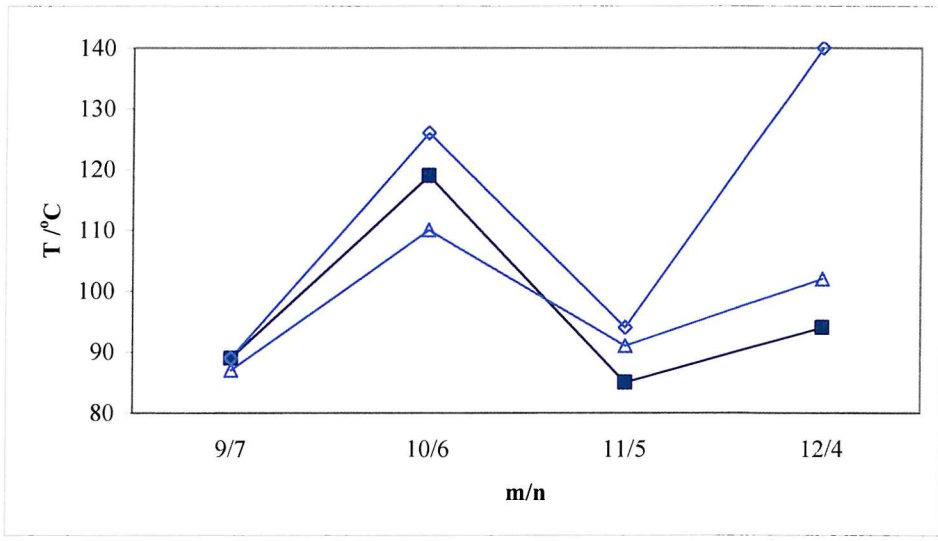

Figure 6.15 T_{NI} as a function of spacer length for the equimolar mixture Cat(OmOCB)$_2$/Cat(OnOCB)$_2$ and the pure symmetric dimers Cat(OmOCB)$_2$ and Cat(OnOCB)$_2$. Here ■ represents T_{NI} for the mixture, ◊ represents T_{NI} for the pure Cat(OmOCB)$_2$ series and Δ T_{NI} for the pure Cat(OnOCB)$_2$ series.

The T_{NI} transitions for the equimolar mixtures compared to T_{NI} for the pure symmetric components naturally look very similar to that of the pure non-symmetric systems. As

such analysis of this data can be brief. The expectation of a mixture would be that the T_{NI} should be the average of the two components weighted by the % composition. Since the components are in a 1:1 ratio we could expect the T_{NI} to simply be the mean of the component T_{NI}s. Within experimental accuracy, this appears to be case for 9/7 and 10/6, the relationship however breaks down for 11/5 and 12/4 where the difference between the spacer lengths becomes larger.

In both pure non-symmetric dimers and the corresponding symmetric dimer equimolar mixtures we see a general trend in the T_{NI} where the more similar the length of the arms, the more closely the materials behave as would be expected, i.e. as an average of the two spacer arms. Deviation from this average of the two pure symmetric systems is apparent for m/n = 11/5 but even more striking for m/n = 12/4. In the latter case, the spacer lengths are so disparate that T_{NI} for the non-symmetric dimer and the symmetric mixture become markedly different. Here the differences of shapes in the conformational distribution of the two components of the mixture appear to become enough to destabilise the nematic, but not enough to initiate phase separation at the T_{NI} transition. We can further comment on this by studying the change in entropy at the nematic – isotropic transition and comparing it to that of the non-symmetric and the symmetric systems (see Section 6.3.3).

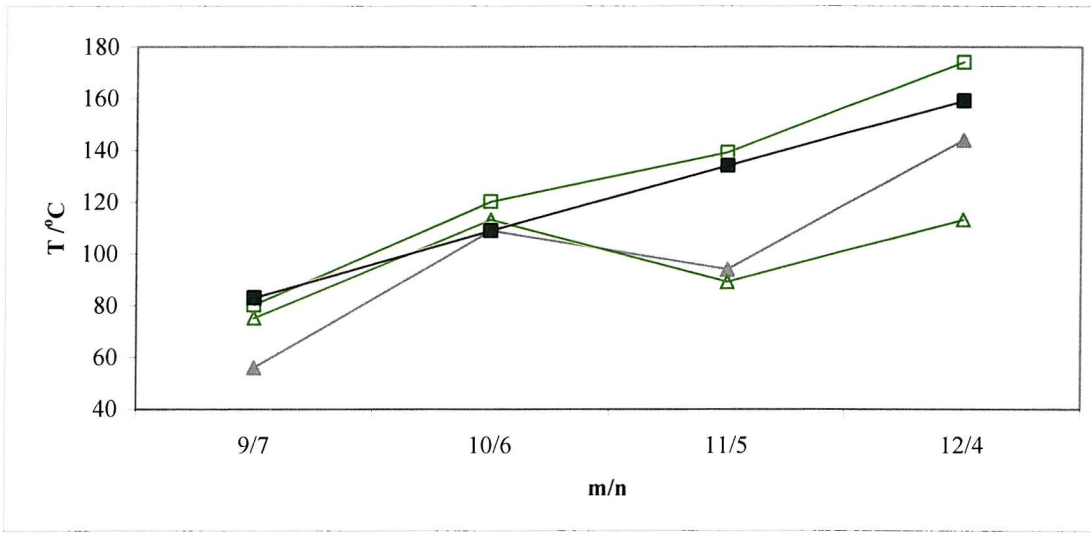

Figure 6.16 Melting points for the equimolar mixture $Cat(OmOCB)_2/Cat(OnOCB)_2$ and the pure symmetric dimers $Cat(OmOCB)_2$ and $Cat(OnOCB)_2$ as a function of spacer length. Here ▲ represents the first melting point for the mixture (Cr_m in Table 6.10), ■ represents the second melting point for the mixture (Cr_n in Table 6.10), Δ represents T_{CrI} for the pure $Cat(OmOCB)_2$ series (Table 6.10) and □ T_{NI} for the pure $Cat(OnOCB)_2$ series (Table 6.10).

Figure 6.16 shows two pairs of very similar trends. Considering the phase diagram of the mixture in Figure 6.12, we can see that the higher melting point of the mixture should be related to the melting point of the shorter spacer length and a lower melting point. relating to the longer spacer length. It is not surprising, therefore, to see that the second melting point in the mixture, Cr_n, relates very closely to the $Cat(OnOCB)_2$ symmetric dimer melting points. It is less clear why the mixture Cr_n melting transition temperatures should increase in an almost perfectly linear fashion. This could perhaps be answered by determining the exact and complete phase diagram. Since there was not enough material to make measurements, this trend will have to remain a curiosity and unexplained.

A brief study of how changing the composition of $Cat(O4OCB)_2$ in $Cat(O12OCB)_2$ affects the T_{NI} for the mixture showed an unexpected result. The T_{NI} and mol fraction for $Cat(O4OCB)_2$ are given in Table 6.11 and these results are plotted in Figure 6.17.

%/% 12/4	mol fraction	T_{NI}
100/0	0.00	101
75/25	0.25	74
50/50	0.50	93
25/75	0.75	118
0/100	1.00	139

Table 6.11 T_{NI} for mol composition of mixtures of $Cat(O4OCB)_2$ in $Cat(O12OCB)_2$ with the corresponding mol fraction of $Cat(O4OCB)_2$ for each composition.

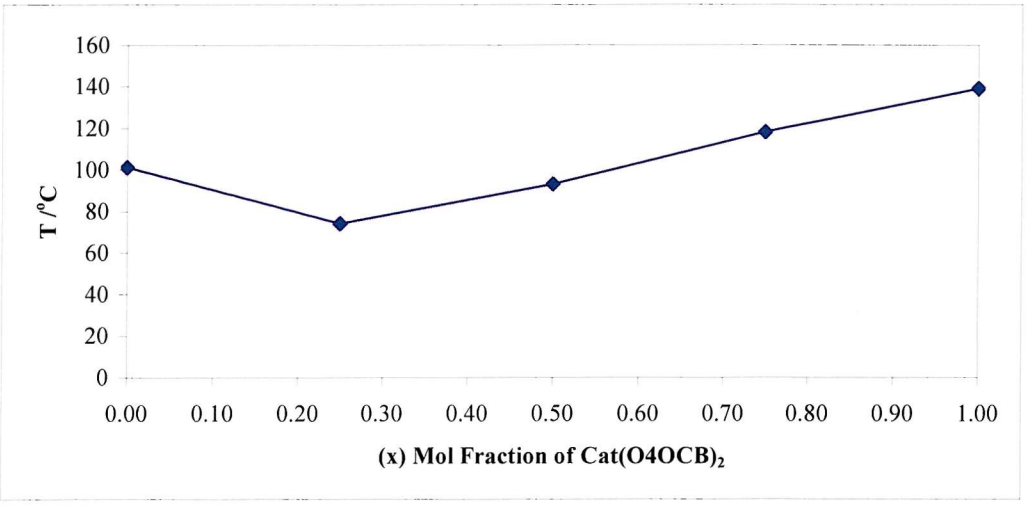

Figure 6.17 The composition dependence of T_{NI} for a mixture of $Cat(O4OCB)_2$ in $Cat(O12OCB)_2$. The composition is written in increasing proportion of $Cat(O4OCB)_2$.

Theory predicts that for a binary mixture of rod-like mesogens increasing T_{NI} for the mixture should exhibit a linear dependence on composition.[11] From Figure 6.17 we can see that from x = 0.25 the increase in T_{NI} is linear, however the drop in T_{NI} from x = 0 to x = 0.25 is unexpected and it is unclear why this should be. The difference in T_{NI} for pure Cat(O12OCB)$_2$ and the value extrapolated from the linear portion of the plot is over 50 °C which is well outside any experimental error. A more thorough investigation of compositions between x = 0 and x = 0.25 would show how quickly the drop in T_{NI} occurs and may give some clue as to why this should happen.

6.4.3 Entropies of transition for Cat(OmOCB)(OnOCB) dimers

The transitional entropy for the kinked dimers with the unsymmetric spacer lengths are given in Tables 6.12 and 6.13. These include data for the Cat(OmOCB)(OnOCB) where n + m = 16 and Cat(O10OCB)(OnOCB) where n = 4 – 6.

m/n	ΔH_{CrN}/ kJmol^{-1}	$\Delta S_{CrN}/R$	ΔH_{NI}/ kJmol^{-1}	$\Delta S_{NI}/R$
12/4	65.9	20.6	7.53	2.36
11/5	56.8	18.5	1.41	0.47
10/6	63.3	19.3	4.8	1.49
9/7	64.7	21.2	1.30	0.43
8/8	50.8	15.8	4.92	1.53

Table 6.12 Transitional entropies for the Cat(OmOCB)(OnOCB) series where n + m = 16.

m/n	ΔH_{NI}/ kJmol^{-1}	$\Delta S_{CrN}/R$	ΔH_{NI}/ kJmol^{-1}	$\Delta S_{NI}/R$
10/4	47.5	15.0	4.10	1.27
10/5	67.0	21.1	2.19	0.73
10/6	19.3	4.8	1.49	1.49

Table 6.13 Transitional entropies for the Cat(O10OCB)(OnOCB) series.

We can see that, generally, the magnitude of the N-I transitional entropy is a little lower than that for the conventional symmetric cyanobiphenyl dimers (which are approximately 2 – 2.5 for even members and 0.6 – 1.2 for odd members). We know that the symmetric Cat(OnOCB)$_2$ series give an odd-even effect in the transitional entropy and this is also the case for the Cat(OmOCB)(OnOCB) and the Cat(O10OCB)(OnOCB) series.

Comparing the results for the Cat(OmOCB)(OnOCB) series to the symmetric Cat(OmOCB)$_2$ series (the longer spacer lengths) we can see that for the odd members

$\Delta S_{NI}/R$ is almost the same whereas for the even members there is a considerable difference becoming more disparate as the difference in spacer lengths increases (see Table 6.13).

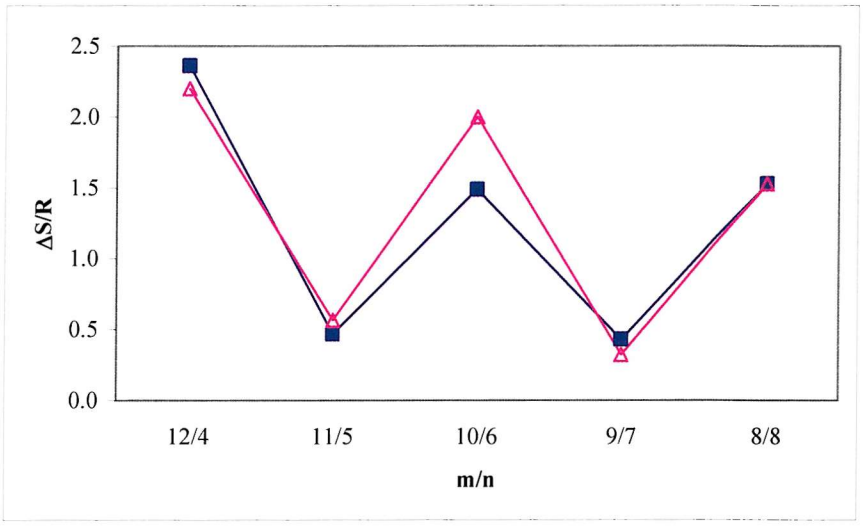

Figure 6.18 The N-I transitional entropies for Cat(OmOCB)(OnOCB) and Cat(OmOCB)$_2$ as a function of spacer length. Here, ■ denotes $\Delta S_{NI}/R$ for Cat(OmOCB)(OnOCB) and Δ denotes $\Delta S_{NI}/R$ for Cat(OmOCB)$_2$

Looking at just the non-symmetric dimers we can see that ΔS/R is very much higher for the 12/4 dimer compared to any of the others (see Figure 6.18). This is unusual as it is slightly higher than the 12/12 and, as we shall see, also larger than the 4/4. It is unclear why this compound should be better ordered in the nematic than either of the symmetric dimers. The group exhibits an odd-even alternation in ΔS/R which for m/n = 11/5 through to 8/8 the alternation remains constant which is not surprising given that the only structural change corresponds to the 1,2-dioxybenzene core being at different positions along the chain.

Theory predicts that for conventional dimers the longer the spacer the more the transitional entropy should increase (i.e. for odd members or for even). Conversely we should, therefore, expect that for the same length chain there would be no difference in the transitional entropy. This lends support for the view of there being a distinct configurational difference between the odd and even dimers we can speculate that this difference may have an impact on the orientational order. We would expect then that, within experimental error, the Cat(OmOCB)$_2$ series would steadily increase their N-I

transitional entropy with increasing spacer length whereas the non-symmetric dimers should remain the same and, with the exception of 12/4 this is the case. If we now compare the shorter chain symmetric dimers, Cat(OnOCB)$_2$ we might expect the reverse to be true. $\Delta S_{NI}/R$ for the symmetric dimers should increase with spacer length whereas that for the non-symmetric dimers should remain the same and, as seen in Figure 6.19 this is the case.

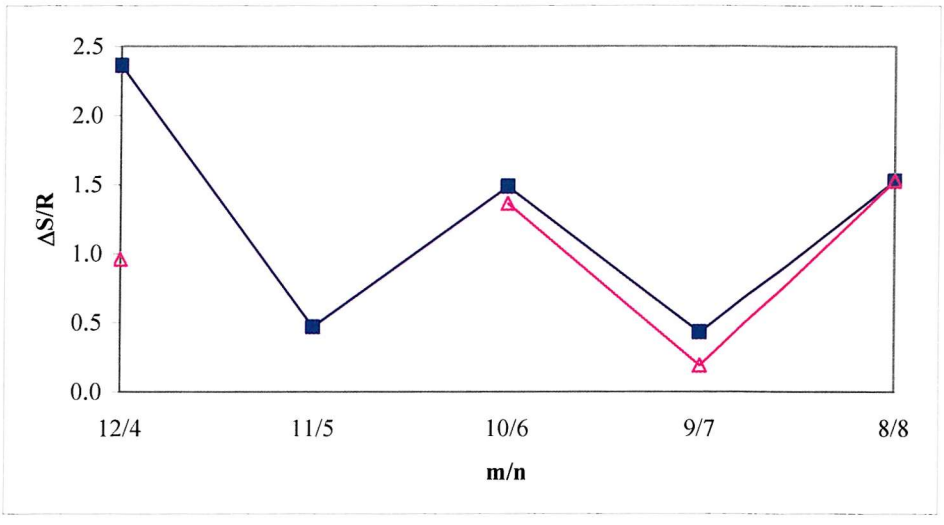

Figure 6.19 The N – I transitional entropy for Cat(OmOCB)(OnOCB) and Cat(OmOCB)$_2$ as a function of spacer length. Here, ■ denotes $\Delta S_{NI}/R$ for Cat(OmOCB)(OnOCB) and Δ denotes $\Delta S_{NI}/R$ for Cat(OmOCB)$_2$

It is interesting to note that in the case of both the m/n = 9/7 and 12/4 non-symmetric dimers have a larger entropy of transition than either of the symmetric dimers.

The entropies of transition were also determined for the mixtures of dimers and these are compared to the pure non-symmetric dimer series. The values for the transitional entropies are given below in Table 6.14. Where two melting transitions were recorded the entropy for the second melting transition is given. This was not always possible as sometimes the melting points were so close together that they gave a single broad exotherm.

m/n	$\Delta H_{Cr(m)I}$/ kJmol^{-1}	$\Delta S_{CrI}/R$	$\Delta H_{Cr(n)I}$/ kJmol^{-1}	$\Delta S_{Cr2N}/R$	ΔH_{NI}/ kJmol^{-1}	$\Delta S_{NI}/R$
12/4	38.3	12.4	25.2	7.2	2.60	0.86
11/5	27.9	8.9	15.4	4.7	1.97	0.66
10/6	31.7	11.2	None observed	None observed	1.47	0.49
9/7	39.8	12.6	None observed	None observed	3.44	1.07
8/8	50.8	15.8	None observed	None observed	4.92	1.53

Table 6.14 Transitional entropies for the equimolar mixtures Cat(OmOCB)$_2$/Cat(OnOCB)$_2$.

The most important result is that no odd-even effect is observed in the mixtures. This is surprising as we have mixtures of two even dimers or odd dimers. Based on our previous observations, we might have expected that the transitional entropy would show some odd-even behaviour as the ordering of each of the individual components shows such an alternation as can be seen in Figure 6.19.

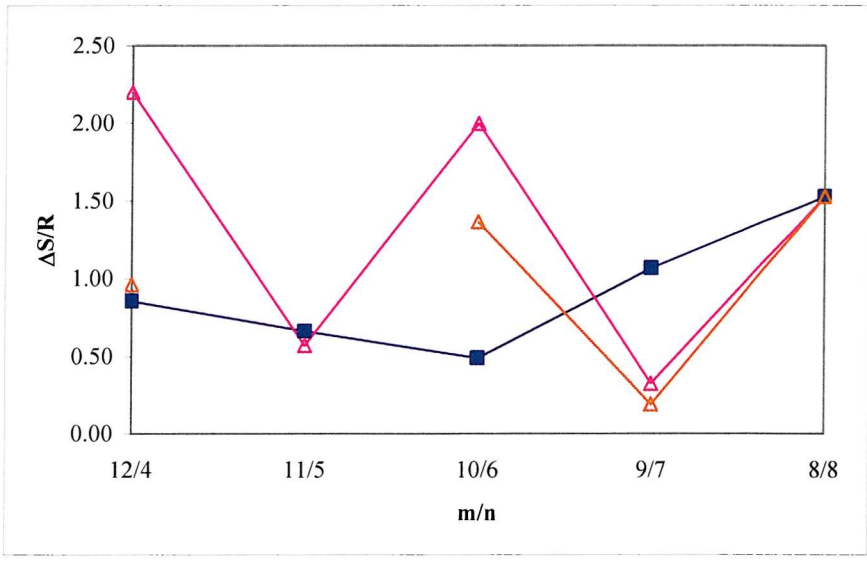

Figure 6.20 The N-I transitional entropy for the equimolar mixture of Cat(OmOCB)$_2$/Cat(OnOCB)$_2$, Cat(OmOCB)$_2$ and Cat(OnOCB)$_2$ as a function of spacer length. Here ■ denotes $\Delta S_{NI}/R$ for the mixture, Δ denotes $\Delta S_{NI}/R$ for Cat(OmOCB)$_2$ and Δ denotes $\Delta S_{NI}/R$ for Cat(OnOCB)$_2$.

Comparing the mixtures with the pure analogues we see that there appears to be very little correlation between the values for $\Delta S_{NI}/R^{pure}$ and $\Delta S_{NI}/R^{mix}$ except for m/n = 11/5. Comparing these mixtures to the pure non-symmetric 1,2-dioxybenzene dimers we see that there is again little correlation between them (see Figure 6.21).

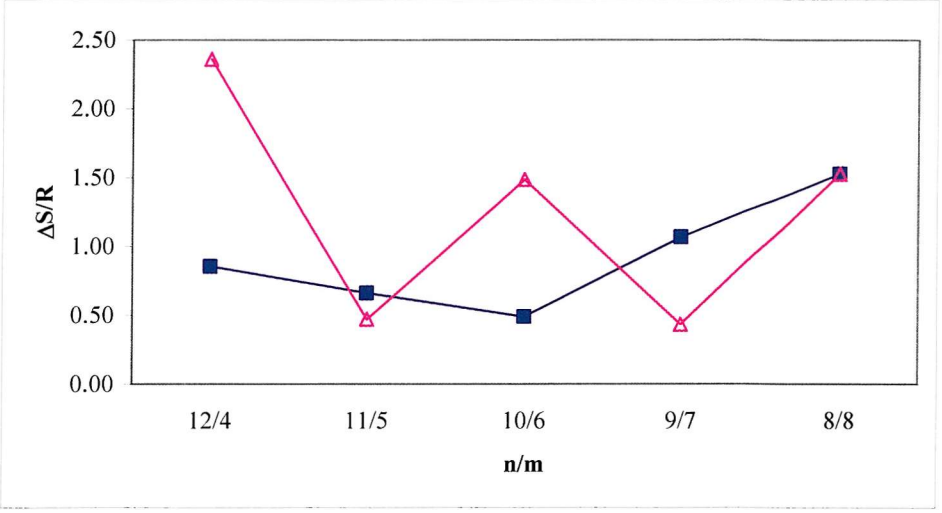

Figure 6.21 The N-I transitional entropy for the equimolar mixture of Cat(OmOCB)$_2$/Cat(OnOCB)$_2$, and Cat(OmOCB)(OnOCB) as a function of spacer length. Here ■ denotes $\Delta S_{NI}/R$ for the mixture, Δ denotes $\Delta S_{NI}/R$ for Cat(OmOCB)(OnOCB).

Finally, we give a brief examination of how the entropy of transition alters with changes in the proportion of the two dimer constituents. Using the most extreme case (namely, m/n = 12/4) where the difference in melting points and N-I transition for the two components is greatest, we have prepared binary mixtures ranging from pure m = 12 to pure n = 4 in 25% increments. The data is given in Table 6.15.

12/4	ΔH_{NI}/ kJmol^{-1}	$\Delta S_{Cr1N}/R$	ΔH_{NI}/ kJmol^{-1}	$\Delta S_{Cr2N}/R$	ΔH_{NI}/ kJmol^{-1}	$\Delta S_{NI}/R$
100/0	88.4	27.7	N/A	N/A	3.29	2.20
75/25	57.0	18.5	6.96	2.07	2.60	0.80
50/50	38.3	12.4	25.2	7.2	2.60	0.86
25/75	20.0	6.5	54.1	14.9	2.58	0.80
0/100	54.2	14.5	N/A	N/A	6.97	0.96

Table 6.15 Transitional entropy for Cat(O12OCB)$_2$/Cat(O4OCB)$_2$ at various compositions.

The data shows that the addition of a small amount of the Cat(O4OCB)$_2$ to Cat(O12OCB)$_2$ has a dramatic effect, but adding further amounts of the short chain dimer makes little change. It would clearly be interesting to investigate the change in $\Delta S_{NI}/R$ on adding increasingly smaller amounts of Cat(O4OCB)$_2$.

We can see the massive decrease in $\Delta S_{NI}/R$ for 100/0 to 25/75 in Figure 6.23. Any subsequent variation in transitional entropy falls within experimental error (taken to be 10%) shown by the error bars in the Figure.

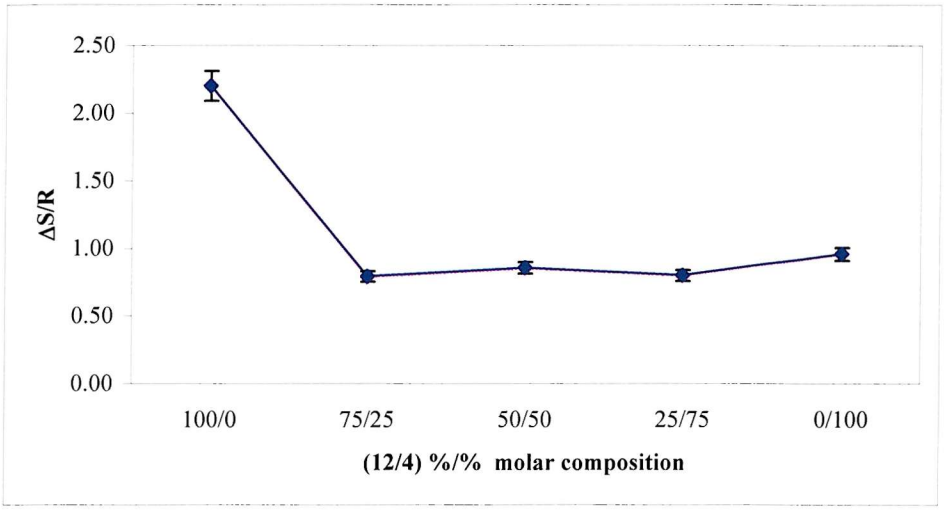

Figure 6.22 Composition dependence of the transitional entropy for $Cat(O12OCB)_2$/$Cat(O4OCB)_2$ with changing composition. The composition is measured as %mol/%mol of 12 and 4 dimers. Error bars show a 10% error in the data normally assumed for DSC measurements.

Theory predicts that for an ideal binary mixture of A and B, where the difference in T_{NI} for the two components is quite large, as the mole fraction of B increased there would be a sharp drop in transitional entropy for N – I transition followed by a steady increase to the value of $\Delta S_{NI}/R$ for pure B.[11] This is for an ideal system and from looking at the T_{NI} (see Figure 6.23) we can see that the mixtures are not behaving ideally in that the pure $Cat(O12OCB)_2$ $\Delta S_{NI}/R$ drops sharply when 25% of $Cat(O4OCB)_2$ is added and then steadily climbs in a linear fashion (as expected).

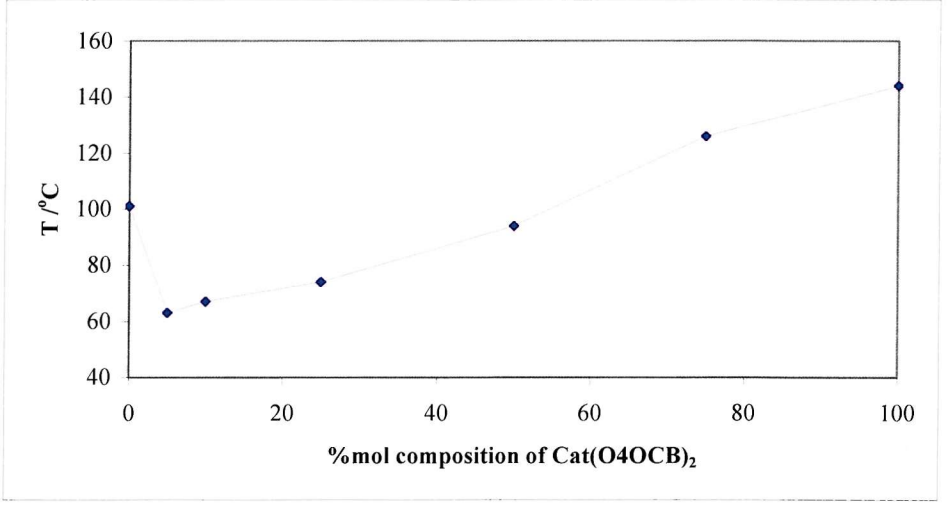

Figure 6.23 T_{NI} transitions in °C for mixtures of $Cat(O12OCB)_2$ and $Cat(O4OCB)_2$ plotted as a function of concentration of the n = 4 dimer.

6.5 Analyzing the physical data for Cat(OnOCB)(OnOBF2)

6.5.1 Optical Microscopy

The optical textures were measured for these materials to determine their phase behaviour and determine the transition temperatures (see Figure 6.24). The materials were set up in much the same way as described in previous chapters, that is the solid was placed on a cover slip, melted and another cover slip placed on top to produce a thin film. This was then studied on a microscope and viewed between crossed polarisers.

These materials were also very easily supercooled and remained in the liquid state after pressure was applied to the slides as described previously. All the samples showed typical nematic textures which were very small and only properly seen under high magnification. In all other respects these samples behaved identically to the Cat(OmOCB)(OnOCB) series.

Figure 6.24 All optical texture pictures were taken on cooling, showing nematic phases Cat(O4OCB)(O4OBF$_2$) taken at 57 °C, 0.92T$_{NI}$ (top left); Cat(O6OCB)(O6OBF$_2$) taken at 35 °C, 0.88T$_{NI}$ (top right); Cat(O8OCB)(O8OBF$_2$) taken at 41 °C, 0.90T$_{NI}$ (middle left); Cat(O9OCB)(O9OBF$_2$) taken at 25 °C, 0.97T$_{NI}$ (middle right); Cat(O10OCB)(O10OBF$_2$) taken at 25 °C, 0.87T$_{NI}$; (bottom left); Cat(O11OCB)(O11OBF$_2$) taken at 25 °C, 0.91T$_{NI}$ (bottom right).

6.5.2 Phase behaviour

This section deals with the phase behaviour of 1,2-dioxybenzene dimers which have the same spacer length but different mesogenic groups. As mentioned previously, the knowledge of the nematic stability of the $CBOnOBF_2$ series and the $Cat(OnOCB)_2$ series suggests that these compounds will be monotropic and this is indeed the case. In a couple of cases (n = 5 and 7) the temperature range of the microscope hotstage limits assignment of sub-room temperature liquid crystal transitions.

n	Cr		N		I	Crystallises
4	•	158	•	(85)	•	<25
5	•	86			•	<25
6	•	106	•	(78)	•	<25
7	•	46			•	<25
8	•	101	•	(74)	•	<25
9	•	56	•	(34)	•	~25
10	•	86	•	(71)	•	47
11	•	65	•	(53)	•	<25

Table 6.16 Transition temperature in °C for $Cat(OnOCB)(OnOBF_2)$. '<25 °C' indicates samples which supercooled to room temperature (taken to be 25 °C) and remained in the nematic phase for several hours.

As with Table 6.6, Table 6.16 also shows the temperatures of crystallisation. Most of the materials supercool to room temperature remaining in the nematic phase for several hours in spite of mechanical stress applied to the cover slips. These materials have been cooled below room temperature in DSC experiments but, as shall be described later, the materials tended to form a nematic glass (again with the exception of n = 5 and 7) rather than crystallising. Crystallisation did occur in these samples at room temperature when left overnight.

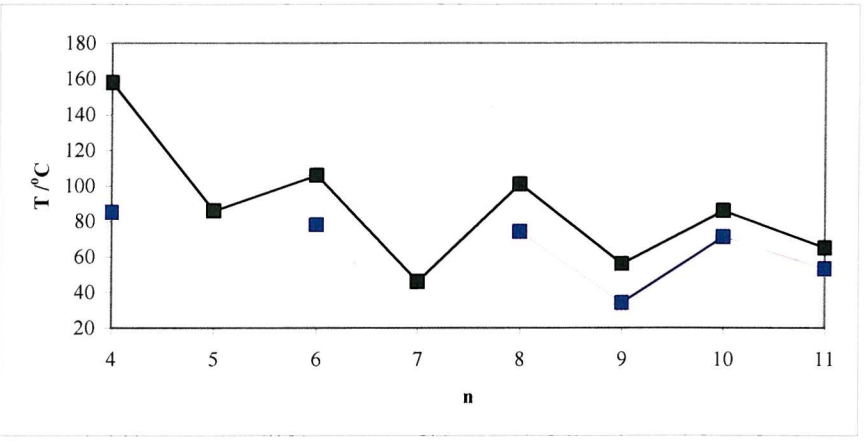

Figure 6.25 The transition temperatures for $Cat(OnOCB)(OnOBF_2)$. Here ■ denotes T_{CrI} and ■ denotes T_{NI}.

Analysis of the data shown in Figure 6.25 shows that, as expected, all of the materials are monotropic and that an odd-even effect is seen in both the nematic-isotropic transition temperatures and the melting points.

No N-I transition was observed for n = 5 and 7 in spite of supercooling the material to below -15 °C in a DSC experiment where it formed an isotropic glass. The remaining compounds show low N – I and melting transitions as expected. The large supercooling range, lower melting points and stability of the monotropic nematic phase at low temperatures makes these materials the best of the monotropic candidates with this structural architecture for investigations of their flexoelectric behaviour.

6.5.2.1 Comparing these results with the symmetric dimers [Cat(OnOCB)2] and the non-symmetric dimers CBOnOBF2

Given the nature of these materials the two series most appropriate for comparison would be the Cat(OnOCB)$_2$ series reported in Chapter 5 and the CBOnOBF$_2$ synthesised by Coles *et al.*[12] Starting with the Cat(OnOCB)$_2$ series we can see in Figure 6.28 that the Cat(OnOCB)(OnOBF$_2$) series behaves fairly similarly.

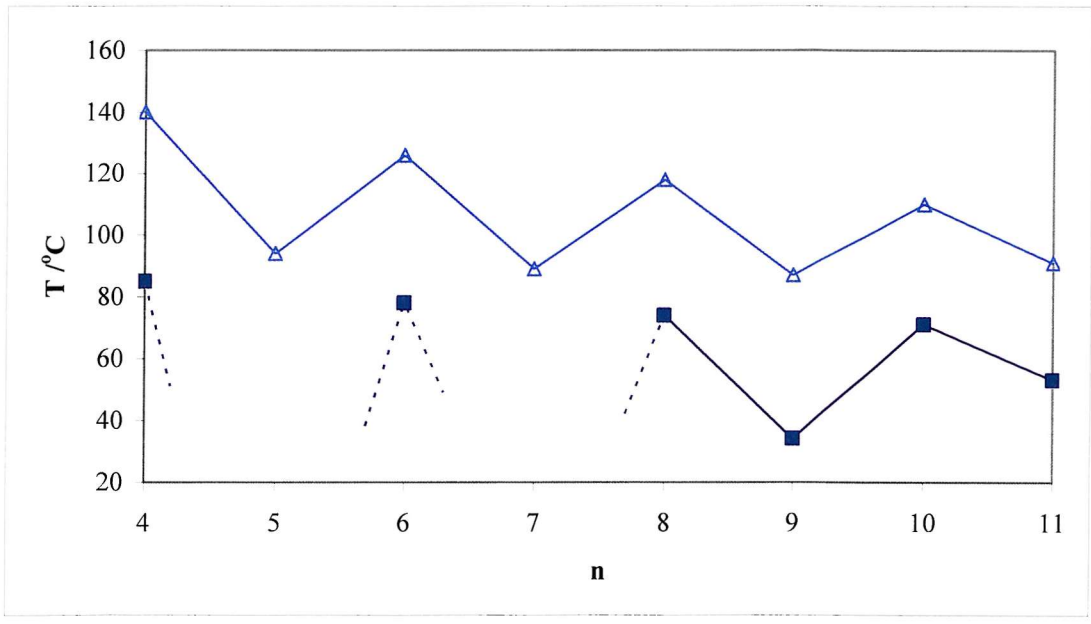

Figure 6.26 The spacer length dependence of T_{NI} for symmetric and non-symmetric 1,2-dioxybenzene dimers. Here Δ denotes T_{NI} Cat(OnOCB)$_2$ and ■ denotes T_{NI} Cat(OnOCB)(OnOBF$_2$).

Both series show an odd-even effect in the N-I transition temperatures which is to be expected since the structure of the materials is very similar. We can expect the materials to behave in a similar manner and can perhaps infer that they have similar geometric environments in the liquid crystal phase. The alternation in T_{NI} for the non-symmetric series is larger than for the Cat(OnOCB)$_2$. This observation is also true comparing the CBOnOCB series with CBOnOBF$_2$ and is likely to be due to the same reason. That is that the mesogenicity of the -OBF$_2$ moiety is smaller than that of the -OCB group and as such is considerably less supportive of the nematic phase for odd members where the geometry of the molecule is less favourable (i.e. less linear).

Commenting on trends in the odd members of the series is difficult as we have no transition data for n = 5 and 7, however we do know the N – I transition temperatures for these members lie below -15 °C. We can, therefore, deduce that the T_{NI} for the odd members increases with increasing chain length compared to the Cat(OnOCB)$_2$ series, a similar comparison again has been made between CBOnOCB and CBOnOBF$_2$. The even members appear to show very little change in T_{NI} as the spacer length increases giving only a 14 °C drop across the series from n = 4 to n = 10 compared to the Cat(OnOCB)$_2$ series which shows a 30 °C drop over the same spacer range.

6.5.3 Entropy of transition

In Chapter 5 (Section 5.3.3) we describe the problem of small transitional entropies which have a long tail section which, depending on whether the area of this tail was included in the measurement when calculating $\Delta S_{NI}/R$ can significantly change the reported result. This problem was also present in these compounds and the same protocol described in Chapter 5 is also adopted here.

	ΔH_{CrI}/ kJmol^{-1}	$\Delta S_{CrN}/R$	ΔH_{NI}/ kJmol^{-1}	$\Delta S_{NI}/R$
4	47.7	14.8	3.67	1.2
5	48.6	16.3	N/A	N/A
6	60.0	19.7	3.23	1.1
7	45.6	17.2	N/A	N/A
8	70.9	22.9	3.54	1.2
9	54.0	20.0	0.97	0.4
10	72.9	24.7	4.23	1.5
11	53.1	19.3	2.10	0.8

Table 6.17 Table of transitional entropies for the Cat(OnOCB)(OnOBF$_2$) series

The entropy changes for the non-symmetric Cat(OnOCB)($OnOBF_2$) for the Cr-I and N-I transitions are given in Table 6.17. We can see that there is an alternation from the odd to even dimers and we might expect this to be very similar to that for the transitions seen for the Cat(OnOCB)$_2$ series and certainly in terms of the trend this is the case (see Figure 6.27).

The absence of values for the transitional entropies for n = 5 and 7 presents a problem when trying to determine trends in the series. Plotting the variation of these values for $\Delta S_{NI}/R$ against the spacer lengths for Cat(OnOCB)$_2$ we can see that the alternation for the symmetric dimers is larger than for the non-symmetric homologues. The transitional entropy for even members of the Cat(OnOCB)($OnOBF_2$) series only start to increase for n > 8 and even then more gradually than that found for the Cat(OnOCB)$_2$ (see Figure 6.27).

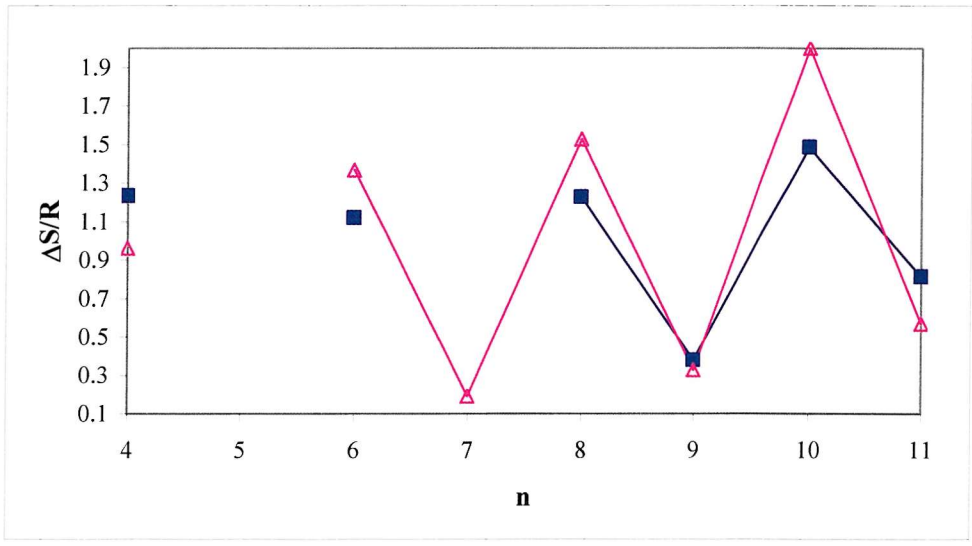

Figure 6.27 Transitional entropies as a function of spacer length for Cat(OnOCB)($OnOBF_2$) and Cat(OnOCB)$_2$ where ■ represents $\Delta S_{NI}/R$ for Cat(OnOCB)($OnOBF_2$) and Δ represents $\Delta S_{NI}/R$ for Cat(OnOCB)$_2$.

The transitional entropies for both series alternate as a function of spacer length and both series show a tendency for $\Delta S_{NI}/R$ to increase with increasing n. This behaviour is in line with the expected behaviour shown by conventional liquid crystal dimers, and, if we compare these non-symmetric kinked dimers to the CBOnOBF_2 non-symmetric conventional dimers the similarity is clearly apparent (see Figure 6.28).

The increase in $\Delta S_{NI}/R$ for the 1,2-dioxybenzene dimers is similar to that of the conventional dimers. The transitional entropy for the even members of the conventional dimer series increases more rapidly than for the kinked dimers but the alternation between odd and even is about the same. For n = 4 the transitional entropy is approximately the same which, interestingly, is also true for n = 11.

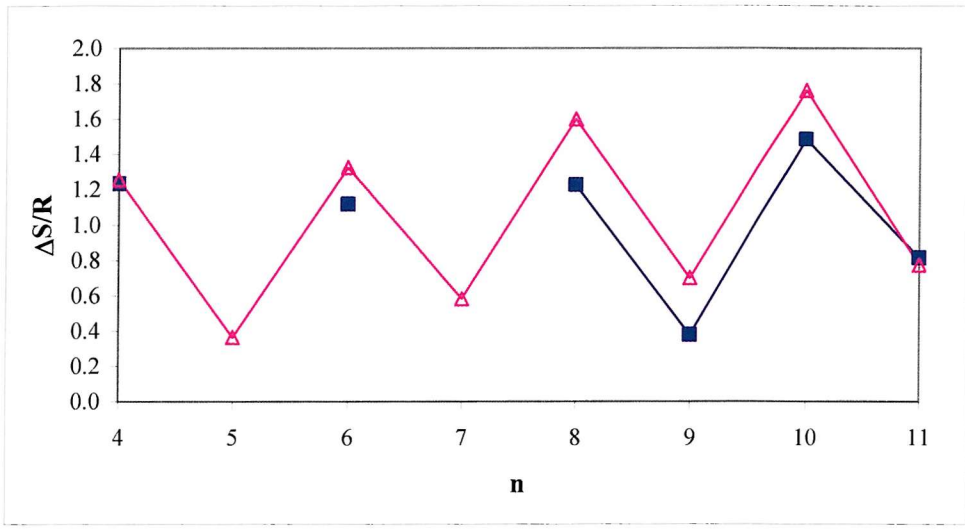

Figure 6.28 Plot of the transitional entropies as a function of spacer length for Cat(OnOCB)($OnOBF_2$) and $CBOnOBF_2$ where ■ represents $\Delta S_{NI}/R$ for Cat(OnOCB)($OnOBF_2$) and △ represents $\Delta S_{NI}/R$ for $CBOnOBF_2$.

6.6 Conclusions

Unfortunately it was not possible to attempt flexoelectric measurements for any of the members of the series discussed in this Chapter. The extent of the monotropic behaviour of these materials makes them largely unsuitable for making measurements on the pure systems. However, investigation of the transitional properties of these materials has afforded an illuminating insight to the structure and property relationship of some non-symmetric compounds which include the 1,2-dioxybenzene core in the structure.

Changing the position of the aromatic disruptor with relation to the mesogenic end groups provided interesting results where even though the total number of carbon atoms in the spacer were kept the same (n + m = 16), there was still a large odd-even effect. This implied that compounds with spacers which were of the same parity but different lengths behaved similarly. This was because there was very little difference in T_{NI}

between dimers of very different spacer length but identical parity and there was a large difference in T_{NI} for dimers with a small difference in spacer length but dissimilar parities. For example Cat(O12OCB)(O4OCB) had a similar T_{NI} to Cat(O10OCB)(O6OCB) and a very different T_{NI} to Cat(O11OCB)(O5OCB). Given the discussions of the possible role of U-shaped dimers in the liquid crystal phase, these results fit that picture well. The anisotropy of the molecule would not be affected so much by altering the length of one spacer with respect to the other compared to what extent the mesogenic groups are parallel with the long axis of the molecule (defined in this case as the line which bisects the arms and the dioxybenzene core). It follows from this that should one spacer arm be odd and the other even then T_{NI} for this molecule would lie between the T_{NI} for odd/odd and even/even (see Figure 6.29). This was demonstrated by comparing the Cat(O10OCB)(O5OCB) with the symmetric $Cat(O7OCB)_2$ and $Cat(O8OCB)_2$.

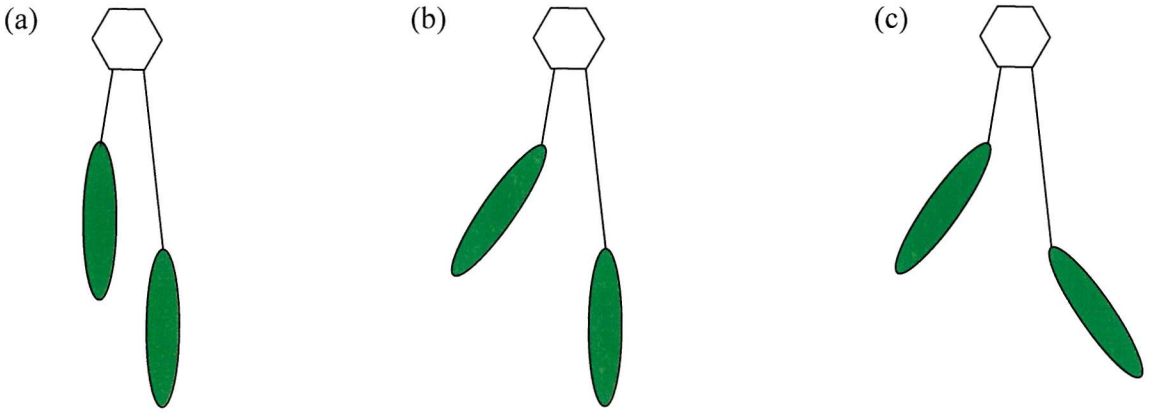

Figure 6.29 Sketch of three non-symmetric dimers showing the orientation of the mesogenic groups with respect to the molecular long axis. (a) where both spacer arms are an even parity, (b) where one spacer arm is even and the other odd and (c) where both spacer arms are odd.

Examining Figure 6.29 and Figure 6.6 we can see that in (a) where both spacer arms are an even parity the mesogenic groups are both parallel to the long axis; this would give the largest T_{NI} and corresponds with $Cat(O8OCB)_2$ in Figure 6.6. In the case of (b) where one spacer arm is even and the other odd, here the anisotropy of the molecule is slightly reduced lowering the T_{NI} slightly corresponding to Cat(O5OCB)(O10OCB) in Figure 6.6. In the case of (c) where both spacer arms are odd, now neither mesogenic group is

parallel to the long axis, reducing the anisotropy further and decreasing T_{NI} more, corresponding to Cat(O7OCB)$_2$.

Comparing the symmetric Cat(OnOCB)$_2$ dimers the non-symmetric dimers showed that in most cases the melting and N – I transitions for the non-symmetric dimer tended to be closer to the symmetric analogue of the longer arm. For example Cat(O11OCB)(O5OCB) had transition temperatures which were closer to Cat(O11OCB)$_2$ than Cat(O5OCB)$_2$. Again using the U-shaped conformer, we can speculate that the close proximity of the short chain mesogenic group to the longer chain would restrict its movement to some extent. This is, of course, not true for the longer chain mesogenic group and thus the molecule is, in the conformational distribution more easily able to behave like the long spacer arm symmetric dimer rather than the short spacer arm dimer. The transitional entropies of the symmetric and non-symmetric dimers are generally similar and follow similar trends. Again the longer spacer arm symmetric dimers tend to be closer comparators to the non-symmetric analogues than the short spacer arms dimers.

Equimolar mixtures of the symmetric dimers containing spacer lengths comparable to pure non-symmetric systems showed N –I transition temperatures very similar to the non-symmetric dimers in all cases but one. The Cat(O12OCB)$_2$/Cat(O4OCB)$_2$ dimer mixture showed a significant decrease in the T_{NI} compared to the analogous non-symmetric dimer. This curious behaviour is not easily explained but could be related to the shape of the molecules being so different that the interactions in the mixture are significantly different to the other mixtures examined in this Chapter.

Curiously the transitional entropy for the mixtures was very different showing no odd-even effect, contrasting greatly with the non-symmetric dimer analogues. Investigating the ordering of the mixtures and the non-symmetric analogue in the nematic phase would be of great interest here. Contrasting the 4/12 mixture and the 11/5 mixture with the pure non-symmetric analogues would be expected to reveal much greater agreement for the latter than the former according to the transitional entropy data (see Figure 6.23).

Investigation of the Cat(OnOCB)(OnOBF$_2$) again showed an odd-even trend in the T_{NI} and the transitional entropies. Given the transition temperatures for the Cat(OnOCB)$_2$ series and the CBOnOBF$_2$ series it was not surprising that this molecular conglomerate series was entirely monotropic. The low melting member of this series could make

potentially good additives for lowering the overall melting point in a mixture whilst still providing the bent shape which could support a director deformation. It is curious that neither n = 5 or 7 show any nematic phase even for temperatures as low as -15 °C. Extrapolation of n = 9 and 11 would predict a N – I transition at ~15 °C and ~-3 °C for n = 7 and 5 respectively.

This Chapter has explored a small number of what is a huge array of potential materials. By altering the relative position of the 1,2-dioxybenzene group in comparison with mesogenic groups we have gathered more information and insight into understanding why the liquid crystal behaviour of these compounds behaves in this way; particularly in terms of the odd-even effect in the T_{NI}. We have also demonstrated that it is possible to tether dissimilar mesogenic groups to the same catechol unit and that these materials too can produce liquid crystal phases albeit monotropic nematics. There is a great deal of scope for further investigation, looking at other mesogenic groups (for example studying ether linked Schiff-base compounds allowing a direct comparison to the work already done[13]). Similarly the core group itself could be altered using, for example, a phthalic acid group producing ester linked materials. Preliminary investigations into these types of compounds have shown that symmetric odd and even cyanobiphenyl dimers are indeed nematogenic.

6.7 References

1. G. S. Attard, R. W. Date, C. T. Imrie, G. R. Luckhurst, S. J. Roskilly, J. M.; Seddon, L. Taylor, *Liq. Cryst.*, **1994**, 16, 529.
2. J. W. Emsley, G. R. Luckhurst, G. N. Shilstone, I. Sage, *Mol. Cryst. Liq. Cryst.*, **1984**, 102, 223.
3. R. W. Date, C. T. Imrie, G. R. Luckhurst, J. M. Seddon, *Liq. Cryst.*, **1992**, 12, 203.
4. F. H. Boardman. Ph.D. Thesis. University of Southampton, 2001.
5. S. Perkins. Ph.D. University of Southampton, 1999.
6. J. B. Orton. Ph.D. Thesis. University of Southampton, 2006.
7. R. P. Sear, G. Jackson,, *Mol. Phys.*, **1994**, 82, 473.
8. J. V. Crivello, M. Deptolla, H. Ringsdorf, *Liq. Cryst.*, **1988**, 3, 235.

9. A. Yoshizawa, H. Kinbara, T. Narumi, A. Yamaguchi, *Liq. Cryst.*, **2005**, 32, 1175.
10. S. Jin, G. Cheng, G. Z. Chen, Z. Ji, *J. Porphyrins and Phthalocyanines*, **2005**, 9, 32.
11. A. Kloczkowski, G. R. Luckhurst, *J. Chem. Soc., Faraday Trans. 2,* , **1988**, 84, 155.
12. S. M. Morris, M. J. Clarke, A. E. Blatch, H. J. Coles, *Phys. Rev. E*, **2007**, 75, 041701.
13. G. S. Attard, A. G. Douglass, *Liq. Cryst.*, **1997**, 22, 349.

Chapter 7

Experimental

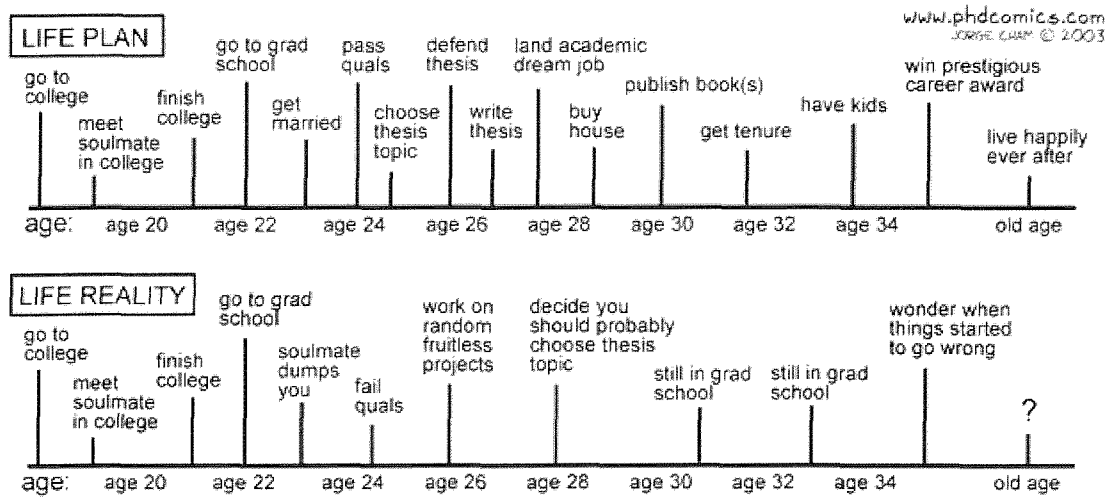

"Piled Higher and Deeper" by Jorge Cham
www.phdcomics.com Used with permission

7. Experimental

The Chapter is divided into five sections. The first (Section 7.1) consists of a general experimental that covers the standard techniques and conditions assumed in Section 7.2 and details of the apparatus used in the physical measurements made throughout the project. Section 7.2 outlines the experimental detail and characterization for each homologous series of compounds studied. Where materials are not novel, literature references are given and any significant differences from the literature data are highlighted. Given that the preparative procedure for each series is largely the same, the procedure for each series is given once using one example from that series. Where more than one method has been attempted, the optimum method is reported. Below each procedure is reported the characterization data for that entire homologous series of compounds. The numbering of the carbon skeleton in each diagram has been designed to assign a different number to a unique carbon NMR environment. Symmetrically related carbons are assigned the same number. Proton and fluorine atoms are assigned via the carbon to which they are attached e.g. the carbon in a cyano group on a cyanobiphenyl is assigned the number 1 and as such all carbon spectra reporting a C_1 will always report a quaternary CN group at approximately the same chemical shift.

Preceding the experimental procedure for each series is a table of the transition temperatures for that series. In each row the number corresponding to the Cr-SmA, Cr-N or Cr-I transition corresponds to the melting point and as such is not repeated in characterization data. In all cases n refers to the number of methylene groups in the carbon chain.

7.1. General Experimental

7.1.1. Organic chemical characterisation information

Where stated, reactions that were carried out under anhydrous conditions were performed in dried glassware under an atmosphere of dry nitrogen. Acetone was distilled over potassium carbonate. Acetonitrile was distilled over calcium hydride. Dimethylformamide (DMF) was distilled over calcium sulphate under vacuum (~0.4mbar). THF was distilled over benzophenone and sodium wire.

TLC were carried out using Merck Kieselgel silica gel 60 F_{254}, visualised by UV illumination (shortwave $\lambda = 254$ nm) and by staining with iodine absorbed on silica, ceric ammonium phosphomoybdic acid and/or basic potassium permanganate solution. Column chromatography was carried out using Fisher 35-70 chromatography grade silica. Column dimensions refer to width x depth of silica.

Infrared spectra were recorded on a Nicolet Impact 400 spectrometer. Spectra were taken either from a liquid placed on sodium chloride plates or as a solid using a 'Goldengate' attachment. Absorptions are described as strong (s), medium (m), weak (w), or broad (brd).

Melting points were recorded on the microscopy/heating stage apparatus detailed in Section 7.1.1. They are reported in the transition temperature table which preceeds each homologous series. The melting point is taken as the crystal-liquid crystal or crystal to isotropic transition (i.e. the number immediately after the Cr column).

^{1}H, ^{19}F and ^{13}C NMR spectra were recorded as solutions in a deuterated solvent (normally $CDCl_3$). Those proton, fluorine or carbon spectra reported at 300, 282 and 75 MHz respectively were run either on a Bruker AC300 or a Bruker AV300 spectrometer. Those proton or carbon spectra reported at 400 or 100 MHz respectively were obtained on a Bruker DPX400 instrument. Chemical shifts are reported using the δ scale using an internal reference (typically $CDCl_3$ is used for proton and carbon spectra run in $CDCl_3$; C_6F_6 is used as a reference for fluorine spectra). Proton spectra are described using the following abbreviations; s (singlet), d (doublet), t (triplet), q (quartet), quin (quintet), br (broad), m (multiplet). The following abbreviations are used in the case of the proton decoupled carbon spectra; q (quarternary), t (methine), d (methylene), s (methyl).

Mass spectra were obtained using either the electron impact ionisation technique (EIMS) or collected by Electro-spray (ESMS). Relative intensities are reported in brackets after the *m/z* value.

7.1.2. Physical chemical characterisation data

The mesophase transitions were recorded using a Linkam TMS 90 Heating Unit, a Linkam hotstage and an Olympus BH-2 Polarising microscope. Transitions were given

on heating at 2°C/min (unless otherwise stated e.g. monotropic T_{NI} transition). Monotropic transitions are denoted by brackets. Error estimated at ±0.2°

Differential scanning calorimetry data were collected using a TA Instruments DSC Q1000, processed using software supplied with the instrument, and then outputted as an Adobe Acrobat® document.

Flexoelectricity measurments were conducted using hybrid aligned nematic cells with approximately a 5 μm^{-1} thickness between the treated plates. The experiments were conducted using an Olympus BX50 microscope which had a THORLABS PDA55 photodiode attachment was connected to a Tektronix TDS224 four channel digital real-time oscilloscope. The applied fields were produced from an HP 8111A pulse/function generator which was amplified using a TREK power amplifier (model 603) which was connected to each cell. The temperature was controlled by a Linkam TMS93 hotstage and controller.

7.2. Chapter 3 experimental

7.2.1. CBOnBr; α-(Cyanobiphenyloxy)alkyl-ω-bromide[1]

n	Temperature /°C					Mass	Yield
	Cr		N		I	g	%
4	•	90	•	61	•	6.36	90%
5	•	87	•	62	•	5.91	87%
6	•	74	•	68	•	2.84	77%
7	•	84	•	72	•	3.15	82%
8	•	85	•	65	•	3.83	97%
9	•	77	•	69	•	3.48	85%
10	•	87	•	71	•	7.31	95%
11	•	77	•	74	•	4.16	92%
12	•	97	•	79	•	4.11	91%

1-(Cyanobiphenyloxy)-butyl-4-bromide

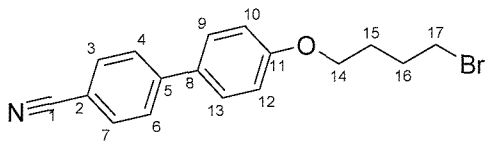

1
$C_{17}H_{16}BrNO$
330.23

Procedure

To a stirred solution of 4'-hydroxy-4-biphenylcarbonitrile (4.00 g, 27.94 mMol, 1 eq) in freshly distilled acetone (40 mL) was added solid potassium carbonate (5.10 g, 36.88 mMol, 1.8 eq) in one portion. The stirred mixture was heated to reflux for 1 h under nitrogen and subsequently allowed to cool to room temperature before 1,4-dibromobutane (24.46 mL, 44.23 g, 204.4 mMol, 10 eq) was added in a single portion. The mixture was then heated at reflux for 3 days, cooled, and was then filtered to remove the inorganic salts these were later washed with DCM. The combined filtrate and washings were then concentrated *in vacuo* to give a yellow crude oil. This was then purified by column chromatography (silica gel, 40 mm x 100 mm; 10-40% DCM / 40-60 petroleum), to give a white powder which was crystallised from ethanol affording the title compound **1** (5.91 g, 17.90 mMol, 87.4%) as a crystalline white solid.

Rf 0.29; 50% DCM / 40-60 petroleum [1 spot by TLC]

^{1}H NMR (400 MHz, $CDCl_3$): δ_H 7.61 (2H, d, J = 8.8 Hz, C_4**H,** C_6**H**), 7.56 (2H, d, J = 8.8 Hz, C_3**H**, C_7**H**), 7.45 (2H, d, 8.9 Hz, C_9**H,** C_{13}**H**), 6.91 (2H, d, J = 9.0 Hz, C_{10}**H**, C_{12}**H**), 3.98 (2H, t, 6.0 Hz, O-C_{14}**H$_2$**), 3.42 (2H, t, 6.5 Hz, C_{17}**H$_2$**Br), 1.86-2.06 (4H, m, 6.5 Hz C_{15}**H$_2$**, C_{16}**H$_2$**) ppm.

^{13}C NMR (100 MHz, $CDCl_3$): δ_C 159.5 (q, **C_{11}**(Ar)), 145.2 (q, **C_5**(Ar)), 132.6 (t, **C_3**(Ar), **C_7**(Ar)), 131.6 (q, **C_8**(Ar)), 128.4 (t, **C_4**(Ar), **C_6**(Ar)), 127.1 (t, **C_9**(Ar), **C_{13}**(Ar)), 119.1 (q, **C_1**(CN)) 115.1 (t, **C_{10}**(Ar), **C_{12}**(Ar)), 110.1 (q, **C_2**(Ar)), 67.0 (s, **C_{14}**(OCH_2)), 33.4 (s, **$C_{15\text{-}17}$**(CH_2)), 29.4 (s, **$C_{15\text{-}17}$**(CH_2)), 27.9 (s, **$C_{15\text{-}17}$**(CH_2)) ppm.

IR (Sol^n in dichloromethane) ν_{max}: 3049(s) (**C-H$_2$**Br), 2983(m) (**C-H$_2$**), 2680(w), 2226 (m) (**C≡N**), 1602(s) (**Ar**), 1493(s) (**Ar**), 1422(m), 1261(s), 731(s) (**C-Br**) cm^{-1}.

EIMS: *m/z* 329 ($[M]^+$, 11%), 195.1 ($[C_{13}H_9NO]^+$, 100%), 166 ($[C_{13}H_{10}]^+$, 5%), 135 ($[C_9H_{10}O]^+$, 79%), 55 ($[C_4H_7]^+$, 32%), 29 ($[C_2H_5]^+$, 7%).

1-(Cyanobiphenyloxy)-pentyl-5-bromide

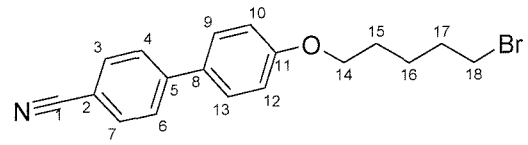

2
$C_{18}H_{18}BrNO$
344.25

Rf 0.29; 50% DCM / 40-60 petroleum [1 spot by TLC]

^{1}H NMR (400 MHz, $CDCl_3$): δ_H 7.61 (2H, d, J = 8.0 Hz, C_4**H**, C_6**H**), 7.56 (2H, d, J = 8.8 Hz, C_3**H**, C_7**H**), 7.45 (2H, d, 8.8 Hz, C_9**H**, C_{13}**H**), 6.92 (2H, d, J = 8.8 Hz, C_{10}**H**, C_{12}**H**), 3.95 (2H, t, 6.3 Hz, O-C_{14}**H_2**), 3.37 (2H, t, 6.5 Hz, C_{18}**H_2**Br), 1.81 (2H, quin, 6.5 Hz C_{15}**H_2** or C_{17}**H_2**), 1.88 (2H, quin, 7.0Hz, C_{15}**H_2** or C_{17}**H_2**), 1.43-1.65 (2H, m, C_{16}**H_2**,) ppm.

^{13}C NMR (100 MHz, $CDCl_3$): δ_C 160.1 (q, **C_{11}**(Ar)), 145.7 (q, **C_5**(Ar)), 133.0 (t, **C_3** (Ar), **C_7**(Ar)), 131.9 (q, **C_8**(Ar)), 128.8 (t, **C_4**(Ar), **C_6**(Ar)), 127.5 (t, **C_9**(Ar), **C_{13}**(Ar)), 119.5 (q, **C_1**(CN)), 115.5 (t, **C_{10}**(Ar), **C_{12}**(Ar)), 110.5 (q, **C_2**(Ar)), 68.1 (s, **C_{14}**(OCH_2)), 34.0 (s, **$C_{15\text{-}17}$**(CH_2)), 32.9 (s, **C_{18}**(CH_2Br)), 28.3 (s, **$C_{15\text{-}17}$**(CH_2)), 24.9 (s, **$C_{15\text{-}17}$**(CH_2)) ppm.

IR (Sol^n in dichloromethane) ν_{max}: 3054(s) (**C-H_2**Br), 2983(m) (**C-H_2**), 2941(w) (**C-H_2**), 2680(w), 2226(m) (**C≡N**), 1602(s) (**Ar**), 1489(s) (**Ar**), 1422 (m), 1261(s), 741(s) (**C-Br**) cm^{-1}.

EIMS: *m/z* 343 ($[M]^+$, 11%), 195 ($[C_{13}H_9NO]^+$, 100%), 151 ($[C_{10}H_{15}O]^+$, 11%), 149 ($[C_{10}H_{13}O]^+$, 11%), 69.1 ($[C_5H_9]^+$, 38%) 41 ($[C_3H_5]^+$, 17%).

1-(Cyanobiphenyloxy)-hexyl-6-bromide

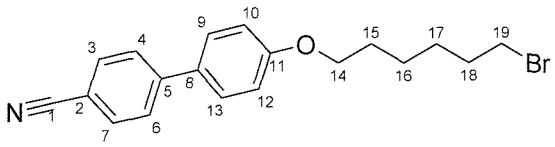

3
$C_{19}H_{20}BrNO$
358.28

Rf 0.36; 50% DCM / 40-60 petroleum [1 spot by TLC]

^{1}H NMR (400 MHz, $CDCl_3$): δ_H 7.61 (2H, d, J = 8.0 Hz, C_4**H**, C_6**H**), 7.56 (2H, d, J = 8.8 Hz, C_3**H**, C_7**H**), 7.45 (2H, d, 9.0 Hz, C_9**H**, C_{13}**H**), 6.91 (2H, d, J = 9.0 Hz,

$C_{10}\mathbf{H}$, $C_{12}\mathbf{H}$), 3.95 (2H, t, 6.5 Hz, O-$C_{14}\mathbf{H_2}$), 3.36 (2H, t, 6.8 Hz, $C_{19}\mathbf{H_2}$Br), 1.72-1.88 (4H, m, $C_{15}\mathbf{H_2}$, $C_{18}\mathbf{H_2}$), 1.40-1.51 (4H, m, $C_{16}\mathbf{H_2}C_{17}\mathbf{H_2}$) ppm.

^{13}C NMR (100 MHz, $CDCl_3$): δ_C 160.1 (q, $\mathbf{C_{11}}$(Ar)), 145.7 (q, $\mathbf{C_5}$(Ar)), 133.0 (t, $\mathbf{C_3}$ (Ar), $\mathbf{C_7}$(Ar)), 131.8 (q, $\mathbf{C_8}$(Ar)), 128.8 (t, $\mathbf{C_4}$(Ar), $\mathbf{C_6}$(Ar)), 127.5 (t, $\mathbf{C_9}$(Ar), $\mathbf{C_{13}}$(Ar)), 119.5 (q, $\mathbf{C_1}$(CN)) 115.5 (t, $\mathbf{C_{10}}$(Ar), $\mathbf{C_{12}}$(Ar)), 110.5 (q, $\mathbf{C_2}$(Ar)), 68.3 (s, $\mathbf{C_{14}}$(OCH_2)), 34.2 (s, $\mathbf{C_{15\text{-}18}}$($CH_2$)), 33.1 (s, $\mathbf{C_{19}}$ (CH_2Br)), 29.5 (s, $\mathbf{C_{15\text{-}18}}$($CH_2$)), 28.3 (s, $\mathbf{C_{15\text{-}18}}$($CH_2$)), 25.7 (s, $\mathbf{C_{15\text{-}18}}$($CH_2$)) ppm.

IR (Sol^n in dichloromethane) ν_{max}: 3049(s) (**C-H$_2$**Br), 2988(m) (**C-H$_2$**), 2680(w), 2302(m), 2222(w) (**C≡N**), 1602(m) (**Ar**), 1493(m) (**Ar**), 1422 (s), 1261(s), 736(s) (**C-Br**) cm^{-1}.

EIMS: *m/z* 357 ($[M]^+$, 22%), 195 ($[C_{13}H_9NO]^+$, 100%), 166 ($[C_{13}H_8]^+$, 13%), 140 ($[C_9H_{16}O]^+$, 10%), 83 ($[C_6H_{11}]^+$, 38%), 55 ($[C_4H_7]^+$, 19%), 41 ($[C_3H_5]^+$, 12%).

1-(Cyanobiphenyloxy)-heptyl-7-bromide

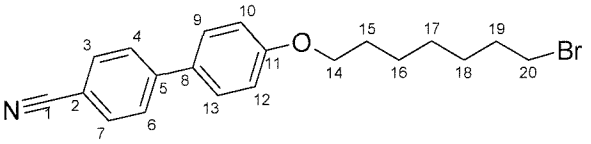

4
$C_{20}H_{22}BrNO$
372.31

Rf 0.37; 50% DCM / 40-60 petroleum

^{1}H NMR (400 MHz, $CDCl_3$): δ_H 7.61 (2H, d, J = 8.0 Hz, $C_4\mathbf{H}$,$C_6\mathbf{H}$), 7.56 (2H, d, J = 9.0 Hz, $C_3\mathbf{H}$, $C_7\mathbf{H}$), 7.45 (2H, d, 9.0 Hz, $C_9\mathbf{H}$, $C_{13}\mathbf{H}$), 6.91 (2H, d, J = 9.0 Hz, $C_{10}\mathbf{H}$, $C_{12}\mathbf{H}$), 3.93 (2H, t, 6.5 Hz, O-$C_{14}\mathbf{H_2}$), 3.34 (2H, t, 7.0 Hz, $C_{20}\mathbf{H_2}$Br), 1.72-1.91 (4H, m, $C_{15}\mathbf{H_2}$,$C_{19}\mathbf{H_2}$), 1.31-1.55 (6H, m, $C_{16}\mathbf{H_2}$, $C_{17}\mathbf{H_2}$, $C_{18}\mathbf{H_2}$) ppm.

^{13}C NMR (100 MHz, $CDCl_3$): δ_C 160.3 (q, $\mathbf{C_{11}}$(Ar)), 145.8 (q, $\mathbf{C_5}$(Ar)), 133.1 (t, $\mathbf{C_3}$, $\mathbf{C_7}$(Ar)), 131.9(q, $\mathbf{C_8}$(Ar)), 128.9 (t, $\mathbf{C_4}$(Ar), $\mathbf{C_6}$(Ar)), 127.6 (t, $\mathbf{C_9}$(Ar), $\mathbf{C_{13}}$(Ar)), 119.6 (q, $\mathbf{C_1}$(CN)) 115.6 (t, $\mathbf{C_{10}}$(Ar), $\mathbf{C_{12}}$(Ar)), 110.6 (q, $\mathbf{C_2}$(Ar)), 68.6 (s, $\mathbf{C_{14}}$(OCH_2)), 34.4 (s, $\mathbf{C_{15\text{-}19}}$($CH_2$)), 32.2 (s, $\mathbf{C_{20}}$(CH_2Br)), 29.6 (s, $\mathbf{C_{15\text{-}19}}$($CH_2$)), 29.0 (s, $\mathbf{C_{15\text{-}19}}$($CH_2$)), 28.6 (s, $\mathbf{C_{15\text{-}19}}$($CH_2$)), 26.4 (s, $\mathbf{C_{15\text{-}19}}$($CH_2$)) ppm.

IR (Solid) ν_{max}: 3049(s) (**C-H$_2$Br**), 2983(m) (**C-H$_2$**), 2931(w) (**C-H$_2$**), 2685 (w), 2222(w) (**C≡N**), 1602(m) (**Ar**), 1493(m), 1261(s), 740(s) (**C-Br**) cm^{-1}.

EIMS: *m/z* 371 ([M]$^+$, 17%), 195 ([$C_{13}H_9NO$]$^+$, 100%), 55 ([C_4H_7]$^+$, 8%)

1-(Cyanobiphenyloxy)-octyl-8-bromide

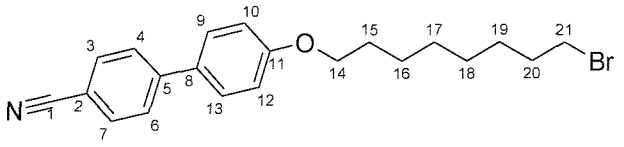

5
C$_{21}$H$_{24}$BrNO
386.34

Rf 0.37; 50% DCM / 40-60 petroleum [1 spot by TLC]

^{1}H NMR (400 MHz, $CDCl_3$): δ_H 7.62 (2H, d, J = 8.0 Hz, C_4**H**, C_6**H**), 7.56 (2H, d, J = 8.5 Hz, C_3**H**, C_7**H**), 7.45 (2H, d, 9.0 Hz, C_9**H**, C_{13}**H**), 6.92 (2H, d, J = 8.5 Hz, C_{10}**H**, C_{12}**H**), 3.94 (2H, t, 6.5 Hz, O-C_{14}**H$_2$**), 3.34 (2H, t, 6.5 Hz, C_{21}**H$_2$**Br), 1.70-1.84 (4H, m, C_{15}**H$_2$**,C_{20}**H$_2$**), 1.21-1.52 (8H, m, C_{16}**H$_2$**, C_{17}**H$_2$**, C_{18}**H$_2$**, C_{19}**H$_2$**) ppm.

^{13}C NMR (100 MHz, $CDCl_3$): δ_C 160.2 (q, **C$_{11}$**(Ar)), 145.7 (q, **C$_5$**(Ar)), 133.0 (t, **C$_3$**, **C$_7$**(Ar)), 131.7 (q, **C$_8$**(Ar)), 128.7 (t, **C$_4$**(Ar), **C$_6$**(Ar)), 127.5 (t, **C$_9$**(Ar), **C$_{13}$**(Ar)), 119.5 (q, **C$_1$**(CN)) 115.5 (t, **C$_{10}$**(Ar), **C$_{12}$**(Ar)), 110.5 (q, **C$_2$**(Ar)), 68.5 (s, **C$_{14}$**(OCH_2)), 34.4 (s, **C$_{15\text{-}20}$**(CH_2)), 33.1 (s, **C$_{21}$**(CH_2Br)), 31.3 (s, **C$_{15\text{-}20}$**(CH_2)), 29.6 (s, **C$_{15\text{-}20}$**(CH_2)), 29.1 (s, **C$_{15\text{-}20}$**(CH_2)), 28.4 (s, **C$_{15\text{-}20}$**(CH_2)), 26.4 (s, **C$_{15\text{-}20}$**(CH_2)) ppm.

IR (Solid) ν_{max}: 3049(s) (**C-H$_2$Br**), 2987(m) (**C-H$_2$**), 2302(m) (**C≡N**), 1602(m) (**Ar**), 1488(m) (**Ar**), 1261(s), 741(s) (C-Br) cm^{-1}.

EIMS: *m/z* 385 ([M]$^+$, 17%), 195 ([$C_{13}H_9NO$]$^+$, 100%), 69 ([C_5H_9]$^+$, 5%), 41 ([C_3H_5]$^+$, 4%)

1-(Cyanobiphenyloxy)-nonyl-9-bromide

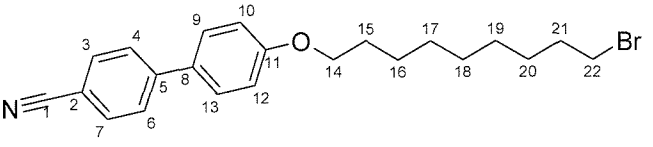

6
C$_{22}$H$_{26}$BrNO
400.36

Rf 0.41; 50% DCM / 40-60 petroleum [1 spot by TLC]

^{1}H NMR (400 MHz, $CDCl_3$): δ_H 7.62 (2H, d, J = 8.5 Hz, C_4**H**, C_6**H**), 7.56 (2H, d, J = 8.5 Hz, C_3**H**, C_7**H**), 7.45 (2H, d, 9.0 Hz, C_9**H**, C_{13}**H**), 6.92 (2H, d, J = 9.0 Hz, C_{10}**H**, C_{12}**H**), 3.94 (2H, t, 6.5 Hz, O-C_{14}**H$_2$**), 3.34 (2H, t, 6.5 Hz, C_{22}**H$_2$**Br), 1.69-1.83 (4H, m, C_{15}**H$_2$**, C_{21}**H$_2$**), 1.20-1.61 (10H, m, C_{16}**H$_2$**, C_{17}**H$_2$**, C_{18}**H$_2$**, C_{19}**H$_2$**, C_{20}**H$_2$**) ppm.

^{13}C NMR (100 MHz, $CDCl_3$): δ_C 160.2 (q, **C_{11}**(Ar)), 145.7 (q, **C_5**(Ar)), 133.0 (t, **C_3**, **C_7**(Ar)), 131.7 (q, **C_8**(Ar)), 128.7 (t, **C_4**(Ar), **C_6**(Ar)), 127.5 (t, **C_9**(Ar), **C_{13}**(Ar)), 119.5 (q, **C_1**(CN)) 115.5 (t, **C_{10}**(Ar), **C_{12}**(Ar)), 110.5 (q, **C_2**(Ar)), 68.5 (s, **C_{14}**(OCH_2)), 34.4 (s, **$C_{15\text{-}21}$**(CH_2)), 33.2 (s, **C_{22}**(CH_2Br)), 29.7 (s, **$C_{15\text{-}21}$**(CH_2)), 29.7 (s, **$C_{15\text{-}21}$**(CH_2)), 29.6 (s, **$C_{15\text{-}21}$**(CH_2)), 29.1 (s, **$C_{15\text{-}21}$**(CH_2)), 28.5 (s, **$C_{15\text{-}21}$**(CH_2)), 26.4 (s, **$C_{15\text{-}21}$**(CH_2)) ppm.

IR (Solid) ν_{max}: 3054(s) (**C-H$_2$**Br), 2983(m) (**C-H$_2$**), 2302(m) (**C≡N**), 1607(m) (**Ar**), 1417(m), 1261(s), 722(s) (**C-Br**) cm^{-1}.

EIMS: *m/z* 399 ($[M]^+$, 38%), 195 ($[C_{13}H_9NO]^+$, 100%), 166 ($[C_{13}H_{10}]^+$, 6%), 55 ($[C_4H_7]^+$, 6%), 41 ($[C_3H_5]^+$, 6%)

1-(Cyanobiphenyloxy)-decyl-10-bromide

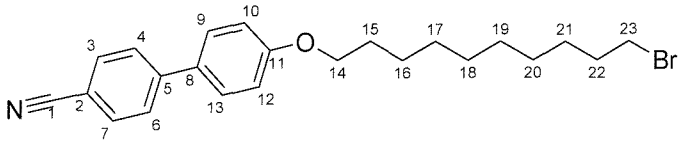

7
$C_{23}H_{28}$rNO
414.39

Rf 0.36; 50% DCM / 40-60 petroleum [1 spot by TLC]

^{1}H NMR (300 MHz, $CDCl_3$): δ_H 7.71 (2H, d, J = 8.0 Hz, C_4**H**, C_6**H**), 7.65 (2H, d, J = 8.4 Hz, C_3**H**, C_7**H**), 7.54 (2H, d, 8.8 Hz, C_9**H**, C_{13}**H**), 7.01 (2H, d, J = 8.8 Hz, C_{10}**H**, C_{12}**H**), 4.02 (2H, t, 6.5 Hz, O-C_{14}**H$_2$**), 3.43 (2H, t, 6.8 Hz, C_{23}**H$_2$**Br), 1.72-2.03 (4H, m, C_{15}**H$_2$**, C_{22}**H$_2$**), 1.28-1.53 (12H, m, C_{16}**H$_2$**C_{21}**H$_2$**) ppm.

^{13}C NMR (75 MHz, $CDCl_3$): δ_C 159.9 (q, **C_{11}**(Ar)), 145.4 (q, **C_5**(Ar)), 132.7 (t, **C_3**(Ar), **C_7**(Ar)), 131.4 (q, **C_8**(Ar)), 128.5 (t, **C_4**(Ar), **C_6**(Ar)), 127.2 (t, **C_9**(Ar), **C_{13}**(Ar)), 119.3 (q, **C_1**(CN)) 115.2 (t, **C_{10}**(Ar), **C_{12}**(Ar)), 110.2 (q, **C_2**(Ar)), 68.3 (s, **C_{14}**(OCH_2)), 34.3 (s, **$C_{15\text{-}22}$**(CH_2)), 33.0 (s, **C_{23}**(CH_2Br)), 29.6 (s, **$C_{15\text{-}22}$**(CH_2)), 29.5 (s, **$C_{15\text{-}22}$**(CH_2)), 29.4 (s, **$C_{15\text{-}22}$**(CH_2)), 28.9 (s, **$C_{15\text{-}22}$**(CH_2)), 26.2 (s, **$C_{15\text{-}22}$**(CH_2)), ppm.

IR (Sol^{n} in dichloromethane) ν_{max}: 2931(m) (**C-H$_2$**), 2855(w) (**C-H$_2$**), 2245(m) , 2222(w) (**C≡N**), 1602(m) (**Ar**), 1488(m) (**Ar**), 1247 (m), 1176(m), 897(s), 732(s) (**C-Br**) cm^{-1}.

EIMS: *m/z* 413 ([M]$^+$, 20%), 195 ([$C_{13}H_9NO$]$^+$, 100%).

1-(Cyanobiphenyloxy)-undecyl-11-bromide 8

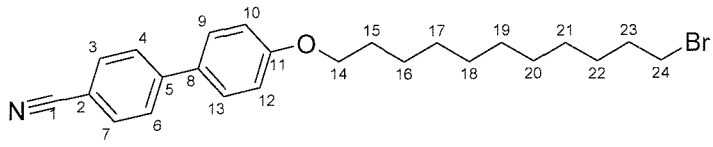

8
$C_{24}H_{30}BrNO$
428.42

Rf 0.29; 50% DCM / 40-60 petroleum [1 spot by TLC]

^{1}H NMR (400 MHz, $CDCl_3$): δ_H 7.62 (2H, d, J = 8.3 Hz, C_4**H**, C_6**H**), 7.56 (2H, d, J = 8.8 Hz, C_3**H**, C_7**H**), 7.45 (2H, d, 8.5 Hz, C_9**H**, C_{13}**H**), 6.92 (2H, d, J = 8.5 Hz, C_{10}**H**, C_{12}**H**), 3.93 (2H, t, 6.5 Hz, O-C_{14}**H$_2$**), 3.34 (2H, t, 6.8 Hz, C_{24}**H$_2$**Br), 1.67-1.83 (4H, m, C_{15}**H$_2$**, C_{23}**H$_2$**), 1.18-1.47 (14H, m, C_{16}**H$_2$**, C_{17}**H$_2$**, C_{18}**H$_2$**, C_{19}**H$_2$**, C_{20}**H$_2$**, C_{21}**H$_2$**, C_{22}**H$_2$**,) ppm.

^{13}C NMR (100 MHz, $CDCl_3$): δ_C 160.2 (q, **C$_{11}$**(Ar)), 145.7 (q, **C$_5$**(Ar)), 134.0 (t, **C$_3$** (Ar), **C$_7$**(Ar)), 131.7 (q, **C$_8$**(Ar)), 128.7 (t, **C$_4$**(Ar), **C$_6$**(Ar)), 127.5 (t, **C$_9$**(Ar), **C$_{13}$**(Ar)), 119.5 (q, **C$_1$**(CN)), 115.5 (t, **C$_{10}$**(Ar), **C$_{12}$**(Ar)), 110.5 (q, **C$_2$**(Ar)), 68.6 (s, **C$_{14}$**(OCH_2)), 34.4 (s, **C$_{15\text{-}23}$**(CH_2)), 33.2 (s, **C$_{24}$**(CH_2Br)), 29.9 (s, **C$_{15\text{-}23}$**(CH_2)), 29.8 (s, **C$_{15\text{-}23}$**(CH_2)), 29.6 (s, **C$_{15\text{-}23}$**(CH_2)), 29.2 (s, **C$_{15\text{-}23}$**(CH_2)), 28.6 (s, **C$_{15\text{-}23}$**(CH_2)), 26.4 (s, **C$_{15\text{-}23}$**(CH_2)) ppm.

IR (Solid) ν_{max}: 3054(s) (**C-H$_2$**Br), 2983(m) (**C-H$_2$**), 2965 (w) (**C-H$_2$**), 2680(w) 2226(m) (**C≡N**), 1602(s) (**Ar**), 1489(s) (**Ar**), 1422 (m), 1261(s), 740(s) (**C-Br**) cm^{-1}.

EIMS: *m/z* 429 ([M]$^+$, 25%), 195 ([$C_{13}H_9NO$]$^+$, 100%), 55 ([C_4H_7]$^+$, 6%)

1-(Cyanobiphenyloxy)-dodecyl-12-bromide

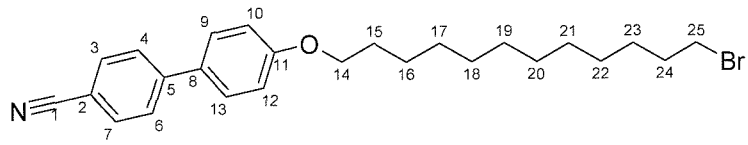

9
$C_{25}H_{32}BrNO$
442.44

Rf 0.29; 50% DCM/40-60 petroleum [1 spot by TLC]

^{1}H NMR (300 MHz, $CDCl_3$): δ_H 7.71 (2H, d, J = 8.3 Hz, C_4**H**, C_6**H**), 7.64 (2H, d, J = 8.6 Hz, C_3**H**, C_7**H**), 7.59 (2H, d, 8.8 Hz, C_9**H**, C_{13}**H**), 6.95 (2H, d, J = 8.8 Hz, C_{10}**H**, C_{12}**H**), 4.02 (2H, t, 6.5 Hz, O-C_{14}**H$_2$**), 3.42 (2H, t, 6.8 Hz, C_{25}**H$_2$**Br), 1.76-1.87 (4H, m, C_{15}**H$_2$**, C_{24}**H$_2$**), 1.25-1.53 (16H, m, C_{16}**H$_2$**, C_{17}**H$_2$**, C_{18}**H$_2$**, C_{19}**H$_2$**, C_{20}**H$_2$**, C_{21}**H$_2$**, C_{22}**H$_2$**, C_{23}**H$_2$**) ppm.

^{13}C NMR (75 MHz, $CDCl_3$): δ_C 160.0 (q, **C$_{11}$**(Ar)), 145.7 (q, **C$_5$**(Ar)), 132.7 (t, **C$_3$** (Ar), **C$_7$**(Ar)), 131.4 (q, **C$_8$**(Ar)), 128.5 (t, **C$_4$**(Ar), **C$_6$**(Ar)), 127.2 (t, **C$_9$**(Ar), **C$_{13}$**(Ar)), 119.8 (q, **C$_1$**(CN)), 115.2 (t, **C$_{10}$**(Ar), **C$_{12}$**(Ar)), 110.2 (q, **C$_2$**(Ar)), 68.3 (s, **C$_{14}$**(OCH_2)), 34.2 (s, **C$_{15\text{-}24}$**(CH_2)), 33.0 (s, **C$_{25}$**(CH_2Br)), 29.7 (s, **C$_{15\text{-}24}$**(CH_2)), 29.6 (s, **C$_{15\text{-}24}$**(CH_2)), 29.5 (s, **C$_{15\text{-}24}$**(CH_2)), 29.4 (s, **C$_{15\text{-}24}$**(CH_2)), 28.9 (s, **C$_{15\text{-}24}$**(CH_2)), 28.3 (s, **C$_{15\text{-}24}$**(CH_2)), 26.2 (s, **C$_{15\text{-}24}$**(CH_2)) ppm.

IR (Solid) ν_{max}: 3054(s) (**C-H$_2$**Br), 2988(s) (**C-H$_2$**), 2686(w), 2519(w), 2411(m), 2226(m) (**C≡N**), 1602(s) (**Ar**), 1489(s) (**Ar**), 1422 (m), 1261(s), 741(s) (**C-Br**) cm^{-1}.

EIMS: *m/z* 443 ($[M]^+$, 25%), 195 ($[C_{13}H_9NO]^+$, 100%), 84 ($[C_6H_{12}]^+$, 11%), 49 ($[C_7H_{14}]^{2+}$, 11%)

7.2.2. CBOnOBF$_2$ α -(4'-cyanobiphenyl-4-oxy-)-ω-(3,4'-difluorbiphenyl-4-oxy-)-alkane

n	Temperature /°C					Mass	Yield
	Cr		N		I	mg	%
4	•	137	•	177	•	212	45%
5	•	92	•	95	•	351	74%
6	•	129	•	160	•	326	67%
7	•	93	•	111	•	201	40%
8	•	123	•	146	•	381	74%
9	•	71	•	111	•	2184	85%
10	•	111	•	132	•	2520	96%
11	•	72	•	111	•	198	68%

1 -(4'-Cyanobiphenyl-4-oxy-)-4-(3,4'-difluorobiphenyl-4-oxy-)-butane

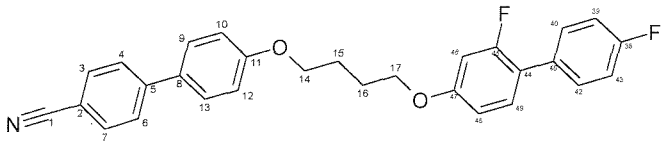

10
$C_{29}H_{23}F_2NO_2$
455.51

To a stirred solution of 2,4'-difluorobiphen-4-ol (227 mg, 1.10 mmol, 1.1 eq) in dry butanone (40 mL) was added potassium carbonate (300mg, 2.15 mmol, 2.15 eq) in one portion and the suspension was heated to reflux for approximately 20 min under nitrogen. The mixture was allowed to cool prior to the addition of 1-(cyanobiphenyloxy)-butyl-4-bromide (330 mg, 1 mmol, 1 eq) in one portion and a catalytic quantity of sodium iodide (80 mg). The reaction mixture was then heated back to reflux for 3 days, cooled and the solvents were removed *in vacuo*. The off-white solid was then partitioned between DCM (50 mL) and water (50 mL). The organic layers were separated and the aqueous layer was washed with DCM (3 x 50 mL). The organic extracts were combined and dried over anhydrous magnesium sulphate. This was then removed by filtration and the filtrate solvent was removed *in vacuo* leaving a white crude product which was purified by column chromatography (silica gel, 40 mm x 70 mm; 50-100% DCM / 40-60 petroleum) to yield **10** the title product as a white microcrystalline solid.

Rf 0.66; 100% DCM [1 spot by TLC]

^{1}H NMR (300 MHz, $CDCl_3$): δ_H 7.62 (2H, d, J = 8.6 Hz, C_4**H**,C_6**H**), 7.56 (2H, d, J = 8.6 Hz, C_3**H**, C_7**H**), 7.46 (2H, d, 8.8 Hz, C_9**H**, C_{13}**H**), 7.34-7.42 (2H, m, C_{40}**H**, C_{42}**H**), 7.22 (1H, t, J = 8.8 Hz, C_{49}**H**), 7.03 (2H, t, J = 8.8 Hz, C_{39}**H**, C_{43}**H**), 6.93 (2H, d, J = 9.0 Hz, C_{10}**H**, C_{12}**H**), 6.68 (1H, dd, (J = 8.6 Hz, 2.6 Hz), C_{48}**H$_2$**), 6.62 (1H, dd, (J = 12.6 Hz, 2.6 Hz), C_{46}**H$_2$**), 4.03 (2H, t, 5.5 Hz, O-C_{14}**H$_2$**), 4.00 (2H, t, 5.2 Hz, O-C_{17}**H$_2$**), 1.89-2.02 (4H, m, C_{15}**H$_2$**, C_{16}**H$_2$**) ppm.

^{13}C NMR (75 MHz, $CDCl_3$): δ_C 163.8 (q, **C_{45}**-F(Ar)), 161.9 (q, **C_{38}**-F(Ar)), 159.6 (q, **C_{11}**(Ar)), 158.4 (q, **C_{47}**(Ar)), 145.2 (q, **C_5**(Ar)), 132.6 (t, **C_3** (Ar), **C_7**(Ar)), 131.5 (q, **C_8**(Ar)), 130.9 (q, **C_{44}**(Ar)), 130.8 (t, **C_{40}**/**C_{42}**(Ar)), 130.4 (t, **C_{40}**/**C_{42}**(Ar)), 128.4 (t, **C_4**(Ar), **C_6**(Ar)), 127.1 (t, **C_9**(Ar), **C_{13}**(Ar)), 119.1 (q, **C_1**(CN)), 115.5 (t, **C_{46}**/**C_{48}**(Ar)), 115.2 (t, **C_{46}**/**C_{48}**(Ar)), 115.1 (t, **C_{10}**(Ar),

C_{12}(Ar)), 110.8 (t, C_{49}(Ar)), 110.1 (q, C_2(Ar)), 102.7 (t, C_{43}/C_{39}(Ar)), 102.3 (t, C_{43}/C_{39}(Ar)) 67.9 (s, C_{14}(OCH_2)), 67.3 (s, C_{17}(OCH_2)), 25.9 (s, $C_{15\text{-}16}$(CH_2)), 25.8 (s, $C_{15\text{-}16}$(CH_2)) ppm.

Note: No Peak found for C_{41}(Ar) Expected around δ_C = 120.4 ppm Signal too weak

IR (Solid) ν_{max}: 2946(m) (**C-H$_2$**), 2868(m) (**C-H$_2$**), 2217 (m) (**C≡N**), 1601(s) (**Ar**), 1568(s) (**Ar**), 1493(s) (**Ar**)

EIMS: *m/z* 455 ($[M]^+$, 23%), 250 ($[C_{18}H_{18}O]^+$, 100%), 208 ($[C_{15}H_{13}O]^+$, 100%), 140 ($[C_8H_9FO]^+$, 6%), 55 ($[C_4H_7]^+$, 11%)

Elemental Analysis: $C_{29}H_{23}F_2NO_2$: (Expected) **C** 76.40, **H** 5.05, **N** 3.07; (Found) **C** 76.22, **H** 5.05, **N** 3.10

1 -(4'-Cyanobiphenyl-4-oxy-)-5-(3,4'-difluorobiphenyl-4-oxy-)-pentane

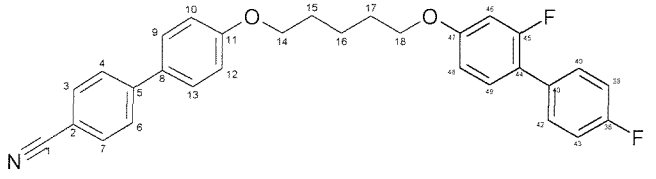

11
$C_{30}H_{25}F_2NO_2$
469.54

Rf 0.67; 100% DCM

^{1}H NMR (300 MHz, $CDCl_3$): δ_H 7.62 (2H, d, J = 8.6 Hz, C_4**H**,C_6**H**), 7.56 (2H, d, J = 8.6 Hz, C_3**H**, C_7**H**), 7.46 (2H, d, 9.0 Hz, C_9**H**, C_{13}**H**), 7.34-7.42 (2H, m, C_{40}**H,** C_{42}**H**), 7.22 (1H, t, J = 8.8 Hz, C_{49}**H**), 7.03 (2H, t, J = 8.8 Hz, C_{39}**H**, C_{43}**H**), 6.93 (2H, d, J = 9.0 Hz, C_{10}**H**, C_{12}**H**), 6.69 (1H, dd, (J = 8.6 Hz, 3.1 Hz), C_{48}**H$_2$**), 6.63 (1H, dd, (J = 12.6 Hz, 2.5 Hz), C_{46}**H$_2$**), 3.98 (2H, t, 6.2 Hz, O-C_{14}**H$_2$**), 3.95 (2H, t, 6.2 Hz, O-C_{18}**H$_2$**), 1.76-1.90 (4H, m, C_{15}**H$_2$**, C_{17}**H$_2$**) 1.55-1.71 (2H, m, C_{16}**H$_2$**) ppm.

^{13}C NMR (75 MHz, $CDCl_3$): δ_C 163.6 (q, C_{45}-F(Ar)), 161.6 (q, C_{38}-F(Ar)), 159.7 (q, C_{11}(Ar)), 158.6 (q, C_{47}(Ar)), 145.2 (q, C_5(Ar)), 132.6 (t, C_3 (Ar), C_7(Ar)), 131.4 (q, C_8(Ar)), 130.9 (q, C_{44}(Ar)), 130.4 (t, C_{40}/C_{42}(Ar)), 130.3 (t, C_{40}/C_{42}(Ar)), 128.4 (t, C_4(Ar), C_6(Ar)), 127.1 (t, C_9(Ar), C_{13}(Ar)), 119.1 (q, C_1(CN)), 115.5 (t, C_{46}/C_{48}(Ar)), 115.2 (t, C_{46}/C_{48}(Ar)), 115.1 (t, C_{10}(Ar), C_{12}(Ar)), 110.8 (t, C_{49}(Ar)), 110.1 (q, C_2(Ar)), 102.7 (t, C_{43}/C_{39}(Ar)), 102.4

(t, C_{43}/C_{39}(Ar)) 68.2 (s, $C_{14}(OCH_2)$), 67.9 (s, $C_{18}(OCH_2)$), 29.0 (s, $C_{15\text{-}17}(CH_2)$), 28.8 (s, $C_{15\text{-}17}(CH_2)$), 22.7 (s, $C_{15\text{-}17}(CH_2)$) ppm.

Note: No Peak found for C_{41}(Ar) Expected around δ_C = 120.4 ppm Signal too weak

IR (Solid) ν_{max}: 2957(m) (**C-H$_2$**), 2869(m) (**C-H$_2$**), 2223 (m) (**C≡N**), 1600(s) (**Ar**), 1566(s) (**Ar**), 1523(s) (**Ar**), 1493(s) (**Ar**) cm^{-1}.

EIMS: *m/z* 469 ($[M]^+$, 29%), 264 ($[C_{19}H_{20}O]^+$, 21%), 206 ($[C_{15}H_{11}O]^+$, 52%), 178 ($[C_{13}H_7O]^+$, 100%), 69 ($[C_5H_9]^+$, 41 ($[C_3H_5]^+$, 28%)

1 -(4'-Cyanobiphenyl-4-oxy-)-6-(3,4'-difluorobiphenyl-4-oxy-)-hexane

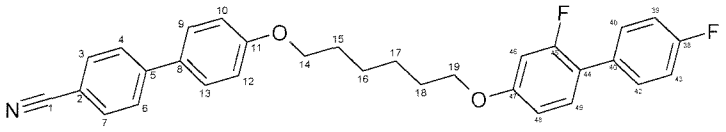

12
$C_{31}H_{27}F_2NO_2$
483.56

Rf 0.68; 100% DCM [1 spot by TLC]

^{1}H NMR (300 MHz, $CDCl_3$): δ_H 7.61 (2H, d, J = 8.6 Hz, C_4**H**,C_6**H**), 7.56 (2H, d, J = 8.6 Hz, C_3**H**, C_7**H**), 7.45 (2H, d, 8.6 Hz, C_9**H**, C_{13}**H**), 7.34-7.42 (2H, m, C_{40}**H,** C_{42}**H**), 7.21 (1H, t, J = 8.8 Hz, C_{49}**H**), 7.03 (2H, t, J = 8.8 Hz, C_{39}**H**, C_{43}**H**), 6.92 (2H, d, J = 8.8 Hz, C_{10}**H**, C_{12}**H**), 6.68 (1H, dd, (J = 8.4 Hz, 2.6 Hz), C_{48}**H$_2$**), 6.62 (1H, dd, (J = 12.6 Hz, 2.5 Hz), C_{46}**H$_2$**), 3.95 (2H, t, 6.4 Hz, O-C_{14}**H$_2$**), 3.92 (2H, t, 6.4 Hz, O-C_{19}**H$_2$**), 1.67-1.88 (4H, m, C_{15}**H$_2$**, C_{18}**H$_2$**) 1.43-1.57 (4H, m, C_{16}**H$_2$**, C_{17}**H$_2$**) ppm.

^{13}C NMR (75 MHz, $CDCl_3$): δ_C 162.6 (q, C_{45}-F(Ar)), 161.4 (q, C_{38}-F(Ar)), 159.7 (q, C_{11}(Ar)), 158.5 (q, C_{47}(Ar)), 144.2 (q, C_5(Ar)), 131.5 (t, C_3 (Ar), C_7(Ar)), 130.7 (q, C_8(Ar)), 130.3 (q, C_{44}(Ar)), 129.8 (t, C_{40}/C_{42}(Ar)), 129.4 (t, C_{40}/C_{42}(Ar)), 127.3 (t, C_4(Ar), C_6(Ar)), 126.1 (t, C_9(Ar), C_{13}(Ar)), 119.3 (q, C_{41}(Ar)), 118.1 (q, C_1(CN)), 114.4 (t, C_{46}/C_{48}(Ar)), 114.1 (t, C_{46}/C_{48}(Ar)), 114.0 (t, C_{10}(Ar), C_{12}(Ar)), 109.8 (t, C_{49}(Ar)), 109.0 (q, C_2(Ar)), 101.7 (t, C_{43}/C_{39}(Ar)), 101.3 (t, C_{43}/C_{39}(Ar)) 67.2 (s, $C_{14}(OCH_2)$), 66.9 (s, $C_{19}(OCH_2)$), 28.1 (s, $C_{15\text{-}18}(CH_2)$), 28.0 (s, $C_{15\text{-}18}(CH_2)$), 24.8 (s, $C_{15\text{-}18}(CH_2)$) ppm.

IR (Solid) ν_{max}: 2940(m) (**C-H$_2$**), 2866(m) (**C-H$_2$**), 2221 (m) (**C≡N**), 1602(s) (**Ar**), 1519(s) (**Ar**), 1493(s) (**Ar**) cm^{-1}.

EIMS: *m/z* 483 ($[M]^+$, 17%), 277 ($[C_{20}H_{22}O]^+$, 4%), 206 ($[C_{15}H_{11}O]^+$, 100%), 177 ($[C_{13}H_6O]^+$, 100%), 83 ($[C_6H_{11}]^+$, 88%), 55 ($[C_4H_7]^+$, 65%)

1 -(4'-Cyanobiphenyl-4-oxy-)-7-(3,4'-difluorobiphenyl-4-oxy-)-heptane

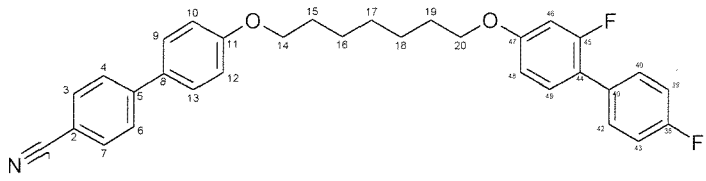

13
$C_{32}H_{29}F_2NO_2$
497.59

Rf 0.69; 100% DCM [1 spot by TLC]

^{1}H NMR (300 MHz, $CDCl_3$): δ_H 7.61 (2H, d, J = 8.6 Hz, C_4**H**,C_6**H**), 7.56 (2H, d, J = 8.6 Hz, C_3**H**, C_7**H**), 7.45 (2H, d, 8.8 Hz, C_9**H**, C_{13}**H**), 7.33-7.42 (2H, m, C_{40}**H,** C_{42}**H**), 7.21 (1H, t, J = 9.5 Hz, C_{49}**H**), 7.03 (2H, t, J = 8.7 Hz, C_{39}**H**, C_{43}**H**), 6.92 (2H, d, J = 8.8 Hz, C_{10}**H**, C_{12}**H**), 6.68 (1H, dd, (J = 8.6 Hz, 2.4 Hz), C_{48}**H$_2$**), 6.62 (1H, dd, (J = 12.6 Hz, 2.4 Hz), C_{46}**H$_2$**), 3.94 (2H, t, 6.4 Hz, O-C_{14}**H$_2$**), 3.91 (2H, t, 6.4 Hz, O-C_{20}**H$_2$**), 1.66-1.85 (4H, m, C_{15}**H$_2$**, C_{19}**H$_2$**) 1.30-1.57 (6H, m, C_{16}**H$_2$**, C_{17}**H$_2$**, C_{18}**H$_2$**) ppm.

^{13}C NMR (75 MHz, $CDCl_3$): δ_C 163.4 (q, C_{45}-F(Ar)), 161.7 (q, C_{38}-F(Ar)), 159.8 (q, C_{11}(Ar)), 157.9 (q, C_{47}(Ar)), 145.3 (q, C_5(Ar)), 132.6 (t, C_3 (Ar), C_7(Ar)), 131.3 (q, C_8(Ar)), 130.9 (q, C_{44}(Ar)), 130.9 (t, C_{40}/C_{42}(Ar)), 130.4 (t, C_{40}/C_{42}(Ar)), 128.3 (t, C_4(Ar), C_6(Ar)), 127.1 (t, C_9(Ar), C_{13}(Ar)), 120.1 (q, C_{41}(Ar)), 119.1 (q, C_1(CN)), 115.5 (t, C_{46}/C_{48}(Ar)), 115.2 (t, C_{46}/C_{48}(Ar)), 115.1 (t, C_{10}(Ar), C_{12}(Ar)), 110.8 (t, C_{49}(Ar)), 110.0 (q, C_2(Ar)), 102.7 (t, C_{43}/C_{39}(Ar)), 102.3 (t, C_{43}/C_{39}(Ar)) 68.3 (s, C_{14}(OCH_2)), 68.0 (s, C_{20}(OCH_2)), 29.1 (s, $C_{15\text{-}19}$(CH_2)), 29.1 (s, $C_{15\text{-}19}$(CH_2)), 26.0 (s, $C_{15\text{-}19}$(CH_2)) ppm.

IR (Solid) ν_{max}: 2939(m) (**C-H$_2$**), 2866(m) (**C-H$_2$**), 2219 (m) (**C≡N**), 1604(s) (**Ar**), 1518(s) (**Ar**), 1491(s) (**Ar**) cm^{-1}.

EIMS: *m/z* 497 ($[M]^+$, 32%), 219 ($[C_{16}H_{12}O]^+$, 5%), 206 ($[C_{15}H_{11}O]^+$, 100%), 151 ($[C_{12}H_7]^+$, 5%), 97 ($[C_7H_{13}]^+$, 13%), 55 ($[C_4H_7]^+$, 34%)

1 -(4'-Cyanobiphenyl-4-oxy-)-8-(3,4'-difluorobiphenyl-4-oxy-)-octane

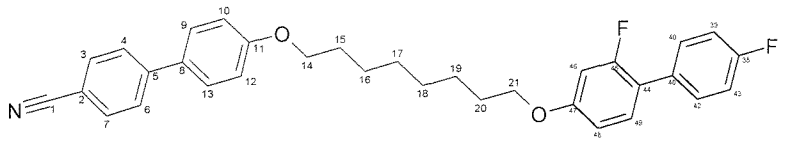

14
$C_{33}H_{31}F_2NO_2$
511.62

Rf 0.70; 100% DCM

^{1}H NMR (300 MHz, $CDCl_3$): δ_H 7.61 (2H, d, J = 8.6 Hz, C_4**H**,C_6**H**), 7.55 (2H, d, J = 8.6 Hz, C_3**H**, C_7**H**), 7.45 (2H, d, 9.0 Hz, C_9**H**, C_{13}**H**), 7.33-7.42 (2H, m, C_{40}**H,** C_{42}**H**), 7.21 (1H, t, J = 9.2 Hz, C_{49}**H**), 7.02 (2H, t, J = 8.9 Hz, C_{39}**H**, C_{43}**H**), 6.92 (2H, d, J = 8.8 Hz, C_{10}**H**, C_{12}**H**), 6.68 (1H, dd, (J = 8.6 Hz, 2.6 Hz), C_{48}**H$_2$**), 6.62 (1H, dd, (J = 12.3 Hz, 2.2 Hz), C_{46}**H$_2$**), 3.94 (2H, t, 6.4 Hz, O-C_{14}**H$_2$**), 3.90 (2H, t, 6.4 Hz, O-C_{21}**H$_2$**), 1.66-1.83 (4H, m, C_{15}**H$_2$**, C_{20}**H$_2$**) 1.27-1.50 (8H, m, C_{16}**H$_2$**, C_{17}**H$_2$**, C_{18}**H$_2$**, C_{19}**H$_2$**) ppm.

^{13}C NMR (75 MHz, $CDCl_3$): δ_C 162.2 (q, C_{45}-F(Ar)), 160.7 (q, C_{38}-F(Ar)), 158.8 (q, C_{11}(Ar)), 157.6 (q, C_{47}(Ar)), 144.3 (q, C_5(Ar)), 131.5 (t, C_3 (Ar), C_7(Ar)), 130.3 (q, C_8(Ar)), 129.8 (q, C_{44}(Ar)), 129.7 (t, C_{40}/C_{42}(Ar)), 129.4 (t, C_{40}/C_{42}(Ar)), 127.3 (t, C_4(Ar), C_6(Ar)), 126.1 (t, C_9(Ar), C_{13}(Ar)), 119.2 (q, C_{41}(Ar)), 118.1 (q, C_1(CN)), 114.5 (t, C_{46}/C_{48}(Ar)), 114.1 (t, C_{46}/C_{48}(Ar)), 114.1 (t, C_{10}(Ar), C_{12}(Ar)), 109.8 (t, C_{49}(Ar)), 109.1 (q, C_2(Ar)), 101.7 (t, C_{43}/C_{39}(Ar)), 101.3 (t, C_{43}/C_{39}(Ar)) 67.4 (s, C_{14}(OCH_2)), 67.1 (s, C_{21}(OCH_2)), 28.2 (s, $C_{15\text{-}20}$(CH_2)), 28.2 (s, $C_{15\text{-}20}$(CH_2)), 24.9 (s, $C_{15\text{-}20}$(CH_2)) ppm.

IR (Solid) ν_{max}: 2936(m) (**C-H$_2$**), 2854(m) (**C-H$_2$**), 2219 (m) (**C≡N**), 1602(s) (**Ar**), 1518(s) (**Ar**), 1492(s) (**Ar**) cm^{-1}.

EIMS: *m/z* 511 ($[M]^+$, 46%), 206 ($[C_{15}H_{11}O]^+$, 100%), 195 ($[C_{13}H_9NO]^+$, 72%), 69 ($[C_5H_9]^+$, 48%), 55 ($[C_4H_7]^+$, 28%)

1 -(4'-Cyanobiphenyl-4-oxy-)-9-(3,4'-difluorobiphenyl-4-oxy-)-nonane

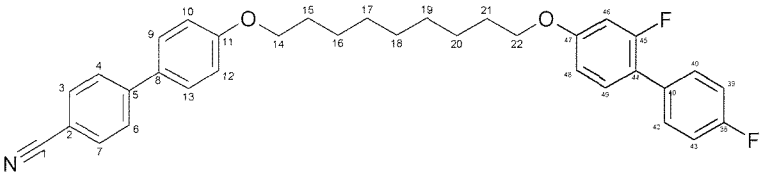

15
$C_{34}H_{33}F_2NO_2$
525.64

Rf 0.71; 100% DCM [1 spot by TLC]

^{1}H NMR (300 MHz, $CDCl_3$): δ_H 7.61 (2H, d, J = 8.6 Hz, C_4**H**,C_6**H**), 7.55 (2H, d, J = 8.6 Hz, C_3**H**, C_7**H**), 7.44 (2H, d, 9.0 Hz, C_9**H**, C_{13}**H**), 7.33-7.41 (2H, m, C_{40}**H**, C_{42}**H**), 7.21 (1H, t, J = 9.2 Hz, C_{49}**H**), 7.02 (2H, t, J = 8.8 Hz, C_{39}**H**, C_{43}**H**), 6.91 (2H, d, J = 8.8 Hz, C_{10}**H**, C_{12}**H**), 6.67 (1H, dd, (J = 8.6 Hz, 2.6 Hz), C_{48}**H**$_2$), 6.62 (1H, dd, (J = 12.3 Hz, 2.6 Hz), C_{46}**H**$_2$), 3.93 (2H, t, 6.4 Hz, O-C_{14}**H**$_2$), 3.90 (2H, t, 6.4 Hz, O-C_{22}**H**$_2$), 1.63-1.82 (4H, m, C_{15}**H**$_2$, C_{21}**H**$_2$) 1.24-1.52 (10H, m, C_{16}**H**$_2$, C_{17}**H**$_2$, C_{18}**H**$_2$, C_{19}**H**$_2$, C_{20}**H**$_2$) ppm.

^{13}C NMR (75 MHz, $CDCl_3$): δ_C 163.7 (q, **C$_{45}$**-F(Ar)), 161.9 (q, **C$_{38}$**-F(Ar)), 159.8 (q, **C$_{11}$**(Ar)), 158.5 (q, **C$_{47}$**(Ar)), 145.3 (q, **C$_5$**(Ar)), 132.6 (t, **C$_3$** (Ar), **C$_7$**(Ar)), 131.3 (q, **C$_8$**(Ar)), 130.8 (q, **C$_{44}$**(Ar)), 130.8 (t, **C$_{40}$**/**C$_{42}$**(Ar)), 130.4 (t, **C$_{40}$**/**C$_{42}$**(Ar)), 128.3 (t, **C$_4$**(Ar), **C$_6$**(Ar)), 127.1 (t, **C$_9$**(Ar), **C$_{13}$**(Ar)), 119.1 (q, **C$_{41}$**(Ar)), 119.1 (q, **C$_1$**(CN)), 115.4 (t, **C$_{46}$**/**C$_{48}$**(Ar)), 115.2 (t, **C$_{46}$**/**C$_{48}$**(Ar)), 115.1 (t, **C$_{10}$**(Ar), **C$_{12}$**(Ar)), 110.9 (t, **C$_{49}$**(Ar)), 110.7 (q, **C$_2$**(Ar)), 102.7 (t, **C$_{43}$**/**C$_{39}$**(Ar)), 102.4 (t, **C$_{43}$**/**C$_{39}$**(Ar)) 68.4 (s, **C$_{14}$**(OCH_2)), 68.2 (s, **C$_{22}$**(OCH_2)), 29.4 (s, **C$_{15\text{-}21}$**(CH_2)), 29.3 (s, **C$_{15\text{-}21}$**(CH_2)), 29.2 (s, **C$_{15\text{-}21}$**(CH_2)), 29.1 (s, **C$_{15\text{-}21}$**(CH_2)), 26.0 (s, **C$_{15\text{-}21}$**(CH_2)) ppm.

IR (Solid) ν_{max}: 2933(m) (**C-H$_2$**), 2852(m) (**C-H$_2$**), 2223 (m) (**C≡N**), 1600(s) (**Ar**), 1519(s) (**Ar**), 1492(s) (**Ar**) cm^{-1}.

EIMS: *m/z* 525 ($[M]^+$, 54%), 330 ($[C_{23}H_{24}NO]^+$, 5%), 206 ($[C_{15}H_{11}O]^+$, 100%), 195 ($[C_{13}H_9NO]^+$, 72%), 83 ($[C_6H_{11}]^+$, 48%), 69 ($[C_5H_9]^+$, 28%)

1 -(4'-Cyanobiphenyl-4-oxy-)-10-(3,4'-difluorobiphenyl-4-oxy-)-decane

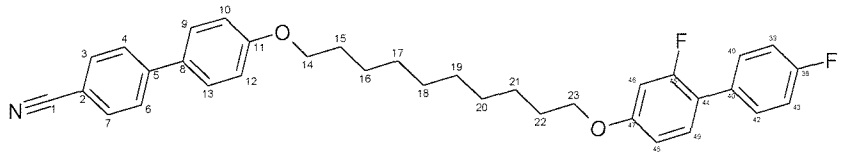

16
$C_{35}H_{35}F_2NO_2$
539.67

Rf 0.72; 100% DCM [1 spot by TLC]

^{1}H NMR (300 MHz, $CDCl_3$): δ_H 7.61 (2H, d, J = 8.6 Hz, C_4**H**,C_6**H**), 7.55 (2H, d, J = 8.8 Hz, C_3**H**, C_7**H**), 7.45 (2H, d, 9.0 Hz, C_9**H**, C_{13}**H**), 7.33-7.42 (2H, m, C_{40}**H**, C_{42}**H**), 7.21 (1H, t, J = 9.2 Hz, C_{49}**H**), 7.02 (2H, t, J = 8.8 Hz, C_{39}**H**, C_{43}**H**), 6.91 (2H, d, J = 9.0 Hz, C_{10}**H**, C_{12}**H**), 6.67 (1H, dd, (J = 8.6 Hz, 2.6

Hz), $C_{48}\mathbf{H_2}$), 6.62 (1H, dd, (J = 12.3 Hz, 2.6 Hz), $C_{46}\mathbf{H_2}$), 3.93 (2H, t, 6.4 Hz, O-$C_{14}\mathbf{H_2}$), 3.90 (2H, t, 6.4 Hz, O-$C_{23}\mathbf{H_2}$), 1.65-1.82 (4H, m, $C_{15}\mathbf{H_2}$, $C_{22}\mathbf{H_2}$) 1.17-1.51 (10H, m, $C_{16}\mathbf{H_2}$, $C_{17}\mathbf{H_2}$, $C_{18}\mathbf{H_2}$, $C_{19}\mathbf{H_2}$, $C_{20}\mathbf{H_2}$, $C_{21}\mathbf{H_2}$) ppm.

^{13}C NMR (75 MHz, $CDCl_3$): δ_C 163.6 (q, $\mathbf{C_{45}}$-F(Ar)), 161.5 (q, $\mathbf{C_{38}}$-F(Ar)), 159.8 (q, $\mathbf{C_{11}}$(Ar)), 158.5 (q, $\mathbf{C_{47}}$(Ar)), 145.3 (q, $\mathbf{C_5}$(Ar)), 132.6 (t, $\mathbf{C_3}$ (Ar), $\mathbf{C_7}$(Ar)), 131.3 (q, $\mathbf{C_8}$(Ar)), 130.8 (q, $\mathbf{C_{44}}$(Ar)), 130.8 (t, $\mathbf{C_{40}}$/$\mathbf{C_{42}}$(Ar)), 130.4 (t, $\mathbf{C_{40}}$/$\mathbf{C_{42}}$(Ar)), 128.3 (t, $\mathbf{C_4}$(Ar), $\mathbf{C_6}$(Ar)), 127.1 (t, $\mathbf{C_9}$(Ar), $\mathbf{C_{13}}$(Ar)), 120.5 (q, $\mathbf{C_{41}}$(Ar)), 119.1 (q, $\mathbf{C_1}$(CN)), 115.4 (t, $\mathbf{C_{46}}$/$\mathbf{C_{48}}$(Ar)), 115.2 (t, $\mathbf{C_{46}}$/$\mathbf{C_{48}}$(Ar)), 115.1 (t, $\mathbf{C_{10}}$(Ar), $\mathbf{C_{12}}$(Ar)), 110.9 (t, $\mathbf{C_{49}}$(Ar)), 110.1 (q, $\mathbf{C_2}$(Ar)), 102.7 (t, $\mathbf{C_{43}}$/$\mathbf{C_{39}}$(Ar)), 102.4 (t, $\mathbf{C_{43}}$/$\mathbf{C_{39}}$(Ar)) 68.4 (s, $\mathbf{C_{14}}$(OCH_2)), 68.2 (s, $\mathbf{C_{23}}$(OCH_2)), 29.5 (s, $\mathbf{C_{15\text{-}22}}$($CH_2$)), 29.3 (s, $\mathbf{C_{15\text{-}22}}$($CH_2$)), 29.2 (s, $\mathbf{C_{15\text{-}22}}$($CH_2$)), 29.1 (s, $\mathbf{C_{15\text{-}22}}$($CH_2$)), 26.0 (s, $\mathbf{C_{15\text{-}22}}$($CH_2$)) ppm.

IR (Solid) ν_{max}: 2918(m) (**C-H$_2$**), 2850(m) (**C-H$_2$**), 2232 (m) (**C≡N**), 1600(s) (**Ar**), 1518(s) (**Ar**), 1472(s) (**Ar**)

EIMS: *m/z* 539 ($[M]^+$, 46%), 344 ($[C_{22}H_{26}OF_2]^+$, 6%), 333 ($[C_{23}H_{27}NO]^+$, 7%), 206, ($[C_{15}H_{11}O]^+$, 100%), 195 ($[C_{13}H_9NO]^+$, 93%), 69 ($[C_5H_9]^+$, 48%), 55 ($[C_4H_7]^+$, 28%)

1 -(4'-Cyanobiphenyl-4-oxy-)-11-(3,4'-difluorobiphenyl-4-oxy-)-undecane

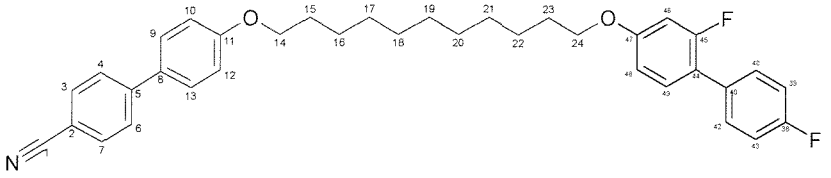

17
$C_{36}H_{37}F_2NO_2$
553.70

Rf 0.73; 100% DCM [1 spot by TLC]

^{1}H NMR (300 MHz, $CDCl_3$): δ_H 7.61 (2H, d, J = 8.6 Hz, $C_4\mathbf{H}$,$C_6\mathbf{H}$), 7.55 (2H, d, J = 8.8 Hz, $C_3\mathbf{H}$, $C_7\mathbf{H}$), 7.44 (2H, d, 8.8 Hz, $C_9\mathbf{H}$, $C_{13}\mathbf{H}$), 7.33-7.41 (2H, m, $C_{40}\mathbf{H}$, $C_{42}\mathbf{H}$), 7.21 (1H, t, J = 9.0 Hz, $C_{49}\mathbf{H}$), 7.02 (2H, t, J = 8.8 Hz, $C_{39}\mathbf{H}$, $C_{43}\mathbf{H}$), 6.91 (2H, d, J = 9.0 Hz, $C_{10}\mathbf{H}$, $C_{12}\mathbf{H}$), 6.67 (1H, dd, (J = 8.4 Hz, 3.2 Hz), $C_{48}\mathbf{H_2}$), 6.62 (1H, dd, (J = 12.3 Hz, 2.2 Hz), $C_{46}\mathbf{H_2}$), 3.93 (2H, t, 6.4 Hz, O-$C_{14}\mathbf{H_2}$), 3.89 (2H, t, 6.4 Hz, O-$C_{24}\mathbf{H_2}$), 1.55-1.82 (4H, m, $C_{15}\mathbf{H_2}$, $C_{23}\mathbf{H_2}$) 1.14-1.51 (12H, m, $C_{16}\mathbf{H_2}$, $C_{17}\mathbf{H_2}$, $C_{18}\mathbf{H_2}$, $C_{19}\mathbf{H_2}$, $C_{20}\mathbf{H_2}$, $C_{21}\mathbf{H_2}$, $C_{22}\mathbf{H_2}$) ppm.

^{13}C NMR (75 MHz, $CDCl_3$): δ_C 163.7 (q, **C_{45}**-F(Ar)), 161.8 (q, **C_{38}**-F(Ar)), 159.9 (q, **C_{11}**(Ar)), 159.9 (q, **C_{47}**(Ar)), 145.3 (q, **C_5**(Ar)), 132.6 (t, **C_3** (Ar), **C_7**(Ar)), 131.8 (q, **C_8**(Ar)), 131.3 (q, **C_{44}**(Ar)), 130.8 (t, **C_{40}**/**C_{42}**(Ar)), 130.4 (t, **C_{40}**/**C_{42}**(Ar)), 128.3 (t, **C_4**(Ar), **C_6**(Ar)), 127.1 (t, **C_9**(Ar), **C_{13}**(Ar)), 120.2 (q, **C_{41}**(Ar)), 119.1 (q, **C_1**(CN)), 115.4 (t, **C_{46}**/**C_{48}**(Ar)), 115.2 (t, **C_{46}**/**C_{48}**(Ar)), 115.1 (t, **C_{10}**(Ar), **C_{12}**(Ar)), 110.9 (t, **C_{49}**(Ar)), 110.1 (q, **C_2**(Ar)), 102.7 (t, **C_{43}**/**C_{39}**(Ar)), 102.4 (t, **C_{43}**/**C_{39}**(Ar)) 68.5 (s, **C_{14}**(OCH_2)), 68.2 (s, **C_{23}**(OCH_2)), 29.5 (s, **$C_{15\text{-}22}$**(CH_2)), 29.3 (s, **$C_{15\text{-}22}$**(CH_2)), 29.2 (s, **$C_{15\text{-}22}$**(CH_2)), 29.1 (s, **$C_{15\text{-}22}$**(CH_2)), 26.0 (s, **$C_{15\text{-}22}$**(CH_2)) ppm.

IR (Solid) ν_{max}: 2918(m) (**C-H_2**), 2849(m) (**C-H_2**), 2224 (m) (**C≡N**), 1602(s) (**Ar**), 1519(s) (**Ar**), 1492(s) (**Ar**) cm^{-1}.

EIMS: *m/z* 553 ($[M]^+$, 46%), 332 ($[C_{23}H_{26}NO]^+$, 7%), 206, ($[C_{15}H_{11}O]^+$, 100%), 195 ($[C_{13}H_9NO]^+$, 87%), 177 ($[C_{12}H_{17}O]^+$, 6%), 69 ($[C_5H_9]^+$, 14%), 55 ($[C_4H_7]^+$, 26%)

7.2.3. CBOnOBF$_3$; α -(4'-cyanobiphenyl-4-oxy-)-ω-(3',4',5'-trifluorbiphenyl-4-oxy-)-alkane

n	Temperature /°C					Mass	Yield
	Cr		N		I	g	%
4	•	126	•	144	•	498	81%
5	•	46	•	55	•	447	46%
6	•	115	•	126	•	462	69%
7	•	86	•	(73)	•	501	88%
8	•	108	•	120	•	120	21%
9	•	79	•	88	•	362	58%
10	•	123	•	(108)	•	456	76%
11	•	77	•	92	•	320	59%

1 -(4'-Cyanobiphenyl-4-oxy-)-4-(3',4',5'-trifluorobiphenyl-4-oxy-)-butane

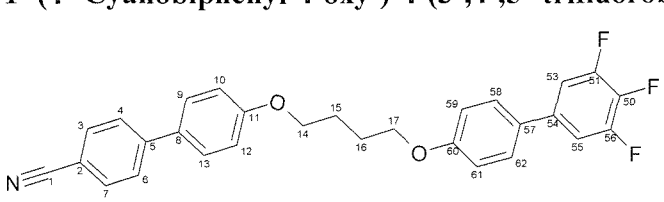

18
$C_{29}H_{24}F_3NO_2$
473.50

Proceedure:

To a stirred solution of 3',4',5'-difluorobiphenyl-4-ol (250 mg, 1.11 mmol, 1eq) in dry butan-2-one (40 mL) was added potassium carbonate (276 mg, 2.00 mmol, 1.8 eq) in one portion and the suspension was then heated to reflux for approximately 20 min under nitrogen. The mixture was allowed to cool prior to the addition of 1-(cyanobiphenyloxy)-butyl-4-bromide (414 mg, 1.11 mmol, 1 eq) in one portion and a catalytic quantity of sodium iodide (80 mg). The reaction mixture was then heated at reflux for 3 days, cooled and the solvents were removed *in vacuo*. The pale yellow solid which remained was partitioned between DCM (50 mL) and water (50 mL). The organic layer was separated and the aqueous layer was washed with further portions of DCM (3 x 50 mL). The organic extracts were combined and dried over anhydrous magnesium sulphate. This was filtered off and the solvent was then removed *in vacuo* leaving a white crude product. This was purified by column chromatography (silica gel, 40 mm x 70 mm; 1-5% ether / 40-60 petroleum) to yield **18** as a white microcrystalline solid.

Rf 0.66; 100% DCM [1 spot by TLC]

^{1}H NMR (300 MHz, $CDCl_3$): δ_H 7.62 (2H, d, J = 8.6 Hz, C_4**H**,C_6**H**), 7.56 (2H, d, J = 8.6 Hz, C_3**H**, C_7**H**), 7.46 (2H, d, J = 8.8 Hz, C_9**H**, C_{13}**H**), 7.34 (2H, d, J = 8.8 Hz, C_{62}**H**, C_{58}**H**), 7.05 (2H, dd, J = 9.1 Hz, 6.5 Hz, C_{53}**H**, C_{55}**H**), 6.93 (2H, t, J = 9.0 Hz, C_{59}**H**, C_{61}**H**), 6.89 (2H, d, J = 8.8 Hz, C_{10}**H**, C_{12}**H**), 3.93 – 4.12 (4H, m, O-C_{14}**H$_2$**, O-C_{17}**H$_2$**), 1.86-2.05 (4H, m, C_{15}**H$_2$**, C_{16}**H$_2$**) ppm.

^{13}C NMR (75 MHz, $CDCl_3$): δ_C 159.9 (q, **C_{60}**(Ar)), 159.2 (q, **C_{11}**(Ar)), 145.2 (q, **C_5**(Ar)), 136.9 (m, **C_{53}**-F(Ar), **C_{55}**-F (Ar)), 132.6 (t, **C_3** (Ar), **C_7**(Ar)), 131.5 (q, **C_8**(Ar)), 130.6 (q, **C_{57}**(Ar)), 128.4 (t, **C_4**(Ar), **C_6**(Ar)), 128.0 (t, **C_{58}**(Ar), **C_{62}**(Ar)), 127.1 (t, **C_9**(Ar), **C_{13}**(Ar)), 119.1 (q, **C_1**(CN)), 115.1 (t, **C_{59}**(Ar), **C_{61}**(Ar)), 115.0 (t, **C_{10}**(Ar), **C_{12}**(Ar)), 110.6 (q, **C_{54}**(Ar)), 110.3 (q, **C_2**(Ar)), 110.1 (q, **C_{57}**(Ar)), 67.6 (s, **C_{14}**(OCH_2)), 26.0 (s, **$C_{15,16}$**(CH_2)) ppm.

IR (Solid) ν_{max}: 2933(m) (**C-H$_2$**), 2873(m) (**C-H$_2$**), 2226 (m) (**C≡N**), 1601(s) (**Ar**), 1537(s) (**Ar**), 1507(s) (**Ar**) cm^{-1}.

EIMS: *m/z* 473 ($[M]^+$, 21%), 279 ($[C_{16}H_{14}F_3O]^+$, 7%), 208, ($[C_{15}H_{11}O]^+$, 100%), 195 ($[C_{13}H_9NO]^+$, 87%), 55 ($[C_4H_7]^+$, 26%)

Elemental Analysis: $C_{29}H_{22}F_3NO_2$: (Expected) **C** 73.50, **H** 5.07, **N** 2.96; (Found) **C** 73.51, **H** 5.07, **N** 2.96

1 -(4'-Cyanobiphenyl-4-oxy-)-5-(3',4',5'-trifluorobiphenyl-4-oxy-)-pentane

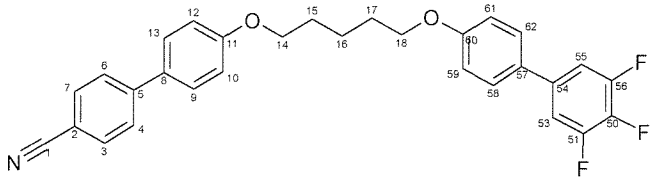

19
$C_{30}H_{26}F_3NO_2$
487.53

Rf 0.67; 100% DCM [1 spot by TLC]

^{1}H NMR (300 MHz, $CDCl_3$): δ_H 7.62 (2H, d, J = 8.6 Hz, C_4**H**,C_6**H**), 7.56 (2H, d, J = 8.6 Hz, C_3**H**, C_7**H**), 7.45 (2H, d, J = 8.8 Hz, C_9**H**, C_{13}**H**), 7.34 (2H, d, J = 8.8 Hz, C_{62}**H**, C_{58}**H**), 7.05 (2H, dd, J = 9.1 Hz, 6.5 Hz, C_{53}**H**, C_{55}**H**), 6.92 (2H, t, J = 9.0 Hz, C_{59}**H**, C_{61}**H**), 6.88 (2H, d, J = 8.8 Hz, C_{10}**H**, C_{12}**H**), 3.90 – 4.01 (4H, m, O-C_{14}**H$_2$**, O-C_{24}**H$_2$**), 1.42-1.61 (4H, m, C_{15}**H$_2$**, C_{17}**H$_2$**), 1.86-2.05 (2H, m, C_{16}**H$_2$**) ppm.

^{13}C NMR (75 MHz, $CDCl_3$): δ_C 159.7 (q, **C_{60}**(Ar)), 159.4 (q, **C_{11}**(Ar)), 145.2 (q, **C_5**(Ar)), 132.6 (t, **C_3** (Ar), **C_7**(Ar)), 131.4 (q, **C_8**(Ar)), 130.5 (q, **C_{57}**(Ar)), 128.4 (t, **C_4**(Ar), **C_6**(Ar)), 127.9 (t, **C_{58}**(Ar), **C_{62}**(Ar)), 127.1 (t, **C_9**(Ar), **C_{13}**(Ar)), 119.1 (q, **C_1**(CN)), 115.1 (t, **C_{59}**(Ar), **C_{61}**(Ar)), 115.0 (t, **C_{10}**(Ar), **C_{12}**(Ar)), 110.6 (q, **C_{54}**(Ar)), 110.3 (q, **C_2**(Ar)), 110.1 (q, **C_{57}**(Ar)), 67.6 (s, **C_{14}**(OCH_2)), 26.0 (s, **$C_{15\text{-}17}$**(CH_2)), 26.0 (s, **$C_{15\text{-}17}$**(CH_2)) ppm.

Note: No Peak found for **C_{53}**-F(Ar) and **C_{55}**-F (Ar) Expected around δ_C = 137 ppm Signal too weak

IR (Solid) ν_{max}: 2946(m) (**C-H$_2$**), 2221 (m) (**C≡N**), 1602(s) (**Ar**), 1537(s) (**Ar**), 1507(s) (**Ar**) cm^{-1}.

EIMS: **Not obtained**

1 -(4'-Cyanobiphenyl-4-oxy-)-6-(3',4',5'-trifluorobiphenyl-4-oxy-)-hexane

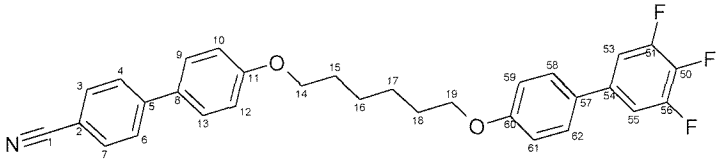

20
$C_{31}H_{28}F_3NO_2$
501.55

Rf 0.68; 100% DCM [1 spot by TLC]

^{1}H NMR (300 MHz, $CDCl_3$): δ_H 7.61 (2H, d, J = 8.6 Hz, C_4**H**,C_6**H**), 7.55 (2H, d, J = 8.6 Hz, C_3**H**, C_7**H**), 7.45 (2H, d, J = 8.8 Hz, C_9**H**, C_{13}**H**), 7.33 (2H, d, J = 8.8 Hz, C_{62}**H**, C_{58}**H**), 7.05 (2H, dd, J = 9.1 Hz, 6.4 Hz, C_{53}**H**, C_{55}**H**), 6.92 (2H, t, J = 9.0 Hz, C_{59}**H**, C_{61}**H**), 6.88 (2H, d, J = 9.0 Hz, C_{10}**H**, C_{12}**H**), 3.96 (2H, t, J = 6.4 Hz, O-C_{14}**H$_2$**), 3.94 (2H, t, J = 6.4 Hz, O-C_{19}**H$_2$**), 1.67-2.05 (4H, m, C_{15}**H$_2$**, C_{18}**H$_2$**), 1.40-1.58 (4H, m, C_{16}**H$_2$**, C_{17}**H$_2$**) ppm.

^{13}C NMR (75 MHz, $CDCl_3$): δ_C 159.8 (q, **C_{60}**(Ar)), 159.5 (q, **C_{11}**(Ar)), 145.3 (q, **C_5**(Ar)), 132.6 (t, **C_3** (Ar), **C_7**(Ar)), 131.4 (q, **C_8**(Ar)), 130.5 (q, **C_{57}**(Ar)), 128.4 (t, **C_4**(Ar), **C_6**(Ar)), 127.9 (t, **C_{58}**(Ar), **C_{62}**(Ar)), 127.1 (t, **C_9**(Ar), **C_{13}**(Ar)), 119.1 (q, **C_1**(CN)), 115.1 (t, **C_{59}**(Ar), **C_{61}**(Ar)), 115.0 (t, **C_{10}**(Ar), **C_{12}**(Ar)), 110.6 (q, **C_{54}**(Ar)), 110.3 (q, **C_2**(Ar)), 110.1 (q, **C_{57}**(Ar)), 68.0 (s, **C_{14}**(OCH_2), **C_{19}**(OCH_2)), 29.2 (s, **$C_{15\text{-}18}$**(CH_2)), 25.9 (s, **$C_{15\text{-}18}$**(CH_2)) ppm.

Note: No Peak found for **C_{53}**-F(Ar) and **C_{55}**-F (Ar) Expected around δ_C = 137 ppm Signal too weak

IR (Solid) ν_{max}: 2940(m) (**C-H$_2$**), 2962(m) (**C-H$_2$**), 2228 (m) (**C≡N**), 1600(s) (**Ar**), 1537(s) (**Ar**), 1505(s) (**Ar**) cm^{-1}.

EIMS: *m/z* 501 ($[M]^+$, 59%), 224, ($[C_{17}H_{15}O]^+$, 100%), 195 ($[C_{13}H_9NO]^+$, 87%), 55 ($[C_4H_7]^+$, 26%)

1 -(4'-Cyanobiphenyl-4-oxy-)-7-(3',4',5'-trifluorobiphenyl-4-oxy-)-heptane

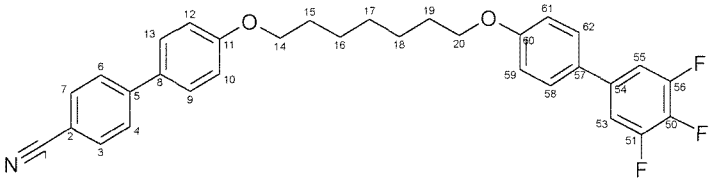

21
$C_{33}H_{30}F_3NO_2$
515.58

Rf 0.69; 100% DCM [1 spot by TLC]

^{1}H NMR (300 MHz, $CDCl_3$): δ_H 7.71 (2H, d, J = 8.6 Hz, C_4**H**,C_6**H**), 7.65 (2H, d, J = 8.7 Hz, C_3**H**, C_7**H**), 7.54 (2H, d, J = 8.6 Hz, C_9**H**, C_{13}**H**), 7.43 (2H, d, J = 8.8 Hz, C_{62}**H**, C_{58}**H**), 7.14 (2H, dd, J = 9.0 Hz, 6.6 Hz, C_{53}**H**, C_{55}**H**), 7.01 (2H, t, J = 8.8 Hz, C_{59}**H**, C_{61}**H**), 6.97 (2H, d, J = 9.0 Hz, C_{10}**H**, C_{12}**H**), 3.98 – 4.09

(2H, m, O-$C_{14}\mathbf{H_2}$, O-$C_{19}\mathbf{H_2}$), 1.69-1.99 (4H, m, $C_{15}\mathbf{H_2}$, $C_{19}\mathbf{H_2}$), 1.69-1.99 (6H, m, $C_{16}\mathbf{H_2}$, $C_{17}\mathbf{H_2}$, $C_{18}\mathbf{H_2}$) ppm.

^{13}C NMR (75 MHz, $CDCl_3$): δ_C 159.8 (q, $\mathbf{C_{60}}$(Ar)), 159.4 (q, $\mathbf{C_{11}}$(Ar)), 145.3 (q, $\mathbf{C_5}$(Ar)), 132.6 (t, $\mathbf{C_3}$ (Ar), $\mathbf{C_7}$(Ar)), 131.3 (q, $\mathbf{C_8}$(Ar)), 130.8 (q, $\mathbf{C_{57}}$(Ar)), 128.3 (t, $\mathbf{C_4}$(Ar), $\mathbf{C_6}$(Ar)), 127.9 (t, $\mathbf{C_{58}}$(Ar), $\mathbf{C_{62}}$(Ar)), 127.1 (t, $\mathbf{C_9}$(Ar), $\mathbf{C_{13}}$(Ar)), 119.1 (q, $\mathbf{C_1}$(CN)), 115.1 (t, $\mathbf{C_{59}}$(Ar), $\mathbf{C_{61}}$(Ar)), 115.0 (t, $\mathbf{C_{10}}$(Ar), $\mathbf{C_{12}}$(Ar)), 110.6 (q, $\mathbf{C_{54}}$(Ar)), 110.4 (q, $\mathbf{C_2}$(Ar)), 110.1 (q, $\mathbf{C_{57}}$(Ar)), 68.0 (s, $\mathbf{C_{14}}$(OCH_2), $\mathbf{C_{20}}$(OCH_2)), 29.2 (s, $\mathbf{C_{15\text{-}19}}$($CH_2$)), 26.2 (s, $\mathbf{C_{15\text{-}19}}$($CH_2$)), 26.0 (s, $\mathbf{C_{15\text{-}19}}$($CH_2$)) ppm.

Note: No Peak found for $\mathbf{C_{53}}$-F(Ar) and $\mathbf{C_{55}}$-F (Ar) Expected around δ_C = 137 ppm Signal too weak

IR (Solid) ν_{max}: 2938(m) (**C-H$_2$**), 2962(m) (**C-H$_2$**), 2221 (m) (**C≡N**), 1698(s) (**Ar**), 1535(s) (**Ar**), 1504(s) (**Ar**) cm^{-1}.

EIMS: *m/z* 515 ($[M]^+$, 59%), 224, ($[C_{17}H_{15}O]^+$, 100%), 195 ($[C_{13}H_9NO]^+$, 87%), 55 ($[C_4H_7]^+$, 26%)

1 -(4'-Cyanobiphenyl-4-oxy-)-8-(3',4',5'-trifluorobiphenyl-4-oxy-)-octane

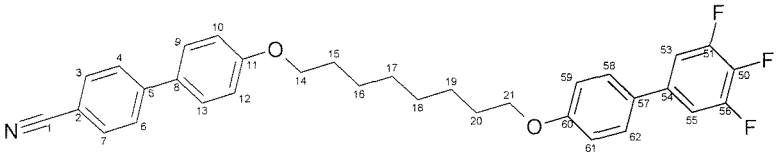

22
$C_{33}H_{30}F_3NO_2$
529.61

Rf 0.70; 100% DCM [1 spot by TLC]

^{1}H NMR (300 MHz, $CDCl_3$): δ_H 7.62 (2H, d, J = 8.6 Hz, $C_4\mathbf{H}$,$C_6\mathbf{H}$), 7.56 (2H, d, J = 8.6 Hz, $C_3\mathbf{H}$, $C_7\mathbf{H}$), 7.45 (2H, d, J = 8.8 Hz, $C_9\mathbf{H}$, $C_{13}\mathbf{H}$), 7.34 (2H, d, J = 8.6 Hz, $C_{62}\mathbf{H}$, $C_{58}\mathbf{H}$), 7.05 (2H, dd, J = 9.0 Hz, 6.4 Hz, $C_{53}\mathbf{H}$, $C_{55}\mathbf{H}$), 6.62 (2H, t, J = 9.0 Hz, $C_{59}\mathbf{H}$, $C_{61}\mathbf{H}$), 6.88 (2H, d, J = 8.8 Hz, $C_{10}\mathbf{H}$, $C_{12}\mathbf{H}$), 3.94 (2H, t, J = 6.4 Hz, O-$C_{14}\mathbf{H_2}$), 3.93 (2H, t, J = 6.4 Hz, O-$C_{21}\mathbf{H_2}$), 1.66-1.84 (4H, m, $C_{15}\mathbf{H_2}$, $C_{20}\mathbf{H_2}$), 1.30-1.55 (8H, m, $C_{16}\mathbf{H_2}$, $C_{17}\mathbf{H_2}$, $C_{18}\mathbf{H_2}$, $C_{19}\mathbf{H_2}$) ppm.

^{13}C NMR (75 MHz, $CDCl_3$): δ_C 159.8 (q, $\mathbf{C_{60}}$(Ar)), 159.5 (q, $\mathbf{C_{11}}$(Ar)), 145.2 (q, $\mathbf{C_5}$(Ar)), 132.6 (t, $\mathbf{C_3}$ (Ar), $\mathbf{C_7}$(Ar)), 131.3 (q, $\mathbf{C_8}$(Ar)), 131.0 (q, $\mathbf{C_{57}}$(Ar)), 128.3 (t, $\mathbf{C_4}$(Ar), $\mathbf{C_6}$(Ar)), 127.9 (t, $\mathbf{C_{58}}$(Ar), $\mathbf{C_{62}}$(Ar)), 127.1 (t, $\mathbf{C_9}$(Ar), $\mathbf{C_{13}}$(Ar)), 119.2 (q, $\mathbf{C_1}$(CN)), 115.1 (t, $\mathbf{C_{59}}$(Ar), $\mathbf{C_{61}}$(Ar)), 115.0 (t, $\mathbf{C_{10}}$(Ar),

C_{12}(Ar)), 110.6 (q, C_{54}(Ar)), 110.3 (q, C_2(Ar)), 110.1 (q, C_{57}(Ar)), 68.1 (s, $C_{14}(OCH_2)$, $C_{21}(OCH_2)$), 29.3 (s, $C_{15\text{-}20}(CH_2)$), 29.2 (s, $C_{15\text{-}20}(CH_2)$), 26.0 (s, $C_{15\text{-}20}(CH_2)$) ppm.

Note: No Peak found for C_{53}-F(Ar) and C_{55}-F (Ar) Expected around δ_C = 137 ppm Signal too weak

IR (Solid) ν_{max}: 2933(m) (**C-H$_2$**), 2954(m) (**C-H$_2$**), 2225 (m) (**C≡N**), 1600(s) (**Ar**), 1539(s) (**Ar**), 1507(s) (**Ar**) cm^{-1}.

EIMS: *m/z* 529 ($[M]^+$, 59%), 224, ($[C_{17}H_{15}O]^+$, 87%), 195 ($[C_{13}H_9NO]^+$, 100%), 69 ($[C_4H_7]^+$, 57%), 55 ($[C_4H_7]^+$, 28%)

1 -(4'-Cyanobiphenyl-4-oxy-)-9-(3',4',5'-trifluorobiphenyl-4-oxy-)-nonane

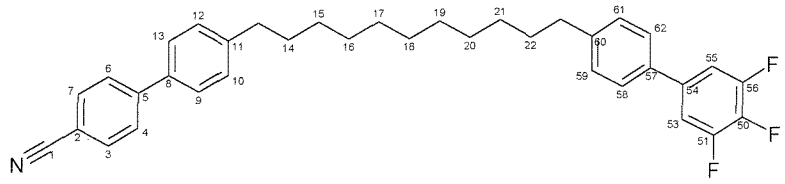

23
$C_{34}H_{32}F_3NO_2$
543.63

Rf 0.71; 100% DCM [1 spot by TLC]

^{1}H NMR (300 MHz, $CDCl_3$): δ_H 7.61 (2H, d, J = 8.6 Hz, C_4**H**,C_6**H**), 7.55 (2H, d, J = 8.6 Hz, C_3**H**, C_7**H**), 7.45 (2H, d, J = 8.8 Hz, C_9**H**, C_{13}**H**), 7.33 (2H, d, J = 8.8 Hz, C_{62}**H**, C_{58}**H**), 7.05 (2H, dd, J = 9.1 Hz, 6.5 Hz, C_{53}**H**, C_{55}**H**), 6.91 (2H, t, J = 9.0 Hz, C_{59}**H**, C_{61}**H**), 6.88 (2H, d, J = 8.8 Hz, C_{10}**H**, C_{12}**H**), 3.93 (2H, t, J = 6.4 Hz, O-C_{14}**H$_2$**), 3.91 (2H, t, J = 6.4 Hz, O-C_{22}**H$_2$**), 1.65-1.82 (4H, m, C_{15}**H$_2$**, C_{21}**H$_2$**), 1.30-1.55 (10H, m, C_{16}**H$_2$**, C_{17}**H$_2$**, C_{18}**H$_2$**, C_{19}**H$_2$**, C_{20}**H$_2$**) ppm.

^{13}C NMR (75 MHz, $CDCl_3$): δ_C 159.8 (q, C_{60}(Ar)), 159.5 (q, C_{11}(Ar)), 145.3 (q, C_5(Ar)), 132.6 (t, C_3 (Ar), C_7(Ar)), 131.3 (q, C_8(Ar)), 130.4 (q, C_{57}(Ar)), 128.3 (t, C_4(Ar), C_6(Ar)), 127.9 (t, C_{58}(Ar), C_{62}(Ar)), 127.1 (t, C_9(Ar), C_{13}(Ar)), 119.1 (q, C_1(CN)), 115.1 (t, C_{59}(Ar), C_{61}(Ar)), 115.0 (t, C_{10}(Ar), C_{12}(Ar)), 110.5 (q, C_{54}(Ar)), 110.3 (q, C_2(Ar)), 110.0 (q, C_{57}(Ar)), 68.1 (s, $C_{14}(OCH_2)$, $C_{22}(OCH_2)$), 29.5 (s, $C_{15\text{-}21}(CH_2)$), 29.3 (s, $C_{15\text{-}21}(CH_2)$), 29.3 (s, $C_{15\text{-}21}(CH_2)$), 26.0 (s, $C_{15\text{-}21}(CH_2)$) ppm.

Note: No Peak found for C_{53}-F(Ar) and C_{55}-F (Ar) Expected around δ_C = 137 ppm Signal too weak

IR (Solid) ν_{max}: 2924(m) (**C-H$_2$**), 2851(m) (**C-H$_2$**), 2217 (m) (**C≡N**), 1600(s) (**Ar**), 1535(s) (**Ar**), 1503(s) (**Ar**) cm^{-1}.

EIMS: *m/z* 543 ([M]$^+$, 59%), 224, ([$C_{17}H_{15}O$]$^+$, 40%), 195 ([$C_{13}H_9NO$]$^+$, 100%), 69 ([C_4H_7]$^+$, 21%), 55 ([C_4H_7]$^+$, 21%)

1 -(4'-Cyanobiphenyl-4-oxy-)-10-(3',4',5'-trifluorobiphenyl-4-oxy-)-decane

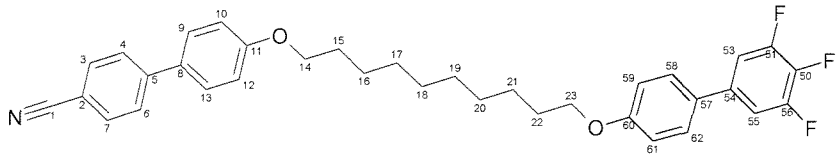

24
$C_{35}H_{34}F_3NO_2$
557.66

Rf 0.72; 100% DCM [1 spot by TLC]

^{1}H NMR (300 MHz, $CDCl_3$): δ_H 7.62 (2H, d, J = 8.6 Hz, C_4**H**,C_6**H**), 7.56 (2H, d, J = 8.6 Hz, C_3**H**, C_7**H**), 7.45 (2H, d, J = 8.8 Hz, C_9**H**, C_{13}**H**), 7.34 (2H, d, J = 8.8 Hz, C_{62}**H**, C_{58}**H**), 7.05 (2H, dd, J = 9.1 Hz, 6.5 Hz, C_{53}**H**, C_{55}**H**), 6.92 (2H, t, J = 9.0 Hz, C_{59}**H**, C_{61}**H**), 6.88 (2H, d, J = 8.8 Hz, C_{10}**H**, C_{12}**H**), 3.81-4.00 (4H, m, O-C_{14}**H$_2$**, O-C_{23}**H$_2$**), 1.62-1.87 (4H, m, C_{15}**H$_2$**, C_{22}**H$_2$**), 1.16-1.57 (12H, m, C_{16}**H$_2$**, C_{17}**H$_2$**, C_{18}**H$_2$**, C_{19}**H$_2$**, C_{20}**H$_2$**, C_{21}**H$_2$**) ppm.

^{13}C NMR (75 MHz, $CDCl_3$): δ_C 158.8 (q, **C_{60}**(Ar)), 158.5 (q, **C_{11}**(Ar)), 144.2 (q, **C_5**(Ar)), 131.6 (t, **C_3** (Ar), **C_7**(Ar)), 130.2 (q, **C_8**(Ar)), 129.4 (q, **C_{57}**(Ar)), 127.3 (t, **C_4**(Ar), **C_6**(Ar)), 126.9 (t, **C_{58}**(Ar), **C_{62}**(Ar)), 126.0 (t, **C_9**(Ar), **C_{13}**(Ar)), 118.2 (q, **C_1**(CN)), 114.0 (t, **C_{59}**(Ar), **C_{61}**(Ar)), 114.0 (t, **C_{10}**(Ar), **C_{12}**(Ar)), 109.5 (q, **C_{54}**(Ar)), 109.2 (q, **C_2**(Ar)), 109.0 (q, **C_{57}**(Ar)), 67.1 (s, **C_{14}**(OCH_2), **C_{23}**(OCH_2)), 28.5 (s, **$C_{15\text{-}22}$**(CH_2)), 28.3 (s, **$C_{15\text{-}22}$**(CH_2)), 28.2 (s, **$C_{15\text{-}22}$**(CH_2)), 25.0 (s, **$C_{15\text{-}22}$**(CH_2)) ppm.

Note: No Peak found for **C_{53}**-F(Ar) and **C_{55}**-F (Ar) Expected around δ_C = 137 ppm Signal too weak

IR (Solid) ν_{max}: 2919(m) (**C-H$_2$**), 2850(m) (**C-H$_2$**), 2229 (m) (**C≡N**), 1600(s) (**Ar**), 1537(s) (**Ar**), 1506(s) (**Ar**) cm^{-1}.

EIMS: *m/z* 557 ([M]$^+$, 56%), 362, ([$C_{27}H_{22}O_2$]$^+$, 5%), 224, ([$C_{17}H_{15}O$]$^+$, 80%), 195 ([$C_{13}H_9NO$]$^+$, 100%), 69 ([C_4H_7]$^+$, 17%), 55 ([C_4H_7]$^+$, 33%)

1 -(4'-Cyanobiphenyl-4-oxy-)-11-(3',4',5'-trifluorobiphenyl-4-oxy-)-undecane

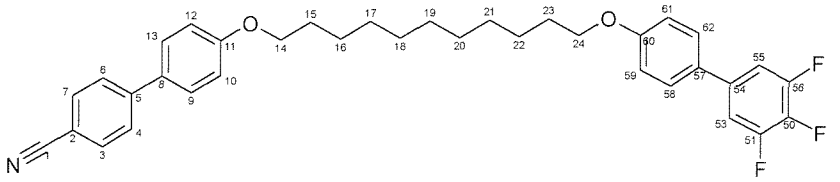

25
$C_{36}H_{36}F_3NO_2$
571.69

Rf 0.73; 100% DCM [1 spot by TLC]

^{1}H NMR (300 MHz, $CDCl_3$): δ_H 7.61 (2H, d, J = 8.6 Hz, C_4**H**,C_6**H**), 7.56 (2H, d, J = 7.8 Hz, C_3**H**, C_7**H**), 7.45 (2H, d, J = 8.8 Hz, C_9**H**, C_{13}**H**), 7.33 (2H, d, J = 8.6 Hz, C_{62}**H**, C_{58}**H**), 7.04 (2H, dd, J = 9.1 Hz, 6.5 Hz, C_{53}**H**, C_{55}**H**), 6.91 (2H, t, J = 8.8 Hz, C_{59}**H**, C_{61}**H**), 6.88 (2H, d, J = 8.8 Hz, C_{10}**H**, C_{12}**H**), 3.83-4.02 (4H, m, O-C_{14}**H$_2$**, O-C_{24}**H$_2$**), 1.64-1.84 (4H, m, C_{15}**H$_2$**, C_{23}**H$_2$**), 1.16-1.52 (14H, m, C_{16}**H$_2$**, C_{17}**H$_2$**, C_{18}**H$_2$**, C_{19}**H$_2$**, C_{20}**H$_2$**, C_{21}**H$_2$**, C_{22}**H$_2$**) ppm.

^{13}C NMR (75 MHz, $CDCl_3$): δ_C 159.8 (q, **C_{60}**(Ar)), 159.5 (q, **C_{11}**(Ar)), 145.3 (q, **C_5**(Ar)), 136.9 (m, **C_{53}**-F(Ar), **C_{55}**-F (Ar)), 132.6 (t, **C_3** (Ar), **C_7**(Ar)), 130.2 (q, **C_8**(Ar)), 130.4 (q, **C_{57}**(Ar)), 128.3 (t, **C_4**(Ar), **C_6**(Ar)), 127.9 (t, **C_{58}**(Ar), **C_{62}**(Ar)), 127.1 (t, **C_9**(Ar), **C_{13}**(Ar)), 119.1 (q, **C_1**(CN)), 115.0 (t, **C_{59}**(Ar), **C_{61}**(Ar)), 115.0 (t, **C_{10}**(Ar), **C_{12}**(Ar)), 110.5 (q, **C_{54}**(Ar)), 110.2 (q, **C_2**(Ar)), 110.0 (q, **C_{57}**(Ar)), 68.1 (s, **C_{14}**(OCH_2), **C_{24}**(OCH_2)), 29.5 (s, **$C_{15\text{-}23}$**(CH_2)), 29.4 (s, **$C_{15\text{-}23}$**(CH_2)), 29.2 (s, **$C_{15\text{-}23}$**(CH_2)), 26.0 (s, **$C_{15\text{-}23}$**(CH_2)) ppm.

IR (Solid) ν_{max}: 2921(m) (**C-H$_2$**), 2850(m) (**C-H$_2$**), 2218 (m) (**C≡N**), 1600(s) (**Ar**), 1537(s) (**Ar**), 1506(s) (**Ar**) cm^{-1}.

EIMS: *m/z* 571 ($[M]^+$, 41%), 324, ($[C_{23}H_{27}F_3O]^+$, 40%), 224, ($[C_{17}H_{15}O]^+$, 90%), 195 ($[C_{13}H_9NO]^+$, 100%), 69 ($[C_4H_7]^+$, 18%), 55 ($[C_4H_7]^+$, 31%)

7.2.4. CBOnOBF$_4$; α -(4'-cyanobiphenyl-4-oxy-)-ω-(3,3',4',5'-tetrafluorobiphenyl-4-oxy-)-alkane

n	Temperature /°C					Mass	Yield
	Cr		N		I	g	%
4	•	113	•	127	•	434	67%
5	•	92	•	(51)	•	419	68%
6	•	96	•	120	•	340	53%
7	•	92	•	(78)	•	3840	41%
8	•	95	•	104	•	250	46%
9	•	63	•	78	•	2480	88%
10	•	93	•	102	•	80	37%
11	•	62	•	80	•	885	41%

1 -(4'-Cyanobiphenyl-4-oxy-)-6-(3,3',4',5'-tetrafluorobiphenyl-4-oxy-)-hexane

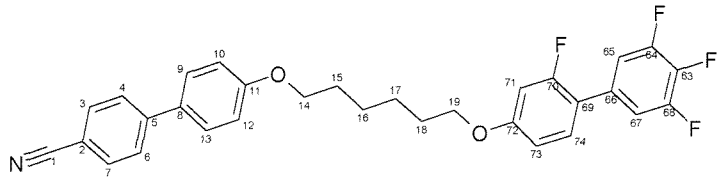

26
$C_{32}H_{27}F_4NO_2$
519.54

Procedure:

To a stirred solution of 2,3',4',5'-tetrafluorobiphen-4-ol (300 mg, 1.24 mMol, 1 eq) in distilled butanone (40 mL) was added solid potassium carbonate (513 mg, 3.72 mMol, 3 eq) in one portion. The mixture was heated to reflux for 40 min and then allowed to cool before the addition of 1-(cyanobiphenyloxy)-hexyl-4-bromide (466 mg, 1.31 mMol, 1.05 eq) in one portion, which dissolved in the butanone immediately. The reaction mixture was then heated to reflux for 3 days. The solvents were removed *in vacuo* and the residue partitioned between DCM and water. The aqueous layer was washed several times with DCM (3 x 30mL) and the combined extracts dried over anhydrous $MgSO_4$ before being concentrated *in vacuo* to give a crude pale yellow solid. The crude material was purified by column chromatography (silica gel, 40 mm x 70 mm, 1-10% ether / 40-60 petroleum) affording the title compound **26** (340 mg, 0.655 mMol 53.2%) as white micro crystalline solid which was dried thoroughly *in vacuo*.

Rf 0.71; 100% DCM [1 spot by TLC]

^{1}H NMR (300 MHz, $CDCl_3$): δ_H 7.71 (2H, d, J = 8.5 Hz, C_4**H**, C_6**H**), 7.65 (2H, d, J = 8.7 Hz, C_3**H**, C_7**H**), 7.55 (2H, d, 8.8 Hz, C_9**H**, C_{13}**H**), 7.28 (1H, t, 8.8 Hz,

C_{74}**H**), 7.10-7.22 (2H, m, C_{65}**H**, C_{67}**H**), 7.02 (2H, d, J = 8.8 Hz, C_{10}**H**, C_{12}**H**), 6.78 (1H, dd, J = 8.6, 2.6 Hz, C_{73}**H**), 6.72 (1H, dd, J = 12.7, 2.6 Hz, C_{71}**H**), 4.06 (4H, t, 6.5 Hz C_{14}**H**$_2$), 4.01 (4H, t, 6.5 Hz C_{19}**H**$_2$), 1.72-1.86 (4H, t, C_{15}**H**$_2$, C_{18}**H**$_2$) 1.55-1.61 (4H, t, C_{16}**H**$_2$, C_{17}**H**$_2$) ppm.

^{13}C NMR (75 MHz, $CDCl_3$): δ_C 159.8 (q, **C**$_{11}$(Ar)), 145.4 (q, **C**$_5$(Ar)), 132.7 (t, **C**$_3$, **C**$_7$(Ar)), 131.5(q, **C**$_8$(Ar)), 130.6(t, **C**$_{74}$(Ar)), 128.5 (t, **C**$_4$(Ar), **C**$_6$(Ar)), 127.2 (t, **C**$_9$(Ar), **C**$_{13}$(Ar)), 119.3 (q, **C**$_1$(CN)), 115.2 (t, **C**$_{10}$(Ar), **C**$_{12}$(Ar)), 113.0 (q, **C**$_{65/67}$(Ar)), 112.7 (q, **C**$_{65/67}$(Ar)), 111.3 (t, **C**$_{31}$(Ar)), 110.2 (q, **C**$_2$(Ar)), 103.0 (t, **C**$_{71/73}$(Ar)), 102.6 (t, **C**$_{71/73}$(Ar)), 68.4 (s, **C**$_{14/19}$(OCH_2)), 68.1 (s, **C**$_{14/19}$(OCH_2)), 29.3 (s, **C**$_{15\text{-}18}$(CH_2)), 29.2 (s, **C**$_{15\text{-}18}$(CH_2)), 25.9 (s, **C**$_{15\text{-}18}$(CH_2)) ppm.

Note: C-F peaks were not found due to extensive coupling to fluorines reducing the intensity of the peaks to below that of the general noise level of the spectra. Peaks for **C**$_{63}$, **C**$_{64}$, **C**$_{66}$, **C**$_{68}$, **C**$_{69}$ and **C**$_{70}$ are consequently not found or reported.

^{19}F NMR (282 MHz, C_6F_6): 42.9 (1F, s, C_{70}**F**), 62.4 (2F, s, C_{64}**F**, C_{68}**F**), -90.1 (1F, s, C_{63}**F**)

IR (Solid) ν_{max}: 2941(m) (**C-H**$_2$), 2868(m) (**C-H**$_2$), 2221 (m) (**C≡N**), 1602(s) (**Ar**), 1535(s) (**Ar**), 1503(s) (**Ar**) cm^{-1}.

EIMS: *m/z* 519 ($[M]^+$, 41%), 242, ($[C_{12}H_7F_4O]^+$, 40%), 195 ($[C_{13}H_9NO]^+$, 100%), 151, ($[C_9H_8FO]^+$, 5%), 83 ($[C_6H_{11}]^+$, 39%), 55 ($[C_4H_7]^+$, 47%)

Elemental Analysis: $C_{32}H_{27}F_4NO_2$: (Expected) **C** 73.91, **H** 5.20, **N** 2.69; (Found) **C** 73.93, **H** 5.11, **N** 2.73

1 -(4'-Cyanobiphenyl-4-oxy-)-4-(3,3',4',5'-tetrafluorobiphenyl-4-oxy-)-butane

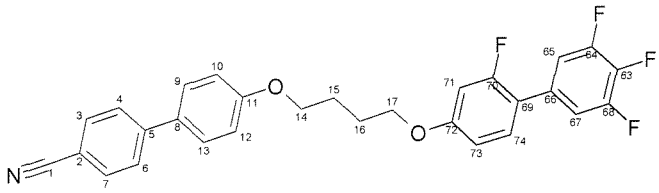

27
$C_{29}H_{21}F_4NO_2$
491.49

Rf 0.71; 100% DCM [1 spot by TLC]

^{1}H NMR (300 MHz, $CDCl_3$): δ_H 7.64 (2H, d, J = 8.5 Hz, C_4**H**, C_6**H**), 7.58 (2H, d, J = 8.8 Hz, C_3**H**, C_7**H**), 7.48 (2H, d, 8.8 Hz, C_9**H**, C_{13}**H**), 7.21 (1H, t, 8.8 Hz, C_{74}**H**), 7.08 (2H, t, J = 8.6, C_{65}**H**, C_{67}**H**), 6.95 (2H, d, J = 8.8 Hz, C_{10}**H**, C_{12}**H**), 6.70 (1H, dd, J = 8.6, 2.4 Hz, C_{73}**H**), 6.63 (1H, dd, J = 12.7, 2.6 Hz, C_{71}**H**), 3.98-4.09 (4H, m, C_{14}**H$_2$**, C_{17}**H$_2$**), 1.91-2.02 (4H, t, C_{15}**H$_2$**, C_{16}**H$_2$**) ppm.

^{13}C NMR (75 MHz, $CDCl_3$): δ_C 159.8 (q, **C_{11}**(Ar)), 145.3 (q, **C_5**(Ar)), 132.7 (t, **C_3**, **C_7**(Ar)), 131.7(q, **C_8**(Ar)), 130.7(t, **C_{74}**(Ar)), 128.5 (t, **C_4**(Ar), **C_6**(Ar)), 127.3 (t, **C_9**(Ar), **C_{13}**(Ar)), 119.3 (q, **C_1**(CN)), 115.2 (t, **C_{10}**(Ar), **C_{12}**(Ar)), 113.0 (q, **$C_{65/67}$**(Ar)), 112.8 (q, **$C_{65/67}$**(Ar)), 111.3 (t, **C_{31}**(Ar)), 110.3 (q, **C_2**(Ar)), 103.0 (t, **$C_{71/73}$**(Ar)), 102.7 (t, **$C_{71/73}$**(Ar)), 68.1 (s, **$C_{14/17}$**(OCH_2)), 68.7 (s, **$C_{14/17}$**(OCH_2)), 26.0 (s, **$C_{15,16}$**(CH_2)) ppm.

Note: C-F peaks were not found due to extensive coupling to fluorines reducing the intensity of the peaks to below that of the general noise level of the spectra. Peaks for **C_{63}**, **C_{64}**, **C_{66}**, **C_{68}**, **C_{69}** and **C_{70}** are consequently not found or reported.

^{19}F NMR (282 MHz, C_6F_6): 47.2 (1F, s, C_{70}**F**), 27.7 (2F, s, C_{64}**F**, C_{68}**F**), -0.56 (1F, s, C_{63}**F**)

IR (Solid) ν_{max}: 2933(m) (**C-H$_2$**), 2859(m) (**C-H$_2$**), 2225 (m) (**C≡N**), 1598(s) (**Ar**), 1533(s) (**Ar**), 1502(s) (**Ar**) cm^{-1}.

EIMS: *m/z* 419 ($[M]^+$, 56%), 297, ($[C_{17}H_{17}F_4O]^+$, 40%), 255, ($[C_{14}H_9F_4O]^+$, 100%), 195 ($[C_{13}H_9NO]^+$, 43%), 151, ($[C_9H_8FO]^+$, 5%), 75 ($[C_6H_3]^+$, 7%), 55 ($[C_4H_7]^+$, 42%)

1 -(4'-Cyanobiphenyl-4-oxy-)-5-(3,3',4',5'-tetrafluorobiphenyl-4-oxy-)-pentane

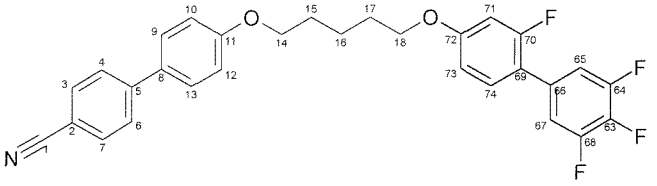

28
$C_{30}H_{23}F_4NO_2$
505.52

Rf 0.72; 100% DCM [1 spot by TLC]

^{1}H NMR (300 MHz, $CDCl_3$): δ_H 7.63 (2H, d, J = 8.6 Hz, C_4**H**, C_6**H**), 7.57 (2H, d, J = 8.8 Hz, C_3**H**, C_7**H**), 7.47 (2H, d, 8.8 Hz, C_9**H**, C_{13}**H**), 7.20 (1H, t, 8.8 Hz, C_{74}**H**), 7.05 (2H, t, J = 8.6, C_{65}**H**, C_{67}**H**), 6.92 (2H, d, J = 8.8 Hz, C_{10}**H**, C_{12}**H**), 6.69 (1H, dd, J = 8.6, 2.4 Hz, C_{73}**H**), 6.63 (1H, dd, J = 12.7, 2.5 Hz, C_{71}**H**), 4.02 (2H, J=6.4, C_{14}**H$_2$**), 3.95 (2H, J=6.5, C_{18}**H$_2$**), 1.78-1.90 (4H, t, C_{15}**H$_2$**, C_{17}**H$_2$**), 1.54-1.71 (2H, m, C_{16}**H$_2$**) ppm.

^{13}C NMR (75 MHz, $CDCl_3$): δ_C 159.8 (q, **C_{11}**(Ar)), 145.4 (q, **C_5**(Ar)), 132.7 (t, **C_3**, **C_7**(Ar)), 131.6(q, **C_8**(Ar)), 130.7(t, **C_{74}**(Ar)), 128.5 (t, **C_4**(Ar), **C_6**(Ar)), 127.3 (t, **C_9**(Ar), **C_{13}**(Ar)), 119.3 (q, **C_1**(CN)), 115.2 (t, **C_{10}**(Ar), **C_{12}**(Ar)), 113.0 (q, **$C_{65/67}$**(Ar)), 112.7 (q, **$C_{65/67}$**(Ar)), 111.3 (t, **C_{31}**(Ar)), 110.2 (q, **C_2**(Ar)), 103.0 (t, **$C_{71/73}$**(Ar)), 102.7 (t, **$C_{71/73}$**(Ar)), 68.1 (s, **$C_{14/18}$**(OCH_2)), 68.7 (s, **$C_{14/18}$**(OCH_2)), 29.1 (s, **$C_{15\text{-}17}$**(CH_2)), 29.0 (s, **$C_{15\text{-}17}$**(CH_2)) 26.0 (s, **$C_{15\text{-}17}$**(CH_2)) ppm.

Note: C-F peaks were not found due to extensive coupling to fluorines reducing the intensity of the peaks to below that of the general noise level of the spectra. Peaks for **C_{63}**, **C_{64}**, **C_{66}**, **C_{68}**, **C_{69}**, **C_{70}** and **C_{72}** are consequently not found or reported.

^{19}F NMR (282 MHz, C_6F_6): 46.5 (1F, s, C_{70}**F**), 27.2 (2F, s, C_{64}**F**, C_{68}**F**), -0.74 (1F, s, C_{63}**F**)

IR (Solid) ν_{max}: 2945(m) (**C-H$_2$**), 2867(m) (**C-H$_2$**), 2221 (m) (**C≡N**), 1602(s) (**Ar**), 1535(s) (**Ar**), 1494(s) (**Ar**) cm^{-1}.

EIMS: *m/z* 505 ($[M]^+$, 53%), 323, ($[C_{18}H_{17}F_4O]^+$, 40%), 311, ($[C_{17}H_{15}F_4O]^+$, 97%), 195 ($[C_{13}H_9NO]^+$, 43%), 178, ($[C_{11}H_{11}FO]^+$, 11%), 69 ($[C_5H_9]^+$, 100%), 41 ($[C_3H_5]^+$, 31%)

1 -(4'-Cyanobiphenyl-4-oxy-)-7-(3,3',4',5'-tetrafluorobiphenyl-4-oxy-)-heptane

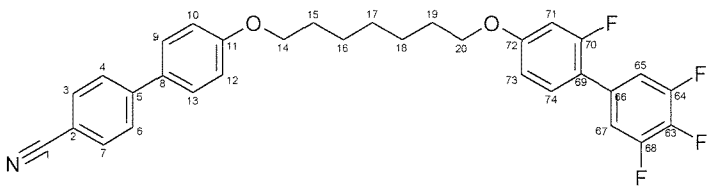

29
$C_{32}H_{27}F_4NO_2$
533.57

Rf 0.73;100% DCM [1 spot by TLC]

^{1}H NMR (400 MHz, $CDCl_3$): δ_H 7.61 (2H, d, J = 8.5 Hz, C_4**H**, C_6**H**), 7.55 (2H, d, J = 8.5 Hz, C_3**H**, C_7**H**), 7.45 (2H, d, 9.0 Hz, C_9**H**, C_{13}**H**), 7.19 (1H, t, 9.0 Hz, C_{74}**H**), 7.04 (2H, t, 7.5 Hz, C_{53}**H**, C_{55}**H**), 6.91 (2H, d, J = 9.0 Hz, C_{10}**H**, C_{12}**H**), 6.68 (2H, dd, J = 9.0, 2.5 Hz, C_{73}**H**), 6.62 (2H, dd, J = 12.5, 2.5 Hz, C_{71}**H**), 3.93 (4H, m, O-C_{14}**H$_2$**, C_{20}**H$_2$**-O), 1.78 (4H, m, 6.5 Hz C_{15}**H$_2$**, C_{19}**H$_2$**), 1.46 (6H, m, C_{16}**H$_2$**, C_{17}**H$_2$**, C_{18}**H$_2$**) ppm.

^{13}C NMR (100 MHz, $CDCl_3$): δ_C 161.5 (q, **C_{72}**(Ar)), 160.1 (q, **C_{11}**(Ar)), 152.8 (q, **C_{66}**(Ar)), 150.3 (q, **C_{69}**(Ar)), 145.4 (q, **C_5**(Ar)), 140.6 (m, **C_{63}**(Ar)), 138.1 (m, **C_{64}**(Ar), **C_{68}**(Ar)), 132.8 (t, **C_3**, **C_7**(Ar)), 132.0(q, **C_8**(Ar)), 130.9(t, **C_{74}**(Ar)), 128.7 (t, **C_4**(Ar), **C_6**(Ar)), 127.5 (t, **C_9**(Ar), **C_{13}**(Ar)), 119.5 (q, **C_1**(CN)), 118.6 (q, **C_{70}**(Ar)), 115.5 (t, **C_{10}**(Ar), **C_{12}**(Ar)), 113.0 (q, **$C_{65/67}$**(Ar)), 113.0 (q, **$C_{65/67}$**(Ar)), 111.3 (t, **C_{31}**(Ar)), 110.2 (q, **C_2**(Ar)), 103.2 (t, **$C_{71/73}$**(Ar)), 102.9 (t, **$C_{71/73}$**(Ar)), 68.8 (s, **$C_{14/20}$**(OCH_2)), 68.5 (s, **$C_{14/20}$**(OCH_2)), 31.3 (s, **$C_{15\text{-}19}$**(CH_2)), 29.6 (s, **$C_{15\text{-}19}$**(CH_2)), 29.5 (s, **$C_{15\text{-}19}$**(CH_2)), 29.4 (s, **$C_{15\text{-}19}$**(CH_2)) 26.4 (s, **$C_{15\text{-}19}$**(CH_2)) ppm.

^{19}F NMR **Not obtained**

IR (Solid) ν_{max}: 2941(m) (**C-H$_2$**), 2854(m) (**C-H$_2$**), 2223 (m) (**C≡N**), 1605(s) (**Ar**), 1533(s) (**Ar**), 1502(s) (**Ar**) cm^{-1}.

EIMS: *m/z* 563 ($[M]^+$, 84%), 338 ($[C_{19}H_{19}F_4O]^+$, 5%), 242 ($[C_{12}H_8OF_4]^+$, 56%), 195 ($[C_{13}H_9NO]^+$, 100%), 166 ($[C_{13}H_{10}]^+$, 5%), 97 ($[C_7H_{13}]^+$, 28%), 55 ($[C_4H_7]^+$, 41%).

1 -(4'-cyanobiphenyl-4-oxy-)-8-(3,3',4',5'-tetrafluorbiphenyl-4-oxy-)-octane

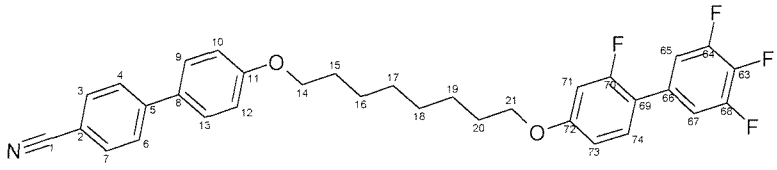

30
$C_{33}H_{29}F_4NO_2$
547.60

Rf 0.73; 100% DCM [1 spot by TLC]

^{1}H NMR (300 MHz, $CDCl_3$): δ_H 7.63 (2H, d, J = 8.6 Hz, C_4**H**, C_6**H**), 7.57 (2H, d, J = 8.8 Hz, C_3**H**, C_7**H**), 7.47 (2H, d, 8.8 Hz, C_9**H**, C_{13}**H**), 7.19 (1H, t, 8.8 Hz, C_{74}**H**), 7.07 (2H, t, J = 8.6, C_{65}**H**, C_{67}**H**), 6.92 (2H, d, J = 8.8 Hz, C_{10}**H**,

C_{12}**H**), 6.69 (1H, dd, J = 8.6, 2.4 Hz, C_{73}**H**), 6.61 (1H, dd, J = 12.7, 2.5 Hz, C_{71}**H**), 3.98 (2H, J=6.4, C_{14}**H**$_2$), 3.88 (2H, J=6.4, C_{21}**H**$_2$), 1.69-1.72 (4H, t, C_{15}**H**$_2$, C_{20}**H**$_2$), 0.75-1.47 (8H, m, C_{16}**H**$_2$, C_{17}**H**$_2$, C_{18}**H**$_2$, C_{19}**H**$_2$) ppm.

^{13}C NMR (75 MHz, $CDCl_3$): δ_C 159.8 (q, **C**$_{11}$(Ar)), 145.4 (q, **C**$_5$(Ar)), 132.7 (t, **C**$_3$, **C**$_7$(Ar)), 131.4(q, **C**$_8$(Ar)), 130.6(t, **C**$_{74}$(Ar)), 128.5 (t, **C**$_4$(Ar), **C**$_6$(Ar)), 127.2 (t, **C**$_9$(Ar), **C**$_{13}$(Ar)), 119.3 (q, **C**$_1$(CN)), 115.2 (t, **C**$_{10}$(Ar), **C**$_{12}$(Ar)), 113.0 (q, **C**$_{65/67}$(Ar)), 112.7 (q, **C**$_{65/67}$(Ar)), 111.3 (t, **C**$_{31}$(Ar)), 110.2 (q, **C**$_2$(Ar)), 103.0 (t, **C**$_{71/73}$(Ar)), 102.6 (t, **C**$_{71/73}$(Ar)), 68.6 (s, **C**$_{14/21}$(OCH_2)), 68.2 (s, **C**$_{14/21}$(OCH_2)), 29.4 (s, **C**$_{15\text{-}20}$(CH_2)), 29.2 (s, **C**$_{15\text{-}20}$(CH_2)), 29.0 (s, **C**$_{15\text{-}20}$(CH_2)), 26.0 (s, **C**$_{15\text{-}20}$(CH_2)), 24.0 (s, **C**$_{15\text{-}20}$(CH_2)) ppm.

Note: C-F peaks were not found due to extensive coupling to fluorines reducing the intensity of the peaks to below that of the general noise level of the spectra. Peaks for **C**$_{63}$, **C**$_{64}$, **C**$_{66}$, **C**$_{68}$, **C**$_{69}$, **C**$_{70}$ and **C**$_{72}$ are consequently not found or reported.

^{19}F NMR (282 MHz, C_6F_6): 46.3 (1F, s, C_{70}**F**), 27.0 (2F, s, C_{64}**F**, C_{68}**F**), -0.83 (1F, s, C_{63}**F**)

IR (Solid) ν_{max}: 2914(m) (**C-H**$_2$), 2850(m) (**C-H**$_2$), 2224 (m) (**C≡N**), 1596(s) (**Ar**), 1536(s) (**Ar**), 1493(s) (**Ar**) cm^{-1}.

EIMS: *m/z* 547 ($[M]^+$, 53%), 352, ($[C_{20}H_{21}F_4O]^+$, 7%), 242, ($[C_{12}H_8F_4O]^+$, 67%), 195 ($[C_{13}H_9NO]^+$, 100%), 178, ($[C_{11}H_{11}FO]^+$, 6%), 69 ($[C_5H_9]^+$, 100%), 55 ($[C_4H_7]^+$, 31%)

1 -(4'-Cyanobiphenyl-4-oxy-)-9-(3,3',4',5'-tetrafluorobiphenyl-4-oxy-)-nonane

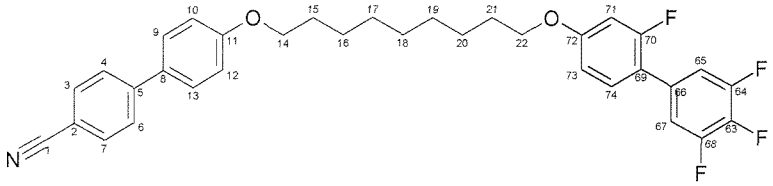

31
$C_{34}H_{31}F_4NO_2$
561.63

Rf 0.74; 100% DCM [1 spot by TLC]

^{1}H NMR (400 MHz, $CDCl_3$): δ_H 7.61 (2H, d, J = 8.0 Hz, C_4**H**, C_6**H**), 7.55 (2H, d, J = 8.0 Hz, C_3**H**, C_7**H**), 7.44 (2H, d, 9.0 Hz, C_9**H**, C_{13}**H**), 7.18 (1H, t, 8.5 Hz, C_{74}**H**), 7.00-7.09 (2H, m, C_{65}**H**, C_{67}**H**), 6.91 (2H, d, J = 9.0 Hz, C_{10}**H**, C_{12}**H**),

6.69 (1H, dd, J = 8.5, 2.5 Hz, C_{73}**H**), 6.62 (1H, dd, J = 8.5, 2.5 Hz, C_{71}**H**), 3.93 (2H, t, J = 6.7 Hz, O-C_{14}**H$_2$**), 3.90 (2H, t, J = 6.6 Hz, O-C_{22}**H$_2$**), 1.68-1.79 (4H, m, 6.5 Hz C_{15}**H$_2$**, C_{21}**H$_2$**), 1.25-1.50 (10H, m, C_{16}**H$_2$**, C_{17}**H$_2$**, C_{18}**H$_2$**, C_{19}**H$_2$**, C_{20}**H$_2$**) ppm.

^{13}C NMR (100 MHz, $CDCl_3$): δ_C 161.1 (q, **C_{72}**(Ar)), 160.2 (q, **C_{11}**(Ar)), 152.7 (q, **C_{66}**(Ar)), 150.2 (q, **C_{69}**(Ar)), 145.7 (q, **C_5**(Ar)), 140.7 (m, **C_{63}**(Ar)), 138.0 (m, **C_{64}**(Ar), **C_{68}**(Ar)), 132.8 (t, **C_3**, **C_7**(Ar)), 131.7(q, **C_8**(Ar)), 130.9(t, **C_{74}**(Ar)), 128.7 (t, **C_4**(Ar), **C_6**(Ar)), 127.5 (t, **C_9**(Ar), **C_{13}**(Ar)), 119.5 (q, **C_1**(CN)), 118.8 (q, **C_{70}**(Ar)), 115.5 (t, **C_{10}**(Ar), **C_{12}**(Ar)), 113.2 (q, **$C_{65/67}$**(Ar)), 113.0 (q, **$C_{65/67}$**(Ar)), 111.6 (t, **C_{31}**(Ar)), 110.5 (q, **C_2**(Ar)), 103.2 (t, **$C_{71/73}$**(Ar)), 103.0 (t, **$C_{71/73}$**(Ar)), 68.8 (s, **$C_{14/22}$**(OCH_2)), 68.6 (s, **$C_{14/22}$**(OCH_2)), 29.9 (s, **$C_{15\text{-}21}$**(CH_2)), 29.7 (s, **$C_{15\text{-}21}$**(CH_2)), 29.6 (s, **$C_{15\text{-}21}$**(CH_2)), 29.5 (s, **$C_{15\text{-}21}$**(CH_2)), 29.4 (s, **$C_{15\text{-}21}$**(CH_2)), 26.4 (s, **$C_{15\text{-}21}$**(CH_2)) ppm.

IR (Solid) ν_{max}: 2926 (m) (**C-H$_2$**), 2845(m) (**C-H$_2$**), 2226 (m) (**C≡N**), 1602(s) (**Ar**), 1541(s) (**Ar**), 1500(s) (**Ar**) cm^{-1}.

EIMS: *m/z* 561 ($[M]^+$, 90%), 366 ($[C_{21}H_{22}F_4O]^+$, 5%), 242 ($[C_{12}H_8OF_4]^+$, 69%), 195 ($[C_{13}H_9NO]^+$, 100%), 69 ($[C_5H_9]^+$, 25%), 55 ($[C_4H_7]^+$, 25%).

1 -(4'-Cyanobiphenyl-4-oxy-)-10-(3,3',4',5'-tetrafluorobiphenyl-4-oxy-)-decane

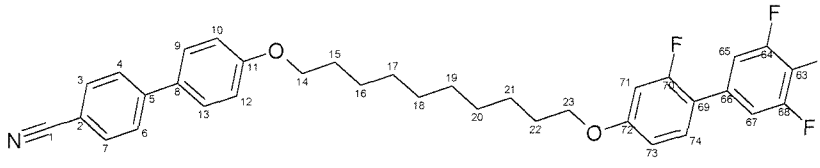

32
$C_{35}H_{33}F_4NO_2$
575.65

Rf 0.74; 100% DCM [1 spot by TLC]

^{1}H NMR (300 MHz, $CDCl_3$): δ_H 7.61 (2H, d, J = 8.5 Hz, C_4**H**, C_6**H**), 7.55 (2H, d, J = 8.5 Hz, C_3**H**, C_7**H**), 7.45 (2H, d, 8.8 Hz, C_9**H**, C_{13}**H**), 7.18 (1H, t, 9.0 Hz, C_{74}**H**), 7.05 (2H, t, J = 7.8 Hz, C_{65}**H**, C_{67}**H**), 6.91 (2H, d, J = 9.0 Hz, C_{10}**H**, C_{12}**H**), 6.68 (1H, dd, J = 8.6, 2.6 Hz, C_{73}**H**), 6.62 (1H, dd, J = 12.8, 2.4 Hz, C_{71}**H**), 3.93 (2H, t, J = 6.5 Hz, O-C_{14}**H$_2$**), 3.90 (2H, t, J = 6.5 Hz, O-C_{23}**H$_2$**), 1.62-1.83 (4H, m, 6.5 Hz C_{15}**H$_2$**, C_{22}**H$_2$**), 1.15-1.54 (12H, m, C_{16}**H$_2$**, C_{17}**H$_2$**, C_{18}**H$_2$**, C_{19}**H$_2$**, C_{20}**H$_2$**, C_{21}**H$_2$**) ppm.

^{13}C NMR (75 MHz, $CDCl_3$): δ_C 159.8 (q, **C_{11}**(Ar)), 145.3 (q, **C_5**(Ar)), 132.6 (t, **C_3**, **C_7**(Ar)), 131.4(q, **C_8**(Ar)), 130.5(t, **C_{74}**(Ar)), 128.3 (t, **C_4**(Ar), **C_6**(Ar)), 127.1 (t, **C_9**(Ar), **C_{13}**(Ar)), 119.1 (q, **C_1**(CN)), 115.1 (t, **C_{10}**(Ar), **C_{12}**(Ar)), 112.9 (q, **$C_{65/67}$**(Ar)), 112.6 (q, **$C_{65/67}$**(Ar)), 111.2 (t, **C_{31}**(Ar)), 110.1 (q, **C_2**(Ar)), 102.8 (t, **$C_{71/73}$**(Ar)), 102.5 (t, **$C_{71/73}$**(Ar)), 68.5 (s, **$C_{14/21}$**(OCH_2)), 68.2 (s, **$C_{14/21}$**(OCH_2)), 29.5 (s, **$C_{15\text{-}20}$**(CH_2)), 29.4 (s, **$C_{15\text{-}20}$**(CH_2)), 29.3 (s, **$C_{15\text{-}20}$**(CH_2)), 29.2 (s, **$C_{15\text{-}20}$**(CH_2)), 29.1 (s, **$C_{15\text{-}20}$**(CH_2)), 26.0 (s, **$C_{15\text{-}20}$**(CH_2)) ppm.

Note: C-F peaks were not found due to extensive coupling to fluorines reducing the intensity of the peaks to below that of the general noise level of the spectra. Peaks for **C_{63}**, **C_{64}**, **C_{66}**, **C_{68}**, **C_{69}**, **C_{70}** and **C_{72}** are consequently not found or reported.

^{19}F NMR (282 MHz, C_6F_6): -115.5 (1F, s, C_{70}**F**), -135.0 (2F, s, C_{64}**F**, C_{68}**F**), -162.5 (1F, s, C_{63}**F**)

IR (Solid) ν_{max}: 2917(m) (**C-H$_2$**), 2850(m) (**C-H$_2$**), 2227 (m) (**C≡N**), 1599(s) (**Ar**), 1536(s) (**Ar**), 1504(s) (**Ar**) cm^{-1}.

EIMS: *m/z* 575 ($[M]^+$, 35%), 195 ($[C_{13}H_9NO]^+$, 100%), 69 ($[C_5H_9]^+$, 26%), 55 ($[C_4H_7]^+$, 39%)

1 -(4'-Cyanobiphenyl-4-oxy-)-11-(3,3',4',5'-tetrafluorobiphenyl-4-oxy-)-undecane

33
$C_{36}H_{35}F_4NO_2$
589.68

Rf 0.75; 100% DCM [1 spot by TLC]

^{1}H NMR (300 MHz, $CDCl_3$): δ_H 7.71 (2H, d, J = 8.6 Hz, C_4**H**, C_6**H**), 7.64 (2H, d, J = 8.8 Hz, C_3**H**, C_7**H**), 7.54 (2H, d, 8.8 Hz, C_9**H**, C_{13}**H**), 7.28 (1H, t, 8.8 Hz, C_{74}**H**), 7.14 (2H, t, J = 8.6, C_{65}**H**, C_{67}**H**), 7.01 (2H, d, J = 8.8 Hz, C_{10}**H**, C_{12}**H**), 6.78 (1H, dd, J = 8.6, 2.4 Hz, C_{73}**H**), 6.70 (1H, dd, J = 12.7, 2.5 Hz, C_{71}**H**), 4.02 (2H, J=6.4, C_{14}**H$_2$**), 3.97 (2H, J=6.4, C_{24}**H$_2$**), 1.78-1.91 (4H, t,

$C_{15}\mathbf{H_2}$, $C_{23}\mathbf{H_2}$), 1.29-1.61 (14H, m, $C_{16}\mathbf{H_2}$, $C_{17}\mathbf{H_2}$, $C_{18}\mathbf{H_2}$, $C_{19}\mathbf{H_2}$, $C_{20}\mathbf{H_2}$, $C_{21}\mathbf{H_2}$, $C_{22}\mathbf{H_2}$) ppm.

^{13}C NMR (75 MHz, $CDCl_3$): δ_C 159.9 (q, $\mathbf{C_{11}}$(Ar)), 145.4 (q, $\mathbf{C_5}$(Ar)), 132.7 (t, $\mathbf{C_3}$, $\mathbf{C_7}$(Ar)), 131.4 (q, $\mathbf{C_8}$(Ar)), 130.6 (t, $\mathbf{C_{74}}$(Ar)), 128.5 (t, $\mathbf{C_4}$(Ar), $\mathbf{C_6}$(Ar)), 127.2 (t, $\mathbf{C_9}$(Ar), $\mathbf{C_{13}}$(Ar)), 119.3 (q, $\mathbf{C_1}$(CN)), 115.2 (t, $\mathbf{C_{10}}$(Ar), $\mathbf{C_{12}}$(Ar)), 113.0 (q, $\mathbf{C_{65/67}}$(Ar)), 112.7 (q, $\mathbf{C_{65/67}}$(Ar)), 111.3 (t, $\mathbf{C_{31}}$(Ar)), 110.2 (q, $\mathbf{C_2}$(Ar)), 103.0 (t, $\mathbf{C_{71/73}}$(Ar)), 102.6 (t, $\mathbf{C_{71/73}}$(Ar)), 68.7 (s, $\mathbf{C_{14/24}}$(OCH_2)), 68.3 (s, $\mathbf{C_{14/24}}$(OCH_2)), 29.7 (s, $\mathbf{C_{15\text{-}23}}$($CH_2$)), 29.5 (s, $\mathbf{C_{15\text{-}23}}$($CH_2$)), 29.4 (s, $\mathbf{C_{15\text{-}23}}$($CH_2$)), 29.2 (s, $\mathbf{C_{15\text{-}23}}$($CH_2$)), 26.2 (s, $\mathbf{C_{15\text{-}23}}$($CH_2$)), 24.1 (s, $\mathbf{C_{15\text{-}23}}$($CH_2$)) ppm.

Note: C-F peaks were not found due to extensive coupling to fluorines reducing the intensity of the peaks to below that of the general noise level of the spectra. Peaks for $\mathbf{C_{63}}$, $\mathbf{C_{64}}$, $\mathbf{C_{66}}$, $\mathbf{C_{68}}$, $\mathbf{C_{69}}$, $\mathbf{C_{70}}$ and $\mathbf{C_{72}}$ are consequently not found or reported.

^{19}F NMR (282 MHz, C_6F_6): 46.6 (1F, s, $C_{70}\mathbf{F}$), 27.2 (2F, s, $C_{64}\mathbf{F}$, $C_{68}\mathbf{F}$), -0.9 (1F, s, $C_{63}\mathbf{F}$)

IR (Solid) ν_{max}: 2918(m) (**C-H$_2$**), 2851(m) (**C-H$_2$**), 2226 (m) (**C≡N**), 1599(s) (**Ar**), 1536(s) (**Ar**), 1504(s) (**Ar**) cm^{-1}.

EIMS: *m/z* 589 ($[M]^+$, 53%), 352, ($[C_{23}H_{27}F_4O]^+$, 11%), 195 ($[C_{13}H_9NO]^+$, 100%), 69 ($[C_5H_9]^+$, 11%), 55 ($[C_4H_7]^+$, 20%)

7.2.5. CBOnOBFOCF$_3$; α -(4'-cyanobiphenyl-4-oxy-)-ω-(3'-fluor-4'-oxytrifluoromethylbiphenyl-4-oxy-)-alkane

n	Temperature /°C					Mass	Yield
	Cr		N		I	mg	%
4	•	135	•	153	•	369	76%
5	•	94	•	(89)	•	454	77%
6	•	129	•	152	•	460	64%
7	•	81	•	104	•	1270	35%
8	•	111	•	133	•	2360	80%
9	•	83	•	104	•	2410	88%
10	•	100	•	128	•	489	63%
11	•	88	•	104	•	518	76%

1 -(4'-Cyanobiphenyl-4-oxy-)-4-(3,3',4',5'-tetrafluorobiphenyl-4-oxy-)-butane

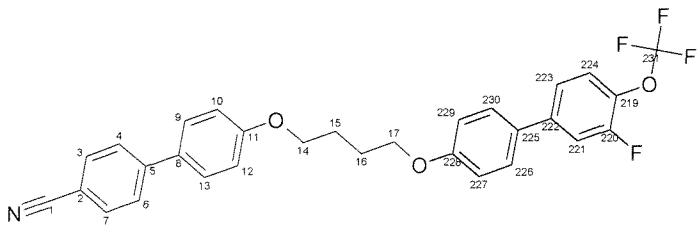

34
$C_{30}H_{23}F_4NO_3$
521.52

Procedure:

To a stirred solution of 3'-fluoro-4'-trifluoromethoxybiphen-4-ol (379 mg, 1.10 mMol, 1 eq) in distilled butan-2-one (40 mL) was added solid potassium carbonate (280 mg, 2.02 mMol, 1.8 eq) in one portion. The mixture was heated to reflux for 1 h then cooled prior to the addition of 1-(cyanobiphenyloxy)-butyl-4-bromide (381 mg, 1.11 mMol, 1.01eq) in one portion and a catalytic quantity of sodium iodide (80 mg). This reaction mixture was heated to reflux for 3 days and then allowed to cool. The solvents were then removed *in vacuo* and the residue was dissolved and partitioned between DCM and water. The aqueous layer was washed several times with DCM (3 x 30mL) and the washed organic exctracts were dried over anhydrous $MgSO_4$ before being concentrated *in vacuo* to give a crude yellow solid. The crude material was purified by column chromatography (silica gel, 35mm x 70mm, 1-5% ether/40-60 pet. ether) affording the title compound **34** (454mg, 0.849 mMol 77.1%) as white powder which was dried thoroughly *in vacuo*.

Rf 0.71; 100% DCM [1 spot by TLC]

^{1}H NMR (300 MHz, $CDCl_3$): δ_H 7.62 (2H, d, J = 8.6 Hz, C_4**H**,C_6**H**), 7.56 (2H, d, J = 8.6 Hz, C_3**H**, C_7**H**), 7.46 (2H, d, J = 8.8 Hz, C_9**H**, C_{13}**H**), 7.39 (2H, d, J = 9.0 Hz, C_{230}**H**, C_{226}**H**), 7.29 (1H, t, J = 12.2 Hz, 2.1 Hz, C_{224}**H**), 7.23 (2H, d, J = 8.8 Hz, C_{221}**H**, C_{223}**H**), 6.93 (1H, d, J = 6.8 Hz, C_{227}**H$_2$**, C_{229}**H$_2$**), 6.90 (2H, d, J = 7.0 Hz, C_{10}**H**, C_{12}**H**), 3.95-4.10 (4H, m, O-C_{14}**H$_2$**, O-C_{17}**H$_2$**), 1.88-2.04 (4H, m, C_{15}**H$_2$**, C_{16}**H$_2$**) ppm.

^{13}C NMR (75 MHz, $CDCl_3$): δ_C 159.6 (q, **C_{11}**(Ar)), 159.2 (q, **C_{228}**(Ar)), 156.2 (q, **C_{219}**(Ar)), 145.2 (q, **C_5**(Ar)), 142.8 (q, **C_{220}**(Ar)), 132.6 (t, **C_3** (Ar), **C_7**(Ar)), 131.5 (q, **C_8**(Ar)), 131.2 (q, **C_{225}**(Ar)), 128.1 (t, **C_{223}**(Ar)), 128.4 (t, **C_4**(Ar), **C_6**(Ar)), 127.1 (t, **C_9**(Ar), **C_{13}**(Ar)), 123.9 (t, **C_{221}**(Ar)), 122.5 (t, **C_{222}**(Ar)), 119.1 (q, **C_1**(CN)), 115.4 (t, **C_{227}**/**C_{229}**(Ar)), 115.1 (t, **C_{227}**/**C_{229}**(Ar)), 115.0 (t,

C_{10}(Ar), C_{12}(Ar)), 110.2 (q, C_2(Ar)), 67.6 (s, $C_{14}(OCH_2)$, $C_{17}(OCH_2)$), 25.9 (s, $C_{15\text{-}16}(CH_2)$) ppm.

IR (Solid) ν_{max}: 2925(m) (**C-H$_2$**), 2863(m) (**C-H$_2$**), 2234 (m) (**C≡N**), 1601(s) (**Ar**), 1527(s) (**Ar**), 1493(s) (**Ar**) cm^{-1}.

EIMS: *m/z* 521 ($[M]^+$, 47%), 327 ($[C_{17}H_{15}F_4O_2]^+$, 69%), 285 ($[C_{114}H_9F_4O_2]^+$, 57%), 250 ($[C_{18}H_{18}O]^+$, 100%), 208 ($[C_{15}H_{13}O]^+$, 100%), 178 ($[C_{12}H_{18}O]^+$, 21%), 55 ($[C_4H_7]^+$, 33%)

Elemental Analysis: $C_{32}H_{27}F_4NO_2$: (Expected) **C** 69.03, **H** 6.33, **N** 2.68; (Found) **C** 68.95, **H** 6.32, **N** 2.68

1 -(4'-Cyanobiphenyl-4-oxy-)-5-(3,3',4',5'-tetrafluorobiphenyl-4-oxy-)-pentane

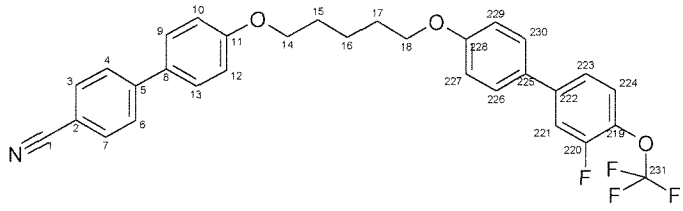

35
$C_{31}H_{25}F_4NO_3$
535.54

Rf 0.72; 100% DCM [1 spot by TLC]

^{1}H NMR (300 MHz, $CDCl_3$): δ_H 7.71 (2H, d, J = 8.6 Hz, C_4**H**,C_6**H**), 7.64 (2H, d, J = 8.6 Hz, C_3**H**, C_7**H**), 7.55 (2H, d, J = 8.8 Hz, C_9**H**, C_{13}**H**), 7.48 (2H, d, J = 6.4 Hz, C_{230}**H**, C_{226}**H**), 7.29-7.41 (3H, m, C_{224}**H**, C_{221}**H**, C_{223}**H**), 7.02 (1H, d, J = 6.8 Hz, C_{227}**H$_2$**, C_{229}**H$_2$**), 6.99 (2H, d, J = 7.8 Hz, C_{10}**H**, C_{12}**H**), 4.07 (2H, t, J = 6.2 Hz, O-C_{14}**H$_2$**), 4.06 (2H, t, J = 6.2 Hz, O-C_{17}**H$_2$**), 1.86-2.00 (4H, m, C_{15}**H$_2$**, C_{17}**H$_2$**), 1.65-1.78 (2H, m, C_{16}**H$_2$**) ppm.

^{13}C NMR (75 MHz, $CDCl_3$): δ_C 159.8 (q, **C_{11}**(Ar)), 159.4 (q, **C_{228}**(Ar)), 156.6 (q, **C_{219}**(Ar)), 145.4 (q, **C_5**(Ar)), 141.7 (q, **C_{220}**(Ar)), 132.7 (t, **C_3** (Ar), **C_7**(Ar)), 131.5 (q, **C_8**(Ar)), 131.3 (q, **C_{225}**(Ar)), 128.5 (t, **C_{223}**(Ar)), 128.3 (t, **C_4**(Ar), **C_6**(Ar)), 127.2 (t, **C_9**(Ar), **C_{13}**(Ar)), 124.0 (t, **C_{221}**(Ar)), 122.6 (t, **C_{222}**(Ar)), 119.3 (q, **C_1**(CN)), 115.5 (t, **C_{227}**/**C_{229}**(Ar)), 115.2 (t, **C_{227}**/**C_{229}**(Ar)), 115.1 (t, **C_{10}**(Ar), **C_{12}**(Ar)), 110.2 (q, **C_2**(Ar)), 68.0 (s, **C_{14}**(OCH_2), **C_{18}**(OCH_2)), 29.1 (s, **$C_{15\text{-}17}$**(CH_2)), 25.9 (s, **$C_{15\text{-}17}$**(CH_2)) ppm.

IR (Solid) ν_{max}: 2952(m) (**C-H$_2$**), 2853(m) (**C-H$_2$**), 2220 (m) (**C≡N**), 1601(s) (**Ar**), 1523(s) (**Ar**), 1492(s) (**Ar**) cm^{-1}.

EIMS: *m/z* 535 ($[M]^+$, 73%), 341 ($[C_{18}H_{17}F_4O_2]^+$, 29%), 272 ($[C_{13}H_8F_4O_2]^+$, 62%), 195 ($[C_{13}H_9NO]^+$, 67%), 170 ($[C_{12}H_9F]^+$, 8%), 69 ($[C_5H_9]^+$, 100%), 41 ($[C_3H_5]^+$, 28%)

1 -(4'-Cyanobiphenyl-4-oxy-)-6-(3,3',4',5'-tetrafluorobiphenyl-4-oxy-)-hexane

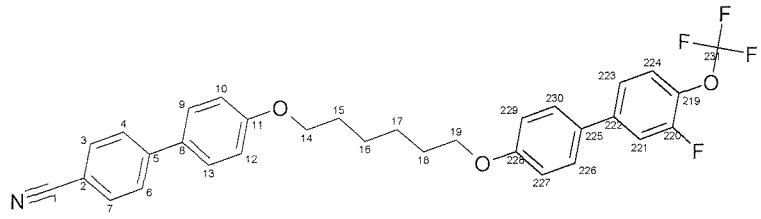

36
$C_{32}H_{27}F_4NO_3$
549.57

Rf 0.72; 100% DCM [1 spot by TLC]

^{1}H NMR (300 MHz, $CDCl_3$): δ_H 7.71 (2H, d, J = 8.6 Hz, C_4**H**,C_6**H**), 7.64 (2H, d, J = 8.6 Hz, C_3**H**, C_7**H**), 7.54 (2H, d, J = 8.8 Hz, C_9**H**, C_{13}**H**), 7.48 (2H, d, J = 6.4 Hz, C_{230}**H**, C_{226}**H**), 7.28-7.41 (3H, m, C_{224}**H**, C_{221}**H**, C_{223}**H**), 7.02 (1H, d, J = 6.8 Hz, C_{227}**H**$_2$, C_{229}**H**$_2$), 7.01 (2H, d, J = 7.8 Hz, C_{10}**H**, C_{12}**H**), 4.04 (2H, t, J = 6.2 Hz, O-C_{14}**H**$_2$), 4.03 (2H, t, J = 6.2 Hz, O-C_{19}**H**$_2$), 1.83-1.94 (4H, m, C_{15}**H**$_2$, C_{18}**H**$_2$), 1.53-1.66 (4H, m, C_{16}**H**$_2$, C_{17}**H**$_2$) ppm.

^{13}C NMR (75 MHz, $CDCl_3$): δ_C 159.9 (q, **C_{11}**(Ar)), 159.5 (q, **C_{228}**(Ar)), 153.2 (q, **C_{219}**(Ar)), 145.4 (q, **C_5**(Ar)), 142.8 (q, **C_{220}**(Ar)), 132.7 (t, **C_3** (Ar), **C_7**(Ar)), 131.5 (q, **C_8**(Ar)), 131.2 (q, **C_{225}**(Ar)), 128.5 (t, **C_{223}**(Ar)), 128.3 (t, **C_4**(Ar), **C_6**(Ar)), 127.2 (t, **C_9**(Ar), **C_{13}**(Ar)), 124.0 (t, **C_{221}**(Ar)), 122.6 (t, **C_{222}**(Ar)), 119.3 (q, **C_1**(CN)), 115.5 (t, **C_{227}**/**C_{229}**(Ar)), 115.2 (t, **C_{227}**/**C_{229}**(Ar)), 115.1 (t, **C_{10}**(Ar), **C_{12}**(Ar)), 110.2 (q, **C_2**(Ar)), 68.1 (s, **C_{14}**(OCH_2), **C_{19}**(OCH_2)), 29.1 (s, **$C_{15\text{-}18}$**(CH_2)), 25.9 (s, **$C_{15\text{-}18}$**(CH_2)) ppm.

^{19}F NMR (282 MHz, C_6F_6): 103 (3F, s, C_{231}**F**$_3$), 33.1 (1F, s, C_{220}**F**)

IR (Solid) ν_{max}: 2937(m) (**C-H**$_2$), 2865(m) (**C-H**$_2$), 2234 (m) (**C≡N**), 1603(s) (**Ar**), 1503(s) (**Ar**) cm^{-1}.

EIMS: *m/z* 549 ($[M]^+$, 100%), 272 ($[C_{13}H_8F_4O_2]^+$, 89%), 195 ($[C_{13}H_9NO]^+$, 88%), 178 ($[C_{12}H_{18}O]^+$, 10%), 55 ($[C_5H_9]^+$, 57%)

1 -(4'-Cyanobiphenyl-4-oxy-)-7-(3,3',4',5'-tetrafluorobiphenyl-4-oxy-)-heptane

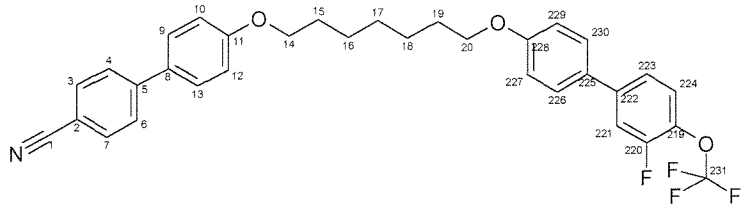

37
$C_{33}H_{29}F_4NO_3$
563.60

Rf 0.73; 100% DCM [1 spot by TLC]

^{1}H NMR (400 MHz, $CDCl_3$): δ_H 7.61 (2H, d, J = 8.5 Hz, C_4**H**, C_6**H**), 7.56 (2H, d, J = 8.5 Hz, C_3**H**, C_7**H**), 7.45 (2H, d, 9.0 Hz, C_9**H**, C_{13}**H**), 7.38 (2H, d, 9.0 Hz, C_{226}**H**, C_{230}**H**), 7.21-7.31 (3H, m, C_{221}**H**, C_{223}**H**, C_{224}**H**), 6.94 (2H, d, J = 8.2 Hz, C_{227}**H**, C_{229}**H**), 6.92 (2H, d, J = 9.0 Hz, C_{10}**H**, C_{12}**H**), 6.89 (2H, d, J = 8.5 Hz, C_{22}**H**, C_{26}**H**), 3.95 (2H, t, 6.5 Hz, O-C_{14}**H$_2$**), 3.91 (2H, t, 6.5 Hz, C_{20}**H$_2$**-O), 1.78 (4H, m, 6.5 Hz C_{15}**H$_2$**, C_{19}**H$_2$**), 1.48 (6H, m, C_{16}**H$_2$**, C_{17}**H$_2$**, C_{18}**H$_2$**) ppm.

^{13}C NMR (75 MHz, $CDCl_3$): δ_C 160.1 (q, **C_{11}**(Ar)), 159.7 (q, **C_{228}**(Ar)), 153.3 (q, **C_{219}**(Ar)), 145.6 (q, **C_5**(Ar)), 143.0 (q, **C_{220}**(Ar)), 132.9 (t, **C_3** (Ar), **C_7**(Ar)), 131.7 (q, **C_8**(Ar)), 131.4 (q, **C_{225}**(Ar)), 128.7 (t, **C_{223}**(Ar)), 128.5 (t, **C_4**(Ar), **C_6**(Ar)), 127.5 (t, **C_9**(Ar), **C_{13}**(Ar)), 124.3 (t, **C_{221}**(Ar)), 122.8 (t, **C_{222}**(Ar)), 119.5 (q, **C_1**(CN)), 115.7 (t, **C_{227}**/**C_{229}**(Ar)), 115.5 (t, **C_{227}**/**C_{229}**(Ar)), 115.4 (t, **C_{10}**(Ar), **C_{12}**(Ar)), 110.4 (q, **C_2**(Ar)), 68.4 (s, **C_{14}**(OCH_2), **C_{20}**(OCH_2)), 29.6 (s, **$C_{15\text{-}19}$**(CH_2)), 29.5 (s, **$C_{15\text{-}19}$**(CH_2)), 26.4 (s, **$C_{15\text{-}19}$**(CH_2)) ppm.

^{19}F NMR (282 MHz, C_6F_6): 103.9 (3F, s, C_{231}**F$_3$**), 33.4 (1F, s, C_{220}**F**)

IR (Solid) ν_{max}: 2937(m) (**C-H$_2$**), 2864(m) (**C-H$_2$**), 2229 (m) (**C≡N**), 1603(s) (**Ar**), 1494(s) (**Ar**) cm^{-1}.

EIMS: *m/z* 563 ($[M]^+$, 100%), 268 ($[C_{19}H_{20}F_4O_2]^+$, 4%), 272 ($[C_{13}H_8F_4O_2]^+$, 91%), 195 ($[C_{13}H_9NO]^+$, 85%), 178 ($[C_{12}H_{18}O]^+$, 7%), 69 ($[C_5H_9]^+$, 57%), 55 ($[C_4H_7]^+$, 51%)

1 -(4'-cyanobiphenyl-4-oxy-)-8-(3,3',4',5'-tetrafluorbiphenyl-4-oxy-)-octane

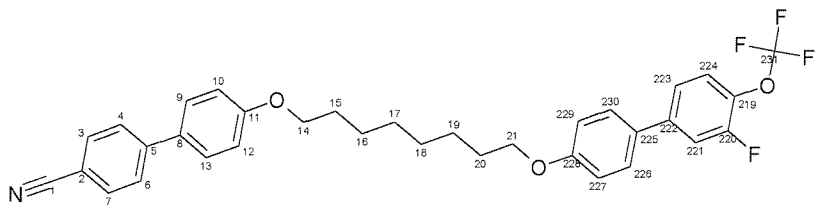

38
$C_{34}H_{31}F_4NO_3$
577.65

Rf 0.74; 100% DCM [1 spot by TLC]

^{1}H NMR (400 MHz, $CDCl_3$): δ_H 7.60 (2H, d, J = 8.5 Hz, C_4**H**, C_6**H**), 7.54 (2H, d, J = 8.5 Hz, C_3**H**, C_7**H**), 7.37 (2H, d, 9.0 Hz, C_9**H**, C_{13}**H**), 7.38 (2H, d, 9.0 Hz, C_{226}**H**, C_{230}**H**), 7.24 (3H, m, C_{221}**H**, C_{223}**H**, C_{224}**H**), 6.92 (2H, d, J = 9.0 Hz, C_{10}**H**, C_{12}**H**), 6.89 (2H, d, J = 8.5 Hz, C_{227}**H**, C_{229}**H**), 3.93 (2H, t, 6.5 Hz, O-C_{14}**H$_2$**), 3.92 (2H, t, 6.5 Hz, C_{21}**H$_2$**-O), 1.78 (4H, m, 6.5 Hz C_{15}**H$_2$**, C_{20}**H$_2$**), 1.48 (8H, m, C_{16}**H$_2$**, C_{17}**H$_2$**, C_{18}**H$_2$**, C_{19}**H$_2$**) ppm.

^{13}C NMR (100 MHz, $CDCl_3$): δ_C 160.2 (q, **C_{11}**(Ar)), 159.8 (q, **C_{228}**(Ar)), 153.7 (q, **C_{219}**(Ar)), 145.6 (q, **C_5**(Ar)), 142.1 (q, **C_{220}**(Ar)), 133.0 (t, **C_3** (Ar), **C_7**(Ar)), 131.7 (q, **C_8**(Ar)), 131.4 (q, **C_{225}**(Ar)), 128.7 (t, **C_{223}**(Ar)), 128.5 (t, **C_4**(Ar), **C_6**(Ar)), 127.5 (t, **C_9**(Ar), **C_{13}**(Ar)), 124.3 (t, **C_{221}**(Ar)), 122.9 (t, **C_{222}**(Ar)), 119.7 (q, **C_1**(CN)), 115.7 (t, **C_{227}**/**C_{229}**(Ar)), 115.5 (t, **C_{227}**/**C_{229}**(Ar)), 115.4 (t, **C_{10}**(Ar), **C_{12}**(Ar)), 110.5 (q, **C_2**(Ar)), 68.4 (s, **C_{14}**(OCH_2), **C_{21}**(OCH_2)), 29.6 (s, **$C_{15\text{-}19}$**(CH_2)), 26.4 (s, **$C_{15\text{-}19}$**(CH_2)) ppm.

^{19}F NMR (282 MHz, C_6F_6): 103.6 (3F, s, C_{231}**F$_3$**), 33.3 (1F, s, C_{220}**F**)

IR (Solid) ν_{max}: 2933(m) (**C-H$_2$**), 2865(m) (**C-H$_2$**), 2225 (m) (**C≡N**), 1602(s) (**Ar**), 1501(s) (**Ar**) cm^{-1}.

EIMS: *m/z* 577 ($[M]^+$, 100%), 272 ($[C_{13}H_8F_4O_2]^+$, 91%), 195 ($[C_{13}H_9NO]^+$, 85%), 166 ($[C_{11}H_{18}O]^+$, 7%), 69 ($[C_5H_9]^+$, 57%), 55 ($[C_4H_7]^+$, 51%)

1 -(4'-Cyanobiphenyl-4-oxy-)-9-(3,3',4',5'-tetrafluorobiphenyl-4-oxy-)-nonane

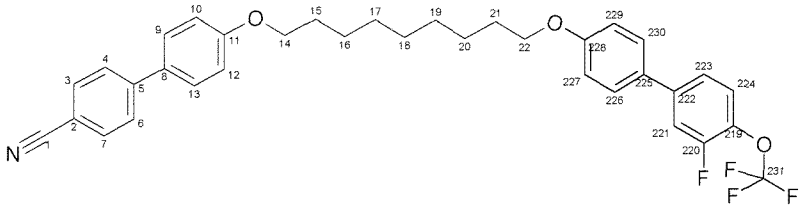

39
$C_{35}H_{33}F_4NO_3$
591.65

Rf 0.74;100% DCM [1 spot by TLC]

^{1}H NMR (400 MHz, $CDCl_3$): δ_H 7.61 (2H, d, J = 8.5 Hz, C_4**H**, C_6**H**), 7.55 (2H, d, J = 8.5 Hz, C_3**H**, C_7**H**), 7.44 (2H, d, 8.8 Hz, C_9**H**, C_{13}**H**), 7.38 (2H, d, 9.0 Hz, C_{226}**H**, C_{230}**H**), 7.20-7.30 (3H, m, C_{221}**H,** C_{223}**H,** C_{224}**H**), 6.90 (2H, d, J = 9.0 Hz, C_{10}**H**, C_{12}**H**), 6.90 (2H, d, J = 9.0 Hz, C_{227}**H**, C_{229}**H**), 3.93 (2H, t, 6.5 Hz, O-C_{14}**H$_2$**), 3.92 (2H, t, 6.5 Hz, C_{22}**H$_2$**-O), 1.69-1.79 (4H, m, C_{15}**H$_2$**, C_{21}**H$_2$**), 1.27-1.45 (10H, m, C_{16}**H$_2$**, C_{17}**H$_2$**, C_{18}**H$_2$**, C_{19}**H$_2$**, C_{20}**H$_2$**) ppm.

^{13}C NMR (100 MHz, $CDCl_3$): δ_C 160.2 (q, **C_{11}**(Ar)), 159.9 (q, **C_{228}**(Ar)), 156.3 (q, **C_{219}**(Ar)), 145.7 (q, **C_5**(Ar)), 142.1 (q, **C_{220}**(Ar)), 133.0 (t, **C_3**(Ar), **C_7**(Ar)), 131.7 (q, **C_8**(Ar)), 131.4 (q, **C_{225}**(Ar)), 128.7 (t, **C_4**(Ar), **C_6**(Ar)), 128.5 (t, **C_{223}**(Ar)), 127.5 (t, **C_9**(Ar), **C_{13}**(Ar)), 124.2 (t, **C_{221}**(Ar)), 122.9 (t, **C_{222}**(Ar), **C_6**(Ar)), 119.5 (q, **C_1**(**C**N)), 115.7 (t, **C_{227}**/**C_{229}** (Ar)), 115.5 (t, **C_{10}**(Ar), **C_{12}**(Ar)), 115.4 (t, **C_{227}**/**C_{229}**(Ar)), 110.5 (q, **C_2**(Ar)), 68.5 (s, **C_{14}** (OCH_2), **C_{22}** (OCH_2)), 29.9 (s, **$C_{15\text{-}21}$**(CH_2)), 29.7 (s, **$C_{15\text{-}21}$**(CH_2)), 29.6 (s, **$C_{15\text{-}21}$**(CH_2)), 26.4 (s, **$C_{15\text{-}21}$**(CH_2)) ppm.

^{19}F NMR (282 MHz, C_6F_6): 103.7 (3F, s, C_{231}**F$_3$**), 33.4 (1F, s, C_{220}**F**)

IR (Solid) ν_{max}: 2917(m) (**C-H$_2$**), 2850(m) (**C-H$_2$**), 2224 (m) (**C≡N**), 1600(s) (**Ar**), 1493(s) (**Ar**) cm^{-1}.

EIMS: *m/z* 591 ($[M]^+$, 100%), 396 ($[C_{22}H_{25}O_2F_4]^+$, 8%), 319 ($[C_{22}H_{25}NO]^+$, 8%), 272 ($[C_{13}H_8O_2F_4]^+$, 93%), 195 ($[C_{13}H_9NO]^+$, 80%), 178 ($[C_7H_4F_4O]^+$, 5%), 69 ($[C_5H_9]^+$, 21%), 55 ($[C_4H_7]^+$, 21%).

1 -(4'-cyanobiphenyl-4-oxy-)-10-(3,3',4',5'-tetrafluorbiphenyl-4-oxy-)-decane

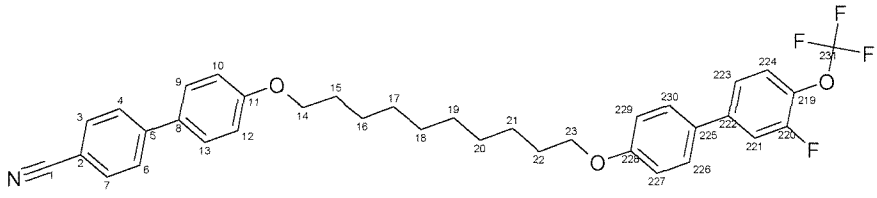

40
$C_{36}H_{35}F_4NO_3$
605.68

Rf 0.76;100% DCM [1 spot by TLC]

^{1}H NMR (400 MHz, $CDCl_3$): δ_H 7.61 (2H, d, J = 8.6 Hz, C_4**H**, C_6**H**), 7.56 (2H, d, J = 8.6 Hz, C_3**H**, C_7**H**), 7.45 (2H, d, J = 8.8 Hz, C_9**H**, C_{13}**H**), 7.38 (2H, d, 9.0 Hz, C_{226}**H**, C_{230}**H**), 7.28 (1H, dd, J = 11.8 Hz, 1.6 Hz, C_{224}**H**), 7.24 (2H, d, J = 5.4 Hz, C_{221}**H**, C_{223}**H**), 6.92 (2H, d, J = 9.0 Hz, C_{10}**H**, C_{12}**H**), 6.89 (2H, d, J = 9.0

Hz, C_{227}**H**, C_{229}**H**), 3.93 (2H, t, 6.5 Hz, O-C_{14}**H$_2$**), 3.92 (2H, t, 6.5 Hz, C_{23}**H$_2$**-O), 1.67-1.83 (4H, m, C_{15}**H$_2$**, C_{22}**H$_2$**), 1.18-1.51 (12H, m, C_{16}**H$_2$**, C_{17}**H$_2$**, C_{18}**H$_2$**, C_{19}**H$_2$**, C_{20}**H$_2$**, C_{21}**H$_2$**) ppm.

^{13}C NMR (100 MHz, $CDCl_3$): δ_C 159.8 (q, **C_{11}**(Ar)), 159.4 (q, **C_{228}**(Ar)), 155.9 (q, **C_{219}**(Ar)), 145.3 (q, **C_5**(Ar)), 141.7 (q, **C_{220}**(Ar)), 132.6 (t, **C_3** (Ar), **C_7**(Ar)), 131.3 (q, **C_8**(Ar)), 131.0 (q, **C_{225}**(Ar)), 128.3 (t, **C_4**(Ar), **C_6**(Ar)), 128.1 (t, **C_{223}**(Ar)), 127.1 (t, **C_9**(Ar), **C_{13}**(Ar)), 123.8 (t, **C_{221}**(Ar)), 122.4 (t, **C_{222}**(Ar), **C_6**(Ar)), 119.1 (q, **C_1**(**C**N)), 115.4 (t, **C_{227}**/**C_{229}** (Ar)), 115.1 (t, **C_{10}**(Ar), **C_{12}**(Ar)), 115.0 (t, **C_{227}**(Ar)/**C_{229}**(Ar)), 110.1 (q, **C_2**(Ar)), 68.2 (s, **C_{14}** (OCH_2), **C_{23}** (OCH_2)), 29.9 (s, **$C_{15\text{-}22}$**(CH_2)), 29.7 (s, **$C_{15\text{-}22}$**(CH_2)), 29.6 (s, **$C_{15\text{-}22}$**(CH_2)), 26.4 (s, **$C_{15\text{-}22}$**(CH_2)) ppm.

IR (Solid) ν_{max}: 2933(m) (**C-H$_2$**), 2851(m) (**C-H$_2$**), 2234 (m) (**C≡N**), 1604(s) (**Ar**), 1502(s) (**Ar**) cm^{-1}.

EIMS: *m/z* 605 ($[M]^+$, 100%), 410 ($[C_{23}H_{23}O_2F_4]^+$, 8%), 333 ($[C_{23}H_{27}NO]^+$, 9%), 272 ($[C_{13}H_8O_2F_4]^+$, 74%), 195 ($[C_{13}H_9NO]^+$, 100%), 178 ($[C_7H_4F_4O]^+$, 5%), 69 ($[C_5H_9]^+$, 31%), 55 ($[C_4H_7]^+$, 18%).

1 -(4'-Cyanobiphenyl-4-oxy-)-11-(3,3',4',5'-tetrafluorobiphenyl-4-oxy-)-undecane

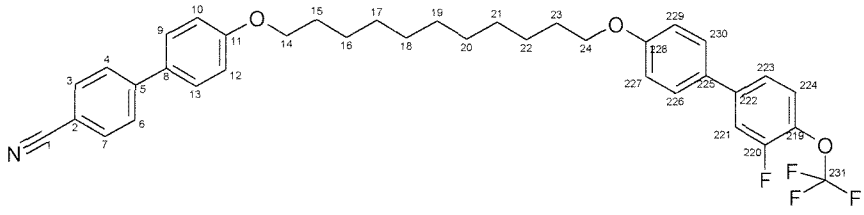

41
$C_{37}H_{37}F_4NO_3$
619.71

Rf 0.75;100% DCM [1 spot by TLC]

^{1}H NMR (400 MHz, $CDCl_3$): δ_H 7.61 (2H, d, J = 8.6 Hz, C_4**H**, C_6**H**), 7.56 (2H, d, J = 8.6 Hz, C_3**H**, C_7**H**), 7.45 (2H, d, J = 8.6 Hz, C_9**H**, C_{13}**H**), 7.38 (2H, d, 8.8 Hz, C_{226}**H**, C_{230}**H**), 7.20-7.32 (1H, m, C_{221}**H**, C_{223}**H**, C_{224}**H**), 6.92 (2H, d, J = 7.0 Hz, C_{10}**H**, C_{12}**H**), 6.89 (2H, d, J = 6.9 Hz, C_{227}**H**, C_{229}**H**), 3.93 (2H, t, 6.4 Hz, O-C_{14}**H$_2$**), 3.92 (2H, t, 6.4 Hz, C_{24}**H$_2$**-O), 1.63-1.82 (4H, m, C_{15}**H$_2$**, C_{23}**H$_2$**), 1.18-1.51 (14H, m, C_{16}**H$_2$**, C_{17}**H$_2$**, C_{18}**H$_2$**, C_{19}**H$_2$**, C_{20}**H$_2$**, C_{21}**H$_2$**, C_{22}**H$_2$**) ppm.

^{13}C NMR (100 MHz, $CDCl_3$): δ_C 159.8 (q, **C_{11}**(Ar)), 159.4 (q, **C_{228}**(Ar)), 154.0 (q, **C_{219}**(Ar)), 145.1 (q, **C_5**(Ar)), 143.3 (q, **C_{220}**(Ar)), 132.6 (t, **C_3** (Ar), **C_7**(Ar)),

131.3 (q, C_8(Ar)), 131.0 (q, C_{225}(Ar)), 128.3 (t, C_4(Ar), C_6(Ar)), 128.1 (t, C_{223}(Ar)), 127.1 (t, C_9(Ar), C_{13}(Ar)), 123.9 (t, C_{221}(Ar)), 122.5 (t, C_{222}(Ar), C_6(Ar)), 119.1 (q, C_1(CN)), 115.4 (t, C_{227}/C_{229} (Ar)), 115.1 (t, C_{10}(Ar), C_{12}(Ar)), 115.0 (t, C_{227}(Ar)/C_{229}(Ar)), 110.1 (q, C_2(Ar)), 68.2 (s, C_{14} (OCH_2), C_{23} (OCH_2)), 29.5 (s, $C_{15\text{-}22}$(CH_2)), 29.4 (s, $C_{15\text{-}22}$(CH_2)), 29.2 (s, $C_{15\text{-}22}$(CH_2)), 26.0 (s, $C_{15\text{-}22}$(CH_2)) ppm.

IR (Solid) ν_{max}: 2915(m) (**C-H$_2$**), 2852(m) (**C-H$_2$**), 2221 (m) (**C≡N**), 1601(s) (**Ar**), 1493(s) (**Ar**) cm^{-1}.

EIMS: *m/z* 619 ($[M]^+$, 65%), 424 ($[C_{24}H_{25}O_2F_4]^+$, 9%), 347 ($[C_{24}H_{29}NO]^+$, 9%), 272 ($[C_{13}H_8O_2F_4]^+$, 86%), 195 ($[C_{13}H_9NO]^+$, 100%), 69 ($[C_5H_9]^+$, 8%), 55 ($[C_4H_7]^+$, 19%).

7.2.6. $F_3COFBOnOBFOCF_3$; α,ω-*bis*-(3'-fluoro-4'-trifluoromethoxybiphenyl-4-yloxy)-alkane

n	Temperature /°C			Mass	Yield
	Cr		I	g	%
7	•	109	•	0.60	37
9	•	92	•	1.11	91

1,7-*bis*-(3'-Fluoro-4'-trifluoromethoxybiphenyl-4-yloxy)-heptane

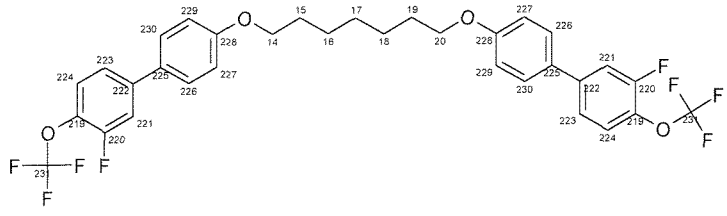

42
$C_{33}H_{28}F_8O_4$
640.58

Procedure:

To a stirred solution of 3'-fluoro-4'-trifluoromethoxybiphenol-4-ol (1.50 g, 5.51 mMol, 2.2 eq) in distilled butan-2-one (40 mL) was added solid potassium carbonate (2.53 g, 18.35 mMol, 7.3 eq) in one portion. The mixture was heated to reflux for 20 min and then allowed to cool before the addition of 1,7-dibromoheptane (0.43 mL, 0.65g, 2.50 mMol, 1 eq) in one portion. The reaction mixture was then heated to reflux for 6 days and then were allowed to cool. Water (30 mL) and DCM (50 mL) were added and the inorganic salts dissolved into the aqueous layer. The layers were separated and the aqueous solution

was washed repeatedly with DCM (3 x 40 mL). The organics were combined and dried over anhydrous $MgSO_4$ and filtered. The organic solvents were removed *in vacuo* to give a crude light brown solid. The crude material was purified by column chromatography (silica gel, 40 mm x 100 mm, 2-10% ether / 40-60 petroleum) affording a white solid, the title compound **42** (596 mg, 0.93 mMol, 37.2%) as fine micro-crystalline white solid.

Rf 0.64; 80% DCM / 40-60 petroleum [1 spot by TLC]

^{1}H NMR (400 MHz, $CDCl_3$): δ_H 7.39 (4H, d, 8.8 Hz, C_{226}**H**,C_{230}**H**), 7.19-7.32 (6H, m, C_{221}**H**, C_{223}**H**, C_{224}**H**), 6.89 (4H, d, J = 8.8 Hz, C_{227}**H**, C_{229}**H**), 3.93 (4H, t, 6.4 Hz, O-C_{14}**H$_2$**, C_{20}**H$_2$**-O), 1.70-1.83 (4H, m, J = 6.5 Hz C_{15}**H$_2$**, C_{19}**H$_2$**), 1.35-1.52 (6H, m, C_{16}**H$_2$**, C_{17}**H$_2$**, C_{18}**H$_2$**) ppm.

^{13}C NMR (100 MHz, $CDCl_3$): δ_C 158.3 (q, **C_{228}**(Ar)), 154.9 (q, **C_{219}**(Ar)), 140.7 (q, **C_{220}**(Ar)), 130.0 (q, **C_{225}**(Ar)), 127.0 (t, **C_{223}**(Ar)), 122.1 (t, **C_{221}**(Ar)), 121.3 (t, **C_{222}**(Ar), **C_6**(Ar)), 114.2 (t, **C_{227}**/**C_{229}** (Ar)), 114.0 (t, **C_{227}**(Ar)/**C_{229}**(Ar)), 67.0 (s, **C_{14}**(OCH_2), **C_{23}**(OCH_2)), 28.7 (s, **$C_{15\text{-}22}$**(CH_2)), 28.1 (s, **$C_{15\text{-}22}$**(CH_2)), 27.2 (s, **$C_{15\text{-}22}$**(CH_2)), 25.1 (s, **$C_{15\text{-}22}$**(CH_2)) ppm.

^{19}F NMR (C_6F_6): **Not Obtained**

IR (Solid) ν_{max}: 2983(m) (**C-H$_2$**), 2302 (m) (**C≡N**), 1607(s) (**Ar**), 1501(s) (**Ar**) cm^{-1}.

EIMS: *m/z* 668 ($[M]^+$, 66%), 396 ($[C_{22}H_{23}F_4O]^+$, 4%), 272 ($[C_{13}H_8O_2F_4]^+$, 100%), 203 ($[C_{12}H_7FO_2]$, 14%), 83 ($[C_6H_{11}]^+$, 11%), 55 ($[C_4H_7]^+$, 12%).

1,9-*bis*-(3'-Fluoro-4'-trifluoromethoxybiphenyl-4-yl)-oxynonane

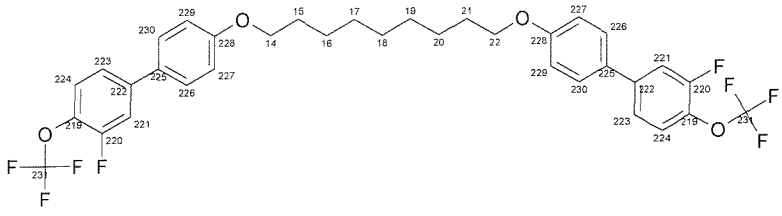

43
$C_{35}H_{32}F_8O_4$
668.63

Rf 0.71; 80% DCM / 40-60 petroleum

^{1}H NMR (400 MHz, $CDCl_3$): δ_H 7.38 (4H, d, 8.8 Hz, C_{226}**H**, C_{230}**H**), 7.17-7.30 (6H, m, C_{221}**H**, C_{223}**H**, C_{224}**H**), 6.89 (4H, d, J = 8.8 Hz, C_{227}**H**, C_{229}**H**), 3.93 (2H, t, 6.5 Hz, O-C_{14}**H$_2$**, C_{22}**H$_2$**-O), 1.78 (4H, quin, J = 6.5 Hz C_{15}**H$_2$**, C_{21}**H$_2$**), 1.28-1.47 (10H, m, C_{16}**H$_2$**, C_{17}**H$_2$**, C_{18}**H$_2$** C_{19}**H$_2$**, C_{20}**H$_2$**) ppm.

^{13}C NMR (100 MHz, $CDCl_3$): δ_C 159.8 (q, $\mathbf{C_{228}}$(Ar)), 156.3 (q, $\mathbf{C_{219}}$(Ar)), 142.1 (q, $\mathbf{C_{220}}$(Ar)), 131.4 (q, $\mathbf{C_{225}}$(Ar)), 128.5 (t, $\mathbf{C_{223}}$(Ar)), 124.3 (t, $\mathbf{C_{221}}$(Ar)), 122.8 (t, $\mathbf{C_{222}}$(Ar), $\mathbf{C_6}$(Ar)), 115.7 (t, $\mathbf{C_{227}}$/$\mathbf{C_{229}}$ (Ar)), 115.5 (t, $\mathbf{C_{227}}$(Ar)/$\mathbf{C_{229}}$(Ar)), 68.2 (s, $\mathbf{C_{14}}$(OCH_2), $\mathbf{C_{23}}$(OCH_2)), 29.9 (s, $\mathbf{C_{15\text{-}22}}$($CH_2$)), 29.7 (s, $\mathbf{C_{15\text{-}22}}$($CH_2$)), 29.6 (s, $\mathbf{C_{15\text{-}22}}$($CH_2$)), 26.4 (s, $\mathbf{C_{15\text{-}22}}$($CH_2$)) ppm.

^{19}F NMR (282 MHz, C_6F_6): **Not Obtained**

IR (Solid) ν_{max}: 2984(m) (**C-H$_2$**), 2301 (m) (**C≡N**), 1600(s) (**Ar**), 1501(s) (**Ar**) cm^{-1}.

EIMS: *m/z* 668 ($[M]^+$, 65%), 396 ($[C_{22}H_{25}F_4O]^+$, 5%), 272 ($[C_{13}H_8O_2F_4]^+$, 100%), 203 ($[C_{12}H_7FO_2]^+$, 16%), 83 ($[C_6H_{11}]^+$, 6%), 55 ($[C_4H_7]^+$, 12%).

7.3. Chapter 4 experimental

7.3.1. 3CHPOnOPCH3; α,ω-bis-(4'-propyl-1'-cyclohexyl-4-phenyloxy)alkane

n	Temperature /°C					Mass	Yield
	Cr		N		I	mg	%
6	•	136	•	150	•	549	71
7	•	88	•	(81)	•	356	45
8	•	109	•	132	•	308	71
9	•	91	•	101	•	259	41
10	•	111	•	129	•	300	34
11	•	95	•	102	•	233	27
12	•	111	•	117	•	510	57

1,6-bis-(4'-Propyl-1'-cyclohexylphenyl-4-oxy)hexane

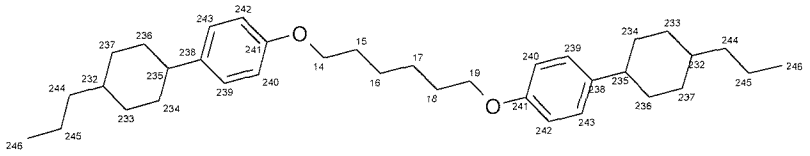

44
$C_{36}H_{54}O_2$
518.83

To a stirred solution of 4-hydroxyphenyl-1-cyclohexyl-4'-propane (0.70 g, 3.21 mMol, 2.15 eq) in butan-2-one (40 mL) was added potassium carbonate (979 mg, 7.06 mMol, 4.73 eq) in one portion. The suspension was heated to reflux and stirred for 20 min before the addition of 1,6-dibromohexane (363 mg, 229 μL, 1.49 mMol, 1 eq) and a catalytic quantity of sodium iodide (80 mg). The solution was stirred at reflux for approximately 3 days and then allowed to cool. The solvents were removed *in vacuo* leaving a creamy-while solid. Water (50 mL) and then DCM (50 mL) were added. The inorganic salts

dissolved into the aqueous layer whilst the organic product dissolved into the DCM. The layers were separated and the aqueous solution was washed repeatedly with DCM (3 x 50 mL). The organics were combined, dried over anhydrous $MgSO_4$ and filtered. The organics were then removed *in vacuo* to give the crude white product. This was then purified by crystalisation from acetonitrile (~100 mL) to yield the title compound **44** as a white microcrystalline solid (549 mg, 1.05 mMol, 71%).

Rf 0.88; 100% DCM

^{1}H NMR (400 MHz, $CDCl_3$): δ_H 7.03 (4H, d, J = 8.5 Hz, $C_{239}\mathbf{H}$, $C_{243}\mathbf{H}$), 6.74 (2H, d, J = 8.8 Hz, $C_{240}\mathbf{H}$, $C_{242}\mathbf{H}$), 3.86 (4H, t, 6.4 Hz, O-$C_{14}\mathbf{H_2}$, O-$C_{19}\mathbf{H_2}$), 2.33 (2H, tt, J = 12.0 Hz, 3.1 Hz, $C_{235}\mathbf{H}$), 1.64-1.86 (12H, m, $C_{15}\mathbf{H_2}$, $C_{18}\mathbf{H_2}$, $C_{234}\mathbf{H_2}$, $C_{236}\mathbf{H_2}$), 1.07-1.50 (18H, m, $C_{16}\mathbf{H_2}$, $C_{17}\mathbf{H_2}$, $C_{232}\mathbf{H}$, $C_{233}\mathbf{H_2}$, $C_{237}\mathbf{H_2}$, $C_{245}\mathbf{H_2}$), 0.89-1.02 (4H, m, $C_{244}\mathbf{H_2}$), 0.83 (6H, t, J = 7.3 Hz, $C_{245}\mathbf{H_2}$) ppm.

^{13}C NMR (100 MHz, $CDCl_3$): δ_C 157.1 (q, $\mathbf{C_{241}}$(Ar)), 139.9 (q, $\mathbf{C_{238}}$(Ar)), 127.5 (t, $\mathbf{C_{239}}$ (Ar), $\mathbf{C_{243}}$(Ar)), 114.2 (t, $\mathbf{C_{240}}$(Ar), $\mathbf{C_{242}}$(Ar)), 67.7 (s, $\mathbf{C_{14}}$(OCH_2), $\mathbf{C_{19}}$(OCH_2)), 43.6 (t, $\mathbf{C_{235}}$(CH)), 39.7 (s, $\mathbf{C_{244}}$(CH_2)), 36.9 (t, $\mathbf{C_{232}}$(CH)), 34.5 (s, $\mathbf{C_{234}}$(CH_2), $\mathbf{C_{236}}$(CH_2)), 33.5 (s, $\mathbf{C_{234}}$(CH_2), $\mathbf{C_{236}}$(CH_2)), 29.2 (s, $\mathbf{C_{15\text{-}18}}$($CH_2$)), 25.8 (s, $\mathbf{C_{15\text{-}18}}$($CH_2$)), 19.9 (s, $\mathbf{C_{245}}$(CH_2)), 14.3 (s, $\mathbf{C_{246}}$(CH_3)) ppm.

IR (Solid) ν_{max}: 2949(m) (**C-H$_2$**), 2913(m) (**C-H$_2$**), 2646(m), 2361(m), 1613(m) (**Ar**), 1561(m) (**Ar**), 1510 (s) cm^{-1}.

EIMS: *m/z* 518 ($[M]^+$, 22%), 433 ($[C_{30}H_{42}O_2]^+$, 100%), 301 ($[C_{21}H_{28}O]^+$, 100%), 218 ($[C_{15}H_{16}O]^+$, 13%), 133 ($[C_{15}H_{10}O]^+$, 100%), 83 ($[C_6H_{11}]^+$, 90%), 55 ($[C_4H_7]^+$, 64%), 41 ($[C_3H_5]^+$, 13%).

Elemental Analysis: $C_{36}H_{54}O_2$: (Expected) **C** 83.26, **H** 10.41, **N** 0.00; (Found) **C** 83.27, **H** 10.41, **N** 0.01

1,7-bis-(4'-Propyl-1'-cyclohexylphenyl-4-oxy)heptane

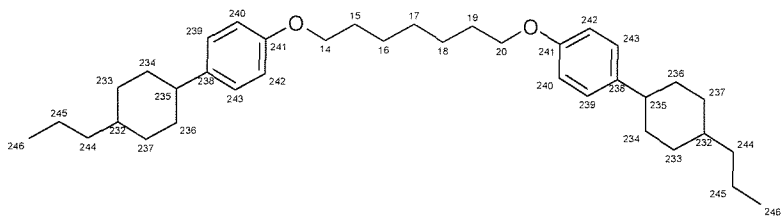

45
$C_{37}H_{56}O_2$
532.86

Rf 0.89; 100% DCM [1 spot by TLC]

^{1}H NMR (400 MHz, $CDCl_3$): δ_H 7.03 (4H, d, J = 8.7 Hz, C_{239}**H,** C_{243}**H**), 6.74 (2H, d, J = 8.7 Hz, C_{240}**H,** C_{242}**H**), 3.85 (4H, t, 6.5 Hz, O-C_{14}**H$_2$,** O-C_{20}**H$_2$**), 2.33 (2H, tt, J = 12.1 Hz, 3.1 Hz, C_{235}**H**), 1.61-1.85 (12H, m, C_{15}**H$_2$,** C_{19}**H$_2$,** C_{234}**H$_2$,** C_{236}**H$_2$**), 1.08-1.49 (20H, m, C_{16}**H$_2$,** C_{17}**H$_2$,** C_{18}**H$_2$,** C_{232}**H,** C_{233}**H$_2$,** C_{237}**H$_2$,** C_{245}**H$_2$**), 0.88-1.03 (4H, m, C_{244}**H$_2$**), 0.83 (6H, t, J = 7.3 Hz, C_{245}**H$_2$**) ppm.

^{13}C NMR (100 MHz, $CDCl_3$): δ_C 157.6 (q, **C_{241}**(Ar)), 140.4 (q, **C_{238}**(Ar)), 128.0 (t, **C_{239}** (Ar), **C_{243}**(Ar)), 114.7 (t, **C_{240}**(Ar), **C_{242}**(Ar)), 68.4 (s, **C_{14}**(OCH_2), **C_{20}**(OCH_2)), 44.2 (t, **C_{235}**(CH)), 40.2 (s, **C_{244}**(CH_2)), 37.4 (t, **C_{232}**(CH)), 35.0 (s, **C_{234}**(CH_2), **C_{236}**(CH_2)), 34.1 (s, **C_{234}**(CH_2), **C_{236}**(CH_2)), 29.7 (s, **$C_{15\text{-}19}$**(CH_2)), 26.4 (s, **$C_{15\text{-}19}$**(CH_2)), 20.4 (s, **C_{245}**(CH_2)), 14.8 (s, **C_{246}**(CH_3)) ppm.

IR (Solid) ν_{max}: 2919(m) (**C-H$_2$**), 2642(m), 2362(m), 1613(m) (**Ar**), 1512(m) (**Ar**) cm^{-1}.

EIMS: *m/z* 279 ($[C_{20}H_{23}O]^+$, 10%), 167 ($[C_{13}H_9]^+$, 30%), 149 ($[C_{10}H_{13}O]^+$, 100%), 83 ($[C_6H_{11}]^+$, 9%), 70 ($[C_4H_6O]^+$, 40%), 57 ($[C_3H_5O]^+$, 30%), 41 ($[C_3H_5]^+$, 23%).

1,8-bis-(4'-Propyl-1'-cyclohexylphenyl-4-oxy)octane

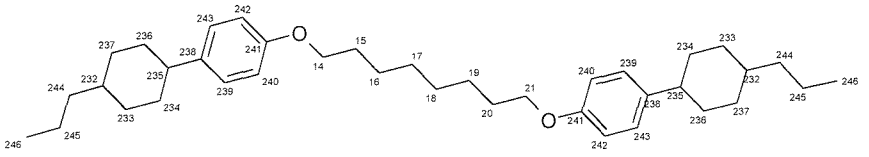

46
$C_{38}H_{58}O_2$
546.88

Rf 0.89; 100% DCM [1 spot by TLC]

^{1}H NMR (400 MHz, $CDCl_3$): δ_H 7.03 (4H, d, J = 8.6 Hz, C_{239}**H,** C_{243}**H**), 6.74 (2H, d, J = 8.7 Hz, C_{240}**H,** C_{242}**H**), 3.85 (4H, t, 6.5 Hz, O-C_{14}**H$_2$,** O-C_{21}**H$_2$**), 2.33 (2H, tt, J = 12.1 Hz, 3.1 Hz, C_{235}**H**), 1.60-1.86 (12H, m, C_{15}**H$_2$,** C_{20}**H$_2$,** C_{234}**H$_2$,** C_{236}**H$_2$**), 1.06-1.49 (22H, m, C_{16}**H$_2$,** C_{17}**H$_2$,** C_{18}**H$_2$,** C_{19}**H$_2$,** C_{232}**H,** C_{233}**H$_2$,** C_{237}**H$_2$,** C_{245}**H$_2$**), 0.88-1.03 (4H, m, C_{244}**H$_2$**), 0.83 (6H, t, J = 7.3 Hz, C_{245}**H$_2$**) ppm.

^{13}C NMR (100 MHz, $CDCl_3$): δ_C 157.6 (q, **C_{241}**(Ar)), 140.4 (q, **C_{238}**(Ar)), 128.0 (t, **C_{239}** (Ar), **C_{243}**(Ar)), 114.7 (t, **C_{240}**(Ar), **C_{242}**(Ar)), 68.4 (s, **C_{14}**(OCH_2), **C_{21}**(OCH_2)), 44.2 (t, **C_{235}**(CH)), 40.2 (s, **C_{244}**(CH_2)), 37.4 (t, **C_{232}**(CH)), 35.0

(s, $\mathbf{C_{234}}(CH_2)$, $\mathbf{C_{236}}(CH_2)$), 34.1 (s, $\mathbf{C_{234}}(CH_2)$, $\mathbf{C_{236}}(CH_2)$), 29.7 (s, $\mathbf{C_{15\text{-}20}}(CH_2)$), 26.4 (s, $\mathbf{C_{15\text{-}20}}(CH_2)$), 20.4 (s, $\mathbf{C_{245}}(CH_2)$), 14.8 (p, $\mathbf{C_{246}}(CH_3)$) ppm.

IR (Solid) ν_{max}: 2920(m) (**C-H$_2$**), 2648(m), 2361(m), 1609(m) (**Ar**), 1561(m) (**Ar**), 1509(m) (**Ar**) cm^{-1}.

EIMS: *m/z* 279 ($[C_{20}H_{23}O]^+$, 6%), 167 ($[C_{13}H_9]^+$, 27%), 149 ($[C_{10}H_{13}O]^+$, 100%), 83 ($[C_6H_{11}]^+$, 8%), 70 ($[C_4H_6O]^+$, 42%), 57 ($[C_3H_5O]^+$, 36%), 41 ($[C_3H_5]^+$, 28%).

1,9-bis-(4'-Propyl-1'-cyclohexylphenyl-4-oxy)nonane

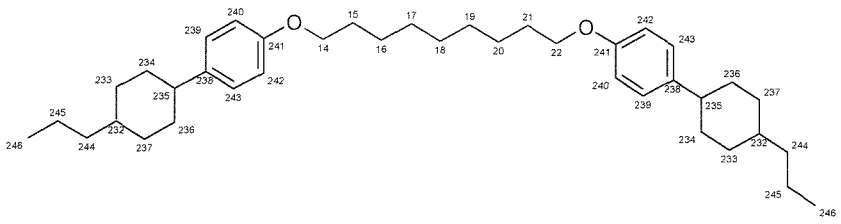

47
$C_{39}H_{60}O_2$
560.91

Rf 0.90; 100% DCM [1 spot by TLC]

^{1}H NMR (400 MHz, $CDCl_3$): δ_H 7.03 (4H, d, J = 8.7 Hz, C_{239}**H,** C_{243}**H**), 6.74 (2H, d, J = 8.7 Hz, C_{240}**H,** C_{242}**H**), 3.85 (4H, t, 6.5 Hz, O-C_{14}**H$_2$,** O-C_{22}**H$_2$**), 2.33 (2H, tt, J = 12.2 Hz, 3.1 Hz, C_{235}**H**), 1.61-1.84 (12H, m, C_{15}**H$_2$**, C_{21}**H$_2$**, C_{234}**H$_2$**, C_{236}**H$_2$**), 1.07-1.48 (24H, m, C_{16}**H$_2$,** C_{17}**H$_2$,** C_{18}**H$_2$,** C_{19}**H$_2$,** C_{20}**H$_2$,** C_{232}**H,** C_{233}**H$_2$,** C_{237}**H$_2$,** C_{245}**H$_2$**), 0.89-1.02 (4H, m, C_{244}**H$_2$**), 0.83 (6H, t, J = 7.4 Hz, C_{245}**H$_2$**) ppm.

^{13}C NMR (100 MHz, $CDCl_3$): δ_C 157.6 (q, $\mathbf{C_{241}}$(Ar)), 140.4 (q, $\mathbf{C_{238}}$(Ar)), 128.0 (t, $\mathbf{C_{239}}$ (Ar), $\mathbf{C_{243}}$(Ar)), 114.7 (t, $\mathbf{C_{240}}$(Ar), $\mathbf{C_{242}}$(Ar)), 68.4 (s, $\mathbf{C_{14}}(OCH_2)$, $\mathbf{C_{22}}(OCH_2)$), 44.2 (t, $\mathbf{C_{235}}$(CH)), 40.2 (s, $\mathbf{C_{244}}(CH_2)$), 37.5 (t, $\mathbf{C_{232}}$(CH)), 35.0 (s, $\mathbf{C_{234}}(CH_2)$, $\mathbf{C_{236}}(CH_2)$), 34.1 (s, $\mathbf{C_{234}}(CH_2)$, $\mathbf{C_{236}}(CH_2)$), 29.9 (s, $\mathbf{C_{15\text{-}21}}(CH_2)$), 29.7 (s, $\mathbf{C_{15\text{-}21}}(CH_2)$), 26.5 (s, $\mathbf{C_{15\text{-}21}}(CH_2)$), 20.4 (s, $\mathbf{C_{245}}(CH_2)$), 14.8 (p, $\mathbf{C_{246}}(CH_3)$) ppm.

IR (Solid) ν_{max}: 2920(m) (**C-H$_2$**), 2648(m), 2361(m), 1609(m) (**Ar**), 1561(m) (**Ar**), 1509(m) (**Ar**) cm^{-1}.

MS: **Not Obtained**

1,10-bis-(4'-Propyl-1'-cyclohexylphenyl-4-oxy)decane

48
$C_{40}H_{62}O_2$
574.94

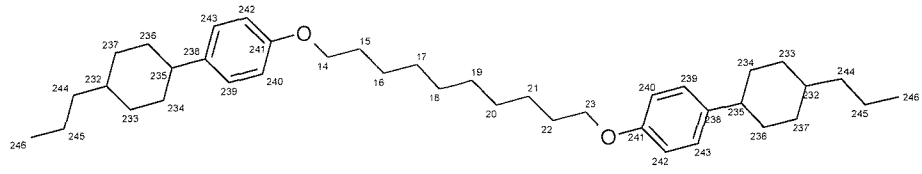

Rf 0.91; 100% DCM [1 spot by TLC]

^{1}H NMR (400 MHz, $CDCl_3$): δ_H 7.03 (4H, d, J = 8.7 Hz, C_{239}**H**, C_{243}**H**), 6.74 (2H, d, J = 8.7 Hz, C_{240}**H**, C_{242}**H**), 3.85 (4H, t, 6.5 Hz, O-C_{14}**H$_2$**, O-C_{23}**H$_2$**), 2.33 (2H, tt, J = 12.1 Hz, 3.1 Hz, C_{235}**H**), 1.61-1.85 (12H, m, C_{15}**H$_2$**, C_{22}**H$_2$**, C_{234}**H$_2$**, C_{236}**H$_2$**), 1.08-1.47 (26H, m, C_{16}**H$_2$**, C_{17}**H$_2$**, C_{18}**H$_2$**, C_{19}**H$_2$**, C_{20}**H$_2$**, C_{232}**H**, C_{233}**H$_2$**, C_{237}**H$_2$**, C_{245}**H$_2$**), 0.89-1.03 (4H, m, C_{244}**H$_2$**), 0.83 (6H, t, J = 7.2 Hz, C_{245}**H$_2$**) ppm.

^{13}C NMR (100 MHz, $CDCl_3$): δ_C 155.2 (q, **C_{241}**(Ar)), 137.9 (q, **C_{238}**(Ar)), 125.5 (t, **C_{239}** (Ar), **C_{243}**(Ar)), 112.2 (t, **C_{240}**(Ar), **C_{242}**(Ar)), 65.9 (s, **C_{14}**(OCH_2), **C_{23}**(OCH_2)), 41.8 (t, **C_{235}**(CH)), 37.7 (s, **C_{244}**(CH_2)), 35.0 (t, **C_{232}**(CH)), 32.5 (s, **C_{234}**(CH_2), **C_{236}**(CH_2)), 31.6 (s, **C_{234}**(CH_2), **C_{236}**(CH_2)), 27.4 (s, **$C_{15\text{-}22}$**(CH_2)), 27.3 (s, **$C_{15\text{-}22}$**(CH_2)), 23.9 (s, **$C_{15\text{-}22}$**(CH_2)), 18.0 (s, **C_{245}**(CH_2)), 12.3 (p, **C_{246}**(CH_3)) ppm.

IR (Solid) ν_{max}: 2919(m) (**C-H$_2$**), 2649(m), 2360(m), 1608(m) (**Ar**), 1560(m) (**Ar**), 1509(m) (**Ar**) cm^{-1}.

MS: **Not Obtained**

1,11-bis-(4'-Propyl-1'-cyclohexylphenyl-4-oxy)undecane

49
$C_{41}H_{64}O_2$
588.97

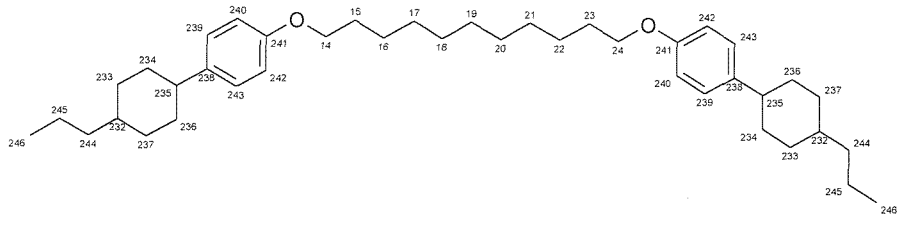

Rf 0.91; 100% DCM [1 spot by TLC]

^{1}H NMR (400 MHz, $CDCl_3$): δ_H 7.03 (4H, d, J = 8.5 Hz, C_{239}**H**, C_{243}**H**), 6.74 (2H, d, J = 8.7 Hz, C_{240}**H**, C_{242}**H**), 3.85 (4H, t, 6.5 Hz, O-C_{14}**H$_2$**, O-C_{24}**H$_2$**), 2.33 (2H, tt, J = 12.1 Hz, 3.0 Hz, C_{235}**H**), 1.60-1.85 (12H, m, C_{15}**H$_2$**, C_{23}**H$_2$**, C_{234}**H$_2$**, C_{236}**H$_2$**), 1.06-1.50 (28H, m, C_{16}**H$_2$**, C_{17}**H$_2$**, C_{18}**H$_2$**, C_{19}**H$_2$**, C_{20}**H$_2$**, C_{21}**H$_2$**,

$C_{232}\mathbf{H}$, $C_{233}\mathbf{H_2}$, $C_{237}\mathbf{H_2}$, $C_{245}\mathbf{H_2}$), 0.88-1.03 (4H, m, $C_{244}\mathbf{H_2}$), 0.83 (6H, t, J = 7.3 Hz, $C_{245}\mathbf{H_2}$) ppm.

^{13}C NMR (100 MHz, $CDCl_3$): δ_C 157.7 (q, $\mathbf{C_{241}}$(Ar)), 140.3 (q, $\mathbf{C_{238}}$(Ar)), 128.0 (t, $\mathbf{C_{239}}$ (Ar), $\mathbf{C_{243}}$(Ar)), 114.7 (t, $\mathbf{C_{240}}$(Ar), $\mathbf{C_{242}}$(Ar)), 68.4 (s, $\mathbf{C_{14}}(OCH_2)$, $\mathbf{C_{24}}(OCH_2)$), 44.2 (t, $\mathbf{C_{235}}$(CH)), 40.2 (s, $\mathbf{C_{244}}(CH_2)$), 37.5 (t, $\mathbf{C_{232}}$(CH)), 35.0 (s, $\mathbf{C_{234}}(CH_2)$, $\mathbf{C_{236}}(CH_2)$), 34.1 (s, $\mathbf{C_{234}}(CH_2)$, $\mathbf{C_{236}}(CH_2)$), 29.9 (s, $\mathbf{C_{15\text{-}23}}(CH_2)$), 27.8 (s, $\mathbf{C_{15\text{-}23}}(CH_2)$), 26.5 (s, $\mathbf{C_{15\text{-}23}}(CH_2)$), 20.5 (s, $\mathbf{C_{245}}(CH_2)$), 14.8 (p, $\mathbf{C_{246}}(CH_3)$) ppm.

IR (Solid) ν_{max}: 2915(m) (**C-H$_2$**), 2649(m), 2362(m), 1610(m) (**Ar**), 1561(m) (**Ar**), 1511(m) (**Ar**) cm^{-1}.

EIMS: *m/z* 279 ($[C_{20}H_{23}O]^+$, 8%), 167 ($[C_{13}H_9]^+$, 29%), 149 ($[C_{10}H_{13}O]^+$, 100%), 83 ($[C_6H_{11}]^+$, 9%), 70 ($[C_4H_6O]^+$, 39%), 57 ($[C_3H_5O]^+$, 31%), 41 ($[C_3H_5]^+$, 24%).

1,12-bis-(4'-Propyl-1'-cyclohexylphenyl-4-oxy)dodecane

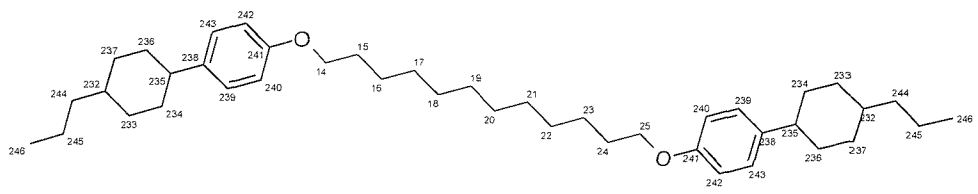

50
$C_{42}H_{66}O_2$
602.99

Rf 0.92; 100% DCM [1 spot by TLC]

^{1}H NMR (400 MHz, $CDCl_3$): δ_H 7.03 (4H, d, J = 8.7 Hz, $C_{239}\mathbf{H}$, $C_{243}\mathbf{H}$), 6.74 (2H, d, J = 8.7 Hz, $C_{240}\mathbf{H}$, $C_{242}\mathbf{H}$), 3.85 (4H, t, 6.5 Hz, O-$C_{14}\mathbf{H_2}$, O-$C_{25}\mathbf{H_2}$), 2.33 (2H, tt, J = 12.1 Hz, 3.0 Hz, $C_{235}\mathbf{H}$), 1.58-1.86 (12H, m, $C_{15}\mathbf{H_2}$, $C_{24}\mathbf{H_2}$, $C_{234}\mathbf{H_2}$, $C_{236}\mathbf{H_2}$), 1.05-1.49 (30H, m, $C_{16}\mathbf{H_2}$, $C_{17}\mathbf{H_2}$, $C_{18}\mathbf{H_2}$, $C_{19}\mathbf{H_2}$, $C_{20}\mathbf{H_2}$, $C_{21}\mathbf{H_2}$, $C_{22}\mathbf{H_2}$, $C_{232}\mathbf{H}$, $C_{233}\mathbf{H_2}$, $C_{237}\mathbf{H_2}$, $C_{245}\mathbf{H_2}$), 0.89-1.04 (4H, m, $C_{244}\mathbf{H_2}$), 0.83 (6H, t, J = 7.2 Hz, $C_{245}\mathbf{H_2}$) ppm.

^{13}C NMR (100 MHz, $CDCl_3$): δ_C 156.9 (q, $\mathbf{C_{241}}$(Ar)), 139.6 (q, $\mathbf{C_{238}}$(Ar)), 127.3 (t, $\mathbf{C_{239}}$ (Ar), $\mathbf{C_{243}}$(Ar)), 114.0 (t, $\mathbf{C_{240}}$(Ar), $\mathbf{C_{242}}$(Ar)), 67.7 (s, $\mathbf{C_{14}}(OCH_2)$, $\mathbf{C_{25}}(OCH_2)$), 43.4 (t, $\mathbf{C_{235}}$(CH)), 39.5 (s, $\mathbf{C_{244}}(CH_2)$), 36.8 (t, $\mathbf{C_{232}}$(CH)), 34.3 (s, $\mathbf{C_{234}}(CH_2)$, $\mathbf{C_{236}}(CH_2)$), 33.4 (s, $\mathbf{C_{234}}(CH_2)$, $\mathbf{C_{236}}(CH_2)$), 29.3 (s, $\mathbf{C_{15\text{-}24}}(CH_2)$), 29.1 (s, $\mathbf{C_{15\text{-}24}}(CH_2)$), 25.8 (s, $\mathbf{C_{15\text{-}24}}(CH_2)$), 19.7 (s, $\mathbf{C_{245}}(CH_2)$), 14.1 (p, $\mathbf{C_{246}}(CH_3)$) ppm.

IR (Solid) ν_{max}: 2915(m) (**C-H$_2$**), 2649(m), 2361(m), 1610(m) (**Ar**), 1561(m) (**Ar**), 1511(m) (**Ar**) cm^{-1}.

EIMS: *m/z* 279 ($[C_{20}H_{23}O]^+$, 8%), 167 ($[C_{13}H_9]^+$, 30%), 149 ($[C_{10}H_{13}O]^+$, 100%), 83 ($[C_6H_{11}]^+$, 9%), 70 ($[C_4H_6O]^+$, 39%), 57 ($[C_3H_5O]^+$, 30%), 41 ($[C_3H_5]^+$, 24%).

7.3.2. CBOnOPCH3; α-(4'-cyanobiphenyl-4-oxy)-ω-(4'-propyl-1'-cyclohexylphenyl-4-oxy)alkane

n	Temperature /°C					Mass	Yield
	Cr		N		I	mg	%
6	•	143	•	187	•	681	60
7	•	119	•	139	•	696	60
8	•	136	•	170	•	370	31
9	•	111	•	134	•	433	35
10	•	113	•	162	•	547	43
11	•	108	•	135	•	1100	85
12	•	100	•	145	•	170	13

1 -(4'-Cyanobiphenyl-4-oxy)-6-(4'-propyl-1'-cyclohexylphenyl-4-oxy)hexane

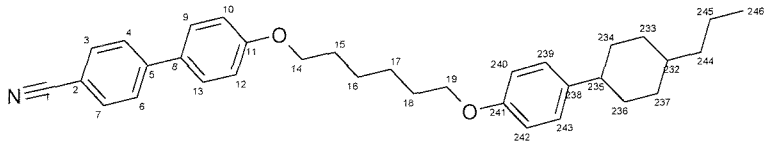

51
$C_{34}H_{43}NO_2$
495.71

To a stirred solution of 4-hydroxyphenyl-1-cyclohexyl-4'-propane (0.60g, 2.75 mMol, 1.20 eq) in butan-2-one (40 mL) was added anhydrous potassium carbonate (834 mg, 6.06 mMol, 2.64 eq) in one portion. The suspension was heated to reflux and stirred for 20 min before the addition of 1-(cyanobiphenyloxy)-hexyl-6-bromide (853 mg, 2.29 mMol, 1 eq) and a catalytic quantity of sodium iodide (80 mg). The solution were stirred at reflux for approximately 3 days and then allowed to cool. The solvents were removed *in vacuo* leaving an off-while solid. Water (50 mL) and then DCM (50 mL) was added. The inorganic salts dissolved into the aqueous layer whilst the organic product dissolved into the DCM. The layers were separated and the aqueous solution was washed repeatedly with DCM (3 x 50 mL). The organics were combined, dried over anhydrous $MgSO_4$ and filtered. The organics were then removed *in vacuo* to give the crude white product. This was then purified by crystalisation from acetonitrile (~200 mL) to yield the title compound **51** (681 mg, 1.38 mMol, 60.1%) as a white microcrystalline solid.

Rf 0.71; 100% DCM [1 spot by TLC]

^{1}H NMR (400 MHz, $CDCl_3$): δ_H 7.61 (2H, d, J = 8.6 Hz, C_4**H**, C_6**H**), 7.56 (2H, d, J = 8.6 Hz, C_3**H**, C_7**H**), 7.44 (2H, d, J = 8.9 Hz, C_9**H**, C_{13}**H**), 7.03 (2H, d, J = 8.4 Hz, C_{239}**H**, C_{243}**H**), 6.92 (2H, d, J = 8.9 Hz, C_{240}**H**, C_{242}**H**), 6.61 (2H, d, J = 8.7 Hz, C_{10}**H**, C_{12}**H**), 3.97 (2H, t, 6.4 Hz, O-C_{14}**H$_2$**), 3.87 (4H, t, 6.4 Hz, O-C_{19}**H$_2$**), 2.33 (1H, tt, J = 12.1 Hz, 3.1 Hz, C_{235}**H**), 1.63-1.85 (8H, m, C_{15}**H$_2$**, C_{18}**H$_2$**, C_{234}**H$_2$**, C_{236}**H$_2$**), 1.40-1.55 (4H, m, C_{16}**H$_2$**, C_{17}**H$_2$**), 1.07-1.55 (7H, m, C_{232}**H**, C_{233}**H$_2$**, C_{237}**H$_2$**, C_{245}**H$_2$**), 0.89-1.02 (2H, m, C_{244}**H$_2$**), 0.82 (3H, t, J = 7.2 Hz, C_{245}**H$_2$**) ppm.

^{13}C NMR (100 MHz, $CDCl_3$): δ_C 160.2 (q, **C_{11}**(Ar)), 157.6 (q, **C_{241}**(Ar)), 145.7 (q, **C_5**(Ar)), 140.4 (q, **C_{238}**(Ar)), 133.0 (t, **C_3**(Ar), **C_7**(Ar)), 131.7 (q, **C_8**(Ar)), 128.7 (t, **C_4**(Ar), **C_6**(Ar)), 128.0 (t, **C_9**(Ar),**C_{13}**(Ar)), 127.5 (t, **C_{239}** (Ar), **C_{243}**(Ar)), 119.5 (q, **C_1**(CN)), 115.5 (t, **C_{10}**(Ar), **C_{12}**(Ar)), 114.7 (t, **C_{240}**(Ar), **C_{242}**(Ar)), 110.5 (q, **C_2**(Ar)), 68.4 (s, **C_{14}**(OCH_2)), 68.2 (s, **C_{19}**(OCH_2)), 44.1 (t, **C_{235}**(CH)), 40.2 (s, **C_{244}**(CH_2)), 37.5 (t, **C_{232}**(CH)), 35.0 (s, **C_{234}**(CH_2), **C_{236}**(CH_2)), 34.0 (s, **C_{233}**(CH_2), **C_{237}**(CH_2)), 29.7 (s, **$C_{15\text{-}18}$**(CH_2)), 29.5 (s, **$C_{15\text{-}18}$**(CH_2)), 26.3 (s, **$C_{15\text{-}18}$**(CH_2)), 20.4 (s, **C_{245}**(CH_2)), 14.8 (s, **C_{246}**(CH_3)) ppm.

IR (Solid) ν_{max}: 2915(m) (**C-H$_2$**), 2649(m), 2361(m), 2222(w) (**C≡N**), 1609(m) (**Ar**), 1561(m) (**Ar**), 1510(m) (**Ar**) cm^{-1}.

EIMS: *m/z* 495 ($[M]^+$, 35%), 410 ($[C_{28}H_{31}NO]^+$, 5%), 278 ($[C_{19}H_{20}NO]^+$, 11%), 195 ($[C_{13}H_9NO]^+$, 97%), 133 ($[C_9H_{10}O]^+$, 100%), 83 ($[C_6H_{10}]^+$, 81%), 55 ($[C_4H_7]^+$, 72%), 41 ($[C_3H_5]^+$, 19%).

Elemental Analysis: $C_{34}H_{43}NO_2$: (Expected) **C** 82.31, **H** 8.67, **N** 2.82; (Found) **C** 82.23, **H** 8.56, **N** 2.71

1 -(4'-Cyanobiphenyl-4-oxy)-7-(4'-propyl-1'-cyclohexylphenyl-4-oxy)heptane

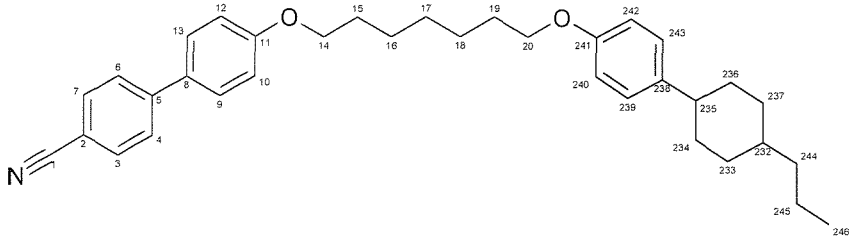

52
$C_{35}H_{45}NO_2$
509.74

Rf 0.72; 100% DCM

^{1}H NMR (400 MHz, $CDCl_3$): δ_H 7.61 (2H, d, J = 8.6 Hz, C_4**H,** C_6**H**), 7.56 (2H, d, J = 8.6 Hz, C_3**H,** C_7**H**), 7.44 (2H, d, J = 8.8 Hz, C_9**H,** C_{13}**H**), 7.03 (2H, d, J = 8.7 Hz, C_{239}**H,** C_{243}**H**), 6.91 (2H, d, J = 8.8 Hz, C_{240}**H,** C_{242}**H**), 6.74 (2H, d, J = 8.7 Hz, C_{10}**H,** C_{12}**H**), 3.93 (2H, t, 6.5 Hz, O-C_{14}**H$_2$**), 3.87 (4H, t, 6.5 Hz, O-C_{20}**H$_2$**), 2.32 (1H, tt, J = 12.1 Hz, 3.1 Hz, C_{235}**H**), 1.61-1.85 (8H, m, C_{15}**H$_2$**, C_{19}**H$_2$**, C_{234}**H$_2$**, C_{236}**H$_2$**), 1.07-1.52 (13H, m, C_{16}**H$_2$**, C_{17}**H$_2$**, C_{18}**H$_2$**, C_{232}**H,** C_{233}**H$_2$,** C_{237}**H$_2$,** C_{245}**H$_2$**), 0.88-1.03 (2H, m, C_{244}**H$_2$**), 0.82 (3H, t, J = 7.3 Hz, C_{245}**H$_2$**) ppm.

^{13}C NMR (100 MHz, $CDCl_3$): δ_C 160.2 (q, **C_{11}**(Ar)), 157.6 (q, **C_{238}**(Ar)), 145.7 (q, **C_5**(Ar)), 140.4 (q, **C_{238}**(Ar)), 133.0 (t, **C_3**(Ar), **C_7**(Ar)), 131.7 (q, **C_8**(Ar)), 128.7 (t, **C_4**(Ar), **C_6**(Ar)), 128.0 (t, **C_9**(Ar), **C_{13}**(Ar)), 127.5 (t, **C_{239}** (Ar), **C_{243}**(Ar)), 119.5 (q, **C_1**(CN)), 115.5 (t, **C_{10}**(Ar), **C_{12}**(Ar)), 114.7 (t, **C_{240}**(Ar), **C_{242}**(Ar)), 110.5 (q, **C_2**(Ar)), 68.4 (s, **C_{14}**(OCH_2)), 68.3 (s, **C_{20}**(OCH_2)), 44.2 (t, **C_{235}**(CH)), 40.2 (s, **C_{244}**(CH_2)), 37.5 (t, **C_{232}**(CH)), 35.0 (s, **C_{234}**(CH_2), **C_{236}**(CH_2)), 34.1 (s, **C_{234}**(CH_2), **C_{236}**(CH_2)), 29.7 (s, **$C_{15\text{-}19}$**(CH_2)), 29.5 (s, **$C_{15\text{-}19}$**(CH_2)), 26.4 (s, **$C_{15\text{-}19}$**(CH_2)), 20.4 (s, **C_{245}**(CH_2)), 14.8 (s, **C_{246}**(CH_3)) ppm.

IR (Solid) ν_{max}: 2916(m) (**C-H$_2$**), 2649(m), 2362(m), 2223(w) (**C≡N**), 1605(m) (**Ar**), 1581(m) (**Ar**), 1510(m) (**Ar**) cm^{-1}.

EIMS: *m/z* 279 ($[C_{20}H_{23}O]^+$, 8%), 193 ($[C_{13}H_7NO]^+$, 29%), 167 ($[C_{13}H_9]^+$, 29%), 149 ($[C_{10}H_{13}O]^+$, 100%), 83 ($[C_6H_{11}]^+$, 9%), 70 ($[C_4H_6O]^+$, 39%), 57 ($[C_3H_5O]^+$, 31%), 41 ($[C_3H_5]^+$, 24%).

1 -(4'-Cyanobiphenyl-4-oxy)-8-(4'-propyl-1'-cyclohexylphenyl-4-oxy)octane

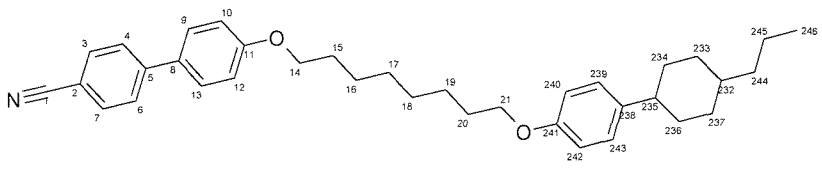

53
$C_{36}H_{45}NO_2$
523.77

Rf 0.73; 100% DCM [1 spot by TLC]

^{1}H NMR (400 MHz, $CDCl_3$): δ_H 7.61 (2H, d, J = 8.6 Hz, C_4**H,** C_6**H**), 7.55 (2H, d, J = 8.6 Hz, C_3**H,** C_7**H**), 7.44 (2H, d, J = 8.8 Hz, C_9**H,** C_{13}**H**), 7.03 (2H, d, J = 8.5 Hz, C_{239}**H,** C_{243}**H**), 6.91 (2H, d, J = 8.8 Hz, C_{240}**H,** C_{242}**H**), 6.74 (2H, d, J =

8.7 Hz, $C_{10}\mathbf{H}$, $C_{12}\mathbf{H}$), 3.93 (2H, t, 6.5 Hz, O-$C_{14}\mathbf{H_2}$), 3.85 (2H, t, 6.5 Hz, O-$C_{21}\mathbf{H_2}$), 2.32 (1H, tt, J = 12.1 Hz, 3.0 Hz, $C_{235}\mathbf{H}$), 1.59-1.86 (8H, m, $C_{15}\mathbf{H_2}$, $C_{20}\mathbf{H_2}$, $C_{234}\mathbf{H_2}$, $C_{236}\mathbf{H_2}$), 1.05-1.49 (15H, m, $C_{16}\mathbf{H_2}$, $C_{17}\mathbf{H_2}$, $C_{18}\mathbf{H_2}$, $C_{19}\mathbf{H_2}$, $C_{232}\mathbf{H}$, $C_{233}\mathbf{H_2}$, $C_{237}\mathbf{H_2}$, $C_{245}\mathbf{H_2}$), 0.88-1.03 (2H, m, $C_{244}\mathbf{H_2}$), 0.82 (3H, t, J = 7.3 Hz, $C_{245}\mathbf{H_2}$) ppm.

^{13}C NMR (100 MHz, $CDCl_3$): δ_C 160.2 (q, $\mathbf{C_{11}}$(Ar)), 157.6 (q, $\mathbf{C_{238}}$(Ar)), 145.7 (q, $\mathbf{C_5}$(Ar)), 140.4 (q, $\mathbf{C_{238}}$(Ar)), 133.0 (t, $\mathbf{C_3}$(Ar), $\mathbf{C_7}$(Ar)), 131.7 (q, $\mathbf{C_8}$(Ar)), 128.7 (t, $\mathbf{C_4}$(Ar), $\mathbf{C_6}$(Ar)), 128.0 (t, $\mathbf{C_9}$(Ar), $\mathbf{C_{13}}$(Ar)), 127.5 (t, $\mathbf{C_{239}}$ (Ar), $\mathbf{C_{243}}$(Ar)), 119.5 (q, $\mathbf{C_1}$(CN)), 115.5 (t, $\mathbf{C_{10}}$(Ar), $\mathbf{C_{12}}$(Ar)), 114.7 (t, $\mathbf{C_{240}}$(Ar), $\mathbf{C_{242}}$(Ar)), 110.5 (q, $\mathbf{C_2}$(Ar)), 68.6 (s, $\mathbf{C_{14}}$(OCH_2)), 68.3 (s, $\mathbf{C_{21}}$(OCH_2)), 44.2 (t, $\mathbf{C_{235}}$(CH)), 40.2 (s, $\mathbf{C_{244}}$(CH_2)), 37.5 (t, $\mathbf{C_{232}}$(CH)), 35.0 (s, $\mathbf{C_{234}}$(CH_2), $\mathbf{C_{236}}$(CH_2)), 34.1 (s, $\mathbf{C_{234}}$(CH_2), $\mathbf{C_{236}}$(CH_2)), 29.8 (s, $\mathbf{C_{15\text{-}20}}$($CH_2$)), 29.7 (s, $\mathbf{C_{15\text{-}20}}$($CH_2$)), 29.6 (s, $\mathbf{C_{15\text{-}20}}$($CH_2$)), 26.4 (s, $\mathbf{C_{15\text{-}20}}$($CH_2$)), 20.4 (s, $\mathbf{C_{245}}$(CH_2)), 14.8 (s, $\mathbf{C_{246}}$(CH_3)) ppm.

IR (Solid) ν_{max}: 2916(m) (**C-H$_2$**), 2650(m), 2362(m), 2232(w) (**C≡N**), 1606(m) (**Ar**), 1582(m) (**Ar**), 1510(m) (**Ar**) cm^{-1}.

EIMS: *m/z* 523 ($[M]^+$, 45%), 438 ($[C_{30}H_{35}NO]^+$, 5%), 305 ($[C_{20}H_{22}NO]^+$, 11%), 218 ($[C_{13}H_{12}NO]^+$, 9%), 195 ($[C_{13}H_9NO]^+$, 100%), 133 ($[C_9H_{10}O]^+$, 98%), 69 ($[C_5H_9]^+$, 72%), 41 ($[C_3H_5]^+$, 19%).

1 -(4'-Cyanobiphenyl-4-oxy)-9-(4'-propyl-1'-cyclohexylphenyl-4-oxy)nonane

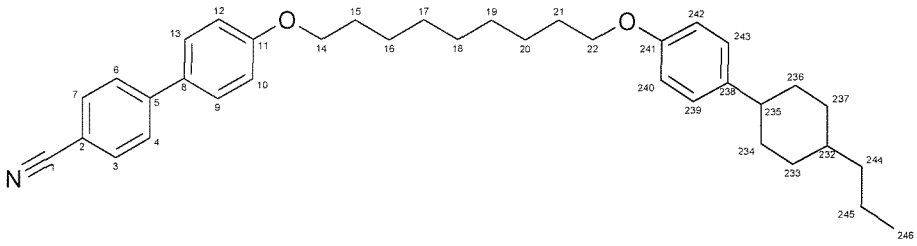

54
$C_{37}H_{47}NO_2$
537.59

Rf 0.75; 100% DCM [1 spot by TLC]

^{1}H NMR (400 MHz, $CDCl_3$): δ_H 7.61 (2H, d, J = 8.6 Hz, $C_4\mathbf{H}$, $C_6\mathbf{H}$), 7.56 (2H, d, J = 8.6 Hz, $C_3\mathbf{H}$, $C_7\mathbf{H}$), 7.44 (2H, d, J = 8.6 Hz, $C_9\mathbf{H}$, $C_{13}\mathbf{H}$), 7.03 (2H, d, J = 8.4 Hz, $C_{239}\mathbf{H}$, $C_{243}\mathbf{H}$), 6.91 (2H, d, J = 8.8 Hz, $C_{240}\mathbf{H}$, $C_{242}\mathbf{H}$), 6.74 (2H, d, J = 8.8 Hz, $C_{10}\mathbf{H}$, $C_{12}\mathbf{H}$), 3.93 (2H, t, 6.5 Hz, O-$C_{14}\mathbf{H_2}$), 3.85 (2H, t, 6.5 Hz, O-

$C_{22}\mathbf{H_2}$), 2.32 (1H, tt, J = 12.1 Hz, 3.1 Hz, $C_{235}\mathbf{H}$), 1.53-1.62 (8H, m, $C_{15}\mathbf{H_2}$, $C_{21}\mathbf{H_2}$, $C_{234}\mathbf{H_2}$, $C_{236}\mathbf{H_2}$), 1.07-1.49 (17H, m, $C_{16}\mathbf{H_2}$, $C_{17}\mathbf{H_2}$, $C_{18}\mathbf{H_2}$, $C_{19}\mathbf{H_2}$, $C_{20}\mathbf{H_2}$, $C_{232}\mathbf{H}$, $C_{233}\mathbf{H_2}$, $C_{237}\mathbf{H_2}$, $C_{245}\mathbf{H_2}$), 0.88-1.03 (2H, m, $C_{244}\mathbf{H_2}$), 0.82 (3H, t, J = 7.2 Hz, $C_{245}\mathbf{H_2}$) ppm.

^{13}C NMR (100 MHz, $CDCl_3$): δ_C 158.0 (q, $\mathbf{C_{11}}$(Ar)), 155.4 (q, $\mathbf{C_{238}}$(Ar)), 143.5 (q, $\mathbf{C_5}$(Ar)), 138.1 (q, $\mathbf{C_{238}}$(Ar)), 130.7 (t, $\mathbf{C_3}$(Ar), $\mathbf{C_7}$(Ar)), 129.4 (q, $\mathbf{C_8}$(Ar)), 126.7 (t, $\mathbf{C_4}$(Ar), $\mathbf{C_6}$(Ar)), 125.7 (t, $\mathbf{C_9}$(Ar), $\mathbf{C_{13}}$(Ar)), 125.2 (t, $\mathbf{C_{239}}$ (Ar), $\mathbf{C_{243}}$(Ar)), 117.2 (q, $\mathbf{C_1}$(CN)), 113.3 (t, $\mathbf{C_{10}}$(Ar), $\mathbf{C_{12}}$(Ar)), 112.4 (t, $\mathbf{C_{240}}$(Ar), $\mathbf{C_{242}}$(Ar)), 108.2 (q, $\mathbf{C_2}$(Ar)), 66.3 (s, $\mathbf{C_{14}}$(OCH_2)), 66.1 (s, $\mathbf{C_{22}}$(OCH_2)), 41.9 (t, $\mathbf{C_{235}}$(CH)), 37.9 (s, $\mathbf{C_{244}}$(CH_2)), 35.2 (t, $\mathbf{C_{232}}$(CH)), 32.8 (s, $\mathbf{C_{234}}$(CH_2), $\mathbf{C_{236}}$(CH_2)), 31.8 (s, $\mathbf{C_{234}}$(CH_2), $\mathbf{C_{236}}$(CH_2)), 27.6 (s, $\mathbf{C_{15\text{-}21}}$($CH_2$)), 27.5 (s, $\mathbf{C_{15\text{-}21}}$($CH_2$)), 27.4 (s, $\mathbf{C_{15\text{-}21}}$($CH_2$)), 27.3 (s, $\mathbf{C_{15\text{-}21}}$($CH_2$)), 24.2 (s, $\mathbf{C_{15\text{-}21}}$($CH_2$)), 18.2 (s, $\mathbf{C_{245}}$(CH_2)), 12.6 (s, $\mathbf{C_{246}}$(CH_3)) ppm.

IR (Solid) ν_{max}: 2916(m) (**C-$\mathbf{H_2}$**), 2650(m), 2362(m), 2232(w) (**C≡N**), 1606(m) (**Ar**), 1582(m) (**Ar**), 1510(m) (**Ar**) cm^{-1}.

EIMS: *m/z* 279 ($[C_{20}H_{23}O]^+$, 8%), 208 ($[C_{15}H_{13}O]^+$, 2%), 167 ($[C_{13}H_9]^+$, 31%), 149 ($[C_{10}H_{13}O]^+$, 100%), 83 ($[C_6H_{11}]^+$, 9%), 70 ($[C_4H_6O]^+$, 37%), 57 ($[C_3H_5O]^+$, 30%), 41 ($[C_3H_5]^+$, 22%).

1 -(4'-Cyanobiphenyl-4-oxy)-10-(4'-propyl-1'-cyclohexylphenyl-4-oxy)decane

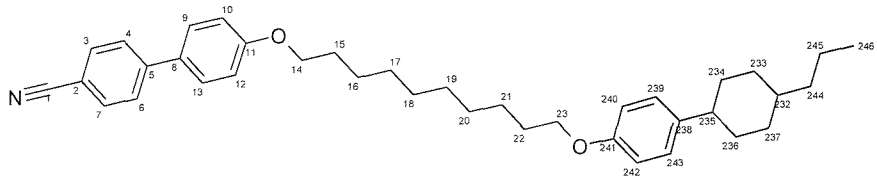

55
$C_{38}H_{49}NO_2$
551.82

Rf 0.76; 100% DCM [1 spot by TLC]

^{1}H NMR (400 MHz, $CDCl_3$): δ_H 7.61 (2H, d, J = 8.6 Hz, $C_4\mathbf{H}$, $C_6\mathbf{H}$), 7.56 (2H, d, J = 8.6 Hz, $C_3\mathbf{H}$, $C_7\mathbf{H}$), 7.45 (2H, d, J = 8.6 Hz, $C_9\mathbf{H}$, $C_{13}\mathbf{H}$), 7.03 (2H, d, J = 8.5 Hz, $C_{239}\mathbf{H}$, $C_{243}\mathbf{H}$), 6.91 (2H, d, J = 8.8 Hz, $C_{240}\mathbf{H}$, $C_{242}\mathbf{H}$), 6.74 (2H, d, J = 8.7 Hz, $C_{10}\mathbf{H}$, $C_{12}\mathbf{H}$), 3.93 (2H, t, 6.5 Hz, O-$C_{14}\mathbf{H_2}$), 3.85 (2H, t, 6.5 Hz, O-$C_{23}\mathbf{H_2}$), 2.32 (1H, tt, J = 12.1 Hz, 3.1 Hz, $C_{235}\mathbf{H}$), 1.60-1.86 (8H, m, $C_{15}\mathbf{H_2}$, $C_{22}\mathbf{H_2}$, $C_{234}\mathbf{H_2}$, $C_{236}\mathbf{H_2}$), 1.05-1.49 (19H, m, $C_{16}\mathbf{H_2}$, $C_{17}\mathbf{H_2}$, $C_{18}\mathbf{H_2}$, $C_{19}\mathbf{H_2}$,

$C_{20}\mathbf{H_2}$, $C_{21}\mathbf{H_2}$, $C_{232}\mathbf{H}$, $C_{233}\mathbf{H_2}$, $C_{237}\mathbf{H_2}$, $C_{245}\mathbf{H_2}$), 0.88-1.03 (2H, m, $C_{244}\mathbf{H_2}$), 0.82 (3H, t, J = 7.3 Hz, $C_{245}\mathbf{H_2}$) ppm.

^{13}C NMR (100 MHz, $CDCl_3$): δ_C 160.7 (q, $\mathbf{C_{11}}$(Ar)), 158.1 (q, $\mathbf{C_{238}}$(Ar)), 146.2 (q, $\mathbf{C_5}$(Ar)), 140.8 (q, $\mathbf{C_{238}}$(Ar)), 133.4 (t, $\mathbf{C_3}$(Ar), $\mathbf{C_7}$(Ar)), 132.1 (q, $\mathbf{C_8}$(Ar)), 129.2 (t, $\mathbf{C_4}$(Ar), $\mathbf{C_6}$(Ar)), 128.4 (t, $\mathbf{C_9}$(Ar), $\mathbf{C_{13}}$(Ar)), 127.9 (t, $\mathbf{C_{239}}$ (Ar), $\mathbf{C_{243}}$(Ar)), 119.9 (q, $\mathbf{C_1}$(CN)), 116.0 (t, $\mathbf{C_{10}}$(Ar), $\mathbf{C_{12}}$(Ar)), 115.1 (t, $\mathbf{C_{240}}$(Ar), $\mathbf{C_{242}}$(Ar)), 110.9 (q, $\mathbf{C_2}$(Ar)), 69.0 (s, $\mathbf{C_{14}}$(OCH_2)), 68.8 (s, $\mathbf{C_{23}}$(OCH_2)), 44.6 (t, $\mathbf{C_{235}}$(CH)), 40.6 (t, $\mathbf{C_{244}}$(CH)), 37.9 (s, $\mathbf{C_{232}}$(CH_2)), 35.5 (s, $\mathbf{C_{234}}$(CH_2), $\mathbf{C_{236}}$(CH_2)), 34.5 (s, $\mathbf{C_{234}}$(CH_2), $\mathbf{C_{236}}$(CH_2)), 30.3 (s, $\mathbf{C_{15\text{-}22}}$($CH_2$)), 30.2 (s, $\mathbf{C_{15\text{-}22}}$($CH_2$)), 30.1 (s, $\mathbf{C_{15\text{-}22}}$($CH_2$)), 26.9 (s, $\mathbf{C_{15\text{-}22}}$($CH_2$)), 26.9 (s, $\mathbf{C_{15\text{-}22}}$($CH_2$)), 20.9 (s, $\mathbf{C_{245}}$(CH_2)), 15.3 (s, $\mathbf{C_{246}}$(CH_3)) ppm.

IR (Solid) ν_{max}: 2919(m) (**C-H$_2$**), 2649(m), 2361(m), 2226(m) (**C≡N**), 1601(m) (**Ar**), 1580(m) (**Ar**), 1512(m) (**Ar**) cm^{-1}.

EIMS: *m/z* 279 ($[C_{20}H_{23}O]^+$, 8%), 195 ($[C_{13}H_9NO]^+$, 1%), 167 ($[C_{13}H_9]^+$, 30%), 149 ($[C_{10}H_{13}O]^+$, 100%), 83 ($[C_6H_{11}]^+$, 9%), 70 ($[C_4H_6O]^+$, 37%), 57 ($[C_3H_5O]^+$, 28%), 41 ($[C_3H_5]^+$, 18%)

1 -(4'-Cyanobiphenyl-4-oxy)-11-(4'-propyl-1'-cyclohexylphenyl-4-oxy)undecane

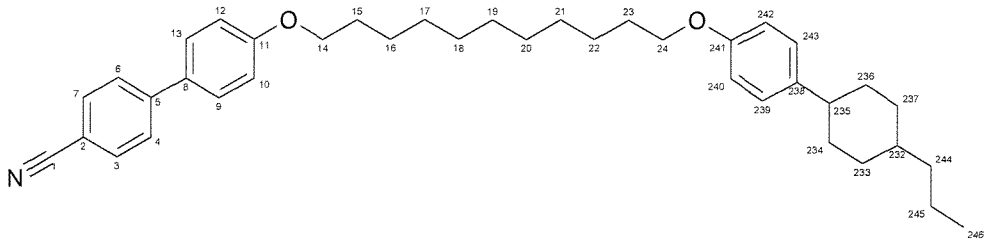

56
$C_{39}H_{51}NO_2$
565.85

Rf 0.77; 100% DCM [1 spot by TLC]

^{1}H NMR (400 MHz, $CDCl_3$): δ_H 7.61 (2H, d, J = 8.6 Hz, $C_4\mathbf{H}$, $C_6\mathbf{H}$), 7.56 (2H, d, J = 8.6 Hz, $C_3\mathbf{H}$, $C_7\mathbf{H}$), 7.45 (2H, d, J = 8.7 Hz, $C_9\mathbf{H}$, $C_{13}\mathbf{H}$), 7.03 (2H, d, J = 8.9 Hz, $C_{239}\mathbf{H}$, $C_{243}\mathbf{H}$), 6.91 (2H, d, J = 8.8 Hz, $C_{240}\mathbf{H}$, $C_{242}\mathbf{H}$), 6.74 (2H, d, J = 8.7 Hz, $C_{10}\mathbf{H}$, $C_{12}\mathbf{H}$), 3.93 (2H, t, 6.5 Hz, O-$C_{14}\mathbf{H_2}$), 3.85 (2H, t, 6.6 Hz, O-$C_{24}\mathbf{H_2}$), 2.32 (1H, tt, J = 12.1 Hz, 3.0 Hz, $C_{235}\mathbf{H}$), 1.58-1.86 (8H, m, $C_{15}\mathbf{H_2}$, $C_{23}\mathbf{H_2}$, $C_{234}\mathbf{H_2}$, $C_{236}\mathbf{H_2}$), 1.03-1.49 (21H, m, $C_{16}\mathbf{H_2}$, $C_{17}\mathbf{H_2}$, $C_{18}\mathbf{H_2}$, $C_{19}\mathbf{H_2}$,

$C_{20}\mathbf{H_2}$, $C_{21}\mathbf{H_2}$, $C_{22}\mathbf{H_2}$, $C_{232}\mathbf{H}$, $C_{233}\mathbf{H_2}$, $C_{237}\mathbf{H_2}$, $C_{245}\mathbf{H_2}$), 0.88-1.03 (2H, m, $C_{244}\mathbf{H_2}$), 0.82 (3H, t, J = 7.3 Hz, $C_{245}\mathbf{H_2}$) ppm.

^{13}C NMR (100 MHz, $CDCl_3$): δ_C 160.3 (q, $\mathbf{C_{11}}$(Ar)), 157.7 (q, $\mathbf{C_{238}}$(Ar)), 145.7 (q, $\mathbf{C_5}$(Ar)), 140.4 (q, $\mathbf{C_{238}}$(Ar)), 133.0 (t, $\mathbf{C_3}$(Ar), $\mathbf{C_7}$(Ar)), 131.7 (q, $\mathbf{C_8}$(Ar)), 128.7 (t, $\mathbf{C_4}$(Ar), $\mathbf{C_6}$(Ar)), 128.0 (t, $\mathbf{C_9}$(Ar), $\mathbf{C_{13}}$(Ar)), 127.5 (t, $\mathbf{C_{239}}$ (Ar), $\mathbf{C_{243}}$(Ar)), 119.5 (q, $\mathbf{C_1}$(CN)), 115.5 (t, $\mathbf{C_{10}}$(Ar), $\mathbf{C_{12}}$(Ar)), 114.7 (t, $\mathbf{C_{240}}$(Ar), $\mathbf{C_{242}}$(Ar)), 110.5 (q, $\mathbf{C_2}$(Ar)), 68.6 (s, $\mathbf{C_{14}}$(OCH_2)), 68.4 (s, $\mathbf{C_{24}}$(OCH_2)), 44.1 (t, $\mathbf{C_{235}}$(CH)), 40.2 (s, $\mathbf{C_{244}}$(CH_2)), 37.5 (t, $\mathbf{C_{232}}$(CH)), 35.0 (s, $\mathbf{C_{234}}$(CH_2), $\mathbf{C_{236}}$(CH_2)), 34.1 (s, $\mathbf{C_{234}}$(CH_2), $\mathbf{C_{236}}$(CH_2)), 30.0 (s, $\mathbf{C_{15\text{-}23}}$($CH_2$)), 29.8 (s, $\mathbf{C_{15\text{-}23}}$($CH_2$)), 29.6 (s, $\mathbf{C_{15\text{-}23}}$($CH_2$)), 26.5 (s, $\mathbf{C_{15\text{-}23}}$($CH_2$)), 26.4 (s, $\mathbf{C_{15\text{-}23}}$($CH_2$)), 20.4 (s, $\mathbf{C_{245}}$(CH_2)), 14.8 (s, $\mathbf{C_{246}}$(CH_3)) ppm.

IR (Solid) ν_{max}: 2918(m) (**C-H$_2$**), 2650(m), 2362(m), 2232(w) (**C≡N**), 1605(m) (**Ar**), 1579(m) (**Ar**), 1511(m) (**Ar**) cm^{-1}.

EIMS: *m/z* 279 ($[C_{20}H_{23}O]^+$, 9%), 207 ($[C_{14}H_9NO]^+$, 5%), 193 ($[C_{13}H_7NO]^+$, 1%), 167 ($[C_{13}H_9]^+$, 30%), 149 ($[C_{10}H_{13}O]^+$, 100%), 83 ($[C_6H_{11}]^+$, 9%), 70 ($[C_4H_6O]^+$, 35%), 57 ($[C_3H_5O]^+$, 28%), 41 ($[C_3H_5]^+$, 20%)

1 -(4'-Cyanobiphenyl-4-oxy)-12-(4'-propyl-1'-cyclohexylphenyl-4-oxy)dodecane

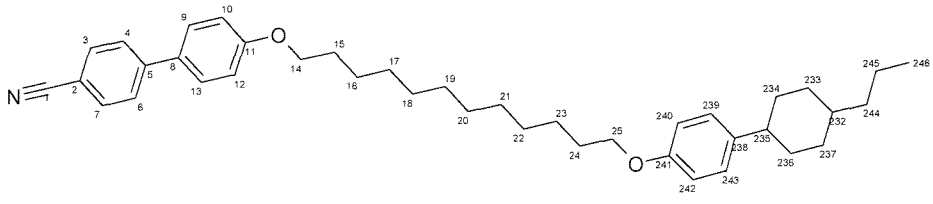

57
$C_{40}H_{53}NO_2$
579.87

Rf 0.78; 100% DCM [1 spot by TLC]

^{1}H NMR (400 MHz, $CDCl_3$): δ_H 7.61 (2H, d, J = 8.6 Hz, $C_4\mathbf{H}$, $C_6\mathbf{H}$), 7.56 (2H, d, J = 8.6 Hz, $C_3\mathbf{H}$, $C_7\mathbf{H}$), 7.45 (2H, d, J = 8.9 Hz, $C_9\mathbf{H}$, $C_{13}\mathbf{H}$), 7.03 (2H, d, J = 8.5 Hz, $C_{239}\mathbf{H}$, $C_{243}\mathbf{H}$), 6.92 (2H, d, J = 8.9 Hz, $C_{240}\mathbf{H}$, $C_{242}\mathbf{H}$), 6.74 (2H, d, J = 8.7 Hz, $C_{10}\mathbf{H}$, $C_{12}\mathbf{H}$), 3.93 (2H, t, 6.5 Hz, O-$C_{14}\mathbf{H_2}$), 3.85 (2H, t, 6.5 Hz, O-$C_{25}\mathbf{H_2}$), 2.32 (1H, tt, J = 12.1 Hz, 3.1 Hz, $C_{235}\mathbf{H}$), 1.60-1.85 (8H, m, $C_{15}\mathbf{H_2}$, $C_{24}\mathbf{H_2}$, $C_{234}\mathbf{H_2}$, $C_{236}\mathbf{H_2}$), 1.05-1.50 (23H, m, $C_{16}\mathbf{H_2}$, $C_{17}\mathbf{H_2}$, $C_{18}\mathbf{H_2}$, $C_{19}\mathbf{H_2}$, $C_{20}\mathbf{H_2}$, $C_{21}\mathbf{H_2}$, $C_{22}\mathbf{H_2}$, $C_{23}\mathbf{H_2}$, $C_{232}\mathbf{H}$, $C_{233}\mathbf{H_2}$, $C_{237}\mathbf{H_2}$, $C_{245}\mathbf{H_2}$), 0.88-1.03 (2H, m, $C_{244}\mathbf{H_2}$), 0.82 (3H, t, J = 7.3 Hz, $C_{245}\mathbf{H_2}$) ppm.

^{13}C NMR (100 MHz, $CDCl_3$): δ_C 160.3 (q, **C_{11}**(Ar)), 157.7 (q, **C_{238}**(Ar)), 145.7 (q, **C_5**(Ar)), 140.4 (q, **C_{238}**(Ar)), 133.0 (t, **C_3**(Ar), **C_7**(Ar)), 131.6 (q, **C_8**(Ar)), 128.7 (t, **C_4**(Ar), **C_6**(Ar)), 128.0 (t, **C_9**(Ar), **C_{13}**(Ar)), 127.5 (t, **C_{239}** (Ar), **C_{243}**(Ar)), 119.5 (q, **C_1**(CN)), 115.5 (t, **C_{10}**(Ar), **C_{12}**(Ar)), 114.7 (t, **C_{240}**(Ar), **C_{242}**(Ar)), 110.5 (q, **C_2**(Ar)), 68.6 (s, **C_{14}**(OCH_2)), 68.4 (s, **C_{25}**(OCH_2)), 44.2 (t, **C_{235}**(CH)), 40.2 (s, **C_{244}**(CH_2)), 37.5 (t, **C_{232}**(CH)), 35.0 (s, **C_{234}**(CH_2), **C_{236}**(CH_2)), 34.1 (s, **C_{234}**(CH_2), **C_{236}**(CH_2)), 29.9 (s, **$C_{15\text{-}24}$**(CH_2)), 29.8 (s, **$C_{15\text{-}24}$**(CH_2)), 29.6 (s, **$C_{15\text{-}24}$**(CH_2)), 26.5 (s, **$C_{15\text{-}24}$**(CH_2)), 26.4 (s, **$C_{15\text{-}24}$**(CH_2)), 20.4 (s, **C_{245}**(CH_2)), 14.8 (s, **C_{246}**(CH_3)) ppm.

IR (Solid) ν_{max}: 2916(m) (**C-H_2**), 2649(m), 2362(m), 2230(w) (**C≡N**), 1606(m) (**Ar**), 1580(m) (**Ar**), 1513(m) (**Ar**) cm^{-1}.

EIMS: *m/z* 279 ($[C_{20}H_{23}O]^+$, 9%), 207 ($[C_{14}H_9NO]^+$, 6%), 195 ($[C_{13}H_9NO]^+$, 1%), 167 ($[C_{13}H_9]^+$, 29%), 149 ($[C_{10}H_{13}O]^+$, 100%), 83 ($[C_6H_{11}]^+$, 9%), 70 ($[C_4H_6O]^+$, 36%), 57 ($[C_3H_5O]^+$, 30%), 41 ($[C_3H_5]^+$, 20%)

7.3.3. CBOnOPCH7; α-(4'-cyanobiphenyl-4-oxy)-ω-(4'-heptyl-1'-cyclohexylphenyl-4-oxy)alkane

n	Temperature /°C							Mass	Yield
	Cr		Sm_A		N		I	mg	%
4	•	127	•	185	•	197	•	620	65
5	•	128	•	(111)	•	(127)	•	650	67
6	•	113	•	151	•	172	•	810	81
7	•	114	•	(104)	•	130	•	530	52
8	•	105	•	123	•	162	•	803	76
9	•	104	•	(81)	•	126	•	2135	72
10	•	124	•	(92)	•	146	•	792	73
11	•	105	•		•	127	•	2350	91
12	•	121	•		•	141	•	967	84

1-(4'-Cyanobiphenyl-4-oxy)-6-(4'-heptyl-1'-cyclohexylphenyl-4-oxy)hexane

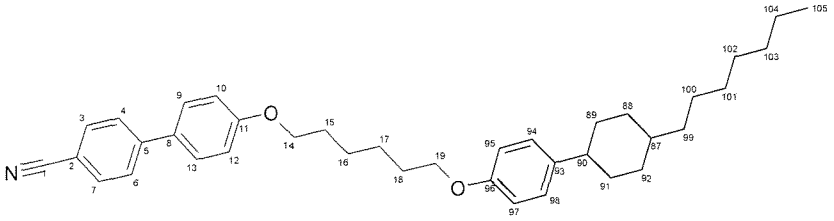

58
$C_{38}H_{49}NO_2$
551.82

Proceedure:

To a stirred solution of 4-hydroxyphenyl-1-cyclohexyl-4'-heptane (500 mg, 1.82 mMol, 1 eq) in butan-2-one (40 mL) was added anhydrous potassium carbonate (452 mg, 3.27 mMol, 1 eq) in one portion. The suspension was heated to reflux and stirred for 20 min before the addition of 1-(cyanobiphenyloxy)-hexyl-6-bromide (651 mg, 1.82 mMol, 1 eq) and a catalytic quantity of sodium iodide (80 mg). The solution was stirred at reflux for approximately 3 days and then allowed to cool. The solvents were removed *in vacuo* leaving an off-while solid. Water (50 mL) and then DCM (50 mL) were added. The inorganic salts dissolved into the aqueous layer whilst the organic product dissolved into the DCM. The layers were separated and the aqueous solution was washed repeatedly with DCM (3 x 50 mL). The organics were combined, dried over anhydrous $MgSO_4$ and filtered. The organics were then removed *in vacuo* to give the crude white product. This was then purified by crystalisation from acetonitrile (~100 mL) to yield the title compound **58** (810 mg, 1.47 mMol, 80.7%) as a white microcrystalline solid.

Rf 0.77; 100% DCM

^{1}H NMR (400 MHz, $CDCl_3$): δ_H 7.61 (2H, d, J = 8.6 Hz, C_4**H,** C_6**H**), 7.56 (2H, d, J = 8.6 Hz, C_3**H,** C_7**H**), 7.44 (2H, d, J = 9.0 Hz, C_9**H,** C_{13}**H**), 7.04 (2H, d, J = 8.6 Hz, C_{94}**H,** C_{98}**H**), 6.91 (2H, d, J = 8.8 Hz, C_{95}**H,** C_{97}**H**), 6.74 (2H, d, J = 8.8 Hz, C_{10}**H,** C_{12}**H**), 3.94 (2H, t, 6.4 Hz, O-C_{14}**H$_2$**), 3.89 (2H, t, 6.4 Hz, O-C_{19}**H$_2$**), 2.33 (1H, tt, J = 11.9 Hz, 2.8 Hz, C_{90}**H**), 1.62-1.86 (8H, m, C_{15}**H$_2$**, C_{18}**H$_2$**, C_{89}**H$_2$**, C_{91}**H$_2$**), 1.41-1.86 (4H, m, C_{16}**H$_2$**, C_{17}**H$_2$**), 1.06-1.41 (15H, m, C_{87}**H,** C_{88}**H$_2$,** C_{92}**H$_2$,** C_{100}**H$_2$,** C_{101}**H$_2$,** C_{102}**H$_2$,** C_{103}**H$_2$,** C_{104}**H$_2$**), 0.89-1.06 (2H, m, C_{99}**H$_2$**), 0.81 (3H, t, J = 7.1 Hz, C_{105}**H$_2$**) ppm.

^{13}C NMR (100 MHz, $CDCl_3$): δ_C 159.8 (q, **C_{11}**(Ar)), 157.2 (q, **C_{96}**(Ar)), 145.3 (q, **C_5**(Ar)), 140.1 (q, **C_{93}**(Ar)), 132.6 (t, **C_3**(Ar), **C_7**(Ar)), 131.3 (q, **C_8**(Ar)), 128.3 (t, **C_4**(Ar), **C_6**(Ar)), 127.6 (t, **C_9**(Ar),**C_{13}**(Ar)), 127.1 (t, **C_{94}** (Ar), **C_{98}**(Ar)), 119.1 (q, **C_1**(CN)), 115.1 (t, **C_{10}**(Ar), **C_{12}**(Ar)), 114.3 (t, **C_{95}**(Ar), **C_{97}**(Ar)), 110.1 (q, **C_2**(Ar)), 68.0 (s, **C_{14}**(OCH_2)), 67.8 (s, **C_{19}**(OCH_2)), 43.8 (t, **C_{90}**(CH)), 37.5 (s, **C_{99}**(CH_2)), 37.5 (t, **C_{87}**(CH)), 34.6 (s, **C_{89}**(CH_2), **C_{91}**(CH_2)), 33.7 (s, **C_{88}**(CH_2), **C_{92}**(CH_2)), 31.9 (s, **$C_{15\text{-}18}$/$C_{100\text{-}105}$** (CH_2)), 30.0 (s, **$C_{15\text{-}18}$/$C_{100\text{-}105}$**(CH_2)), 29.4 (s, **$C_{15\text{-}18}$/$C_{100\text{-}105}$**(CH_2)), 29.3 (s, **$C_{15\text{-}18}$/$C_{100\text{-}}$**

$_{105}(CH_2)$), 29.2 (s, $\mathbf{C_{15\text{-}18}/C_{100\text{-}105}}(CH_2)$), 27.0 (s, $\mathbf{C_{15\text{-}18}/C_{100\text{-}105}}(CH_2)$), 25.9 (s, $\mathbf{C_{15\text{-}18}/C_{100\text{-}105}}(CH_2)$), 22.7 (s, $\mathbf{C_{15\text{-}18}/C_{100\text{-}105}}(CH_2)$), 14.1 (s, $\mathbf{C_{105}}(CH_3)$) ppm.

IR (Solid) ν_{max}: 2915(m) (**C-H$_2$**), 2845(m), 2227(m) (**C≡N**), 1604(m) (**Ar**), 1576(w) (**Ar**), 1510(s) (**Ar**), 1467(s) cm^{-1}.

EIMS: *m/z* 279 ($[C_{20}H_{23}O]^+$, 9%), 207 ($[C_{14}H_9NO]^+$, 5%), 167 ($[C_{13}H_9]^+$, 30%), 149 ($[C_{10}H_{13}O]^+$, 100%), 83 ($[C_6H_{11}]^+$, 9%), 70 ($[C_4H_6O]^+$, 35%), 57 ($[C_3H_5O]^+$, 29%), 41 ($[C_3H_5]^+$, 20%)

Elemental Analysis: $C_{38}H_{49}NO_2$: (Expected) **C** 82.64, **H** 8.88, **N** 2.54; (Found) **C** 82.63, **H** 8.87, **N** 2.53

1-(4'-Cyanobiphenyl-4-oxy)-6-(4'-heptyl-1'-cyclohexylphenyl-4-oxy)butane

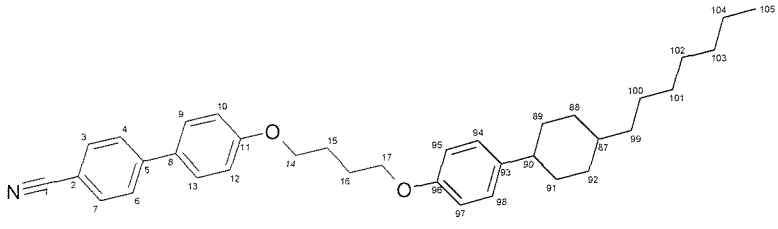

59
$C_{36}H_{45}NO_2$
523.77

Rf 0.78; 100% DCM [1 spot by TLC]

^{1}H NMR (400 MHz, $CDCl_3$): δ_H 7.61 (2H, d, J = 8.6 Hz, C_4**H,** C_6**H**), 7.56 (2H, d, J = 8.6 Hz, C_3**H,** C_7**H**), 7.44 (2H, d, J = 8.9 Hz, C_9**H,** C_{13}**H**), 7.04 (2H, d, J = 8.4 Hz, C_{94}**H,** C_{98}**H**), 6.92 (2H, d, J = 8.8 Hz, C_{95}**H,** C_{97}**H**), 6.75 (2H, d, J = 8.7 Hz, C_{10}**H,** C_{12}**H**), 4.01 (2H, t, 5.6 Hz, O-C_{14}**H$_2$**), 3.95 (2H, t, 5.6 Hz, O-C_{17}**H$_2$**), 2.33 (1H, tt, J = 12.1 Hz, 3.1 Hz, C_{90}**H**), 1.69-2.00 (8H, m, C_{15}**H$_2$**, C_{16}**H$_2$**, C_{89}**H$_2$**, C_{91}**H$_2$**), 1.05-1.44 (15H, m, C_{87}**H,** C_{88}**H$_2$,** C_{92}**H$_2$,** C_{100}**H$_2$,** C_{101}**H$_2$,** C_{102}**H$_2$,** C_{103}**H$_2$,** C_{104}**H$_2$**), 0.87-1.05 (2H, m, C_{99}**H$_2$**), 0.82 (3H, t, J = 7.2 Hz, C_{105}**H$_2$**) ppm.

^{13}C NMR (100 MHz, $CDCl_3$): δ_C 159.7 (q, $\mathbf{C_{11}}$(Ar)), 157.1 (q, $\mathbf{C_{96}}$(Ar)), 145.3 (q, $\mathbf{C_5}$(Ar)), 140.2 (q, $\mathbf{C_{93}}$(Ar)), 132.6 (t, $\mathbf{C_3}$(Ar), $\mathbf{C_7}$(Ar)), 131.4 (q, $\mathbf{C_8}$(Ar)), 128.3 (t, $\mathbf{C_4}$(Ar), $\mathbf{C_6}$(Ar)), 127.6 (t, $\mathbf{C_9}$(Ar),$\mathbf{C_{13}}$(Ar)), 127.1 (t, $\mathbf{C_{94}}$ (Ar), $\mathbf{C_{98}}$(Ar)), 119.1 (q, $\mathbf{C_1}$(CN)), 115.1 (t, $\mathbf{C_{10}}$(Ar), $\mathbf{C_{12}}$(Ar)), 114.3 (t, $\mathbf{C_{95}}$(Ar), $\mathbf{C_{97}}$(Ar)), 110.1 (q, $\mathbf{C_2}$(Ar)), 67.7 (s, $\mathbf{C_{14}}(OCH_2)$), 67.4 (s, $\mathbf{C_{17}}(OCH_2)$), 43.8 (t, $\mathbf{C_{90}}$(CH)), 37.4 (s, $\mathbf{C_{99}}(CH_2)$), 37.4 (t, $\mathbf{C_{87}}$(CH)), 34.6 (s, $\mathbf{C_{89}}(CH_2)$,

$\mathbf{C_{91}}(CH_2)$), 33.6 (s, $\mathbf{C_{88}}(CH_2)$, $\mathbf{C_{92}}(CH_2)$), 31.9 (s, $\mathbf{C_{15\text{-}16}/C_{100\text{-}105}}$ (CH_2)), 30.0 (s, $\mathbf{C_{15\text{-}16}/C_{100\text{-}105}}(CH_2)$), 29.4 (s, $\mathbf{C_{15\text{-}16}/C_{100\text{-}105}}(CH_2)$), 27.0 (s, $\mathbf{C_{15\text{-}16}/C_{100\text{-}105}}(CH_2)$), 26.0 (s, $\mathbf{C_{15\text{-}16}/C_{100\text{-}105}}(CH_2)$), 22.7 (s, $\mathbf{C_{15\text{-}16}/C_{100\text{-}105}}(CH_2)$), 14.1 (s, $\mathbf{C_{105}}(CH_3)$) ppm.

IR (Solid) ν_{max}: 2915(m) (**C-H$_2$**), 2867(m), 2225(m) (**C≡N**), 1597(m) (**Ar**), 1529(w) (**Ar**), 1493 (s) cm^{-1}.

EIMS: *m/z* 523 ($[M]^+$, 22%), 329 ($[C_{23}H_{34}O]^+$, 39%), 274 ($[C_{19}H_{30}O]^+$, 8%), 250 ($[C_{17}H_{28}O]^+$, 100%), 208 ($[C_{14}H_{10}NO]^+$, 73%), 195 ($[C_{13}H_9NO]^+$, 74%), 133 ($[C_9H_{10}O]^+$, 38%), 55 ($[C_4H_7]^+$, 24%), 41 ($[C_3H_5]^+$, 6%).

1-(4'-Cyanobiphenyl-4-oxy)-5-(4'-heptyl-1'-cyclohexylphenyl-4-oxy)pentane

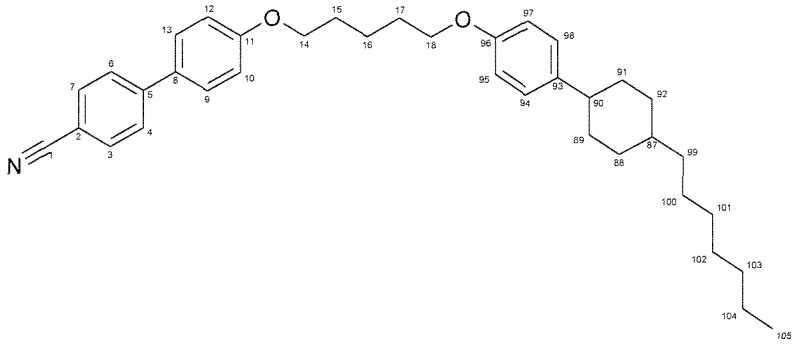

60
$C_{37}H_{47}NO_2$
537.79

Rf 0.78; 100% DCM [1 spot by TLC]

^{1}H NMR (400 MHz, $CDCl_3$): δ_H 7.60 (2H, d, J = 8.6 Hz, C_4**H**, C_6**H**), 7.55 (2H, d, J = 8.6 Hz, C_3**H**, C_7**H**), 7.44 (2H, d, J = 9.0 Hz, C_9**H**, C_{13}**H**), 7.04 (2H, d, J = 8.6 Hz, C_{94}**H**, C_{98}**H**), 6.91 (2H, d, J = 8.8 Hz, C_{95}**H**, C_{97}**H**), 6.74 (2H, d, J = 8.8 Hz, C_{10}**H**, C_{12}**H**), 3.96 (2H, t, 6.3 Hz, O-C_{14}**H$_2$**), 3.89 (2H, t, 6.3 Hz, O-C_{18}**H$_2$**), 2.32 (1H, tt, J = 12.0 Hz, 2.9 Hz, C_{90}**H**), 1.67-1.87 (8H, m, C_{15}**H$_2$**, C_{17}**H$_2$**, C_{89}**H$_2$**, C_{91}**H$_2$**), 1.52-1.67 (8H, m, C_{15}**H$_2$**, C_{17}**H$_2$**, C_{18}**H$_2$**, C_{89}**H$_2$**, C_{91}**H$_2$**), 1.04-1.43 (15H, m, C_{87}**H**, C_{88}**H$_2$**, C_{92}**H$_2$**, C_{100}**H$_2$**, C_{101}**H$_2$**, C_{102}**H$_2$**, C_{103}**H$_2$**, C_{104}**H$_2$**), 0.86-1.05 (2H, m, C_{99}**H$_2$**), 0.81 (3H, t, J = 7.2 Hz, C_{105}**H$_2$**) ppm.

^{13}C NMR (100 MHz, $CDCl_3$): δ_C 159.8 (q, $\mathbf{C_{11}}$(Ar)), 157.1 (q, $\mathbf{C_{96}}$(Ar)), 145.3 (q, $\mathbf{C_5}$(Ar)), 140.1 (q, $\mathbf{C_{93}}$(Ar)), 132.6 (t, $\mathbf{C_3}$(Ar), $\mathbf{C_7}$(Ar)), 131.4 (q, $\mathbf{C_8}$(Ar)), 128.3 (t, $\mathbf{C_4}$(Ar), $\mathbf{C_6}$(Ar)), 127.6 (t, $\mathbf{C_9}$(Ar),$\mathbf{C_{13}}$(Ar)), 127.1 (t, $\mathbf{C_{94}}$ (Ar),

C_{98}(Ar)), 119.1 (q, C_1(CN)), 115.1 (t, C_{10}(Ar), C_{12}(Ar)), 114.3 (t, C_{95}(Ar), C_{97}(Ar)), 110.1 (q, C_2(Ar)), 68.0 (s, $C_{14}(OCH_2)$), 67.7 (s, $C_{18}(OCH_2)$), 43.8 (t, C_{90}(CH)), 37.5 (s, $C_{99}(CH_2)$), 37.4 (t, C_{87}(CH)), 34.6 (s, $C_{89}(CH_2)$, $C_{91}(CH_2)$), 33.7 (s, $C_{88}(CH_2)$, $C_{92}(CH_2)$), 31.9 (s, $C_{15\text{-}17}/C_{100\text{-}105}$ (CH_2)), 30.0 (s, $C_{15\text{-}17}/C_{100\text{-}105}(CH_2)$), 29.4 (s, $C_{15\text{-}17}/C_{100\text{-}105}(CH_2)$), 29.1 (s, $C_{15\text{-}17}/C_{100\text{-}105}(CH_2)$), 29.0 (s, $C_{15\text{-}17}/C_{100\text{-}105}(CH_2)$), 27.0 (s, $C_{15\text{-}17}/C_{100\text{-}105}(CH_2)$), 22.8 (s, $C_{15\text{-}16}/C_{100\text{-}105}(CH_2)$), 22.7 (s, $C_{15\text{-}16}/C_{100\text{-}105}(CH_2)$), 14.1 (s, $C_{105}(CH_3)$) ppm.

IR (Solid) ν_{max}: 2916(m) (**C-H$_2$**), 2846(m), 2226(m) (**C≡N**), 1604(m) (**Ar**), 1511(w) (**Ar**), 1466 (s) cm^{-1}.

EIMS: *m/z* 537 ($[M]^+$, 9%), 343 ($[C_{24}H_{36}O]^+$, 39%), 274 ($[C_{19}H_{30}O]^+$, 8%), 264 ($[C_{18}H_{30}O]^+$, 100%), 208 ($[C_{14}H_{10}NO]^+$, 31%), 195 ($[C_{13}H_9NO]^+$, 92%), 133 ($[C_9H_{10}O]^+$, 38%), 69 ($[C_4H_7]^+$, 24%), 55 ($[C_4H_7]^+$, 24%), 41 ($[C_3H_5]^+$, 6%).

1-(4'-Cyanobiphenyl-4-oxy)-7-(4'-heptyl-1'-cyclohexylphenyl-4-oxy)heptane

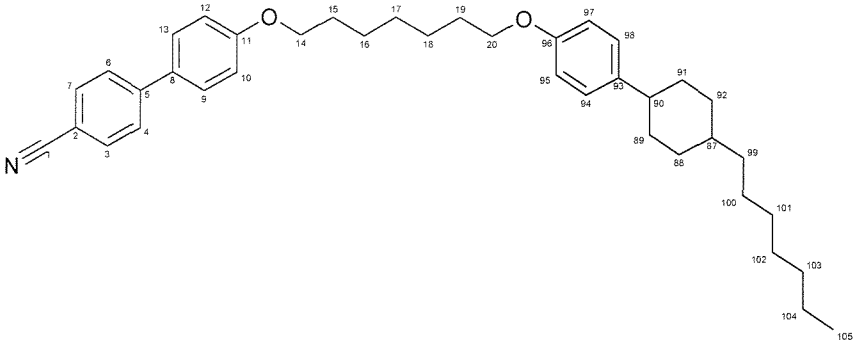

61
$C_{39}H_{51}NO_2$
565.85

Rf 0.80; 100% DCM [1 spot by TLC]

^{1}H NMR (400 MHz, $CDCl_3$): δ_H 7.61 (2H, d, J = 8.6 Hz, C_4**H**, C_6**H**), 7.56 (2H, d, J = 8.6 Hz, C_3**H**, C_7**H**), 7.45 (2H, d, J = 8.8 Hz, C_9**H**, C_{13}**H**), 7.03 (2H, d, J = 8.6 Hz, C_{94}**H**, C_{98}**H**), 6.91 (2H, d, J = 8.8 Hz, C_{95}**H**, C_{97}**H**), 6.74 (2H, d, J = 8.6 Hz, C_{10}**H**, C_{12}**H**), 3.94 (2H, t, 6.5 Hz, O-C_{14}**H$_2$**), 3.86 (2H, t, 6.5 Hz, O-C_{20}**H$_2$**), 2.32 (1H, tt, J = 12.1 Hz, 3.2 Hz, C_{90}**H**), 1.61-1.89 (8H, m, C_{15}**H$_2$**, C_{19}**H$_2$**, C_{89}**H$_2$**, C_{91}**H$_2$**), 1.06-1.41 (21H, m, C_{16}**H$_2$**, C_{17}**H$_2$**, C_{18}**H$_2$**, C_{87}**H**, C_{88}**H$_2$**, C_{92}**H$_2$**, C_{100}**H$_2$**, C_{101}**H$_2$**, C_{102}**H$_2$**, C_{103}**H$_2$**, C_{104}**H$_2$**), 0.89-1.06 (2H, m, C_{99}**H$_2$**), 0.82 (3H, t, J = 7.0 Hz, C_{105}**H$_2$**) ppm.

^{13}C NMR (100 MHz, $CDCl_3$): δ_C 159.8 (q, **C_{11}**(Ar)), 157.2 (q, **C_{96}**(Ar)), 145.3 (q, **C_5**(Ar)), 140.0 (q, **C_{93}**(Ar)), 132.5 (t, **C_3**(Ar), **C_7**(Ar)), 131.3 (q, **C_8**(Ar)), 128.3 (t, **C_4**(Ar), **C_6**(Ar)), 127.6 (t, **C_9**(Ar),**C_{13}**(Ar)), 127.1 (t, **C_{94}** (Ar), **C_{98}**(Ar)), 119.1 (q, **C_1**(CN)), 115.1 (t, **C_{10}**(Ar), **C_{12}**(Ar)), 114.3 (t, **C_{95}**(Ar), **C_{97}**(Ar)), 110.1 (q, **C_2**(Ar)), 68.1 (s, **C_{14}**(OCH_2)), 67.9 (s, **C_{20}**(OCH_2)), 43.7 (t, **C_{90}**(CH)), 37.5 (s, **C_{99}**(CH_2)), 37.4 (t, **C_{87}**(CH)), 34.6 (s, **C_{89}**(CH_2), **C_{91}**(CH_2)), 33.7 (s, **C_{88}**(CH_2), **C_{92}**(CH_2)), 31.9 (s, **$C_{15\text{-}19}$/$C_{100\text{-}105}$** (CH_2)), 30.0 (s, **$C_{15\text{-}19}$/$C_{100\text{-}105}$**(CH_2)), 29.4 (s, **$C_{15\text{-}19}$/$C_{100\text{-}105}$**(CH_2)), 29.3 (s, **$C_{15\text{-}19}$/$C_{100\text{-}105}$**(CH_2)), 29.1 (s, **$C_{15\text{-}19}$/$C_{100\text{-}105}$**(CH_2)), 27.0 (s, **$C_{15\text{-}19}$/$C_{100\text{-}105}$**(CH_2)), 26.0 (s, **$C_{15\text{-}19}$/$C_{100\text{-}105}$**(CH_2)), 22.7 (s, **$C_{15\text{-}19}$/$C_{100\text{-}105}$**(CH_2)), 14.1 (s, **C_{105}**(CH_3)) ppm.

IR (Solid) ν_{max}: 2915(m) (**C-H_2**), 2846(m), 2229(m) (**C≡N**), 1604(m) (**Ar**), 1577(w) (**Ar**), 1510(s) (**Ar**), 1469(s) cm^{-1}.

EIMS: *m/z* 279 ($[C_{20}H_{23}O]^+$, 8%), 207 ($[C_{14}H_9NO]^+$, 4%), 167 ($[C_{13}H_9]^+$, 29%), 149 ($[C_{10}H_{13}O]^+$, 100%), 83 ($[C_6H_{11}]^+$, 9%), 70 ($[C_4H_6O]^+$, 38%), 57 ($[C_3H_5O]^+$, 31%), 41 ($[C_3H_5]^+$, 22%)

1-(4'-Cyanobiphenyl-4-oxy)-8-(4'-heptyl-1'-cyclohexylphenyl-4-oxy)octane

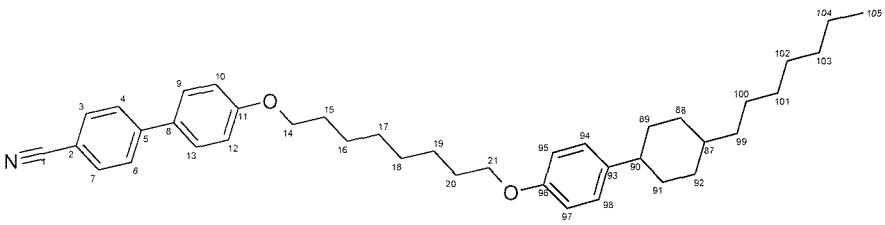

62
$C_{40}H_{53}NO_2$
579.83

Rf 0.80; 100% DCM [1 spot by TLC]

^{1}H NMR (400 MHz, $CDCl_3$): δ_H 7.61 (2H, d, J = 8.6 Hz, C_4**H**, C_6**H**), 7.55 (2H, d, J = 8.6 Hz, C_3**H**, C_7**H**), 7.44 (2H, d, J = 8.8 Hz, C_9**H**, C_{13}**H**), 7.03 (2H, d, J = 8.6 Hz, C_{94}**H**, C_{98}**H**), 6.91 (2H, d, J = 8.8 Hz, C_{95}**H**, C_{97}**H**), 6.74 (2H, d, J = 8.6 Hz, C_{10}**H**, C_{12}**H**), 3.93 (2H, t, 6.5 Hz, O-C_{14}**H_2**), 3.85 (2H, t, 6.5 Hz, O-C_{21}**H_2**), 2.32 (1H, tt, J = 12.1 Hz, 2.9 Hz, C_{90}**H**), 1.63-1.85 (8H, m, C_{15}**H_2**, C_{20}**H_2**, C_{89}**H_2**, C_{91}**H_2**), 1.07-1.49 (23H, m, C_{16}**H_2**, C_{17}**H_2**, C_{18}**H_2**, C_{19}**H_2**, C_{87}**H**, C_{88}**H_2**, C_{92}**H_2**, C_{100}**H_2**, C_{101}**H_2**, C_{102}**H_2**, C_{103}**H_2**, C_{104}**H_2**), 0.87-1.04 (2H, m, C_{99}**H_2**), 0.81 (3H, t, J = 7.0 Hz, C_{105}**H_2**) ppm.

^{13}C NMR (100 MHz, $CDCl_3$): δ_C 159.8 (q, **C_{11}**(Ar)), 157.2 (q, **C_{96}**(Ar)), 145.3 (q, **C_5**(Ar)), 140.0 (q, **C_{93}**(Ar)), 132.5 (t, **C_3**(Ar), **C_7**(Ar)), 131.3 (q, **C_8**(Ar)), 128.3 (t, **C_4**(Ar), **C_6**(Ar)), 127.6 (t, **C_9**(Ar),**C_{13}**(Ar)), 127.1 (t, **C_{94}** (Ar), **C_{98}**(Ar)), 119.1 (q, **C_1**(CN)), 115.1 (t, **C_{10}**(Ar), **C_{12}**(Ar)), 114.3 (t, **C_{95}**(Ar), **C_{97}**(Ar)), 110.1 (q, **C_2**(Ar)), 68.1 (s, **C_{14}**(OCH_2)), 67.9 (s, **C_{21}**(OCH_2)), 43.7 (t, **C_{90}**(CH)), 37.5 (s, **C_{99}**(CH_2)), 37.4 (t, **C_{87}**(CH)), 34.6 (s, **C_{89}**(CH_2), **C_{91}**(CH_2)), 33.7 (s, **C_{88}**(CH_2), **C_{92}**(CH_2)), 31.9 (s, **$C_{15\text{-}20}$/$C_{100\text{-}105}$** (CH_2)), 30.0 (s, **$C_{15\text{-}20}$/$C_{100\text{-}105}$**(CH_2)), 29.4 (s, **$C_{15\text{-}20}$/$C_{100\text{-}105}$**(CH_2)), 29.3 (s, **$C_{15\text{-}20}$/$C_{100\text{-}105}$**(CH_2)), 29.3 (s, **$C_{15\text{-}20}$/$C_{100\text{-}105}$**(CH_2)), 29.2 (s, **$C_{15\text{-}20}$/$C_{100\text{-}105}$**(CH_2)), 27.0 (s, **$C_{15\text{-}20}$/$C_{100\text{-}105}$**(CH_2)), 26.0 (s, **$C_{15\text{-}20}$/$C_{100\text{-}105}$**(CH_2)), 22.7 (s, **$C_{15\text{-}20}$/$C_{100\text{-}105}$**(CH_2)), 14.1 (s, **C_{105}**(CH_3)) ppm.

IR (Solid) ν_{max}: 2913(s) (**C-H_2**), 2846(s), 2227(m) (**C≡N**), 1604(m) (**Ar**), 1578(w) (**Ar**), 1511(s) (**Ar**), 1468(s) cm^{-1}.

EIMS: *m/z* 279 ($[C_{20}H_{23}O]^+$, 10%), 208 ($[C_{14}H_{10}NO]^+$, 1%), 193 ($[C_{13}H_7NO]^+$, 1%), 167 ($[C_{13}H_9]^+$, 32%), 149 ($[C_{10}H_{13}O]^+$, 100%), 83 ($[C_6H_{11}]^+$, 9%), 70 ($[C_4H_6O]^+$, 35%), 57 ($[C_3H_5O]^+$, 30%), 41 ($[C_3H_5]^+$, 21%)

1-(4'-Cyanobiphenyl-4-oxy)-9-(4'-heptyl-1'-cyclohexylphenyl-4-oxy)nonane

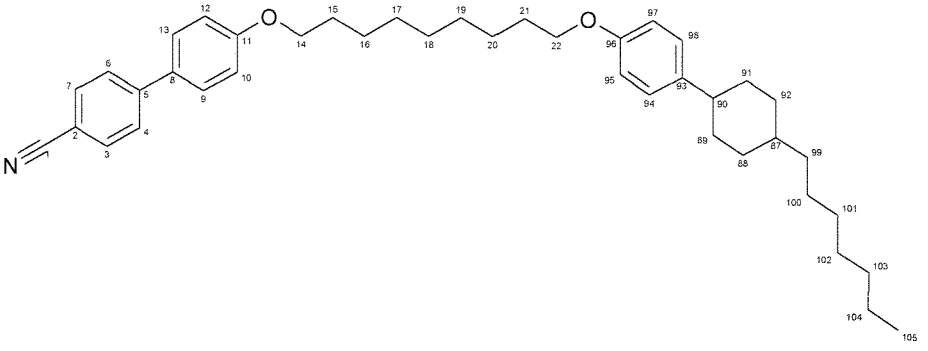

63
$C_{41}H_{55}NO_2$
593.90

Rf 0.81; 100% DCM [1 spot by TLC]

^{1}H NMR (400 MHz, $CDCl_3$): δ_H 7.61 (2H, d, J = 8.6 Hz, C_4**H,** C_6**H**), 7.56 (2H, d, J = 8.5 Hz, C_3**H,** C_7**H**), 7.45 (2H, d, J = 9.0 Hz, C_9**H,** C_{13}**H**), 7.03 (2H, d, J = 8.4 Hz, C_{94}**H,** C_{98}**H**), 6.92 (2H, d, J = 9.0 Hz, C_{95}**H,** C_{97}**H**), 6.74 (2H, d, J = 8.8 Hz, C_{10}**H,** C_{12}**H**), 3.93 (2H, t, 6.6 Hz, O-C_{14}**H_2**), 3.85 (2H, t, 6.5 Hz, O-C_{22}**H_2**), 2.32 (1H, tt, J = 12.1 Hz, 3.0 Hz, C_{90}**H**), 1.62-1.85 (8H, m, C_{15}**H_2**,

$C_{21}\mathbf{H_2}$, $C_{89}\mathbf{H_2}$, $C_{91}\mathbf{H_2}$), 1.06-1.52 (25H, m, $C_{16}\mathbf{H_2}$, $C_{17}\mathbf{H_2}$, $C_{18}\mathbf{H_2}$, $C_{19}\mathbf{H_2}$, $C_{20}\mathbf{H_2}$, $C_{87}\mathbf{H}$, $C_{88}\mathbf{H_2}$, $C_{92}\mathbf{H_2}$, $C_{100}\mathbf{H_2}$, $C_{101}\mathbf{H_2}$, $C_{102}\mathbf{H_2}$, $C_{103}\mathbf{H_2}$, $C_{104}\mathbf{H_2}$), 0.86-1.05 (2H, m, $C_{99}\mathbf{H_2}$), 0.82 (3H, t, J = 7.1 Hz, $C_{105}\mathbf{H_2}$) ppm.

^{13}C NMR (100 MHz, $CDCl_3$): δ_C 160.2 (q, $\mathbf{C_{11}}$(Ar)), 157.6 (q, $\mathbf{C_{96}}$(Ar)), 145.7 (q, $\mathbf{C_5}$(Ar)), 140.4 (q, $\mathbf{C_{93}}$(Ar)), 133.0 (t, $\mathbf{C_3}$(Ar), $\mathbf{C_7}$(Ar)), 131.7 (q, $\mathbf{C_8}$(Ar)), 128.7 (t, $\mathbf{C_4}$(Ar), $\mathbf{C_6}$(Ar)), 128.0 (t, $\mathbf{C_9}$(Ar),$\mathbf{C_{13}}$(Ar)), 127.5 (t, $\mathbf{C_{94}}$ (Ar), $\mathbf{C_{98}}$(Ar)), 119.5 (q, $\mathbf{C_1}$(CN)), 115.5 (t, $\mathbf{C_{10}}$(Ar), $\mathbf{C_{12}}$(Ar)), 114.7 (t, $\mathbf{C_{95}}$(Ar), $\mathbf{C_{97}}$(Ar)), 110.5 (q, $\mathbf{C_2}$(Ar)), 68.6 (s, $\mathbf{C_{14}}$(OCH_2)), 68.3 (s, $\mathbf{C_{22}}$(OCH_2)), 44.2 (t, $\mathbf{C_{90}}$(CH)), 37.9 (s, $\mathbf{C_{99}}$(CH_2)), 37.8 (t, $\mathbf{C_{87}}$(CH)), 35.0 (s, $\mathbf{C_{89}}$(CH_2), $\mathbf{C_{91}}$(CH_2)), 34.1 (s, $\mathbf{C_{88}}$(CH_2), $\mathbf{C_{92}}$(CH_2)), 32.3 (s, $\mathbf{C_{15\text{-}21}}$/$\mathbf{C_{100\text{-}105}}$ (CH_2)), 30.4 (s, $\mathbf{C_{15\text{-}21}}$/$\mathbf{C_{100\text{-}105}}$($CH_2$)), 29.9 (s, $\mathbf{C_{15\text{-}21}}$/$\mathbf{C_{100\text{-}105}}$($CH_2$)), 29.8 (s, $\mathbf{C_{15\text{-}21}}$/$\mathbf{C_{100\text{-}105}}$($CH_2$)), 29.8 (s, $\mathbf{C_{15\text{-}21}}$/$\mathbf{C_{100\text{-}105}}$($CH_2$)), 29.7 (s, $\mathbf{C_{15\text{-}21}}$/$\mathbf{C_{100\text{-}105}}$($CH_2$)), 29.6 (s, $\mathbf{C_{15\text{-}21}}$/$\mathbf{C_{100\text{-}105}}$($CH_2$)), 27.4 (s, $\mathbf{C_{15\text{-}21}}$/$\mathbf{C_{100\text{-}105}}$($CH_2$)), 26.5 (s, $\mathbf{C_{15\text{-}21}}$/$\mathbf{C_{100\text{-}105}}$($CH_2$)), 26.4 (s, $\mathbf{C_{15\text{-}21}}$/$\mathbf{C_{100\text{-}105}}$($CH_2$)), 23.1 (s, $\mathbf{C_{15\text{-}21}}$/$\mathbf{C_{100\text{-}105}}$($CH_2$)), 14.5 (s, $\mathbf{C_{105}}$(CH_3)) ppm.

IR (Solid) ν_{max}: 2914(s) (**C-H$_2$**), 2846(s), 2229(m) (**C≡N**), 1604(m) (**Ar**), 1578(w) (**Ar**), 1511(s) (**Ar**), 1468(s) cm^{-1}.

EIMS: *m/z* 279 ($[C_{20}H_{23}O]^+$, 10%), 207 ($[C_{14}H_9NO]^+$, 6%), 167 ($[C_{13}H_9]^+$, 32%), 149 ($[C_{10}H_{13}O]^+$, 100%), 83 ($[C_6H_{11}]^+$, 9%), 70 ($[C_4H_6O]^+$, 35%), 57 ($[C_3H_5O]^+$, 28%), 41 ($[C_3H_5]^+$, 20%)

1-(4'-Cyanobiphenyl-4-oxy)-10-(4'-heptyl-1'-cyclohexylphenyl-4-oxy)decane

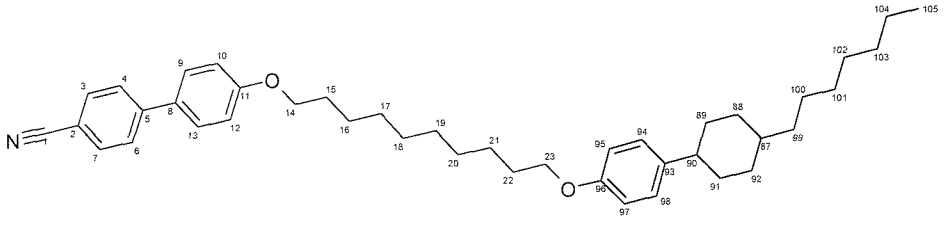

64
$C_{42}H_{57}NO_2$
607.93

Rf 0.82; 100% DCM [1 spot by TLC]

^{1}H NMR (400 MHz, $CDCl_3$): δ_H 7.61 (2H, d, J = 8.6 Hz, $C_4\mathbf{H}$, $C_6\mathbf{H}$), 7.56 (2H, d, J = 8.6 Hz, $C_3\mathbf{H}$, $C_7\mathbf{H}$), 7.45 (2H, d, J = 8.8 Hz, $C_9\mathbf{H}$, $C_{13}\mathbf{H}$), 7.03 (2H, d, J = 8.6 Hz, $C_{94}\mathbf{H}$, $C_{98}\mathbf{H}$), 6.92 (2H, d, J = 9.0 Hz, $C_{95}\mathbf{H}$, $C_{97}\mathbf{H}$), 6.74 (2H, d, J = 8.6

Hz, $C_{10}\mathbf{H}$, $C_{12}\mathbf{H}$), 3.93 (2H, t, 6.6 Hz, O-$C_{14}\mathbf{H_2}$), 3.85 (2H, t, 6.6 Hz, O-$C_{23}\mathbf{H_2}$), 2.32 (1H, tt, J = 12.3 Hz, 3.1 Hz, $C_{90}\mathbf{H}$), 1.63-1.85 (8H, m, $C_{15}\mathbf{H_2}$, $C_{22}\mathbf{H_2}$, $C_{89}\mathbf{H_2}$, $C_{91}\mathbf{H_2}$), 1.07-1.45 (27H, m, $C_{16}\mathbf{H_2}$, $C_{17}\mathbf{H_2}$, $C_{18}\mathbf{H_2}$, $C_{19}\mathbf{H_2}$, $C_{20}\mathbf{H_2}$, $C_{21}\mathbf{H_2}$, $C_{87}\mathbf{H}$, $C_{88}\mathbf{H_2}$, $C_{92}\mathbf{H_2}$, $C_{100}\mathbf{H_2}$, $C_{101}\mathbf{H_2}$, $C_{102}\mathbf{H_2}$, $C_{103}\mathbf{H_2}$, $C_{104}\mathbf{H_2}$), 0.89-1.07 (2H, m, $C_{99}\mathbf{H_2}$), 0.82 (3H, t, J = 7.0 Hz, $C_{105}\mathbf{H_2}$) ppm.

^{13}C NMR (100 MHz, $CDCl_3$): δ_C 159.8 (q, $\mathbf{C_{11}}$(Ar)), 157.2 (q, $\mathbf{C_{96}}$(Ar)), 145.3 (q, $\mathbf{C_5}$(Ar)), 140.0 (q, $\mathbf{C_{93}}$(Ar)), 132.6 (t, $\mathbf{C_3}$(Ar), $\mathbf{C_7}$(Ar)), 131.3 (q, $\mathbf{C_8}$(Ar)), 128.3 (t, $\mathbf{C_4}$(Ar), $\mathbf{C_6}$(Ar)), 127.7 (t, $\mathbf{C_9}$(Ar),$\mathbf{C_{13}}$(Ar)), 127.0 (t, $\mathbf{C_{94}}$ (Ar), $\mathbf{C_{98}}$(Ar)), 119.1 (q, $\mathbf{C_1}$(CN)), 115.1 (t, $\mathbf{C_{10}}$(Ar), $\mathbf{C_{12}}$(Ar)), 114.3 (t, $\mathbf{C_{95}}$(Ar), $\mathbf{C_{97}}$(Ar)), 110.1 (q, $\mathbf{C_2}$(Ar)), 68.2 (s, $\mathbf{C_{14}}$(OCH_2)), 68.0 (s, $\mathbf{C_{23}}$(OCH_2)), 43.7 (t, $\mathbf{C_{90}}$(CH)), 37.5 (s, $\mathbf{C_{99}}$(CH_2)), 37.4 (t, $\mathbf{C_{87}}$(CH)), 34.6 (s, $\mathbf{C_{89}}$(CH_2), $\mathbf{C_{91}}$(CH_2)), 33.7 (s, $\mathbf{C_{88}}$(CH_2), $\mathbf{C_{92}}$(CH_2)), 31.9 (s, $\mathbf{C_{15\text{-}22}/C_{100\text{-}105}}$ (CH_2)), 30.0 (s, $\mathbf{C_{15\text{-}22}/C_{100\text{-}105}}$($CH_2$)), 29.5 (s, $\mathbf{C_{15\text{-}22}/C_{100\text{-}105}}$($CH_2$)), 29.4 (s, $\mathbf{C_{15\text{-}22}/C_{100\text{-}105}}$($CH_2$)), 29.2 (s, $\mathbf{C_{15\text{-}22}/C_{100\text{-}105}}$($CH_2$)), 27.0 (s, $\mathbf{C_{15\text{-}22}/C_{100\text{-}105}}$($CH_2$)), 26.1 (s, $\mathbf{C_{15\text{-}22}/C_{100\text{-}105}}$($CH_2$)), 22.7 (s, $\mathbf{C_{15\text{-}22}/C_{100\text{-}105}}$($CH_2$)), 14.1 (s, $\mathbf{C_{105}}$(CH_3)) ppm.

IR (Solid) ν_{max}: 2914(s) (**C-H$_2$**), 2845(s), 2226(m) (**C≡N**), 1600(m) (**Ar**), , 1511(s) (**Ar**), 1465(s) cm^{-1}.

EIMS: *m/z* 607 ($[M]^+$, 22%), 466 ($[C_{34}H_{43}NO]^+$, 6%), 333 ($[C_{23}H_{38}O]^+$, 11%), 274 ($[C_{19}H_{30}O]^+$, 14%), 195 ($[C_{13}H_9NO]^+$, 100%), 133 ($[C_9H_{10}O]^+$, 68%), 55 ($[C_4H_7]^+$, 24%), 41 ($[C_3H_5]^+$, 11%).

1-(4'-Cyanobiphenyl-4-oxy)-11-(4'-heptyl-1'-cyclohexylphenyl-4-oxy)undecane

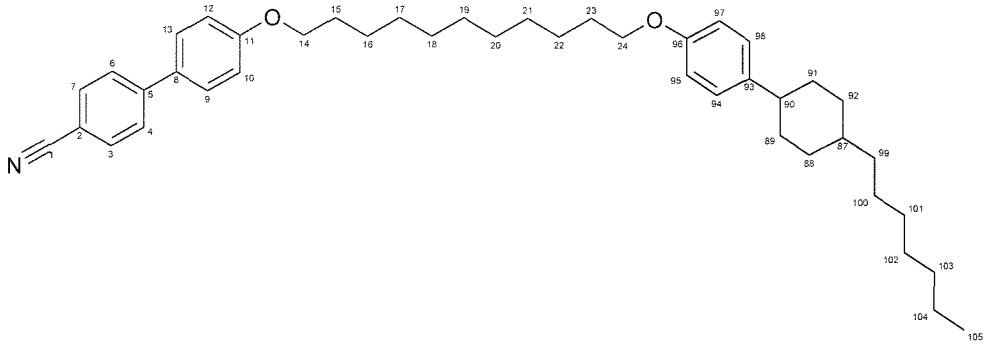

65
$C_{43}H_{59}NO_2$
621.96

Rf 0.84; 100% DCM [1 spot by TLC]

^{1}H NMR (400 MHz, $CDCl_3$): δ_H 7.61 (2H, d, J = 8.6 Hz, C_4**H,** C_6**H**), 7.56 (2H, d, J = 8.6 Hz, C_3**H,** C_7**H**), 7.45 (2H, d, J = 8.8 Hz, C_9**H,** C_{13}**H**), 7.03 (2H, d, J = 8.6 Hz, C_{94}**H,** C_{98}**H**), 6.92 (2H, d, J = 8.8 Hz, C_{95}**H,** C_{97}**H**), 6.74 (2H, d, J = 8.8 Hz, C_{10}**H,** C_{12}**H**), 3.93 (2H, t, 6.6 Hz, O-C_{14}**H$_2$**), 3.85 (2H, t, 6.5 Hz, O-C_{24}**H$_2$**), 2.32 (1H, tt, J = 12.0 Hz, 2.6 Hz, C_{90}**H**), 1.60-1.84 (8H, m, C_{15}**H$_2$**, C_{23}**H$_2$**, C_{89}**H$_2$**, C_{91}**H$_2$**), 1.06-1.44 (29H, m, C_{16}**H$_2$**, C_{17}**H$_2$**, C_{18}**H$_2$**, C_{19}**H$_2$**, C_{20}**H$_2$**, C_{21}**H$_2$**, C_{22}**H$_2$**, C_{87}**H,** C_{88}**H$_2$,** C_{92}**H$_2$,** C_{100}**H$_2$,** C_{101}**H$_2$,** C_{102}**H$_2$,** C_{103}**H$_2$,** C_{104}**H$_2$**), 0.87-1.05 (2H, m, C_{99}**H$_2$**), 0.82 (3H, t, J = 6.4 Hz, C_{105}**H$_2$**) ppm.

^{13}C NMR (100 MHz, $CDCl_3$): δ_C 159.7 (q, **C_{11}**(Ar)), 157.1 (q, **C_{96}**(Ar)), 145.2 (q, **C_5**(Ar)), 139.9 (q, **C_{93}**(Ar)), 132.5 (t, **C_3**(Ar), **C_7**(Ar)), 131.2 (q, **C_8**(Ar)), 128.3 (t, **C_4**(Ar), **C_6**(Ar)), 127.6 (t, **C_9**(Ar),**C_{13}**(Ar)), 127.1 (t, **C_{94}** (Ar), **C_{98}**(Ar)), 119.0 (q, **C_1**(CN)), 115.1 (t, **C_{10}**(Ar), **C_{12}**(Ar)), 114.3 (t, **C_{95}**(Ar), **C_{97}**(Ar)), 110.0 (q, **C_2**(Ar)), 68.2 (s, **C_{14}**(OCH_2)), 68.0 (s, **C_{24}**(OCH_2)), 43.7 (t, **C_{90}**(CH)), 37.4 (s, **C_{99}**(CH_2)), 37.4 (t, **C_{87}**(CH)), 34.6 (s, **C_{89}**(CH_2), **C_{91}**(CH_2)), 33.7 (s, **C_{88}**(CH_2), **C_{92}**(CH_2)), 31.9 (s, **$C_{15\text{-}23}$/$C_{100\text{-}105}$** (CH_2)), 30.0 (s, **$C_{15\text{-}23}$/$C_{100\text{-}105}$**(CH_2)), 29.5 (s, **$C_{15\text{-}23}$/$C_{100\text{-}105}$**(CH_2)), 29.4 (s, **$C_{15\text{-}23}$/$C_{100\text{-}105}$**(CH_2)), 29.4 (s, **$C_{15\text{-}23}$/$C_{100\text{-}105}$**(CH_2)), 29.3 (s, **$C_{15\text{-}23}$/$C_{100\text{-}105}$**(CH_2)), 29.2 (s, **$C_{15\text{-}23}$/$C_{100\text{-}105}$**(CH_2)), 27.0 (s, **$C_{15\text{-}23}$/$C_{100\text{-}105}$**(CH_2)), 26.1 (s, **$C_{15\text{-}23}$/$C_{100\text{-}105}$**(CH_2)), 26.0 (s, **$C_{15\text{-}23}$/$C_{100\text{-}105}$**(CH_2)), 22.6 (s, **$C_{15\text{-}23}$/$C_{100\text{-}105}$**(CH_2)), 14.1 (s, **C_{105}**(CH_3)) ppm.

IR (Solid) ν_{max}: 2915(s) (**C-H$_2$**), 2847(s), 2230(m) (**C≡N**), 1604(m) (**Ar**), 1510(s) (**Ar**), 1471(s) cm^{-1}.

EIMS: *m/z* 279 ($[C_{20}H_{23}O]^+$, 10%), 207 ($[C_{14}H_9NO]^+$, 5%), 167 ($[C_{13}H_9]^+$, 31%), 149 ($[C_{10}H_{13}O]^+$, 100%), 83 ($[C_6H_{11}]^+$, 9%), 70 ($[C_4H_6O]^+$, 33%), 57 ($[C_3H_5O]^+$, 28%), 41 ($[C_3H_5]^+$, 19%)

1-(4'-Cyanobiphenyl-4-oxy)-12-(4'-heptyl-1'-cyclohexylphenyl-4-oxy)dodecane

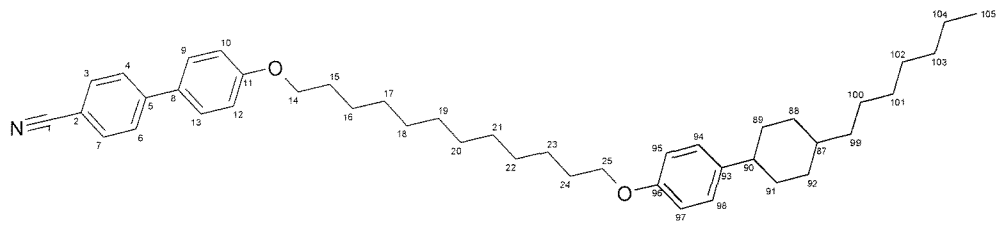

66
$C_{44}H_{61}NO_2$
635.98

Rf 0.85; 100% DCM [1 spot by TLC]

^{1}H NMR (400 MHz, $CDCl_3$): δ_H 7.61 (2H, d, J = 8.6 Hz, C_4**H,** C_6**H**), 7.55 (2H, d, J = 8.6 Hz, C_3**H,** C_7**H**), 7.44 (2H, d, J = 9.0 Hz, C_9**H,** C_{13}**H**), 7.03 (2H, d, J = 8.4 Hz, C_{94}**H,** C_{98}**H**), 6.91 (2H, d, J = 8.8 Hz, C_{95}**H,** C_{97}**H**), 6.74 (2H, d, J = 8.8 Hz, C_{10}**H,** C_{12}**H**), 3.93 (2H, t, 6.6 Hz, O-C_{14}**H$_2$**), 3.84 (2H, t, 6.5 Hz, O-C_{25}**H$_2$**), 2.32 (1H, tt, J = 12.1 Hz, 2.7 Hz, C_{90}**H**), 1.56-1.85 (8H, m, C_{15}**H$_2$**, C_{24}**H$_2$**, C_{89}**H$_2$**, C_{91}**H$_2$**), 1.05-1.47 (31H, m, C_{16}**H$_2$**, C_{17}**H$_2$**, C_{18}**H$_2$**, C_{19}**H$_2$**, C_{20}**H$_2$**, C_{21}**H$_2$**, C_{22}**H$_2$**, C_{23}**H$_2$**, C_{87}**H,** C_{88}**H$_2$,** C_{92}**H$_2$,** C_{100}**H$_2$,** C_{101}**H$_2$,** C_{102}**H$_2$,** C_{103}**H$_2$,** C_{104}**H$_2$**), 0.86-1.06 (2H, m, C_{99}**H$_2$**), 0.81 (3H, t, J = 6.6 Hz, C_{105}**H$_2$**) ppm.

^{13}C NMR (100 MHz, $CDCl_3$): δ_C 159.8 (q, **C_{11}**(Ar)), 157.3 (q, **C_{96}**(Ar)), 145.3 (q, **C_5**(Ar)), 140.0 (q, **C_{93}**(Ar)), 132.5 (t, **C_3**(Ar), **C_7**(Ar)), 131.3 (q, **C_8**(Ar)), 128.3 (t, **C_4**(Ar), **C_6**(Ar)), 127.6 (t, **C_9**(Ar),**C_{13}**(Ar)), 127.1 (t, **C_{94}** (Ar), **C_{98}**(Ar)), 119.1 (q, **C_1**(CN)), 115.1 (t, **C_{10}**(Ar), **C_{12}**(Ar)), 114.3 (t, **C_{95}**(Ar), **C_{97}**(Ar)), 110.1 (q, **C_2**(Ar)), 68.2 (s, **C_{14}**(OCH_2)), 68.0 (s, **C_{25}**(OCH_2)), 43.7 (t, **C_{90}**(CH)), 37.5 (s, **C_{99}**(CH_2)), 37.4 (t, **C_{87}**(CH)), 34.6 (s, **C_{89}**(CH_2), **C_{91}**(CH_2)), 33.7 (s, **C_{88}**(CH_2), **C_{92}**(CH_2)), 31.9 (s, **$C_{15\text{-}24}$/$C_{100\text{-}105}$** (CH_2)), 30.0 (s, **$C_{15\text{-}24}$/$C_{100\text{-}105}$**(CH_2)), 29.5 (s, **$C_{15\text{-}24}$/$C_{100\text{-}105}$**(CH_2)), 29.4 (s, **$C_{15\text{-}24}$/$C_{100\text{-}105}$**(CH_2)), 29.4 (s, **$C_{15\text{-}24}$/$C_{100\text{-}105}$**(CH_2)), 29.2 (s, **$C_{15\text{-}24}$/$C_{100\text{-}105}$**(CH_2)), 27.0 (s, **$C_{15\text{-}24}$/$C_{100\text{-}105}$**(CH_2)), 26.1 (s, **$C_{15\text{-}24}$/$C_{100\text{-}105}$**(CH_2)), 26.0 (s, **$C_{15\text{-}24}$/$C_{100\text{-}105}$**(CH_2)), 22.7 (s, **$C_{15\text{-}24}$/$C_{100\text{-}105}$**(CH_2)), 14.1 (s, **C_{105}**(CH_3)) ppm.

IR (Solid) ν_{max}: 2912(s) (**C-H$_2$**), 2846(s), 2228(m) (**C≡N**), 1600(m) (**Ar**), 1511(s) (**Ar**), 1500(s) (**Ar**), 1465(s) cm^{-1}.

EIMS: *m/z* 635 ($[M]^+$, 28%), 494 ($[C_{36}H_{47}NO]^+$, 6%), 361 ($[C_{25}H_{42}O]^+$, 11%), 274 ($[C_{19}H_{30}O]^+$, 18%), 195 ($[C_{13}H_9NO]^+$, 100%), 133 ($[C_9H_{10}O]^+$, 62%), 55 ($[C_4H_7]^+$, 24%), 41 ($[C_3H_5]^+$, 11%).

7.4. Chapter 5 experimental

7.4.1. Cat(OnOCB)$_2$; 1,2-bis-[α-(4'-cyanobiphen-4-yloxy)alkyl-ω-oxy]benzene

n	Temperature /°C					Mass	Yield
	Cr		N		I	mg	%
4	•	174	•	(140)	•	736	46%
5	•	139	•	(94)	•	1436	46%
6	•	120	•	126	•	650	34%
7	•	80	•	89	•	120	24%
8	•	126	•	(115)	•	1270	68%
9	•	75	•	87	•	700	45%
10	•	113	•	(110)	•	1140	92%
11	•	89	•	91	•	1400	60%
12	•	113	•	(102)	•	1430	63%

1,2-bis-[1-(4'-Cyanobiphen-4-yloxy)butyl-4-oxy]benzene

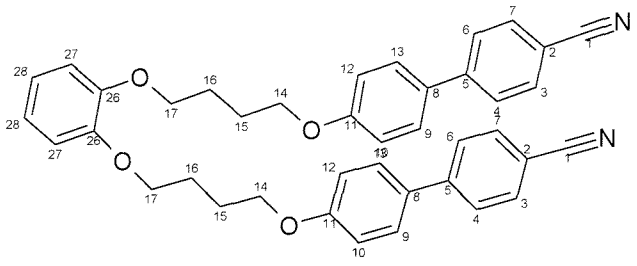

67
$C_{40}H_{36}N_2O_4$
608.74

Procedure:

To a stirred solution of catechol, (0.253 g, 2.28 mMol, 1 eq) in dry, nitrogen purged (30 min) DMF (40 mL) was added solid potassium carbonate (3.77 g, 27.3 mMol, 10 eq) in one portion. The mixture was warmed to 80°C for 10 min, turning blue and then pale brown before being allowed to cool prior to the addition of 1-(cyanobiphenyloxy)-butyl-4-bromide (2.00 g, 4.55 mMol, 2 eq) in one portion and a catalytic quantity of sodium iodide (80 mg). The reaction mixture was then heated to 80°C for 4 days under an N_2 atmosphere. The reaction mixture was allowed to cool and water (40 mL) was added causing a brown/white precipitate to form. The precipitate was filtered through celite and washed with copious amounts of water. The residue, which was only partly soluble in DCM, was extracted from the celite by soxhlet and refluxing DCM. The organic extracts were dried over anhydrous $MgSO_4$ and filtered. The organic solvents were removed *in vacuo* to give a crude yellow solid. The crude material was purified by column

chromatography (silica gel, 40 mm x 100 mm, DCM) affording the title compound **67**, (736 mg, 1.23 mMol, 46.2%) as crystalline white solid.

NB: subsequent homologues were synthesised via an identical route however they were found to be soluble in DCM and consequently the soxhlet extraction step was unnecessary and so omitted.

Rf 0.34; 100% DCM [1 spot by TLC]

^{1}H NMR (300 MHz, $CDCl_3$): δ_H 7.69 (4H, d, J = 8.4 Hz, C_4**H**, C_6**H**), 7.62 (4H, d, J = 8.6 Hz, C_3**H**, C_7**H**), 7.51 (4H, d, 8.8 Hz, C_9**H**, C_{13}**H**), 6.98 (4H, d, J = 8.8 Hz, C_{10}**H**, C_{12}**H**), 6.93 (4H, s, C_{27}**H**, C_{28}**H**), 4.06-4.14 (8H, m, 6.4 Hz, O-C_{14}**H**$_2$, C_{17}**H**$_2$-O), 2.00-2.08 (8H, m, C_{15}**H**$_2$, C_{16}**H**$_2$) ppm.

^{13}C NMR (75 MHz, $CDCl_3$): δ_C 159.8 (q, **C**$_{11}$(Ar_{CB})), 149.1 (q, **C**$_{26}$(Ar_{Cat})), 145.3 (q, **C**$_5$(Ar_{CB})), 132.7 (t, **C**$_3$(Ar_{CB}), **C**$_7$(Ar_{CB})), 131.5 (q, **C**$_8$(Ar_{CB})), 128.5 (t, **C**$_9$(Ar_{CB}), **C**$_{13}$(Ar_{CB})), 127.2 (t, **C**$_4$(Ar_{CB}), **C**$_6$(Ar_{CB})), 121.4 (t, **C**$_{28}$(Ar_{Cat})), 119.2 (q, **C**$_1$(CN)), 115.2 (t, **C**$_{10}$(Ar_{CB}), **C**$_{12}$(Ar_{CB})), 114.1 (t, **C**$_{27}$ (Ar_{Cat})), 110.2 (q, **C**$_2$(Ar_{CB})), 68.8 (s, **C**$_{17}$ (Cat-O-**C**H_2)), 67.8 (s, **C**$_{14}$ (CB-O-**C**H_2)), 26.2 (s, **C**$_{15,16}$(CH_2)), 26.1 (s, **C**$_{15,16}$(CH_2)) ppm.

IR (Solid) ν_{max}: 2998(s) (**C-H**$_2$), 2248(m) (**C≡N**), 1592(m) (**Ar**) cm^{-1}.

ESMS: *m/z* 331 ($[M+Na]^+$, 26%), 347 ($[M+K]^+$, 9%)

Elemental Analysis: $C_{46}H_{36}N_2O_4$: (Expected) **C** 78.92, **H** 5.96, **N** 4.60; (Found) **C** 78.89, **H** 5.95, **N** 4.60

1,2-bis-[1-(4'Cyanobiphen-4-yloxy)pentyl-5-oxy]benzene

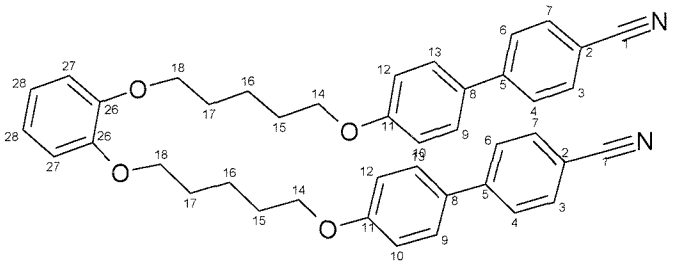

68
$C_{42}H_{40}N_2O_4$
636.80

Rf 0.39; 100% DCM [1 spot by TLC]

^{1}H NMR (400 MHz, $CDCl_3$): δ_H 7.59 (4H, d, J = 8.0 Hz, C_4**H**, C_6**H**), 7.53 (4H, d, J = 8.5 Hz, C_3**H**, C_7**H**), 7.42 (4H, d, 8.7 Hz, C_9**H**, C_{13}**H**), 6.89 (4H, d, J = 8.8 Hz, C_{10}**H**, C_{12}**H**), 6.82 (4H, s, C_{27}**H**, C_{28}**H**), 3.97 (4H, t, 6.4 Hz, O-C_{14}**H**$_2$), 3.94

(4H, t, 6.4 Hz, $C_{18}\mathbf{H_2}$-O), 1.77-1.88 (8H, m, $C_{15}\mathbf{H_2}$, $C_{17}\mathbf{H_2}$), 1.57-1.67 (4H, m, $C_{16}\mathbf{H_2}$) ppm.

^{13}C NMR (100 MHz, $CDCl_3$): δ_C 162.3 (q, $\mathbf{C_{11}}(Ar_{CB})$), 151.7 (q, $\mathbf{C_{26}}(Ar_{Cat})$), 147.8 (q, $\mathbf{C_5}(Ar_{CB})$), 135.2 (t, $\mathbf{C_3}(Ar_{CB})$, $\mathbf{C_7}(Ar_{CB})$), 133.9 (q, $\mathbf{C_8}(Ar_{CB})$), 130.9 (t, $\mathbf{C_9}(Ar_{CB})$, $\mathbf{C_{13}}(Ar_{CB})$), 129.6 (t, $\mathbf{C_4}(Ar_{CB})$, $\mathbf{C_6}(Ar_{CB})$), 123.8 (t, $\mathbf{C_{28}}(Ar_{Cat})$), 121.7 (q, $\mathbf{C_1}$(CN)), 117.7 (t, $\mathbf{C_{10}}(Ar_{CB})$, $\mathbf{C_{12}}(Ar_{CB})$), 116.8 (t, $\mathbf{C_{27}}$ (Ar_{Cat})), 112.7 (q, $\mathbf{C_2}(Ar_{CB})$), 71.6 (s, $\mathbf{C_{18}}$(Cat-O-$\mathbf{C}H_2$)), 70.6 (s, $\mathbf{C_{14}}$(CB-O-$\mathbf{C}H_2$)), 31.7 (s, $\mathbf{C_{15\text{-}17}}(CH_2)$), 31.6 (s, $\mathbf{C_{15\text{-}17}}(CH_2)$), 26.4 (s, $\mathbf{C_{15\text{-}17}}(CH_2)$) ppm.

IR (Solid) ν_{max}: 2997(s) (**C-H$_2$**), 2250(s) (**C≡N**), 1593(m) (**Ar**) cm^{-1}.

EIMS: *m/z* 636.4 ($[M]^+$, 45%), 442.3 ($[C_{29}H_{32}NO_3]^+$, 5%), 373.2 ($[C_{24}H_{23}NO_3]^+$, 5%), 264.2 ($[C_{18}H_{19}NO_3]^+$, 99%), 195.1 ($[C_{13}H_9NO]^+$, 73%), 69.1 ($[C_5H_9]^+$, 100%) 41 ($[C_3H_8]^+$, 35%)

Elemental Analysis: $C_{46}H_{40}N_2O_4$: (Expected) **C** 79.22, **H** 6.33, **N** 4.40; (Found) **C** 78.99, **H** 6.29, **N** 4.36

1,2-bis-[1-(4'-Cyanobiphen-4-yloxy)hexyl-6-oxy]benzene

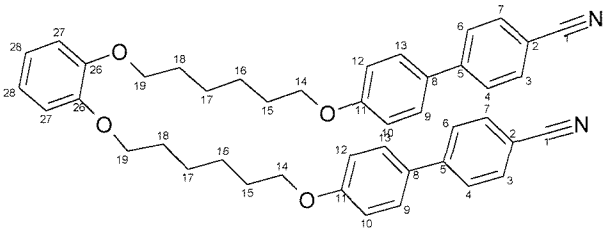

69
$C_{44}H_{44}N_2O_4$
664.85

Rf 0.41; 100% DCM [1 spot by TLC]

^{1}H NMR (400 MHz, $CDCl_3$): δ_H 7.60 (4H, d, J = 8.0 Hz, $C_4\mathbf{H}$, $C_6\mathbf{H}$), 7.54 (4H, d, J = 8.5 Hz, $C_3\mathbf{H}$, $C_7\mathbf{H}$), 7.42 (4H, d, 8.8 Hz, $C_9\mathbf{H}$, $C_{13}\mathbf{H}$), 6.89 (4H, d, J = 9.0 Hz, $C_{10}\mathbf{H}$, $C_{12}\mathbf{H}$), 6.83 (4H, s, $C_{27}\mathbf{H}$, $C_{28}\mathbf{H}$), 3.94 (4H, t, 6.5 Hz, O-$C_{14}\mathbf{H_2}$), 3.93 (4H, t, 6.5 Hz, $C_{19}\mathbf{H_2}$-O), 1.72-1.84 (8H, m, $C_{15}\mathbf{H_2}$, $C_{18}\mathbf{H_2}$), 1.43-1.57 (8H, m, $C_{16}\mathbf{H_2}$, $C_{17}\mathbf{H_2}$) ppm.

^{13}C NMR (100 MHz, $CDCl_3$): δ_C 160.2 (q, $\mathbf{C_{11}}(Ar_{CB})$), 149.6 (q, $\mathbf{C_{26}}(Ar_{Cat})$), 145.6 (q, $\mathbf{C_5}(Ar_{CB})$), 133.0 (t, $\mathbf{C_3}(Ar_{CB})$, $\mathbf{C_7}(Ar_{CB})$), 131.7 (q, $\mathbf{C_8}(Ar_{CB})$), 128.7 (t, $\mathbf{C_9}(Ar_{CB})$, $\mathbf{C_{13}}(Ar_{CB})$), 127.5 (t, $\mathbf{C_4}(Ar_{CB})$, $\mathbf{C_6}(Ar_{CB})$), 121.6 (t, $\mathbf{C_{28}}(Ar_{Cat})$), 119.5 (q, $\mathbf{C_1}$(CN)), 115.5 (t, $\mathbf{C_{10}}(Ar_{CB})$, $\mathbf{C_{12}}(Ar_{CB})$), 114.6 (t, $\mathbf{C_{27}}$ (Ar_{Cat})),

110.5 (q, $\mathbf{C_2}(Ar_{CB})$), 69.5 (s, $\mathbf{C_{19}}(Cat\text{-}O\text{-}\mathbf{C}H_2)$), 68.4 (s, $\mathbf{C_{14}}(CB\text{-}O\text{-}\mathbf{C}H_2)$), 29.7 (s, $\mathbf{C_{15\text{-}18}}(CH_2)$), 29.6 (s, $\mathbf{C_{15\text{-}18}}(CH_2)$), 26.3 (s, $\mathbf{C_{15\text{-}18}}(CH_2)$), 26.3 (s, $\mathbf{C_{15\text{-}18}}(CH_2)$) ppm.

IR (Solid) ν_{max}: 2997(s) (**C-H$_2$**), 2250(s) (**C≡N**), 1593(m) (**Ar**) cm^{-1}.

ESMS: *m/z* 687 ($[M+Na]^+$, 100%), 703 ($[M+K]^+$, 100%).

Elemental Analysis: $C_{44}H_{44}N_2O_4$: (Expected) **C** 79.49, **H** 6.67, **N** 4.21; (Found) **C** 79.42, **H** 6.63, **N** 4.17

1,2-bis-[1-(4'-Cyanobiphen-4-yloxy)heptyl-7-oxy]benzene

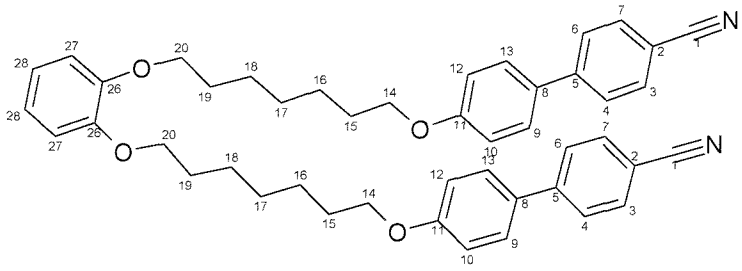

70
$C_{46}H_{48}N_2O_4$
692.91

Rf 0.44; 100% DCM [1 spot by TLC]

^{1}H NMR (400 MHz, $CDCl_3$): δ_H 7.59 (4H, d, J = 8.5 Hz, $C_4\mathbf{H}$, $C_6\mathbf{H}$), 7.52 (4H, d, J = 8.8 Hz, $C_3\mathbf{H}$, $C_7\mathbf{H}$), 7.42 (4H, d, 8.8 Hz, $C_9\mathbf{H}$, $C_{13}\mathbf{H}$), 6.89 (4H, d, J = 9.0 Hz, $C_{10}\mathbf{H}$, $C_{12}\mathbf{H}$), 6.81 (4H, s, $C_{27}\mathbf{H}$, $C_{28}\mathbf{H}$), 3.93 (4H, t, 6.5 Hz, O-$C_{14}\mathbf{H_2}$), 3.89 (4H, t, 6.5 Hz, $C_{20}\mathbf{H_2}$-O), 1.69-1.80 (8H, m, $C_{15}\mathbf{H_2}$, $C_{19}\mathbf{H_2}$), 1.32-1.50 (12H, m, $C_{16}\mathbf{H_2}$, $C_{17}\mathbf{H_2}$, $C_{18}\mathbf{H_2}$) ppm.

^{13}C NMR (100 MHz, $CDCl_3$): δ_C 158.8 (q, $\mathbf{C_{11}}(Ar_{CB})$), 148.2 (q, $\mathbf{C_{26}}(Ar_{Cat})$), 144.2 (q, $\mathbf{C_5}(Ar_{CB})$), 131.5 (t, $\mathbf{C_3}(Ar_{CB})$, $\mathbf{C_7}(Ar_{CB})$), 130.2 (q, $\mathbf{C_8}(Ar_{CB})$), 127.3 (t, $\mathbf{C_9}(Ar_{CB})$, $\mathbf{C_{13}}(Ar_{CB})$), 126.0 (t, $\mathbf{C_4}(Ar_{CB})$, $\mathbf{C_6}(Ar_{CB})$), 120.1 (t, $\mathbf{C_{28}}(Ar_{Cat})$), 118.1 (q, $\mathbf{C_1}(CN)$), 114.1 (t, $\mathbf{C_{10}}(Ar_{CB})$, $\mathbf{C_{12}}(Ar_{CB})$), 113.2 (t, $\mathbf{C_{27}}$ (Ar_{Cat})), 109.1 (q, $\mathbf{C_2}(Ar_{CB})$), 68.2 (s, $\mathbf{C_{20}}(Cat\text{-}O\text{-}\mathbf{C}H_2)$), 67.1 (s, $\mathbf{C_{14}}(CB\text{-}O\text{-}\mathbf{C}H_2)$), 28.3 (s, $\mathbf{C_{15\text{-}19}}(CH_2)$), 28.2 (s, $\mathbf{C_{15\text{-}19}}(CH_2)$), 24.9 (s, $\mathbf{C_{15\text{-}19}}(CH_2)$) ppm.

IR (Solid) ν_{max}: 2983(s) (**C-H$_2$**), 2222(s) (**C≡N**), 1602(m) (**Ar**), 1543(m) (**Ar**) cm^{-1}.

ESMS: *m/z* 743 ($[M+NH_4]^+$, 4%), 715.4 ($[M+Na]^+$, 100%), 1408.3 ($[2M+Na]^+$ 9%).

Elemental Analysis: $C_{46}H_{48}N_2O_4$: (Expected) **C** 79.74, **H** 6.98, **N** 4.04; (Found) **C** 80.01, **H** 7.04, **N** 7.07

1,2-bis-[1-(4'-Cyanobiphen-4-yloxy)octyl-8-oxy]benzene 14

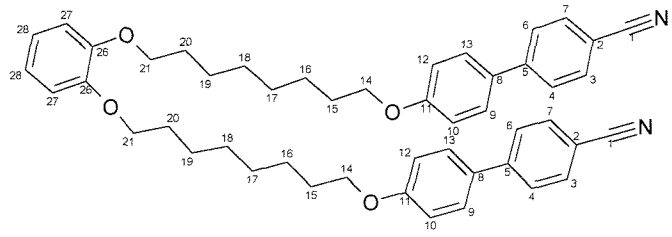

71
$C_{48}H_{52}N_2O_4$
720.96

Rf 0.45; 100% DCM [1 spot by TLC]

^{1}H NMR (300 MHz, $CDCl_3$): δ_H 7.59 (4H, d, J = 8.6 Hz, C_4**H**, C_6**H**), 7.52 (4H, d, J = 8.8 Hz, C_3**H**, C_7**H**), 7.43 (4H, d, 8.8 Hz, C_9**H**, C_{13}**H**), 6.89 (4H, d, J = 8.8 Hz, C_{10}**H**, C_{12}**H**), 6.81 (4H, s, C_{27}**H**, C_{28}**H**), 3.92 (4H, t, 6.5 Hz, O-C_{14}**H$_2$**), 3.91 (4H, t, 6.5 Hz, C_{21}**H$_2$**-O), 1.66-1.72 (8H, m, C_{15}**H$_2$**, C_{20}**H$_2$**), 1.33-1.43 (16H, m, C_{16}**H$_2$**, C_{17}**H$_2$**, C_{18}**H$_2$**, C_{19}**H$_2$**) ppm.

^{13}C NMR (100 MHz, $CDCl_3$): δ_C 158.8 (q, **C_{11}**(Ar_{CB})), 148.2 (q, **C_{26}**(Ar_{Cat})), 144.2 (q, **C_5**(Ar_{CB})), 131.5 (t, **C_3**(Ar_{CB}), **C_7**(Ar_{CB})), 130.2 (q, **C_8**(Ar_{CB})), 127.3 (t, **C_9**(Ar_{CB}), **C_{13}**(Ar_{CB})), 126.0 (t, **C_4**(Ar_{CB}), **C_6**(Ar_{CB})), 120.0 (t, **C_{28}**(Ar_{Cat})), 118.1 (q, **C_1**(CN)), 114.1 (t, **C_{10}**(Ar_{CB}), **C_{12}**(Ar_{CB})), 113.2 (t, **C_{27}** (Ar_{Cat})), 109.0 (q, **C_2**(Ar_{CB})), 68.2 (s, **C_{21}**(Cat-O-**C**H_2)), 67.1 (s, **C_{14}**(CB-O-**C**H_2)), 28.3 (s, **$C_{15\text{-}20}$**(CH_2)), 28.2 (s, **$C_{15\text{-}20}$**(CH_2)), 25.0 (s, **$C_{15\text{-}20}$**(CH_2)) ppm.

IR (Solid) ν_{max}: 2982(s) (**C-H$_2$**), 2222(s) (**C≡N**), 1601(m) (**Ar**), 1542(m) (**Ar**) cm^{-1}.

ESMS: *m/z* 743 ($[M+Na]^+$, 100%)

Elemental Analysis: $C_{48}H_{52}N_2O_4$: (Expected) **C** 79.97, **H** 7.27, **N** 3.88; (Found) **C** 79.79, **H** 7.22, **N** 3.79

1,2-bis-[1-(4'-Cyanobiphen-4-yloxy)nonyl-9-oxy]benzene

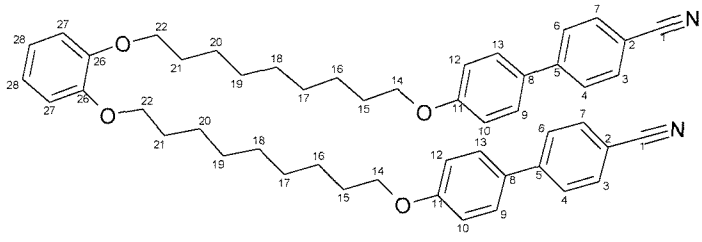

72
$C_{50}H_{56}N_2O_4$
749.01

Rf 0.45; 100% DCM [1 spot by TLC]

^{1}H NMR (300 MHz, $CDCl_3$): δ_H 7.70 (4H, d, J = 8.6 Hz, C_4**H**, C_6**H**), 7.63 (4H, d, J = 8.6 Hz, C_3**H**, C_7**H**), 7.53 (4H, d, 8.6 Hz, C_9**H**, C_{13}**H**), 6.89 (4H, d, J = 8.8 Hz, C_{10}**H**, C_{12}**H**), 6.91 (4H, s, C_{27}**H,** C_{28}**H**), 4.01 (8H, t, 6.5 Hz, O-C_{14}**H$_2$**, C_{22}**H$_2$**-O), 1.75-1.89 (8H, m, C_{15}**H$_2$**, C_{21}**H$_2$**), 1.43-1.57 (8H, m, C_{16}**H$_2$**, C_{17}**H$_2$**, C_{18}**H$_2$**, C_{19}**H$_2$**, C_{20}**H$_2$**) ppm.

^{13}C NMR (75 MHz, $CDCl_3$): δ_C 159.9 (q, **C_{11}**(Ar_{CB})), 149.3 (q, **C_{26}**(Ar_{Cat})), 145.4 (q, **C_5**(Ar_{CB})), 132.7 (t, **C_3**(Ar_{CB}), **C_7**(Ar_{CB})), 131.4 (q, **C_8**(Ar_{CB})), 128.4 (t, **C_9**(Ar_{CB}), **C_{13}**(Ar_{CB})), 127.2 (t, **C_4**(Ar_{CB}), **C_6**(Ar_{CB})), 121.2 (t, **C_{28}**(Ar_{Cat})), 119.3 (q, **C_1**(CN)), 115.2 (t, **C_{10}**(Ar_{CB}), **C_{12}**(Ar_{CB})), 114.1 (t, **C_{27}** (Ar_{Cat})), 110.2 (q, **C_2**(Ar_{CB})), 69.3 (s, **C_{22}**(Cat-O-**C**H_2)), 68.3 (s, **C_{14}**(CB-O-**C**H_2)), 29.7 (s, **$C_{15\text{-}21}$**(CH_2)), 29.9 (s, **$C_{15\text{-}21}$**(CH_2)), 29.4 (s, **$C_{15\text{-}21}$**(CH_2)), 26.2 (s, **$C_{15\text{-}21}$**(CH_2)) ppm.

IR (Solid) ν_{max}: 2921(s) (**C-H$_2$**), 2855(s) (**C-H$_2$**), 2250(s) (**C≡N**), 1602(m) (**Ar**), 1493(m) (**Ar**) cm^{-1}.

EIMS: *m/z* 748.3 ($[M]^+$, 100%), 429.2 ($[C_{28}H_{31}NO_3]^+$, 17%), 319.1 ($[C_{24}H_{23}NO_3]^+$, 5%), 195.1 ($[C_{13}H_9NO]^+$, 94%), 110 ($[C_6H_6O_2]^+$, 50%), 69.1 ($[C_5H_9]^+$, 42%)

1,2-bis-[1-(4'-Cyanobiphen-4-yloxy)decyl-10-oxy]benzene

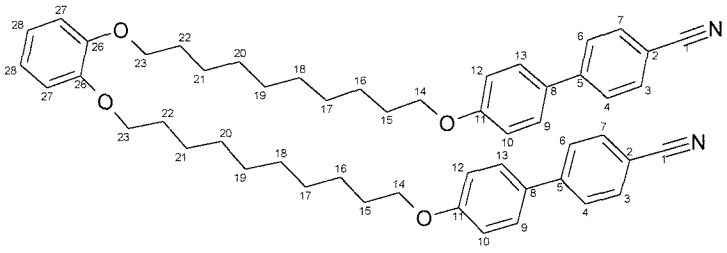

73
$C_{52}H_{60}N_2O_4$
777.07

Rf 0.51; 100% DCM [1 spot by TLC]

^{1}H NMR (400 MHz, $CDCl_3$): δ_H 7.61 (4H, d, J = 8.8 Hz, C_4**H**, C_6**H**), 7.55 (4H, d, J = 8.8 Hz, C_3**H**, C_7**H**), 7.44 (4H, d, 8.6 Hz, C_9**H**, C_{13}**H**), 6.91 (4H, d, J = 9.0 Hz, C_{10}**H**, C_{12}**H**), 6.81 (4H, s, C_{27}**H**, C_{28}**H**), 3.92 (4H, t, 6.5 Hz, O-C_{14}**H$_2$**), 3.91 (4H, t, 6.8 Hz, C_{23}**H$_2$**-O), 1.68-1.78 (8H, m, C_{15}**H$_2$**, C_{22}**H$_2$**), 1.21-1.52 (24H, m, C_{16}**H$_2$**, C_{17}**H$_2$**, C_{18}**H$_2$**, C_{19}**H$_2$**, C_{20}**H$_2$**, C_{21}**H$_2$**) ppm.

^{13}C NMR (100 MHz, $CDCl_3$): δ_C 160.2 (q, **C_{11}**(Ar_{CB})), 149.7 (q, **C_{26}**(Ar_{Cat})), 145.9 (q, **C_5**(Ar_{CB})), 133.0 (t, **C_3**(Ar_{CB}), **C_7**(Ar_{CB})), 131.7 (q, **C_8**(Ar_{CB})), 128.7 (t,

$\mathbf{C_9}(Ar_{CB})$, $\mathbf{C_{13}}(Ar_{CB})$), 127.5 (t, $\mathbf{C_4}(Ar_{CB})$, $\mathbf{C_6}(Ar_{CB})$), 121.5 (t, $\mathbf{C_{28}}(Ar_{Cat})$), 119.5 (q, $\mathbf{C_1}$(CN)), 115.5 (t, $\mathbf{C_{10}}(Ar_{CB})$, $\mathbf{C_{12}}(Ar_{CB})$), 114.6 (t, $\mathbf{C_{27}}$ (Ar_{Cat})), 110.5 (q, $\mathbf{C_2}(Ar_{CB})$), 69.7 (s, $\mathbf{C_{23}}$(Cat-O-$\mathbf{C}H_2$)), 68.6 (s, $\mathbf{C_{14}}$(CB-O-$\mathbf{C}H_2$)), 29.9 (s, $\mathbf{C_{15\text{-}22}}(CH_2)$), 29.9 (s, $\mathbf{C_{15\text{-}22}}(CH_2)$), 29.8 (s, $\mathbf{C_{15\text{-}22}}(CH_2)$), 29.8 (s, $\mathbf{C_{15\text{-}22}}(CH_2)$), 29.6 (s, $\mathbf{C_{15\text{-}22}}(CH_2)$), 26.5 (s, $\mathbf{C_{15\text{-}22}}(CH_2)$) ppm.

IR (Solid) ν_{max}: 2926(s) (**C-H$_2$**), 2855(s) (**C-H$_2$**), 2245(s) (**C≡N**), 2226(s) (**C≡N**), 1602(m) (**Ar**), 1497(m) (**Ar**) cm^{-1}.

EIMS: *m/z* 776.3 ($[M]^+$, 9%), 528.1 ($[impurity]^+$, 31%), 333 ($[C_{22}H_{36}O_2]^+$, 8%), 195.1 ($[C_{13}H_9NO]^+$, 100%), 69.1 ($[C_5H_9]^+$, 100%), 110 ($[C_6H_6O_2]^+$, 11%), 55 ($[C_4H_8]^+$, 20%)

Elemental Analysis: $C_{52}H_{60}N_2O_4$: (Expected) **C** 80.38, **H** 7.78, **N** 3.60; (Found) **C** 80.16, **H** 7.72, **N** 3.58

1,2-bis-[1-(4'-Cyanobiphen-4-yloxy)undecyl-11-oxy]benzene

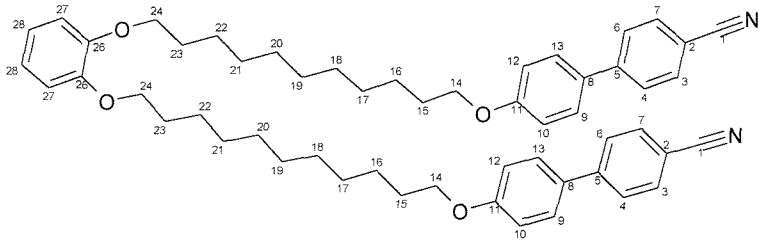

74
$C_{54}H_{64}N_2O_4$
805.12

Rf 0.51; 100% DCM [1 spot by TLC]

H NMR (300 MHz, $CDCl_3$): δ_H 7.70 (4H, d, J = 8.7 Hz, C_4**H**, C_6**H**), 7.65 (4H, d, J = 8.7 Hz, C_3**H**, C_7**H**), 7.53 (4H, d, 8.8 Hz, C_9**H**, C_{13}**H**), 6.99 (4H, d, J = 8.7 Hz, C_{10}**H**, C_{12}**H**), 6.90 (4H, s, C_{27}**H**, C_{28}**H**), 4.01 (4H, t, 6.5 Hz, O-$C_{14}\mathbf{H_2}$), 4.00 (4H, t, 6.8 Hz, $C_{24}\mathbf{H_2}$-O), 1.76-1.88 (8H, m, $C_{15}\mathbf{H_2}$, $C_{23}\mathbf{H_2}$), 1.38-1.53 (28H, m, $C_{16}\mathbf{H_2}$, $C_{17}\mathbf{H_2}$, $C_{18}\mathbf{H_2}$, $C_{19}\mathbf{H_2}$, $C_{20}\mathbf{H_2}$, $C_{21}\mathbf{H_2}$, $C_{22}\mathbf{H_2}$) ppm.

^{13}C NMR (75 MHz, $CDCl_3$): δ_C 159.9 (q, $\mathbf{C_{11}}(Ar_{CB})$), 149.3 (q, $\mathbf{C_{26}}(Ar_{Cat})$), 145.4 (q, $\mathbf{C_5}(Ar_{CB})$), 132.7 (t, $\mathbf{C_3}(Ar_{CB})$, $\mathbf{C_7}(Ar_{CB})$), 131.4 (q, $\mathbf{C_8}(Ar_{CB})$), 128.5 (t, $\mathbf{C_9}(Ar_{CB})$, $\mathbf{C_{13}}(Ar_{CB})$), 127.2 (t, $\mathbf{C_4}(Ar_{CB})$, $\mathbf{C_6}(Ar_{CB})$), 121.2 (t, $\mathbf{C_{28}}(Ar_{Cat})$), 119.3 (q, $\mathbf{C_1}$(CN)), 115.2 (t, $\mathbf{C_{10}}(Ar_{CB})$, $\mathbf{C_{12}}(Ar_{CB})$), 114.2 (t, $\mathbf{C_{27}}$ (Ar_{Cat})), 110.2 (q, $\mathbf{C_2}(Ar_{CB})$), 69.4 (s, $\mathbf{C_{24}}$(Cat-O-$\mathbf{C}H_2$)), 68.3 (s, $\mathbf{C_{14}}$(CB-O-$\mathbf{C}H_2$)),

29.7 (s, $\mathbf{C_{15\text{-}23}}(CH_2)$), 29.6 (s, $\mathbf{C_{15\text{-}23}}(CH_2)$), 29.5 (s, $\mathbf{C_{15\text{-}23}}(CH_2)$), 29.4 (s, $\mathbf{C_{15\text{-}23}}(CH_2)$) 26.2 (s, $\mathbf{C_{15\text{-}23}}(CH_2)$) ppm.

IR (Solid) ν_{max}: 2979(s) (**C-H$_2$**), 2299(s) (**C≡N**), 1604(m) (**Ar**), 1548(m) (**Ar**) cm^{-1}.

ESMS: *m/z* 804 ($[M]^+$, 25%), 827 ($[M+Na]^+$, 100%), 843 ($[M+K]^+$, 20%)

Elemental Analysis: $C_{54}H_{64}N_2O_4$: (Expected) **C** 80.56, **H** 8.01, **N** 3.48; (Found) **C** 80.26, **H** 7.99, **N** 3.38

1,2-bis-[1-(4'-Cyanobiphen-4-yloxy)dodecyl-12-oxy]benzene

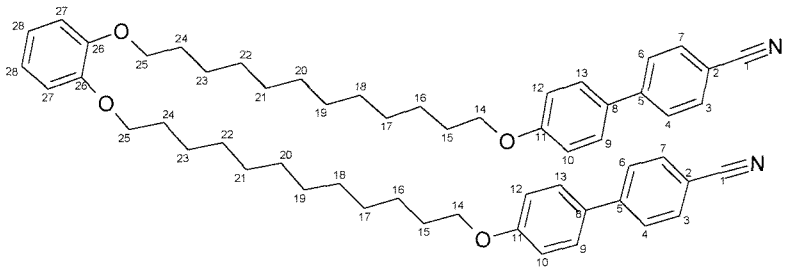

75
$C_{56}H_{68}N_2O_4$
833.18

Rf 0.52; 100% DCM [1 spot by TLC]

^{1}H NMR (100 MHz, $CDCl_3$): δ_H 7.70 (4H, d, J = 8.7 Hz, $C_4\mathbf{H}$, $C_6\mathbf{H}$), 7.64 (4H, d, J = 8.6 Hz, $C_3\mathbf{H}$, $C_7\mathbf{H}$), 7.54 (4H, d, 8.8 Hz, $C_9\mathbf{H}$, $C_{13}\mathbf{H}$), 7.01 (4H, d, J = 8.8 Hz, $C_{10}\mathbf{H}$, $C_{12}\mathbf{H}$), 6.90 (4H, s, $C_{27}\mathbf{H}$, $C_{28}\mathbf{H}$), 4.02 (4H, t, 6.5 Hz, O-$C_{14}\mathbf{H_2}$), 4.01 (4H, t, 6.8 Hz, $C_{25}\mathbf{H_2}$-O), 1.75-1.88 (8H, m, $C_{15}\mathbf{H_2}$, $C_{24}\mathbf{H_2}$), 1.23-1.45 (32H, m, $C_{16}\mathbf{H_2}$, $C_{17}\mathbf{H_2}$, $C_{18}\mathbf{H_2}$, $C_{19}\mathbf{H_2}$, $C_{20}\mathbf{H_2}$, $C_{21}\mathbf{H_2}$, $C_{22}\mathbf{H_2}$, $C_{23}\mathbf{H_2}$) ppm.

^{13}C NMR (75 MHz, $CDCl_3$): δ_C 159.9 (q, $\mathbf{C_{11}}(Ar_{CB})$), 149.8 (q, $\mathbf{C_{26}}(Ar_{Cat})$), 145.4 (q, $\mathbf{C_5}(Ar_{CB})$), 132.7 (t, $\mathbf{C_3}(Ar_{CB})$, $\mathbf{C_7}(Ar_{CB})$), 131.4 (q, $\mathbf{C_8}(Ar_{CB})$), 128.5 (t, $\mathbf{C_9}(Ar_{CB})$, $\mathbf{C_{13}}(Ar_{CB})$), 127.2 (t, $\mathbf{C_4}(Ar_{CB})$, $\mathbf{C_6}(Ar_{CB})$), 121.2 (t, $\mathbf{C_{28}}(Ar_{Cat})$), 119.3 (q, $\mathbf{C_1}$(CN)), 115.2 (t, $\mathbf{C_{10}}(Ar_{CB})$, $\mathbf{C_{12}}(Ar_{CB})$), 114.2 (t, $\mathbf{C_{27}}$ (Ar_{Cat})), 110.2 (q, $\mathbf{C_2}(Ar_{CB})$), 69.4 (s, $\mathbf{C_{25}}$(Cat-O-$\mathbf{C}H_2$)), 68.3 (s, $\mathbf{C_{14}}$(CB-O-$\mathbf{C}H_2$)), 29.8 (s, $\mathbf{C_{15\text{-}24}}(CH_2)$), 29.6 (s, $\mathbf{C_{15\text{-}24}}(CH_2)$), 29.5 (s, $\mathbf{C_{15\text{-}24}}(CH_2)$), 29.4 (s, $\mathbf{C_{15\text{-}24}}(CH_2)$) 26.2 (s, $\mathbf{C_{15\text{-}24}}(CH_2)$) ppm.

IR (Solid) ν_{max}: 2982(s) (**C-H$_2$**), 2680(w), 2302(s) (**C≡N**), 1603(m) (**Ar**), 1547(m) (**Ar**) cm^{-1}.

ESMS: *m/z* 832 ($[M]^+$, 25%), 855 ($[M+Na]^+$, 100%), 871 ($[M+K]^+$, 13%)

7.4.2. Res(OnOCB)$_2$; 1,2-bis-[α-(4'-cyanobiphen-4-yloxy)alkyl-ω-oxy]benzene

n	Temperature /°C						Mass	Yield
	Cr		Sm_A		N	I	g	%
4	•	138	•		•	(129)	•	282	38
5	•	146	•		•	(109)	•	245	37
6	•	125	•		•	(116)	•	587	74
7	•	124	•		•	(105)	•	512	59
8	•	99	•		•	104	•	469	52
9	•	124	•		•	(102)	•	654	70
10	•	107	•		•	(102)	•	621	64
11	•	107	•		•	(93)	•	713	71
12	•	106	•	(83)	•	(92)	•	262	24

1,3-bis-[1-(4'-cyanobiphen-4-yloxy)butyl-4-oxy]benzene

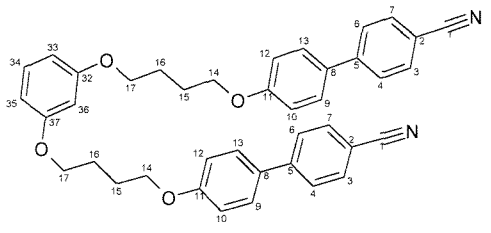

76
$C_{40}H_{36}N_2O_4$
608.74

To a stirred solution of resorcinol, (143 mg, 1.28 mMol, 1 eq) in dry, nitrogen purged (30 min) DMF (50 mL) was added solid caesium carbonate (3.20 g, 9.84 mMol, 7.6 eq) in one portion. The mixture was warmed to 80°C for 30 min, turning dark brown before being allowed to cool prior to the addition of 1-(cyanobiphenyloxy)-butyl-4-bromide (851 mg, 2.58 mMol, 2 eq) in one portion and a catalytic quantity of sodium iodide (80 mg). The reaction mixture was then heated to 80°C for 3 days under an N_2 atmosphere. The reaction mixture was allowed to cool and the solvent was removed *in vacuo* giving a brown solid. The solid was partitioned between water (50 mL) and DCM (50 mL). The aqueous layer was washed with DCM (3 x 50 mL) and the organics were combined, dried over anhydrous $MgSO_4$ and filtered. The organic solvents were removed *in vacuo* to give a crude off-white solid. The crude material was purified by column chromatography (silica gel, 40 mm x 100 mm, 50-100% DCM / petroleum) affording the title compound **76**, (282 mg, 0.49 mMol, 37.7 %) as white microcrystalline solid.

Rf 0.45; 100% DCM [1 spot by TLC]

^{1}H NMR (300 MHz, $CDCl_3$): δ_H 7.61 (4H, d, J = 8.6 Hz, C_4**H**, C_6**H**), 7.55 (4H, d, J = 8.6 Hz, C_3**H**, C_7**H**), 7.45 (4H, d, J = 8.8 Hz, C_9**H**, C_{13}**H**), 7.09 (1H, t, J = 8.1 Hz, C_{36}**H**), 6.91 (4H, d, J = 8.8 Hz, C_{10}**H**, C_{12}**H**), 6.33-6.51 (3H, m, C_{33}**H**, C_{34}**H**, C_{35}**H**), 4.01 (4H, t, 5.6 Hz, C_{17}**H$_2$**-O), 3.95 (4H, t, 5.6 Hz, O-C_{14}**H$_2$**), 1.79-2.02 (8H, m, C_{15}**H$_2$**, C_{16}**H$_2$**) ppm.

^{13}C NMR (75 MHz, $CDCl_3$): δ_C 160.2 (q, **C$_{11}$**(Ar_{CB})), 159.7 (q, **C$_{26}$**(Ar_{Res})), 145.3 (q, **C$_5$**(Ar_{CB})), 132.6 (t, **C$_3$**(Ar_{CB}), **C$_7$**(Ar_{CB})), 131.5 (q, **C$_8$**(Ar_{CB})), 129.9 (q, **C$_{36}$**(Ar_{Res})), 128.4 (t, **C$_9$**(Ar_{CB}), **C$_{13}$**(Ar_{CB})), 127.1 (t, **C$_4$**(Ar_{CB}), **C$_6$**(Ar_{CB})), 119.2 (q, **C$_1$**(CN)), 115.2 (t, **C$_{10}$**(Ar_{CB}), **C$_{12}$**(Ar_{CB})), 110.1 (q, **C$_2$**(Ar_{CB})), 106.8 (t, **C$_{33}$** (Ar_{Res}), **C$_{35}$** (Ar_{Res})), 67.7 (s, **C$_{14}$/C$_{17}$** (Res-O-**C**H$_2$)), 67.4 (s, **C$_{14}$/C$_{17}$** (CB-O-**C**H$_2$)), 26.0 (s, **C$_{15,16}$**(CH_2)), 26.0 (s, **C$_{15,16}$**(CH_2)) ppm.

IR (Solid) ν_{max}: 2947(s) (**C-H$_2$**), 2870(s) (**C-H$_2$**), 2218(m) (**C≡N**), 1600(m) (**Ar**), 1520(m) (**Ar**), 1491(s) (**Ar**) cm^{-1}.

EIMS: *m/z* 608 ($[M]^+$, 1%), 414 ($[C_{27}H_{36}NO_3]^+$, 12%), 250 ($[C_{17}H_{17}NO_3]^+$, 55%), 208 ($[C_{14}H_{10}NO]^+$, 100%), 195 ($[C_{13}H_9NO]^+$, 100%), 69 ($[C_5H_9]^+$, 100%), 123 ($[C_7H_8O_2]^+$, 18%), 55 ($[C_4H_8]^+$, 20%), 29 ($[C_2H_1]^+$, 20%).

Elemental Analysis: $C_{40}H_{36}N_2O_4$: (Expected) **C** 78.85, **H** 5.91, **N** 4.60; (Found) **C** 77.11, **H** 6.15, **N** 4.91

1,3-bis-[1-(4'-cyanobiphen-4-yloxy)pentyl-5-oxy]benzene

77
$C_{42}H_{40}N_2O_4$
636.80

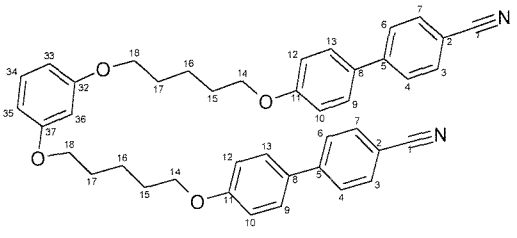

Rf 0.50; 100% DCM [1 spot by TLC]

^{1}H NMR (300 MHz, $CDCl_3$): δ_H 7.61 (4H, d, J = 8.6 Hz, C_4**H**, C_6**H**), 7.55 (4H, d, J = 8.6 Hz, C_3**H**, C_7**H**), 7.45 (4H, d, J = 9.0 Hz, C_9**H**, C_{13}**H**), 7.08 (1H, t, J = 7.9 Hz, C_{36}**H**), 6.91 (4H, d, J = 8.8 Hz, C_{10}**H**, C_{12}**H**), 6.36-6.48 (3H, m, C_{33}**H**, C_{34}**H**, C_{35}**H**), 3.97 (4H, t, 6.3 Hz, C_{18}**H$_2$**-O), 3.91 (4H, t, 6.3 Hz, O-C_{14}**H$_2$**), 1.71-1.89 (8H, m, C_{15}**H$_2$**, C_{17}**H$_2$**), 1.52-1.67 (4H, m, C_{16}**H$_2$**) ppm.

^{13}C NMR (75 MHz, $CDCl_3$): δ_C 160.3 (q, $\mathbf{C_{11}}(Ar_{CB})$), 159.7 (q, $\mathbf{C_{26}}(Ar_{Res})$), 145.3 (q, $\mathbf{C_5}(Ar_{CB})$), 132.6 (t, $\mathbf{C_3}(Ar_{CB})$, $\mathbf{C_7}(Ar_{CB})$), 131.4 (q, $\mathbf{C_8}(Ar_{CB})$), 129.8 (q, $\mathbf{C_{32}}(Ar_{Res})$, $\mathbf{C_{37}}(Ar_{Res})$), 128.3 (t, $\mathbf{C_9}(Ar_{CB})$, $\mathbf{C_{13}}(Ar_{CB})$), 127.1 (t, $\mathbf{C_4}(Ar_{CB})$, $\mathbf{C_6}(Ar_{CB})$), 119.1 (q, $\mathbf{C_1}$(CN)), 115.1 (t, $\mathbf{C_{10}}(Ar_{CB})$, $\mathbf{C_{12}}(Ar_{CB})$), 110.1 (q, $\mathbf{C_2}(Ar_{CB})$), 106.7 (t, $\mathbf{C_{33}}$ (Ar_{Res}), $\mathbf{C_{35}}$ (Ar_{Res})), 101.6 (t, $\mathbf{C_{36}}$ (Ar_{Res})), 68.0 (s, $\mathbf{C_{14}}$/$\mathbf{C_{18}}$ (Res-O-$\mathbf{C}H_2$)), 67.7 (s, $\mathbf{C_{14}}$/$\mathbf{C_{18}}$ (CB-O-$\mathbf{C}H_2$)), 29.0 (s, $\mathbf{C_{15\text{-}17}}(CH_2)$), 29.0 (s, $\mathbf{C_{15\text{-}17}}(CH_2)$), 22.8 (s, $\mathbf{C_{16}}(CH_2)$) ppm.

IR (Solid) ν_{max}: 2945(s) (**C-H$_2$**), 2866(s) (**C-H$_2$**), 2219(m) (**C≡N**), 1601(m) (**Ar**), 1519(m) (**Ar**), 1491(s) (**Ar**) cm^{-1}.

EIMS: *m/z* 636 ($[M]^+$, 20%), 442 ($[C_{29}H_{40}NO_3]^+$, 19%), 264 ($[C_{18}H_{19}NO_3]^+$, 28%), 208 ($[C_{14}H_{10}NO]^+$, 22%), 195 ($[C_{13}H_9NO]^+$, 78%), 110 ($[C_6H_6O_2]^+$, 12%), 69 ($[C_5H_9]^+$, 100%), 41 ($[C_3H_5]^+$, 20%).

1,3-bis-[1-(4'-cyanobiphen-4-yloxy)hexyl-6-oxy]benzene

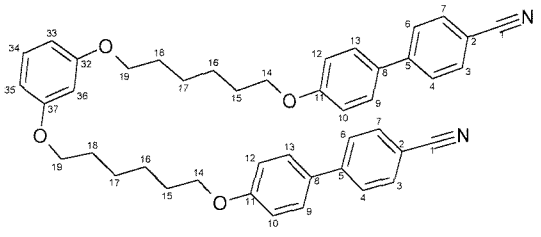

Rf 0.52; 100% DCM [1 spot by TLC]

^{1}H NMR (300 MHz, $CDCl_3$): δ_H 7.61 (4H, d, J = 8.6 Hz, $C_4\mathbf{H}$, $C_6\mathbf{H}$), 7.56 (4H, d, J = 8.6 Hz, $C_3\mathbf{H}$, $C_7\mathbf{H}$), 7.45 (4H, d, J = 8.8 Hz, $C_9\mathbf{H}$, $C_{13}\mathbf{H}$), 7.08 (1H, t, J = 7.7 Hz, $C_{36}\mathbf{H}$), 6.91 (4H, d, J = 9.0 Hz, $C_{10}\mathbf{H}$, $C_{12}\mathbf{H}$), 6.33-6.47 (3H, m, $C_{33}\mathbf{H}$, $C_{34}\mathbf{H}$, $C_{35}\mathbf{H}$), 3.95 (4H, t, 6.4 Hz, $C_{19}\mathbf{H_2}$-O), 3.88 (4H, t, 6.3 Hz, O-$C_{14}\mathbf{H_2}$), 1.64-1.85 (8H, m, $C_{15}\mathbf{H_2}$, $C_{18}\mathbf{H_2}$), 1.40-1.55 (8H, m, $C_{16}\mathbf{H_2}$, $C_{15}\mathbf{H_2}$) ppm.

^{13}C NMR (75 MHz, $CDCl_3$): δ_C 160.3 (q, $\mathbf{C_{11}}(Ar_{CB})$), 159.8 (q, $\mathbf{C_{26}}(Ar_{Res})$), 145.3 (q, $\mathbf{C_5}(Ar_{CB})$), 132.6 (t, $\mathbf{C_3}(Ar_{CB})$, $\mathbf{C_7}(Ar_{CB})$), 131.3 (q, $\mathbf{C_8}(Ar_{CB})$), 129.8 (q, $\mathbf{C_{32}}(Ar_{Res})$, $\mathbf{C_{37}}(Ar_{Res})$), 128.3 (t, $\mathbf{C_9}(Ar_{CB})$, $\mathbf{C_{13}}(Ar_{CB})$), 127.1 (t, $\mathbf{C_4}(Ar_{CB})$, $\mathbf{C_6}(Ar_{CB})$), 119.1 (q, $\mathbf{C_1}$(CN)), 115.1 (t, $\mathbf{C_{10}}(Ar_{CB})$, $\mathbf{C_{12}}(Ar_{CB})$), 110.1 (q, $\mathbf{C_2}(Ar_{CB})$), 106.7 (t, $\mathbf{C_{33}}$ (Ar_{Res}), $\mathbf{C_{35}}$ (Ar_{Res})), 101.6 (t, $\mathbf{C_{36}}$ (Ar_{Res})), 68.0 (s,

$\mathbf{C_{14}/C_{19}}$ (Res-O-$\mathbf{C}H_2$)), 67.8 (s, $\mathbf{C_{14}/C_{19}}$ (CB-O-$\mathbf{C}H_2$)), 29.2 (s, $\mathbf{C_{15\text{-}18}}(CH_2)$), 29.2 (s, $\mathbf{C_{15\text{-}18}}(CH_2)$), 25.9 (s, $\mathbf{C_{15\text{-}18}}(CH_2)$) ppm.

IR (Solid) ν_{max}: 2934(s) (**C-H$_2$**), 2866(s) (**C-H$_2$**), 2220(m) (**C≡N**), 1600(m) (**Ar**), 1518(m) (**Ar**), 1492(s) (**Ar**) cm^{-1}.

EIMS: *m/z* 664 ($[M]^+$, 20%), 277 ($[C_{19}H_{20}NO_3]^+$, 28%), 195 ($[C_{13}H_9NO]^+$, 78%), 178 ($[C_{13}H_8N]^+$, 7%), 110 ($[C_6H_6O_2]^+$, 12%), 69 ($[C_5H_9]^+$, 100%), 41 ($[C_3H_5]^+$, 20%).

1,3-bis-[1-(4'-cyanobiphen-4-yloxy)heptyl-7-oxy]benzene

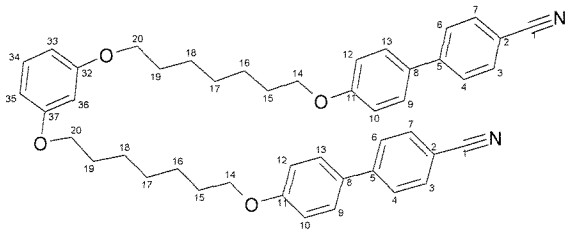

78
$C_{46}H_{48}N_2O_4$
692.91

Rf 0.55; 100% DCM [1 spot by TLC]

^{1}H NMR (300 MHz, $CDCl_3$): δ_H 7.60 (4H, d, J = 8.6 Hz, $C_4\mathbf{H}$, $C_6\mathbf{H}$), 7.55 (4H, d, J = 8.6 Hz, $C_3\mathbf{H}$, $C_7\mathbf{H}$), 7.44 (4H, d, J = 8.8 Hz, $C_9\mathbf{H}$, $C_{13}\mathbf{H}$), 7.07 (1H, t, J = 8.0 Hz, $C_{36}\mathbf{H}$), 6.91 (4H, d, J = 8.8 Hz, $C_{10}\mathbf{H}$, $C_{12}\mathbf{H}$), 6.34-6.46 (3H, m, $C_{33}\mathbf{H}$, $C_{34}\mathbf{H}$, $C_{35}\mathbf{H}$), 3.93 (4H, t, 6.5 Hz, $C_{20}\mathbf{H_2}$-O), 3.86 (4H, t, 6.4 Hz, O-$C_{14}\mathbf{H_2}$), 1.60-1.84 (8H, m, $C_{15}\mathbf{H_2}$, $C_{19}\mathbf{H_2}$), 1.25-1.56 (12H, m, $C_{16}\mathbf{H_2}$, $C_{17}\mathbf{H_2}$, $C_{18}\mathbf{H_2}$) ppm.

^{13}C NMR (75 MHz, $CDCl_3$): δ_C 160.4 (q, $\mathbf{C_{11}}(Ar_{CB})$), 159.8 (q, $\mathbf{C_{26}}(Ar_{Res})$), 145.3 (q, $\mathbf{C_5}(Ar_{CB})$), 132.6 (t, $\mathbf{C_3}(Ar_{CB})$, $\mathbf{C_7}(Ar_{CB})$), 131.3 (q, $\mathbf{C_8}(Ar_{CB})$), 129.8 (q, $\mathbf{C_{32}}(Ar_{Res})$, $\mathbf{C_{37}}(Ar_{Res})$), 128.3 (t, $\mathbf{C_9}(Ar_{CB})$, $\mathbf{C_{13}}(Ar_{CB})$), 127.1 (t, $\mathbf{C_4}(Ar_{CB})$, $\mathbf{C_6}(Ar_{CB})$), 119.1 (q, $\mathbf{C_1}$(CN)), 115.1 (t, $\mathbf{C_{10}}(Ar_{CB})$, $\mathbf{C_{12}}(Ar_{CB})$), 110.1 (q, $\mathbf{C_2}(Ar_{CB})$), 106.7 (t, $\mathbf{C_{33}}$ (Ar_{Res}), $\mathbf{C_{35}}$ (Ar_{Res})), 101.5 (t, $\mathbf{C_{36}}$ (Ar_{Res})), 68.1 (s, $\mathbf{C_{14}/C_{20}}$ (Res-O-$\mathbf{C}H_2$)), 67.9 (s, $\mathbf{C_{14}/C_{20}}$ (CB-O-$\mathbf{C}H_2$)), 29.2 (s, $\mathbf{C_{15\text{-}19}}(CH_2)$), 29.2 (s, $\mathbf{C_{15\text{-}19}}(CH_2)$), 29.1 (s, $\mathbf{C_{15\text{-}19}}(CH_2)$), 26.0 (s, $\mathbf{C_{15\text{-}19}}(CH_2)$) ppm.

IR (Solid) ν_{max}: 2935(s) (**C-H$_2$**), 2852(s) (**C-H$_2$**), 2220(m) (**C≡N**), 1601(m) (**Ar**), 1538(m) (**Ar**), 1492(s) (**Ar**) cm^{-1}.

MS: **Not obtained**

1,3-bis-[1-(4'-cyanobiphen-4-yloxy)octyl-8-oxy]benzene

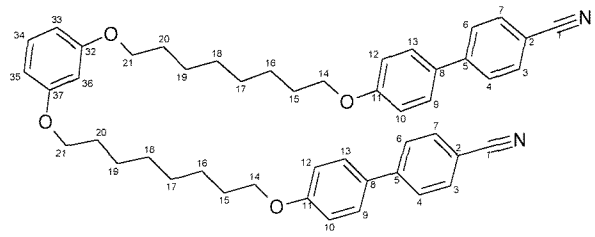

79
$C_{48}H_{52}N_2O_4$
720.96

Rf 0.58; 100% DCM [1 spot by TLC]

^{1}H NMR (300 MHz, $CDCl_3$): δ_H 7.61 (4H, d, J = 8.6 Hz, C_4**H**, C_6**H**), 7.55 (4H, d, J = 8.6 Hz, C_3**H**, C_7**H**), 7.44 (4H, d, J = 8.8 Hz, C_9**H**, C_{13}**H**), 7.07 (1H, t, J = 7.5 Hz, C_{36}**H**), 6.91 (4H, d, J = 8.8 Hz, C_{10}**H**, C_{12}**H**), 6.33-6.46 (3H, m, C_{33}**H,** C_{34}**H,** C_{35}**H**), 3.93 (4H, t, 6.5 Hz, C_{21}**H$_2$**-O), 3.86 (4H, t, 6.4 Hz, O-C_{14}**H$_2$**), 1.61-1.81 (8H, m, C_{15}**H$_2$**, C_{20}**H$_2$**), 1.24-1.51 (16H, m, C_{16}**H$_2$**, C_{17}**H$_2$**, C_{18}**H$_2$**, C_{19}**H$_2$**) ppm.

^{13}C NMR (75 MHz, $CDCl_3$): δ_C 160.4 (q, **C_{11}**(Ar_{CB})), 159.8 (q, **C_{26}**(Ar_{Res})), 145.3 (q, **C_5**(Ar_{CB})), 132.6 (t, **C_3**(Ar_{CB}), **C_7**(Ar_{CB})), 131.3 (q, **C_8**(Ar_{CB})), 129.8 (q, **C_{32}**(Ar_{Res}) , **C_{37}**(Ar_{Res})), 128.3 (t, **C_9**(Ar_{CB}), **C_{13}**(Ar_{CB})), 127.1 (t, **C_4**(Ar_{CB}), **C_6**(Ar_{CB})), 119.1 (q, **C_1**(CN)), 115.1 (t, **C_{10}**(Ar_{CB}), **C_{12}**(Ar_{CB})), 110.1 (q, **C_2**(Ar_{CB})), 106.7 (t, **C_{33}** (Ar_{Res}), **C_{35}** (Ar_{Res})), 101.6 (t, **C_{36}** (Ar_{Res})), 68.2 (s, **C_{14}/C_{21}** (Res-O-**C**H_2)), 68.0 (s, **C_{14}/C_{21}** (CB-O-**C**H_2)), 29.3 (s, **$C_{15\text{-}20}$**(CH_2)), 26.0 (s, **$C_{15\text{-}20}$**(CH_2)) ppm.

IR (Solid) ν_{max}: 2934(s) (**C-H$_2$**), 2851(s) (**C-H$_2$**), 2219(m) (**C≡N**), 1600(m) (**Ar**), 1523(m) (**Ar**), 1492(s) (**Ar**) cm^{-1}.

EIMS: *m/z* 279 ($[C_{20}H_{23}O]^+$, 9%), 207 ($[C_{14}H_9NO]^+$, 5%), 167 ($[C_{13}H_9]^+$, 29%), 149 ($[C_{10}H_{13}O]^+$, 100%), 83 ($[C_6H_{11}]^+$, 9%), 70 ($[C_4H_6O]^+$, 38%), 57 ($[C_3H_5O]^+$, 30%), 41 ($[C_3H_5]^+$, 22%)

1,3-bis-[1-(4'-cyanobiphen-4-yloxy)nonyl-9-oxy]benzene

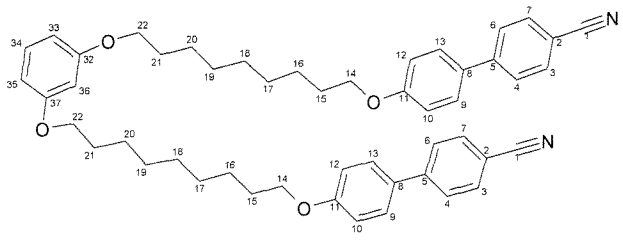

80
$C_{50}H_{56}N_2O_4$
749.01

Rf 0.59; 100% DCM [1 spot by TLC]

^{1}H NMR (400 MHz, $CDCl_3$): δ_H 7.60 (4H, d, J = 8.6 Hz, C_4**H**, C_6**H**), 7.55 (4H, d, J = 8.0 Hz, C_3**H**, C_7**H**), 7.44 (4H, d, J = 8.8 Hz, C_9**H**, C_{13}**H**), 7.07 (1H, t, J = 8.1 Hz, C_{36}**H**), 6.91 (4H, d, J = 8.8 Hz, C_{10}**H**, C_{12}**H**), 6.35-6.44 (3H, m, C_{33}**H,** C_{34}**H,** C_{35}**H**), 3.93 (4H, t, 6.5 Hz, C_{22}**H$_2$**-O), 3.85 (4H, t, 6.5 Hz, O-C_{14}**H$_2$**), 1.61-1.80 (8H, m, C_{15}**H$_2$**, C_{21}**H$_2$**), 1.20-1.50 (20H, m, C_{16}**H$_2$**, C_{17}**H$_2$**, C_{18}**H$_2$**, C_{19}**H$_2$**, C_{20}**H$_2$**) ppm.

^{13}C NMR (100 MHz, $CDCl_3$): δ_C 160.8 (q, **C_{11}**(Ar_{CB})), 160.2 (q, **C_{26}**(Ar_{Res})), 145.7 (q, **C_5**(Ar_{CB})), 133.0 (t, **C_3**(Ar_{CB}), **C_7**(Ar_{CB})), 131.7 (q, **C_8**(Ar_{CB})), 130.2 (q, **C_{32}**(Ar_{Res}) , **C_{37}**(Ar_{Res})), 128.7 (t, **C_9**(Ar_{CB}), **C_{13}**(Ar_{CB})), 127.5 (t, **C_4**(Ar_{CB}), **C_6**(Ar_{CB})), 119.5 (q, **C_1**(CN)), 115.5 (t, **C_{10}**(Ar_{CB}), **C_{12}**(Ar_{CB})), 110.5 (q, **C_2**(Ar_{CB})), 107.1 (t, **C_{33}** (Ar_{Res}), **C_{35}** (Ar_{Res})), 101.9 (t, **C_{36}** (Ar_{Res})), 68.6 (s, **C_{14}/C_{22}** (Res-O-**C**H_2)), 68.4 (s, **C_{14}/C_{22}** (CB-O-**C**H_2)), 29.9 (s, **$C_{15\text{-}21}$**(CH_2)), 29.7 (s, **$C_{15\text{-}21}$**(CH_2)), 29.6 (s, **$C_{15\text{-}21}$**(CH_2)), 26.4 (s, **$C_{15\text{-}21}$**(CH_2)) ppm.

IR (Solid) ν_{max}: 2934(s) (**C-H$_2$**), 2849(s) (**C-H$_2$**), 2222(m) (**C≡N**), 1602(m) (**Ar**), 1577(m) (**Ar**), 1519(w) (**Ar**), 1491(s) (**Ar**) cm^{-1}.

EIMS: *m/z* 748 ($[M]^+$, 8%), 429 ($[C_{28}H_{30}NO_3]^+$, 4%), 319 ($[C_{22}H_{25}NO]^+$, 12%), 195 ($[C_{13}H_9NO]^+$, 100%), 178 ($[C_{13}H_8N]^+$, 27%), 110 ($[C_6H_6O_2]^+$, 25%), 69 ($[C_5H_9]^+$, 17%).

1,3-bis-[1-(4'-cyanobiphen-4-yloxy)alkyl-10-oxy]benzene

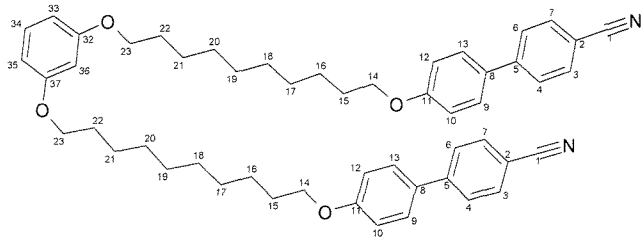

81
$C_{52}H_{60}N_2O_4$
777.07

Rf 0.61; 100% DCM [1 spot by TLC]

^{1}H NMR (400 MHz, $CDCl_3$): δ_H 7.60 (4H, d, J = 8.6 Hz, C_4**H**, C_6**H**), 7.55 (4H, d, J = 8.0 Hz, C_3**H**, C_7**H**), 7.44 (4H, d, J = 8.8 Hz, C_9**H**, C_{13}**H**), 7.07 (1H, t, J = 8.1 Hz, C_{36}**H**), 6.91 (4H, d, J = 8.8 Hz, C_{10}**H**, C_{12}**H**), 6.35-6.44 (3H, m, C_{33}**H**, C_{34}**H**, C_{35}**H**), 3.93 (4H, t, 6.5 Hz, C_{23}**H$_2$**-O), 3.85 (4H, t, 6.5 Hz, O-C_{14}**H$_2$**), 1.60-1.81 (8H, m, C_{15}**H$_2$**, C_{22}**H$_2$**), 1.16-1.51 (20H, m, C_{16}**H$_2$**, C_{17}**H$_2$**, C_{18}**H$_2$**, C_{19}**H$_2$**, C_{20}**H$_2$**, C_{21}**H$_2$**) ppm.

^{13}C NMR (100 MHz, $CDCl_3$): δ_C 161.3 (q, **C_{11}**(Ar_{CB})), 160.7 (q, **C_{26}**(Ar_{Res})), 146.2 (q, **C_5**(Ar_{CB})), 133.4 (t, **C_3**(Ar_{CB}), **C_7**(Ar_{CB})), 132.1 (q, **C_8**(Ar_{CB})), 130.6 (q, **C_{32}**(Ar_{Res}) , **C_{37}**(Ar_{Res})), 129.2 (t, **C_9**(Ar_{CB}), **C_{13}**(Ar_{CB})), 127.9 (t, **C_4**(Ar_{CB}), **C_6**(Ar_{CB})), 119.9 (q, **C_1**(CN)), 116.0 (t, **C_{10}**(Ar_{CB}), **C_{12}**(Ar_{CB})), 110.9 (q, **C_2**(Ar_{CB})), 107.5 (t, **C_{33}** (Ar_{Res}), **C_{35}** (Ar_{Res})), 102.4 (t, **C_{36}** (Ar_{Res})), 69.0 (s, **C_{14}**/**C_{23}** (Res-O-**C**H_2)), 68.8 (s, **C_{14}**/**C_{23}** (CB-O-**C**H_2)), 30.3 (s, **$C_{15\text{-}22}$**(CH_2)), 30.2 (s, **$C_{15\text{-}22}$**(CH_2)), 30.1 (s, **$C_{15\text{-}22}$**(CH_2)), 30.0 (s, **$C_{15\text{-}22}$**(CH_2)), 26.9 (s, **$C_{15\text{-}22}$**(CH_2)) ppm.

IR (Solid) ν_{max}: 2933(s) (**C-H$_2$**), 2849(s) (**C-H$_2$**), 2233(m) (**C≡N**), 1595(m) (**Ar**), 1519(w) (**Ar**), 1492(s) (**Ar**) cm^{-1}.

EIMS: *m/z* 279 ($[C_{20}H_{23}O]^+$, 9%), 207 ($[C_{14}H_9NO]^+$, 13%), 167 ($[C_{13}H_9]^+$, 32%), 149 ($[C_{10}H_{13}O]^+$, 100%), 83 ($[C_6H_{11}]^+$, 12%), 70 ($[C_4H_6O]^+$, 49%), 57 ($[C_3H_5O]^+$, 33%), 41 ($[C_3H_5]^+$, 28%)

1,3-bis-[1-(4'-cyanobiphen-4-yloxy)undecyl-11-oxy]benzene

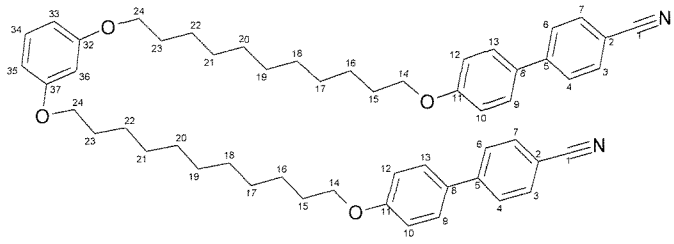

82
$C_{54}H_{64}N_2O_4$
805.12

Rf 0.63; 100% DCM [1 spot by TLC]

^{1}H NMR (400 MHz, $CDCl_3$): δ_H 7.60 (4H, d, J = 8.6 Hz, C_4**H**, C_6**H**), 7.55 (4H, d, J = 8.6 Hz, C_3**H**, C_7**H**), 7.44 (4H, d, J = 8.9 Hz, C_9**H**, C_{13}**H**), 7.07 (1H, t, J = 8.0 Hz, C_{36}**H**), 6.91 (4H, d, J = 8.8 Hz, C_{10}**H**, C_{12}**H**), 6.35-6.44 (3H, m, C_{33}**H,** C_{34}**H,** C_{35}**H**), 3.93 (4H, t, 6.5 Hz, C_{24}**H$_2$**-O), 3.85 (4H, t, 6.6 Hz, O-C_{14}**H$_2$**), 1.60-1.79 (8H, m, C_{15}**H$_2$**, C_{23}**H$_2$**), 1.15-1.51 (20H, m, C_{16}**H$_2$**, C_{17}**H$_2$**, C_{18}**H$_2$**, C_{19}**H$_2$**, C_{20}**H$_2$**, C_{21}**H$_2$**, C_{22}**H$_2$**) ppm.

^{13}C NMR (100 MHz, $CDCl_3$): δ_C 160.8 (q, **C_{11}**(Ar_{CB})), 160.2 (q, **C_{26}**(Ar_{Res})), 145.7 (q, **C_5**(Ar_{CB})), 133.0 (t, **C_3**(Ar_{CB}), **C_7**(Ar_{CB})), 131.7 (q, **C_8**(Ar_{CB})), 130.2 (q, **C_{32}**(Ar_{Res}) , **C_{37}**(Ar_{Res})), 128.7 (t, **C_9**(Ar_{CB}), **C_{13}**(Ar_{CB})), 127.5 (t, **C_4**(Ar_{CB}), **C_6**(Ar_{CB})), 119.5 (q, **C_1**(CN)), 115.5 (t, **C_{10}**(Ar_{CB}), **C_{12}**(Ar_{CB})), 110.5 (q, **C_2**(Ar_{CB})), 107.1 (t, **C_{33}** (Ar_{Res}), **C_{35}** (Ar_{Res})), 101.9 (t, **C_{36}** (Ar_{Res})), 68.6 (s, **C_{14}/C_{23}** (Res-O-**C**H_2)), 68.4 (s, **C_{14}/C_{24}** (CB-O-**C**H_2)), 30.1 (s, **$C_{15\text{-}23}$**(CH_2)), 29.9 (s, **$C_{15\text{-}23}$**(CH_2)), 29.9 (s, **$C_{15\text{-}23}$**(CH_2)), 29.8 (s, **$C_{15\text{-}23}$**(CH_2)), 29.7 (s, **$C_{15\text{-}23}$**(CH_2)), 29.7 (s, **$C_{15\text{-}23}$**(CH_2)), 29.6 (s, **$C_{15\text{-}23}$**(CH_2)), 26.5 (s, **$C_{15\text{-}23}$**(CH_2)), 26.4 (s, **$C_{15\text{-}23}$**(CH_2)) ppm.

IR (Solid) ν_{max}: 2918(s) (**C-H$_2$**), 2850(s) (**C-H$_2$**), 2222(m) (**C≡N**), 1601(m) (**Ar**), 1521(w) (**Ar**), 1492(s) (**Ar**) cm^{-1}.

EIMS: *m/z* 279 ($[C_{20}H_{23}O]^+$, 9%), 207 ($[C_{14}H_9NO]^+$, 8%), 167 ($[C_{13}H_9]^+$, 29%), 149 ($[C_{10}H_{13}O]^+$, 100%), 83 ($[C_6H_{11}]^+$, 9%), 70 ($[C_4H_6O]^+$, 37%), 57 ($[C_3H_5O]^+$, 29%), 41 ($[C_3H_5]^+$, 21%)

1,3-bis-[1-(4'-cyanobiphen-4-yloxy)dodecyl-dodec-oxy]benzene

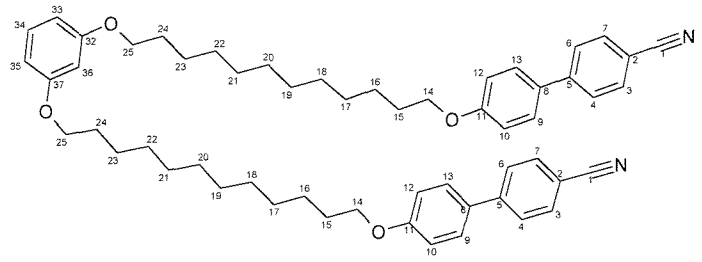

83
$C_{56}H_{68}N_2O_4$
833.18

Rf 0.64; 100% DCM [1 spot by TLC]

^{1}H NMR (300 MHz, $CDCl_3$): δ_H 7.61 (4H, d, J = 8.5 Hz, C_4**H**, C_6**H**), 7.55 (4H, d, J = 8.6 Hz, C_3**H**, C_7**H**), 7.45 (4H, d, J = 8.8 Hz, C_9**H**, C_{13}**H**), 7.07 (1H, t, J = 8.1 Hz, C_{36}**H**), 6.91 (4H, d, J = 8.8 Hz, C_{10}**H**, C_{12}**H**), 6.34-6.45 (3H, m, C_{33}**H**, C_{34}**H**, C_{35}**H**), 3.93 (4H, t, 6.5 Hz, C_{24}**H$_2$**-O), 3.85 (4H, t, 6.6 Hz, O-C_{14}**H$_2$**), 1.60-1.81 (8H, m, C_{15}**H$_2$**, C_{23}**H$_2$**), 1.11-1.52 (32H, m, C_{16}**H$_2$**, C_{17}**H$_2$**, C_{18}**H$_2$**, C_{19}**H$_2$**, C_{20}**H$_2$**, C_{21}**H$_2$**, C_{22}**H$_2$**, C_{23}**H$_2$**) ppm.

^{13}C NMR (75 MHz, $CDCl_3$): δ_C 160.4 (q, **C_{11}**(Ar_{CB})), 159.8 (q, **C_{26}**(Ar_{Res})), 145.3 (q, **C_5**(Ar_{CB})), 132.6 (t, **C_3**(Ar_{CB}), **C_7**(Ar_{CB})), 131.2 (q, **C_8**(Ar_{CB})), 129.8 (q, **C_{32}**(Ar_{Res}) , **C_{37}**(Ar_{Res})), 128.3 (t, **C_9**(Ar_{CB}), **C_{13}**(Ar_{CB})), 127.1 (t, **C_4**(Ar_{CB}), **C_6**(Ar_{CB})), 119.1 (q, **C_1**(CN)), 115.1 (t, **C_{10}**(Ar_{CB}), **C_{12}**(Ar_{CB})), 110.0 (q, **C_2**(Ar_{CB})), 106.6 (t, **C_{33}** (Ar_{Res}), **C_{35}** (Ar_{Res})), 101.5 (t, **C_{36}** (Ar_{Res})), 68.2 (s, **C_{14}**/**C_{23}** (Res-O-**C**H_2)), 68.0 (s, **C_{14}**/**C_{24}** (CB-O-**C**H_2)), 29.6 (s, **$C_{15\text{-}23}$**(CH_2)), 29.4 (s, **$C_{15\text{-}23}$**(CH_2)), 29.3 (s, **$C_{15\text{-}23}$**(CH_2)), 29.2 (s, **$C_{15\text{-}23}$**(CH_2)), 26.1 (s, **$C_{15\text{-}23}$**(CH_2)) ppm.

IR (Solid) ν_{max}: 2935(s) (**C-H$_2$**), 2918(s) (**C-H$_2$**), 2651(s), 2236(m) (**C≡N**), 1597(m) (**Ar**), 1521(w) (**Ar**), 1493(s) (**Ar**) cm^{-1}.

EIMS: *m/z* 279 ($[C_{20}H_{23}O]^+$, 9%), 207 ($[C_{14}H_9NO]^+$, 10%), 167 ($[C_{13}H_9]^+$, 29%), 149 ($[C_{10}H_{13}O]^+$, 100%), 83 ($[C_6H_{11}]^+$, 11%), 70 ($[C_4H_6O]^+$, 46%), 57 ($[C_3H_5O]^+$, 32%), 41 ($[C_3H_5]^+$, 27%)

7.5. Chapter 6 experimental

7.5.1. Cat(OH)(OnOCB); 1-[α-(4'cyanobiphen-4-yloxy)alkyl-ω-oxy]-2-hydroxybenzene

n	Temperature /°C					Mass	Yield
	Cr		N		I	g	%
4	•	195	•		•	121	10
5	•	98	•	(43)	•	202	18
6	•	147	•		•	531	98
7	•	109	•	(60)	•	620	99
8	•	131	•		•	539	93
9	•	100	•	(65)	•	1645	87
10	•	123	•	(93)	•	1410	72
11	•	100	•	(65)	•	600	94
12	•	125	•	(79)	•	601	91

1-[1-(4'Cyanobiphen-4-yloxy)decyl-10-oxy]-2-hydroxybenzene

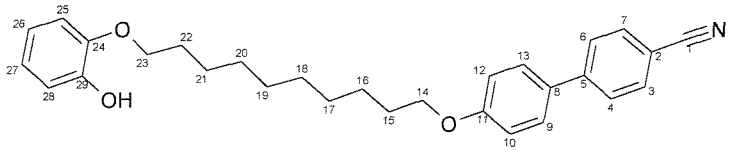

84
$C_{29}H_{35}NO_3$
443.59

Procedure:

To a solution of catechol (330 mg, 3.00 mMol, 2 eq) in nitrogen purged acetonitrile (40 mL) was added potassium carbonate (414 mg, 3.00 mMol, 2 eq) as one portion. This mixture was stirred at reflux for 30 min and then cooled to room temperature for the addition of the 1-(cyanobiphenyloxy)-dodecyl-12-bromide (663 mg, 1.50 mMol, 1 eq). and a catalytic quantity of sodium iodide (80 mg). The reaction mixture was brought back to reflux and stirred at this temperature for 30 h. The reaction was cooled to room temperature and water (100 mL); this precipitated a brown solid which was separated by filtration through celite. The solid was dissolved in DCM, dried over $MgSO_4$, filtered and the solvent was removed *in vacuo*. The crude material was further purified by column chromatography (40 x 40 mm, silica, 100% DCM) to give the title product **84** as a white microcrystalline solid (601 mg, 1.35 mMol, 91.0%).

Rf 0.50; 100% DCM [1 spot by TLC]

^{1}H NMR (300 MHz, $CDCl_3$): δ_H 7.61 (2H, d, J = 8.5 Hz, C_4**H**, C_6**H**), 7.56 (2H, d, J = 8.5 Hz, C_3**H**, C_7**H**), 7.45 (2H, d, 9.0 Hz, C_9**H**, C_{13}**H**), 6.92 (2H, d, J = 8.8 Hz, C_{10}**H**, C_{12}**H**), 6.68-6.88 (4H, m, C_{27}**H**, C_{28}**H**, C_{29}**H**, C_{30}**H**), 5.56 (1H, s, Cat-**OH**), 3.87-4.01 (4H, m, O-C_{14}**H$_2$**, C_{23}**H$_2$**-O), 3.90-3.99 (4H, m, 6.8 Hz, C_{23}**H$_2$**-O, C_{14}**H$_2$**-O), 1.65-1.81 (4H, m, C_{15}**H$_2$**, C_{22}**H$_2$**), 1.15-1.50 (12H, m, C_{16}**H$_2$**, C_{17}**H$_2$**, C_{18}**H$_2$**, C_{19}**H$_2$**, C_{20}**H$_2$**, C_{21}**H$_2$**) ppm.

^{13}C NMR (75 MHz, $CDCl_3$): δ_C 159.8 (q, **C_{11}**(Ar_{CB})), 146.0 (q, **C_{26}**(Ar_{Cat})), 145.8 (q, **C_5**(Ar_{CB})), 145.3 (q, **C_{31}**(Ar_{Cat})), 132.6 (t, **C_3**(Ar_{CB}), **C_7**(Ar_{CB})), 131.3 (q, **C_8**(Ar_{CB})), 128.3 (t, **C_9**(Ar_{CB}), **C_{13}**(Ar_{CB})), 127.1 (t, **C_4**(Ar_{CB}), **C_6**(Ar_{CB})), 121.3 (t, **C_{28}**(Ar_{Cat})), 120.1 (q, **C_{29}**(Ar_{Cat})), 119.1 (q, **C_1**(CN)), 115.1 (t, **C_{10}**(Ar_{CB}), **C_{12}**(Ar_{CB})), 114.4 (t, **C_{27}** (Ar_{Cat})), 111.6 (q, **C_{30}**(Ar_{Cat})), 110.1 (q, **C_2**(Ar_{CB})), 68.9 (s, **C_{17}** (Cat-O-**C**H_2)), 68.2 (s, **C_{14}** (CB-O-CH_2)), 29.5 (s, **$C_{15\text{-}22}$** (CH_2)), 29.3 (s, **$C_{15\text{-}22}$** (CH_2)), 29.2 (s, **$C_{15\text{-}22}$** (CH_2)), 26.0 (s, **$C_{15\text{-}22}$** (CH_2)) ppm.

IR (Solid) ν_{max}: 3442(br) (**C-OH**), 2923(s) (**C-H$_2$**), 2852(s) (**C-H$_2$**), 2223(m) (**C≡N**), 1597(m) (**Ar**), 1501(w) (**Ar**) cm^{-1}.

ESMS *m/z* 442 ([M – H]$^-$, 100%), 886 ([2M – H]$^-$, 7%)

Elemental Analysis: $C_{29}H_{35}NO_3$: (Expected) **C** 78.45, **H** 7.44, **N** 3.16; (Found) **C** 78.66, **H** 7.57, **N** 3.19

1-[1-(4'Cyanobiphen-4-yloxy)butyl-4-oxy]-2-hydroxybenzene

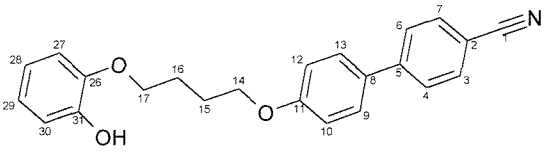

85
$C_{23}H_{21}NO_3$
359.43

Rf 0.50; 100% DCM [1 spot by TLC]

^{1}H NMR (100 MHz, $CDCl_3$): δ_H 7.62 (2H, d, J = 8.6 Hz, C_4**H**, C_6**H**), 7.56 (2H, d, J = 8.6 Hz, C_3**H**, C_7**H**), 7.46 (2H, d, 9.0 Hz, C_9**H**, C_{13}**H**), 6.93 (2H, d, J = 8.8 Hz, C_{10}**H**, C_{12}**H**), 6.70-6.89 (4H, m, C_{27}**H**, C_{28}**H**, C_{29}**H**, C_{30}**H**), 5.52 (1H, br.s, Cat-**OH**), 4.07 (2H, t, 6.0 Hz, O-C_{14}**H$_2$**), 4.03 (2H, t, 6.8 Hz C_{17}**H$_2$**-O), 1.84-2.06 (4H, m, C_{15}**H$_2$**, C_{16}**H$_2$**) ppm.

^{13}C NMR (75 MHz, $CDCl_3$): δ_C 159.5 (q, $\mathbf{C_{11}}(Ar_{CB})$), 145.8 (q, $\mathbf{C_{26}}(Ar_{Cat})$), 145.2 (q, $\mathbf{C_5}(Ar_{CB})$), 132.6 (t, $\mathbf{C_3}(Ar_{CB})$, $\mathbf{C_7}(Ar_{CB})$), 131.6 (q, $\mathbf{C_8}(Ar_{CB})$), 128.2 (t, $\mathbf{C_9}(Ar_{CB})$, $\mathbf{C_{13}}(Ar_{CB})$), 127.1 (t, $\mathbf{C_4}(Ar_{CB})$, $\mathbf{C_6}(Ar_{CB})$), 121.6 (t, $\mathbf{C_{28}}(Ar_{Cat})$), 120.1 (q, $\mathbf{C_{29}}(Ar_{Cat})$), 119.1 (q, $\mathbf{C_1}(CN)$), 115.1 (t, $\mathbf{C_{10}}(Ar_{CB})$, $\mathbf{C_{12}}(Ar_{CB})$), 114.6 (t, $\mathbf{C_{27}}(Ar_{Cat})$), 111.7 (q, $\mathbf{C_{30}}(Ar_{Cat})$), 110.2 (q, $\mathbf{C_2}(Ar_{CB})$), 68.4 (s, $\mathbf{C_{17}}$ (Cat-O-$\mathbf{C}H_2$)), 67.5 (s, $\mathbf{C_{14}}$ (CB-O-$\mathbf{C}H_2$)), 26.1 (s, $\mathbf{C_{15,16}}$ (CH_2)), 26.0 (s, $\mathbf{C_{15,16}}$ (CH_2)) ppm.

Note: No peak found for $\mathbf{C_{31}}$OH(Ar) expected around δ_C = 145 ppm.

IR **Not Obtained**

MS **Not Obtained**

1-[1-(4'Cyanobiphen-4-yloxy)pentyl-5-oxy]-2-hydroxybenzene 86

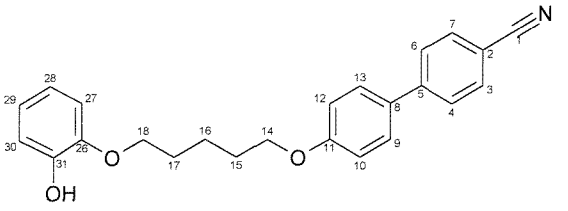

86
$C_{24}H_{23}NO_3$
373.46

Rf 0.51; 100% DCM [1 spot by TLC]

^{1}H NMR (100 MHz, $CDCl_3$): δ_H 7.61 (2H, d, J = 8.4 Hz, $C_4\mathbf{H}$, $C_6\mathbf{H}$), 7.56 (2H, d, J = 8.4 Hz, $C_3\mathbf{H}$, $C_7\mathbf{H}$), 7.45 (2H, d, 9.0 Hz, $C_9\mathbf{H}$, $C_{13}\mathbf{H}$), 6.92 (2H, d, J = 8.8 Hz, $C_{10}\mathbf{H}$, $C_{12}\mathbf{H}$), 6.69-6.89 (4H, m, $C_{27}\mathbf{H}$, $C_{28}\mathbf{H}$, $C_{29}\mathbf{H}$, $C_{30}\mathbf{H}$), 5.57 (1H, s, Cat-O**H**), 4.01 (2H, t, 5.8 Hz, O-$C_{14}\mathbf{H_2}$), 3.97 (2H, t, 5.7 Hz $C_{17}\mathbf{H_2}$-O), 1.76-1.92 (4H, m, $C_{15}\mathbf{H_2}$, $C_{17}\mathbf{H_2}$), 1.54-1.69 (2H, m, $C_{16}\mathbf{H_2}$) ppm.

^{13}C NMR (75 MHz, $CDCl_3$): δ_C 159.6 (q, $\mathbf{C_{11}}(Ar_{CB})$), 145.8 (q, $\mathbf{C_{26}}(Ar_{Cat})$), 145.3 (q, $\mathbf{C_5}(Ar_{CB})$), 132.6 (t, $\mathbf{C_3}(Ar_{CB})$, $\mathbf{C_7}(Ar_{CB})$), 131.5 (q, $\mathbf{C_8}(Ar_{CB})$), 128.4 (t, $\mathbf{C_9}(Ar_{CB})$, $\mathbf{C_{13}}(Ar_{CB})$), 127.1 (t, $\mathbf{C_4}(Ar_{CB})$, $\mathbf{C_6}(Ar_{CB})$), 121.5 (t, $\mathbf{C_{28}}(Ar_{Cat})$), 120.1 (q, $\mathbf{C_{29}}(Ar_{Cat})$), 119.1 (q, $\mathbf{C_1}(CN)$), 115.1 (t, $\mathbf{C_{10}}(Ar_{CB})$, $\mathbf{C_{12}}(Ar_{CB})$), 114.6 (t, $\mathbf{C_{27}}(Ar_{Cat})$), 111.7 (q, $\mathbf{C_{30}}(Ar_{Cat})$), 110.1 (q, $\mathbf{C_2}(Ar_{CB})$), 68.6 (s, $\mathbf{C_{18}}$ (Cat-O-$\mathbf{C}H_2$)), 67.8 (s, $\mathbf{C_{14}}$ (CB-O-$\mathbf{C}H_2$)), 28.9 (s, $\mathbf{C_{15\text{-}17}}$ (CH_2)), 28.9 (s, $\mathbf{C_{15\text{-}17}}$ (CH_2)), 22.7 (s, $\mathbf{C_{15\text{-}17}}$ (CH_2)) ppm.

Note: No peak found for $\mathbf{C_{31}}$OH(Ar) expected around δ_C = 145 ppm.

IR **Not Obtained**

MS **Not Obtained**

1-[1-(4'cyanobiphen-4-yloxy)hexyl-6-oxy]-2-hydroxybenzene

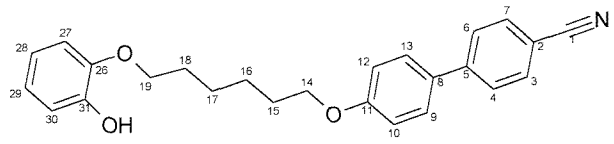

87
$C_{25}H_{25}NO_3$
387.48

Rf 0.51; 100% DCM

^{1}H NMR (100 MHz, $CDCl_3$): δ_H 7.61 (2H, d, J = 8.4 Hz, C_4**H**, C_6**H**), 7.56 (2H, d, J = 8.5 Hz, C_3**H**, C_7**H**), 7.45 (2H, d, 8.8 Hz, C_9**H**, C_{13}**H**), 6.92 (2H, d, J = 8.8 Hz, C_{10}**H**, C_{12}**H**), 6.69-6.89 (4H, m, C_{27}**H**, C_{28}**H**, C_{29}**H**, C_{30}**H**), 5.56 (1H, s, Cat-O**H**), 3.99 (2H, t, 6.6 Hz, O-C_{14}**H_2**), 3.95 (2H, t, 6.6 Hz C_{18}**H_2**-O), 1.69-1.87 (4H, m, C_{15}**H_2**, C_{18}**H_2**), 1.39-1.60 (4H, m, C_{16}**H_2**, C_{17}**H_2**) ppm.

^{13}C NMR (75 MHz, $CDCl_3$): δ_C 159.7 (q, **C_{11}**(Ar_{CB})), 145.9 (q, **C_{26}**(Ar_{Cat})), 145.8 (q, **C_5**(Ar_{CB})), 145.3 (q, **C_{31}**(Ar_{Cat})), 132.6 (t, **C_3**(Ar_{CB}), **C_7**(Ar_{CB})), 131.4 (q, **C_8**(Ar_{CB})), 128.3 (t, **C_9**(Ar_{CB}), **C_{13}**(Ar_{CB})), 127.1 (t, **C_4**(Ar_{CB}), **C_6**(Ar_{CB})), 121.4 (t, **C_{28}**(Ar_{Cat})), 120.1 (q, **C_{29}**(Ar_{Cat})), 119.1 (q, **C_1**(CN)), 115.1 (t, **C_{10}**(Ar_{CB}), **C_{12}**(Ar_{CB})), 114.5 (t, **C_{27}** (Ar_{Cat})), 111.7 (q, **C_{30}**(Ar_{Cat})), 110.1 (q, **C_2**(Ar_{CB})), 68.7 (s, **C_{19}** (Cat-O-**C**H_2)), 67.9 (s, **C_{14}** (CB-O-**C**H_2)), 28.9 (s, **$C_{15\text{-}18}$** (CH_2)), 28.9 (s, **$C_{15\text{-}18}$** (CH_2)), 22.7 (s, **$C_{15\text{-}18}$** (CH_2)) ppm.

IR (Solid) ν_{max}: 3418(br) (**O-H**), 2948(s) (**C-H_2**), 2850(s) (**C-H_2**), 2229(m) (**C≡N**), 1600(m) (**Ar**), 1504(w) (**Ar**) cm^{-1}.

ESMS *m/z* 386 ([M – H]$^-$, 100%), 773 ([2M – H]$^-$, 14%).

1-[1-(4'Cyanobiphen-4-yloxy)heptyl-7-oxy]-2-hydroxybenzene

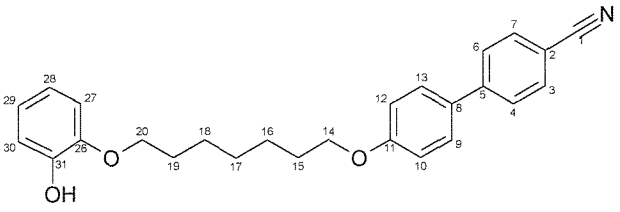

88
$C_{26}H_{27}NO_3$
401.51

Rf 0.50; 100% DCM [1 spot by TLC]

^{1}H NMR (100 MHz, $CDCl_3$): δ_H 7.61 (2H, d, J = 8.4 Hz, C_4**H**, C_6**H**), 7.56 (2H, d, J = 8.6 Hz, C_3**H**, C_7**H**), 7.45 (2H, d, 8.8 Hz, C_9**H**, C_{13}**H**), 6.92 (2H, d, J = 8.8 Hz, C_{10}**H**, C_{12}**H**), 6.69-6.89 (4H, m, C_{27}**H**, C_{28}**H**, C_{29}**H**, C_{30}**H**), 5.56 (1H, s, Cat-O**H**), 3.99 (2H, t, 6.6 Hz, O-C_{14}**H**$_2$), 3.95 (2H, t, 6.4 Hz C_{20}**H**$_2$-O), 1.67-1.88 (4H, m, C_{15}**H**$_2$, C_{19}**H**$_2$), 1.40-1.58 (6H, m, C_{16}**H**$_2$, C_{17}**H**$_2$, C_{18}**H**$_2$) ppm.

^{13}C NMR (75 MHz, $CDCl_3$): δ_C 159.8 (q, **C**$_{11}$(Ar_{CB})), 145.9 (q, **C**$_{26}$(Ar_{Cat})), 145.8 (q, **C**$_5$(Ar_{CB})), 145.3 (q, **C**$_{31}$(Ar_{Cat})), 132.6 (t, **C**$_3$(Ar_{CB}), **C**$_7$(Ar_{CB})), 131.3 (q, **C**$_8$(Ar_{CB})), 128.3 (t, **C**$_9$(Ar_{CB}), **C**$_{13}$(Ar_{CB})), 127.1 (t, **C**$_4$(Ar_{CB}), **C**$_6$(Ar_{CB})), 121.4 (t, **C**$_{28}$(Ar_{Cat})), 120.1 (q, **C**$_{29}$(Ar_{Cat})), 119.1 (q, **C**$_1$(CN)), 115.1 (t, **C**$_{10}$(Ar_{CB}), **C**$_{12}$(Ar_{CB})), 114.5 (t, **C**$_{27}$ (Ar_{Cat})), 111.7 (q, **C**$_{30}$(Ar_{Cat})), 110.1 (q, **C**$_2$(Ar_{CB})), 68.8 (s, **C**$_{20}$ (Cat-O-**C**H_2)), 68.0 (s, **C**$_{14}$ (CB-O-**C**H_2)), 29.2 (s, **C**$_{15\text{-}19}$ (CH_2)), 29.1 (s, **C**$_{15\text{-}19}$ (CH_2)), 29.1 (s, **C**$_{15\text{-}19}$ (CH_2)), 26.0 (s, **C**$_{15\text{-}19}$ (CH_2)) ppm.

IR (Solid) ν_{max}: 2934(s) (**C-H**$_2$), 2866(s) (**C-H**$_2$), 2228(m) (**C≡N**), 1699(m) (**Ar**), 1500(s) (**Ar**) cm^{-1}.

ESMS *m/z* 400 ([M – H]$^-$, 100%), 802 ([2M – H]$^-$, 6%).

1-[1-(4'Cyanobiphen-4-yloxy)octyl-8-oxy]-2-hydroxybenzene

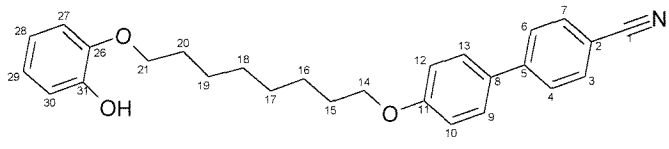

89
$C_{27}H_{29}NO_3$
415.54

Rf 0.50; 100% DCM [1 spot by TLC]

^{1}H NMR (100 MHz, $CDCl_3$): δ_H 7.61 (2H, d, J = 8.5 Hz, C_4**H**, C_6**H**), 7.56 (2H, d, J = 8.5 Hz, C_3**H**, C_7**H**), 7.45 (2H, d, 9.0 Hz, C_9**H**, C_{13}**H**), 6.92 (2H, d, J = 8.8 Hz, C_{10}**H**, C_{12}**H**), 6.68-6.88 (4H, m, C_{27}**H**, C_{28}**H**, C_{29}**H**, C_{30}**H**), 5.57 (1H, s, Cat-O**H**), 3.97 (2H, t, 6.4 Hz, O-C_{14}**H**$_2$), 3.94 (2H, t, 6.4 Hz C_{21}**H**$_2$-O), 1.65-1.83 (4H, m, C_{15}**H**$_2$, C_{20}**H**$_2$), 1.40-1.58 (8H, m, C_{16}**H**$_2$, C_{17}**H**$_2$, C_{18}**H**$_2$, C_{19}**H**$_2$) ppm.

^{13}C NMR (75 MHz, $CDCl_3$): δ_C 159.8 (q, **C**$_{11}$(Ar_{CB})), 145.9 (q, **C**$_{26}$(Ar_{Cat})), 145.8 (q, **C**$_5$(Ar_{CB})), 145.3 (q, **C**$_{31}$(Ar_{Cat})), 132.6 (t, **C**$_3$(Ar_{CB}), **C**$_7$(Ar_{CB})), 131.3 (q, **C**$_8$(Ar_{CB})), 128.3 (t, **C**$_9$(Ar_{CB}), **C**$_{13}$(Ar_{CB})), 127.1 (t, **C**$_4$(Ar_{CB}), **C**$_6$(Ar_{CB})), 121.4 (t, **C**$_{28}$(Ar_{Cat})), 120.1 (q, **C**$_{29}$(Ar_{Cat})), 119.1 (q, **C**$_1$(CN)), 115.1 (t,

$C_{10}(Ar_{CB})$, $C_{12}(Ar_{CB})$), 114.5 (t, C_{27} (Ar_{Cat})), 111.7 (q, $C_{30}(Ar_{Cat})$), 110.1 (q, $C_2(Ar_{CB})$), 68.8 (s, C_{21} (Cat-O-CH_2)), 68.1 (s, C_{14} (CB-O-CH_2)), 29.3 (s, $C_{15\text{-}20}$ (CH_2)), 29.2 (s, $C_{15\text{-}20}$ (CH_2)), 26.0 (s, $C_{15\text{-}20}$ (CH_2)) ppm.

IR (Solid) ν_{max}: 2934(s) (**C-H$_2$**), 2866(s) (**C-H$_2$**), 2228(m) (**C≡N**), 1699(m) (**Ar**), 1500(s) (**Ar**) cm^{-1}.

ESMS *m/z* 414 ([M – H]$^-$, 100%), 830 ([2M – H]$^-$, 7%).

1-[1-(4'Cyanobiphen-4-yloxy)nonyl-9-oxy]-2-hydroxybenzene

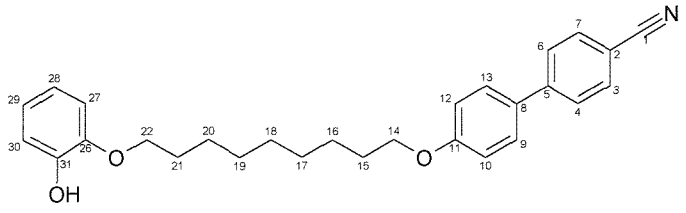

90
$C_{28}H_{31}NO_3$
429.56

Rf 0.51; 100% DCM [1 spot by TLC]

^{1}H NMR (100 MHz, $CDCl_3$): δ_H 7.61 (2H, d, J = 8.4 Hz, C_4**H**, C_6**H**), 7.56 (2H, d, J = 8.5 Hz, C_3**H**, C_7**H**), 7.45 (2H, d, 9.0 Hz, C_9**H**, C_{13}**H**), 6.92 (2H, d, J = 9.0 Hz, C_{10}**H**, C_{12}**H**), 6.67-6.88 (4H, m, C_{27}**H,** C_{28}**H**, C_{29}**H**, C_{30}**H**), 5.57 (1H, s, Cat-O**H**), 3.96 (2H, t, 6.6 Hz, O-C_{14}**H$_2$**), 3.93 (2H, t, 6.6 Hz C_{22}**H$_2$**-O), 1.64-1.82 (4H, m, C_{15}**H$_2$**, C_{21}**H$_2$**), 1.19-1.54 (10H, m, C_{16}**H$_2$**, C_{17}**H$_2$**, C_{18}**H$_2$**, C_{19}**H$_2$**, C_{20}**H$_2$**) ppm.

^{13}C NMR (75 MHz, $CDCl_3$): δ_C 161.2 (q, $C_{11}(Ar_{CB})$), 159.8 (q, $C_{26}(Ar_{Cat})$), 145.8 (q, $C_5(Ar_{CB})$), 145.3 (q, $C_{31}(Ar_{Cat})$), 132.6 (t, $C_3(Ar_{CB})$, $C_7(Ar_{CB})$), 131.3 (q, $C_8(Ar_{CB})$), 128.3 (t, $C_9(Ar_{CB})$, $C_{13}(Ar_{CB})$), 127.1 (t, $C_4(Ar_{CB})$, $C_6(Ar_{CB})$), 121.3 (t, $C_{28}(Ar_{Cat})$), 120.1 (q, $C_{29}(Ar_{Cat})$), 119.1 (q, C_1(CN)), 115.1 (t, $C_{10}(Ar_{CB})$, $C_{12}(Ar_{CB})$), 114.5 (t, C_{27} (Ar_{Cat})), 111.7 (q, $C_{30}(Ar_{Cat})$), 110.1 (q, $C_2(Ar_{CB})$), 68.8 (s, C_{21} (Cat-O-CH_2)), 68.1 (s, C_{14} (CB-O-CH_2)), 29.4 (s, $C_{15\text{-}21}$ (CH_2)), 29.3 (s, $C_{15\text{-}21}$ (CH_2)), 29.2 (s, $C_{15\text{-}21}$ (CH_2)), 29.1 (s, $C_{15\text{-}21}$ (CH_2)), 28.5 (s, $C_{15\text{-}21}$ (CH_2)), 26.0 (s, $C_{15\text{-}21}$ (CH_2)) ppm.

IR (Solid) ν_{max}: 3416(br) (**O-H**), 2932(s) (**C-H$_2$**), 2863(s) (**C-H$_2$**), 2226(m) (**C≡N**), 1596(m) (**Ar**), 1500(s) (**Ar**) cm^{-1}.

ESMS *m/z* 428 ([M – H]$^-$, 100%), 858 ([2M – H]$^-$, 5%).

1-[1-(4'Cyanobiphen-4-yloxy)undecyl-11-oxy]-2-hydroxybenzene

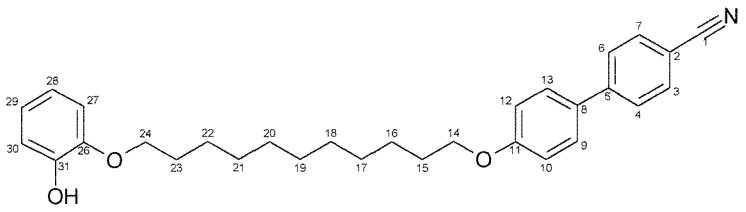

91
$C_{30}H_{35}NO_3$
457.62

Rf 0.52; 100% DCM [1 spot by TLC]

^{1}H NMR (100 MHz, $CDCl_3$): δ_H 7.61 (2H, d, J = 8.5 Hz, C_4**H**, C_6**H**), 7.55 (2H, d, J = 8.5 Hz, C_3**H**, C_7**H**), 7.45 (2H, d, 9.0 Hz, C_9**H**, C_{13}**H**), 6.91 (2H, d, J = 9.0 Hz, C_{10}**H**, C_{12}**H**), 6.67-6.88 (4H, m, C_{27}**H**, C_{28}**H**, C_{29}**H**, C_{30}**H**), 5.57 (1H, s, Cat-O**H**), 3.97-4.00 (4H, m, O-C_{14}**H$_2$**, Hz C_{23}**H$_2$**-O), 1.65-1.80 (4H, m, C_{15}**H$_2$**, C_{22}**H$_2$**), 1.17-1.55 (12H, m, C_{16}**H$_2$**, C_{17}**H$_2$**, C_{18}**H$_2$**, C_{19}**H$_2$**, C_{20}**H$_2$**, C_{21}**H$_2$**) ppm.

^{13}C NMR (75 MHz, $CDCl_3$): δ_C 159.8 (q, **C_{11}**(Ar_{CB})), 146.0 (q, **C_{26}**(Ar_{Cat})), 145.8 (q, **C_5**(Ar_{CB})), 145.3 (q, **C_{31}**(Ar_{Cat})), 132.6 (t, **C_3**(Ar_{CB}), **C_7**(Ar_{CB})), 131.3 (q, **C_8**(Ar_{CB})), 128.3 (t, **C_9**(Ar_{CB}), **C_{13}**(Ar_{CB})), 127.1 (t, **C_4**(Ar_{CB}), **C_6**(Ar_{CB})), 121.3 (t, **C_{28}**(Ar_{Cat})), 120.1 (q, **C_{29}**(Ar_{Cat})), 119.1 (q, **C_1**(CN)), 115.1 (t, **C_{10}**(Ar_{CB}), **C_{12}**(Ar_{CB})), 114.5 (t, **C_{27}** (Ar_{Cat})), 111.7 (q, **C_{30}**(Ar_{Cat})), 110.1 (q, **C_2**(Ar_{CB})), 68.9 (s, **C_{21}** (Cat-O-**C**H_2)), 68.2 (s, **C_{14}** (CB-O-**C**H_2)), 29.5 (s, **C_{15-21}** (CH_2)), 29.4 (s, **C_{15-21}** (CH_2)), 29.3 (s, **C_{15-21}** (CH_2)), 26.0 (s, **C_{15-21}** (CH_2)) ppm.

IR (Solid) ν_{max}: 3373(br) (**O-H**), 2915(s) (**C-H$_2$**), 2847(s) (**C-H$_2$**), 2234(m) (**C≡N**), 1594(s) (**Ar**), 1529(s) (**Ar**), 1493(s) (**Ar**) cm^{-1}.

ESMS *m/z* 456 ($[M - H]^-$, 100%), 914 ($[2M - H]^-$, 5%).

1-[1-(4'Cyanobiphen-4-yloxy)dodecyl-12-oxy]-2-hydroxybenzene

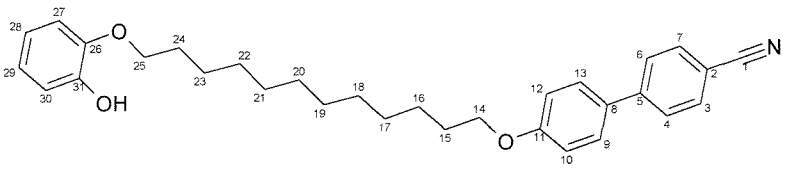

92
$C_{31}H_{37}NO_3$
471.65

Rf 0.50; 100% DCM [1 spot by TLC]

^{1}H NMR (100 MHz, $CDCl_3$): δ_H 7.61 (2H, d, J = 8.5 Hz, C_4**H**, C_6**H**), 7.56 (2H, d, J = 8.5 Hz, C_3**H**, C_7**H**), 7.45 (2H, d, 8.8 Hz, C_9**H**, C_{13}**H**), 6.91 (2H, d, J = 9.0 Hz,

C_{10}**H**, C_{12}**H**), 6.69-6.88 (4H, m, C_{27}**H**, C_{28}**H**, C_{29}**H**, C_{30}**H**), 5.57 (1H, s, Cat-O**H**), 3.87-4.00 (4H, m, O-C_{14}**H**$_2$, Hz C_{25}**H**$_2$-O), 1.66-1.81 (4H, m, C_{15}**H**$_2$, C_{24}**H**$_2$), 1.12-1.56 (14H, m, C_{16}**H**$_2$, C_{17}**H**$_2$, C_{18}**H**$_2$, C_{19}**H**$_2$, C_{20}**H**$_2$, C_{21}**H**$_2$, C_{22}**H**$_2$, C_{23}**H**$_2$) ppm.

^{13}C NMR (75 MHz, $CDCl_3$): δ_C 159.8 (q, **C**$_{11}$(Ar_{CB})), 145.7 (q, **C**$_{26}$(Ar_{Cat})), 145.8 (q, **C**$_5$(Ar_{CB})), 145.3 (q, **C**$_{31}$(Ar_{Cat})), 132.6 (t, **C**$_3$(Ar_{CB}), **C**$_7$(Ar_{CB})), 131.3 (q, **C**$_8$(Ar_{CB})), 128.3 (t, **C**$_9$(Ar_{CB}), **C**$_{13}$(Ar_{CB})), 127.1 (t, **C**$_4$(Ar_{CB}), **C**$_6$(Ar_{CB})), 121.3 (t, **C**$_{28}$(Ar_{Cat})), 120.1 (q, **C**$_{29}$(Ar_{Cat})), 119.1 (q, **C**$_1$(CN)), 115.1 (t, **C**$_{10}$(Ar_{CB}), **C**$_{12}$(Ar_{CB})), 114.4 (t, **C**$_{27}$ (Ar_{Cat})), 111.7 (q, **C**$_{30}$(Ar_{Cat})), 110.1 (q, **C**$_2$(Ar_{CB})), 68.9 (s, **C**$_{21}$ (Cat-O-CH_2)), 68.2 (s, **C**$_{14}$ (CB-O-CH_2)), 29.5 (s, **C**$_{15\text{-}21}$ (CH_2)), 29.4 (s, **C**$_{15\text{-}21}$ (CH_2)), 29.3 (s, **C**$_{15\text{-}21}$ (CH_2)), 26.0 (s, **C**$_{15\text{-}21}$ (CH_2)) ppm.

IR (Solid) ν_{max}: 3450(br) (**O-H**), 2934(s) (**C-H**$_2$), 2847(s) (**C-H**$_2$), 2222(m) (**C≡N**), 1596(s) (**Ar**), 1491(s) (**Ar**) cm^{-1}.

ESMS *m/z* 470 ([M – H]$^-$, 100%), 942 ([2M – H]$^-$, 6%).

7.5.2. Cat(OMe)(O10OCB); 1-[α-(4'cyanobiphen-4-yloxy)decyl-ω-oxy]-3-methoxybenzene

n	Temperature /°C					Mass	Yield
	Cr		N		I	mg	%
10	•	67	•	46	•	43	42

1-[1-(4'cyanobiphen-4-yloxy)decyl-10-oxy]-2-methoxybenzene

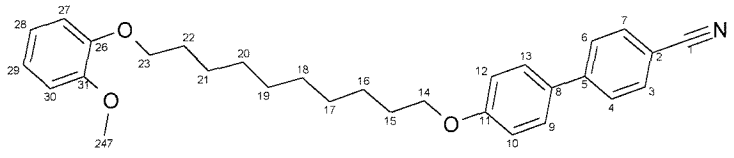

93
$C_{30}H_{36}N_2O_4$
457.62

To a solution of **67** (100 mg, 0.23 mmol, 1 eq) in tetrahyrdofuran (20 mL) was added activated sodium hydride (62 mg as a 44.5% solution in mineral oil, 1.13 mmol, 5 eq) at room temperature in 1 portion. The mixture was stirred at room temperature for 20 mins during which time hydrogen was evolved. Methyl iodide (~1 mL, approx 70 eq) was then added and the mixture was stirred at reflux for 24 h. The solvents were then removed *in vaccuo* and product was dissolved in DCM (30 mL) and this solution was then washed

with water (50 mL). The water layer was extracted with more DCM (3 x 40 mL). The organics were combined, dried over magnesium sulphate and the solvents were removed *in vacuo* to yield a yellow crude product which was crystallised from neat ethyl acetate to give a pale yellow crystalline solid **93** (43 mg, 0.93 mmol, 41.5%).

Rf 0.56; 100% DCM [1 spot by TLC]

^{1}H NMR (300 MHz, $CDCl_3$): δ_H 7.61 (2H, d, J = 8.5 Hz, $C_4\mathbf{H}$, $C_6\mathbf{H}$), 7.56 (2H, d, J = 8.5 Hz, $C_3\mathbf{H}$, $C_7\mathbf{H}$), 7.45 (2H, d, 8.8 Hz, $C_9\mathbf{H}$, $C_{13}\mathbf{H}$), 6.92 (2H, d, J = 8.8 Hz, $C_{10}\mathbf{H}$, $C_{12}\mathbf{H}$), 6.82 (4H, s, $C_{27}\mathbf{H}$, $C_{28}\mathbf{H}$, $C_{29}\mathbf{H}$, $C_{30}\mathbf{H}$), 3.79 (4H, t, O-$C_{14}\mathbf{H_2}$, $C_{23}\mathbf{H_2}$-O), 3.79 (3H, t, O-$C_{247}\mathbf{H_3}$), 1.64-1.84 (4H, m, $C_{15}\mathbf{H_2}$, $C_{22}\mathbf{H_2}$), 1.15-1.53 (12H, m, $C_{16}\mathbf{H_2}$, $C_{17}\mathbf{H_2}$, $C_{18}\mathbf{H_2}$, $C_{19}\mathbf{H_2}$, $C_{20}\mathbf{H_2}$, $C_{21}\mathbf{H_2}$) ppm.

^{13}C NMR (75 MHz, $CDCl_3$): δ_C 158.0 (q, $\mathbf{C_{11}}(Ar_{CB})$), 147.7 (q, $\mathbf{C_{26}}(Ar_{Cat})$), 146.8 (q, $\mathbf{C_5}(Ar_{CB})$), 143.5 (q, $\mathbf{C_{31}}(Ar_{Cat})$), 130.8 (t, $\mathbf{C_3}(Ar_{CB})$, $\mathbf{C_7}(Ar_{CB})$), 129.5 (q, $\mathbf{C_8}(Ar_{CB})$), 126.5 (t, $\mathbf{C_9}(Ar_{CB})$, $\mathbf{C_{13}}(Ar_{CB})$), 125.3 (t, $\mathbf{C_4}(Ar_{CB})$, $\mathbf{C_6}(Ar_{CB})$), 119.1 (t, $\mathbf{C_{28}}(Ar_{Cat})$, $\mathbf{C_{29}}(Ar_{Cat})$), 117.3 (q, $\mathbf{C_1}(CN)$), 113.3 (t, $\mathbf{C_{10}}(Ar_{CB})$, $\mathbf{C_{12}}(Ar_{CB})$), 111.4 (t, $\mathbf{C_{27}}(Ar_{Cat})$), 110.1 (q, $\mathbf{C_{30}}(Ar_{Cat})$), 108.3 (q, $\mathbf{C_2}(Ar_{CB})$), 67.2 (s, $\mathbf{C_{23}}$ (Cat-O-CH_2)), 66.4 (s, $\mathbf{C_{14}}$ (CB-O-CH_2)), 54.2 (p, $\mathbf{C_{247}}$ (CB-O-CH_2)), 27.9 (s, $\mathbf{C_{15\text{-}22}}$ (CH_2)), 27.7 (s, $\mathbf{C_{15\text{-}22}}$ (CH_2)), 27.6 (s, $\mathbf{C_{15\text{-}22}}$ (CH_2)), 27.6 (s, $\mathbf{C_{15\text{-}22}}$ (CH_2)), 27.4 (s, $\mathbf{C_{15\text{-}22}}$ (CH_2)), 24.2 (s, $\mathbf{C_{15\text{-}22}}$ (CH_2)), 24.2 (s, $\mathbf{C_{15\text{-}22}}$ (CH_2)) ppm.

IR **Not Obtained**

MS **Not Obtained**

7.5.3. Cat(OmOCB)(OnOCB); 1-[α-(4'cyanobiphenyl-4-oxy)alkyl$_1$-ω-oxy]-2-[α'-(4'cyanobiphenyl-4-oxy)alkyl$_2$-ω'-oxy-]-benzene

m	n	Temperature /°C					Mass	Yield
		Cr		N		I	mg	%
12	4	•	121	•	(111)	•	20	10
11	5	•	99	•	(85)	•	101	51
10	6	•	124	•	(118)	•	148	46
9	7	•	107	•	(89)	•	59	16
8	8	•	126	•	(118)	•	1270	68

1-[10-(4'-Cyanobiphen-4-yloxy)decyl-1-oxy-]-2-[6-(4'-cyanobiphen-4-yloxy)hexyl-1-oxy-]-benzene

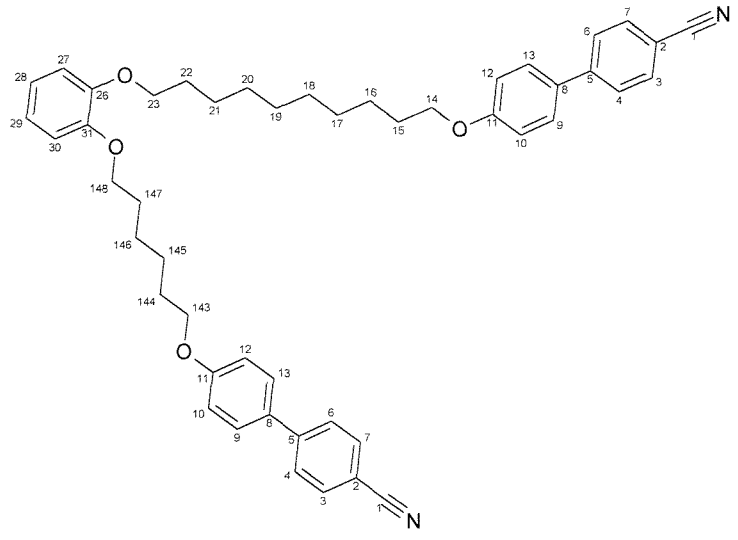

94
$C_{48}H_{52}N_2O_4$
720.96

Procedure:

To a suspension of activated sodium hydride (122 mg, 2.25 mMol, 44.5% solution in mineral oil, 5 eq) in DMF (40 mL) was added compound 1-[1-(4'cyanobiphen-4-yloxy)decyl-10-oxy]-2-hydroxybenzene (203 mg, 0.45 mMol, 1 eq) in the presence of nitrogen. This mixture was stirred at 100°C for 30 min and the solution became dark green before being cooled to room temperature. 1-(cyanobiphenyloxy)-hexyl-6-bromide (333 mg, 340 mMol, 2.1 eq) was then added followed by a catalytic quantity of sodium iodide (80 mg). Almost immediately on adding the catalyst the solution changed colour to yellow/orange. The reaction mixture was brought back to 100°C and stirred at this temperature for 3 days after which the hydroxy-benzene had been consumed as found by TLC. The reaction mixture was cooled to room temperature and the remaining hydride was quenched using ice water. The addition of water precipitated a white solid which was separated by filtration through celite. The solid was dissolved in DCM, dried over $MgSO_4$, filtered and the solvent was removed *in vacuo*. The crude material was purified by column chromatography (40 x 70 mm, silica, 50% DCM / 40-60 petroleum) to yield an off-white microcrystalline solid **94** (148 mg, 0.21 mMol, 46%).

Rf 0.47; 100% DCM

^{1}H NMR (300 MHz, $CDCl_3$): δ_H 7.61 (4H, d, J = 8.6 Hz, C_4**H**, C_6**H**), 7.54 (4H, d, J = 8.6 Hz, C_3**H**, C_7**H**), 7.43 (4H, d, J = 8.8 Hz, C_9**H**, C_{13}**H**), 6.90 (4H, d, J = 8.8

Hz, $C_{10}\mathbf{H}$, $C_{12}\mathbf{H}$), 6.81 (4H, s, $C_{25}\mathbf{H}$), 3.82-4.01 (4H, m, O-$C_{14}\mathbf{H_2}$, $C_{22}\mathbf{H_2}$-O, $C_{143}\mathbf{H_2}$-O, O-$C_{148}\mathbf{H_2}$,), 1.09-1.90 (8H, m, $C_{15}\mathbf{H_2}$, $C_{22}\mathbf{H_2}$, $C_{144}\mathbf{H_2}$, $C_{147}\mathbf{H_2}$), 1.09-1.90 (16H, m, 8H, m, $C_{16}\mathbf{H_2}$, $C_{17}\mathbf{H_2}$, $C_{18}\mathbf{H_2}$, $C_{19}\mathbf{H_2}$, $C_{20}\mathbf{H_2}$, $C_{21}\mathbf{H_2}$, $C_{145}\mathbf{H_2}$, $C_{146}\mathbf{H_2}$) ppm.

^{13}C NMR (75 MHz, $CDCl_3$): δ_C 159.8 (q, $\mathbf{C_{11}}(Ar_{CB})$), 149.3 (q, $\mathbf{C_{26}}/\mathbf{C_{31}}(Ar_{Cat})$), 149.1 (q, $\mathbf{C_{26}}/\mathbf{C_{31}}(Ar_{Cat})$), 145.3 (q, $\mathbf{C_5}(Ar_{CB})$), 132.6 (t, $\mathbf{C_3}(Ar_{CB})$, $\mathbf{C_7}(Ar_{CB})$), 131.3 (q, $\mathbf{C_8}(Ar_{CB})$), 128.3 (t, $\mathbf{C_9}(Ar_{CB})$, $\mathbf{C_{13}}(Ar_{CB})$), 127.1 (t, $\mathbf{C_4}(Ar_{CB})$, $\mathbf{C_6}(Ar_{CB})$), 121.2 (t, $\mathbf{C_{27}}/\mathbf{C_{30}}(Ar_{Cat})$), 121.0 (t, $\mathbf{C_{27}}/\mathbf{C_{30}}(Ar_{Cat})$), 119.1 (q, $\mathbf{C_1}(\mathbf{C}N)$), 115.1 (t, $\mathbf{C_{10}}(Ar_{CB})$, $\mathbf{C_{12}}(Ar_{CB})$), 114.2 (t, $\mathbf{C_{28}}/\mathbf{C_{29}}(Ar_{Cat})$), 114.1 (t, $\mathbf{C_{28}}/\mathbf{C_{29}}(Ar_{Cat})$), 110.1 (q, $\mathbf{C_2}(Ar_{CB})$), 69.2 (s, $\mathbf{C_{22}}/\mathbf{C_{149}}$(Cat-O-$\mathbf{C}H_2$)), 69.1 (s, $\mathbf{C_{22}}/\mathbf{C_{149}}$(Cat-O-$\mathbf{C}H_2$)), 68.2 (s, $\mathbf{C_{14}}/\mathbf{C_{143}}$(CB-O-$\mathbf{C}H_2$)), 68.0 (s, $\mathbf{C_{14}}/\mathbf{C_{143}}$(CB-O-$\mathbf{C}H_2$)), 29.2-29.5 (s, $\mathbf{C_{15\text{-}22}}(CH_2)$, $\mathbf{C_{144\text{-}147}}(CH_2)$), 26.1 (s, $\mathbf{C_{15\text{-}22}}(CH_2)$, $\mathbf{C_{144\text{-}147}}(CH_2)$) , 25.8 (s, $\mathbf{C_{15\text{-}22}}(CH_2)$, $\mathbf{C_{144\text{-}147}}(CH_2)$) ppm.

IR (Solid) ν_{max}: 2919(s) (**C-H$_2$**), 2850(s) (**C-H$_2$**), 2217(s) (**C≡N**), 1599(s) (**Ar**), 1492(s) (**Ar**) cm^{-1}.

EIMS: *m/z* 720 ($[M]^+$, 11%), 333 ($[C_{23}H_{28}NO]^+$, 6%), 278 ($[C_{19}H_{20}NO_3]^+$, 79%), 278 ($[C_{19}H_{20}NO_3]^+$, 10%), 208 ($[C_{17}H_{16}NO_3]^+$, 17%), 195 ($[C_{13}H_9NO]^+$, 100%), 110 ($[C_6H_6O_2]^+$, 27%), 69 ($[C_5H_9]^+$, 50%), 55 ($[C_5H_9]^+$, 55%), 41 ($[C_5H_9]^+$, 24%).

Elemental Analysis: $C_{29}H_{35}NO_3$: (Expected) **C** 79.89, **H** 7.21, **N** 3.88; (Found) **C** 80.46, **H** 7.27, **N** 3.80

1-[9-(4'-Cyanobiphen-4-yloxy)nonyl-1-oxy-]-2-[7-(4'-cyanobiphen-4-yloxy)heptyl-1-oxy-]-benzene

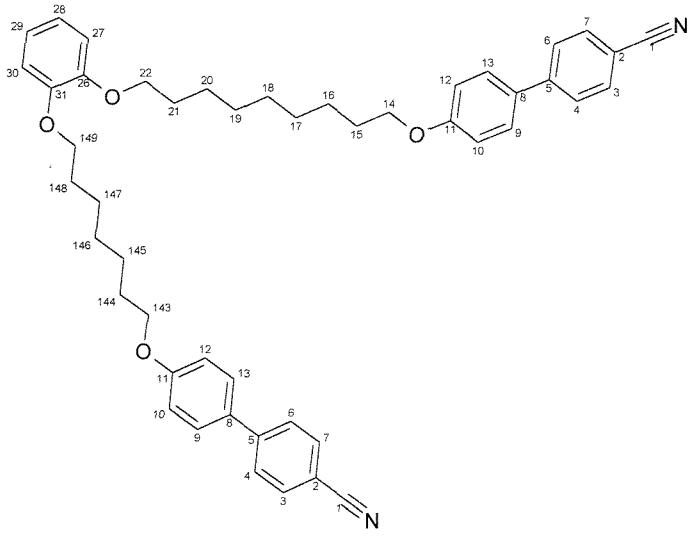

95
$C_{48}H_{52}N_2O_4$
720.96

Rf 0.45; 100% DCM [1 spot by TLC]

^{1}H NMR (400 MHz, $CDCl_3$): δ_H 7.61 (4H, d, J = 8.6 Hz, C_4**H**, C_6**H**), 7.55 (4H, d, J = 8.6 Hz, C_3**H**, C_7**H**), 7.44 (4H, d, J = 8.8 Hz, C_9**H**, C_{13}**H**), 6.91 (4H, d, J = 8.8 Hz, C_{10}**H**, C_{12}**H**), 6.82 (4H, s, C_{25}**H**), 3.84-4.02 (4H, t, J = 6.5 Hz, O-C_{14}**H$_2$**, C_{22}**H$_2$**-O, C_{143}**H$_2$**-O, O-C_{149}**H$_2$**,), 1.09-1.90 (24H, m, 8H, m, C_{15}**H$_2$**, C_{16}**H$_2$**, C_{17}**H$_2$**, C_{18}**H$_2$**, C_{19}**H$_2$**, C_{20}**H$_2$**, C_{21}**H$_2$**, C_{144}**H$_2$**, C_{145}**H$_2$**, C_{146}**H$_2$**, C_{147}**H$_2$**, C_{148}**H$_2$**) ppm.

^{13}C NMR (100 MHz, $CDCl_3$): δ_C 159.8 (q, **C_{11}**(Ar_{CB})), 149.2 (q, **C_{26}**/**C_{31}**(Ar_{Cat})), 149.0 (q, **C_{26}**/**C_{31}**(Ar_{Cat})), 145.3 (q, **C_5**(Ar_{CB})), 132.6 (t, **C_3**(Ar_{CB}), **C_7**(Ar_{CB})), 131.3 (q, **C_8**(Ar_{CB})), 128.3 (t, **C_9**(Ar_{CB}), **C_{13}**(Ar_{CB})), 127.1 (t, **C_4**(Ar_{CB}), **C_6**(Ar_{CB})), 121.1 (t, **C_{27}**/**C_{30}**(Ar_{Cat})), 121.0 (t, **C_{27}**/**C_{30}**(Ar_{Cat})), 119.1 (q, **C_1**(**C**N)), 115.1 (t, **C_{10}**(Ar_{CB}), **C_{12}**(Ar_{CB})), 114.2 (t, **C_{28}**/**C_{29}** (Ar_{Cat})), 114.2 (t, **C_{28}**/**C_{29}** (Ar_{Cat})), 110.1 (q, **C_2**(Ar_{CB})), 69.2 (s, **C_{22}**, **C_{149}**(Cat-O-**C**H_2)), 68.1 (s, **C_{14}**, **C_{143}**(CB-O-**C**H_2)), 29.0-29.5 (s, **$C_{15\text{-}21}$**(CH_2), **$C_{144\text{-}148}$**(CH_2)), 26.1 (s, **$C_{15\text{-}21}$**(CH_2), **$C_{144\text{-}147}$**(CH_2)) ppm.

IR (Solid) ν_{max}: 2930(s) (**C-H$_2$**), 2908(s) (**C-H$_2$**), 2221(s) (**C≡N**), 1602(s) (**Ar**), 1492(s) (**Ar**) cm^{-1}.

MS: **Not Obtained**

1-[11-(4'-Cyanobiphen-4-yloxy)undecyl-1-oxy-]-2-[5-(4'-cyanobiphen-4-yloxy)pentyl-1-oxy-]-benzene

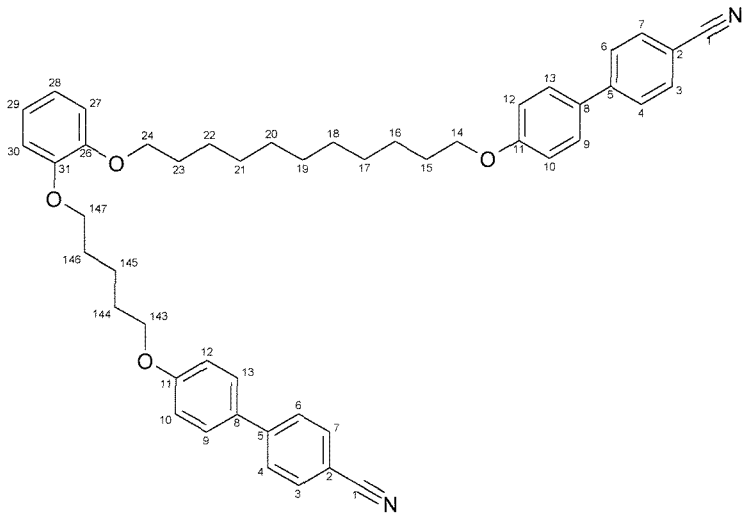

96
$C_{48}H_{52}N_2O_4$
720.96

Rf 0.47; 100% DCM [1 spot by TLC]

^{1}H NMR (300 MHz, $CDCl_3$): δ_H 7.60 (4H, d, J = 8.6 Hz, C_4**H**, C_6**H**), 7.55 (4H, d, J = 8.6 Hz, C_3**H**, C_7**H**), 7.44 (4H, d, J = 8.8 Hz, C_9**H**, C_{13}**H**), 6.90 (4H, d, J = 8.8 Hz, C_{10}**H**, C_{12}**H**), 6.82 (4H, s, C_{25}**H**), 3.84-4.02 (4H, m, O-C_{14}**H$_2$**, C_{24}**H$_2$**-O, C_{143}**H$_2$**-O, O-C_{147}**H$_2$**,), 1.12-1.90 (24H, m, C_{15}**H$_2$**, C_{16}**H$_2$**, C_{17}**H$_2$**, C_{18}**H$_2$**, C_{19}**H$_2$**, C_{20}**H$_2$**, C_{21}**H$_2$**, C_{22}**H$_2$**, C_{23}**H$_2$**, C_{144}**H$_2$**, C_{145}**H$_2$**, C_{146}**H$_2$**) ppm.

^{13}C NMR (75 MHz, $CDCl_3$): δ_C 159.8 (q, **C_{11}**(Ar_{CB})), 149.3 (q, **C_{26}**/**C_{31}**(Ar_{Cat})), 149.1 (q, **C_{26}**/**C_{31}**(Ar_{Cat})), 145.3 (q, **C_5**(Ar_{CB})), 132.6 (t, **C_3**(Ar_{CB}), **C_7**(Ar_{CB})), 131.3 (q, **C_8**(Ar_{CB})), 128.3 (t, **C_9**(Ar_{CB}), **C_{13}**(Ar_{CB})), 127.1 (t, **C_4**(Ar_{CB}), **C_6**(Ar_{CB})), 121.3 (t, **C_{27}**/**C_{30}**(Ar_{Cat})), 121.0 (t, **C_{27}**/**C_{30}**(Ar_{Cat})), 119.1 (q, **C_1**(**C**N)), 115.1 (t, **C_{10}**(Ar_{CB}), **C_{12}**(Ar_{CB})), 114.3 (t, **C_{28}**/**C_{29}**(Ar_{Cat})), 114.0 (t, **C_{28}**/**C_{29}**(Ar_{Cat})), 110.1 (q, **C_2**(Ar_{CB})), 69.2 (s, **C_{22}**/**C_{147}**(Cat-O-**C**H$_2$)), 69.1 (s, **C_{22}**/**C_{147}**(Cat-O-**C**H$_2$)), 68.2 (s, **C_{14}**/**C_{143}**(CB-O-**C**H$_2$)), 68.0 (s, **C_{14}**/**C_{143}**(CB-O-**C**H$_2$)), 29.0-29.7 (s, **$C_{15\text{-}23}$**(CH_2), **$C_{144\text{-}146}$**(CH_2)), 26.0 (s, **$C_{15\text{-}23}$**(CH_2), **$C_{144\text{-}146}$**(CH_2)) , 22.8 (s, **$C_{15\text{-}23}$**(CH_2), **$C_{144\text{-}146}$**(CH_2)) ppm.

IR (Solid) ν_{max}: 2916(s) (**C-H$_2$**), 2851(s) (**C-H$_2$**), 2219(s) (**C≡N**), 1599(s) (**Ar**), 1492(s) (**Ar**) cm^{-1}.

EIMS: *m/z* 279 ($[C_{20}H_{23}O]^+$, 9%), 207 ($[C_{14}H_9NO]^+$, 4%), 167 ($[C_{13}H_9]^+$, 30%), 149 ($[C_{10}H_{13}O]^+$, 100%), 112 ($[C_6H_6O_2]^+$, 9%), 83 ($[C_6H_{11}]^+$, 8%), 70 ($[C_4H_6O]^+$, 30%), 57 ($[C_3H_5O]^+$, 26%), 41 ($[C_3H_5]^+$, 16%)

1-[12-(4'cyanobiphen-4-yloxy)undecyl-1-oxy-]-2-[4-(4'-cyanobiphen-4-yloxy)butyl-1-oxy-]-benzene

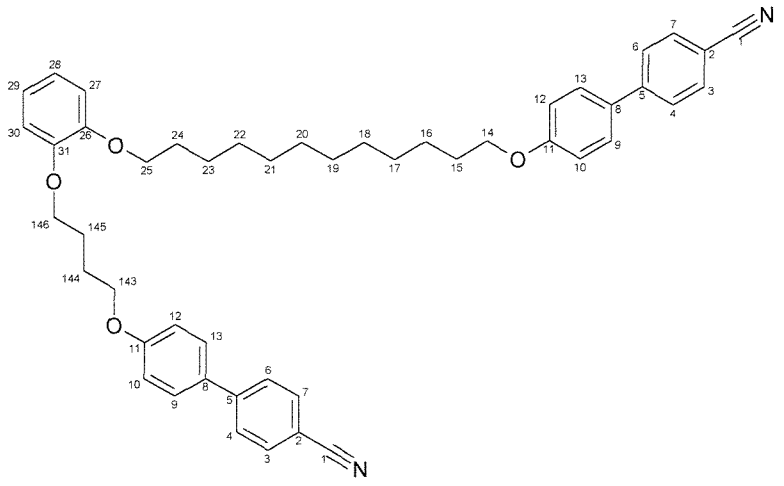

97
$C_{48}H_{52}N_2O_4$
720.96

Rf 0.51; 100% DCM [1 spot by TLC]

^{1}H NMR (300 MHz, $CDCl_3$): δ_H 7.60 (4H, d, J = 8.4 Hz, C_4**H**, C_6**H**), 7.55 (4H, d, J = 8.4 Hz, C_3**H**, C_7**H**), 7.44 (4H, d, J = 8.8 Hz, C_9**H**, C_{13}**H**), 6.90 (4H, d, J = 8.8 Hz, C_{10}**H**, C_{12}**H**), 6.82 (4H, s, C_{25}**H**), 3.82-4.05 (4H, m, O-C_{14}**H$_2$**, C_{25}**H$_2$**-O, C_{143}**H$_2$**-O, O-C_{146}**H$_2$**,), 1.06-1.94 (24H, m, C_{15}**H$_2$**, C_{16}**H$_2$**, C_{17}**H$_2$**, C_{18}**H$_2$**, C_{19}**H$_2$**, C_{20}**H$_2$**, C_{21}**H$_2$**, C_{22}**H$_2$**, C_{23}**H$_2$**, C_{24}**H$_2$**, C_{144}**H$_2$**, C_{145}**H$_2$**) ppm.

^{13}C NMR (75 MHz, $CDCl_3$): δ_C 159.8 (q, **C_{11}**(Ar_{CB})), 149.3 (q, **C_{26}**/**C_{31}**(Ar_{Cat})), 148.9 (q, **C_{26}**/**C_{31}**(Ar_{Cat})), 145.3 (q, **C_5**(Ar_{CB})), 132.6 (t, **C_3**(Ar_{CB}), **C_7**(Ar_{CB})), 131.3 (q, **C_8**(Ar_{CB})), 128.3 (t, **C_9**(Ar_{CB}), **C_{13}**(Ar_{CB})), 127.1 (t, **C_4**(Ar_{CB}), **C_6**(Ar_{CB})), 121.3 (t, **C_{27}**/**C_{30}**(Ar_{Cat})), 121.0 (t, **C_{27}**/**C_{30}**(Ar_{Cat})), 119.1 (q, **C_1**(**C**N)), 115.1 (t, **C_{10}**(Ar_{CB}), **C_{12}**(Ar_{CB})), 114.3 (t, **C_{28}**/**C_{29}**(Ar_{Cat})), 113.9 (t, **C_{28}**/**C_{29}**(Ar_{Cat})), 110.1 (q, **C_2**(Ar_{CB})), 69.2 (s, **C_{25}**/**C_{146}**(Cat-O-**C**H$_2$)), 68.8 (s, **C_{25}**/**C_{146}**(Cat-O-**C**H$_2$)), 68.2 (s, **C_{14}**/**C_{143}**(CB-O-**C**H$_2$)), 68.0 (s, **C_{14}**/**C_{143}**(CB-O-**C**H$_2$)), 29.2-29.6 (s, **$C_{15\text{-}24}$**(CH_2), **$C_{144,145}$**(CH_2)), 26.0 (s, **$C_{15\text{-}24}$**(CH_2), **$C_{144,145}$**(CH_2)) ppm.

IR (Solid) ν_{max}: 2923(s) (**C-H$_2$**), 2848(s) (**C-H$_2$**), 2219(s) (**C≡N**), 1600(s) (**Ar**), 1578(s) (**Ar**), 1492(s) (**Ar**) cm^{-1}.

EIMS: *m/z* 720 ($[M]^+$, 3%), 526 ($[C_{36}H_{45}NO_3]^+$, 22%), 250 ($[C_{17}H_{16}NO_3]^+$, 70%), 208 ($[C_{17}H_{16}NO_3]^+$, 38%), 195 ($[C_{13}H_9NO]^+$, 100%), 110 ($[C_6H_6O_2]^+$, 27%), 55 ($[C_4H_7]^+$, 100%), 41 ($[C_3H_5]^+$, 100%).

1-[10-(4'cyanobiphen-4-yloxy)decyl-1-oxy-]-2-[4-(4'-cyanobiphen-4-yloxy)butyl-1-oxy-]-benzene

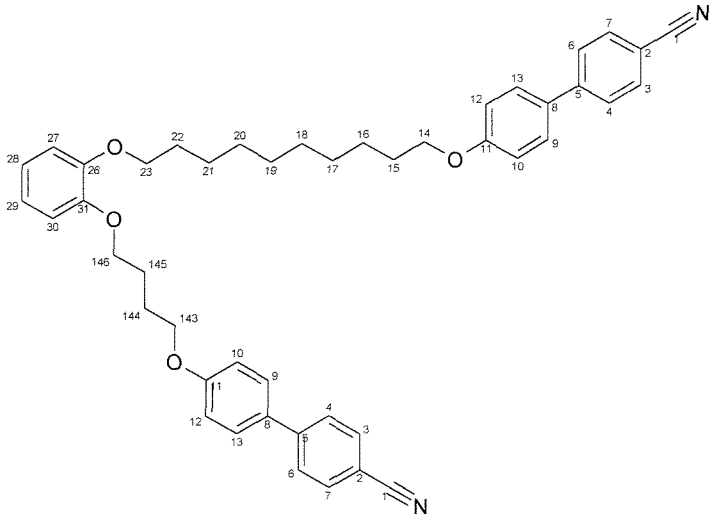

98
$C_{48}H_{52}N_2O_4$
692.91

Rf 0.49; 100% DCM [1 spot by TLC]

^{1}H NMR (400 MHz, $CDCl_3$): δ_H 7.61 (4H, d, J = 8.6 Hz, C_4**H**, C_6**H**), 7.56 (4H, d, J = 8.5 Hz, C_3**H**, C_7**H**), 7.45 (4H, d, J = 8.8 Hz, C_9**H**, C_{13}**H**), 6.91 (4H, d, J = 8.5 Hz, C_{10}**H**, C_{12}**H**), 6.35-6.45 (4H, m, C_{25}**H**), 3.93 (4H, t, J = 6.5 Hz, O-C_{14}**H$_2$**, C_{23}**H$_2$**-O, C_{143}**H$_2$**-O, O-C_{146}**H$_2$**,), 1.63-1.81 (8H, m, C_{15}**H$_2$**, C_{22}**H$_2$**, C_{144}**H$_2$**, C_{145}**H$_2$**), 1.23-1.52 (12H, m, C_{16}**H$_2$**, C_{17}**H$_2$**, C_{18}**H$_2$**, C_{19}**H$_2$**, C_{20}**H$_2$**, C_{21}**H$_2$**) ppm.

^{13}C NMR (100 MHz, $CDCl_3$): δ_C 158.8 (q, **C_{11}**(Ar_{CB})), 148.3 (q, **C_{26}**/**C_{31}**(Ar_{Cat})), 147.9 (q, **C_{26}**/**C_{31}**(Ar_{Cat})), 144.2 (q, **C_5**(Ar_{CB})), 131.5 (t, **C_3**(Ar_{CB}), **C_7**(Ar_{CB})), 130.3 (q, **C_8**(Ar_{CB})), 127.3 (t, **C_9**(Ar_{CB}), **C_{13}**(Ar_{CB})), 126.1 (t, **C_4**(Ar_{CB}), **C_6**(Ar_{CB})), 120.3 (t, **C_{27}**/**C_{30}**(Ar_{Cat})), 120.0 (t, **C_{27}**/**C_{30}**(Ar_{Cat})), 118.1 (q, **C_1**(**C**N)), 114.1 (t, **C_{10}**(Ar_{CB}), **C_{12}**(Ar_{CB})), 113.3 (t, **C_{28}**/**C_{29}**(Ar_{Cat})), 112.9 (t, **C_{28}**/**C_{29}**(Ar_{Cat})), 109.1 (q, **C_2**(Ar_{CB})), 68.1 (s, **C_{23}**/**C_{146}**(Cat-O-**C**H$_2$)), 67.8 (s, **C_{23}**/**C_{146}**(Cat-O-**C**H$_2$)), 67.1 (s, **C_{14}**/**C_{143}**(CB-O-**C**H$_2$)), 66.7 (s, **C_{14}**/**C_{143}**(CB-O-**C**H$_2$)), 29.0-29.5 (s, **$C_{15\text{-}22}$**(CH_2), **$C_{144,145}$**(CH_2)), 25.1 (s, **$C_{15\text{-}22}$**(CH_2), **$C_{144,145}$**(CH_2)), 25.0 (s, **$C_{15\text{-}22}$**(CH_2), **$C_{144,145}$**(CH_2)) ppm.

IR (Solid) ν_{max}: 2923(s) (**C-H$_2$**), 2850(s) (**C-H$_2$**), 2222(m) (**C≡N**), 1599(s) (**Ar**), 1492(s) (**Ar**) cm^{-1}.

MS **Not Obtained**

1-[10-(4'-Cyanobiphen-4-yloxy)decyl-1-oxy-]-2-[5-(4'-cyanobiphen-4-yloxy)pentyl-1-oxy-]-benzene

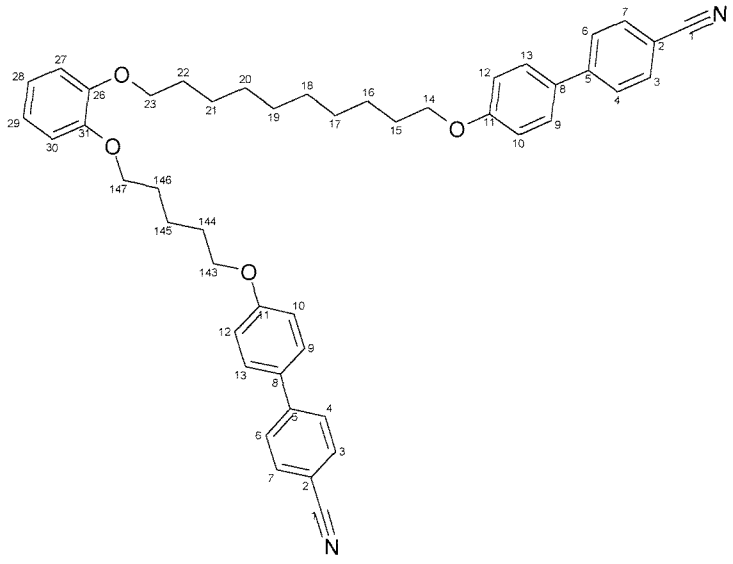

99
$C_{48}H_{52}N_2O_4$
706.93

Rf 0.50; 100% DCM [1 spot by TLC]

^{1}H NMR (400 MHz, $CDCl_3$): δ_H 7.61 (4H, d, J = 8.6 Hz, C_4**H**, C_6**H**), 7.55 (4H, d, J = 8.6 Hz, C_3**H**, C_7**H**), 7.44 (4H, d, J = 8.8 Hz, C_9**H**, C_{13}**H**), 6.91 (4H, d, J = 8.8 Hz, C_{10}**H**, C_{12}**H**), 6.82 (4H, s, C_{25}**H**), 3.84-4.02 (4H, t, J = 6.5 Hz, O-C_{14}**H$_2$**, C_{23}**H$_2$**-O, C_{143}**H$_2$**-O, O-C_{147}**H$_2$**,), 1.23-1.52 (22H, m, 8H, m, C_{15}**H$_2$**, C_{16}**H$_2$**, C_{17}**H$_2$**, C_{18}**H$_2$**, C_{19}**H$_2$**, C_{20}**H$_2$**, C_{21}**H$_2$**, C_{22}**H$_2$**, C_{144}**H$_2$**, C_{145}**H$_2$**, C_{146}**H$_2$**) ppm.

^{13}C NMR (100 MHz, $CDCl_3$): δ_C 158.8 (q, **C_{11}**(Ar_{CB})), 148.2 (q, **C_{26}**/**C_{31}**(Ar_{Cat})), 149.0 (q, **C_{26}**/**C_{31}**(Ar_{Cat})), 145.3 (q, **C_5**(Ar_{CB})), 132.6 (t, **C_3**(Ar_{CB}), **C_7**(Ar_{CB})), 131.3 (q, **C_8**(Ar_{CB})), 128.3 (t, **C_9**(Ar_{CB}), **C_{13}**(Ar_{CB})), 127.1 (t, **C_4**(Ar_{CB}), **C_6**(Ar_{CB})), 121.2 (t, **C_{27}**/**C_{30}**(Ar_{Cat})), 121.0 (t, **C_{27}**/**C_{30}**(Ar_{Cat})), 119.1 (q, **C_1**(**C**N)), 115.1 (t, **C_{10}**(Ar_{CB}), **C_{12}**(Ar_{CB})), 114.2 (t, **C_{28}**/**C_{29}** (Ar_{Cat})), 114.0 (t, **C_{28}**/**C_{29}** (Ar_{Cat})), 110.0 (q, **C_2**(Ar_{CB})), 69.2 (s, **C_{23}**/**C_{147}**(Cat-O-**C**H$_2$)), 69.0 (s, **C_{23}**/**C_{147}**(Cat-O-**C**H$_2$)), 68.1 (s, **C_{14}**/**C_{143}**(CB-O-**C**H$_2$)), 68.0 (s, **C_{14}**/**C_{143}**(CB-O-**C**H$_2$)), 29.0-

29.5 (s, $\mathbf{C_{15\text{-}23}}(CH_2)$, $\mathbf{C_{144\text{-}146}}(CH_2)$), 26.1 (s, $\mathbf{C_{15\text{-}23}}(CH_2)$, $\mathbf{C_{144\text{-}146}}(CH_2)$), 22.7 (s, $\mathbf{C_{15\text{-}23}}(CH_2)$, $\mathbf{C_{144\text{-}146}}(CH_2)$) ppm.

IR (Solid) ν_{max}: 2919(s) (**C-H₂**), 2848(s) (**C-H₂**), 2220(s) (**C≡N**), 1597(s) (**Ar**), 1492(s) (**Ar**) cm^{-1}.

EIMS: *m/z* 706 ($[M]^+$, 20%), 512 ($[C_{35}H_{43}NO_3]^+$, 5%), 458 ($[C_{31}H_{37}NO_3]^+$, 5%), 333 ($[C_{23}H_{28}NO]^+$, 6%), 264 ($[C_{18}H_{18}NO_3]^+$, 79%), 195 ($[C_{13}H_9NO]^+$, 50%), 110 ($[C_6H_6O_2]^+$, 27%), 69 ($[C_5H_9]^+$, 100%).

7.5.4. F_2BOnBr; α-(2,4'-difluorobipheny-4-oxy)alkyl-ω-bromide

n	Temperature /°C mp	Mass g	Yield %
4	oil	0.916	46
5	oil	1.18	68
6	53	1.12	63
7	oil	1.51	81
8	53	0.97	50
9	oil	1.01	51
10	53	1.12	54
11	oil	0.431	20

1-(2,4'-Difluorobipheny-4-oxy)octyl-8-bromide

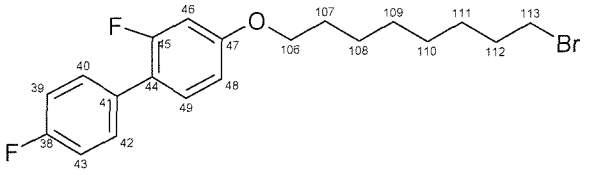

100
$C_{20}H_{23}BrF_2O$
397.31

Procedure

To a stirred solution of 2,4'-diflurobiphenyl-4-ol (1.00 g, 4.85 mMol) in acetone (40 mL) was added solid potassium carbonate (1.74 g, 10.67 mMol, 2.2 eq) as one portion. The stirred mixture was heated to reflux for 1 h under nitrogen and subsequently allowed to cool to room temperature before the addition of 1,8-dibromooctane (8.9 mL, 48.5 mMol, 10 eq) in a single portion. The mixture was then heated back to reflux and stirred for an additional 4 days. The filtrate was then concentrated *in vacuo* and the remaining suspension was partitioned between water (50 mL) and DCM (50 mL). The organic layer was removed and the aqueous layer was washed with DCM (3 x 40 mL). The organics were combined, dried over $MgSO_4$, filtered and the solvent was removed *in vacuo*. Most of the excess dibromooctane was removed by distillation (87°C, 18 mbar) to give the

crude dark yellow product. This was purified by flash column chromatography (silica gel, 40 mm x 70 mm; 0-20% DCM / 40-60 petroleum) to give **100** as a translucent white solid (0.97 g, 2.44 mMol, 50.5%).

Rf 0.64 ;10% DCM / 40-60 petroleum [1 spot by TLC]

^{1}H NMR (300 MHz, $CDCl_3$): δ_H 7.33-7.43 (2H, m, C_{40}**H**, C_{42}**H**), 7.21 (1H, t, J = 9.0 Hz, C_{49}**H**), 7.03 (2H, t, J = 8.9 Hz, C_{39}**H**, C_{43}**H**), 6.68 (1H, dd, (J = 8.6 Hz, 2.6 Hz), C_{48}**H$_2$**), 6.62 (1H, dd, (J = 12.6 Hz, 2.6 Hz), C_{46}**H$_2$**), 3.90 (2H, t, 6.5 Hz, O-C_{106}**H$_2$**), 3.34 (2H, t, 6.8 Hz, C_{113}**H$_2$**Br), 1.65-1.87 (4H, m, C_{107}**H$_2$**, C_{112}**H$_2$**), 1.21-1.50 (8H, m, C_{108}**H$_2$**, C_{109}**H$_2$**, C_{110}**H$_2$**, C_{111}**H$_2$**) ppm.

^{13}C NMR (75 MHz, $CDCl_3$): δ_C 163.7 (q, **C$_{45}$**-F(Ar)), 162.0 (q, **C$_{38}$**-F(Ar)), 159.9 (q, **C$_{47}$**(Ar)), 131.7 (q, **C$_{44}$**(Ar)), 130.8 (t, **C$_{40}$/C$_{42}$**(Ar)), 130.4 (t, **C$_{40}$/C$_{42}$**(Ar)), 120.8 (q, **C$_{41}$**(Ar)), 115.4 (t, **C$_{46}$/C$_{48}$**(Ar)), 115.2 (t, **C$_{46}$/C$_{48}$**(Ar)), 110.9 (t, **C$_{49}$**(Ar)), 102.7 (t, **C$_{43}$/C$_{39}$**(Ar)), 102.4 (t, **C$_{43}$/C$_{39}$**(Ar)) 68.4 (s, **C$_{106}$**(OCH_2)), 33.9 (s, **C$_{113}$** (CH_2Br)), 32.8 (s, **C$_{107\text{-}112}$** (CH_2Br)), 29.1 (s, **C$_{107\text{-}112}$** (CH_2)), 28.7 (s, **C$_{107\text{-}112}$** (CH_2)), 28.1 (s, **C$_{107\text{-}112}$** (CH_2)), 25.9 (s, **C$_{107\text{-}112}$** (CH_2)) ppm.

^{19}F NMR (282 MHz, C_6F_6): δ_C -115.5 (C-**F**(Ar)), -115.9 (C-**F**(Ar))

IR (Film) ν_{max}: 2920(s) (**C-H$_2$**), 2852(m), 1622(s) (**Ar**), 1600(s) (**Ar**), 1572(m), 741(s) (**C-Br**) cm^{-1}.

EIMS *m/z* 397 ($[M]^+$, 9%), 316 ($[C_{20}H_{23}F_2O]^+$, 5%), 206, ($[C_{15}H_{11}O]^+$, 100%), 177 ($[C_{12}H_{17}O]^+$, 16%), 69 ($[C_5H_9]^+$, 15%), 55 ($[C_4H_7]^+$, 13%)

Elemental Analysis: $C_{20}H_{23}BrF_2O$: (Expected) **C** 60.41, **H** 5.79, **N** 0.00; (Found) **C** 60.47, **H** 5.79, **N** 0.00

1 -(2,4'-Difluorobipheny-4-oxy)butyl-4-bromide

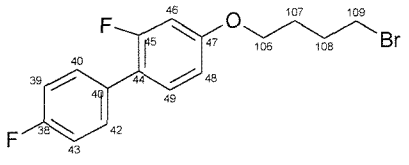

101
$C_{16}H_{15}BrF_2O$
341.20

Rf 0.55 ;10% DCM / 40-60 petroleum [1 spot by TLC]

^{1}H NMR (300 MHz, $CDCl_3$): δ_H 7.33-7.42 (2H, m, C_{40}**H**, C_{42}**H**), 7.20 (2H, t, J = 9.0 Hz, C_{49}**H**), 7.02 (1H, t, J = 9.0 Hz, C_{39}**H**, C_{43}**H**), 6.62 (1H, dd, (J = 8.4 Hz, 3.3 Hz), C_{48}**H$_2$**), 6.63 (1H, dd, (J = 12.6 Hz, 3.3 Hz), C_{46}**H$_2$**), 3.94 (2H, t, 6.0

Hz, O-$C_{106}\mathbf{H_2}$), 3.94 (2H, t, 6.5 Hz, $C_{109}\mathbf{H_2}$Br), 1.78-2.08 (4H, m, $C_{107}\mathbf{H_2}$, $C_{108}\mathbf{H_2}$) ppm.

^{13}C NMR (75 MHz, $CDCl_3$): δ_C 163.7 (q, $\mathbf{C_{45}}$-F(Ar)), 161.7 (q, $\mathbf{C_{38}}$-F(Ar)), 159.4 (q, $\mathbf{C_{47}}$(Ar)), 131.6 (q, $\mathbf{C_{44}}$(Ar)), 130.9 (t, $\mathbf{C_{40}}$/$\mathbf{C_{42}}$(Ar)), 130.4 (t, $\mathbf{C_{40}}$/$\mathbf{C_{42}}$(Ar)), 120.5 (q, $\mathbf{C_{41}}$(Ar)), 115.4 (t, $\mathbf{C_{46}}$/$\mathbf{C_{48}}$(Ar)), 115.1 (t, $\mathbf{C_{46}}$/$\mathbf{C_{48}}$(Ar)), 110.8 (t, $\mathbf{C_{49}}$(Ar)), 102.8 (t, $\mathbf{C_{43}}$/$\mathbf{C_{39}}$(Ar)), 102.4 (t, $\mathbf{C_{43}}$/$\mathbf{C_{39}}$(Ar)) 67.3 (s, $\mathbf{C_{106}}$(OCH_2)), 33.2 (s, $\mathbf{C_{109}}$ (CH_2Br)), 29.4 (s, $\mathbf{C_{107,108}}$ (CH_2)), 27.8 (s, $\mathbf{C_{107,108}}$ (CH_2)) ppm.

^{19}F NMR (282 MHz, C_6F_6): δ_C -115.4 (C-**F**(Ar)), -115.8 (C-**F**(Ar))

IR (Film) ν_{max}: 2911(s) (**C-H$_2$**), 2849(m), 1622(w) (**Ar**), 1572(w), 741(s) (**C-Br**) cm^{-1}.

MS **Not Obtained**

1 -(2,4'-Difluorobipheny-4-oxy)pentyl-5-bromide

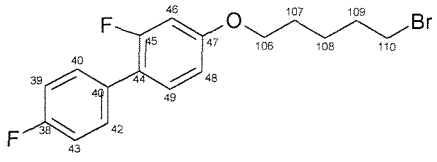

102
$C_{17}H_{17}BrF_2O$
355.23

Rf 0.55 ;10% DCM / 40-60 petroleum [1 spot by TLC]

^{1}H NMR (300 MHz, $CDCl_3$): δ_H 7.33-7.43 (2H, m, C_{40}**H**, C_{42}**H**), 7.22 (2H, t, J = 9.0 Hz, C_{49}**H**), 7.03 (1H, t, J = 8.8 Hz, C_{39}**H**, C_{43}**H**), 6.69 (2H, dd, (J = 8.6 Hz, 2.6 Hz), $C_{48}\mathbf{H_2}$), 6.63 (2H, dd, (J = 12.5 Hz, 2.4 Hz), $C_{46}\mathbf{H_2}$), 3.92 (2H, t, 6.7 Hz, O-$C_{106}\mathbf{H_2}$), 3.42 (2H, t, 6.0 Hz, $C_{109}\mathbf{H_2}$Br), 1.70-1.94 (4H, m, $C_{107}\mathbf{H_2}$, $C_{109}\mathbf{H_2}$), 1.57 (2H, m, $C_{108}\mathbf{H_2}$) ppm.

^{13}C NMR (75 MHz, $CDCl_3$): δ_C 163.7 (q, $\mathbf{C_{45}}$-F(Ar)), 161.8 (q, $\mathbf{C_{38}}$-F(Ar)), 159.7 (q, $\mathbf{C_{47}}$(Ar)), 131.8 (q, $\mathbf{C_{44}}$(Ar)), 130.9 (t, $\mathbf{C_{40}}$/$\mathbf{C_{42}}$(Ar)), 130.4 (t, $\mathbf{C_{40}}$/$\mathbf{C_{42}}$(Ar)), 120.5 (q, $\mathbf{C_{41}}$(Ar)), 115.4 (t, $\mathbf{C_{46}}$/$\mathbf{C_{48}}$(Ar)), 115.2 (t, $\mathbf{C_{46}}$/$\mathbf{C_{48}}$(Ar)), 110.8 (t, $\mathbf{C_{49}}$(Ar)), 102.7 (t, $\mathbf{C_{43}}$/$\mathbf{C_{39}}$(Ar)), 102.4 (t, $\mathbf{C_{43}}$/$\mathbf{C_{39}}$(Ar)), 68.0 (s, $\mathbf{C_{106}}$(OCH_2)), 33.4 (s, $\mathbf{C_{110}}$ (CH_2Br)), 32.4 (s, $\mathbf{C_{107\text{-}109}}$ (CH_2)), 28.3 (s, $\mathbf{C_{107\text{-}109}}$ (CH_2)), 24.8 (s, $\mathbf{C_{107\text{-}109}}$ (CH_2)) ppm.

^{19}F NMR (282 MHz, C_6F_6): δ_C -115.5 (C-**F**(Ar)), -116.0 (C-**F**(Ar))

IR (Film) ν_{max}: 2916(s) (**C-H$_2$**), 2850(m) (**C-H$_2$**), 1623(w) (**Ar**), 1599(s) (**Ar**), 1571(m), 742(s) (**C-Br**) cm^{-1}.

EIMS *m/z* 354 ([M]$^+$, 9%), 274 ([$C_{17}H_{17}F_2O$]$^+$, 10%), 206, ([$C_{15}H_{11}O$]$^+$, 100%), 177 ([$C_{12}H_{17}O$]$^+$, 26%), 69 ([C_5H_9]$^+$, 48%), 41 ([C_3H_5]$^+$, 21%)

1 -(2,4'-Difluorobipheny-4-oxy)hexyl-6-bromide

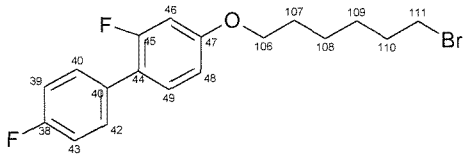

103
$C_{18}H_{19}BrF_2O$
369.25

Rf 0.57 ;10% DCM / 40-60 petroleum [1 spot by TLC]

^{1}H NMR (300 MHz, $CDCl_3$): δ_H 7.32-7.52 (2H, m, C_{40}**H,** C_{42}**H**), 7.21 (1H, t, J = 8.8 Hz, C_{49}**H**), 7.03 (2H, t, J = 8.8 Hz, C_{39}**H**, C_{43}**H**), 6.65 (2H, dd, (J = 8.5 Hz, 3.3 Hz), C_{48}**H$_2$**), 6.65 (2H, dd, (J = 12.3 Hz, 2.9 Hz), C_{46}**H$_2$**), 3.91 (2H, t, 6.4 Hz, O-C_{106}**H$_2$**), 3.36 (2H, t, 6.8 Hz, C_{111}**H$_2$**Br), 1.66-1.90 (4H, m, C_{107}**H$_2$**, C_{110}**H$_2$**), 1.37-1.52 (4H, m, C_{108}**H$_2$**, C_{109}**H$_2$**) ppm.

^{13}C NMR (75 MHz, $CDCl_3$): δ_C 163.7 (q, **C_{45}**-F(Ar)), 161.8 (q, **C_{38}**-F(Ar)), 159.7 (q, **C_{47}**(Ar)), 131.8 (q, **C_{44}**(Ar)), 130.8 (t, **C_{40}**/**C_{42}**(Ar)), 130.4 (t, **C_{40}**/**C_{42}**(Ar)), 120.5 (q, **C_{41}**(Ar)), 115.5 (t, **C_{46}**/**C_{48}**(Ar)), 115.2 (t, **C_{46}**/**C_{48}**(Ar)), 110.9 (t, **C_{49}**(Ar)), 102.7 (t, **C_{43}**/**C_{39}**(Ar)), 102.4 (t, **C_{43}**/**C_{39}**(Ar)) 68.2 (s, **C_{106}**(OCH_2)), 33.7 (s, **C_{111}** (CH_2Br)), 32.7 (s, **$C_{107\text{-}110}$** (CH_2)), 29.0 (s, **$C_{107\text{-}110}$** (CH_2)), 27.9 (s, **$C_{107\text{-}110}$** (CH_2)), 25.3 (s, **$C_{107\text{-}110}$** (CH_2)) ppm.

^{19}F NMR (282 MHz, C_6F_6): δ_C -115.5 (C-**F**(Ar)), -115.9 (C-**F**(Ar)) ppm.

IR (solid) ν_{max}: 2937(s) (**C-H$_2$**), 2857(m), 1623(m) (**Ar**), 1600(s) (**Ar**), 1520 (w) (**Ar**), 740(s) (**C-Br**) cm^{-1}.

EIMS *m/z* 368 ([M]$^+$, 9%), 288 ([$C_{18}H_{19}F_2O$]$^+$, 6%), 206, ([$C_{15}H_{11}O$]$^+$, 100%), 177 ([$C_{12}H_{17}O$]$^+$, 20%), 69 ([C_5H_9]$^+$, 2%), 55 ([C_4H_7]$^+$, 19%)

1 -(2,4'-Difluorobipheny-4-oxy)heptyl-7-bromide

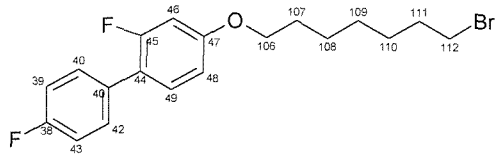

104
$C_{19}H_{21}BrF_2O$
383.28

Rf 0.62 ;10% DCM / 40-60 petroleum [1 spot by TLC]

^{1}H NMR (300 MHz, $CDCl_3$): δ_H 7.30-7.48 (2H, m, C_{40}**H**, C_{42}**H**), 7.21 (1H, t, J = 9.0 Hz, C_{49}**H**), 7.02 (2H, t, J = 8.8 Hz, C_{39}**H**, C_{43}**H**), 6.67 (2H, dd, J = 9.0 Hz, 2.6 Hz, C_{48}**H$_2$**), 6.61 (2H, dd, J = 12.3 Hz, 2.3 Hz, C_{46}**H$_2$**), 3.89 (2H, t, 6.4 Hz, O-C_{106}**H$_2$**), 3.34 (2H, t, 6.8 Hz, C_{112}**H$_2$**Br), 1.64-1.87 (4H, m, C_{107}**H$_2$**, C_{111}**H$_2$**), 1.24-1.53 (6H, m, C_{108}**H$_2$**, C_{109}**H$_2$**, C_{110}**H$_2$**) ppm.

^{13}C NMR (75 MHz, $CDCl_3$): δ_C 163.7 (q, **C_{45}**-F(Ar)), 161.8 (q, **C_{38}**-F(Ar)), 159.7 (q, **C_{47}**(Ar)), 131.8 (q, **C_{44}**(Ar)), 130.9 (t, **C_{40}/C_{42}**(Ar)), 130.4 (t, **C_{40}/C_{42}**(Ar)), 120.3 (q, **C_{41}**(Ar)), 115.4 (t, **C_{46}/C_{48}**(Ar)), 115.2 (t, **C_{46}/C_{48}**(Ar)), 110.8 (t, **C_{49}**(Ar)), 102.7 (t, **C_{43}/C_{39}**(Ar)), 102.4 (t, **C_{43}/C_{39}**(Ar)) 68.3 (s, **C_{106}**(OCH_2)), 33.8 (s, **C_{112}** (CH_2Br)), 32.7 (s, **$C_{107\text{-}111}$** (CH_2)), 29.0 (s, **$C_{107\text{-}111}$** (CH_2)), 28.5 (s, **$C_{107\text{-}111}$** (CH_2)), 28.0 (s, **$C_{107\text{-}111}$** (CH_2)), 25.9 (s, **$C_{107\text{-}111}$** (CH_2)) ppm.

^{19}F NMR (282 MHz, C_6F_6): δ_C -115.4 (C-**F**(Ar)), -115.8 (C-**F**(Ar)) ppm.

IR (Film) ν_{max}: 2930(s) (**C-H$_2$**), 2854(m) (**C-H$_2$**), 1622(s) (**Ar**), 1602(m) (**Ar**), 1568(w), 740(s) (**C-Br**) cm^{-1}.

EIMS *m/z* 384 ($[M]^+$, 10%), 302 ($[C_{19}H_{21}F_2O]^+$, 5%), 206, ($[C_{15}H_{11}O]^+$, 100%), 177 ($[C_{12}H_{17}O]^+$, 17%), 55 ($[C_4H_7]^+$, 21%)

1 -(2,4'-Difluorobipheny-4-oxy)nonyl-9-bromide

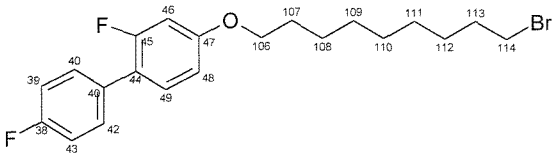

105
$C_{21}H_{25}BrF_2O$
411.33

Rf 0.67 ;10% DCM / 40-60 petroleum [1 spot by TLC]

^{1}H NMR (300 MHz, $CDCl_3$): δ_H 7.32-7.44 (2H, m, C_{40}**H**, C_{42}**H**), 7.21 (1H, t, J = 8.8 Hz, C_{49}**H**), 7.02 (2H, t, J = 8.8 Hz, C_{39}**H**, C_{43}**H**), 6.67 (1H, dd, (J = 8.6 Hz, 2.5 Hz), C_{48}**H$_2$**), 6.62 (1H, dd, (J = 12.4 Hz, 2.6 Hz), C_{46}**H$_2$**), 3.89 (2H, t, 6.5

Hz, O-$C_{106}\mathbf{H_2}$), 3.33 (2H, t, 6.8 Hz, $C_{114}\mathbf{H_2}$Br), 1.63-1.86 (4H, m, $C_{107}\mathbf{H_2}$, $C_{113}\mathbf{H_2}$), 1.14-1.49 (10H, m, $C_{108}\mathbf{H_2}$, $C_{109}\mathbf{H_2}$, $C_{110}\mathbf{H_2}$, $C_{111}\mathbf{H_2}$, $C_{112}\mathbf{H_2}$) ppm.

^{13}C NMR (75 MHz, $CDCl_3$): δ_C 163.7 (q, $\mathbf{C_{45}}$-F(Ar)), 161.8 (q, $\mathbf{C_{38}}$-F(Ar)), 159.9 (q, $\mathbf{C_{47}}$(Ar)), 131.8 (q, $\mathbf{C_{44}}$(Ar)), 130.8 (t, $\mathbf{C_{40}}$/$\mathbf{C_{42}}$(Ar)), 130.4 (t, $\mathbf{C_{40}}$/$\mathbf{C_{42}}$(Ar)), 120.5 (q, $\mathbf{C_{41}}$(Ar)), 115.4 (t, $\mathbf{C_{46}}$/$\mathbf{C_{48}}$(Ar)), 115.2 (t, $\mathbf{C_{46}}$/$\mathbf{C_{48}}$(Ar)), 110.9 (t, $\mathbf{C_{49}}$(Ar)), 102.7 (t, $\mathbf{C_{43}}$/$\mathbf{C_{39}}$(Ar)), 102.4 (t, $\mathbf{C_{43}}$/$\mathbf{C_{39}}$(Ar)) 68.4 (s, $\mathbf{C_{106}}$(OCH_2)), 34.0 (s, $\mathbf{C_{113}}$ (CH_2Br)), 32.8 (s, $\mathbf{C_{107\text{-}112}}$ (CH_2)), 29.3 (s, $\mathbf{C_{107\text{-}112}}$ (CH_2)), 28.7 (s, $\mathbf{C_{107\text{-}112}}$ (CH_2)), 28.1 (s, $\mathbf{C_{107\text{-}112}}$ (CH_2)), 26.0 (s, $\mathbf{C_{107\text{-}112}}$ (CH_2)) ppm.

^{19}F NMR (282 MHz, C_6F_6): δ_C -115.5 (C-**F**(Ar)), -115.9 (C-**F**(Ar))

IR (Film) ν_{max}: 2922(s) (**C-H$_2$**), 2852(m), 1622(s) (**Ar**), 1600(s) (**Ar**), 1571(m), 740(s) (**C-Br**) cm^{-1}.

EIMS *m/z* 412 ($[M]^+$, 9%), 330 ($[C_{21}H_{25}F_2O]^+$, 5%), 206, ($[C_{15}H_{11}O]^+$, 100%), 177 ($[C_{12}H_{17}O]^+$, 13%), 69 ($[C_5H_9]^+$, 10%), 55 ($[C_4H_7]^+$, 13%), 55 ($[C_4H_7]^+$, 11%).

1 -(2,4'-Difluorobipheny-4-oxy)decyl-10-bromide

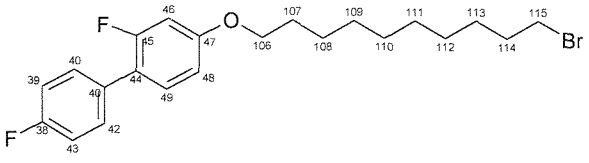

106
$C_{22}H_{27}BrF_2O$
425.36

Rf 0.67 ;10% DCM / 40-60 petroleum [1 spot by TLC]

^{1}H NMR (300 MHz, $CDCl_3$): δ_H 7.32-7.45 (2H, m, $C_{40}\mathbf{H}$, $C_{42}\mathbf{H}$), 7.21 (1H, t, J = 8.8 Hz, $C_{49}\mathbf{H}$), 7.03 (2H, t, J = 8.9 Hz, $C_{44}\mathbf{H}$, $C_{46}\mathbf{H}$), 6.68 (1H, dd, (J = 8.6 Hz, 3.1 Hz), $C_{48}\mathbf{H_2}$), 6.62 (1H, dd, (J = 12.6 Hz, 2.1 Hz), $C_{46}\mathbf{H_2}$), 3.90 (2H, t, 6.9 Hz, O-$C_{106}\mathbf{H_2}$), 3.33 (2H, t, 6.9 Hz, $C_{114}\mathbf{H_2}$Br), 1.65-1.85 (4H, m, $C_{107}\mathbf{H_2}$, $C_{114}\mathbf{H_2}$), 1.13-1.48 (12H, m, $C_{108}\mathbf{H_2}$, $C_{109}\mathbf{H_2}$, $C_{110}\mathbf{H_2}$, $C_{111}\mathbf{H_2}$, $C_{112}\mathbf{H_2}$, $C_{113}\mathbf{H_2}$) ppm.

^{13}C NMR (75 MHz, $CDCl_3$): δ_C 163.8 (q, $\mathbf{C_{45}}$-F(Ar)), 161.9 (q, $\mathbf{C_{38}}$-F(Ar)), 159.8 (q, $\mathbf{C_{47}}$(Ar)), 132.0 (q, $\mathbf{C_{44}}$(Ar)), 130.8 (t, $\mathbf{C_{40}}$/$\mathbf{C_{42}}$(Ar)), 130.4 (t, $\mathbf{C_{40}}$/$\mathbf{C_{42}}$(Ar)), 120.5 (q, $\mathbf{C_{41}}$(Ar)), 115.4 (t, $\mathbf{C_{46}}$/$\mathbf{C_{48}}$(Ar)), 115.2 (t, $\mathbf{C_{46}}$/$\mathbf{C_{48}}$(Ar)), 110.9 (t, $\mathbf{C_{49}}$(Ar)), 102.7 (t, $\mathbf{C_{43}}$/$\mathbf{C_{39}}$(Ar)), 102.3 (t, $\mathbf{C_{43}}$/$\mathbf{C_{39}}$(Ar)) 68.4 (s, $\mathbf{C_{106}}$(OCH_2)), 34.0 (s, $\mathbf{C_{115}}$ (CH_2Br)), 32.8 (s, $\mathbf{C_{107\text{-}114}}$ (CH_2)), 29.5 (s, $\mathbf{C_{107\text{-}114}}$ (CH_2)), 29.4

(s, $\mathbf{C_{107\text{-}114}}$ (CH_2)), 28.7 (s, $\mathbf{C_{107\text{-}114}}$ (CH_2)), 28.2 (s, $\mathbf{C_{107\text{-}114}}$ (CH_2)), 26.0 (s, $\mathbf{C_{107\text{-}114}}$ (CH_2)) ppm.

^{19}F NMR (282 MHz, C_6F_6): δ_C -115.5 (C-**F**(Ar)), -115.9 (C-**F**(Ar))

IR (Film) ν_{max}: 2921(s) (**C-H$_2$**), 2852(m), 1622(s) (**Ar**), 1601(s) (**Ar**), 1572(m), 742(s) (**C-Br**) cm^{-1}.

EIMS *m/z* 438 ([M]$^+$, 9%), 345 ([$C_{21}H_{25}F_2O$]$^+$, 5%), 206, ([$C_{15}H_{11}O$]$^+$, 100%), 177 ([$C_{12}H_{17}O$]$^+$, 10%), 69 ([C_5H_9]$^+$, 11%), 55 ([C_4H_7]$^+$, 21%), 55 ([C_4H_7]$^+$, 21%), 41 ([C_3H_5]$^+$, 21%).

1 -(2,4'-Difluorobipheny-4-oxy)undecyl-11-bromide

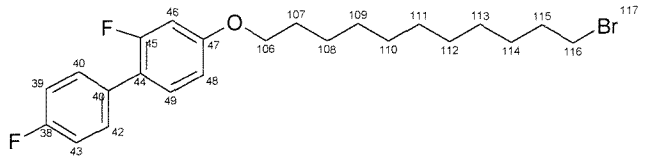

107
$C_{23}H_{29}BrF_2O$
439.39

Rf 0.34; 100% 40-60 petroleum [1 spot by TLC]

^{1}H NMR (300 MHz, $CDCl_3$): δ_H 7.34-7.43 (2H, m, C_{43}**H,** C_{47}**H**), 7.21 (1H, t, J = 8.8 Hz, C_{49}**H**), 7.03 (2H, t, J = 8.8 Hz, C_{39}**H**, C_{43}**H**), 6.68 (1H, dd, (J = 8.4 Hz, 2.6 Hz), C_{48}**H$_2$**), 6.62 (1H, dd, (J = 12.4 Hz, 2.4 Hz), C_{46}**H$_2$**), 3.90 (2H, t, 6.5 Hz, O-C_{106}**H$_2$**), 3.34 (2H, t, 6.9 Hz, C_{114}**H$_2$**Br), 1.65-1.86 (4H, m, C_{107}**H$_2$**, C_{115}**H$_2$**), 1.14-1.50 (14H, m, C_{108}**H$_2$**, C_{109}**H$_2$**, C_{110}**H$_2$**, C_{111}**H$_2$**, C_{112}**H$_2$**, C_{113}**H$_2$**, C_{114}**H$_2$**) ppm.

^{13}C NMR (75 MHz, $CDCl_3$): δ_C 163.7 (q, $\mathbf{C_{45}}$-F(Ar)), 161.8 (q, $\mathbf{C_{38}}$-F(Ar)), 159.9 (q, $\mathbf{C_{47}}$(Ar)), 131.8 (q, $\mathbf{C_{44}}$(Ar)), 130.8 (t, $\mathbf{C_{40}}$/$\mathbf{C_{42}}$(Ar)), 130.4 (t, $\mathbf{C_{40}}$/$\mathbf{C_{42}}$(Ar)), 120.1 (q, $\mathbf{C_{41}}$(Ar)), 115.4 (t, $\mathbf{C_{46}}$/$\mathbf{C_{48}}$(Ar)), 115.2 (t, $\mathbf{C_{46}}$/$\mathbf{C_{48}}$(Ar)), 110.9 (t, $\mathbf{C_{49}}$(Ar)), 102.7 (t, $\mathbf{C_{43}}$/$\mathbf{C_{39}}$(Ar)), 102.4 (t, $\mathbf{C_{43}}$/$\mathbf{C_{39}}$(Ar)) 68.4 (s, $\mathbf{C_{106}}$(OCH_2)), 34.0 (s, $\mathbf{C_{116}}$ (CH_2Br)), 32.8 (s, $\mathbf{C_{107\text{-}115}}$ (CH_2)), 29.4 (s, $\mathbf{C_{107\text{-}115}}$ (CH_2)), 29.3 (s, $\mathbf{C_{107\text{-}115}}$ (CH_2)), 29.1 (s, $\mathbf{C_{107\text{-}115}}$ (CH_2)), 28.7 (s, $\mathbf{C_{107\text{-}115}}$ (CH_2)), 28.2 (s, $\mathbf{C_{107\text{-}115}}$ (CH_2)), 26.0 (s, $\mathbf{C_{107\text{-}115}}$ (CH_2)) ppm.

^{19}F NMR (282 MHz, C_6F_6): δ_C -115.5 (C-**F**(Ar)), -115.9 (C-**F**(Ar))

IR (Film) ν_{max}: 2924(s) (**C-H$_2$**), 2850(m), 1620(s) (**Ar**), 1604(s) (**Ar**), 1572(m), 743(s) (**C-Br**) cm^{-1}.

EIMS *m/z* 345 ($[C_{21}H_{25}F_2O]^+$, 3%), 207, ($[C_{15}H_{11}O]^+$, 10%), 167 ($[C_{12}H_{21}]^+$, 10%), 149 ($[C_{10}H_{15}O]^+$, 10%), 69 ($[C_5H_9]^+$, 13%), 55 ($[C_4H_7]^+$, 23%), 57 ($[C_4H_9]^+$, 22%), 41 ($[C_3H_5]^+$, 20%).

7.5.5. Cat(OnOCB)(OnOBF$_2$); 1-[α-(4'cyanobiphen-4-yloxy)alkyl-ω-oxy-]-2-[α-(2,4'-difluorobiphenyl-4-yloxy)alkyl-ω-oxy-]-benzene

n	Temperature /°C					Mass	Yield
	Cr		N		I	mg	%
4	•	158	•	(85)	•	269	24
5	•	86	•		•	129	38
6	•	106	•	(78)	•	160	48
7	•	46	•		•	100	30
8	•	101	•	(74)	•	97	30
9	•	56	•	(34)	•	403	49
10	•	86	•	(71)	•	176	21
11	•	65	•	(53)	•	290	23

1-[1-(4'-Cyanobiphen-4-yloxy)octyl-8-oxy-]-2-[1-(2,4'-difluorobiphenyl-4-yloxy) octyl-8-oxy]benzene

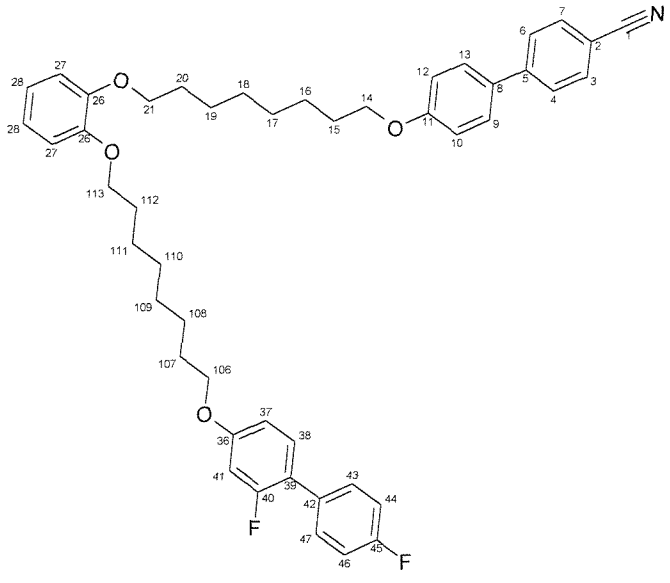

108
$C_{47}H_{51}F_2NO_4$
731.93

Procedure:

To a suspension of activated sodium hydride (131 mg, 2.40 mMol, 44.5% solution in mineral oil, 5 eq) in DMF (40 mL) was added 1-[1-(4'cyanobiphen-4-yloxy)octyl-8-oxy]-2-hydroxybenzene (201 mg, 0.48 mMol, 1 eq) in the presence of nitrogen. This mixture

was stirred at 100°C for 30 min and then cooled to room temperature for the addition of the 1-(2,4'-difluorobipheny-4-oxy)octyl-8-bromide (420 mg, 1.06 mMol, 2.2 eq) and subsequently a catalytic quantity of sodium iodide (80 mg). Almost immediately on adding the catalyst the solution changed colour to yellow/orange. The reaction mixture was brought back to 100°C and stirred at this temperature for 5 days. The reaction was cooled to room temperature and the remaining hydride was quenched using ice water. The aqueous mixture was washed with DCM (3 x 50 mL). The combined DCM extracts were dried over $MgSO_4$, filtered and the solvents, including the DMF, were removed *in vacuo*. The crude material was purified by column chromatography (40 x 70 mm, silica, 20 - 50% DCM / 40-60 petroleum to yield a white microcrystalline solid **108** (97 mg, 0.14 mMol, 30%).

Rf 0.72; 100% DCM [1 spot by TLC]

^{1}H NMR (400 MHz, $CDCl_3$): δ_H 7.60 (2H, d, J = 8.5 Hz, C_4**H**, C_6**H**), 7.55 (2H, d, J = 8.6 Hz, C_3**H**, C_7**H**), 7.44 (2H, d, J = 8.8, C_9**H**, C_{13}**H**), 7.31-7.40 (2H, m, C_{40}**H**, C_{42}**H**), 7.18 (1H, dd, J = 11.3, 8.6 Hz, Hz, C_{49}**H**), 7.03 (2H, t, J = 8.8 Hz, C_{39}**H**, C_{43}**H**), 6.89 (2H, d, J = 8.1 Hz, C_{10}**H**, C_{12}**H**), 6.82 (4H, s, C_{26}**H**, C_{27}**H**, C_{28}**H**, C_{29}**H**), 6.65 (1H, dd, J = 8.6, 3.0 Hz, C_{48}**H**), 6.59 (1H, dd, J = 12.0, 2.6 Hz, C_{46}**H**), 3.80-4.01 (8H, m, O-C_{14}**H$_2$**, O-C_{21}**H$_2$**, O-C_{106}**H$_2$**, O-C_{113}**H$_2$**), 1.70-1.81 (8H, m, C_{15}**H$_2$**, C_{20}**H$_2$**, C_{107}**H$_2$**, C_{112}**H$_2$**), 1.36-1.59 (16H, m, C_{16}**H$_2$**, C_{17}**H$_2$**, C_{18}**H$_2$**, C_{19}**H$_2$**, C_{108}**H$_2$**, C_{109}**H$_2$**, C_{110}**H$_2$**, C_{111}**H$_2$**)** ppm.

^{13}C NMR (75 MHz, $CDCl_3$): δ_C 159.8 (q, **C_{11}**(Ar)), 158.5 (q, **C_{47}**(Ar)), 149.2 (q, **C_{26}**(Ar), **C_{31}**(Ar)), 145.3 (q, **C_5**(Ar)), 132.6 (t, **C_3** (Ar), **C_7**(Ar)), 131.3 (q, **C_8**(Ar)), 130.8 (q, **C_{44}**(Ar)), 130.8 (t, **C_{40}**/**C_{42}**(Ar)), 130.3 (t, **C_{40}**/**C_{42}**(Ar)), 128.3 (t, **C_4**(Ar), **C_6**(Ar)), 127.1 (t, **C_9**(Ar), **C_{13}**(Ar)), 121.1 (t, **C_{27}**, **C_{30}**(Ar_{Cat})), 119.1 (q, **C_1**(CN)), 115.4 (t, **C_{46}**/**C_{48}**(Ar)), 115.2 (t, **C_{46}**/**C_{48}**(Ar)), 115.1 (t, **C_{10}**(Ar), **C_{12}**(Ar)), 114.6 (t, **C_{28}**/**C_{29}** (Ar_{Cat})), 114.2 (t, **C_{28}**/**C_{29}** (Ar_{Cat})), 110.9 (t, **C_{49}**(Ar)), 110.1 (q, **C_2**(Ar)), 102.7 (t, **C_{43}**/**C_{39}**(Ar)), 102.3 (t, **C_{43}**/**C_{39}**(Ar)), 69.2 (s, **C_{14}**, **C_{106}**(OCH_2)), 68.3 (s, **C_{21}**/**C_{113}**(OCH_2)), 68.0 (s, **C_{21}**/**C_{113}**(OCH_2)), 29.3 (s, **$C_{15\text{-}21}$**(CH_2), **$C_{107\text{-}112}$**(CH_2)), 29.2 (s, **$C_{15\text{-}17}$**(CH_2) , **$C_{107\text{-}112}$**(CH_2)), 29.1 (s, **$C_{15\text{-}17}$**(CH_2) , **$C_{107\text{-}112}$**(CH_2)), 26.0 (s, **$C_{15\text{-}17}$**(CH_2) , **$C_{107\text{-}112}$**(CH_2)) ppm.

Note: No Peak found for C_{38}(Ar), C_{41}(Ar), C_{45}(Ar)

IR **Not Obtained**

MS: **Not Obtained**

Elemental Analysis: $C_{47}H_{51}F_2NO_4$: (Expected) **C** 77.06, **H** 6.97, **N** 1.91; (Found) **C** 77.00, **H** 7.00, **N** 1.93

1-[1-(4'-Cyanobiphen-4-yloxy)butyl-4-oxy-]-2-[1-(2,4'-difluorobiphenyl-4-yloxy) butyl-4-oxy]benzene

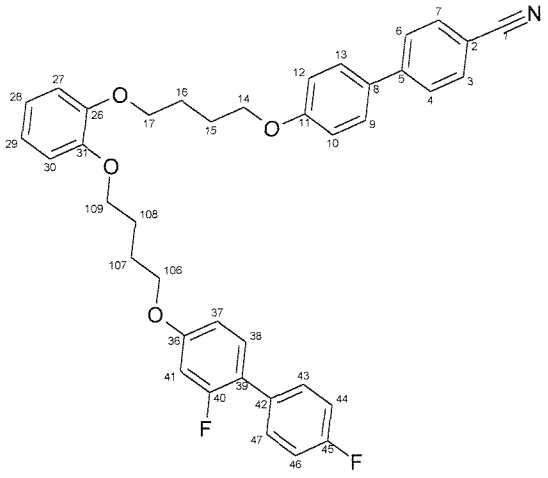

109
$C_{39}H_{35}F_2NO_4$
619.71

Rf 0.61; 100% DCM [1 spot by TLC]

^{1}H NMR (300 MHz, $CDCl_3$): δ_H 7.28-7.66 (9H, m, C_3**H**, C_4**H**, C_6**H**, C_7**H**, C_9**H**, C_{13}**H**, C_{40}**H**, C_{42}**H**, C_{49}**H**), 7.01 (2H, t, J = 8.8 Hz, C_{39}**H**, C_{43}**H**), 6.74-6.95 (6H, m, C_{10}**H**, C_{12}**H**, C_{26}**H**, C_{27}**H**, C_{28}**H**, C_{29}**H**), 6.74-6.95 (2H, m, C_{46}**H**, C_{48}**H**), 3.89-4.03 (8H, m, O-C_{14}**H$_2$**, O-C_{17}**H$_2$**, O-C_{106}**H$_2$**, O-C_{109}**H$_2$**), 1.83-2.06 (8H, m, C_{15}**H$_2$**, C_{16}**H$_2$**, C_{107}**H$_2$**, C_{108}**H$_2$**) ppm.

^{13}C NMR (75 MHz, $CDCl_3$): δ_C 159.7 (q, **C_{11}**(Ar)), 158.4 (q, **C_{47}**(Ar)), 149.0 (q, **C_{26}**(Ar), **C_{31}**(Ar)), 145.2 (q, **C_5**(Ar)), 132.6 (t, **C_3** (Ar), **C_7**(Ar)), 131.4 (q, **C_8**(Ar)), 130.8 (q, **C_{44}**(Ar)), 130.8 (t, **C_{40}**/**C_{42}**(Ar)), 130.3 (t, **C_{40}**/**C_{42}**(Ar)), 128.4 (t, **C_4**(Ar), **C_6**(Ar)), 127.0 (t, **C_9**(Ar), **C_{13}**(Ar)), 121.6 (t, **C_{27}**/**C_{30}**(Ar_{Cat})), 121.3 (t, **C_{27}**/**C_{30}**(Ar_{Cat})), 119.1 (q, **C_1**(CN)), 115.5 (t, **C_{46}**/**C_{48}**(Ar)), 115.2 (t, **C_{46}**/**C_{48}**(Ar)), 115.1 (t, **C_{10}**(Ar), **C_{12}**(Ar)), 114.6 (t, **C_{28}**/**C_{29}** (Ar_{Cat})), 114.1 (t, **C_{28}**/**C_{29}** (Ar_{Cat})), 111.7 (t, **C_{49}**(Ar)), 110.9 (q, **C_2**(Ar)), 102.7 (t, **C_{43}**/**C_{39}**(Ar)), 102.3 (t, **C_{43}**/**C_{39}**(Ar)), 68.7 (s, **C_{14}**/**C_{106}**(OCH_2)), 68.4 (s, **C_{14}**/**C_{106}**(OCH_2)),

68.0 (s, $\mathbf{C_{17}/C_{109}}(OCH_2)$), 67.5 (s, $\mathbf{C_{17}/C_{109}}(OCH_2)$), 26.1 (s, $\mathbf{C_{15,16}}(CH_2)$), 26.0 (s, $\mathbf{C_{15,16}}(CH_2)$) ppm.

Note: No Peak found for $\mathbf{C_{38}}$(Ar), $\mathbf{C_{41}}$(Ar), $\mathbf{C_{45}}$(Ar)

^{19}F NMR (282 MHz, C_6F_6): δ_C -115.5 (C-**F**(Ar)), -116.0 (C-**F**(Ar)) ppm

IR (Solid) ν_{max}: 2951(m) (**C-H$_2$**), 2872(m) (**C-H$_2$**), 2223 (m) (**C≡N**), 1596(s) (**Ar**), 1492(s) (**Ar**) cm^{-1}.

EIMS: *m/z* 619 ([M]$^+$, 23%), 414 ([$C_{25}H_{25}F_2O_3$]$^+$, 3%), 250 ([$C_{18}H_{18}O$]$^+$, 100%), 208 ([$C_{15}H_{13}O$]$^+$, 100%), 178 ([$C_{10}H_7FO_2$]$^+$, 92%), 151 ([C_9H_8FO]$^+$, 28%), 55 ([C_4H_7]$^+$, 12%)

1-[1-(4'-Cyanobiphen-4-yloxy)pentyl-5-oxy-]-2-[1-(2,4'-difluorobiphenyl-4-yloxy) pentyl-5-oxy]benzene

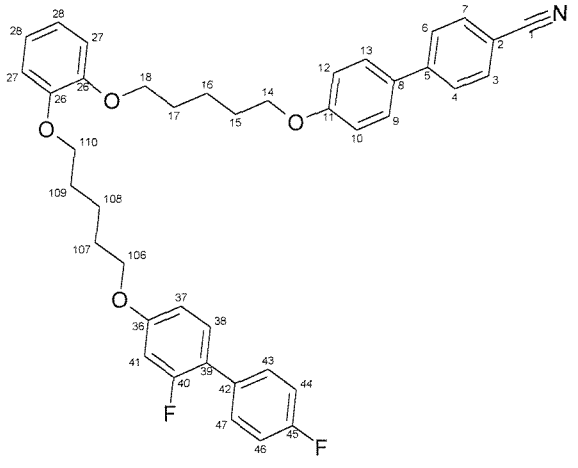

111
$C_{41}H_{39}F_2NO_4$
647.77

Rf 0.64; 100% DCM [1 spot by TLC]

^{1}H NMR (300 MHz, $CDCl_3$): δ_H 7.59 (2H, d, J = 8.5 Hz, C_4**H**, C_6**H**), 7.53 (2H, d, J = 8.6 Hz, C_3**H**, C_7**H**), 7.41 (2H, d, J = 8.8, C_9**H**, C_{13}**H**), 7.31-7.39 (2H, m, C_{40}**H**, C_{42}**H**), 7.18 (1H, t, J = 8.4 Hz, C_{49}**H**), 7.01 (2H, t, J = 8.8 Hz, C_{39}**H**, C_{43}**H**), 6.88 (2H, d, J = 8.8 Hz, C_{10}**H**, C_{12}**H**), 6.83 (4H, s, C_{26}**H**, C_{27}**H**, C_{28}**H**, C_{29}**H**), 6.64 (1H, dd, J = 8.6, 3.1 Hz, C_{48}**H**), 6.59 (1H, dd, J = 12.0, 2.6 Hz, C_{46}**H**), 3.83-4.02 (8H, m, O-C_{14}**H$_2$**, O-C_{18}**H$_2$**, O-C_{106}**H$_2$**, O-C_{110}**H$_2$**), 1.73-1.91 (8H, m, C_{15}**H$_2$**, C_{17}**H$_2$**, C_{107}**H$_2$**, C_{109}**H$_2$**), 1.73-1.91 (4H, m, C_{16}**H$_2$**, C_{108}**H$_2$**) ppm.

^{13}C NMR (75 MHz, $CDCl_3$): δ_C 159.7 (q, C_{11}(Ar)), 158.4 (q, C_{47}(Ar)), 149.1 (q, C_{26}(Ar), C_{31}(Ar)), 145.2 (q, C_5(Ar)), 132.5 (t, C_3 (Ar), C_7(Ar)), 131.3 (q, C_8(Ar)), 130.8 (q, C_{44}(Ar)), 130.8 (t, C_{40}/C_{42}(Ar)), 130.3 (t, C_{40}/C_{42}(Ar)), 128.3 (t, C_4(Ar), C_6(Ar)), 127.0 (t, C_9(Ar), C_{13}(Ar)), 121.6 (t, C_{27}, C_{30}(Ar_{Cat})), 119.1 (q, C_1(CN)), 115.5 (t, C_{46}/C_{48}(Ar)), 115.2 (t, C_{46}/C_{48}(Ar)), 115.1 (t, C_{10}(Ar), C_{12}(Ar)), 114.6 (t, C_{28}/C_{29} (Ar_{Cat})), 114.2 (t, C_{28}/C_{29} (Ar_{Cat})), 110.8 (t, C_{49}(Ar)), 110.1 (q, C_2(Ar)), 102.7 (t, C_{43}/C_{39}(Ar)), 102.4 (t, C_{43}/C_{39}(Ar)), 69.0 (s, C_{14}, C_{106}(OCH_2)), 68.3 (s, C_{18}/C_{110}(OCH_2)), 68.0 (s, C_{18}/C_{110}(OCH_2)), 29.1 (s, $C_{15\text{-}17}$(CH_2)), 29.0 (s, $C_{15\text{-}17}$(CH_2)), 28.9 (s, $C_{15\text{-}17}$(CH_2)), 22.8 (s, $C_{15\text{-}17}$(CH_2)) ppm.

Note: No Peak found for C_{38}(Ar), C_{41}(Ar), C_{45}(Ar)

^{19}F NMR (282 MHz, C_6F_6): δ_C -115.4 (C-**F**(Ar)), -115.8 (C-**F**(Ar)) ppm

IR (Solid) ν_{max}: 2944(m) (**C-H$_2$**), 2872(m) (**C-H$_2$**), 2217(m) (**C≡N**), 1600(s) (**Ar**), 1491(s) (**Ar**) cm^{-1}.

EIMS *m/z* 345 ($[C_{21}H_{25}F_2O]^+$, 1%), 279 ($[C_{20}H_{19}O]^+$, 6%), 207 ($[C_{15}H_{11}O]^+$, 10%), 167 ($[C_{12}H_{21}]^+$, 32%), 149 ($[C_{10}H_{15}O]^+$, 100%), 69 ($[C_5H_9]^+$, 10%), 57 ($[C_4H_9]^+$, 29%), 41 ($[C_3H_5]^+$, 19%).

1-[1-(4'-Cyanobiphen-4-yloxy)hexyl-6-oxy-]-2-[1-(2,4'-difluorobiphenyl-4-yloxy) hexyl-6-oxy]benzene 7

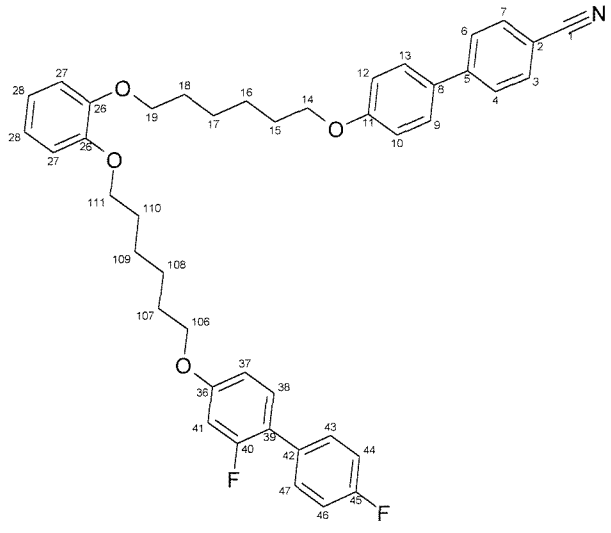

112
$C_{43}H_{43}F_2NO_4$
675.83

Rf 0.64; 100% DCM

^{1}H NMR (400 MHz, $CDCl_3$): δ_H 7.60 (2H, d, J = 8.4 Hz, C_4**H**, C_6**H**), 7.54 (2H, d, J = 8.5 Hz, C_3**H**, C_7**H**), 7.43 (2H, d, J = 8.8, C_9**H**, C_{13}**H**), 7.32-7.40 (2H, m, C_{40}**H**, C_{42}**H**), 7.18 (1H, dd, J = 11.3, 8.6 Hz, Hz, C_{49}**H**), 7.01 (2H, t, J = 8.8 Hz, C_{39}**H**, C_{43}**H**), 6.89 (2H, d, J = 7.5 Hz, C_{10}**H**, C_{12}**H**), 6.82 (4H, s, C_{26}**H**, C_{27}**H**, C_{28}**H**, C_{29}**H**), 6.65 (1H, dd, J = 8.6, 3.1 Hz, C_{48}**H**), 6.60 (1H, dd, J = 12.0, 2.6 Hz, C_{46}**H**), 3.79-3.99 (8H, m, O-C_{14}**H$_2$**, O-C_{19}**H$_2$**, O-C_{106}**H$_2$**, O-C_{111}**H$_2$**), 1.68-1.83 (8H, m, C_{15}**H$_2$**, C_{18}**H$_2$**, C_{107}**H$_2$**, C_{110}**H$_2$**), 1.39-1.54 (8H, m, C_{16}**H$_2$**, C_{17}**H$_2$**, C_{108}**H$_2$**, C_{109}**H$_2$**) ppm.

^{13}C NMR (75 MHz, $CDCl_3$): δ_C 159.8 (q, **C_{11}**(Ar)), 158.5 (q, **C_{47}**(Ar)), 149.2 (q, **C_{26}**(Ar), **C_{31}**(Ar)), 145.3 (q, **C_5**(Ar)), 132.5 (t, **C_3** (Ar), **C_7**(Ar)), 131.3 (q, **C_8**(Ar)), 130.8 (q, **C_{44}**(Ar)), 130.8 (t, **C_{40}**/**C_{42}**(Ar)), 130.3 (t, **C_{40}**/**C_{42}**(Ar)), 128.3 (t, **C_4**(Ar), **C_6**(Ar)), 127.0 (t, **C_9**(Ar), **C_{13}**(Ar)), 121.2 (t, **C_{27}**, **C_{30}**(Ar_{Cat})), 119.1 (q, **C_1**(CN)), 115.5 (t, **C_{46}**/**C_{48}**(Ar)), 115.2 (t, **C_{46}**/**C_{48}**(Ar)), 115.1 (t, **C_{10}**(Ar), **C_{12}**(Ar)), 114.6 (t, **C_{28}**/**C_{29}** (Ar_{Cat})), 114.2 (t, **C_{28}**/**C_{29}** (Ar_{Cat})), 110.8 (t, **C_{49}**(Ar)), 110.1 (q, **C_2**(Ar)), 102.7 (t, **C_{43}**/**C_{39}**(Ar)), 102.3 (t, **C_{43}**/**C_{39}**(Ar)), 69.1 (s, **C_{14}**, **C_{106}**(OCH_2)), 68.3 (s, **C_{19}**/**C_{111}**(OCH_2)), 68.0 (s, **C_{17}**/**C_{111}**(OCH_2)), 29.3 (s, **$C_{15\text{-}18}$**(CH_2)), 29.2 (s, **$C_{15\text{-}18}$**(CH_2)), 28.1 (s, **$C_{15\text{-}18}$**(CH_2)), 25.9 (s, **$C_{15\text{-}18}$**(CH_2)) ppm.

Note: No Peak found for **C_{38}**(Ar), **C_{41}**(Ar), **C_{45}**(Ar)

^{19}F NMR (282 MHz, C_6F_6): δ_C -115.4 (C-**F**(Ar)), -115.9 (C-**F**(Ar)) ppm

IR (Solid) ν_{max}: 2940(m) (**C-H$_2$**), 2861(m) (**C-H$_2$**), 2223(m) (**C≡N**), 1601(s) (**Ar**), 1491(s) (**Ar**) cm^{-1}.

EIMS *m/z* 279 ($[C_{20}H_{19}O]^+$, 8%), 207 ($[C_{15}H_{11}O]^+$, 11%), 167 ($[C_{12}H_{21}]^+$, 33%), 149 ($[C_{10}H_{15}O]^+$, 100%), 69 ($[C_5H_9]^+$, 9%), 57 ($[C_4H_9]^+$, 24%), 41 ($[C_3H_5]^+$, 19%).

1-[1-(4'-Cyanobiphen-4-yloxy)heptyl-7-oxy-]-2-[1-(2,4'-difluorobiphenyl-4-yloxy) heptyl-7-oxy]benzene

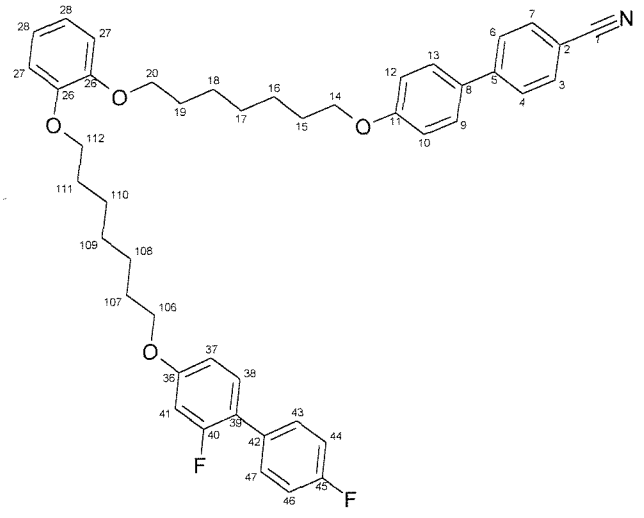

113
$C_{45}H_{47}F_2NO_4$
703.88

Rf 0.69; 100% DCM [1 spot by TLC]

^{1}H NMR (400 MHz, $CDCl_3$): δ_H 7.60 (2H, d, J = 8.5 Hz, C_4**H**, C_6**H**), 7.54 (2H, d, J = 8.5 Hz, C_3**H**, C_7**H**), 7.43 (2H, d, J = 9.0, C_9**H**, C_{13}**H**), 7.32-7.40 (2H, m, C_{40}**H**, C_{42}**H**), 7.19 (1H, t, J = 8.8 Hz, Hz, C_{49}**H**), 7.02 (2H, t, J = 8.8 Hz, C_{39}**H**, C_{43}**H**), 6.89 (2H, d, J = 8.8 Hz, C_{10}**H**, C_{12}**H**), 6.82 (4H, s, C_{26}**H**, C_{27}**H**, C_{28}**H**, C_{29}**H**), 6.65 (1H, dd, J = 8.6, 3.1 Hz, C_{48}**H**), 6.60 (1H, dd, J = 12.0, 2.6 Hz, C_{46}**H**), 3.80-3.98 (8H, m, O-C_{14}**H**$_2$, O-C_{20}**H**$_2$, O-C_{106}**H**$_2$, O-C_{112}**H**$_2$), 1.64-1.84 (8H, m, C_{15}**H**$_2$, C_{19}**H**$_2$, C_{107}**H**$_2$, C_{111}**H**$_2$), 1.24-1.54 (12H, m, C_{16}**H**$_2$, C_{17}**H**$_2$, C_{18}**H**$_2$, C_{108}**H**$_2$, C_{109}**H**$_2$, C_{110}**H**$_2$) ppm.

^{13}C NMR (75 MHz, $CDCl_3$): δ_C 159.8 (q, **C$_{11}$**(Ar)), 158.5 (q, **C$_{47}$**(Ar)), 149.2 (q, **C$_{26}$**(Ar), **C$_{31}$**(Ar)), 145.1 (q, **C$_5$**(Ar)), 132.5 (t, **C$_3$** (Ar), **C$_7$**(Ar)), 131.3 (q, **C$_8$**(Ar)), 130.8 (q, **C$_{44}$**(Ar)), 130.4 (t, **C$_{40}$**/**C$_{42}$**(Ar)), 130.3 (t, **C$_{40}$**/**C$_{42}$**(Ar)), 128.3 (t, **C$_4$**(Ar), **C$_6$**(Ar)), 127.1 (t, **C$_9$**(Ar), **C$_{13}$**(Ar)), 121.1 (t, **C$_{27}$**, **C$_{30}$**(Ar_{Cat})), 119.1 (q, **C$_1$**(CN)), 115.4 (t, **C$_{46}$**/**C$_{48}$**(Ar)), 115.2 (t, **C$_{46}$**/**C$_{48}$**(Ar)), 115.1 (t, **C$_{10}$**(Ar), **C$_{12}$**(Ar)), 114.6 (t, **C$_{28}$**/**C$_{29}$** (Ar_{Cat})), 114.2 (t, **C$_{28}$**/**C$_{29}$** (Ar_{Cat})), 110.9 (t, **C$_{49}$**(Ar)), 110.2 (q, **C$_2$**(Ar)), 102.7 (t, **C$_{43}$**/**C$_{39}$**(Ar)), 102.3 (t, **C$_{43}$**/**C$_{39}$**(Ar)), 69.2 (s, **C$_{14}$**, **C$_{106}$**(OCH_2)), 68.4 (s, **C$_{20}$**/**C$_{112}$**(OCH_2)), 68.1 (s, **C$_{20}$**/**C$_{112}$**(OCH_2)), 29.3 (s, **C$_{15\text{-}19}$**(CH_2)), 29.1 (s, **C$_{15\text{-}19}$**(CH_2)), 28.1 (s, **C$_{15\text{-}19}$**(CH_2)), 26.0 (s, **C$_{15\text{-}19}$**(CH_2)) ppm.

Note: No Peak found for C_{38}(Ar), C_{41}(Ar), C_{45}(Ar)

^{19}F NMR (282 MHz, C_6F_6): δ_C -115.4 (C-**F**(Ar)), -115.9 (C-**F**(Ar)) ppm

IR (Solid) ν_{max}: 2940(m) (**C-H$_2$**), 2861(m) (**C-H$_2$**), 2223(m) (**C≡N**), 1601(s) (**Ar**), 1491(s) (**Ar**) cm^{-1}.

EIMS *m/z* 345 ($[C_{21}H_{25}F_2O]^+$, 1%), 279 ($[C_{20}H_{19}O]^+$, 6%), 207 ($[C_{15}H_{11}O]^+$, 11%), 167 ($[C_{12}H_{21}]^+$, 33%), 149 ($[C_{10}H_{15}O]^+$, 100%), 69 ($[C_5H_9]^+$, 11%), 55 ($[C_4H_7]^+$, 21%), 41 ($[C_3H_5]^+$, 16%).

1-[1-(4'-Cyanobiphen-4-yloxy)nonyl-9-oxy-]-2-[1-(2,4'-difluorobiphenyl-4-yloxy) nonyl-9-oxy-]-benzene

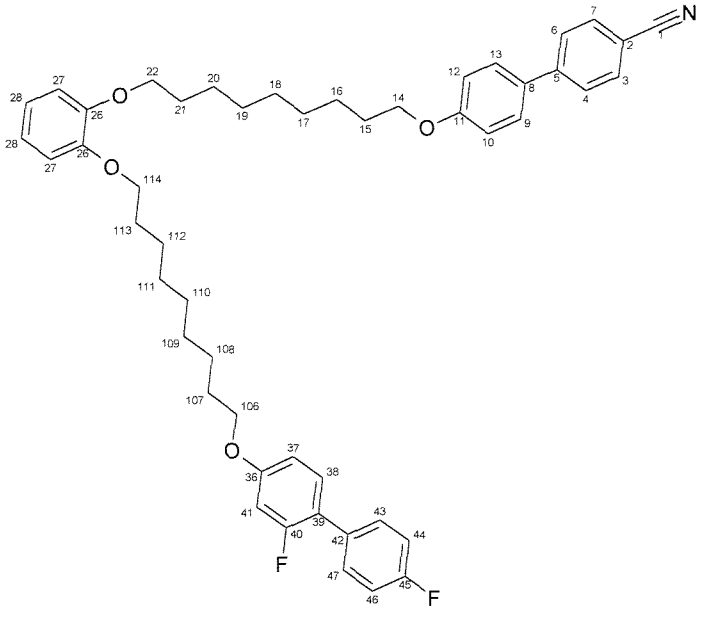

114
$C_{49}H_{55}F_2NO_4$
759.99

Rf 0.75; 100% DCM [1 spot by TLC]

^{1}H NMR (300 MHz, $CDCl_3$): δ_H 7.60 (2H, d, J = 8.5 Hz, C_4**H**, C_6**H**), 7.54 (2H, d, J = 8.5 Hz, C_3**H**, C_7**H**), 7.43 (2H, d, J = 9.0, C_9**H**, C_{13}**H**), 7.32-7.41 (2H, m, C_{40}**H**, C_{42}**H**), 7.20 (1H, t, J = 8.8 Hz, Hz, C_{49}**H**), 7.02 (2H, t, J = 8.8 Hz, C_{39}**H**, C_{43}**H**), 6.90 (2H, d, J = 8.8 Hz, C_{10}**H**, C_{12}**H**), 6.81 (4H, s, C_{26}**H**, C_{27}**H**, C_{28}**H**, C_{29}**H**), 6.66 (1H, dd, J = 8.4, 2.3 Hz, C_{48}**H**), 6.61 (1H, dd, J = 12.4, 2.4 Hz, C_{46}**H**), 3.80-3.98 (8H, m, O-C_{14}**H$_2$**, O-C_{22}**H$_2$**, O-C_{106}**H$_2$**, O-C_{114}**H$_2$**), 1.63-1.81 (8H, m, C_{15}**H$_2$**, C_{21}**H$_2$**, C_{107}**H$_2$**, C_{113}**H$_2$**), 1.24-1.54 (20H, m, C_{16}**H$_2$**, C_{17}**H$_2$**, C_{18}**H$_2$**, C_{19}**H$_2$**, C_{20}**H$_2$**, C_{108}**H$_2$**, C_{109}**H$_2$**, C_{110}**H$_2$**, C_{111}**H$_2$**, C_{112}**H$_2$**) ppm.

^{13}C NMR (75 MHz, $CDCl_3$): δ_C 159.8 (q, $\mathbf{C_{11}}$(Ar)), 158.5 (q, $\mathbf{C_{47}}$(Ar)), 149.3 (q, $\mathbf{C_{26}}$(Ar), $\mathbf{C_{31}}$(Ar)), 145.1 (q, $\mathbf{C_5}$(Ar)), 132.6 (t, $\mathbf{C_3}$ (Ar), $\mathbf{C_7}$(Ar)), 131.3 (q, $\mathbf{C_8}$(Ar)), 130.8 (q, $\mathbf{C_{44}}$(Ar)), 130.3 (t, $\mathbf{C_{40}}$/$\mathbf{C_{42}}$(Ar)), 130.3 (t, $\mathbf{C_{40}}$/$\mathbf{C_{42}}$(Ar)), 128.3 (t, $\mathbf{C_4}$(Ar), $\mathbf{C_6}$(Ar)), 127.1 (t, $\mathbf{C_9}$(Ar), $\mathbf{C_{13}}$(Ar)), 121.1 (t, $\mathbf{C_{27}}$, $\mathbf{C_{30}}$(Ar_{Cat})), 119.1 (q, $\mathbf{C_1}$(CN)), 115.4 (t, $\mathbf{C_{46}}$/$\mathbf{C_{48}}$(Ar)), 115.2 (t, $\mathbf{C_{46}}$/$\mathbf{C_{48}}$(Ar)), 115.1 (t, $\mathbf{C_{10}}$(Ar), $\mathbf{C_{12}}$(Ar)), 114.6 (t, $\mathbf{C_{28}}$/$\mathbf{C_{29}}$ (Ar_{Cat})), 114.2 (t, $\mathbf{C_{28}}$/$\mathbf{C_{29}}$ (Ar_{Cat})), 110.9 (t, $\mathbf{C_{49}}$(Ar)), 110.1 (q, $\mathbf{C_2}$(Ar)), 102.7 (t, $\mathbf{C_{43}}$/$\mathbf{C_{39}}$(Ar)), 102.3 (t, $\mathbf{C_{43}}$/$\mathbf{C_{39}}$(Ar)), 69.3 (s, $\mathbf{C_{14}}$, $\mathbf{C_{106}}$(OCH_2)), 68.4 (s, $\mathbf{C_{22}}$/$\mathbf{C_{114}}$(OCH_2)), 68.2 (s, $\mathbf{C_{22}}$/$\mathbf{C_{114}}$(OCH_2)), 29.1-29.6 (s, $\mathbf{C_{15\text{-}21}}$($CH_2$), $\mathbf{C_{107\text{-}113}}$($CH_2$)), 26.0 (s, $\mathbf{C_{15\text{-}21}}$($CH_2$), $\mathbf{C_{107\text{-}113}}$($CH_2$)) ppm.

Note: No Peak found for $\mathbf{C_{38}}$(Ar), $\mathbf{C_{41}}$(Ar), $\mathbf{C_{45}}$(Ar)

^{19}F NMR (282 MHz, C_6F_6): δ_C -115.5 (C-**F**(Ar)), -115.9 (C-**F**(Ar)) ppm

IR (Solid) ν_{max}: 2913(m) (**C-H$_2$**), 2847(m) (**C-H$_2$**), 2224(m) (**C≡N**), 1599(s) (**Ar**), 1493(s) (**Ar**) cm^{-1}.

EIMS *m/z* 279 ($[C_{20}H_{19}O]^+$, 4%), 207 ($[C_{15}H_{11}O]^+$, 15%), 167 ($[C_{12}H_{21}]^+$, 29%), 149 ($[C_{10}H_{15}O]^+$, 100%), 69 ($[C_5H_9]^+$, 10%), 57 ($[C_4H_9]^+$, 23%), 41 ($[C_3H_5]^+$, 21%).

1-[1-(4'-Cyanobiphen-4-yloxy)decyl-10-oxy-]-2-[1-(2,4'-difluorobiphenyl-4-yloxy) decyl-10-oxy]benzene

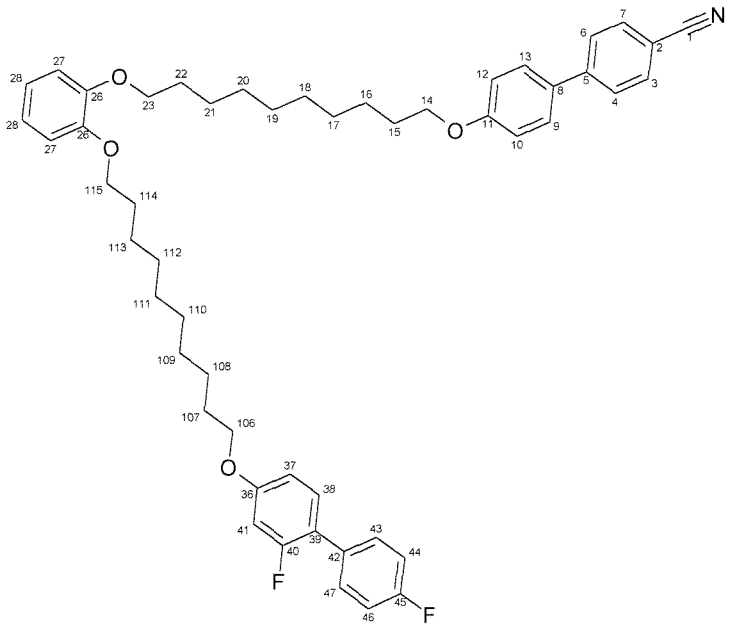

115
$C_{51}H_{59}F_2NO_4$
788.04

Rf 0.78; 100% DCM [1 spot by TLC]

^{1}H NMR (300 MHz, $CDCl_3$): δ_H 7.60 (2H, d, J = 8.5 Hz, C_4**H**, C_6**H**), 7.55 (2H, d, J = 8.5 Hz, C_3**H**, C_7**H**), 7.44 (2H, d, J = 8.8, C_9**H**, C_{13}**H**), 7.32-7.41 (2H, m, C_{40}**H**, C_{42}**H**), 7.20 (1H, t, J = 8.9 Hz, Hz, C_{49}**H**), 7.02 (2H, t, J = 8.8 Hz, C_{39}**H**, C_{43}**H**), 6.90 (2H, d, J = 8.8 Hz, C_{10}**H**, C_{12}**H**), 6.81 (4H, s, C_{26}**H**, C_{27}**H**, C_{28}**H**, C_{29}**H**), 6.66 (1H, dd, J = 8.6, 2.6 Hz, C_{48}**H**), 6.61 (1H, dd, J = 12.5, 2.6 Hz, C_{46}**H**), 3.83-3.99 (8H, m, O-C_{14}**H**$_2$, O-C_{23}**H**$_2$, O-C_{106}**H**$_2$, O-C_{115}**H**$_2$), 1.58-1.83 (8H, m, C_{15}**H**$_2$, C_{22}**H**$_2$, C_{107}**H**$_2$, C_{114}**H**$_2$), 1.17-1.52 (20H, m, C_{16}**H**$_2$, C_{17}**H**$_2$, C_{18}**H**$_2$, C_{19}**H**$_2$, C_{20}**H**$_2$, C_{21}**H**$_2$, C_{108}**H**$_2$, C_{109}**H**$_2$, C_{110}**H**$_2$, C_{111}**H**$_2$, C_{112}**H**$_2$, C_{113}**H**$_2$) ppm.

^{13}C NMR (75 MHz, $CDCl_3$): δ_C 159.8 (q, **C**$_{11}$(Ar)), 158.5 (q, **C**$_{47}$(Ar)), 149.3 (q, **C**$_{26}$(Ar), **C**$_{31}$(Ar)), 145.3 (q, **C**$_5$(Ar)), 132.6 (t, **C**$_3$ (Ar), **C**$_7$(Ar)), 131.3 (q, **C**$_8$(Ar)), 130.8 (q, **C**$_{44}$(Ar)), 130.4 (t, **C**$_{40}$/**C**$_{42}$(Ar)), 130.3 (t, **C**$_{40}$/**C**$_{42}$(Ar)), 128.3 (t, **C**$_4$(Ar), **C**$_6$(Ar)), 127.1 (t, **C**$_9$(Ar), **C**$_{13}$(Ar)), 121.1 (t, **C**$_{27}$, **C**$_{30}$(Ar_{Cat})), 119.1 (q, **C**$_1$(CN)), 115.4 (t, **C**$_{46}$/**C**$_{48}$(Ar)), 115.2 (t, **C**$_{46}$/**C**$_{48}$(Ar)), 115.1 (t, **C**$_{10}$(Ar), **C**$_{12}$(Ar)), 114.6 (t, **C**$_{28}$/**C**$_{29}$ (Ar_{Cat})), 114.2 (t, **C**$_{28}$/**C**$_{29}$ (Ar_{Cat})), 110.9 (t, **C**$_{49}$(Ar)), 110.1 (q, **C**$_2$(Ar)), 102.7 (t, **C**$_{43}$/**C**$_{39}$(Ar)), 102.3 (t,

C_{43}/C_{39}(Ar)), 69.3 (s, C_{14}, $C_{106}(OCH_2)$), 68.4 (s, $C_{23}/C_{115}(OCH_2)$), 68.2 (s, $C_{23}/C_{115}(OCH_2)$), 29.1-29.6 (s, $C_{15\text{-}22}(CH_2)$, $C_{107\text{-}114}(CH_2)$), 26.0 (s, $C_{15\text{-}22}(CH_2)$, $C_{107\text{-}114}(CH_2)$) ppm.

Note: No Peak found for C_{38}(Ar), C_{41}(Ar), C_{45}(Ar)

^{19}F NMR (282 MHz, C_6F_6): δ_C -115.5 (C-**F**(Ar)), -115.9 (C-**F**(Ar)) ppm

IR (Solid) ν_{max}: 2916(m) (**C-H$_2$**), 2846(m) (**C-H$_2$**), 2248(m) (**C≡N**), 1601(s) (**Ar**), 1493(s) (**Ar**) cm^{-1}.

EIMS *m/z* 345 ($[C_{21}H_{25}F_2O]^+$, 3%), 279 ($[C_{20}H_{19}O]^+$, 5%), 207 ($[C_{15}H_{11}O]^+$, 10%), 167 ($[C_{12}H_{21}]^+$, 31%), 149 ($[C_{10}H_{15}O]^+$, 100%), 69 ($[C_5H_9]^+$, 11%), 57 ($[C_4H_9]^+$, 26%), 41 ($[C_3H_5]^+$, 18%).

1-[1-(4'-Cyanobiphen-4-yloxy)undecyl-11-oxy-]-2-[1-(2,4'-difluorobiphenyl-4-yloxy)undecyl-11-oxy]benzene

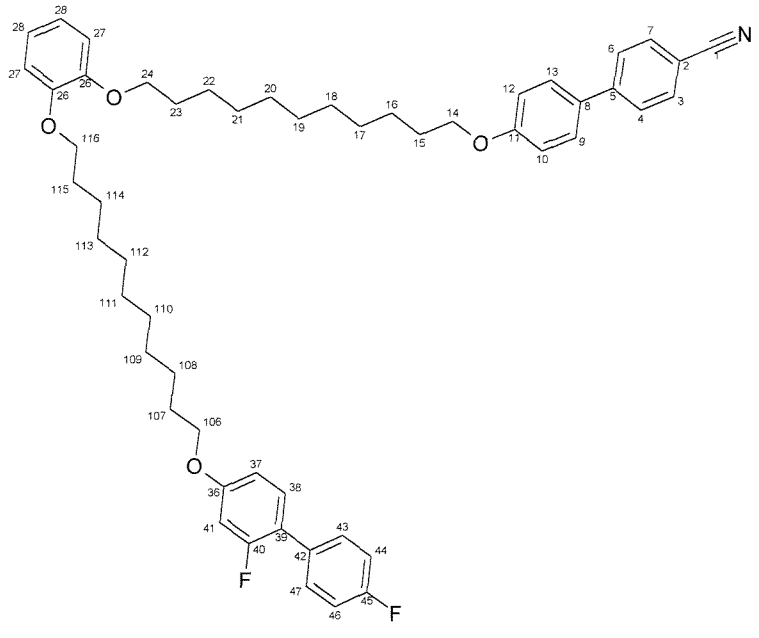

116
$C_{53}H_{63}F_2NO_4$
816.09

Rf 0.80; 100% DCM

^{1}H NMR (300 MHz, $CDCl_3$): δ_H 7.60 (2H, d, J = 8.6 Hz, C_4**H**, C_6**H**), 7.55 (2H, d, J = 8.6 Hz, C_3**H**, C_7**H**), 7.44 (2H, d, J = 8.8, C_9**H**, C_{13}**H**), 7.32-7.41 (2H, m, C_{40}**H**, C_{42}**H**), 7.20 (1H, t, J = 8.9 Hz, Hz, C_{49}**H**), 7.02 (2H, t, J = 8.8 Hz, C_{39}**H**, C_{43}**H**), 6.91 (2H, d, J = 8.8 Hz, C_{10}**H**, C_{12}**H**), 6.81 (4H, s, C_{26}**H**, C_{27}**H**, C_{28}**H**, C_{29}**H**), 6.67 (1H, dd, J = 8.5, 2.5 Hz, C_{48}**H**), 6.61 (1H, dd, J = 12.5, 2.4

Hz, $C_{46}\mathbf{H}$), 3.82-4.00 (8H, m, O-$C_{14}\mathbf{H_2}$, O-$C_{24}\mathbf{H_2}$, O-$C_{106}\mathbf{H_2}$, O-$C_{116}\mathbf{H_2}$), 1.59-1.85 (8H, m, $C_{15}\mathbf{H_2}$, $C_{23}\mathbf{H_2}$, $C_{107}\mathbf{H_2}$, $C_{115}\mathbf{H_2}$), 1.12-1.51 (20H, m, $C_{16}\mathbf{H_2}$, $C_{17}\mathbf{H_2}$, $C_{18}\mathbf{H_2}$, $C_{19}\mathbf{H_2}$, $C_{20}\mathbf{H_2}$, $C_{21}\mathbf{H_2}$, $C_{22}\mathbf{H_2}$, $C_{108}\mathbf{H_2}$, $C_{109}\mathbf{H_2}$, $C_{110}\mathbf{H_2}$, $C_{111}\mathbf{H_2}$, $C_{112}\mathbf{H_2}$, $C_{113}\mathbf{H_2}$, $C_{114}\mathbf{H_2}$) ppm.

^{13}C NMR (75 MHz, $CDCl_3$): δ_C 159.8 (q, $\mathbf{C_{11}}$(Ar)), 149.2 (q, $\mathbf{C_{26}}$(Ar), $\mathbf{C_{31}}$(Ar)), 145.3 (q, $\mathbf{C_5}$(Ar)), 132.6 (t, $\mathbf{C_3}$ (Ar), $\mathbf{C_7}$(Ar)), 131.2 (q, $\mathbf{C_8}$(Ar)), 130.8 (q, $\mathbf{C_{44}}$(Ar)), 130.8 (t, $\mathbf{C_{40}}$/$\mathbf{C_{42}}$(Ar)), 130.4 (t, $\mathbf{C_{40}}$/$\mathbf{C_{42}}$(Ar)), 128.3 (t, $\mathbf{C_4}$(Ar), $\mathbf{C_6}$(Ar)), 127.1 (t, $\mathbf{C_9}$(Ar), $\mathbf{C_{13}}$(Ar)), 121.0 (t, $\mathbf{C_{27}}$, $\mathbf{C_{30}}$(Ar_{Cat})), 119.1 (q, $\mathbf{C_1}$(CN)), 115.5 (t, $\mathbf{C_{46}}$/$\mathbf{C_{48}}$(Ar)), 115.2 (t, $\mathbf{C_{46}}$/$\mathbf{C_{48}}$(Ar)), 115.1 (t, $\mathbf{C_{10}}$(Ar), $\mathbf{C_{12}}$(Ar)), 114.5 (t, $\mathbf{C_{28}}$/$\mathbf{C_{29}}$ (Ar_{Cat})), 114.1 (t, $\mathbf{C_{28}}$/$\mathbf{C_{29}}$ (Ar_{Cat})), 110.9 (t, $\mathbf{C_{49}}$(Ar)), 110.0 (q, $\mathbf{C_2}$(Ar)), 102.7 (t, $\mathbf{C_{43}}$/$\mathbf{C_{39}}$(Ar)), 102.3 (t, $\mathbf{C_{43}}$/$\mathbf{C_{39}}$(Ar)), 69.3 (s, $\mathbf{C_{14}}$, $\mathbf{C_{106}}$(OCH_2)), 68.4 (s, $\mathbf{C_{23}}$/$\mathbf{C_{115}}$(OCH_2)), 68.2 (s, $\mathbf{C_{23}}$/$\mathbf{C_{115}}$(OCH_2)), 29.0-29.6 (s, $\mathbf{C_{15\text{-}22}}$($CH_2$), $\mathbf{C_{107\text{-}114}}$($CH_2$)), 26.0 (s, $\mathbf{C_{15\text{-}22}}$($CH_2$), $\mathbf{C_{107\text{-}114}}$($CH_2$)) ppm.

Note: No Peak found for $\mathbf{C_{38}}$(Ar), $\mathbf{C_{41}}$(Ar), $\mathbf{C_{45}}$(Ar) , $\mathbf{C_{47}}$(Ar)

^{19}F NMR (282 MHz, C_6F_6): δ_C -115.5 (C-**F**(Ar)), -115.9 (C-**F**(Ar)) ppm

IR (Solid) ν_{max}: 2919(m) (**C-H$_2$**), 2848(m) (**C-H$_2$**), 2227(m) (**C≡N**), 1603(s) (**Ar**), 1509(s) (**Ar**) cm^{-1}.

EIMS *m/z* 279 ($[C_{20}H_{19}O]^+$, 9%), 207 ($[C_{15}H_{11}O]^+$, 12%), 167 ($[C_{12}H_{21}]^+$, 27%), 149 ($[C_{10}H_{15}O]^+$, 100%), 69 ($[C_5H_9]^+$, 13%), 57 ($[C_4H_9]^+$, 29%), 41 ($[C_3H_5]^+$, 22%).

7.6. References

1 J. V. Crivello, M. Deptolla, H. Ringsdorf, *Liq. Cryst.*, **1988**, 3, 235.

Appendix A

Describing Mathematically the Splay and Bend Deformations

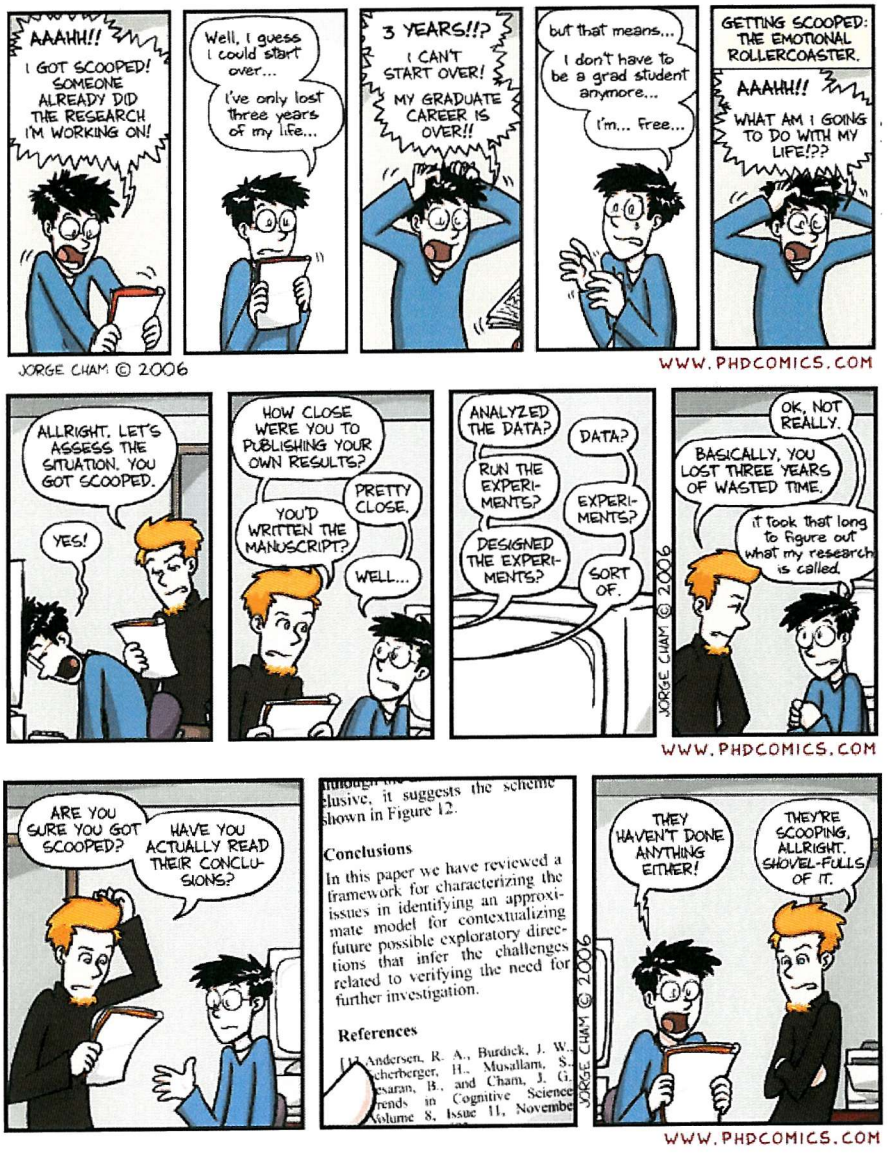

"Piled Higher and Deeper" by Jorge Cham
www.phdcomics.com

Used with permission

A. Appendix A

The del operator (∇) is given by

$$\nabla = \begin{pmatrix} \frac{\delta}{\delta x} \\ \frac{\delta}{\delta y} \\ \frac{\delta}{\delta z} \end{pmatrix}.$$

So for a director n with components $\mathbf{n}_x$, $\mathbf{n}_y$ and $\mathbf{n}_z$

$$\mathbf{n} = \begin{pmatrix} \mathbf{n}_x \\ \mathbf{n}_y \\ \mathbf{n}_z \end{pmatrix},$$

$\mathbf{n}\nabla$ is defined as

$$\mathbf{n}\nabla = \begin{pmatrix} \frac{\delta \mathbf{n}_x}{\delta x} \\ \frac{\delta \mathbf{n}_y}{\delta y} \\ \frac{\delta \mathbf{n}_z}{\delta z} \end{pmatrix}$$

and the dot product of 'del' and $\mathbf{n}$ as

$$(\nabla \cdot \mathbf{n}) = \frac{\delta \mathbf{n}_x}{\delta x} + \frac{\delta \mathbf{n}_y}{\delta y} + \frac{\delta \mathbf{n}_z}{\delta z}.$$

Which can also be described as $\mathrm{div}(\mathbf{n})$ since

$$\mathrm{div}(\mathbf{n}) = (\nabla \cdot \mathbf{n})$$

Therefore, for the splay deformation, we get $\mathbf{n}(\nabla\cdot\mathbf{n})$ by combining the previous two results so that

$$\mathbf{n}(\nabla\cdot\mathbf{n})=\begin{pmatrix}\mathbf{n}_x\left(\frac{\delta\mathbf{n}_x}{\delta x}+\frac{\delta\mathbf{n}_y}{\delta y}+\frac{\delta\mathbf{n}_z}{\delta z}\right)\\ \mathbf{n}_y\left(\frac{\delta\mathbf{n}_x}{\delta x}+\frac{\delta\mathbf{n}_y}{\delta y}+\frac{\delta\mathbf{n}_z}{\delta z}\right)\\ \mathbf{n}_y\left(\frac{\delta\mathbf{n}_x}{\delta x}+\frac{\delta\mathbf{n}_y}{\delta y}+\frac{\delta\mathbf{n}_z}{\delta z}\right)\end{pmatrix}.$$

The dot product is commutative and thus

$$(\nabla\cdot\mathbf{n})=(\mathbf{n}\cdot\nabla).$$

This is not true for the cross product and therefore

$$(\nabla\times\mathbf{n})=\begin{pmatrix}\left(\frac{\delta\mathbf{n}_y}{\delta z}-\frac{\delta\mathbf{n}_z}{\delta y}\right)\\ \left(\frac{\delta\mathbf{n}_x}{\delta z}-\frac{\delta\mathbf{n}_z}{\delta x}\right)\\ \left(\frac{\delta\mathbf{n}_x}{\delta y}-\frac{\delta\mathbf{n}_y}{\delta x}\right)\end{pmatrix},$$

which can also be written as $\mathrm{rot}(\mathbf{n})$ or $\mathrm{curl}(\mathbf{n})$ since

$$\mathrm{rot}(\mathbf{n})=\mathrm{curl}(\mathbf{n})=(\nabla\times\mathbf{n})$$

And therefore in the Meyer definition of the flexoelectric polarisation, the bend deformation is given as

$$(\nabla\times\mathbf{n})\times\mathbf{n}=\begin{pmatrix}\mathbf{n}_z\left(\frac{\delta\mathbf{n}_x}{\delta z}-\frac{\delta\mathbf{n}_z}{\delta x}\right)-\mathbf{n}_y\left(\frac{\delta\mathbf{n}_x}{\delta y}-\frac{\delta\mathbf{n}_y}{\delta x}\right)\\ \mathbf{n}_y\left(\frac{\delta\mathbf{n}_y}{\delta z}-\frac{\delta\mathbf{n}_z}{\delta y}\right)-\mathbf{n}_x\left(\frac{\delta\mathbf{n}_x}{\delta y}-\frac{\delta\mathbf{n}_y}{\delta x}\right)\\ \mathbf{n}_y\left(\frac{\delta\mathbf{n}_y}{\delta z}-\frac{\delta\mathbf{n}_z}{\delta y}\right)-\mathbf{n}_x\left(\frac{\delta\mathbf{n}_x}{\delta z}-\frac{\delta\mathbf{n}_z}{\delta x}\right)\end{pmatrix},$$

which we will see is different to that which is based on the Frank definition used in the elastic constants which is given as

$$\mathbf{n}\times(\nabla\times\mathbf{n})=\begin{pmatrix}\mathbf{n}_y\left(\frac{\delta\mathbf{n}_x}{\delta y}-\frac{\delta\mathbf{n}_y}{\delta x}\right)-\mathbf{n}_z\left(\frac{\delta\mathbf{n}_x}{\delta z}-\frac{\delta\mathbf{n}_z}{\delta x}\right)\\ \mathbf{n}_x\left(\frac{\delta\mathbf{n}_x}{\delta y}-\frac{\delta\mathbf{n}_y}{\delta x}\right)-\mathbf{n}_y\left(\frac{\delta\mathbf{n}_y}{\delta z}-\frac{\delta\mathbf{n}_z}{\delta y}\right)\\ \mathbf{n}_x\left(\frac{\delta\mathbf{n}_x}{\delta z}-\frac{\delta\mathbf{n}_z}{\delta x}\right)-\mathbf{n}_y\left(\frac{\delta\mathbf{n}_y}{\delta z}-\frac{\delta\mathbf{n}_z}{\delta y}\right)\end{pmatrix}.$$

However we can see that

$$\mathbf{n}\times(\nabla\times\mathbf{n})(-1)=(\nabla\times\mathbf{n})\times\mathbf{n},$$

which expands to give

$$\begin{pmatrix}\mathbf{n}_y\left(\frac{\delta\mathbf{n}_x}{\delta y}-\frac{\delta\mathbf{n}_y}{\delta x}\right)-\mathbf{n}_z\left(\frac{\delta\mathbf{n}_x}{\delta z}-\frac{\delta\mathbf{n}_z}{\delta x}\right)\\ \mathbf{n}_x\left(\frac{\delta\mathbf{n}_x}{\delta y}-\frac{\delta\mathbf{n}_y}{\delta x}\right)-\mathbf{n}_y\left(\frac{\delta\mathbf{n}_y}{\delta z}-\frac{\delta\mathbf{n}_z}{\delta y}\right)\\ \mathbf{n}_x\left(\frac{\delta\mathbf{n}_x}{\delta z}-\frac{\delta\mathbf{n}_z}{\delta x}\right)-\mathbf{n}_y\left(\frac{\delta\mathbf{n}_y}{\delta z}-\frac{\delta\mathbf{n}_z}{\delta y}\right)\end{pmatrix}*(-1)=\begin{pmatrix}-\mathbf{n}_y\left(\frac{\delta\mathbf{n}_x}{\delta y}-\frac{\delta\mathbf{n}_y}{\delta x}\right)+\mathbf{n}_z\left(\frac{\delta\mathbf{n}_x}{\delta z}-\frac{\delta\mathbf{n}_z}{\delta x}\right)\\ -\mathbf{n}_x\left(\frac{\delta\mathbf{n}_x}{\delta y}-\frac{\delta\mathbf{n}_y}{\delta x}\right)+\mathbf{n}_y\left(\frac{\delta\mathbf{n}_y}{\delta z}-\frac{\delta\mathbf{n}_z}{\delta y}\right)\\ -\mathbf{n}_x\left(\frac{\delta\mathbf{n}_x}{\delta z}-\frac{\delta\mathbf{n}_z}{\delta x}\right)+\mathbf{n}_y\left(\frac{\delta\mathbf{n}_y}{\delta z}-\frac{\delta\mathbf{n}_z}{\delta y}\right)\end{pmatrix}=\begin{pmatrix}\mathbf{n}_z\left(\frac{\delta\mathbf{n}_x}{\delta z}-\frac{\delta\mathbf{n}_z}{\delta x}\right)-\mathbf{n}_y\left(\frac{\delta\mathbf{n}_x}{\delta y}-\frac{\delta\mathbf{n}_y}{\delta x}\right)\\ \mathbf{n}_y\left(\frac{\delta\mathbf{n}_y}{\delta z}-\frac{\delta\mathbf{n}_z}{\delta y}\right)-\mathbf{n}_x\left(\frac{\delta\mathbf{n}_x}{\delta y}-\frac{\delta\mathbf{n}_y}{\delta x}\right)\\ \mathbf{n}_y\left(\frac{\delta\mathbf{n}_y}{\delta z}-\frac{\delta\mathbf{n}_z}{\delta y}\right)-\mathbf{n}_x\left(\frac{\delta\mathbf{n}_x}{\delta z}-\frac{\delta\mathbf{n}_z}{\delta x}\right)\end{pmatrix}$$

So for the Meyer definition

$$\mathbf{P}=e_1\mathbf{n}(\nabla\cdot\mathbf{n})+e_3(\nabla\times\mathbf{n})\times\mathbf{n}$$

$$\mathbf{P}=e_1\begin{pmatrix}\mathbf{n}_x\left(\frac{\delta\mathbf{n}_x}{\delta x}+\frac{\delta\mathbf{n}_y}{\delta y}+\frac{\delta\mathbf{n}_z}{\delta z}\right)\\ \mathbf{n}_y\left(\frac{\delta\mathbf{n}_x}{\delta x}+\frac{\delta\mathbf{n}_y}{\delta y}+\frac{\delta\mathbf{n}_z}{\delta z}\right)\\ \mathbf{n}_y\left(\frac{\delta\mathbf{n}_x}{\delta x}+\frac{\delta\mathbf{n}_y}{\delta y}+\frac{\delta\mathbf{n}_z}{\delta z}\right)\end{pmatrix}+e_3\begin{pmatrix}\mathbf{n}_z\left(\frac{\delta\mathbf{n}_x}{\delta z}-\frac{\delta\mathbf{n}_z}{\delta x}\right)-\mathbf{n}_y\left(\frac{\delta\mathbf{n}_x}{\delta y}-\frac{\delta\mathbf{n}_y}{\delta x}\right)\\ \mathbf{n}_y\left(\frac{\delta\mathbf{n}_y}{\delta z}-\frac{\delta\mathbf{n}_z}{\delta y}\right)-\mathbf{n}_x\left(\frac{\delta\mathbf{n}_x}{\delta y}-\frac{\delta\mathbf{n}_y}{\delta x}\right)\\ \mathbf{n}_y\left(\frac{\delta\mathbf{n}_y}{\delta z}-\frac{\delta\mathbf{n}_z}{\delta y}\right)-\mathbf{n}_x\left(\frac{\delta\mathbf{n}_x}{\delta z}-\frac{\delta\mathbf{n}_z}{\delta x}\right)\end{pmatrix}$$

And for the alternative definition

$$\mathbf{P}=e_1\mathbf{n}(\nabla\cdot\mathbf{n})+e_3\mathbf{n}\times(\nabla\times\mathbf{n})$$

$$\mathbf{P}=e_1\begin{pmatrix}\mathbf{n}_x\left(\frac{\delta\mathbf{n}_x}{\delta x}+\frac{\delta\mathbf{n}_y}{\delta y}+\frac{\delta\mathbf{n}_z}{\delta z}\right)\\ \mathbf{n}_y\left(\frac{\delta\mathbf{n}_x}{\delta x}+\frac{\delta\mathbf{n}_y}{\delta y}+\frac{\delta\mathbf{n}_z}{\delta z}\right)\\ \mathbf{n}_y\left(\frac{\delta\mathbf{n}_x}{\delta x}+\frac{\delta\mathbf{n}_y}{\delta y}+\frac{\delta\mathbf{n}_z}{\delta z}\right)\end{pmatrix}+e_3\begin{pmatrix}\mathbf{n}_y\left(\frac{\delta\mathbf{n}_x}{\delta y}-\frac{\delta\mathbf{n}_y}{\delta x}\right)-\mathbf{n}_z\left(\frac{\delta\mathbf{n}_x}{\delta z}-\frac{\delta\mathbf{n}_z}{\delta x}\right)\\ \mathbf{n}_x\left(\frac{\delta\mathbf{n}_x}{\delta y}-\frac{\delta\mathbf{n}_y}{\delta x}\right)-\mathbf{n}_y\left(\frac{\delta\mathbf{n}_y}{\delta z}-\frac{\delta\mathbf{n}_z}{\delta y}\right)\\ \mathbf{n}_x\left(\frac{\delta\mathbf{n}_x}{\delta z}-\frac{\delta\mathbf{n}_z}{\delta x}\right)-\mathbf{n}_y\left(\frac{\delta\mathbf{n}_y}{\delta z}-\frac{\delta\mathbf{n}_z}{\delta y}\right)\end{pmatrix}$$

Appendix B

Diagrams of How Small and Large Angle Tilts in the Optic Axis Affect the Results Observed Through the Microscope

"Piled Higher and Deeper" by Jorge Cham
www.phdcomics.com

Used with permission

B. Appendix B

In order to make measurements on the angular dependance of the optic axis on the applied field, we examined in Chapter 2 how, practically, the intensity of light as a way of reading the degree of tilt in the axis. We noted that for small anglar tilt we could easily measure this by determining the dark state (corresponding the the helix axis being lined up with one of the crossed polarisers) and rotated the sample through 22.5°. The light intensity is related to the optic axis through a sine squared relationship and as such, 22.5° corresponds the position on the trigonomic curve which is most sensitive to small rotations in the same. Thus subsequently when the sample is rotated about this point, the most accurate measure us achieved.

We explored how the helix axis and optic axes (for positive and negative fields from an A.C. square-wave source) moved throughout the experiment examining these axis form the point of view of looking down the microscope (the crossed polarisers are represented by the x and y axes) and where they are on a the squared sine wave. In Chapter 2 this was done for small angles (i.e. an example where $+\varphi$ to $-\varphi$ is less than 45°). We also comment that these measurements become difficult when $+\varphi$ to $-\varphi$ exceeds 45°.

Below we show the large angle example demonstrating why the intensity gets smaller and consequently becomes much harder to read on the oscilloscope. With each diagram is the angles for the helix axis (HA) and the + and – optic axes. For comparison, the short angle example (as seen in Chapter 2) is also given.

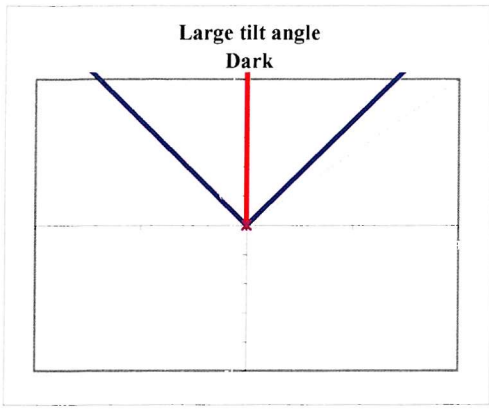

HA = 0°; -φ(E) = -35°, +φ(E) = 35°;

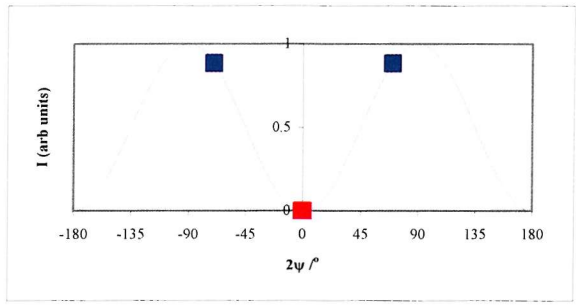

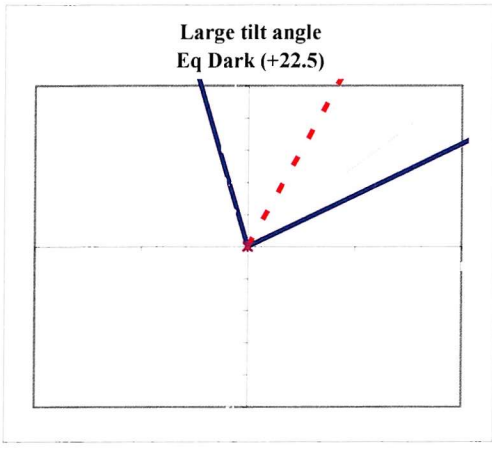

HA = 22.5°; -φ(E) = -12.5°;+φ(E) = 57.5°;

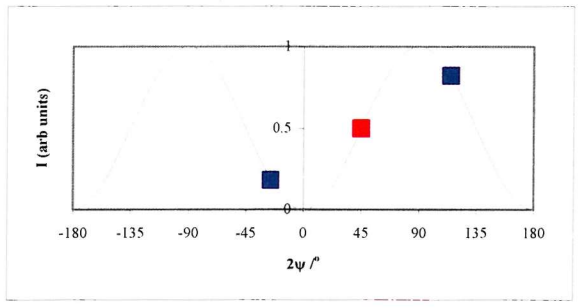

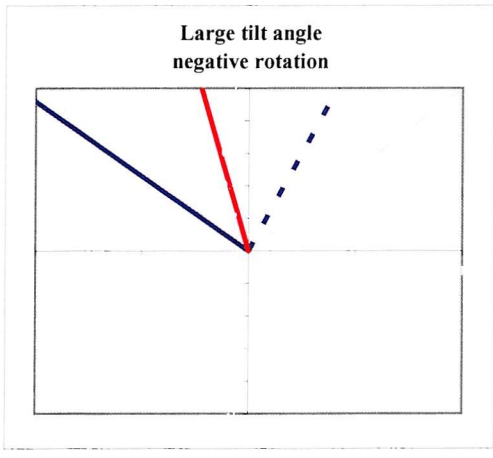

HA = -22.5°; -φ(E) = -47.5°;+φ(E) = 22.5°;

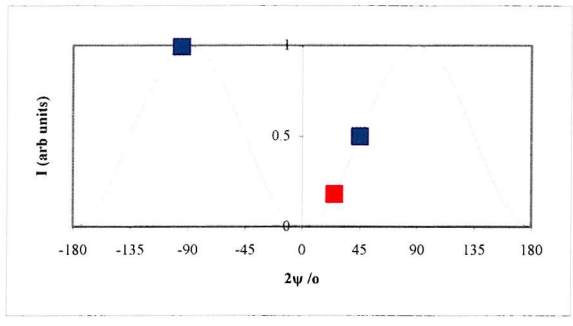

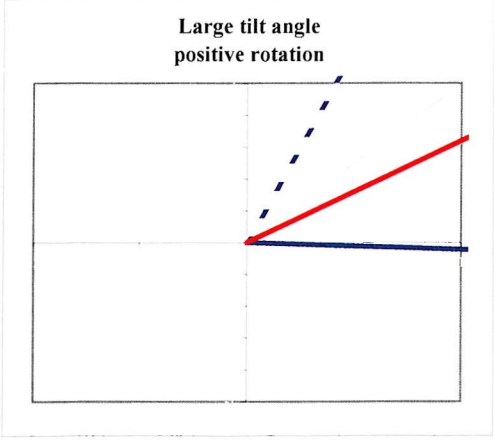

HA = 57.5°; -φ(E) = 22.5°;+φ(E) = 92.5°;

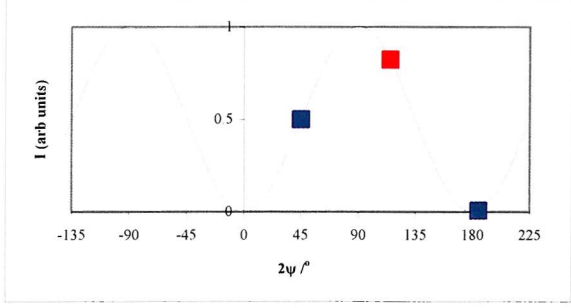

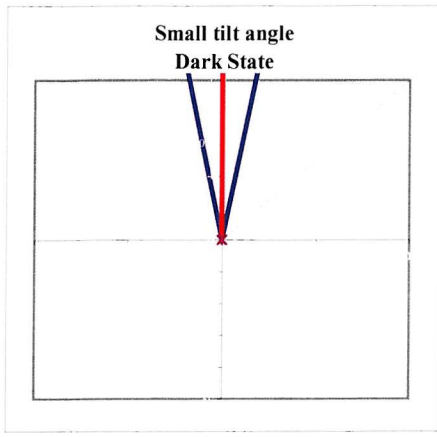

HA = 0; -φ(E) = -10°, +φ(E) = 10°;

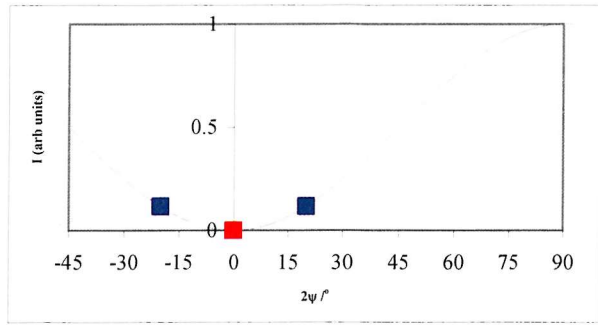

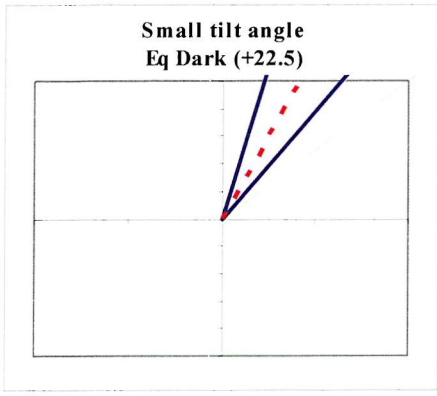

HA = 22.5°; -φ(E) = 12.5°;+φ(E) = 32.5°;

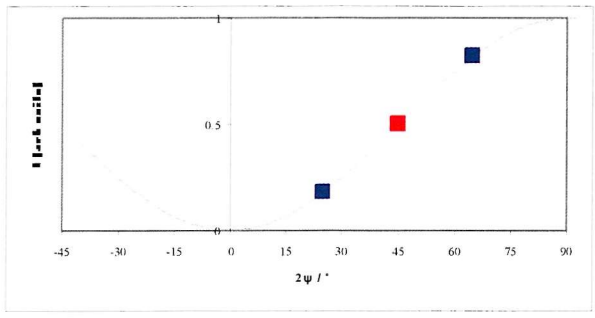

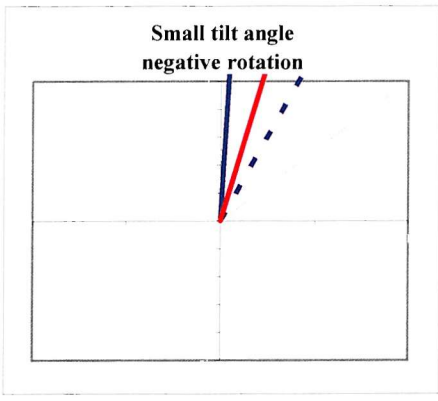

HA = 32.5°; -φ(E) = 22.5°;+φ(E) = 42.5°;

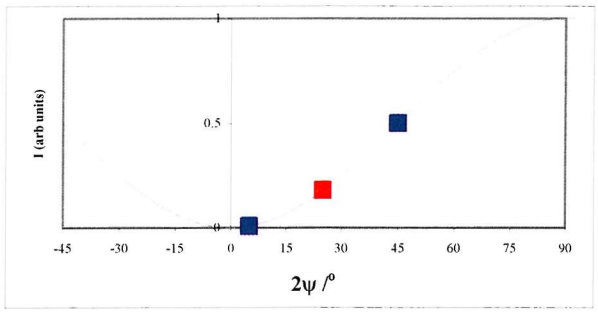

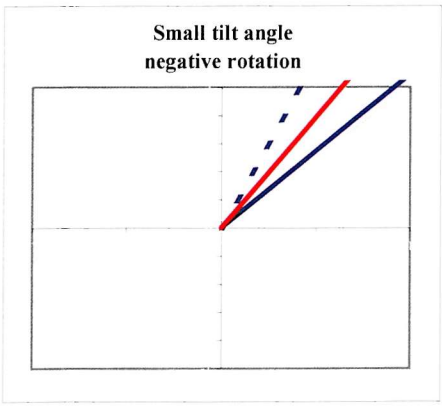

HA = 57.5°; -φ(E) = 22.5°;+φ(E) = 92.5°;

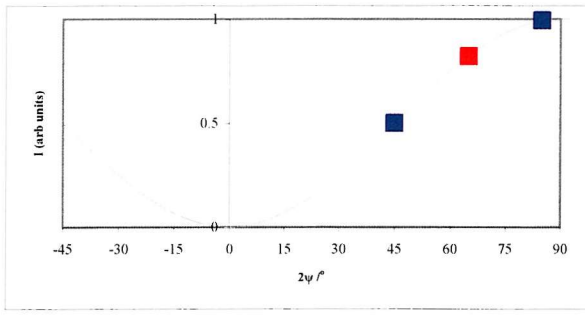

Appendix C

Primary Data for ULH Flexoelastic Experiments Obtaining Tan(φ)/E

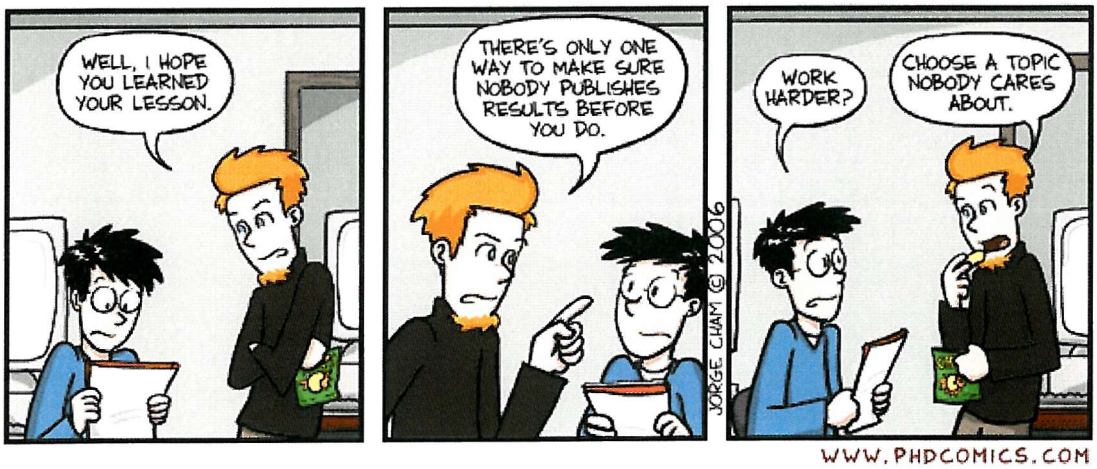

"Piled Higher and Deeper" by Jorge Cham
www.phdcomics.com

Used with permission

C. Appendix C

C.1. Chapter 3

C.1.1. $CBOnOBF_2$

compound **CBO7OBF2** est HTP 0.163399 nm^{-1}

Vc unwin	40 V	**Gradient**	0.0686 $V^{-1}\mu m$	T_{NI}	119 °C
pitch	299.1081 nm	**K**	unknown pN	**T**	111.2 °C
Thickness	4.88 µm	**e/K**	1.441039 V^{-1}	T/T_{NI}	0.98
		eP/K	4.31E-04 $V^{-1}\mu m$		

#	real V	Electric field per micron	Max Angle	Min Angle	tilt angle	tan ϕ
1	3.9	0.79918	55.8	49.5	3.15	0.06
2	7.8	1.598361	59.9	46.4	6.75	0.12
3	11.7	2.397541	62.4	43.2	9.6	0.17
4	15.6	3.196721	65.7	40.5	12.6	0.22
5	19.5	3.995902	69	38.5	15.25	0.27
6	23.4	4.795082	72	35.8	18.1	0.33
7	27.3	5.594262	75.7	33.7	21	0.38
8	31.2	6.393443	78.5	31.4	23.55	0.44
9	35.1	7.192623	0	0	0	0
10	39.0	7.991803	0	0	0	0

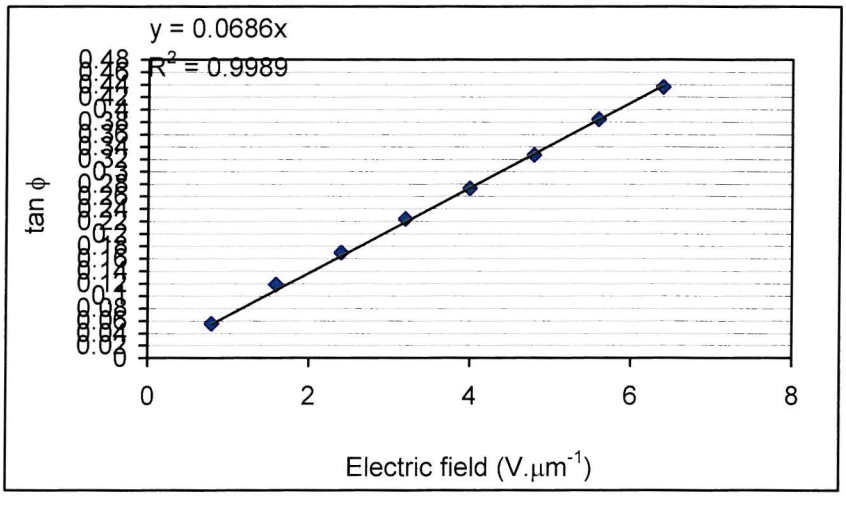

compound **CBO8OBF2** est HTP 0.1634 nm^{-1}

Vc unwin	30 V	**Gradient**	0.0421 $V^{-1}\mu m$	T_{NI}	150 °C
pitch	452.1637 nm	**K**	0 pN	**T**	141.5 °C
Thickness	4.94 µm	**e/K**	0.58501 V^{-1}	T/T_{NI}	0.98
		eP/K	2.65E-04 $V^{-1}\mu m$		

#	real V	Electric field per micron	Max Angle	Min Angle	tilt angle	tan ϕ
1	2.9	0.587045	0	0	0	0
2	5.8	1.174089	0	0	0	0
3	8.7	1.761134	66.4	56.7	4.85	0.08
4	11.6	2.348178	66.3	53.7	6.3	0.11
5	14.5	2.935223	70.7	55.1	7.8	0.14
6	17.4	3.522267	71.5	54.4	8.55	0.15
7	20.3	4.109312	75	56.2	9.4	0.17
8	23.2	4.696356	78.6	57.7	10.45	0.18
9	26.1	5.283401	0	0	0	0
10	29.0	5.870445	0	0	0	0

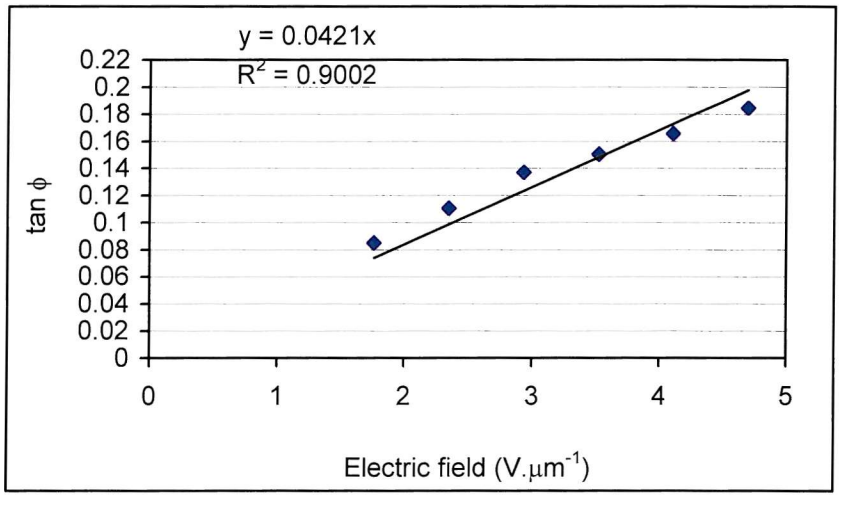

compound **CBO9OBF2** est HTP 0.1634 nm^{-1}

Vc unwin	36 V	**Gradient**	0.064 $V^{-1}\mu m$	$\mathbf{T_{NI}}$	143 °C
pitch	293.0648 nm	**K**	0 pN	**T**	134.7 °C
Thickness	4.96 µm	**e/K**	1.37213 V^{-1}	$\mathbf{T/T_{NI}}$	0.98
		eP/K	4.02E-04 $V^{-1}\mu m$		

#	real V	Electric field per micron	Max Angle	Min Angle	tilt angle	tan ϕ
1	3.5	0.705645	0	0	0	0
2	7.0	1.41129	0	0	0	0
3	10.5	2.116935	385.8	371.5	7.15	0.125443
4	14.0	2.822581	389.8	369.8	10	0.176327
5	17.5	3.528226	394.6	368.2	13.2	0.234548
6	21.0	4.233871	398.3	367.9	15.2	0.271694
7	24.5	4.939516	0	0	0	0
8	28.0	5.645161	0	0	0	0
9	31.5	6.350806	0	0	0	0
10	35.0	7.056452	0	0	0	0

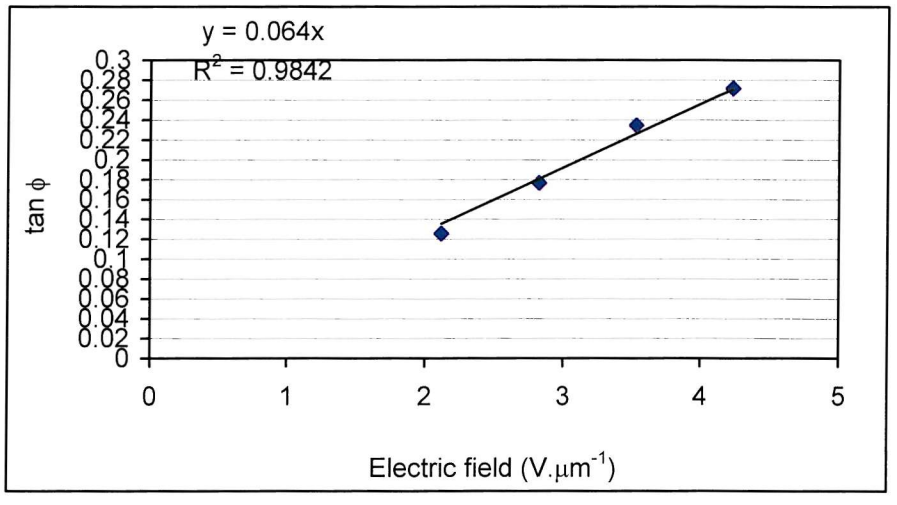

compound **CBO10OBF2** HTP 0.1634 nm^{-1}

Vc unwin	30 V	**Gradient**	0.0399 $V^{-1}\mu m$	$\mathbf{T_{NI}}$	146 °C
pitch	235.6 nm	**K**	unknown pN	**T**	138 °C
Thickness	4.91 µm	**e/K**	1.06429 V^{-1}	$\mathbf{T/T_{NI}}$	0.98
		eP/K	2.51E-04 $V^{-1}\mu m$		

#	real V	Electric field per micron	Max Angle	Min Angle	tilt angle	tan ϕ
1	2.9	0.590631	0	0	0	0
2	5.8	1.181263	0	0	0	0
3	8.7	1.771894	55.5	46.1	4.7	0.08
4	11.6	2.362525	56.7	44.2	6.25	0.11
5	14.5	2.953157	58.7	44.3	7.2	0.13
6	17.4	3.543788	60.1	43.5	8.3	0.15
7	20.3	4.13442	61.5	42.5	9.5	0.17
8	23.2	4.725051	61.4	40.5	10.45	0.18
9	26.1	5.315682	64.7	42.5	11.1	0.2

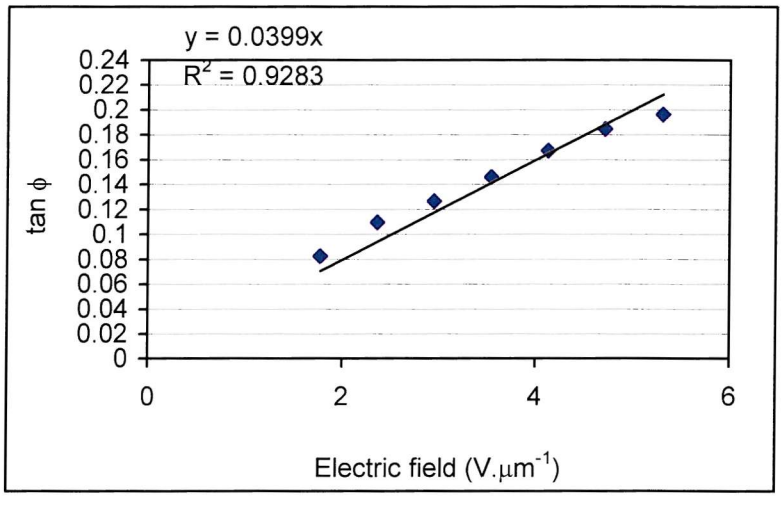

compound **CBO11OBF2** HTP 0.163399 nm^{-1}

Vc unwin	44.1 V	**Gradient**	0.0835 $V^{-1}\mu m$	T_{NI}	111 °C
pitch	0.323298 nm	**K**	0 pN	**T**	103.3 °C
Thickness	4.96 μm	**e/K**	1.622795 V^{-1}	T/T_{NI}	0.98
		eP/K	0.524646 $V^{-1}\mu m$		

#	Voltage	Electric field per micron	Max Angle	Min Angle	tilt angle	tan ϕ
1	4.3	0.87	368.4	358.3	5.05	0.088
2	8.6	1.74	371.9	353.8	9.05	0.159
3	12.9	2.61	376.6	349.9	13.35	0.237
4	17.2	3.48	380.5	347.8	16.35	0.293
5	21.6	4.34	384.5	343.9	20.30	0.370
6	25.9	5.21	388.9	341.7	23.60	0.437
7	30.2	6.08	391.2	337.2	27.00	0.510
8	34.5	6.95	389.2	330.7	29.25	0.560
9	38.8	7.821	0	0	0	0
10	43.1	8.690	0	0	0	0

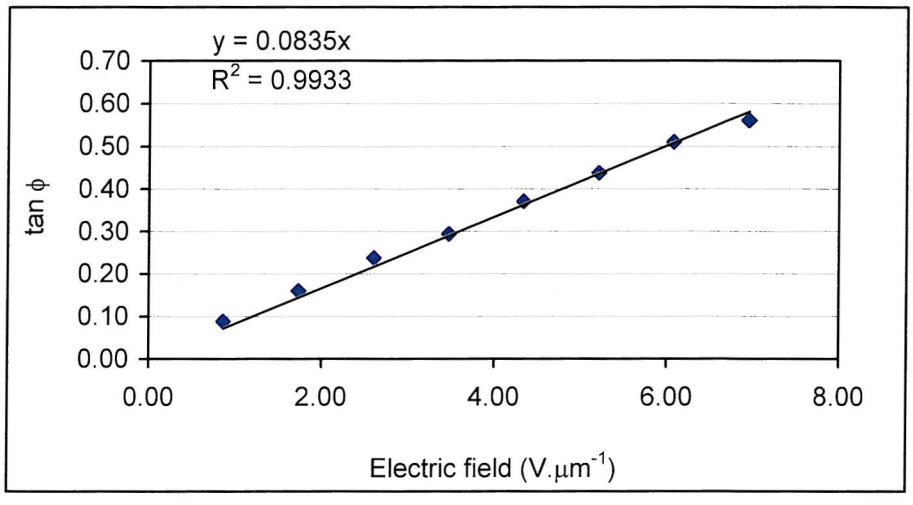

C.1.2. $CBOnOBF_3$

compound **CBO6OBF3** Est HTP 0.163399 nm^{-1}

Vc unwind	30 V	**Gradient**	0.0471 $V^{-1}\mu m$	**T_{NI}**	136 °C
pitch	412.4 nm	**K**	Unknown pN	**T**	128 °C
Thickness	5.05 µm	**e/K**	0.717628 V^{-1}	**T/T_{NI}**	0.98
		eP/K	2.96E-04 $V^{-1}\mu m$		

#	real V	Electric field per micron	Max Angle	Min Angle	tilt angle	tan φ
1	2.9	0.574257426	0	0	0	0
2	5.8	1.148514851	0	0	0	0
3	8.7	1.722772277	44	35.7	4.15	0.073
4	11.6	2.297029703	45.4	34.4	5.5	0.096
5	14.5	2.871287129	48.6	34.2	7.2	0.126
6	17.4		46.9	31.8	7.55	
7	20.3	4.01980198	48.8	28.2	10.3	0.182
8	23.2	4.594059406	56.5	31.4	12.55	0.223
9	26.1	5.168316832	54.2	25.4	14.4	0.257
10	29.0	5.742574257	64.9	25.5	19.7	0.358

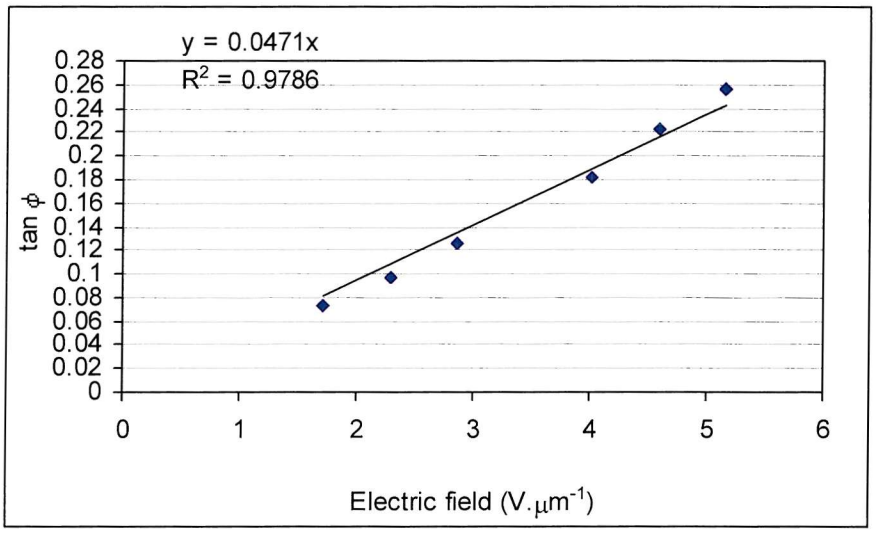

compound	**CBO7OBF3**	est HTP	0.1634 nm^{-1}		
Vc unwind	40 V	**Gradient**	0.0787 $V^{-1}\mu m$	T_{NI}	73 °C
pitch	379.0782 nm	**K**	unknown pN	**T**	66.1 °C
Thickness	5.05 µm	**e/K**	1.30444 V^{-1}	T/T_{NI}	0.98
		eP/K	4.94E-04 $V^{-1}\mu m$		

#	real V	Electric field per micron	Max Angle	Min Angle	tilt angle	tan ϕ
1	3.9	0.7722772	57	46.9	5.05	0.088368
2	7.8	1.5445545	59.6	44.1	7.75	0.136094
3	11.7	2.3168317	64.4	41.3	11.55	0.204361
4	15.6	3.0891089	68.3	40.7	13.8	0.245624
5	19.5	3.8613861	70.6	39.6	15.5	0.277325
6	23.4	4.6336634	72.2	39.2	16.5	0.296213
7	27.3	5.4059406	74.7	39.5	17.6	0.317219
8	31.2	6.1782178	74.4	39.2	17.6	0.317219
9	35.1	6.950495	71	37.9	16.55	0.297163
10	39.0	7.7227723	0	0	0	0

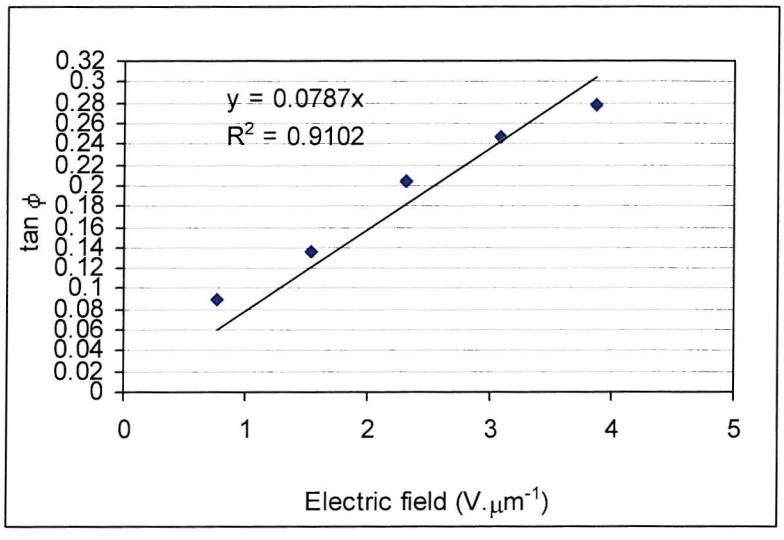

compound **CBO8OBF3** est HTP 0.163399 nm^{-1}

Vc unwin	20 V	**Gradient**	0.0636 $V^{-1}\mu m$	$\mathbf{T_{NI}}$	130 °C
pitch	247 nm	**K**	unknown pN	**T**	122 °C
Thickness	5.05 µm	**e/K**	1.620277 V^{-1}	$\mathbf{T/T_{NI}}$	0.98
		eP/K	4.00E-04 $V^{-1}\mu m$		

#	real V	Electric field per micron	Max Angle	Min Angle	tilt angle	tan ϕ
1	1.9	0.376238	0	0	0	0
2	3.8	0.752475	61	57.2	1.9	0.033173
3	5.7	1.128713	61	53.5	3.75	0.065543
4	7.6	1.50495	61	52.2	4.4	0.076946
5	9.5	1.881188	62.9	52.4	5.25	0.091887
6	11.4	2.257426	62	46.7	7.65	0.134317
7	13.3	2.633663	62.6	42	10.3	0.181731
8	15.2	3.009901	60	37.5	11.25	0.198912
9	17.1	3.386139	64.4	38.9	12.75	0.226277
10	19.0	3.762376	64	36.4	13.8	0.245624

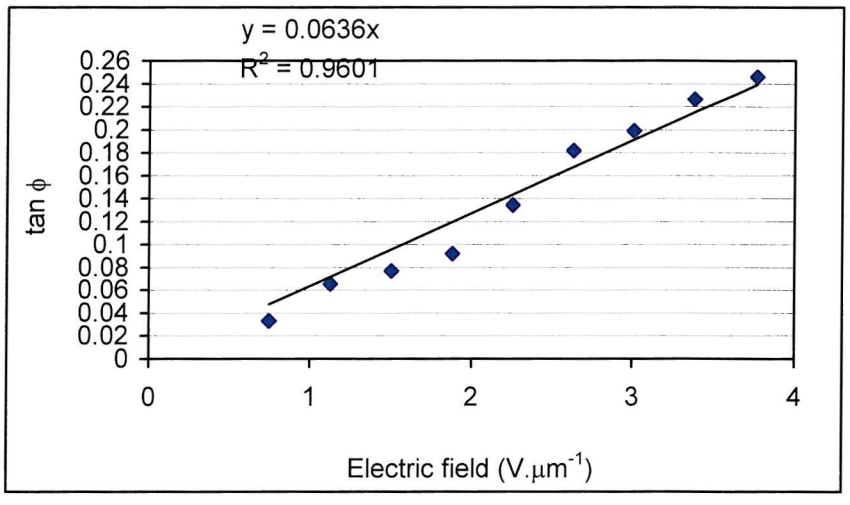

compound **CBO9OBF3** est HTP 0.163399 nm^{-1}

Vc unwin	30 V	**Gradient**	0.0918 $V^{-1}\mu m$	**T_{NI}**	88 °C
pitch	348.4854 nm	**K**	unknown pN	**T**	80.8 °C
Thickness	5.05 µm	**e/K**	1.655152 V^{-1}	**T/T_{NI}**	0.98
		eP/K	5.77E-04 $V^{-1}\mu m$		

#	real V	Electric field per micron	Max Angle	Min Angle	tilt angle	tan ϕ
1	2.9	0.574257	360.1	354.4	2.85	0.049783
2	5.8	1.148515	361.9	350.7	5.6	0.098051
3	8.7	1.722772	366.1	349.1	8.5	0.149451
4	11.6	2.29703	370	347.3	11.35	0.200727
5	14.5	2.871287	377.2	346.4	15.4	0.275446
6	17.4	3.445545	381.3	345	18.15	0.327817
7	20.3	4.019802	383	342.7	20.15	0.366938
8	23.2	4.594059	386.6	341.4	22.6	0.41626
9	26.1	5.168317	0	0	0	0
10	29.0	5.742574	0	0	0	0

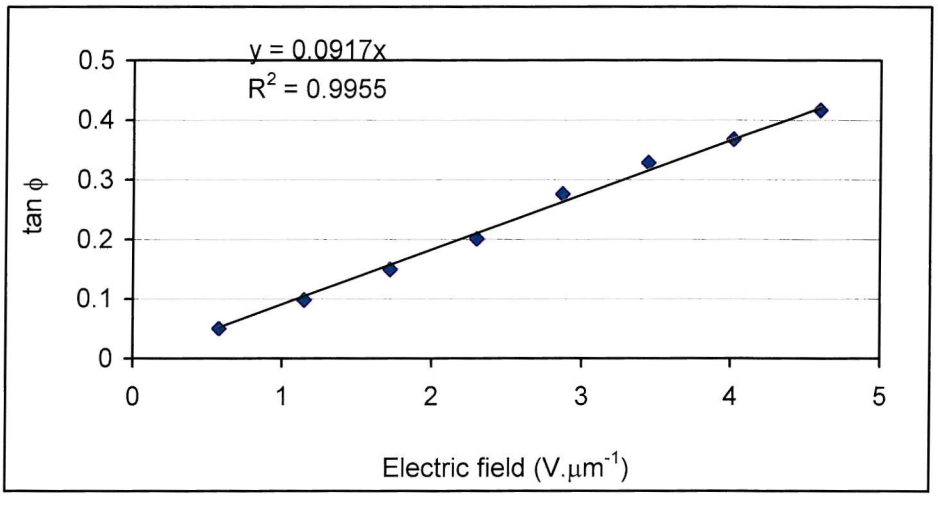

compound **CBO10OBF3**		HTP	0.1634 nm^{-1}		
Vc unwin	40 V	**Gradient**	0.0444 $V^{-1}\mu m$	T_{NI}	112 °C
pitch	369.3134 nm	**K**	unknown pN	**T**	104.3 °C
Thickness	5.05 µm	**e/K**	0.75538 V^{-1}	T/T_{NI}	0.98
		eP/K	2.79E-04 $V^{-1}\mu m$		

#	real V	Electric field per micron	Max Angle	Min Angle	tilt angle	tan ϕ
1	3.9	0.772277	0	0	0	0
2	7.8	1.544554	30.9	22.4	4.25	0.07
3	11.7	2.316832	33.2	21.1	6.05	0.11
4	15.6	3.089109	34	19.3	7.35	0.13
5	19.5	3.861386	37.9	18.2	9.85	0.17
6	23.4	4.633663	0	0	0	0
7	27.3	5.405941	0	0	0	0
8	31.2	6.178218	0	0	0	0
9	35.1	6.950495	0	0	0	0
10	39.0	7.722772	0	0	0	0

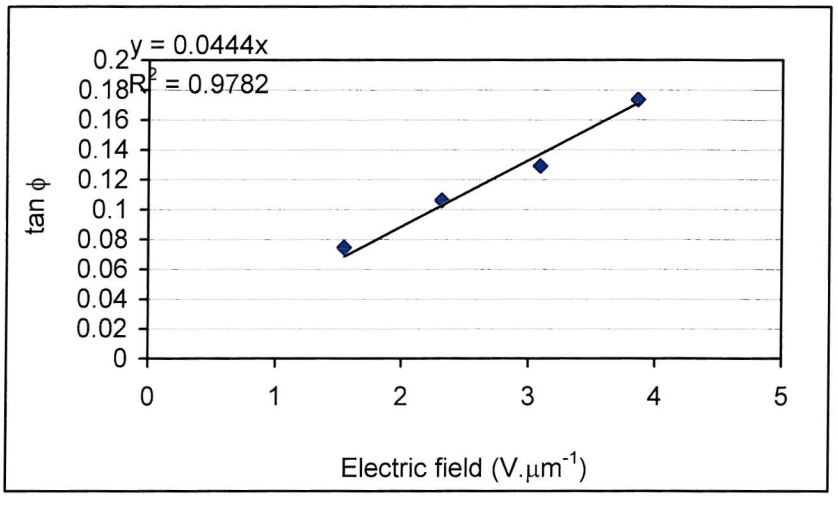

compound **CBO11OBF3** est HTP 0.163399 nm^{-1}

Vc unwin	40	V	**Gradient**	0.068	$V^{-1}\mu m$	T_{NI}	92 °C
pitch	271.3	nm	**K**	unknown	pN	**T**	84.7 °C
Thickness	5.05	µm	**e/K**	1.575051	V^{-1}	T/T_{NI}	0.98
			eP/K	4.27E-04	$V^{-1}\mu m$		

#	real V	Electric field per micron	Max Angle	Min Angle	tilt angle	tan ϕ
1	3.9	0.772277	368.2	359.9	4.15	0.073
2	7.8	1.544554	382	355.7	13.15	0.234
3	11.7	2.316832	383.4	352.3	15.55	0.278
4	15.6	3.089109	387.2	349.6	18.8	0.34
5	19.5	3.861386	389.3	346.9	21.2	0.388
6	23.4	4.633663	391.2	346.7	22.25	0.409
7	27.3	5.405941	0	0	0	0
8	31.2	6.178218	0	0	0	0
9	35.1	6.950495	0	0	0	0
10	39.0	7.722772	0	0	0	0

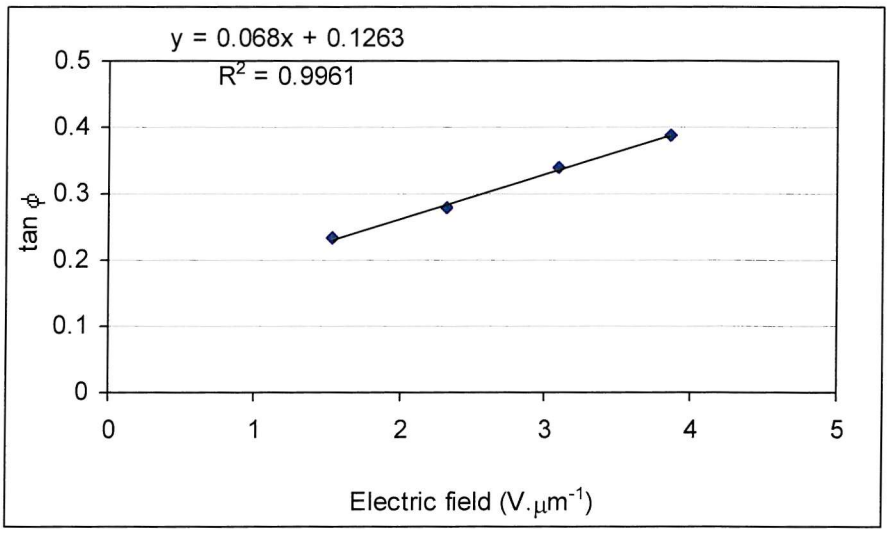

C.1.3. $CBOnOBF_4$

compound **CBO4OBF4** est HTP 0.163399 nm^{-1}

Vc unwin	40 V	**Gradient**	0.0429 $V^{-1}\mu m$	T_{NI}	138 °C
pitch	288.8 nm	**K**	0 pN	**T**	129.8 °C
Thickness	4.95 µm	**e/K**	0.933376 V^{-1}	T/T_{NI}	0.98
		eP/K	2.70E-04 $V^{-1}\mu m$		

#	real V	Electric field per micron	Max Angle	Min Angle	tilt angle	tan ϕ
1	3.9	0.787879	346	341.5	2.25	0.04
2	7.8	1.575758	352.8	342.8	5	0.09
3	11.7	2.363636	355.5	341.5	7	0.12
4	15.6	3.151515	354.2	337.8	8.2	0.14
5	19.5	3.939394	356.4	336.9	9.75	0.17
6	23.4	4.727273	357	334.1	11.45	0.2
7	27.3	5.515152	359.4	333.2	13.1	0.23
8	31.2	6.30303	360.9	332.3	14.3	0.25
9	35.1	7.090909	360.8	329.7	15.55	0.28
10	39.0	7.878788	0	0	0	0

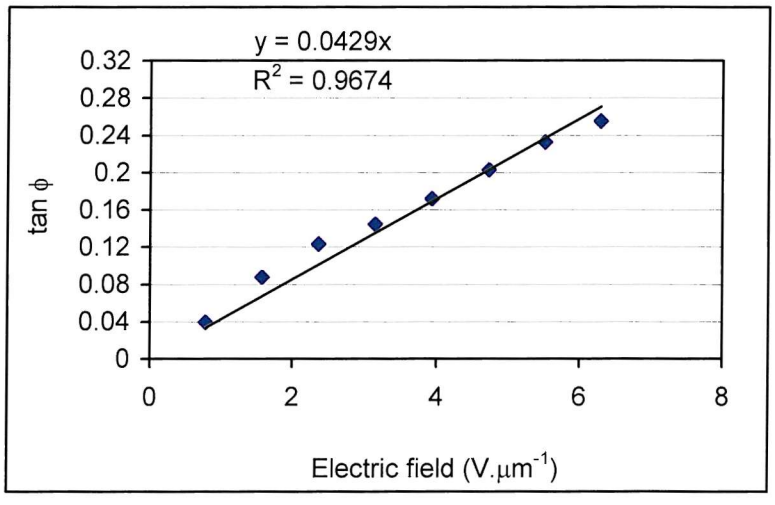

compound **CBO6OBF4** est HTP 0.163399 nm^{-1}

Vc unwin	50 V	**Gradient**	0.0879 $V^{-1}\mu m$	$\mathbf{T_{NI}}$	104 °C
pitch	233.7 nm	**K**	unknown pN	**T**	96.5 °C
Thickness	4.96 µm	**e/K**	2.363673 V^{-1}	$\mathbf{T/T_{NI}}$	0.98
		eP/K	5.52E-04 $V^{-1}\mu m$		

#	real V	Electric field per micron	Max Angle	Min Angle	tilt angle	tan ϕ
1	11.1	2.237903	353.4	345.5	3.95	0.069
2	13.5	2.721774	357.5	345.7	5.9	0.103
3	15.0	3.024194	357.9	342.5	7.7	0.135
4	17.5	3.528226	359.6	340.6	9.5	0.167
5	20.0	4.032258	360	334.1	12.95	0.23
6	25.0	5.040323	367.5	324	21.75	0.399
7	11.1	6.915323	0	0	0	0
8	11.1	7.903226	0	0	0	0
9	11.1	8.891129	0	0	0	0
10	11.1	9.879032	0	0	0	0

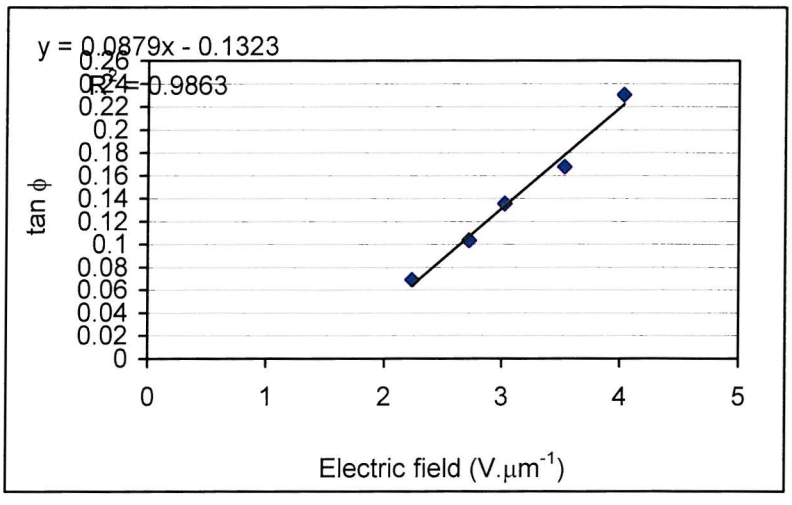

compound **CBO7OBF4** HTP 0.163399 nm^{-1}

Vc unwin	80	V	**Gradient**	0.0598	$V^{-1}\mu m$	T_{NI}	78 °C
pitch	299.2	nm	**K**	unknown	pN	**T**	70.98 °C
Thickness	4.97	µm	**e/K**	1.25582	V^{-1}	T/T_{NI}	0.98
			eP/K	3.76E-04	$V^{-1}\mu m$		

#	real V	Electric field per micror	Max Angle	Min Angle	tilt angl	tan ϕ
1	7.9	1.589537	374.7	364.8	4.95	0.09
2	15.8	3.179074	380.4	361	9.7	0.17
3	23.7	4.768612	385	355.7	14.65	0.26
4	31.6	6.358149	391	351.6	19.7	0.36
5	39.5	7.947686	396.4	346.6	24.9	0.46
6	47.4	9.537223	401.7	341.9	29.9	0.58
7	55.3	11.12676	405.9	338.9	33.5	0.66
8	63.2	12.7163	411.8	335	38.4	0.79
9	71.1	14.30584	418.4	333.7	42.35	0.91
10	79.0	15.89537	0	0	0	0

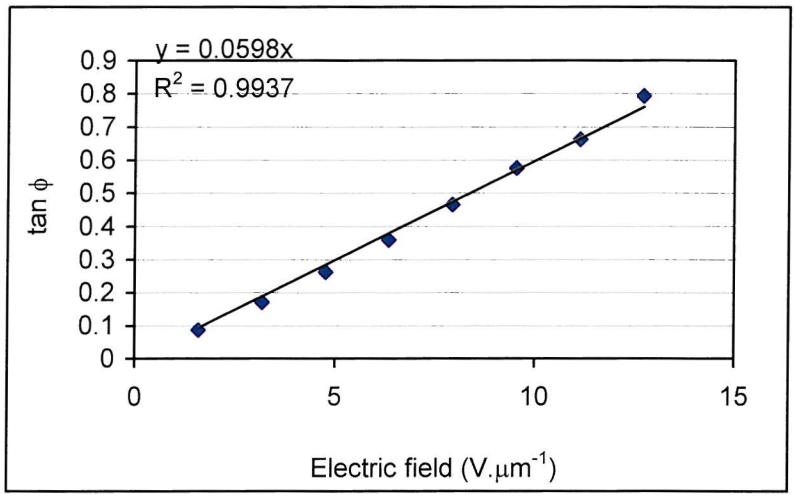

compound **CBO8OBF4** est HTP 0.163399 nm^{-1}

Vc unwin	80	V	**Gradient**	0.0511	$V^{-1}\mu m$	T_{NI}	104 °C
pitch	250.6	nm	**K**	unknown	pN	**T**	96.5 °C
Thickness	4.95	µm	**e/K**	1.281283	V^{-1}	T/T_{NI}	0.98
			eP/K	3.21E-04	$V^{-1}\mu m$		

#	real V	Electric field per micron	Max Angle	Min Angle	tilt angle	tan ϕ
1	7.9	1.59596	44.6	35	4.8	0.08
2	10.0	2.020202	46	34.6	5.7	0.1
3	12.5	2.525253	47.4	33.2	7.1	0.12
4	15.0	3.030303	52.2	34.1	9.05	0.16
5	3.5	0.707071	51.4	44	3.7	0.06
6	4.0	0.808081	51.9	42.8	4.55	0.08
7	4.5	0.909091	50.4	40.7	4.85	0.08
8	5.0	1.010101	50.9	39.8	5.55	0.1
9	6.0	1.212121	51.8	38.8	6.5	0.11
10	7.0	1.414141	51.4	37.8	6.8	0.12

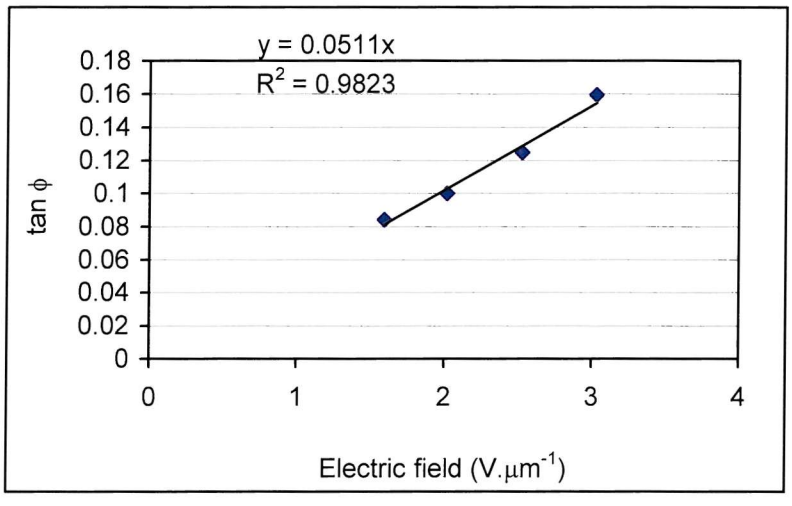

compound **CBO9OBF4** est HTP 0.163399 nm^{-1}

Vc unwin	100 V	**Gradient**	0.0781 $V^{-1}\mu m$	T_{NI}	78 °C
pitch	0.324674 nm	**K**	unknown pN	**T**	70.98 °C
Thickness	4.96 µm	**e/K**	1.511413 V^{-1}	T/T_{NI}	0.98
		eP/K	4.91E-04 $V^{-1}\mu m$		

#	real V	Electric field per micron	Max Angle	Min Angle	tilt angle	tan ϕ
1	7.9	1.592742	29.1	17.1	6	0.11
2	15.8	3.185484	34	7.3	13.35	0.24
3	23.7	4.778226	42.8	2	20.4	0.37
4	31.6	6.370968	54.7	-1.6	28.15	0.54
5	39.5	7.96371	55.5	-6.1	30.8	0.6
6	3.1	0.614919	25.1	15.5	4.8	0.08
7	4.0	0.806452	23.7	14	4.85	0.08
8	5.0	1.008065	26.8	12.4	7.2	0.13
9	6.0	1.209677	31	12	9.5	0.17
10	7.0	1.41129	32.9	11.4	10.75	0.19

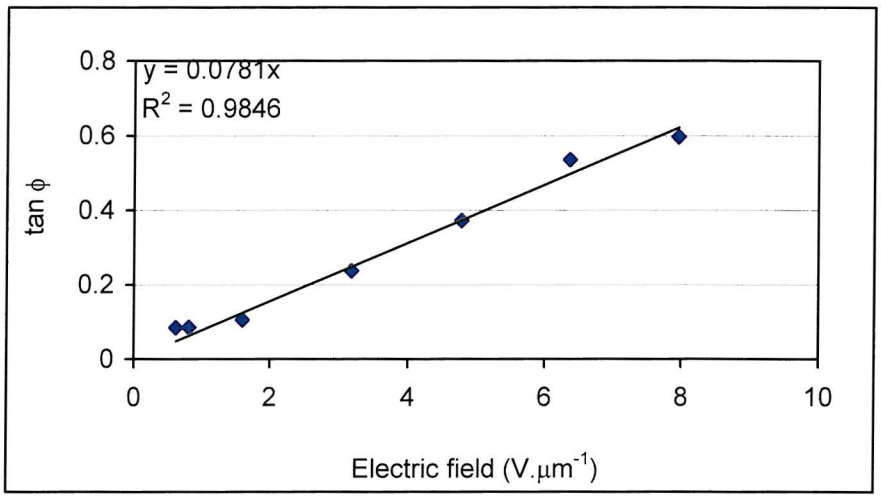

compound	**CBO10OBF4**		est HTP	0.163399	nm^{-1}		
Vc unwind	80	V	**Gradient**	0.0408	$V^{-1}\mu m$	**T_{NI}**	102 °C
pitch	288.3703	nm	**K**	unknown	pN	**T**	94.5 °C
Thickness	4.97	µm	**e/K**	0.888975	V^{-1}	**T/T_{NI}**	0.98
			eP/K	2.56E-04	$V^{-1}\mu m$		

#	real V	Electric field per micron	Max Angle	Min Angle	tilt angle	tan ϕ
1	7.9	1.589537	10.4	3.2	3.6	0.063
2	15.8	3.179074	372.5	355.9	8.3	0.146
3	23.7	4.768612	375.2	351.6	11.8	0.209
4	31.6	6.358149	379.9	349.9	15	0.268
5	39.5	7.947686	381.8	347.2	17.3	0.311
6	42.4	8.531187	383	345.4	18.8	0.34
7	55.3	11.12676	0	0	0	0
8	63.2	12.7163	0	0	0	0
9	71.1	14.30584	0	0	0	0
10	79.0	15.89537	0	0	0	0

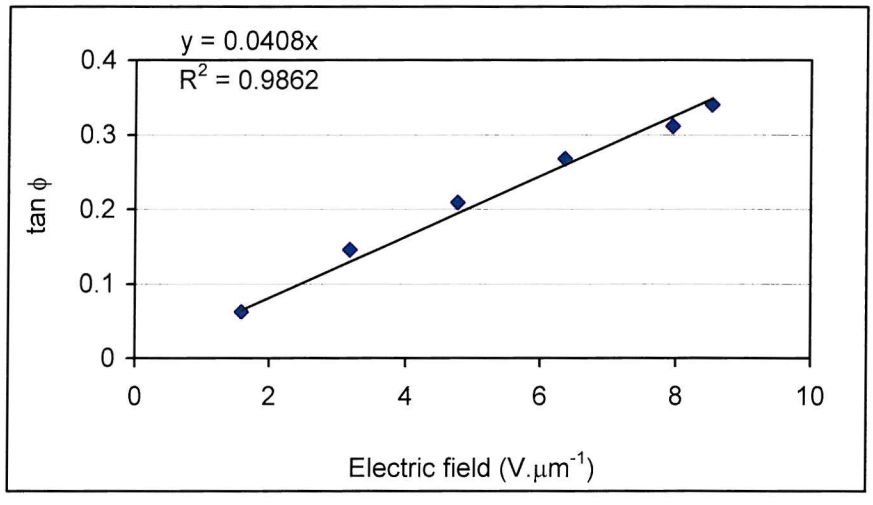

compound	**CBO11OBF4**		HTP	0.163399	nm^{-1}		
Vc unwind	40	V	**Gradient**	0.0548	$V^{-1}\mu m$	**T_{NI}**	80 °C
pitch	196.8	nm	**K**	unknown	pN	**T**	72.9 °C
Thickness	4.7	µm	**e/K**	1.749399	V^{-1}	**T/T_{NI}**	0.98
			eP/K	3.44E-04	$V^{-1}\mu m$		

#	real V	Electric field per micron	Max Angle	Min Angle	tilt angle	tan ϕ
1	3.9	0.829787	364.6	359.8	2.4	0.042
2	7.8	1.659574	367.7	357.7	5	0.087
3	11.7	2.489362	370.2	355.2	7.5	0.132
4	15.6	3.319149	373.2	353.2	10	0.176
5	19.5	4.148936	375.8	351.2	12.3	0.218
6	23.4	4.978723	379	348.9	15.05	0.269
7	27.3	5.808511	382.3	346.5	17.9	0.323
8	31.2	6.638298	385	344	20.5	0.374
9	35.1	7.468085	387.5	341.4	23.05	0.426
10	39.0	8.297872	393.3	338.5	27.4	0.518

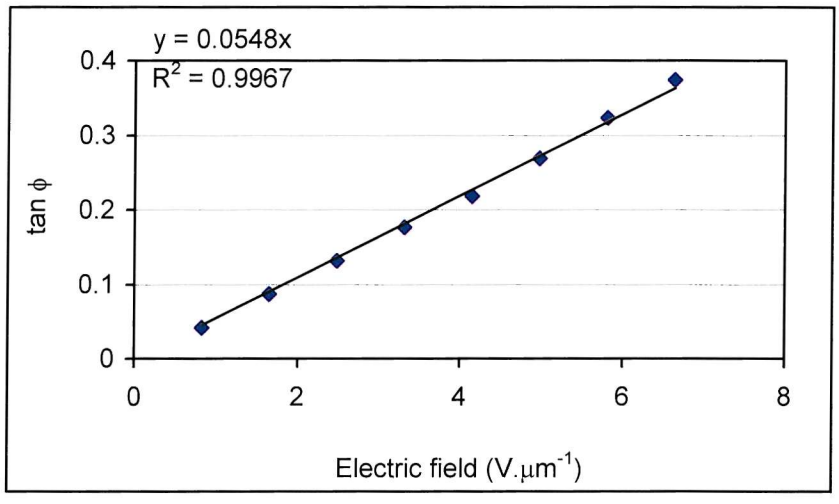

C.1.4. CBOnOBFOCF$_3$

compound **CBO4OBFOCF3** est HTP 0.163399 nm^{-1}

Vc unwin	28 V	**Gradient**	0.0442 $V^{-1}\mu m$	$\mathbf{T_{NI}}$	153 °C
pitch	452.1812 nm	**K**	0 pN	**T**	144.5 °C
Thickness	4.95 µm	**e/K**	0.614171 V^{-1}	$\mathbf{T/T_{NI}}$	0.98
		eP/K	2.78E-04 $V^{-1}\mu m$		

#	real V	Electric field per micron	Max Angle	Min Angle	tilt angle	tan ϕ
1	3.9	0.787879	35.6	28	3.8	0.07
2	7.8	1.575758	43.7	24.6	9.55	0.17
3	11.7	2.363636	45.1	23.3	10.9	0.19
4	15.6	3.151515	46.2	23.1	11.55	0.2
5	19.5	3.939394	48.5	20.6	13.95	0.25
6	23.4	4.727273	49.5	20.4	14.55	0.26
7	27.3	5.515152	0	0	0	0
8	31.2	6.30303	0	0	0	0
9	35.1	7.090909	0	0	0	0
10	39.0	7.878788	0	0	0	0

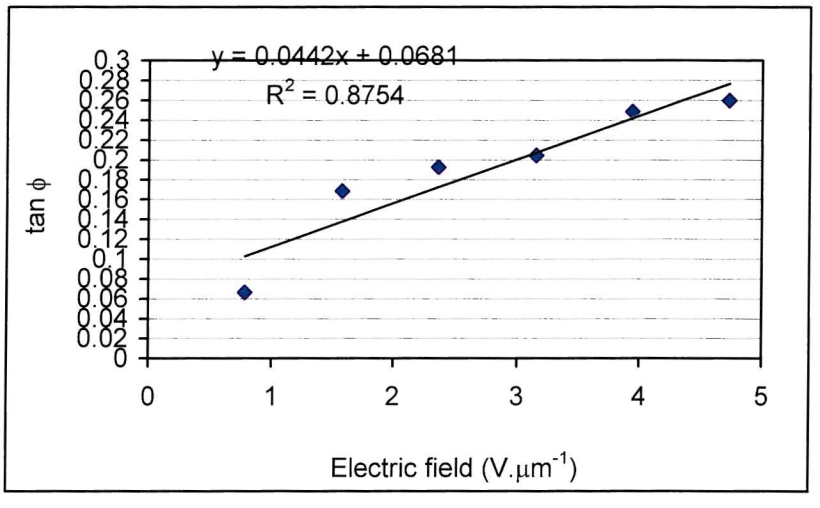

compound **CBO5OBFOCF** est HTP 0.163399 nm^{-1}

Vc unwin	80 V	**Gradient**	0.0704 $V^{-1}\mu m$	T_{NI}	89 °C
pitch	322 nm	**K**	0 pN	**T**	81.8 °C
Thickness	4.97 µm	**e/K**	1.371762 V^{-1}	T/T_{NI}	0.98
		eP/K	4.42E-04 $V^{-1}\mu m$		

#	real V	Electric field per micron	Max Angle	Min Angle	tilt angle	tan ϕ
1	7.9	1.589537	385.4	367.8	8.8	0.15
2	15.8	3.179074	394.3	363.9	15.2	0.27
3	23.7	4.768612	397.6	357.5	20.05	0.36
4	31.6	6.358149	401.8	353.8	24	0.45
5	39.5	7.947686	405.1	348.1	28.5	0.54
6	47.4	9.537223	410.3	343	33.65	0.67
7	55.3	11.12676	412.5	337.3	37.6	0.77
8	63.2	12.7163	0	0	0	0
9	71.1	14.30584	0	0	0	0
10	79.0	15.89537	0	0	0	0

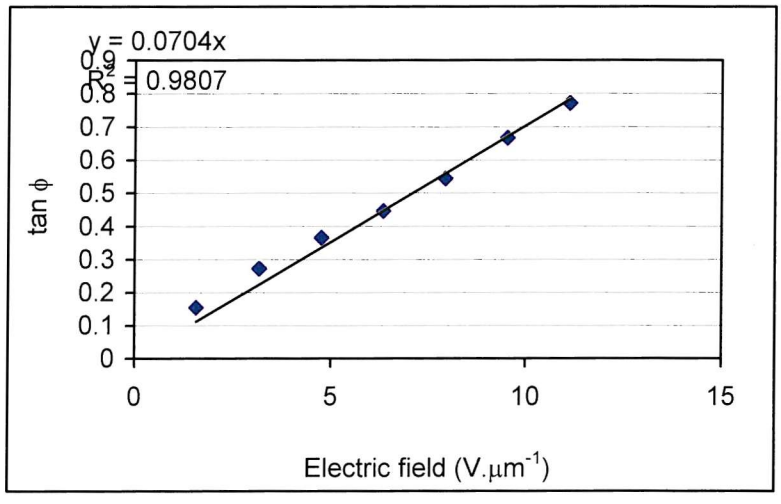

compound **CBO6OBFOCF3** est HTP 0.163399 nm^{-1}

Vc unwin	30	V	**Gradient**	0.0344	$V^{-1}\mu m$	T_{NI}	154 °C
pitch	274.3	nm	**K**	unknown	pN	**T**	145.5 °C
Thickness	4.95	µm	**e/K**	0.787984	V^{-1}	T/T_{NI}	0.98
			eP/K	2.16E-04	$V^{-1}\mu m$		

#	real V	Electric field per micron	Max Angle	Min Angle	tilt angle	tan ϕ
1	2.9	0.585859	0	0	0	0
2	5.8	1.171717	0	0	0	0
3	8.7	1.757576	0	0	0	0
4	11.6	2.343434	0	0	0	0
5	14.5	2.929293	64.8	51.3	6.75	0.118
6	17.4	3.515152	64.2	47.7	8.25	0.145
7	20.3	4.10101	67.4	47.8	9.8	0.173
8	23.2	4.686869	67	47	10	0.176
9	26.1	5.272727	0	0	0	0
10	29.0	5.858586	0	0	0	0

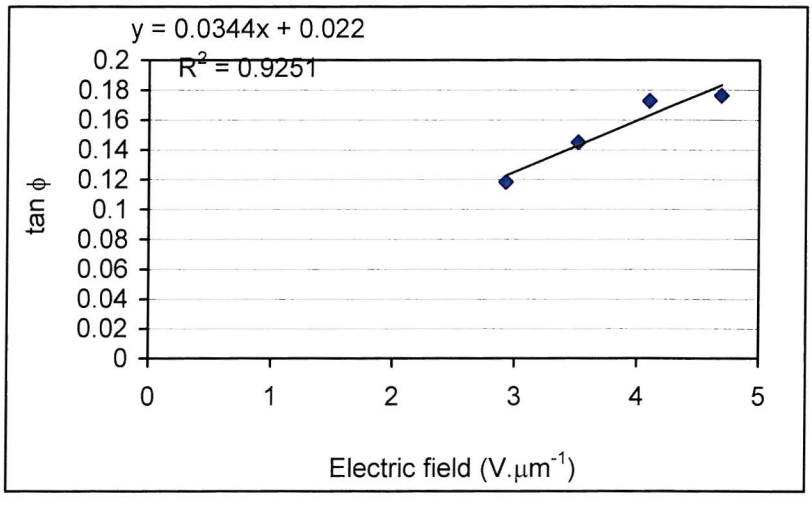

compound **CBO7OBFOCF3** est HTP 0.163399 nm^{-1}

Vc unwin	33 V	**Gradient**	0.0829 $V^{-1}\mu m$	**T_{NI}**	133 °C
pitch	285.0726 nm	**K**	0 pN	**T**	124.9 °C
Thickness	4.96 µm	**e/K**	1.82717 V^{-1}	**T/T_{NI}**	0.98
		eP/K	5.21E-04 $V^{-1}\mu m$		

#	real V	Electric field per micron	Max Angl	Min Angle	tilt angle	tan ϕ
1	3.2	0.645161	0	0	0	0
2	6.4	1.290323	0	0	0	0
3	9.6	1.935484	338.8	320.5	9.15	0.161
4	12.8	2.580645	339.5	315.4	12.05	0.213
5	16.0	3.225806	341.2	310.6	15.3	0.274
6	19.2	3.870968	344.2	308.8	17.7	0.319
7	22.4	4.516129	346.8	306.1	20.35	0.371
8	25.6	5.16129	348.9	304.9	22	0.404
9	28.8	5.806452	349.1	304.1	22.5	0.414
10	32.0	6.451613	0	0	0	0

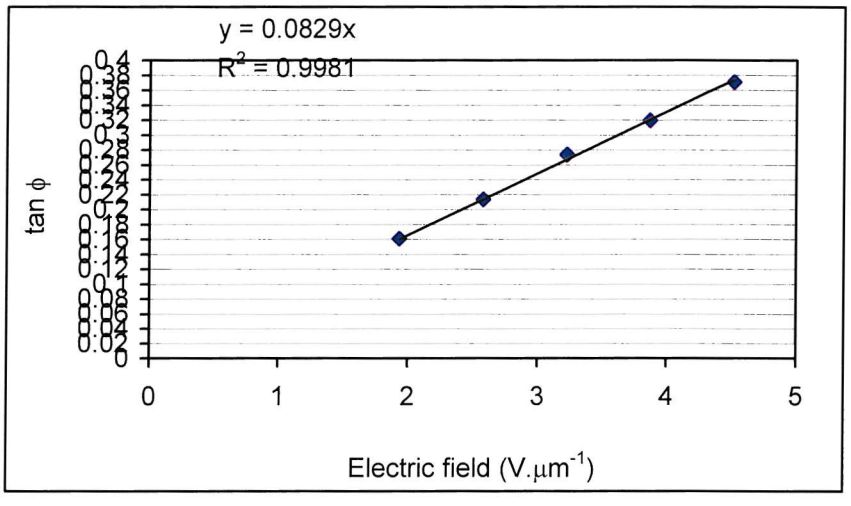

compound **CBO8OBFOCF3** est HTP 0.163399 nm^{-1}

Vc unwin	40 V	**Gradient**	0.0279 $V^{-1}\mu m$	**T_{NI}**	104 °C
pitch	400.5282 nm	**K**	unknown pN	**T**	96.5 °C
Thickness	4.95 µm	**e/K**	0.437674 V^{-1}	**T/T_{NI}**	0.98
		eP/K	1.75E-04 $V^{-1}\mu m$		

#	real V	Electric field per micron	Max Angle	Min Angle	tilt angle	tan ϕ
1	3.9	0.787879	57	53.4	1.8	0.03
2	7.8	1.575758	57.8	51	3.4	0.06
3	11.7	2.363636	58.6	49.4	4.6	0.08
4	15.6	3.151515	61.5	49.5	6	0.11
5	19.5	3.939394	62.4	49.4	6.5	0.11
6	23.4	4.727273	62.8	48	7.4	0.13
7	27.3	5.515152	63.6	47	8.3	0.15
8	31.2	6.30303	65.5	47	9.25	0.16
9	35.1	7.090909	0	0	0	0

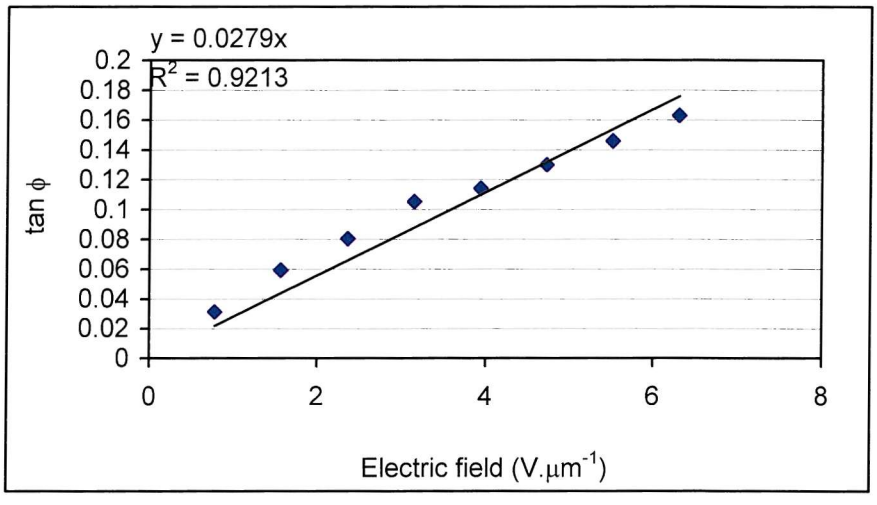

compound **CBO9OBFOCF3** est HTP 0.1634 nm^{-1}

Vc unwin	30 V	**Gradient**	0.1112 $V^{-1}\mu m$	$\mathbf{T_{NI}}$	115 °C
pitch	300.4 nm	**K**	unknown pN	**T**	107.2 °C
Thickness	5.05 µm	**e/K**	2.326 V^{-1}	$\mathbf{T/T_{NI}}$	0.98
		eP/K	6.99E-04 $V^{-1}\mu m$		

#	real V	Electric field per micron	Max Angle	Min Angl	tilt angl	tan ϕ
1	2.9	0.574257	32.3	24.3	4	0.07
2	5.8	1.148515	36	21.7	7.15	0.125
3	8.7	1.722772	41.2	19	11.1	0.196
4	11.6	2.29703	43.8	10.3	16.75	0.301
5	14.5	2.871287	47.9	12	17.95	0.324
6	17.4	3.445545	52.9	9.6	21.65	0.397
7	20.3	4.019802	52	5	23.5	0.435
8	23.2	4.594059	59.8	6.5	26.65	0.502
9	26.1	5.168317	62.3	2.9	29.7	0.57

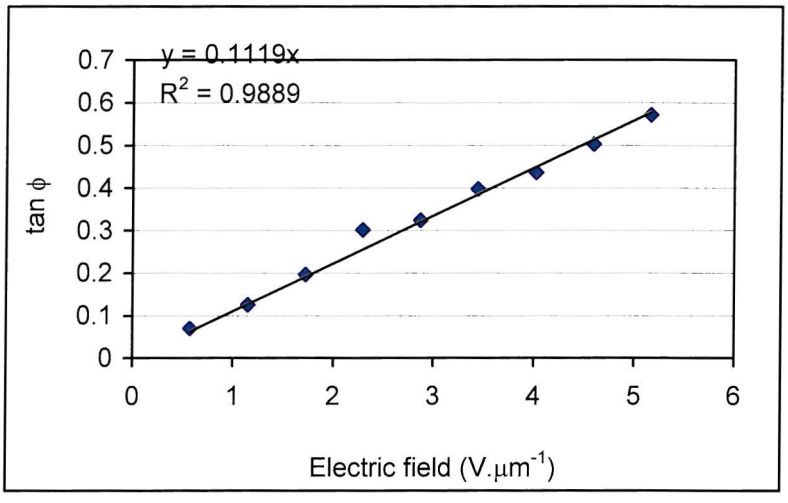

compound **CBO10OBFOCF3** est HTP 0.163399 nm^{-1}

Vc unwin	40	V	**Gradient**	0.0367	$V^{-1}\mu m$	$\mathbf{T_{NI}}$	140 °C
pitch	334.5873	nm	**K**	unknown	pN	**T**	131.7 °C
Thickness	5.05	µm	**e/K**	0.689186	V^{-1}	$\mathbf{T/T_{NI}}$	0.98
			eP/K	2.31E-04	$V^{-1}\mu m$		

#	real V	Electric field per micron	Max Angle	Min Angle	tilt angle	tan ϕ
1	3.9	0.772277	0	0	0	0
2	7.8	1.544554	0	0	0	0
3	11.7	2.316832	0	0	0	0
4	15.6	3.089109	0	0	0	0
5	19.5	3.861386	0	0	0	0
6	23.4	4.633663	0	0	0	0
7	27.3	5.405941	30	7	11.5	0.2
8	31.2	6.178218	30.7	4.5	13.1	0.23
9	35.1	6.950495	30.9	3.2	13.85	0.25
10	39.0	7.722772	0	0	0	0

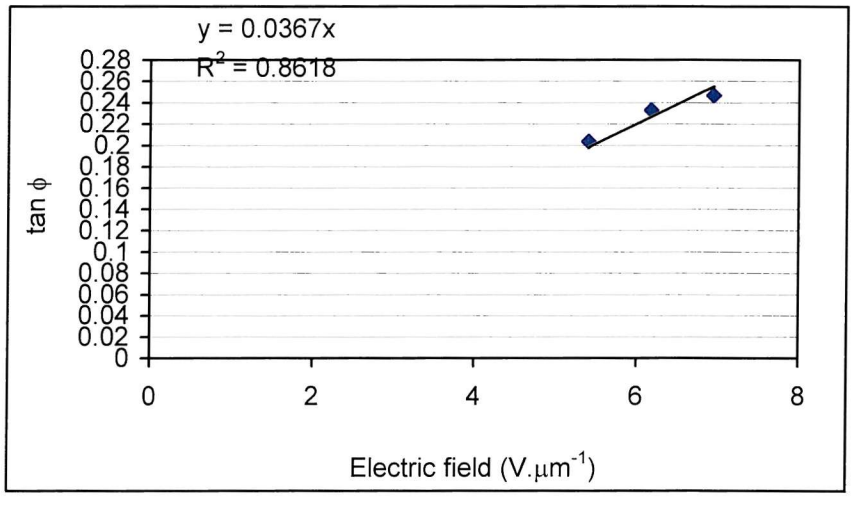

compound **CBO11OBFOCF3** est HTP 0.163399 nm^{-1}

Vc unwin	40	V	**Gradient**	0.1233	$V^{-1}\mu m$	$\mathbf{T_{NI}}$	104 °C
pitch	309.9979	nm	**K**	unknown	pN	**T**	96.5 °C
Thickness	5.05	µm	**e/K**	2.499103	V^{-1}	$\mathbf{T/T_{NI}}$	0.98
			eP/K	7.75E-04	$V^{-1}\mu m$		

#	real V	Electric field per micron	Max Angle	Min Angle	tilt angle	tan ϕ
1	3.9	0.772277	29.8	18.5	5.65	0.1
2	7.8	1.544554	35.2	13	11.1	0.2
3	11.7	2.316832	39.2	8.1	15.55	0.28
4	3.0	0.594059	23.4	13.4	5	0.09
5	5.0	0.990099	31.4	16.6	7.4	0.13
6	6.3	1.237624	33.2	16.4	8.4	0.15
7	8.8	1.732673	36.7	13	11.85	0.21
8	10.0	1.980198	38	10.5	13.75	0.24
9	12.5	2.475248	0	0	0	0
10	39.0	7.722772	0	0	0	0

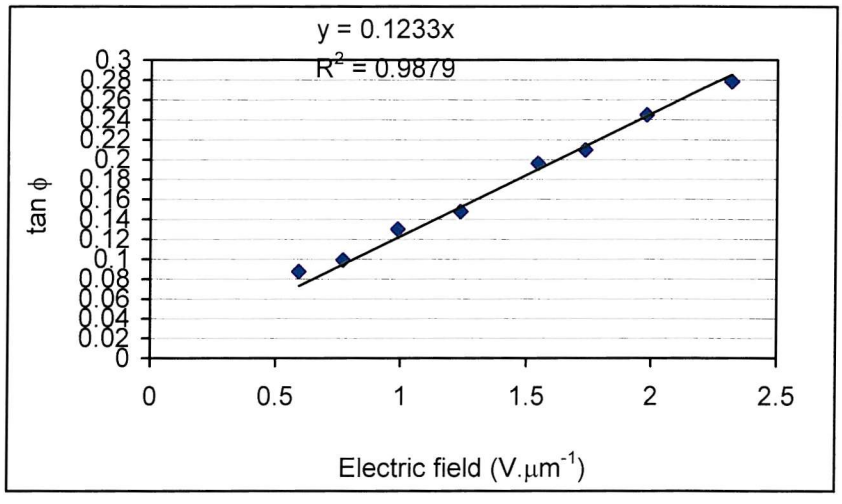

C.2. Chapter 4

C.2.1. 3CHPOnOPCH3 in E7

compound **E7** HTP E7 0.1 nm^{-1}

Vc unwin	16 V	**Gradient**	0.0302 $V^{-1}\mu m$	**T_{NI}**	80 °C
pitch	491 nm	**K**	11.6 pN	**T**	72.9 °C
Thickness	10 µm	**e/K**	0.38653 V^{-1}	**T/T_{NI}**	0.98
		e	4.48377 pCm^{-1}		
		eP/K	1.90E-04 $V^{-1}\mu m$		

#	real V	Electric field per micron	Max Angle	Min Angle	tilt angle	tan ϕ
1	1.5	0.15	0	0	0	0
2	3.0	0.3	79.2	77.8	0.7	0.012
3	4.5	0.45	79.4	77.5	0.95	0.017
4	6.0	0.6	79.8	77.2	1.3	0.023
5	7.5	0.75	79.8	76.9	1.45	0.025
6	9.0	0.9	82	78.7	1.65	0.029
7	10.5	1.05	82.1	78.5	1.8	0.031
8	12.0	1.2	82.2	78.3	1.95	0.034
9	13.5	1.35	82.3	78.1	2.1	0.037
10	15.0	1.5	0	0	0	0

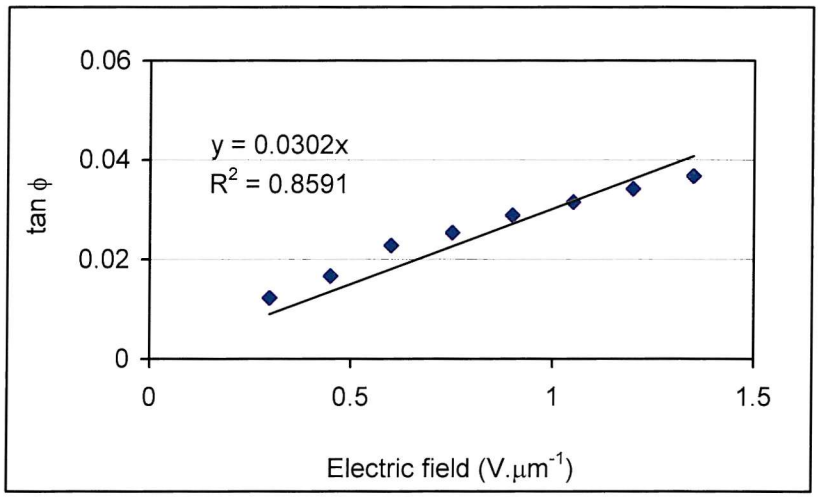

compound	**20% 3CHPO6OPCH3 in E7**	HTP E7	100 μm^{-1}	

Vc unwind	24 V	**Gradient**	0.0305 $V^{-1}\mu m$	**T_{NI}**	66 °C
pitch	522.9 nm	**K**	11.6 pN	**T**	59.2 °C
Thickness	4.94 µm	**e/K**	0.36647 V^{-1}	**T/T_{NI}**	0.98
		e	4.251055 pCm^{-1}		
		eP/K	1.92E-04 $V^{-1}\mu m$		

#	real V	Electric field per micron	Max Angle	Min Angle	tilt angle	tan ϕ
1	2.3	0.465587	276.4	274.4	1	0.02
2	4.6	0.931174	277	273.4	1.8	0.03
3	6.9	1.396761	277.7	272.4	2.65	0.05
4	9.2	1.862348	278.3	271.4	3.45	0.06
5	11.5	2.327935	278.2	270	4.1	0.07
6	13.8	2.793522	278.5	269.7	4.4	0.08
7	16.1	3.259109	279.8	268.6	5.6	0.1
8	18.4	3.724696	282.2	268	7.1	0.12
9	20.7	4.190283	282.7	268.9	6.9	0.12
10	23.0	4.65587	0	0	0	0

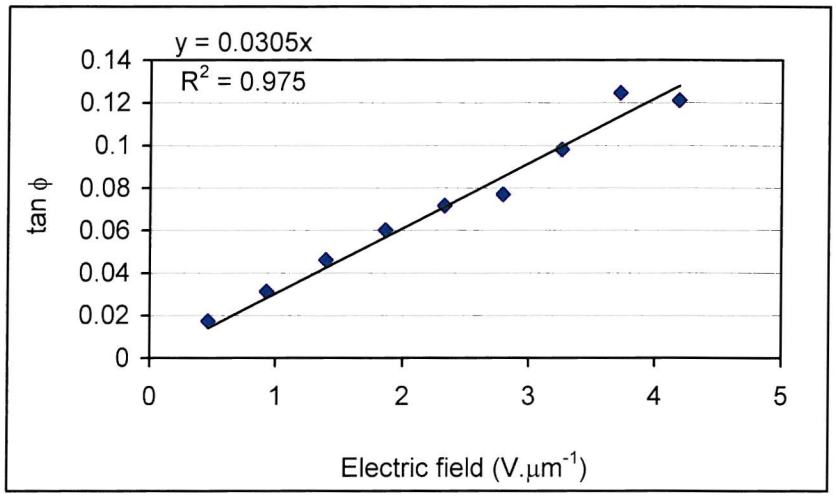

compound **20% 3CHPO7OPCH3 in E'** HTP E7 100 μm^{-1}

Vc unwind	28 V	**Gradient**	0.0233	$V^{-1}\mu m$	$\mathbf{T_{NI}}$	35	°C
pitch	597 nm	**K**	11.6	pN	**T**	28.8	°C
Thickness	4.94 µm	**e/K**	0.245429	V^{-1}	$\mathbf{T/T_{NI}}$	0.98	
		e	2.846973	pCm^{-1}			
		eP/K	1.46E-04	$V^{-1}\mu m$			

#	real V	Electric field per micron	Max Angle	Min Angle	tilt angl	tan ϕ
1	2.7	0.546559	275.3	273.5	0.9	0.02
2	5.4	1.093117	276.5	273.3	1.6	0.03
3	8.1	1.639676	275.7	271.9	1.9	0.03
4	10.8	2.186235	276.9	270.4	3.25	0.06
5	13.5	2.732794	277.3	269.7	3.8	0.07
6	16.2	3.279352	277.8	268.7	4.55	0.08
7	18.9	3.825911	278.4	268	5.2	0.09
8	21.6	4.37247	278.4	267.7	5.35	0.09
9	24.3	4.919028	279.2	267.4	5.9	0.1
10	27.0	5.465587	279.3	267.1	6.1	0.11

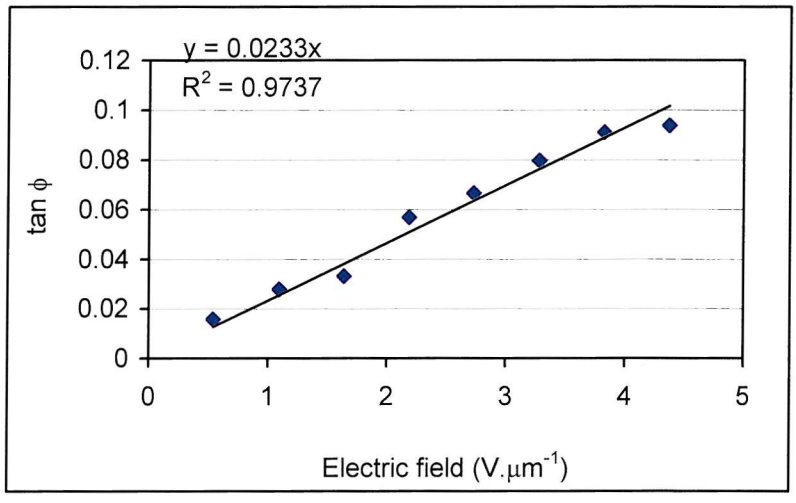

compound **20% 3CHPO8OPCH3 in E7** HTP E7 100 μm^{-1}

Vc unwin	22 V	**Gradient**	0.0261 $V^{-1}\mu m$	$\mathbf{T_{NI}}$	71 °C
pitch	526.5 nm	**K**	11.6 pN	**T**	64.1 °C
Thickness	4.94 μm	**e/K**	0.311474 V^{-1}	$\mathbf{T/T_{NI}}$	0.98
		e	3.6131 pCm^{-1}		
		eP/K	1.64E-04 $V^{-1}\mu m$		

#	real V	Electric field per micron	Max Angle	Min Angle	tilt angle	tan ϕ
1	2.1	0.425101	275.6	274.1	0.75	0.01
2	4.2	0.850202	275.9	273.3	1.3	0.02
3	6.3	1.275304	276.9	272.7	2.1	0.04
4	8.4	1.700405	277.5	272.4	2.55	0.04
5	10.5	2.125506	278.3	271.4	3.45	0.06
6	12.6	2.550607	278.6	270.8	3.9	0.07
7	14.7	2.975709	279.5	270.7	4.4	0.08
8	16.8	3.40081	279.5	269.9	4.8	0.08
9	18.9	3.825911	280.1	269.7	5.2	0.09

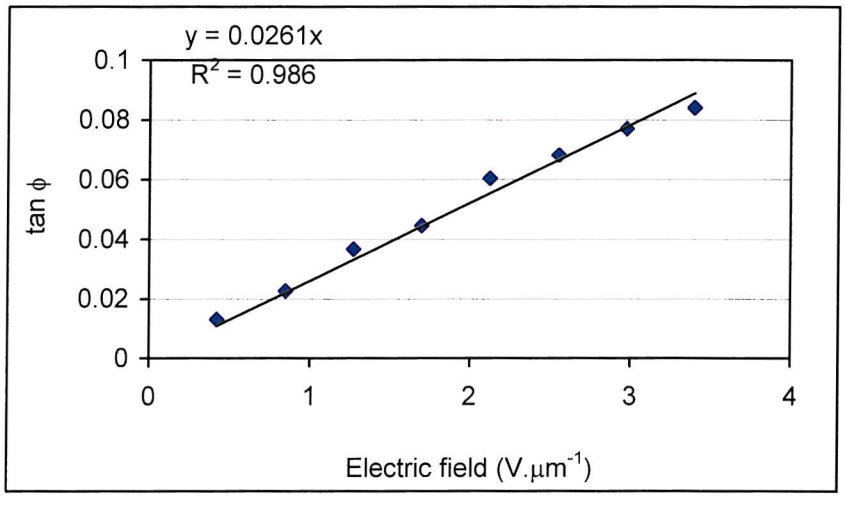

compound **20% 3CHPO9OPCH3 in E'** HTP E7 100 μm^{-1}

Vc unwin	20 V	**Gradient**	0.0107 $V^{-1}\mu m$	T_{NI}	35 °C
pitch	558.5 nm	**K**	11.6 pN	**T**	28.8 °C
Thickness	2.94 µm	**e/K**	0.12037 V^{-1}	T/T_{NI}	0.98
		e	1.39627 pCm^{-1}		
		eP/K	6.7E-05 $V^{-1}\mu m$		

#	real V	Electric field per micron	Max Angle	Min Angle	tilt angle	tan ϕ
1	1.9	0.646259	273.4	271.9	0.75	0.013
2	3.8	1.292517	274.3	271	1.65	0.029
3	5.7	1.938776	274.4	269.5	2.45	0.043
4	7.6	2.585034	275.6	269.4	3.1	0.054
5	9.5	3.231293	276	268.7	3.65	0.064
6	11.4	3.877551	276.5	268.2	4.15	0.073
7	13.3	4.52381	276.9	267.5	4.7	0.082
8	15.2	5.170068	277.3	267	5.15	0.09
9	17.1	5.816327	277.3	266.1	5.6	0.098
10	19.0	6.462585	277.3	265	6.15	0.108

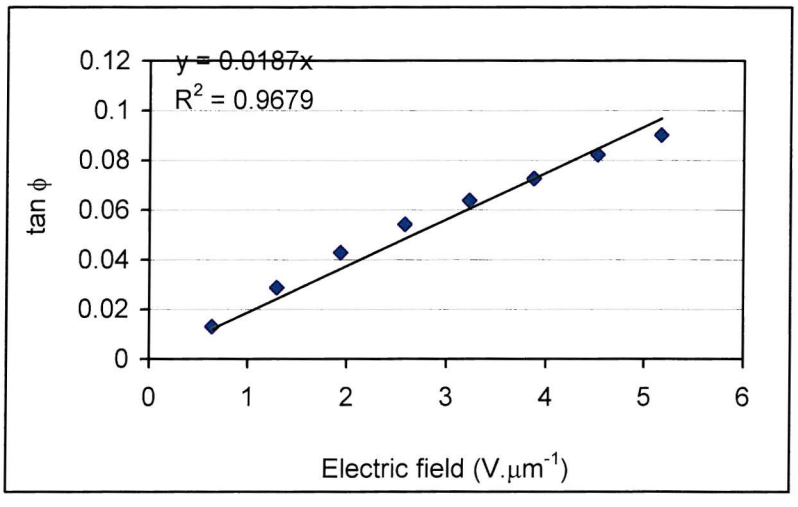

compound **20% 3CHPO10OPCH3 in I** HTP E7 100 μm^{-1}

Vc unwin	22 V	**Gradient**	0.0373 $V^{-1}\mu m$	$\mathbf{T_{NI}}$	35 °C
pitch	590.3 nm	**K**	11.6 pN	**T**	28.8 °C
Thickness	4.95 μm	**e/K**	0.39706 V^{-1}	$\mathbf{T/T_{NI}}$	0.98
		e	4.60586 pCm^{-1}		
		eP/K	2.34E-04 $V^{-1}\mu m$		

#	real V	Electric field per micron	Max Angle	Min Angle	tilt angle	tan ϕ
1	2.1	0.424242	301.8	300.7	0.55	0.0096
2	4.2	0.848485	303.2	299.4	1.9	0.0332
3	6.3	1.272727	304.8	298.2	3.3	0.0577
4	8.4	1.69697	307.6	298.6	4.5	0.0787
5	10.5	2.121212	308.5	297.7	5.4	0.0945
6	12.6	2.545455	309.2	296.9	6.15	0.1078
7	14.7	2.969697	309.9	296.3	6.8	0.1192
8	16.8	3.393939	310.3	295.8	7.25	0.1272
9	18.9	3.818182	310.6	295.6	7.5	0.1317
10	21.0	4.242424	309.2	293.7	7.75	0.1361

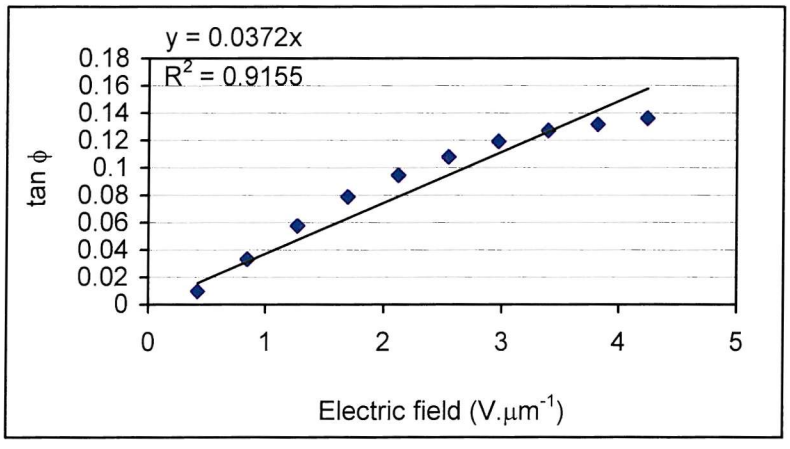

compound **20% 3CHPO11OPCH3 in E7** HTP E7 100 μm^{-1}

Vc unwin	24 V	**Gradient**	0.0259 $V^{-1}\mu m$	$\mathbf{T_{NI}}$	66 °C
pitch	497.7 nm	**K**	11.6 pN	**T**	59.2 °C
Thickness	4.94 µm	**e/K**	0.326955 V^{-1}	$\mathbf{T/T_{NI}}$	0.98
		e	3.79268 pCm^{-1}		
		eP/K	1.63E-04 $V^{-1}\mu m$		

#	real V	Electric field per micron	Max Angle	Min Angle	tilt angle	tan ϕ
1	2.3	0.465587	288.7	287.1	0.8	0.01
2	4.6	0.931174	289	285.7	1.65	0.03
3	6.9	1.396761	294	289.8	2.1	0.04
4	9.2	1.862348	291.2	285.7	2.75	0.05
5	11.5	2.327935	288.9	281.6	3.65	0.06
6	13.8	2.793522	293.2	284.3	4.45	0.08
7	16.1	3.259109	291	281.4	4.8	0.08
8	18.4	3.724696	290.7	280.5	5.1	0.09
9	20.7	4.190283	290.7	280.3	5.2	0.09
10	23.0	4.65587	0	0	0	0

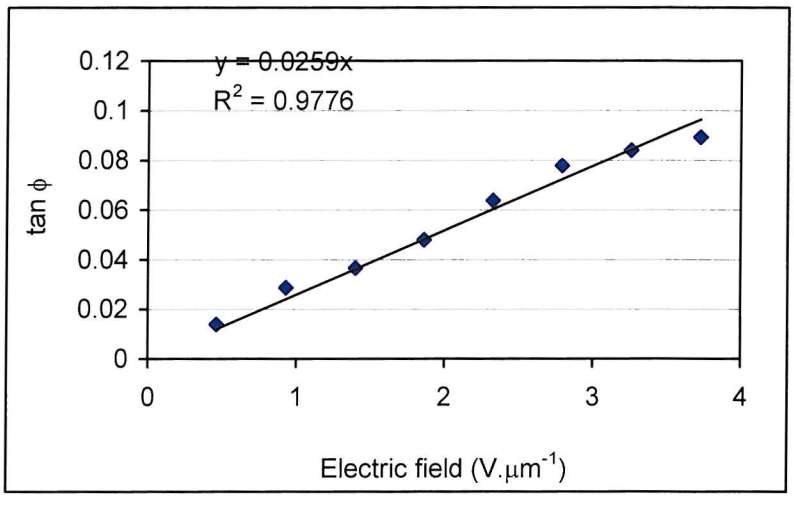

compound **20% 3CHPO12OPCH3 in** HTP E7 100 μm^{-1}

Vc unwin	16 V	**Gradient**	0.0383 $V^{-1}\mu m$	$\mathbf{T_{NI}}$	66 °C
pitch	536 nm	**K**	11.6 pN	**T**	59.2 °C
Thickness	4.99 μm	**e/K**	0.44866 V^{-1}	$\mathbf{T/T_{NI}}$	0.98
		e	5.20448 pCm^{-1}		
		eP/K	2.41E-04 $V^{-1}\mu m$		

#	real V	Electric field per micron	Max Angle	Min Angle	tilt angle	tan ϕ
1	1.5	0.300601	269.5	268.2	0.65	0.01
2	3.0	0.601202	270.5	267.6	1.45	0.03
3	4.5	0.901804	271.2	266.7	2.25	0.04
4	6.0	1.202405	272	266.7	2.65	0.05
5	7.5	1.503006	272.6	265.5	3.55	0.06
6	9.0	1.803607	273.2	265.2	4	0.07
7	10.5	2.104208	273.4	264.3	4.55	0.08
8	12.0	2.40481	273.8	263.8	5	0.09
9	13.5	2.705411	274.1	263.6	5.25	0.09
10	15.0	3.006012	274.5	263.2	5.65	0.1

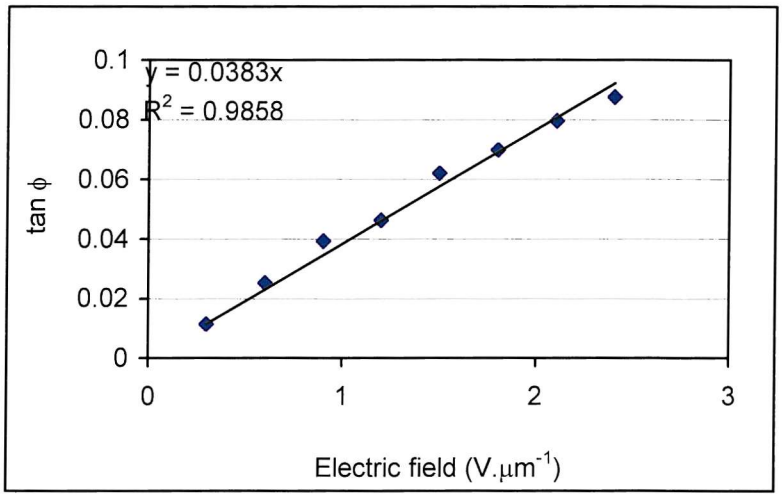

C.2.2. CBOnOPCH3

compound **CBO6OPCH3** HTP 163.3987 μm^{-1}

Vc unwin	30 V	**Gradient**	0.0269 $V^{-1}\mu m$	$\mathbf{T_{NI}}$	187 °C
pitch	308.7 nm	**K**	unknown pN	**T**	177.8 °C
Thickness	4.83 µm	**e/K**	0.547432 V^{-1}	$\mathbf{T/T_{NI}}$	0.98
		eP/K	1.69E-04 $V^{-1}\mu m$		

#	real V	Electric field per micron	Max Angle	Min Angle	tilt angle	tan ϕ
1	2.9	0.600414	257.8	255.8	1	0.02
2	5.8	1.200828	260.7	256.5	2.1	0.04
3	8.7	1.801242	268	262	3	0.05
4	11.6	2.401656	268.9	261.3	3.8	0.07
5	14.5	3.00207	269.6	259.7	4.95	0.09
6	17.4	3.602484	270.4	259	5.7	0.1
7	20.3	4.202899	271	258.8	6.1	0.11
8	23.2	4.803313	271.6	257.3	7.15	0.13
9	26.1	5.403727	271	257	7	0.12
10	29.0	6.004141	266.5	251.5	7.5	0.13

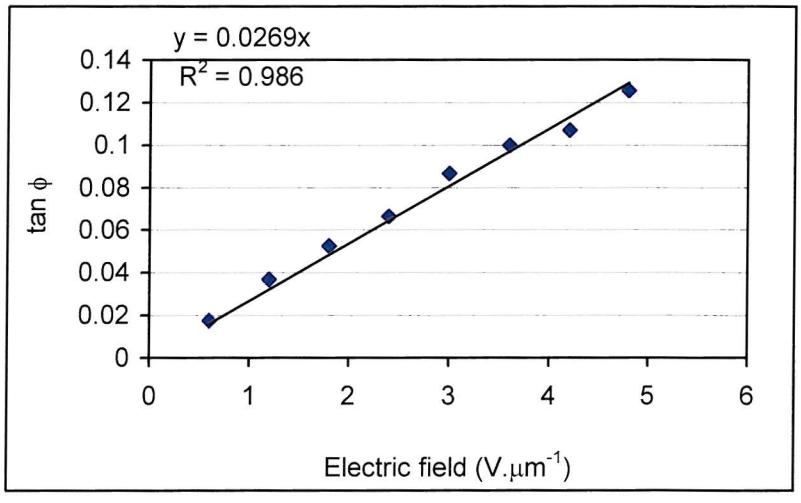

compound **CBO7OPCH3** HTP 0.163399 nm^{-1}

Vc unwin	32	V	**Gradient**	0.0389	$V^{-1}\mu m$	T_{NI}	139 °C
pitch	295.5	nm	**K**	unknown	pN	**T**	130.8 °C
Thickness	4.9	µm	**e/K**	0.82723	V^{-1}	T/T_{NI}	0.98
			eP/K	2.44E-04	$V^{-1}\mu m$		

#	real V	Electric field per micron	Max Angle	Min Angle	tilt angle	tan ϕ
1	3.1	0.632653	283.3	280.5	1.4	0.02
2	6.2	1.265306	284.8	279	2.9	0.05
3	9.3	1.897959	280	270.7	4.65	0.08
4	12.4	2.530612	285.2	273.7	5.75	0.1
5	15.5	3.163265	286.5	271.1	7.7	0.14
6	18.6	3.795918	287.4	271	8.2	0.14
7	21.7	4.428571	288.7	269	9.85	0.17
8	24.8	5.061224	290.9	269.8	10.55	0.19
9	27.9	5.693878	293	269.7	11.65	0.21
10	31.0	6.326531	294.1	268.8	12.65	0.22

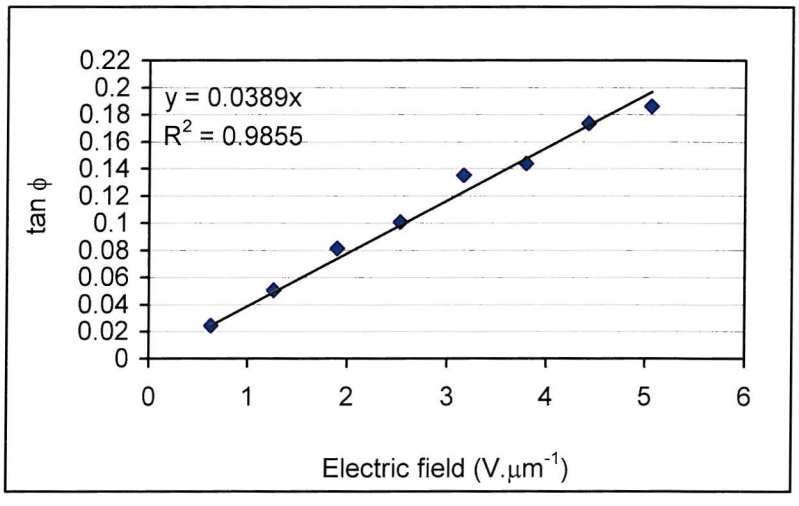

compound **CBO8OPCH3**	HTP	0.1634 nm^{-1}			
Vc unwin	35 V	**Gradient**	0.0277 $V^{-1}\mu m$	T_{NI}	170 °C
pitch	268.7 nm	**K**	unknown pN	**T**	161.1 °C
Thickness	4.89 µm	**e/K**	0.64776 V^{-1}	T/T_{NI}	0.98
		eP/K	1.74E-04 $V^{-1}\mu m$		

#	real V	Electric field per micron	Max Angle	Min Angle	tilt angle	tan ϕ
1	3.4	0.695297	271	268.8	1.1	0.02
2	6.8	1.390593	272.4	267.6	2.4	0.04
3	10.2	2.08589	273.4	266.4	3.5	0.06
4	13.6	2.781186	274.3	265.1	4.6	0.08
5	17.0	3.476483	275.1	263.8	5.65	0.1
6	20.4	4.171779	276.7	263.5	6.6	0.12
7	23.8	4.867076	277.7	263.1	7.3	0.13
8	27.2	5.562372	278.2	262.7	7.75	0.14
9	30.6	6.257669	278.7	263	7.85	0.14
10	34.0	6.952965	278.5	261.8	8.35	0.15

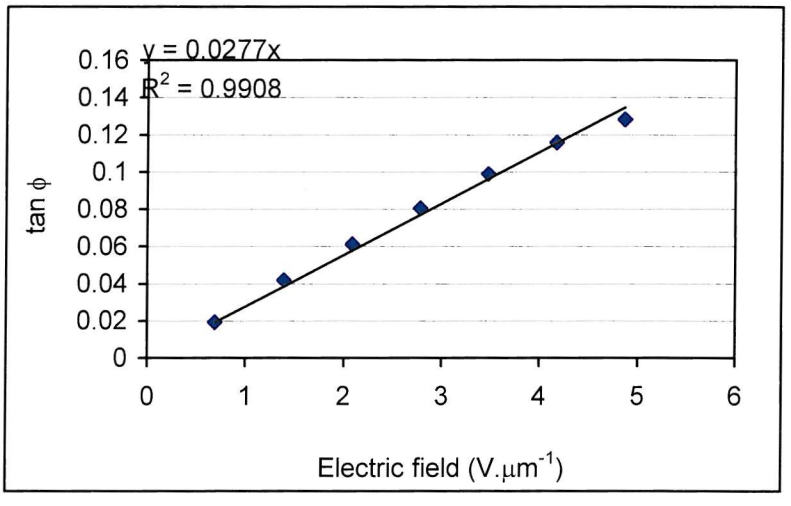

compound **CBO9OPCH3** HTP 0.163399 nm^{-1}

Vc unwin	45 V	**Gradient**	0.0307 $V^{-1}\mu m$	$\mathbf{T_{NI}}$	138 °C
pitch	232.9 nm	**K**	unknown pN	**T**	129.8 °C
Thickness	4.92 μm	**e/K**	0.828204 V^{-1}	$\mathbf{T/T_{NI}}$	0.98
		eP/K	1.93E-04 $V^{-1}\mu m$		

#	real V	Electric field per micron	Max Angle	Min Angle	tilt angle	tan ϕ
1	4.4	0.894309	268.5	265.2	1.65	0.03
2	8.8	1.788618	265.5	258.5	3.5	0.06
3	13.2	2.682927	267.3	257.3	5	0.09
4	17.6	3.577236	269	255.7	6.65	0.12
5	22.0	4.471545	270.5	254.8	7.85	0.14
6	26.4	5.365854	271.7	253	9.35	0.16
7	30.8	6.260163	273.1	251.4	10.85	0.19
8	35.2	7.154472	275	251.1	11.95	0.21
9	39.6	8.04878	278.7	252.3	13.2	0.23
10	44.0	8.943089	0	0	0	0

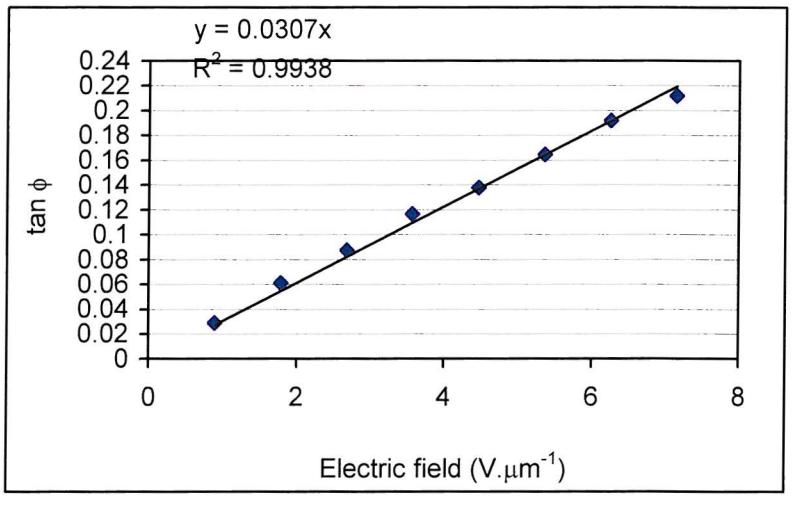

compound **CBO10OPCH3** HTP 0.163399 nm^{-1}

Vc unwin	20	V	**Gradient**	0.0423	$V^{-1}\mu m$	T_{NI}	152 °C
pitch	312.8	nm	**K**	unknown	pN	**T**	143.5 °C
Thickness	4.88	µm	**e/K**	0.849801	V^{-1}	T/T_{NI}	0.98
			eP/K	0.000266	$V^{-1}\mu m$		

#	real V	Electric field per micron	Max Angle	Min Angle	tilt angle	tan ϕ
1	1.9	0.389344	0	0	0	0
2	3.8	0.778689	0	0	0	0
3	5.7	1.168033	0	0	0	0
4	7.6	1.557377	302	294.4	3.8	0.07
5	9.5	1.946721	303.5	294.7	4.4	0.08
6	11.4	2.336066	306.8	294.9	5.95	0.1
7	13.3	2.72541	307	293.6	6.7	0.12
8	15.2	3.114754	308.5	293.5	7.5	0.13
9	17.1	3.504098	310	293.4	8.3	0.15
10	19.0	3.893443	311.9	294.7	8.6	0.15

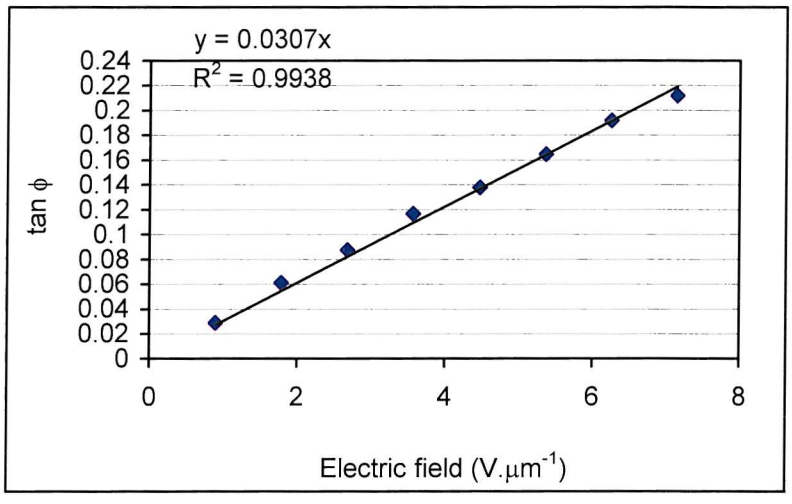

compound **CBO11OPCH3** est HTP 0.163399 nm^{-1}

Vc unwind	33	V	Gradient	0.0391	$V^{-1}\mu m$	T_{NI}	135 °C
pitch	295.7	nm	K	0	pN	T	126.8 °C
Thickness	4.97	µm	e/K	0.830949	V^{-1}	T/T_{NI}	0.98
			eP/K	2.46E-04	$V^{-1}\mu m$		

#	real V	Electric field per micron	Max Angle	Min Angle	tilt angle	tan ϕ
1	3.2	0.643863	244	240.7	1.65	0.028806
2	6.4	1.287726	245.4	239	3.2	0.055909
3	9.6	1.93159	246.6	237.3	4.65	0.081336
4	12.8	2.575453	247.7	235.5	6.1	0.106869
5	16.0	3.219316	249.9	235.1	7.4	0.129877
6	19.2	3.863179	251.2	234	8.6	0.151236
7	22.4	4.507042	252	232.4	9.8	0.17273
8	25.6	5.150905	253.5	231.5	11	0.19438
9	28.8	5.794769	254	230.2	11.9	0.210733
10	32.0	6.438632	255.3	228.9	13.2	0.234548

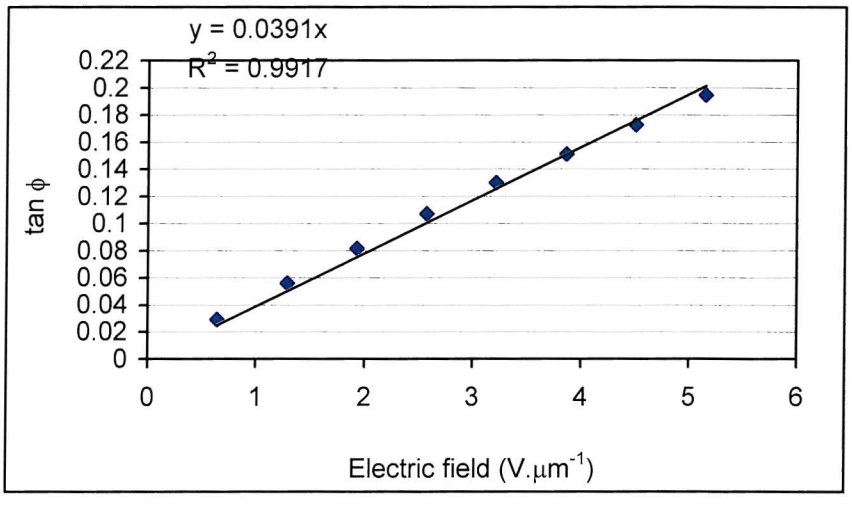

compound **CBO12OPCH3** HTP 163.3987 μm^{-1}

Vc unwin	39 V	**Gradient**	0.023 $V^{-1}\mu m$	T_{NI}	145 °C
pitch	204 nm	**K**	0 pN	**T**	136.6 °C
Thickness	4.9 µm	**e/K**	0.707654 V^{-1}	T/T_{NI}	0.98
		eP/K	1.45E-04 $V^{-1}\mu m$		

#	real V	Electric field per micron	Max Angle	Min Angle	tilt angle	tan ϕ
1	3.8	0.77551	277.7	275.3	1.2	0.02
2	7.6	1.55102	277.9	273.5	2.2	0.04
3	11.4	2.326531	279.7	272.9	3.4	0.06
4	15.2	3.102041	280.9	272.8	4.05	0.07
5	19.0	3.877551	283.2	272.8	5.2	0.09
6	22.8	4.653061	284.4	271.7	6.35	0.11
7	26.6	5.428571	284.6	270.8	6.9	0.12
8	30.4	6.204082	285.5	269.7	7.9	0.14
9	34.2	6.979592	283.5	266	8.75	0.15
10	38.0	7.755102	281	259.9	10.55	0.19

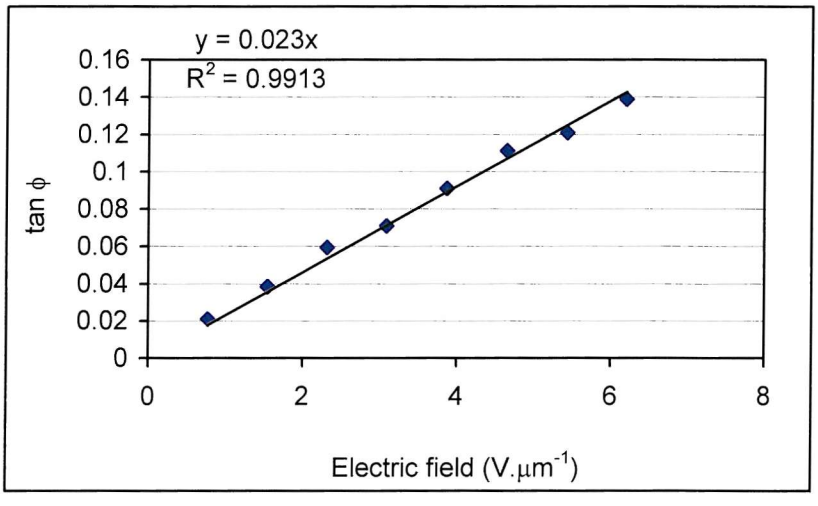

C.2.3. CBO11OPCH3/3CHPO11OPCH3

compound **3CHPO7OPCH3/OCB 20/80** est HTP 163 μm^{-1}

Vc unwin	30 V	**Gradient**	0.0418 $V^{-1}\mu m$	**T_{NI}**	131 °C
pitch	242 nm	**K**	unknown pN	**T**	122.9 °C
Thickness	4.95 µm	**e/K**	1.08542 V^{-1}	**T/T_{NI}**	0.98
		eP/K	2.63E-04 $V^{-1}\mu m$		

#	real V	Electric field per micron	Max Angle	Min Angle	tilt angle	tan ϕ
1	2.9	0.585859	0	0	0	0
2	5.8	1.171717	284.9	278.9	3	0.05
3	8.7	1.757576	285.2	275.8	4.7	0.08
4	11.6	2.343434	284.6	273.6	5.5	0.1
5	14.5	2.929293	288.4	275	6.7	0.12
6	17.4	3.515152	291.7	274	8.85	0.16
7	20.3	4.10101	290.5	271.9	9.3	0.16
8	23.2	4.686869	286.9	269.6	8.65	0.15
9	26.1	5.272727	289	268.7	10.15	0.18
10	29.0	5.858586	289.5	269	10.25	0.18

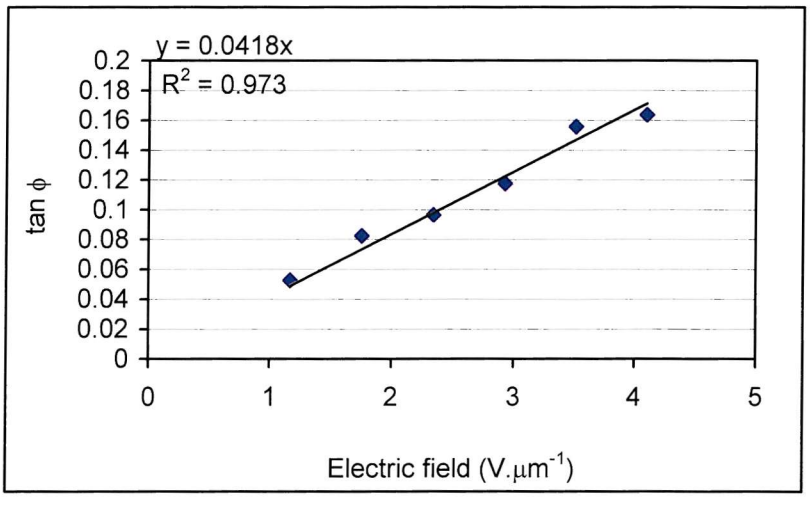

compound **3CHPO11OPCH3/OCB 40/6(** HTP 163 μm^{-1}

Vc unwin(	28 V	**Gradient**	0.0323 $V^{-1}\mu m$	$\mathbf{T_{NI}}$	126 °C
pitch	313 nm	**K**	0 pN	**T**	118 °C
Thickness	4.95 µm	**e/K**	0.64898 V^{-1}	$\mathbf{T/T_{NI}}$	0.98
		eP/K	2.03E-04 $V^{-1}\mu m$		

#	real V	Electric field per micron	Max Angle	Min Angl	tilt angle	tan ϕ
1	2.7	0.545455	0	0	0	0
2	5.4	1.090909	293	288.5	2.25	0.04
3	8.1	1.636364	294.3	287.5	3.4	0.06
4	10.8	2.181818	294.9	286.6	4.15	0.07
5	13.5	2.727273	297.1	286.6	5.25	0.09
6	16.2	3.272727	298.1	285.5	6.3	0.11
7	18.9	3.818182	299	285	7	0.12
8	21.6	4.363636	299.7	284.3	7.7	0.14
9	24.3	4.909091	301.3	283.7	8.8	0.15
10	27.0	5.454545	302	283.7	9.15	0.16

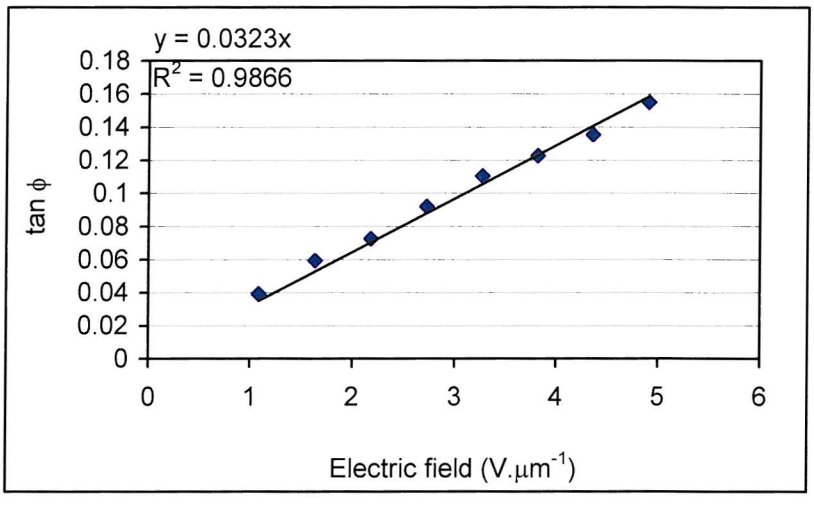

compound **3CHPO11OPCH3/OCB 60/4(** HTP 163 μm^{-1}

Vc unwin(	45 V	**Gradient**	0.0114 $V^{-1}\mu m$	$\mathbf{T_{NI}}$	120 °C
pitch	312.7 nm	**K**	0 pN	**T**	112 °C
Thickness	4.95 μm	**e/K**	0.229052 V^{-1}	$\mathbf{T/T_{NI}}$	0.98
		eP/K	7.16E-05 $V^{-1}\mu m$		

#	real V	Electric field per micror	Max Angle	Min Angle	tilt angle	tan ϕ
1	4.4	0.888889	252.9	251.7	0.6	0.01
2	8.8	1.777778	253.4	251	1.2	0.021
3	13.2	2.666667	254.3	250.4	1.95	0.034
4	17.6	3.555556	255.2	249.7	2.75	0.048
5	22.0	4.444444	255.5	249	3.25	0.057
6	26.4	5.333333	256.2	249.4	3.4	0.059
7	30.8	6.222222	256.5	248.9	3.8	0.066
8	35.2	7.111111	256.3	247	4.65	0.081
9	39.6	8	255.4	245.5	4.95	0.087
10	44.0	8.888889	254.6	243.3	5.65	0.099

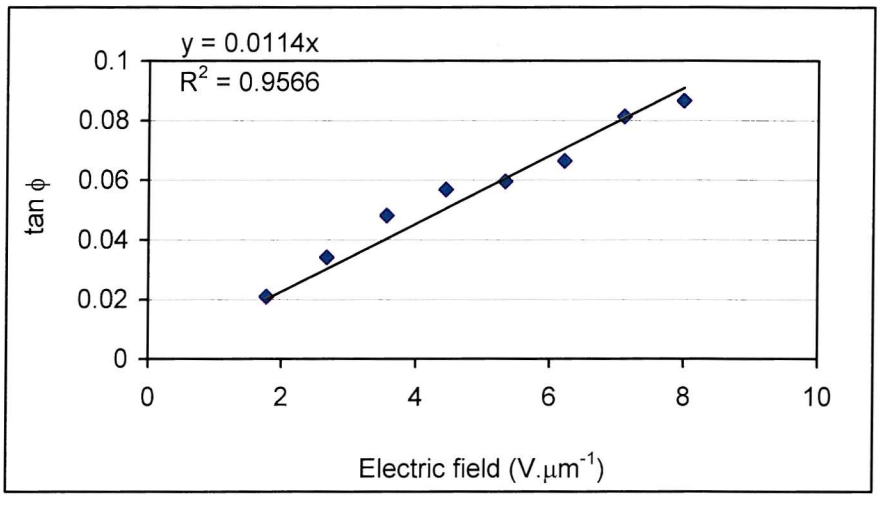

C.2.4. CBOnOPCH7

compound **CBO4OPCH7** est HTP 163.399 μm^{-1}

Vc unwin	13	V	**Gradient**	0.03	$V^{-1}\mu m$	T_{NI}	199 °C
pitch	283.1	nm	**K**	unknown	pN	**T**	189.6 °C
Thickness	4.97	µm	**e/K**	0.66577	V^{-1}	T/T_{NI}	0.98
			eP/K	1.88E-04	$V^{-1}\mu m$		

#	real V	Electric field per micron	Max Angle	Min Angl	tilt angle	tan ϕ
1	1.2	0.241449	250.2	248.7	0.75	0.013
2	2.4	0.482897	250.1	247	1.55	0.027
3	3.6	0.724346	251.3	247	2.15	0.038
4	4.8	0.965795	252	246	3	0.052
5	6.0	1.207243	252.9	245.6	3.65	0.064
6	7.2	1.448692	252.2	244	4.1	0.072
7	8.4	1.690141	253.1	244.1	4.5	0.079
8	9.6	1.93159	253.6	243.4	5.1	0.089
9	10.8	2.173038	254.3	243	5.65	0.099
10	12.0	2.414487	254.8	242.4	6.2	0.109

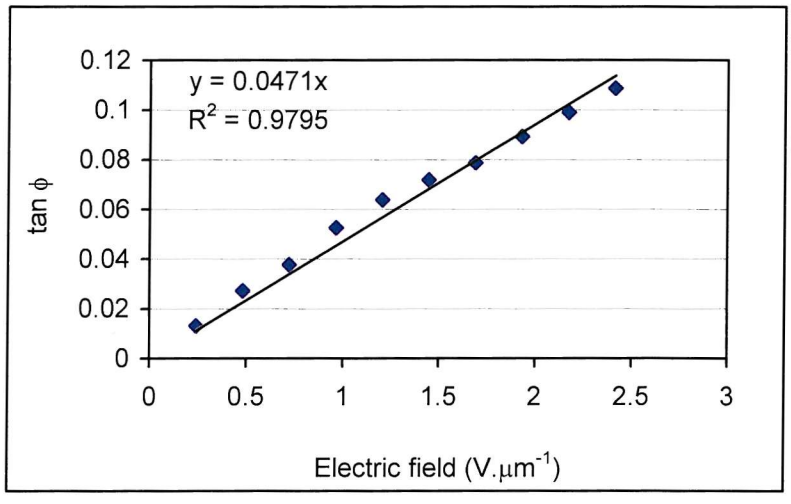

compound **CBO6OPCH7** est HTP 163.3987 μm^{-1}

Vc unwind	28	V	Gradient	0.0332	$V^{-1}\mu m$	T_{NI}	172 °C
pitch	274	nm	K	unknown	pN	T	163.1 °C
Thickness	4.97	µm	e/K	0.761675	V^{-1}	T/T_{NI}	0.98
			eP/K	2.09E-04	$V^{-1}\mu m$		

#	real V	Electric field per micron	Max Angle	Min Angle	tilt angle	tan ϕ
1	2.7	0.54326	271.9	269.6	1.15	0.02
2	5.4	1.086519	272.8	268.5	2.15	0.04
3	8.1	1.629779	274	267.2	3.4	0.06
4	10.8	2.173038	274.9	266.4	4.25	0.07
5	13.5	2.716298	275.6	265	5.3	0.09
6	16.2	3.259557	276.8	264	6.4	0.11
7	18.9	3.802817	277.5	263.2	7.15	0.13
8	21.6	4.346076	277.5	262	7.75	0.14
9	24.3	4.889336	278	261.5	8.25	0.14
10	27.0	5.432596	278.8	261.4	8.7	0.15

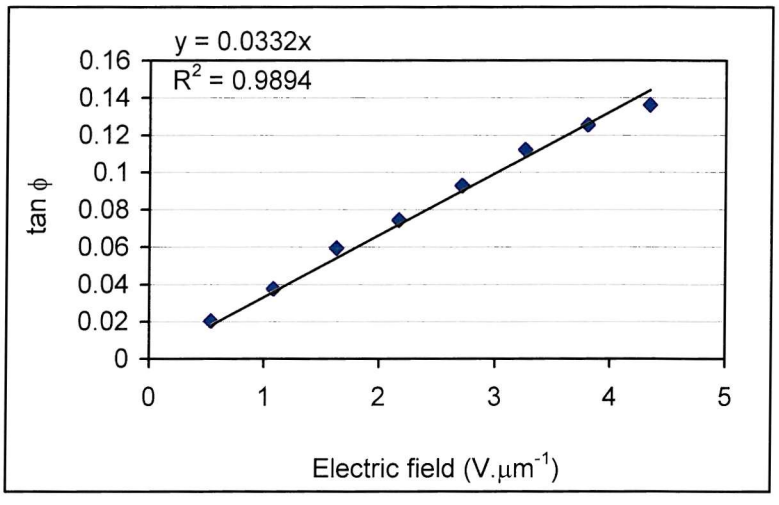

compound **CBO7OPCH7** est HTP 163.3987 μm^{-1}

Vc unwin	25 V	**Gradient**	0.0342 $V^{-1}\mu m$	$\mathbf{T_{NI}}$	124 °C
pitch	322 nm	**K**	0 pN	**T**	116 °C
Thickness	4.96 μm	**e/K**	0.667691 V^{-1}	$\mathbf{T/T_{NI}}$	0.98
		eP/K	0.000215 $V^{-1}\mu m$		

#	real V	Electric field per micron	Max Angle	Min Angle	tilt angle	tan ϕ
1	2.4	0.483871	258.5	256.4	1.05	0.02
2	4.8	0.967742	259.9	255.9	2	0.03
3	7.2	1.451613	260.3	254.4	2.95	0.05
4	9.6	1.935484	261.4	253.5	3.95	0.07
5	12.0	2.419355	262.5	252.7	4.9	0.09
6	14.4	2.903226	263.5	251.9	5.8	0.1
7	16.8	3.387097	264.1	251.6	6.25	0.11
8	19.2	3.870968	265.2	249.9	7.65	0.13
9	21.6	4.354839	265.8	249	8.4	0.15
10	24.0	4.83871	268.6	250	9.3	0.16

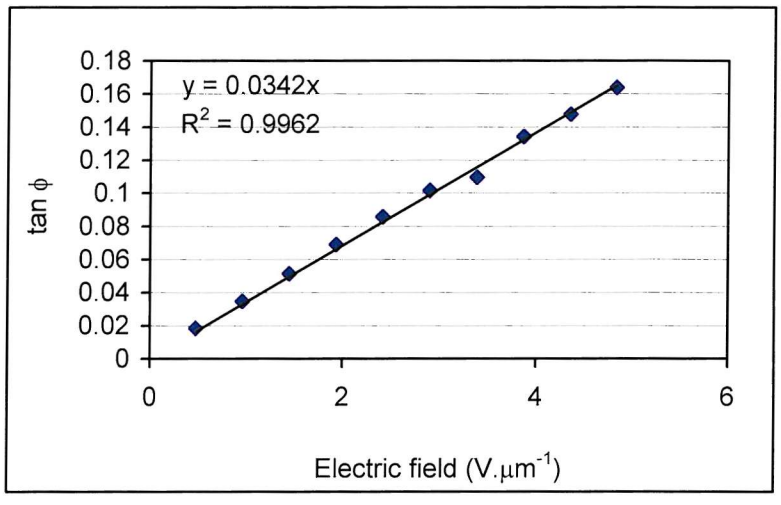

compound **CBO8OPCH7** est HTP 163.3987 μm^{-1}

Vc unwin	26	V	**Gradient**	0.0347	$V^{-1}\mu m$	T_{NI}	153 °C
pitch	321	nm	**K**	unknown	pN	**T**	144.5 °C
Thickness	4.97	µm	**e/K**	0.679311	V^{-1}	T/T_{NI}	0.98
			eP/K	2.18E-04	$V^{-1}\mu m$		

#	real V	Electric field per micron	Max Angle	Min Angle	tilt angle	tan ϕ
1	2.5	0.503018	262.2	259.7	1.25	0.02
2	5.0	1.006036	263.7	259.3	2.2	0.04
3	7.5	1.509054	264	257.6	3.2	0.06
4	10.0	2.012072	265.4	256.6	4.4	0.08
5	12.5	2.515091	265.5	255.1	5.2	0.09
6	15.0	3.018109	265	253	6	0.11
7	17.5	3.521127	265	251.5	6.75	0.12
8	20.0	4.024145	264.6	249.4	7.6	0.13
9	22.5	4.527163	263.1	246.8	8.15	0.14
10	25.0	5.030181	255.3	238.2	8.55	0.15

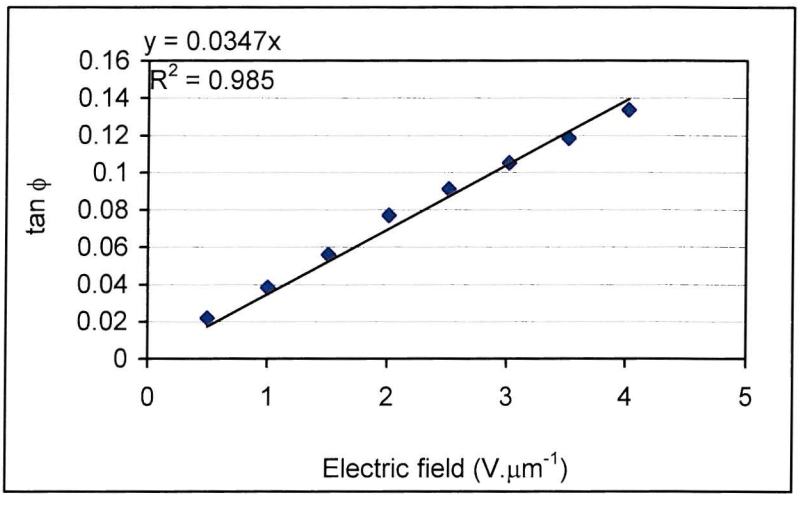

compound **CBO9OPCH7** est HTP 163.39869 μm^{-1}

Vc unwin	26 V	**Gradient**	0.0435 $V^{-1}\mu m$	T_{NI}	140 °C
pitch	317.3 nm	**K**	unknown pN	**T**	132 °C
Thickness	4.97 µm	**e/K**	0.0008615 V^{-1}	T/T_{NI}	0.98
		eP/K	2.733E-07 $V^{-1}\mu m$		

#	real V	Electric field per micron	Max Angle	Min Angle	tilt angle	tan ϕ
1	2.5	0.503018	311.6	308.9	1.35	0.02
2	5.0	1.006036	314.9	309.5	2.7	0.05
3	7.5	1.509054	315.8	308.5	3.65	0.06
4	10.0	2.012072	317	306.4	5.3	0.09
5	12.5	2.515091	317.5	305.3	6.1	0.11
6	15.0	3.018109	319.7	304.1	7.8	0.14
7	17.5	3.521127	315.6	297.9	8.85	0.16
8	20.0	4.024145	321.7	301.5	10.1	0.18
9	22.5	4.527163	322.8	300.2	11.3	0.2
10	25.0	5.030181	323.7	299.1	12.3	0.22

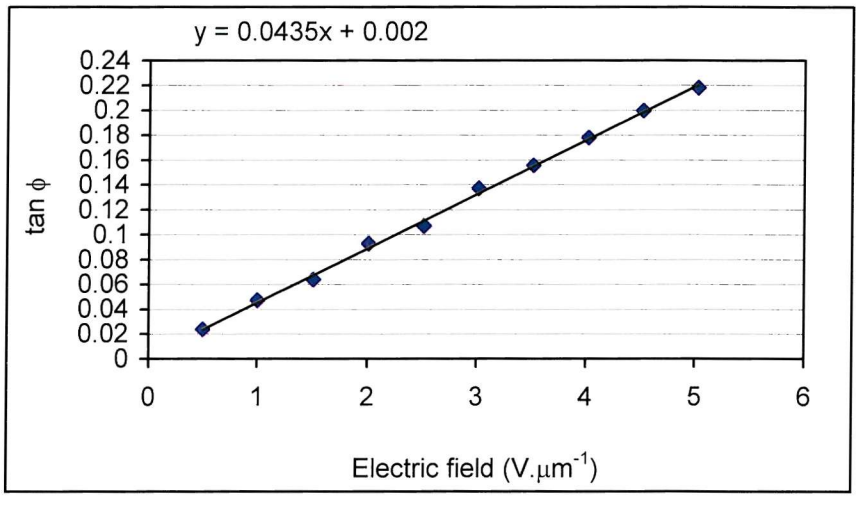

compound **CBO10OPCH7** est HTP 163.39869 μm^{-1}

Vc unwin	26 V	**Gradient**	0.0356 $V^{-1}\mu m$	**T_{NI}**	146 °C
pitch	314.6 nm	**K**	unknown pN	**T**	138 °C
Thickness	4.97 µm	**e/K**	0.7109782 V^{-1}	**T/T_{NI}**	0.98
		eP/K	2.24E-04 $V^{-1}\mu m$		

#	real V	Electric field per micron	Max Angle	Min Angle	tilt angle	tan φ
1	2.5	0.503018	301.8	298.7	1.55	0.027
2	5.0	1.006036	301.9	297.7	2.1	0.037
3	7.5	1.509054	305.5	299.4	3.05	0.053
4	10.0	2.012072	308.2	299.7	4.25	0.074
5	12.5	2.515091	312.3	301.8	5.25	0.092
6	15.0	3.018109	316.4	304.1	6.15	0.108
7	17.5	3.521127	318	304.7	6.65	0.117
8	20.0	4.024145	321.3	304.6	8.35	0.147
9	22.5	4.527163	322	303.5	9.25	0.163
10	25.0	5.030181	327.6	303.4	12.1	0.214

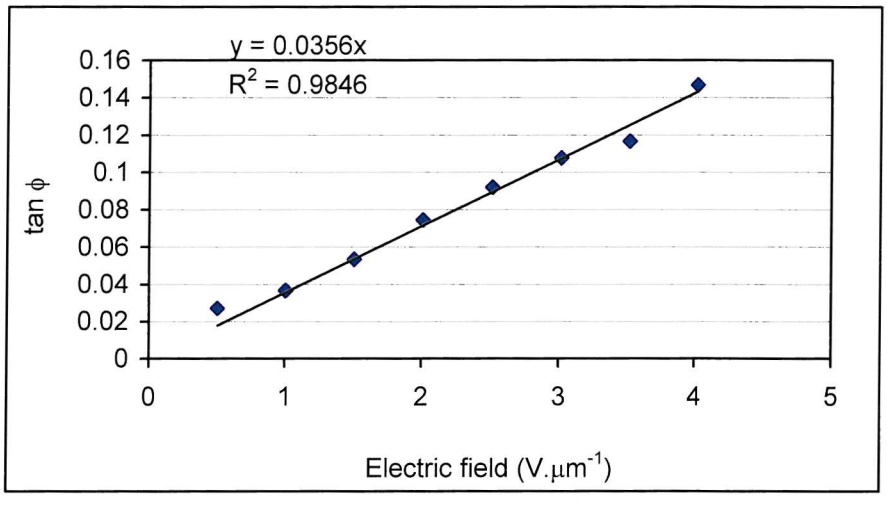

compound **CBO11OPCH7** est HTP 163.39869 μm^{-1}

Vc unwin	26 V	**Gradient**	0.0394 $V^{-1}\mu m$	T_{NI}	127 °C
pitch	305.2 nm	**K**	0 pN	**T**	119 °C
Thickness	4.57 μm	**e/K**	0.811141 V^{-1}	T/T_{NI}	0.98
		eP/K	0.0002476 $V^{-1}\mu m$		

#	real V	Electric field per micron	Max Angle	Min Angle	tilt angle	tan ϕ
1	2.5	0.547046	251.9	249.3	1.3	0.023
2	5.0	1.094092	252.7	247.8	2.45	0.043
3	7.5	1.641138	253.3	245.8	3.75	0.066
4	10.0	2.188184	254.4	244	5.2	0.091
5	12.5	2.73523	254.7	242.5	6.1	0.107
6	15.0	3.282276	257.8	242.6	7.6	0.133
7	17.5	3.829322	256.6	239.9	8.35	0.147
8	20.0	4.376368	258.9	239.6	9.65	0.17
9	22.5	4.923414	260	238.2	10.9	0.193
10	25.0	5.47046	261.3	236.7	12.3	0.218

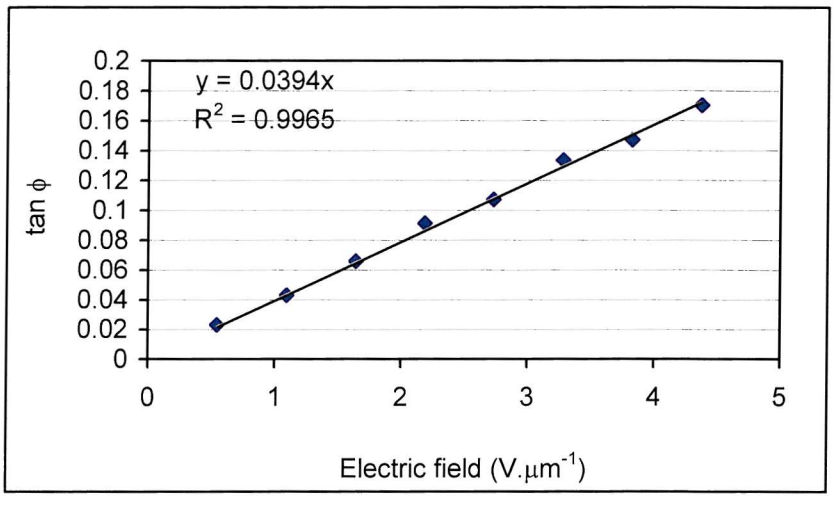

compound **CBO12OPCH7** est HTP 163.399 μm^{-1}

Vc unwin	43	V	**Gradient**	0.0217	$V^{-1}\mu m$	$\mathbf{T_{NI}}$	137 °C
pitch	136.1	nm	**K**	unknown	pN	**T**	129 °C
Thickness	4.97	µm	**e/K**	1.0015	V^{-1}	$\mathbf{T/T_{NI}}$	0.98
			eP/K	1.36E-04	$V^{-1}\mu m$		

#	real V	Electric field per micron	Max Angle	Min Angl	tilt angle	tan ϕ
1	4.2	0.84507	247.6	245.6	1	0.017
2	8.4	1.690141	247.8	243.3	2.25	0.039
3	12.6	2.535211	250.1	243	3.55	0.062
4	16.8	3.380282	250.5	241.6	4.45	0.078
5	21.0	4.225352	251.4	240.4	5.5	0.096
6	25.2	5.070423	252.4	239.8	6.3	0.11
7	29.4	5.915493	256.8	242.5	7.15	0.125
8	33.6	6.760563	262.6	246.6	8	0.141
9	37.8	7.605634	254.7	238	8.35	0.147
10	42.0	8.450704	254.5	236.6	8.95	0.157

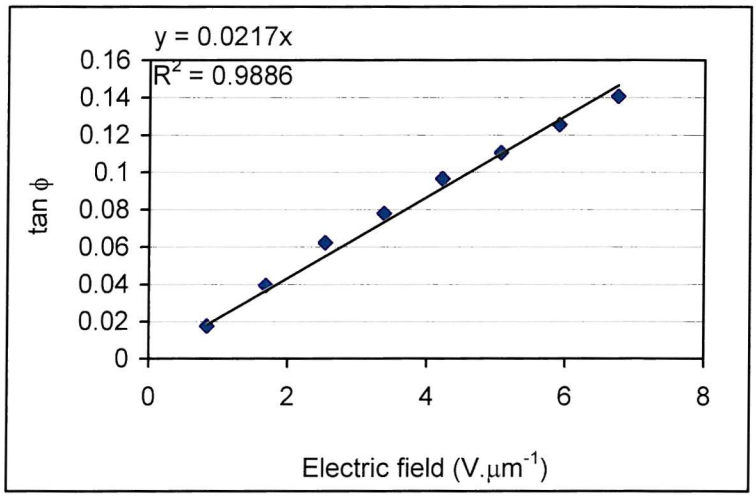

Appendix D

Orientational Ordering Data for Anthracene Dissolved in Liquid Crystal Hosts

"Piled Higher and Deeper" by Jorge Cham
www.phdcomics.com

Used with permission

D. Appendix D

D.1. CBO9OCB

The order parameters S_{zz}, S_{xx}, S_{yy} and the biaxial ordering S_{xx}-S_{yy} for per-deuterated anthracene dissolved in CBO9OCB.

Temperature /°C	$(T_{NI}-T)$	$\Delta\upsilon_{\beta}$ /kHz	$\Delta\upsilon_{\alpha,\gamma}$ /kHz	S_{zz}	S_{xx}	S_{yy}	S_{xx}-S_{yy}
170	-1	0.0	0.0	0.000	0.000	0.000	0.000
168	0	56.9	-15.1	0.291	-0.068	-0.223	0.156
167	1	62.2	-16.9	0.319	-0.076	-0.243	0.168
166	2	65.0	-18.4	0.334	-0.082	-0.252	0.171
165	3	67.8	-19.8	0.349	-0.088	-0.262	0.174
164	4	70.1	-21.0	0.362	-0.092	-0.269	0.177
163	5	72.1	-22.2	0.373	-0.097	-0.276	0.178
162	6	73.9	-23.2	0.383	-0.101	-0.281	0.180
161	7	75.4	-24.2	0.391	-0.105	-0.286	0.180
160	8	76.9	-25.2	0.400	-0.110	-0.290	0.181
159	9	78.3	-26.0	0.407	-0.113	-0.295	0.182
158	10	79.7	-26.9	0.415	-0.116	-0.299	0.182
156	12	81.9	-28.4	0.428	-0.122	-0.305	0.183

Plot of S_{zz} and S_{xx}-S_{yy} for per-deuterated anthracene dissolved in CBO9OCB.

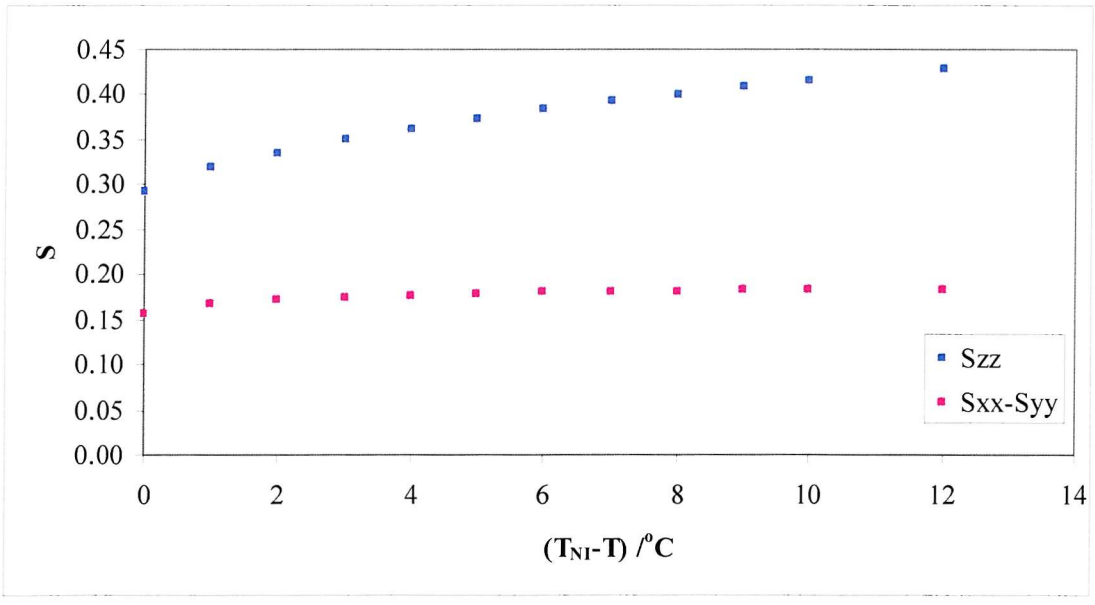

Plot of S_{zz}, S_{xx} and S_{yy} for per-deuterated anthracene dissolved in CBO9OCB.

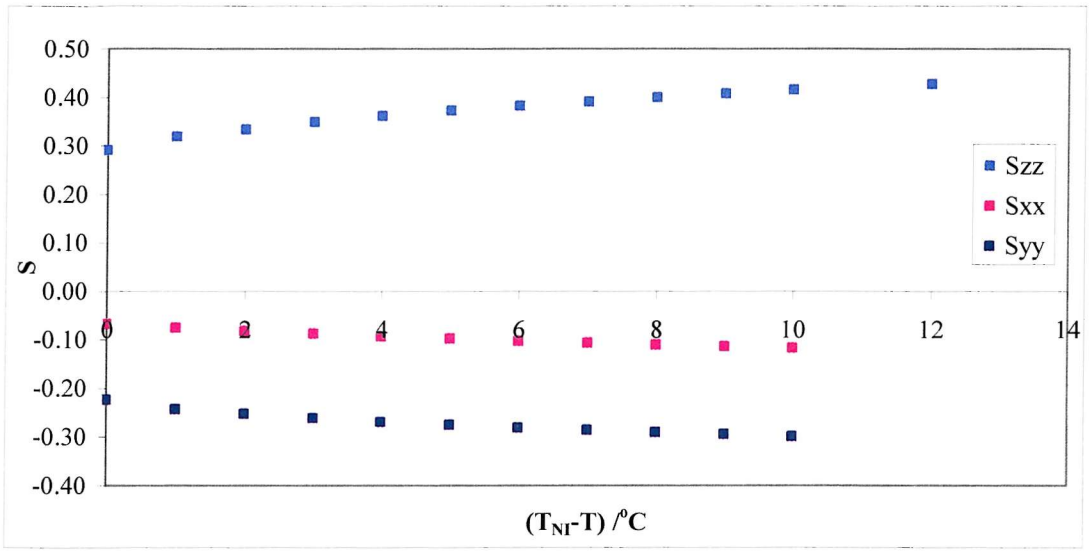

D.2. CBO9OBF$_2$

The order parameters S_{zz}, S_{xx}, S_{yy} and the biaxial ordering S_{xx}-S_{yy} for per-deuterated anthracene dissolved in CBO9OBF$_2$.

Temperature /°C	(T_{NI}-T)	$\Delta\upsilon_\beta$ /kHz	$\Delta\upsilon_{\alpha,\gamma}$ /kHz	S_{zz}	S_{xx}	S_{yy}	S_{xx}-S_{yy}
111	-1	0.0	0.0	0.000	0.000	0.000	0.000
110	0	48.0	-13.9	0.247	-0.062	-0.186	0.124
109	1	55.7	-16.7	0.287	-0.074	-0.214	0.140
108	2	60.1	-18.7	0.311	-0.082	-0.229	0.147
108	2	60.1	-18.7	0.311	-0.082	-0.229	0.147
107	3	63.5	-20.3	0.329	-0.089	-0.241	0.152
106	4	66.2	-21.7	0.344	-0.094	-0.250	0.155
105	5	68.5	-22.9	0.357	-0.099	-0.257	0.158
104	6	70.6	-24.1	0.368	-0.104	-0.264	0.160
103	7	72.4	-25.1	0.378	-0.108	-0.270	0.162
102	8	74.1	-26.1	0.388	-0.112	-0.275	0.163
101	9	75.6	-27.1	0.396	-0.116	-0.280	0.163
102	8	74.1	-26.2	0.388	-0.113	-0.275	0.162
101	9	75.7	-27.1	0.396	-0.116	-0.280	0.164
100	10	77.2	-28.1	0.405	-0.120	-0.284	0.164
99	11	78.6	-29.0	0.413	-0.124	-0.289	0.165
98	12	79.8	-29.8	0.420	-0.127	-0.292	0.165
96	14	82.2	-31.4	0.433	-0.134	-0.299	0.166
94	16	84.3	-33.0	0.445	-0.140	-0.305	0.165
92	18	86.3	-34.5	0.457	-0.146	-0.311	0.164
92	18	86.3	-34.5	0.457	-0.146	-0.311	0.164
90	20	88.1	-35.9	0.467	-0.152	-0.315	0.164
88	22	89.8	-37.3	0.477	-0.157	-0.320	0.162
86	24	91.4	-38.6	0.486	-0.162	-0.324	0.161
84	26	92.9	-39.9	0.495	-0.168	-0.328	0.160
82	28	94.3	-41.1	0.503	-0.172	-0.331	0.159
80	30	95.7	-42.3	0.512	-0.177	-0.335	0.157
78	32	96.9	-43.7	0.519	-0.183	-0.337	0.154
76	34	98.3	-44.9	0.527	-0.187	-0.340	0.153
74	36	99.3	-46.0	0.534	-0.192	-0.342	0.150
72	38	100.5	-47.1	0.541	-0.196	-0.345	0.149
72	38	100.5	-47.1	0.541	-0.196	-0.345	0.149
70	40	101.5	-48.3	0.547	-0.201	-0.346	0.146
68	42	101.6	-49.3	0.549	-0.205	-0.344	0.140

Plot of S_{zz} and S_{xx}-S_{yy} for per-deuterated anthracene dissolved in CBO9OBF$_2$.

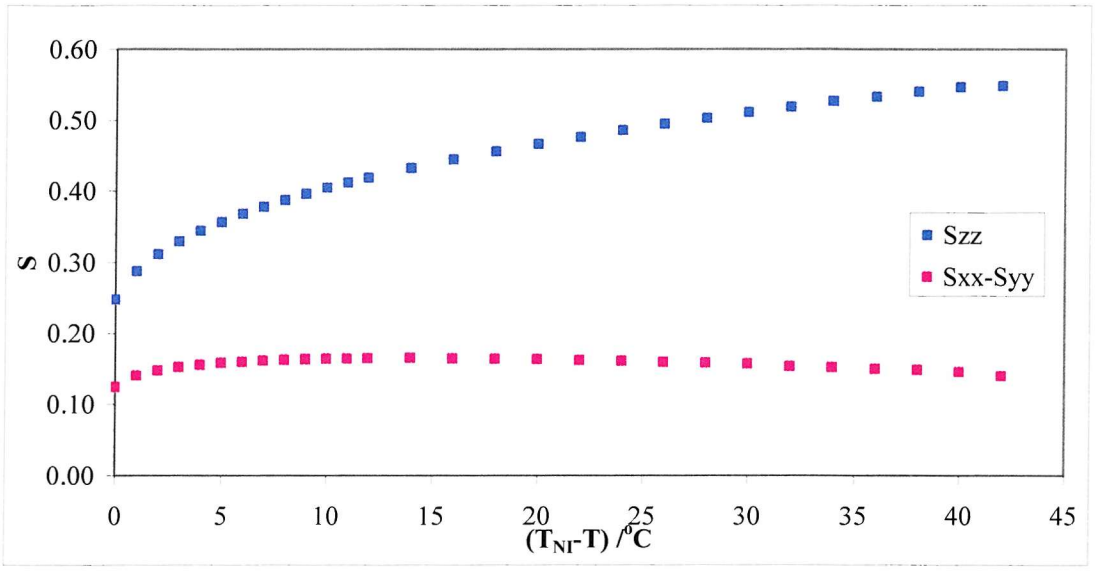

Plot of S_{zz}, S_{xx} and S_{yy} for per-deuterated anthracene dissolved in CBO9OBF$_2$.

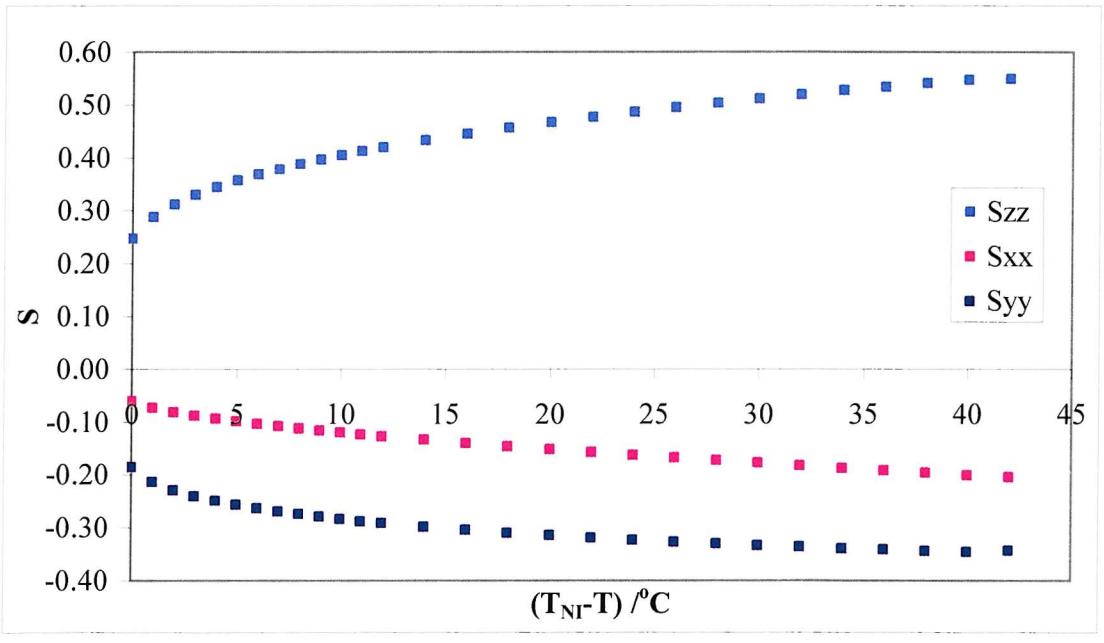

D.3. CBO9OBFOCF$_3$

The order parameters S_{zz}, S_{xx}, S_{yy} and the biaxial ordering S_{xx}-S_{yy} for per-deuterated anthracene dissolved in CBO9OBFOCF$_3$.

Temperature /°C	(T_{NI}-T)	$\Delta\upsilon_\beta$ /kHz	$\Delta\upsilon_{\alpha,\gamma}$ /kHz	S_{zz}	S_{xx}	S_{yy}	S_{xx}-S_{yy}
102	0	45.6	-15.0	0.237	-0.065	-0.172	0.107
101	1	55.1	-18.3	0.287	-0.079	-0.207	0.128
100	2	59.9	-20.5	0.312	-0.089	-0.224	0.135
99	3	63.3	-22.3	0.331	-0.096	-0.235	0.139
98	4	66.1	-23.8	0.346	-0.102	-0.244	0.142
97	5	68.7	-25.2	0.361	-0.108	-0.253	0.145
96	6	70.9	-26.5	0.373	-0.113	-0.260	0.146
95	7	72.9	-27.7	0.384	-0.118	-0.266	0.148
94	8	74.7	-28.8	0.394	-0.123	-0.271	0.149
93	9	76.3	-29.9	0.403	-0.127	-0.276	0.149
92	10	77.9	-30.9	0.412	-0.131	-0.281	0.150
91	11	79.3	-31.9	0.420	-0.135	-0.285	0.150
90	12	80.7	-32.8	0.428	-0.139	-0.289	0.150
88	14	83.1	-34.7	0.442	-0.146	-0.295	0.149
86	16	85.3	-36.4	0.454	-0.153	-0.301	0.148
84	18	87.4	-38.0	0.466	-0.159	-0.307	0.148
82	20	89.4	-39.6	0.478	-0.166	-0.312	0.146
80	22	91.0	-41.1	0.488	-0.172	-0.316	0.144
78	24	92.8	-42.6	0.498	-0.178	-0.321	0.143

Plot of S_{zz} and S_{xx}-S_{yy} for per-deuterated anthracene dissolved in CBO9OBFOCF$_3$.

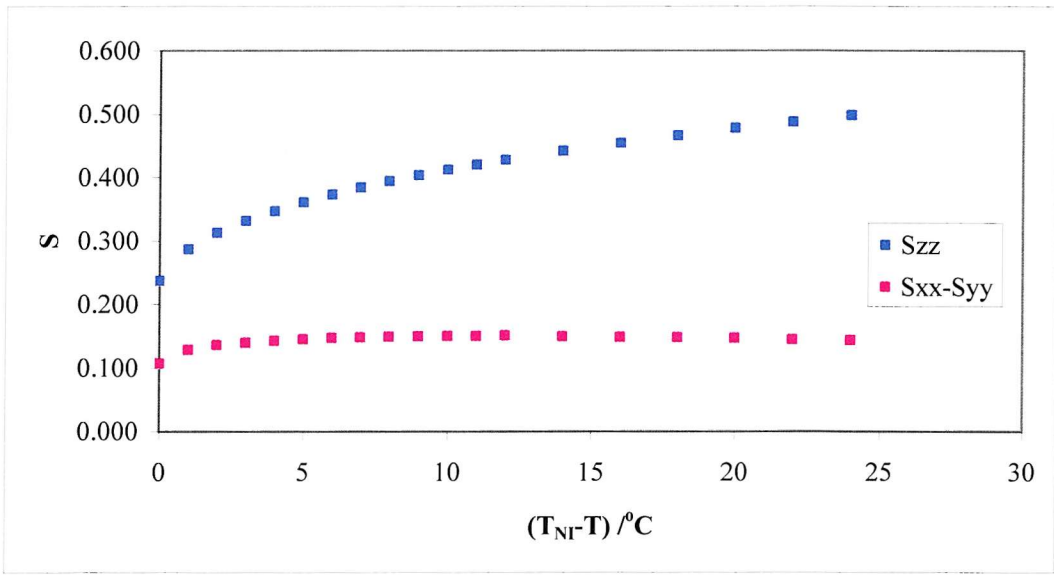

Plot of S_{zz}, S_{xx} and S_{yy} for per-deuterated anthracene dissolved in CBO9OBFOCF$_3$.

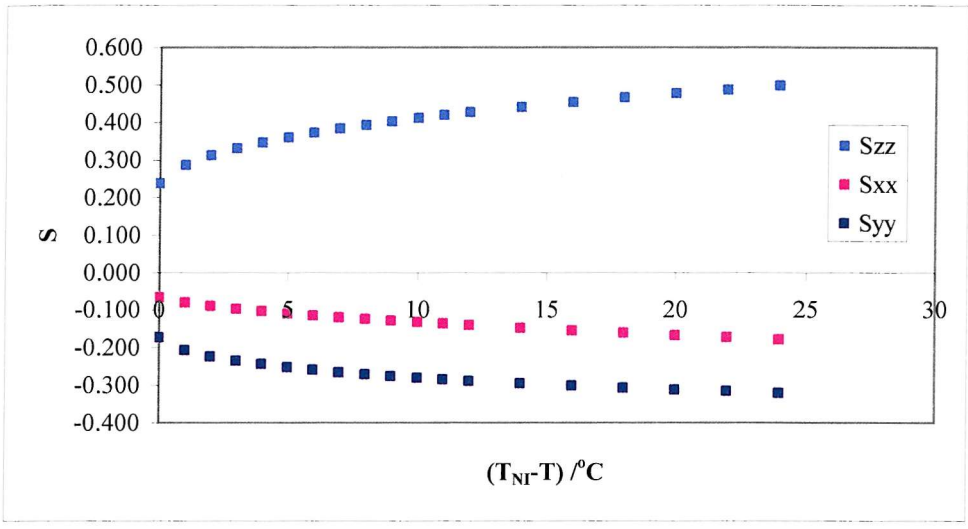

D.4. CBO9OBF$_3$

The order parameters S_{zz}, S_{xx}, S_{yy} and the biaxial ordering S_{xx}-S_{yy} for per-deuterated anthracene dissolved in CBO9OBF$_3$.

Temperature /°C	$(T_{NI}-T)$	$\Delta\upsilon_\beta$ /kHz	$\Delta\upsilon_{\alpha,\gamma}$ /kHz	S_{zz}	S_{xx}	S_{yy}	S_{xx}-S_{yy}
86	-1	0.0	0.0	0.000	0.000	0.000	0.000
85	0	37.8	-11.0	0.195	-0.049	-0.146	0.097
84	1	44.4	-13.1	0.229	-0.058	-0.171	0.113
83	2	51.3	-15.7	0.265	-0.069	-0.196	0.127
82	4	59.1	-19.1	0.307	-0.083	-0.224	0.140
81	3	55.7	-17.5	0.289	-0.077	-0.212	0.135
80	5	61.9	-20.3	0.322	-0.088	-0.234	0.145
80	5	61.9	-20.5	0.322	-0.089	-0.233	0.144
80	5	62.0	-20.7	0.323	-0.090	-0.233	0.143
79	6	64.4	-21.7	0.335	-0.094	-0.242	0.148
79	6	64.5	-21.9	0.336	-0.095	-0.242	0.147
78	7	66.7	-22.9	0.348	-0.099	-0.249	0.150
78	7	66.7	-22.9	0.348	-0.099	-0.249	0.150
77	8	68.7	-24.1	0.359	-0.104	-0.255	0.152
77	8	68.7	-24.1	0.359	-0.104	-0.255	0.152
76	9	70.5	-25.1	0.369	-0.108	-0.261	0.153
76	9	70.5	-25.1	0.369	-0.108	-0.261	0.153
75	10	72.1	-26.0	0.378	-0.112	-0.266	0.155
75	10	72.3	-26.1	0.379	-0.112	-0.267	0.155
74	11	73.6	-26.5	0.386	-0.114	-0.272	0.158
74	11	73.8	-26.9	0.387	-0.115	-0.272	0.157
73	12	75.3	-27.7	0.395	-0.119	-0.277	0.158
72	13	76.5	-28.3	0.402	-0.121	-0.281	0.160
70	15	79.0	-29.8	0.416	-0.127	-0.289	0.161

Plot of S_{zz} and S_{xx}-S_{yy} for per-deuterated anthracene dissolved in CBO9OBF$_3$.

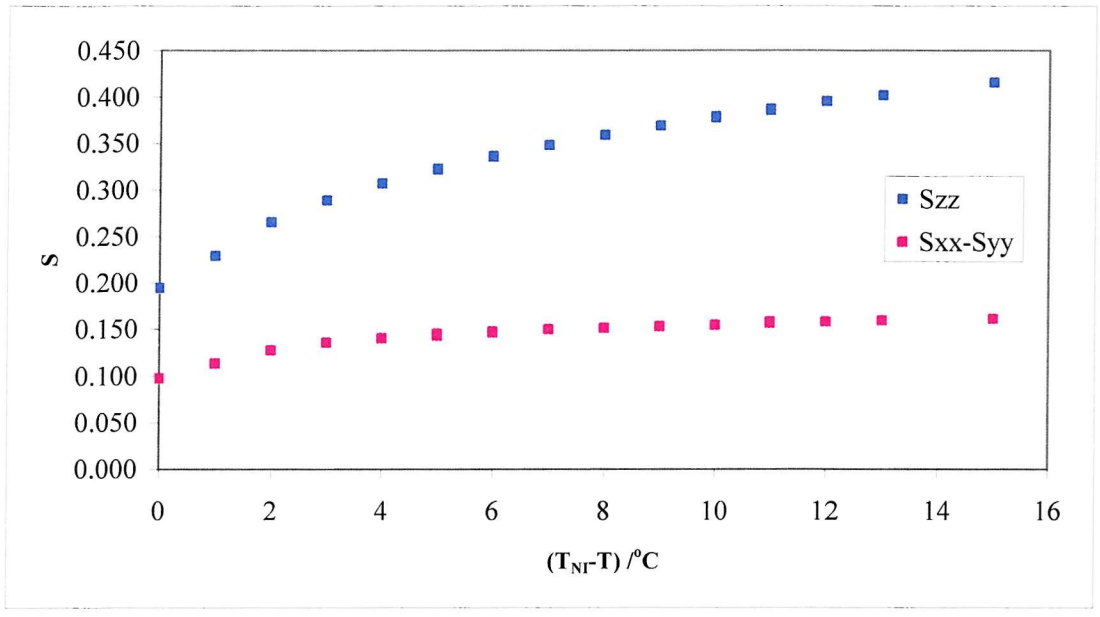

Plot of S_{zz}, S_{xx} and S_{yy} for per-deuterated anthracene dissolved in CBO9OBF$_3$.

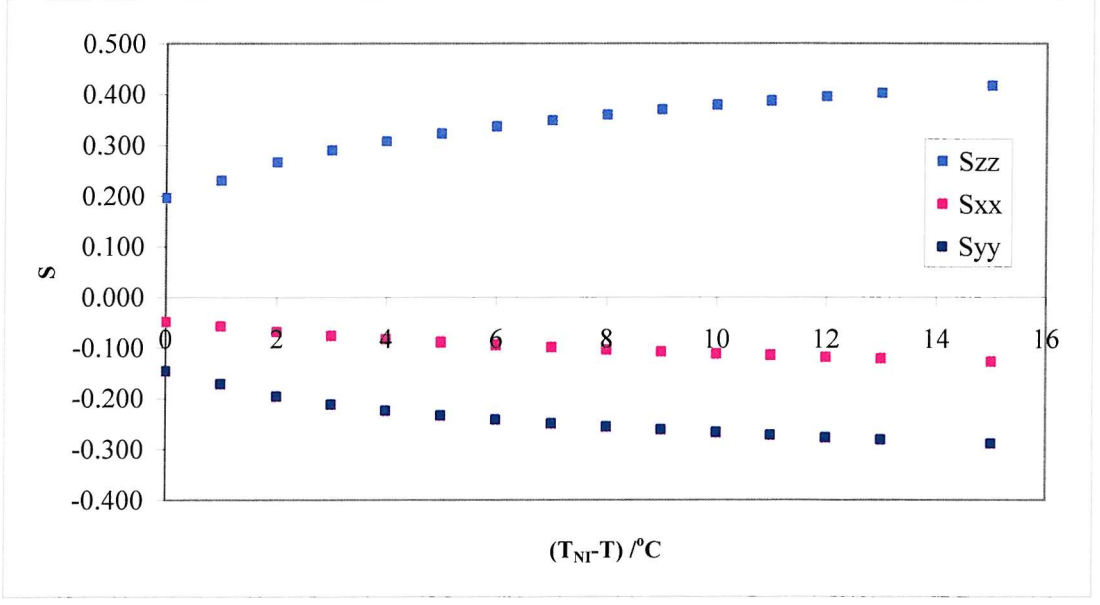

D.5. CBO9OBF$_4$

The order parameters S_{zz}, S_{xx}, S_{yy} and the biaxial ordering S_{xx}-S_{yy} for per-deuterated anthracene dissolved in CBO9OBF$_3$.

Temperature /°C	(T_{NI}-T)	$\Delta\upsilon_\beta$ /kHz	$\Delta\upsilon_{\alpha,\gamma}$ /kHz	S_{zz}	S_{xx}	S_{yy}	S_{xx}-S_{yy}
75	0	36.5	-9.5	0.186	-0.043	-0.144	0.101
74	1	48.1	-13.1	0.247	-0.059	-0.188	0.129
73	2	53.4	-15.1	0.274	-0.067	-0.207	0.140
72	3	57.3	-16.7	0.295	-0.074	-0.221	0.147
71	4	60.5	-18.1	0.312	-0.080	-0.232	0.153
70	5	63.2	-19.3	0.327	-0.085	-0.242	0.157
69	6	65.5	-20.5	0.339	-0.090	-0.249	0.160
68	7	67.7	-21.6	0.351	-0.094	-0.257	0.163
67	8	69.6	-22.6	0.361	-0.098	-0.263	0.165
66	9	71.3	-23.6	0.371	-0.102	-0.268	0.166
65	10	73.1	-24.6	0.381	-0.107	-0.274	0.168

Plot of S_{zz} and S_{xx}-S_{yy} for per-deuterated anthracene dissolved in CBO9OBF$_4$.

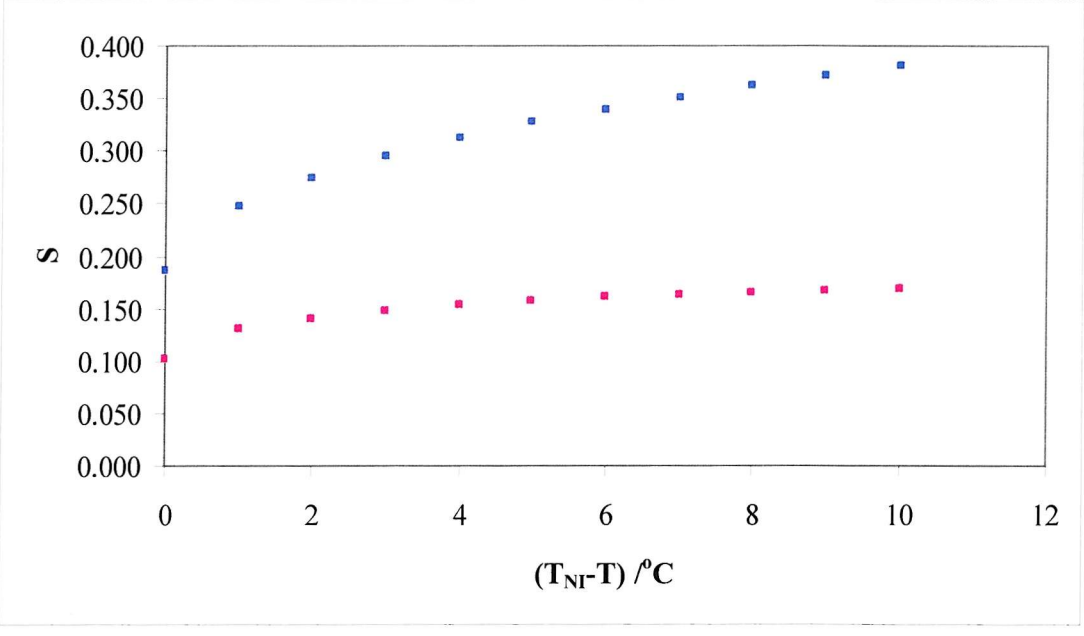

Plot of S_{zz}, S_{xx} and S_{yy} for per-deuterated anthracene dissolved in CBO9OBF$_4$.

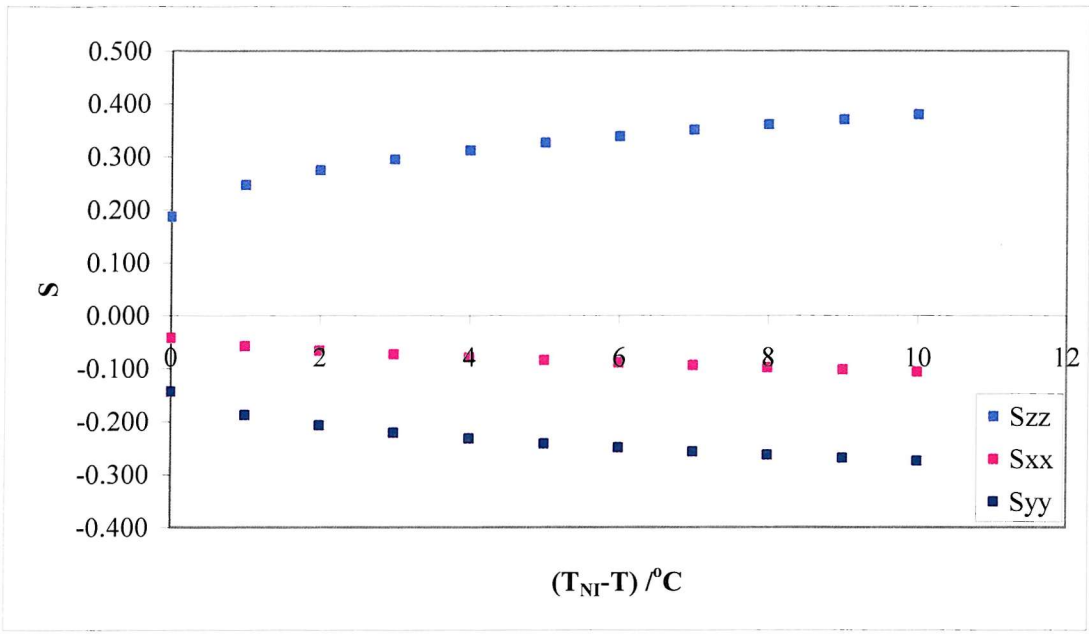

Appendix E

Crystal Structures and Data

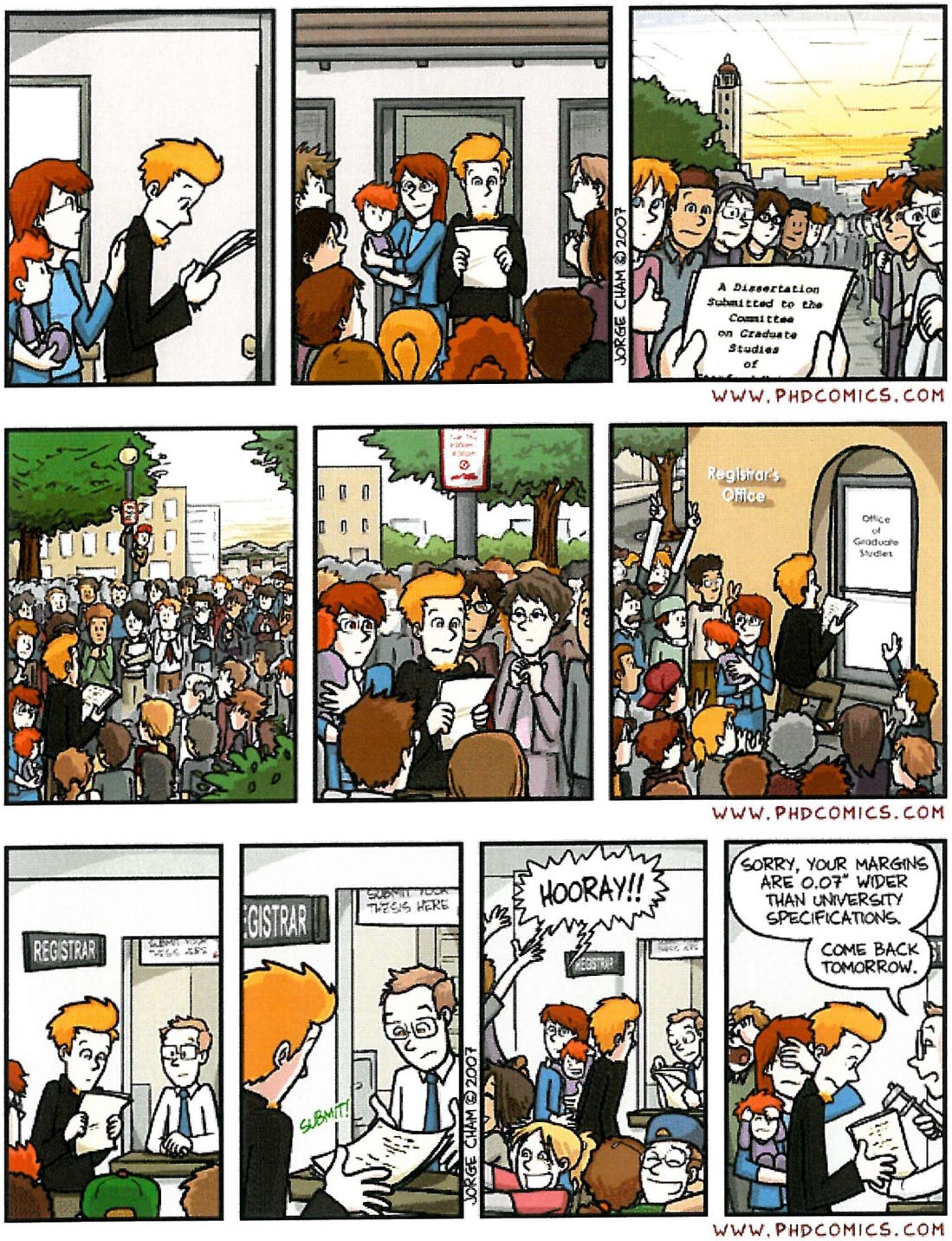

"Piled Higher and Deeper" by Jorge Cham
www.phdcomics.com

Used with permission

E. Appendix E

E.1. Chapter 3

E.1.1. CBOnOBFOCF$_3$

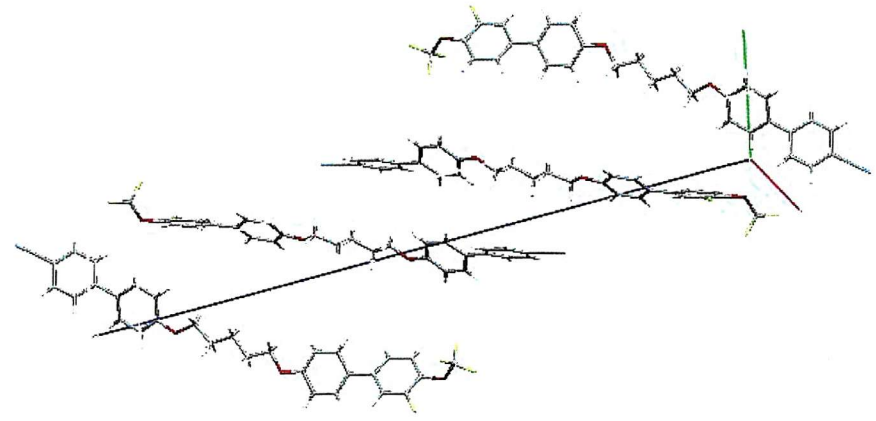

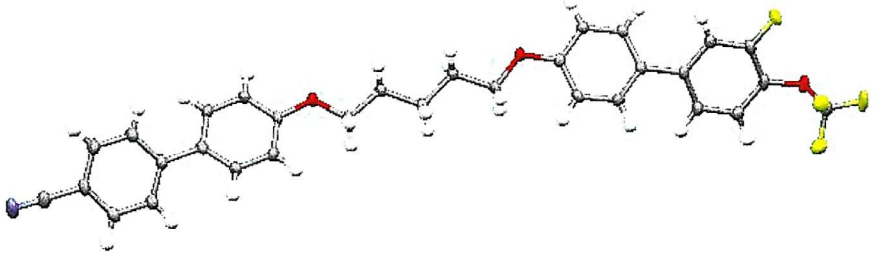

Crystal structure of CBO5OBFOCF$_3$ (top) view of the unit cell with six dimer molecules, (bottom) numbered asymmetric unit where ellipsoids represent greater than 50% probability level of atomic position within the cell.

$C_{31}H_{25}NO_4$	a = 6.60560(10) Å	T = 120(2) K
RMM = 535.54	b = 9.0388(2) Å	λ = 1.436 Å
monoclinic P2(1)/n	c = 41.6066(7) Å	Dc = 1.213 Mg/m^3
V = 2477.7(9) Å^3	α = 90.00°	μ = 0.112 mm^{-1}
Z = 4	β = 94.1130°	0.10 x 0.10 x 0.06 mm^3
R_1 = 0.043	γ = 90.00°	White shard

E.2. Chapter 5

E.2.1. Cat(O4OCB)$_2$

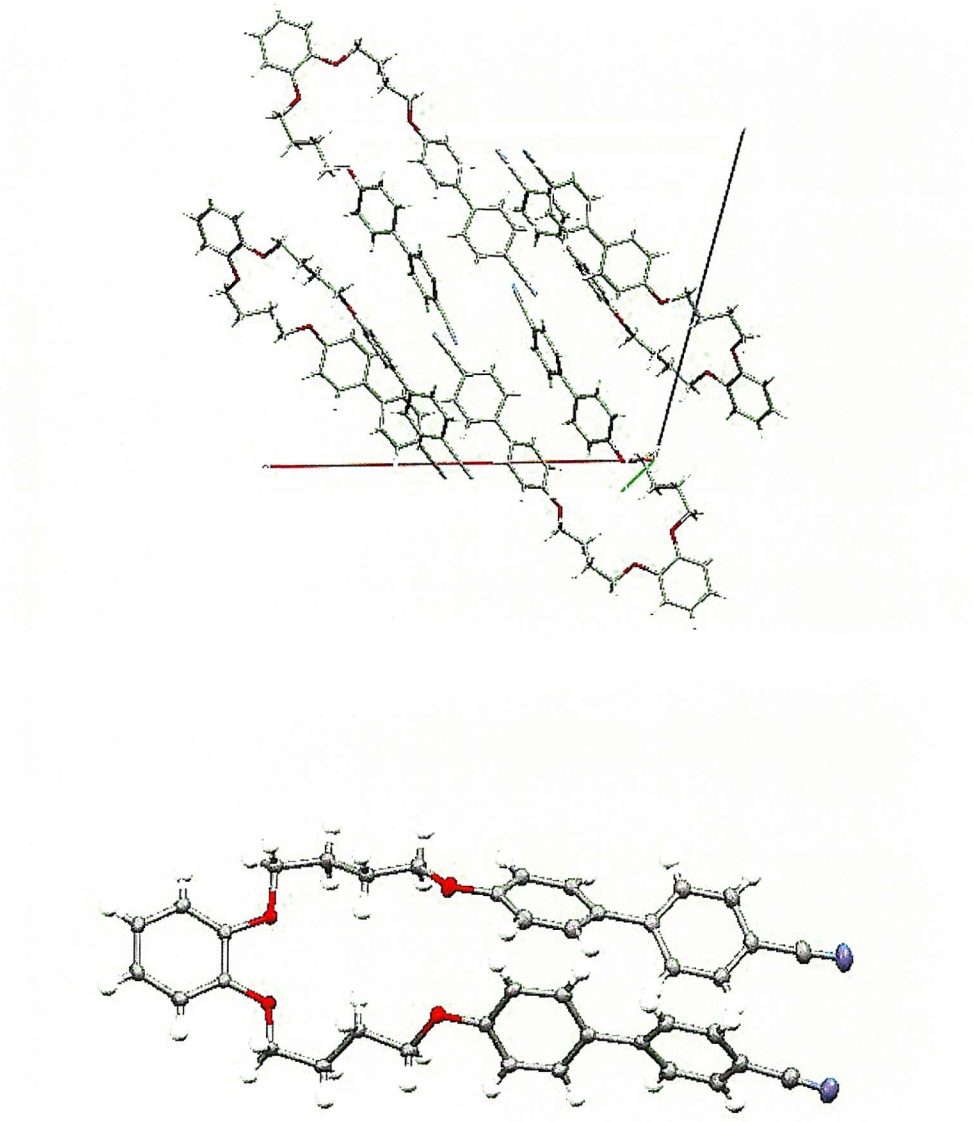

Crystal structure of Cat(O4OCB)$_2$ (top) view of the unit cell with six dimer molecules, (bottom) numbered asymmetric unit where ellipsoids represent greater than 50% probability level of atomic position within the cell.

$C_{40}H_{36}N_2O_4$	a = 20.6189(3) Å	T = 120(2) K
RMM = 604.78	b = 8.8790(10) Å	λ = 0.71073 Å
Monoclinic P2(1)/c	c = 18.1867(3) Å	Dc = 1.278 Mg/m^3
V = 3164.7(4) Å^3	α = 90.00°	μ = 0.076 mm^{-1}
Z = 4	β = 108.102 (10)°	0.60 x 0.40 x 0.12 mm^3
R_1 = 0.0464	γ = 90.00°	White shard

E.2.2. Cat(O8OCB)$_2$

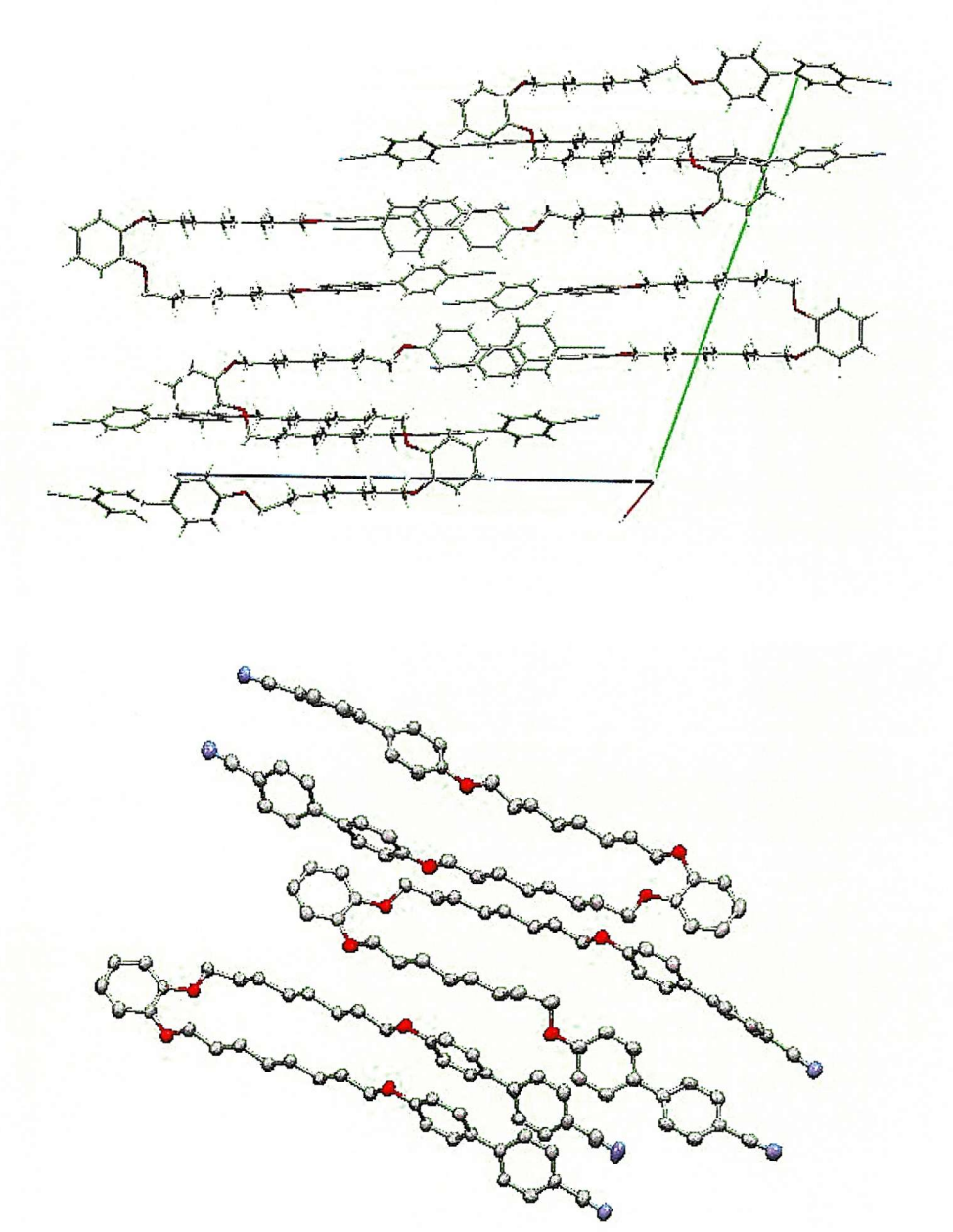

Crystal structure of Cat(O8OCB)$_2$ (top) view of the unit cell with six dimer molecules, (bottom) numbered asymmetric unit where ellipsoids represent greater than 50% probability level of atomic position within the cell.

$C_{49}H_{52}N_2O_4$	a = 9.4379(3) Å	T = 120(2) K
RMM = 720.92	b = 24.5343(10) Å	λ = 0.71073 Å
Triclinic P-1	c = 27.8878(11) Å	Dc = 1.213 Mg/m^3
V = 5920.8(4) Å^3	α = 109.848(2)°	μ = 0.076 mm^{-1}
Z = 6	β = 96.750(2)°	0.10 x 0.10 x 0.06 mm^3
R_1 = 0.0576	γ = 97.960(2)°	Pale beige shard

E.2.3. Cat(O9OCB)$_2$

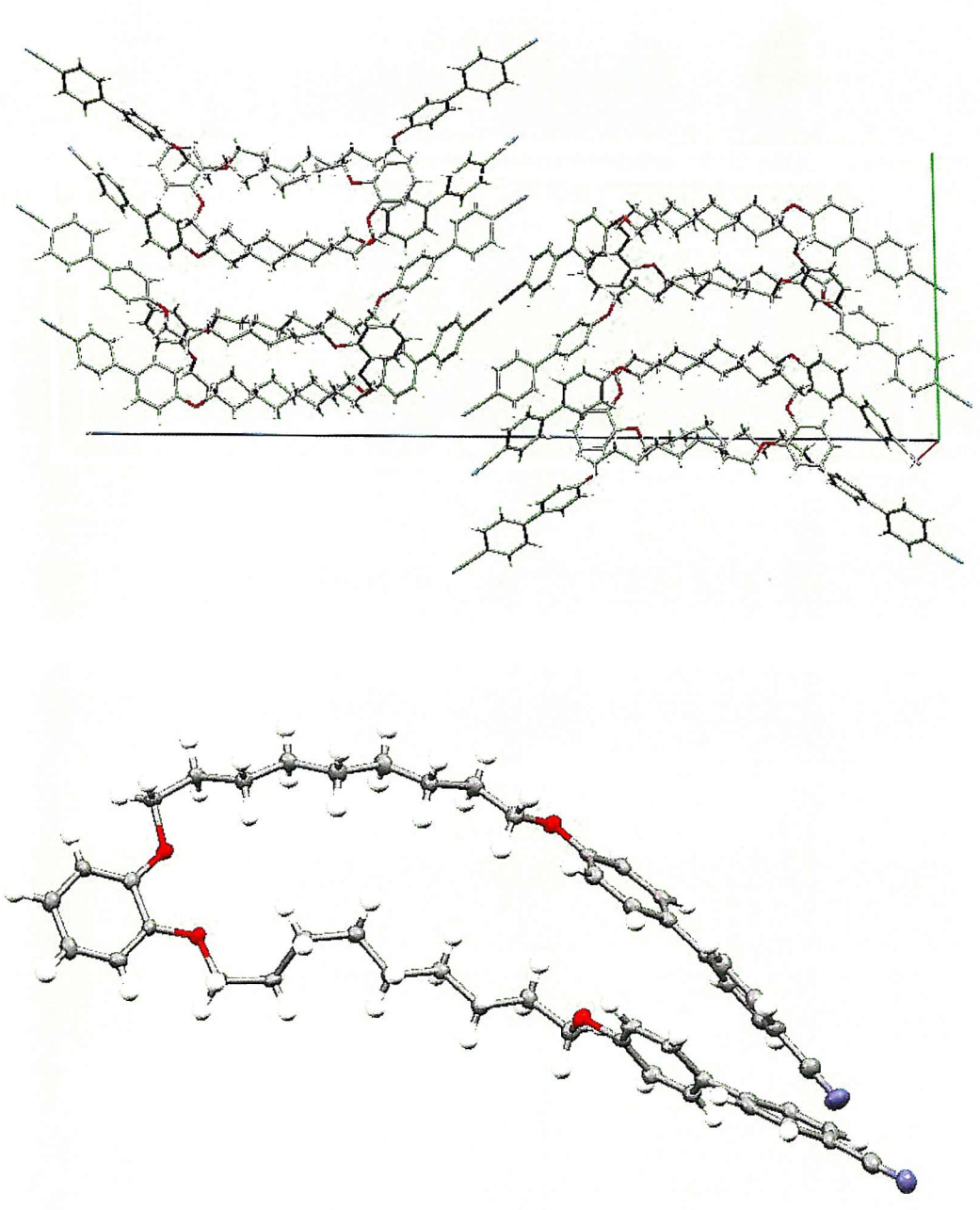

Crystal structure of Cat(O9OCB)$_2$ (top) view of the unit cell with six dimer molecules, (bottom) numbered asymmetric unit where ellipsoids represent greater than 50% probability level of atomic position within the cell.

$C_{50}H_{56}N_2O_4$	a = 8.8233(2) Å	T = 120(2) K
RMM = 749.01	b = 17.7886(4) Å	λ = 0.71073 Å
Orthorhombic Pbca	c = 52.8278(12) Å	Dc = 1.200 Mg/m^3
V = 8291.5(4) Å^3	α = 90.00°	μ = 0.075 mm^{-1}
Z = 8	β = 90.00°	0.05 x 0.05 x 0.02 mm^3
R_1 = 0.1294	γ = 90.000°	White shard